Symposium on the Geology and Mineral Deposits of the Challis 1°×2° Quadrangle, Idaho

U. S. GEOLOGICAL SURVEY BULLETIN 1658 A–S

Symposium on the Geology and Mineral Deposits of the Challis 1°×2° Quadrangle, Idaho

Edited by D. H. McINTYRE

Papers presented at the
Northwest Mining
Association Convention,
Spokane, Washington,
Dec. 1–2, 1983

U. S. GEOLOGICAL SURVEY BULLETIN 1658 A–S

DEPARTMENT OF THE INTERIOR
DONALD PAUL HODEL, *Secretary*

U.S. GEOLOGICAL SURVEY
Dallas L. Peck, Director

UNITED STATES GOVERNMENT PRINTING OFFICE, WASHINGTON: 1985

For sale by the Branch of Distribution
U.S. Geological Survey
604 South Pickett Street
Alexandria, VA 22304

Library of Congress Cataloging in Publication Data
Symposium on the Geology and Mineral Deposits of the Challis 1°×2° Quadrangle, Idaho (1983 : Spokane, Wash.)
(U.S. Geological Survey bulletin ; 1658A–S)
"Papers presented at the Northwest Mining Association Convention, Spokane, Washington, Dec. 1–2, 1983."
Bibliography: p.
Supt. of Docs. No.: I 19.3:1658A–S
1. Geology—Idaho—Challis Region—Congresses. 2. Mines and mineral resources—Idaho—Challis Region—Congresses.
I. McIntyre, David H. II. Northwest Mining Association (U.S.). Convention (1983 : Spokane, Wash.) III. Title. IV. Series.
QE75.B9 no. 1658A–S 557.3 s
[557.95'7] 85–600112

[QE104.C46]

CONTENTS

[LETTERS INDICATE CHAPTERS]

INTRODUCTION

The symposium on the geology and mineral deposits of the Challis 1°×2° quadrangle, presented at the Northwest Mining Association convention in Spokane, Wash., on December 1–2, 1983, was the seventh public meeting in which the results of studies made under the Conterminous United States Mineral Assessment Program (CUSMAP) have been discussed. The chapters in this volume are slightly expanded, written versions of the talks presented as part of the symposium.

CUSMAP was initiated in 1977 to provide an up-to-date assessment of the mineral resource potential of the lower 48 States. Under CUSMAP, more than 66,000 square miles in 12 states have been assessed to date, and additional assessments will be completed on another 60,000 square miles in the near future.

One of the major objectives of CUSMAP is the development and application of new concepts for the identification of mineral resource potential in heretofore untested but possibly mineralized areas. CUSMAP is providing new information on present and potential mineral supplies and is producing important data to guide our national minerals policy, for minerals exploration, and for land-use planning by Federal, State, and local governments. The results of the CUSMAP assessments are published in folio format. In addition to a mineral resource appraisal report and map, a folio may include geologic, geochemical, geophysical, and other maps and reports. A summary report for each quadrangle is published as a U.S. Geological Survey Circular. Basic data developed during the studies are published in a wide range of other technical reports.

The Challis CUSMAP project began in 1979. At that time, modern geologic mapping was available for 15 percent of the quadrangle. Major emphasis, therefore, was placed on improvement of the geologic data base, a necessary prerequisite to a meaningful mineral resource appraisal. A wide range of geologic settings is present; 41 mineral commodities have been produced or occur in anomalous but subeconomic quantities.

The chapters in this volume are summaries of parts of the work done on the Challis project prior to December 1983. In many respects, the chapters should be considered progress reports because work on some of the topics discussed is continuing. And, because the articles originated as scripts for oral presentation, not all the customary conventions for formal written presentation could be followed. For example, not all geographic terms mentioned in the text are shown on the figures. However, the text provides sufficient information about their location to guide the interested reader.

Symposium on the Geology and Mineral Deposits of the Challis 1°×2° Quadrangle, Idaho

Chapter A

Summary of the Geology, Mineral Deposits, and Resource Potential for Selected Commodities in the Challis Quadrangle

By FREDERICK S. FISHER

CONTENTS

FIGURES

TABLE

Abstract

At least four major metallogenic events are represented in the Challis quadrangle. The earliest of these was syngenetic deposition of cobalt, copper, iron, gold, and minor silver and lead in Precambrian sedimentary rocks about 1.7 to 1.5 b.y. (billion years) ago. The second event, syngenetic deposition of silver, barium, lead, vanadium, zinc, and lesser amounts of gold, copper, molybdenum, tungsten, and tin, took place in Cambrian to Permian time. The third event was introduction of niobium, tantalum, thorium, uranium, and the rare-earth elements in pegmatites and primary minerals of the Idaho batholith, which was emplaced in several phases during the Cretaceous between 112 and 70 m.y. (million years) ago. The final event was the introduction of beryllium, uranium, thorium, molybdenum, tin, gold, silver, mercury, antimony, and fluorine during Tertiary igneous activity about 47 to 29 m.y. ago. Blacksand and gold placer deposits accumulated during Pleistocene and Holocene time.

Previously deposited metals were remobilized during igneous and tectonic activity in the Precambrian, Cretaceous, and Tertiary. Ore minerals occur in veins, replacements, disseminations, stockworks, and skarns associated both with the Idaho batholith and its satellite plutons and with many types of Tertiary intrusive bodies. Most metals in these deposits are believed to have been derived from crustal sources, most likely the metalliferous Precambrian and Paleozoic sedimentary rocks.

Much of the area along the trans-Challis fault system has moderate to high resource potential for silver and gold, as does the northwestern side of the Twin Peaks caldera. The southwestern and western sides of the Thunder Mountain cauldron complex have a high resource potential for silver, gold, mercury, molybdenum, and tungsten. Roof pendants of metamorphosed Paleozoic rocks in the Idaho batholith have a high resource potential for tungsten. The greatest resource potential in the Challis quadrangle is in Paleozoic sedimentary rocks, which in the Bayhorse area have a high potential for silver, gold, copper, fluorspar, lead, and zinc. Elsewhere in the quadrangle, argillite and micritic limestone beds in the Devonian Milligen Formation and the Paleozoic Salmon River assemblage have a high resource potential for silver, barite, molybdenum, lead, antimony, vanadium, tungsten, and zinc in veins, replacements, and stratabound syngenetic deposits.

INTRODUCTION

The Challis quadrangle is in central Idaho north of the Snake River Plain (fig. A1). The largest community in the quadrangle is Challis, with a population of 794. Other settlements are Stanley, Lowman, Garden Valley, and Yellow Pine, all with populations of less than 100.

More than 95 percent of the quadrangle is federally owned land, encompassing parts of the Salmon, Challis, Boise, Sawtooth, and Payette National Forests. Nearly one-third of the area is within the River-Of-No-Return Wilderness and the Sawtooth National Recreation Area (fig. A4). Extensive tracts, chiefly in the southeastern part of the quadrangle, are managed by the U.S. Bureau of Land Management.

Most of the quadrangle is mountainous. Elevations range from a low of 3,000 ft (feet) in the valley of the South Fork of the Payette River where it exits the quadrangle in the southwest to a high of 11,815 ft at the summit of Castle Peak in the White Cloud Peaks (fig. A2). Local relief of 3,000–4,000 ft is common throughout the area, and canyons and valleys are steep sided.

Much of the terrane is moderately to heavily forested and generally below timberline; however, parts of the White Cloud Peaks and Sawtooth Range and other scattered peaks rise well above timberline and have subalpine climates.

Principal industries in the area are farming, ranching, lumbering, mining, and recreation.

GEOLOGIC SETTING

The rocks in the quadrangle can be subdivided into five main groups (fig. A2). Precambrian sedimentary and metamorphic rocks crop out mainly in the northern and eastern parts of the area. Paleozoic sedimentary rocks are mostly in the south-central and east with scattered exposures through the central parts of the quadrangle. The Cretaceous Idaho batholith occupies the western half of the quadrangle, and the Tertiary Challis volcanic field covers most of the eastern half. Tertiary intrusive batholiths and stocks are mainly in the central part of the quadrangle.

Four major structural features predominate: first, a northeast-trending structural grain expressed by extensive high-angle faults, fracture systems, dike swarms, and grabens; second, a north- and northwest-trending system of high-angle faults; third, caldera and collapse features associated with the Challis volcanic field; and fourth, extensive thrust faults in the Paleozoic formations.

RESOURCE INVESTIGATIONS

At the start of the Challis CUSMAP (Conterminous United States Mineral Assessment Program) project in 1979, only about 15 percent of the quadrangle had published geologic maps less than 50 years old, and about half of the quadrangle had never been mapped geologically. Regional geophysical data were incomplete, and geochemical studies had been conducted only in parts of the River-Of-No-Return Wilderness and the Sawtooth National Recreational Area.

Field studies made during the Challis project have resulted in modern geologic maps for the entire quadrangle (Fisher, McIntyre, and Johnson, 1983), gravity and aeromagnetic maps for the entire quadrangle (Webring and Mabey, 1981; Mabey, 1982; Mabey and Webring, chap. E, this volume), and extensive geochemical surveys

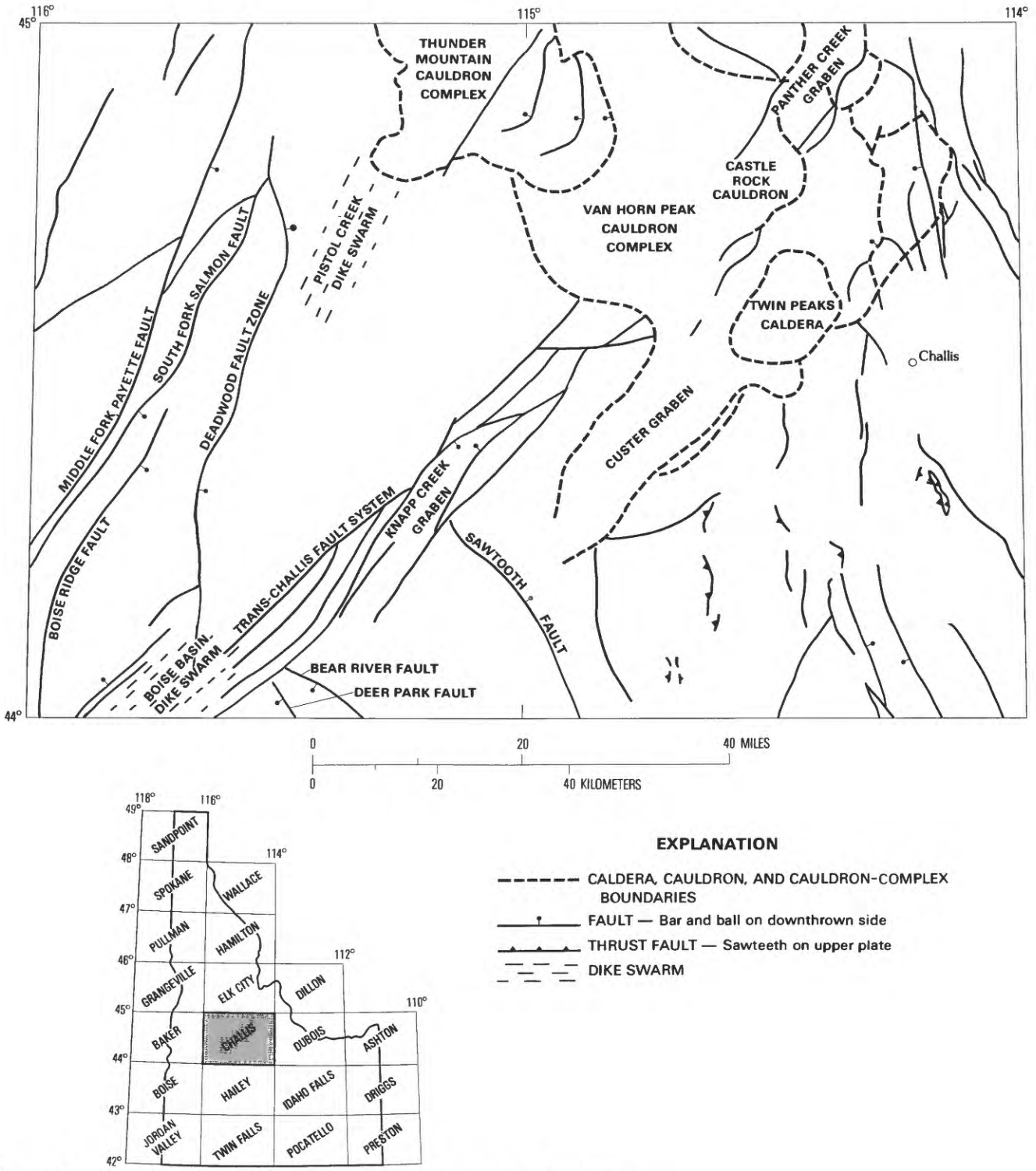

Figure A1. Map showing selected geologic features in the Challis quadrangle.

(Callahan and others, 1981a, 1981b; Shacklette and Erdman, 1982; Erdman and others, 1983; Fisher and May, 1983; Fisher and others, 1983).

Some of the highlights of these field studies are summarized here. The discovery and delineation of the caldera complexes and development of the framework stratigraphy of the Challis volcanic field (McIntyre and others, 1982; Fisher, McIntyre, and Johnson, 1983) resulted from studies spearheaded by E. B. Ekren, D. H. McIntyre, R. F. Hardyman, and B. F. Leonard, all with the U.S. Geological Survey, Denver, Colo. Detailed mapping and petrological studies by Thor Kiilsgaard (U.S. Geological Survey, Spokane, Wash.) and Earl Bennett (Idaho Bureau of Mines and Geology, Moscow, Idaho)

in the western half of the quadrangle have shown that the Atlanta lobe of the Idaho batholith is composed of six rock types emplaced in at least three stages during a considerable time span (Kiilsgaard and Lewis, chap. B, this volume). Kiilsgaard and Bennett also discovered, delineated, and described a previously unrecognized bimodal group of epizonal granitic and dioritic Tertiary plutons, some of batholithic size, within areas thought to be composed of Cretaceous rocks of the Idaho batholith (Bennett, 1980). Mapping in the central and south-central parts of the quadrangle by W. E. Hall and S. W. Hobbs (Fisher, McIntyre, and Johnson, 1983) unraveled a highly complicated sequence of thrust faults bounding large areas of allochthonous Paleozoic terranes. Also, the stratigraphic studies in these terranes have described host rocks for major ore deposits including both veins and replacements and also newly recognized stratabound syngenetic occurrences (Hall, chap. J, this volume; Hobbs, chaps. D, K, this volume). Together these field studies have led to the recognition of a major northeast-trending fault zone more than 100 mi (miles) (160 km or kilometers) long, marked by dike swarms, grabens, faults, and calderas, that transects the quadrangle and extends well into Montana (fig. A3).

These newly discovered features—the fault zone, the caldera complexes, the six phases of the Idaho batholith, the Tertiary plutons, and the thrust faults and allochthons—have had a profound influence on the character, type, and location of ore deposits in the quadrangle and are the subjects of the succeeding chapters in this volume.

The evaluation of the mineral resource potential of the Challis quadrangle is still in progress, and final resource appraisal maps will be completed when the project is concluded at the end of 1985. The resource appraisal method being used is best described as "simple subjective;" it relies mainly on the opinions of highly qualified economic geologists and is firmly grounded on a solid geologic-map base. In a broad sense, we are following many of the principles recently outlined by Taylor and Steven (1983).

Forty-one commodities either have been produced or are present in anomalous but subeconomic quantities within the quadrangle (table A1), and hundreds of mines and prospects are scattered across the quadrangle (fig. A4). Descriptions and locations of all the mines and prospects in the Challis quadrangle are given in Mitchell and others (1981).

The number and diversity of deposits containing the 12 most abundant metallic commodities in the quadrangle are shown in figure A5. Precious-metal deposits make up the largest group, followed in order by lead, copper, and zinc; but the remaining 7 commodities account for more than 300 deposits. The other 12 commodities (table A1) have been produced from fewer than 10 deposits each, or as byproducts, and are not shown on figure A5.

Because of the large number and variety of mineral deposits within the quadrangle, an attempt was made to identify the most important commodities and to focus efforts on them. First, a list of all commodities known to occur in the area was compiled (table A1); second, those commodities were ranked into four groups according to significance (loosely defined here as national importance) (fig. A6), using the net import reliance tables as determined by the U.S. Bureau of Mines (U.S. Bureau of Mines, 1983). Finally, 10 geologists having more than 100 years of combined experience in the area were asked to rank the listed commodities into one of five groups based on their beliefs as to the likelihood of new deposits of a given commodity occurring within the quadrangle. Their responses were averaged, and each commodity was then plotted on figure A6 according to significance and likelihood of occurrence. Those commodities in the shaded area have received generally more geologic study by the Challis CUSMAP project.

METALLOGENIC EVENTS

At least four major metallogenic events are represented in the Challis quadrangle. These occurred during Precambrian, Paleozoic, Cretaceous, and Tertiary time. The relationship of these events to major igneous, sedimentary, and tectonic features in the Challis quadrangle are shown on figure A7.

Precambrian

The earliest metallogenic event occurred in the Precambrian. Nearly 1 b.y. of sedimentary history are represented by argillic rocks of the Middle Proterozoic Yellowjacket Formation and quartzite and siltite of the Lemhi Group and the Hoodoo Quartzite, Swauger, Lawson Creek, and the Late Proterozoic Wilbert Formations. Precambrian igneous activity consisted of intrusion of granitoid plutons about 1.5 to 1.3 b.y. ago (Evans, 1981). Mafic tuffs and dikes dated at about 1.7 b.y. are also present within the Yellowjacket sequence (Hughes, 1982). Rocks of the Yellowjacket Formation range from argillaceous quartzite to argillite. They have been interpreted as having been deposited in a rift basin bordering the craton and representing depositional environments ranging from basinal to deepwater clastic fan deposits and turbidites (Modreski, chap. R, this volume; Hughes, 1982). Metals deposited during Yellowjacket time were probably formed by some type of sea-floor hot springs related to the mafic volcanic activity. The principal metals were cobalt, copper, and iron, lesser amounts of gold, and probably some silver and lead. The metals are mostly stratabound and were probably deposited syngenetically with the enclosing sediments.

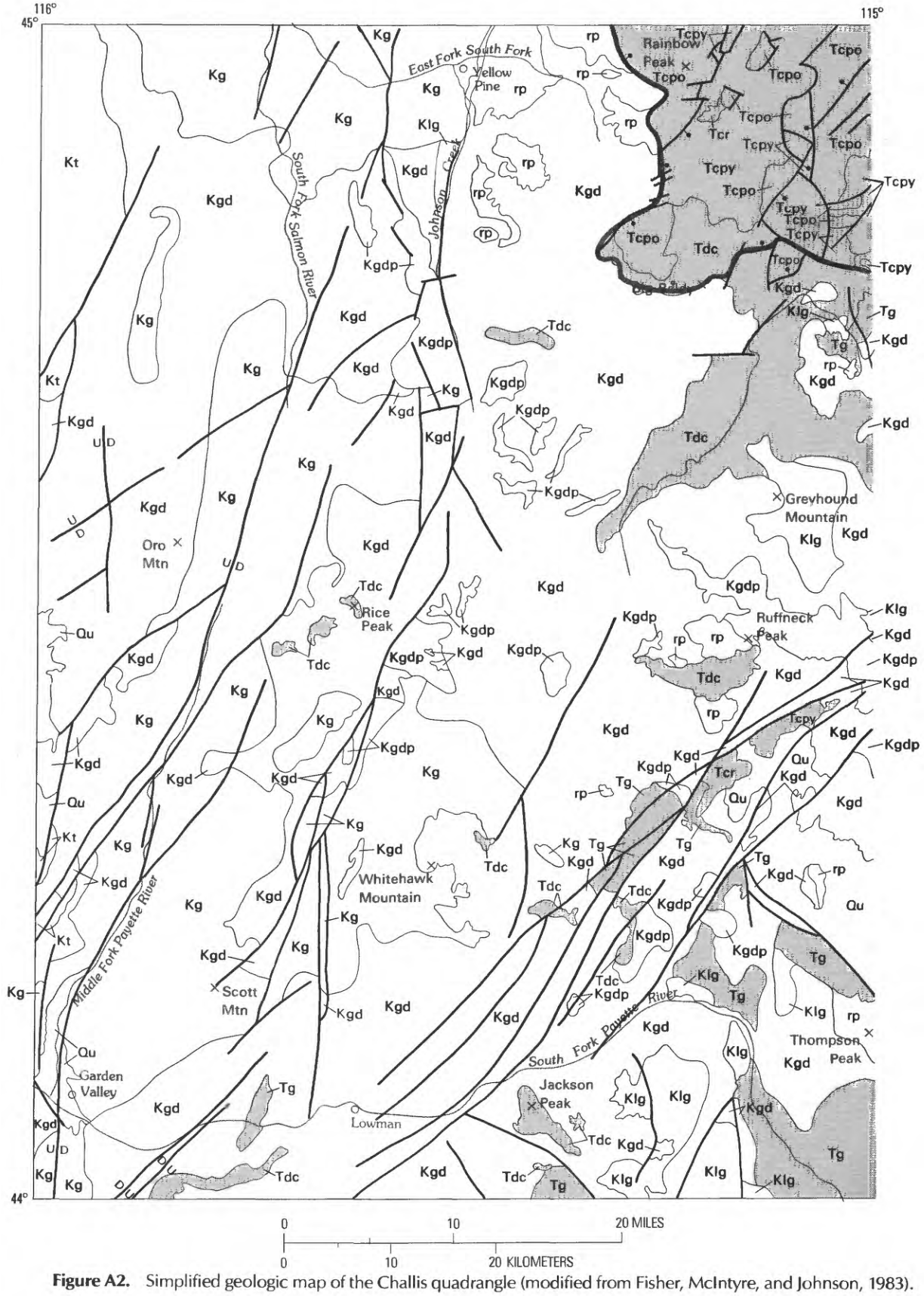

Figure A2. Simplified geologic map of the Challis quadrangle (modified from Fisher, McIntyre, and Johnson, 1983).

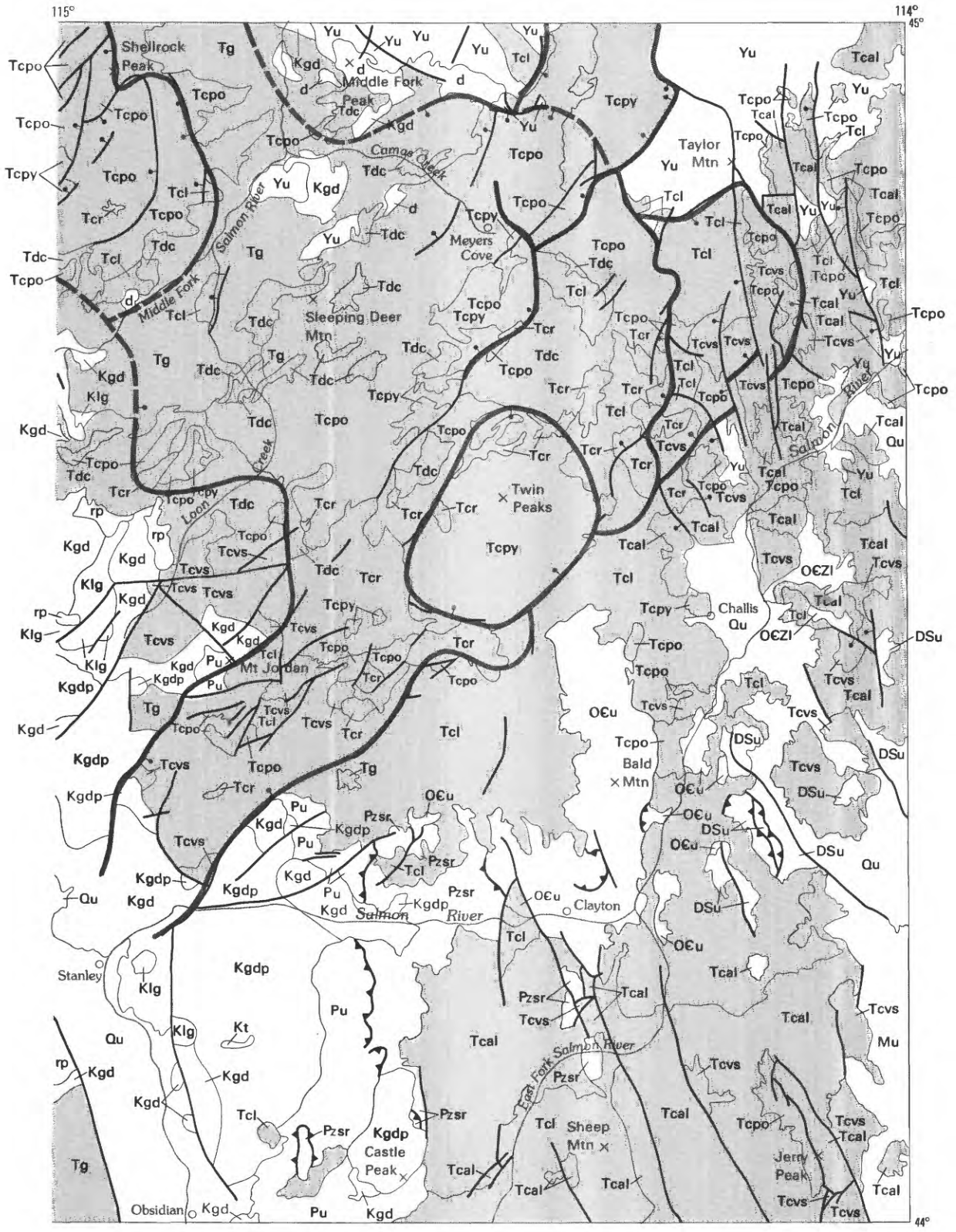

Figure A2. Continued.

CORRELATION OF MAP UNITS

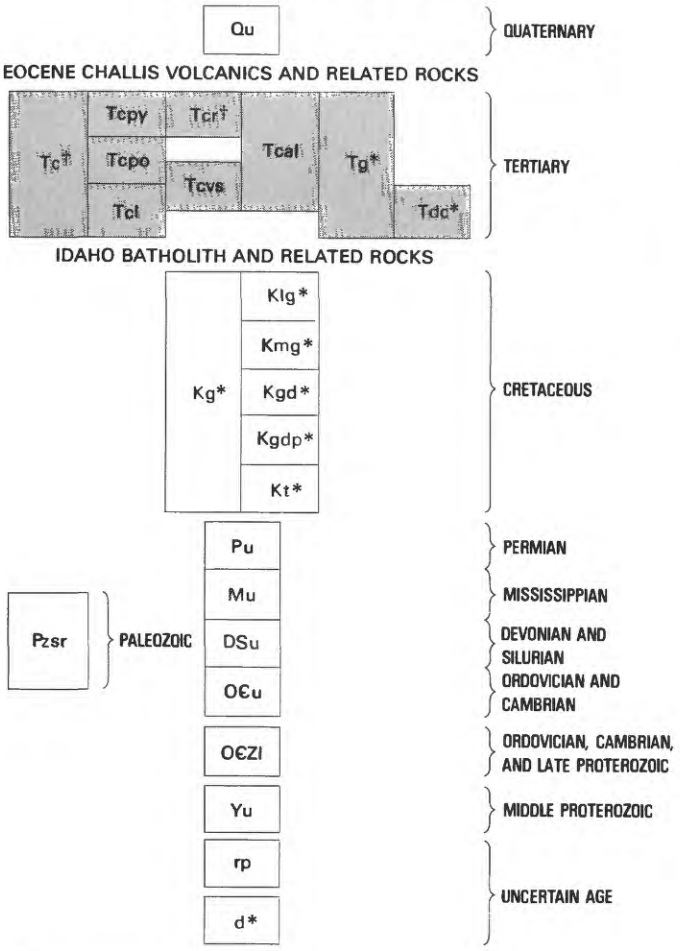

*Intrusive rocks
†Rocks with both intrusive and extrusive characteristics

DESCRIPTION OF MAP UNITS

Qu — QUATERNARY DEPOSITS, UNDIVIDED—Includes floodplain, terrace, landslide, and glacial deposits. Materials include boulders, cobbles, pebbles, sand, silt, clay, peat, and travertine

Tc — CHALLIS VOLCANICS, UNDIVIDED (EOCENE)

Tcpy — YOUNGER PYROCLASTIC ROCKS AND SEDIMENTS—Associated with development of Twin Peaks caldera, Panther Creek graben, and late stages of Thunder Mountain cauldron complex. Welded and nonwelded ash-flow and ash-fall tuffs, lavas, pumice flows, flow breccias, caldera-slump breccias, and reworked tuffaceous sediments. Mostly rhyolite and rhyodacite

Tcpo — OLDER PYROCLASTIC ROCKS AND SEDIMENTS—Associated with development of Van Horn Peak cauldron complex, Custer graben, and early stages of Thunder Mountain cauldron complex. Welded and nonwelded ash-flow and ash-fall tuffs, lavas, flow breccias, and reworked tuffaceous sediments. Mostly thyolite, quartz latite, and rhyodacite, with lesser amounts of dacite and andesite

Tcl — LAVAS, FLOW BBRECCIAS, AND AGGLOMERATES—Principally andesite, dacite, and latite, with lesser amounts of basalt. Phenocryst rich to phenocryst poor, varying combinations of plagioclase, biotite, amphibole, clinopyroxene, orthopyroxene, and less common olivine and quartz

Tcr — RHYOLITE INTRUSIVE BODIES—Dikes, plugs, domes, and stocks. Phenocryst rich to phenocryst poor. Typically contain quartz, alkali feldspar, and sparse plagioclase and biotite phenocrysts

Tcvs — VOLCANICLASTIC AND SEDIMENTARY ROCKS—Includes subaqueously deposited pyroclastic flows, mudflow breccia and conglomerate, volcanic sandstone and mudstone. Volcanic components of these rocks contain plagioclase, biotite, and amphibole. Quartz and pyroxene are sparse as phenocrysts

Tcal — POTASSIUM-RICH ANDESITE, LATITE, AND BASALT LAVAS—Predominantly aphyric, reddish-brown, blocky to platy lavas that contain interbedded oxidized breccia. Olivine and pyroxene phenocrysts in some samples along with lesser amounts of plagioclase

Tg — GRANITE—Pink to gray, medium- to coarse-grained granite characterized by pink perthitic feldspar that commonly forms phenocrysts. May contain miarolitic cavities locally lined with smoky-quartz crystals

Tdc — DIORITE COMPLEX—Complex suite of rocks ranging from nonporphyritic diorite to porphyritic granodiorite, which is more common. Characterized by abundance of hornblende, euhedral biotite, and magnetite, which together make up as much as 35 percent of rock

Kg — IDAHO BATHOLITH AND RELATED ROCKS (CRETACEOUS)— Granitic rocks, undivided

Klg — Leucocratic granite—Light-gray to white, fine- to medium- grained, with distinctive anhedral texture. Principal minerals are quartz (33 percent), potassium feldspar (29 percent), and plagioclase (An_{26-30}, 33 percent). Biotite may constitute as much as 2 percent of rock. Garnet is common. Occurs as dikes and irregular stocks that are resistant to erosion and tend to form high points and ridges

Kmg — Muscovite-biotite granodiorite—Gray to light-gray, medium to coarse-grained, equigranular to porphyritic; contains books of muscovite visible in hand specimen and comprising as much as 5 percent of rock

Kgd — Biotite granodiorite and granite—Gray to light-gray, medium- to coarse-grained, equigranular to porphyritic. Plagioclase (An_{22-36}) is chief component of rock, with lesser quantities of quartz and potassium feldspar; biotite, as much as 5 percent, is principal mafic mineral; hornblende is absent

Kgdp — Porphyritic biotite granite and granodiorite—Coarsely porphyritic granitoid rock with metacrysts of pink potassium feldspar (microcline) 3-10 cm long in medium- to coarse-grained matrix that contains roughly equal amounts of microcline, plagioclase, and quartz. Rock generally contains 5-15 percent biotite and variable amounts of hornblende

Kt — Tonalite—Gray to dark-gray, medium- to coarse-grained, equigranular to porphyritic. Plagioclase is dominant mineral of rock, which may contain biotite or hornblende and ranges from massive to highly foliated

Pu — PERMIAN ROCKS, UNDIVIDED—Includes carbonaceous argillite, siltite, limestone, calcareous sandstone, and fine-grained quartzite of the Dollarhide and Grand Prize Formations. Parts of sequence are graded, have abundant crossbedding, convolute structures, and prominent banding. Thickness about 2,400 m

Pzsr	SALMON RIVER ASSEMBLAGE PALEOZOIC—Medium- to dark-gray, thin- to thick-bedded, well laminated argillite, siltstone, calcareous siltstone, and fine-grained calcareous sandstone. Faint to prominent lamination in most places, with cross lamination, current bedding, and sole structures in many fine-grained, thin sandstone beds. Dark colors related to amount of carbonaceous material, which ranges from none to a few impure coaly seams. Thickness unknown, but in places 1,400 m are present
Mu	MISSISSIPPIAN ROCKS, UNDIVIDED—Includes limestone, cherty limestone, mudstone, siltstone, sandstone, and conglomerate. In places highly fossiliferous, containing crinoidal debris, corals, and brachiopods. Thickness about 3,600 m
DSu	DEVONIAN AND SILURIAN ROCKS, UNDIVIDED—Includes dolomite, siltstone, sandstone, and quartzite. Dolomite units moderately to highly resistant and form blocky ledges and locally cliffs. Thickness about 1,800 m
O€u	ORDOVICIAN AND CAMBRIAN ROCKS, UNDIVIDED—Includes shale, argillite, phyllite, dolomite, and quartzite. Locally deformed and recrystallized. Thickness unknown but probably more than 3,500 m
O€Zl	INTERBEDDED QUARTZITE, DOLOMITE, AND ARGILLITE OF LEATON GULCH (ORDOVICIAN, CAMBRIAN, AND LATE PROTEROZOIC)—Predominantly quartzitic strata containing subordinate dolomite interbeds and some thin to thick (100 m) interbeds of argillite. Ripple marks, flute casts, and magnetite are locally abundant. Many argillite layers are metamorphosed to phyllite close to thrust faults. Thickness unknown but probably several hundred meters
Yu	MIDDLE PROTEROZOIC, UNDIVIDED—Includes quartzite, phyllite, argillite, siltite, and sandstone. Locally common ripple marks, cross laminations, load casts, and mud cracks. Thickness unknown but probably greater than 10,000 m
rp	ROOF PENDANTS AND XENOLITHS OF METAMORPHIC ROCK IN IDAHO BATHOLITH, UNDIVIDED (UNCERTAIN AGE)—Includes schist, quartzite, and calc-silicate rocks. At some localities graphite, garnet, and andalustite are common constituents
d	DIORITE, QUARTZ DIORITE, AND SYENITE (UNCERTAIN AGE)—Composite masses and mixed sequences of intrusive rocks of uncertain age. Rocks range from fresh to altered; where altered, epidote, chlorite, sericite, and calcite are common
	CONTACT
	FAULT
	THRUST FAULT—Sawteeth on upper plate
	CALDERA BOUNDARY—Dashed where inferred; bar and ball on downthrown side

Figure A2. Continued.

Table A1. Mineral commodities produced from or present in anomalous concentrations within the Challis quadrangle.

PRODUCED	
Silver	Niobium
Arsenic	Lead
Gold	Rare-earth elements
Barium	Sand and gravel
Bismuth	Antimony
Cadmium	Selenium
Cobalt	Stone
Copper	Tantalum
Fluorspar	Tellurium
Semiprecious gemstones	Thorium
Mercury	Uranium
Molybdenum	Tungsten
	Zinc

ANOMALOUS CONCENTRATIONS	
Beryllium	Nickel
Clay	Sulfur
Iron	Silica
Garnet	Tin
Graphite	Titanium
Limestone	Vanadium
Mica	Zirconium
Manganese	Zeolites

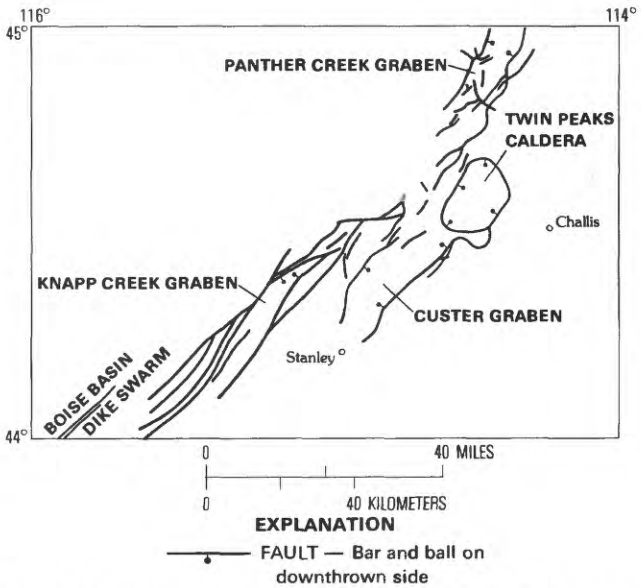

Figure A3. Principal features of the trans-Challis fault system (modified from Fisher, McIntyre, and Johnson, 1983).

Rocks of the Yellowjacket and Hoodoo Formations were complexly folded and metamorphosed to greenschist facies probably between 1.4 and 1.2 b.y. ago (Hughes, 1982). The cobalt-copper-iron ores in the Yellowjacket Formation were remobilized and recrystallized at this time. The Blackbird deposit, north of the Challis quadrangle, and the Iron Creek deposit (fig. A8) are examples of these remobilized Precambrian deposits.

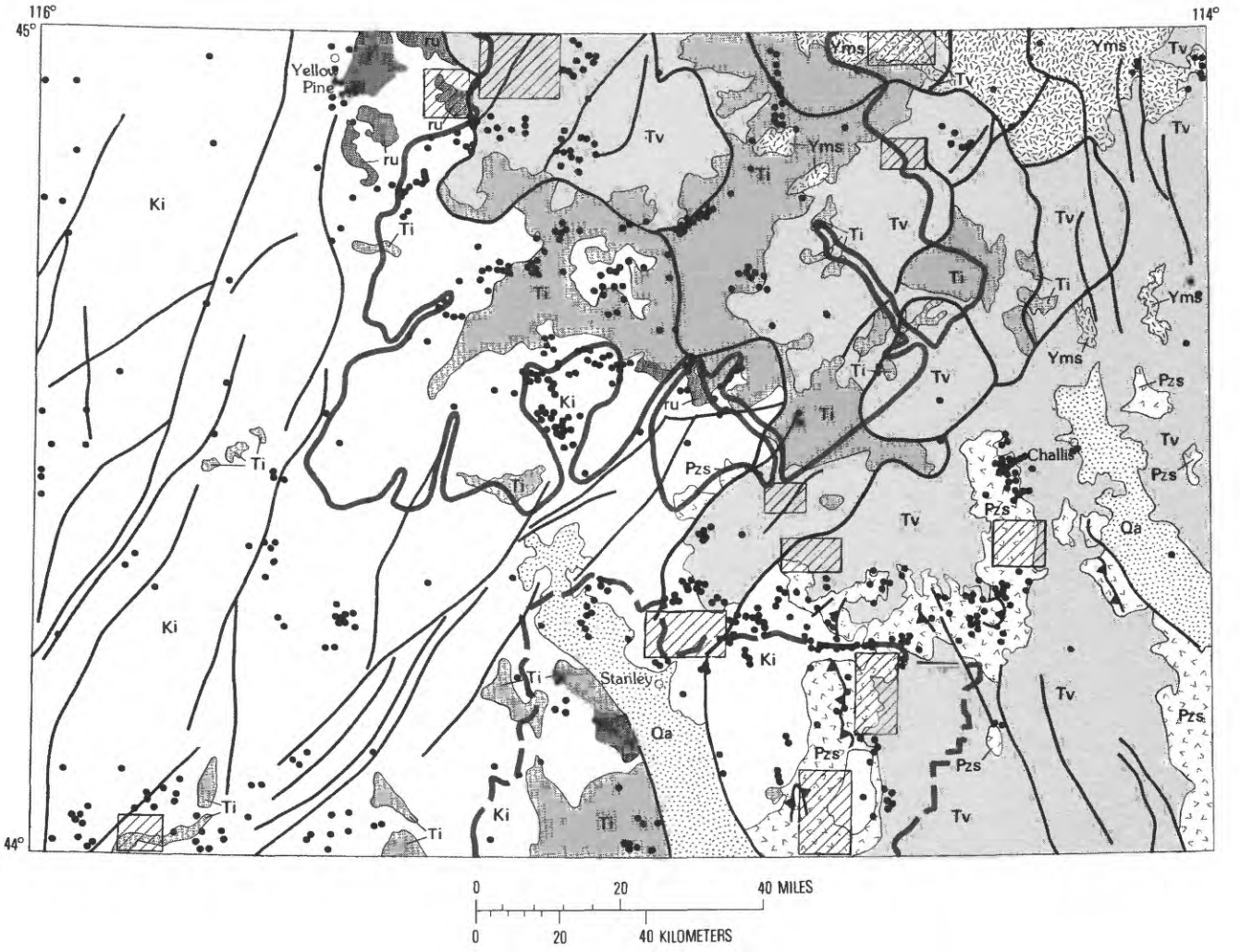

Figure A4. Map showing locations of mines and prospects, and wilderness and recreation areas in the Challis quadrangle.

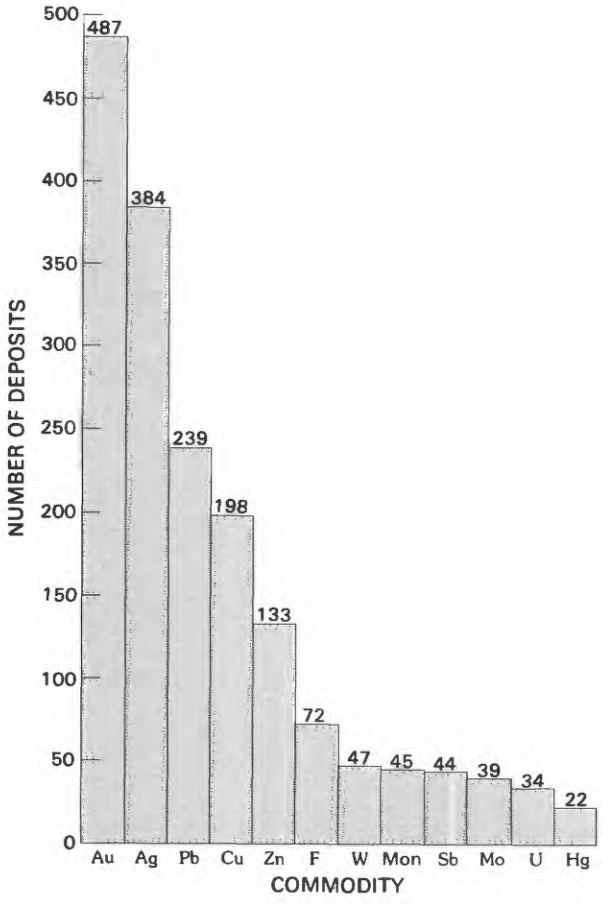

Figure A5. Number of mineral deposits arranged by commodity, Challis quadrangle. Mon., monazite.

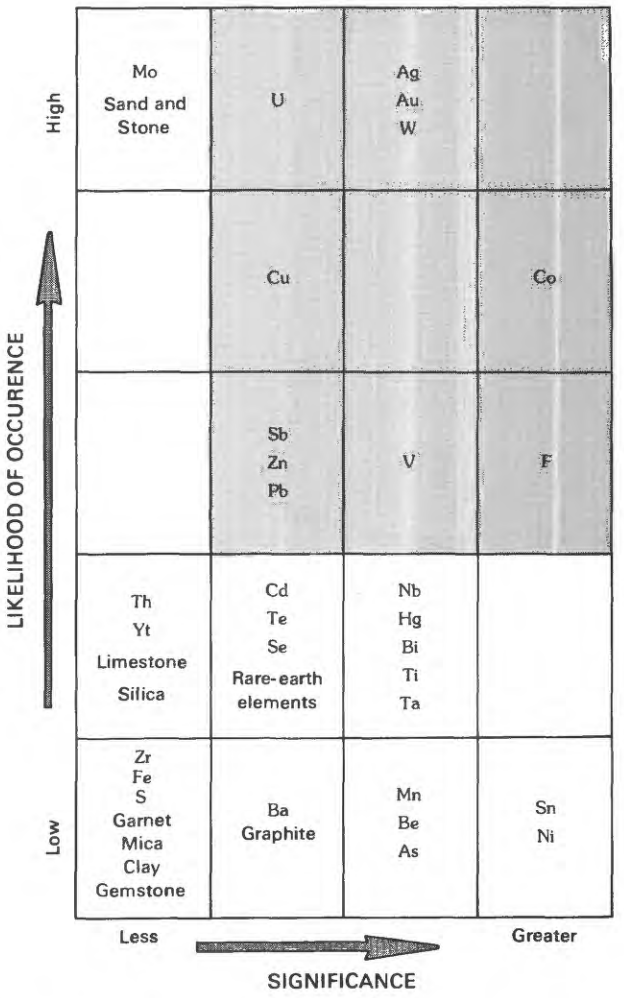

Figure A6. Chart comparing the significance as defined by the net import reliance tables (U.S. Bureau of Mines, 1983) and chance of discovery of mineral commodities in the Challis quadrangle.

Rocks of the Yellowjacket and Hoodoo Formations were complexly folded and metamorphosed to greenschist facies probably between 1.4 and 1.2 b.y. ago (Hughes, 1982). The cobalt-copper-iron ores in the Yellowjacket Formation were remobilized and recrystallized at this time. The Blackbird deposit, north of the Challis quadrangle, and the Iron Creek deposit (fig. A8) are examples of these remobilized Precambrian deposits.

Paleozoic

During the Paleozoic Era (fig. A7), silver, barium, lead, vanadium, and zinc were deposited syngenetically in many types of sedimentary rocks (Fisher and May, 1983; Skipp and others, 1979; Ketner, 1983). These metals, along with lesser amounts of gold, copper, molybdenum, and tungsten, are present in lower Paleozoic quartzite, limestone, dolomite, siltstone, and shale in the Bayhorse district (Hobbs, chap. K, this volume) and in middle and upper Paleozoic dark limestone, argillite, shale, and siltstone of the Milligen Formation, Copper Basin, Grand Prize, and Dollarhide Formations, and in the Paleozoic Salmon River assemblage and the Wood River Formation in the southern parts of the quadrangle (Hall and others, 1978; Skipp and others, 1979). The only Paleozoic igneous activity recorded in the quadrangle was the intrusion of some diorite and gabbro stocks in the north near the Yellowjacket region about 400 m.y. (million years) ago. Tectonic activity in the region was associated with the Late Devonian–Early Mississippian Antler orogeny, during which the Paleozoic rocks were widely folded and thrust eastward (Dover, 1980). Presumably, some refolding of the Precambrian rocks also occurred at that time.

Examples of syngenetic Paleozoic deposits are the zinc and barite ores at the Hoodoo mine (fig. A8) in the Paleozoic Salmon River assemblage. Other examples of syngenetic mineral deposits in the Salmon River assemblage are the vanadium-silver concentrations described by Fisher and May (1983) and possibly the lead-silver ores at the Livingston mine (fig. A8). The Lower Permian fine-grained carbonaceous basinal sedimentary rocks have potential

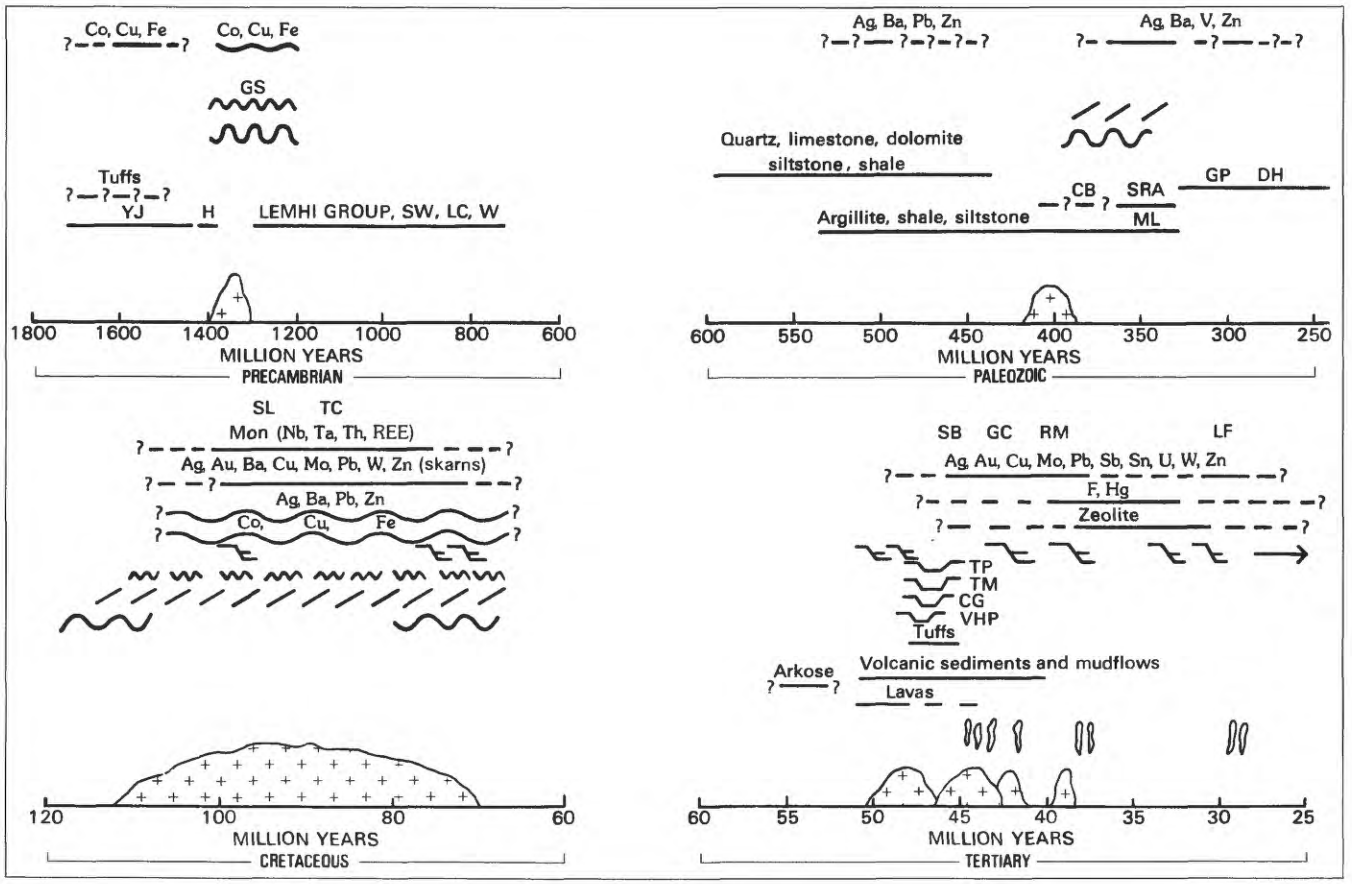

EXPLANATION

Co, Cu, Fe — TIME INTERVAL DURING WHICH METALS WERE DEPOSITED — Queried where uncertain

Co, Cu, Fe — TIME INTERVAL DURING WHICH METALS WERE REMOBILIZED

PERIOD OF METAMORPHISM

PERIOD OF THRUST FAULTING

PERIOD OF FOLDING

PERIOD OF ROCK FORMATION — Abbreviations explained at right

PERIOD OF HIGH-ANGLE FAULTING

PERIOD OF CALDERA FORMATION

DIKE

STOCK

GS, green-schist facies
YJ, Yellowjacket Formation
H, Hoodoo quartzite
SW, Swauger Formation
LC, Lawson Creek Formation
W, Wilbert Formation
CB, Copper Basin Formation
SRA, Salmon River assemblage
ML, Milligen Formation
GP, Grand Prize Formation
DH, Dollarhide Formation
SL, Skylark vein
TC, Thompson Creek mine
SB, Sunbeam mine
GC, General Custer vein
RM, Red Mountain prospect
LF, Little Falls molybdenum deposit
TP, Twin Peaks caldera
TM, Thunder Mountain caldera
CG, Custer graben
VHP, Van Horn Peak cauldron complex
REE, Rare-earth elements
Mon, Monazite

Figure A7. Diagram showing the temporal relationships of the major geologic and tectonic features and metallic mineral deposits in the Challis quadrangle.

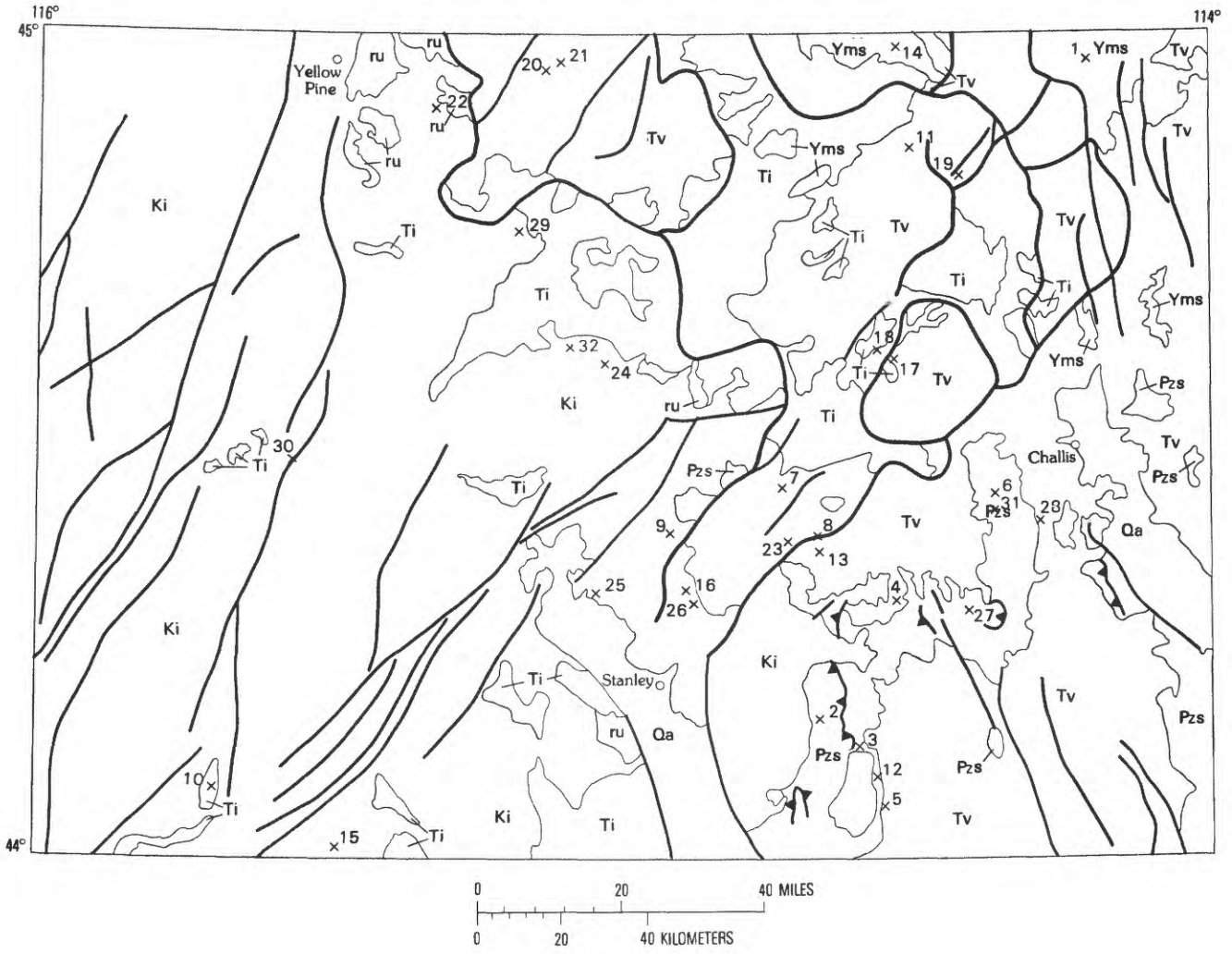

EXPLANATION

Qa	QUATERNARY ALLUVIUM—Includes flood plain, terrace, and alluvial-fan deposits
Ti	TERTIARY INTRUSIVE VOLCANIC ROCKS — Dikes, stocks, and batholiths of dioritic, granitic, or rhyolitic composition
Tv	TERTIARY EXTRUSIVE VOLCANIC ROCKS — Tuffs, lsvas, snd volcanic sedimentsry rocks of rhyolite, rhyodscite, dacite, and sndesite
Ki	CRETACEOUS INTRUSIVE ROCKS OF THE IDAHO BATHOLITH — Tonalite, granodiorite, granite, muscovite-biotite grsnite, and leucocratic granite
Pzs	PALEOZOIC SEDIMENTARY ROCKS — Limestone, dolomite, shale, siltstone, argillite, quartzite, sandstone, and slate
Yms	MIDDLE PROTEROZOIC METAMORPHIC AND SEDIMENTARY ROCKS — Argillite, slate, quartzite, sandstone, siltite, schist, and phyllite
ru	ROCKS OF UNCERTAIN AGE—Argillite, carbonate, quartzite, and phyllite

CONTACT
FAULT
THRUST FAULT — Sswteeth on upper plste
CALDERA BOUNDARY
× MINE OR PROSPECT

1. Iron Creek mine
2. Hoodoo mine
3. Livingston mine
4. Thompson Creek mine
5. Little Boulder Creek deposit
6. Skylark vein
7. Sunbeam mine
8. General Custer vein
9. Red Mountain deposit
10. Little Falls deposit
11. Meyers Cove district
12. Boulder Creek district
13. Lucky Boy mine
14. Yellowjacket mine
15. Mammoth mine
16. Golden Day mine
17. Parker Mountain deposit
18. Snowshoe Creek deposit
19. Singheiser mine
20. Sunnyside mine
21. Dewey mine
22. West End deposit
23. Yankee Fork placer deposits
24. Loon Creek placer deposits
25. Stanley Creek placer deposits
26. Valley Creek placer deposits
27. Clayton Silver mine
28. Bayhorse district
29. Virginia Beth deposit
30. Hall-Interstate mine
31. Ramshorn vein
32. Seafoam district

Figure A8. Map showing mining districts and selected principal mines in the Challis quadrangle.

deposits of zinc, lead, and barite in the Grand Prize and Dollarhide Formations (Hall, chap. J, this volume; Skipp and others, 1979). All of these syngenetic ores show varying degrees of remobilization during Late Cretaceous and Tertiary igneous activity.

Cretaceous

The intrusion of several phases of the Idaho batholith and satellite stocks from about 112 to 70 m.y. ago dominated the Cretaceous Period (fig. A7). Folding and eastward thrusting of Paleozoic rocks were widespread before and during batholith intrusion and culminated during the Sevier orogeny in Late Cretaceous time (Skipp and Hall, 1975). Some normal faulting also occurred during this time, and contact metamorphism was locally intense (Anderson, 1948).

Intrusion of various phases of the batholith probably remobilized yet again the Precambrian cobalt-copper-iron deposits; certainly the Paleozoic syngenetic silver, barium, lead, and zinc deposits were also remobilized to varying degrees. Skarn deposits containing silver, gold, barium, copper, molybdenum, lead, tungsten, and zinc were formed at this time in roof pendants and adjacent to the batholith, as were the Thompson Creek and Little Boulder Creek porphyry molybdenum deposits (fig. A8). The most widely accepted date for the Thompson Creek deposit is 88 m.y. (Marvin and others, 1973). Vein and replacement lead-silver deposits in the Bayhorse district, specifically the Skylark vein (fig. A8), have been dated at 95 m.y. (McIntyre and others, 1976; recalculated). The source of the metals in the skarns, the porphyry molybdenum, and the vein-replacement deposits is a matter of conjecture. In my opinion, the metals in these deposits were derived from the metalliferous Paleozoic and Precambrian rocks by hydrothermal systems associated with the various intrusive phases of the batholith, and the batholith itself contributed little metallic content to the ore deposits of the region. The batholith did, however, contribute euxenite and columbite in pegmatites, and monazite as a primary disseminated mineral. These minerals contain valuable concentrations of niobium, tantalum, thorium, uranium, and the rare-earth elements, and accumulated in placer deposits as a result of late Tertiary weathering followed by concentration during the Pleistocene and Holocene (Schmidt and Mackin, 1970).

Tertiary

Tertiary time was characterized by the deposition of the Eocene Challis Volcanics, the development of the Challis volcanic field, and the emplacement of several batholiths and many stocks (fig. A7). Prior to the igneous activity, however, the Idaho batholith was being eroded, and arkosic sediments were deposited in local areas. These sediments eventually were the traps for stratabound uranium deposits in the Stanley region (Choate, 1962). Volcanism began with the widespread eruption of lavas of intermediate composition about 51 m.y. ago (McIntyre and others, 1982). Lavas were intermittently erupted for another 5 to 6 m.y. About 48 m.y. ago the character of volcanic activity changed and ash-flow eruptions predominated. These eruptions led to the development of the cauldron complexes, starting with the Van Horn Peak cauldron complex, which was closely followed and probably partly concurrent with the formation of the Custer graben, and the Thunder Mountain and Twin Peaks calderas (Ekren, chap. C, this volume). The size and shape of the calderas were closely related to pre-existing graben-bounding northeast-trending faults. Northeast and northwest-trending high-angle faults began to form at least 51 m.y. ago, as dated by lavas that ponded against pre-existing fault scarps (McIntyre and others, 1982).

Intrusive activity from 50 to about 43 m.y. ago resulted in the emplacement of the Casto pluton (more accurately called a batholith), the Sawtooth batholith, and many other smaller stocks and countless dikes (Bennett, 1980). From 43 to 39 m.y. ago, extensive rhyolitic intrusions and high-level domes and dikes were emplaced (Hardyman and Fisher, chap. N, this volume). "High-level" is a term used in this report for rhyolite intrusive bodies emplaced at or very near the Earth's surface. Some of these bodies may have breached; in plan view their shapes may be circular, linear, or very irregular. Limited age data suggest that at least some of the intrusive activity in the Boise Basin dike swarm occurred as recently as 29 m.y. ago (Kiilsgaard and Bennett, chap. M, this volume).

A great diversity of deposits is associated with Tertiary igneous activity (fig. A7). The oldest date we have so far in the Tertiary is 45 m.y. for the Sunbeam gold-silver deposit (Johnson and McIntyre, 1983). The General Custer epithermal gold-silver vein deposit is dated at 43 m.y., the Red Mountain gold-molybdenum deposit in high-level rhyolite at 39 m.y., and the Little Falls vein-fracture molybdenum deposit at 29 m.y. (Johnson and McIntyre, 1983). To the best of our knowledge, then, most of these metals were deposited in a minimum time span of 18 m.y. A broad paragenetic sequence of three stages within that time period can be postulated: a base-metal stage, overlapped and followed by a fluorite and possibly mercury episode, in turn overlapped and followed by zeolite development. This sequence is strictly conjecture at present, as we do not have detailed dating of the different stages. However, the major fluorspar and zeolite deposits and possibly also the mercury deposits all are spatially separate from the main areas of base- and precious-metal deposits.

Hundreds of deposits within the quadrangle are examples of Tertiary mineralization. A few examples are:

the lead-silver-antimony-tin veins in the Wood River Formation in the southern part of the quadrangle; tungsten-antimony-gold deposits at Yellow Pine; stratabound and vein uranium deposits near Stanley; vein fluorspar deposits near Meyers Cove, Challis, and Stanley; mercury vein-replacement deposits in roof pendants near Yellow Pine; and many of the epithermal gold-silver vein deposits in the quadrangle.

The source of the metals for the extensive Tertiary mineralization is still an enigma. Did the Tertiary plutons, much as the Idaho batholith, simply provide a driving mechanism for convecting hydrothermal systems, or were the plutons themselves metalliferous? Geochemical evidence suggests that the Tertiary granites were enriched in beryllium, uranium, thorium, molybdenum, and tin (Bennett, 1980). However, as suggested by Howe and Hall (chap. P, this volume), the sulfur isotopes indicate a crustal source for the sulfur.

SPATIAL DISTRIBUTION OF SELECTED MINERAL COMMODITIES

Examination of the distribution of the major commodities shows certain definite spatial associations with major structural and stratigraphic features. These associations are discussed here by commodity, in order of fluorspar, mercury, gold, silver, molybdenum, zinc, lead, and copper.

Fluorspar

Fluorspar deposits are present in three major areas in the Challis quadrangle, the Meyers Cove, Stanley, and Challis-Bayhorse districts (fig. A9). Elsewhere throughout the quadrangle fluorspar is a common gangue mineral associated with both base- and precious-metal deposits.

In the Meyers Cove district (Anderson, 1943; Cox, 1954), the fluorspar deposits are tabular veins paralleling fracture zones, with some stringers and lenses cutting obliquely across the fracture zones. The deposits form well-defined lodes along the fractures, generally with some minor replacement. Individual lodes may be 8 to 30 m long. The ore minerals are fluorite with or without minor stibnite in a gangue of barite, calcite, and chalcedony. The deposits are within a zone 1 km wide by 3 km long. Host rocks are the 47-m.y.-old tuffs of Camas Creek.

In the Stanley district (Choate, 1962; Tschanz and others, 1974) fluorspar is present in tabular zones containing veins and stringers; individual veins are as much as 1 m wide, and the composite width of veins and stringers is as much as 5 m. All of the deposits are associated with faults and shears and are spatially related to rhyolite dikes. The veins are mostly open-space fillings with minor replacement. Two main assemblages are present: a quartz-pyrite-gold-fluorite assemblage, and simply quartz and fluorite. The host rock for all of the fluorspar deposits near Stanley is the Idaho batholith.

Fluorspar in the Bayhorse-Challis district is widely distributed in dolomitic rocks and is controlled in part by faults and in part by breccia zones (Snyder, 1978; Hobbs, chap. K, this volume). Two types of fluorspar deposits are present. The first type is fissure veins ranging from small veinlets measured in centimeters to zones several meters wide containing lodes tens of meters long; the second type is stratabound zones of breccia a few tens to several meters wide in a stratigraphic interval as much as 7 m thick within the Ordovician(?) Bayhorse Dolomite. The stratabound deposits have been interpreted as open-space filling of collapse breccia (Snyder, 1978), and alternatively as Mississippi Valley/Appalachian-type deposits modified by later igneous and tectonic events (Hoagland, 1979). The mineralogy of both the vein and stratabound deposits is grossly similar; fluorite is present along with earlier formed base-metal sulfides and sulfosalts of silver and copper in a silica gangue.

Thus fluorspar is a fairly common gangue mineral in both base- and precious-metal deposits throughout the quadrangle, but, more important, the main fluorspar-producing deposits are spatially separate from the major base-metal deposits, as in the Meyers Cove and Stanley districts. In the Bayhorse district base metals are common but are markedly earlier than the fluorspar. Therefore, fluorspar mineralization may have occurred separately and later than the base- and precious-metal mineralization. This event was probably the result of the emanations of volatile elements late in the crystallization history of the Tertiary magmas.

Mercury

Mercury occurs in several areas in the quadrangle, including the Boulder Creek district where it is associated with base- and precious-metal deposits, and the Stanley area where trace amounts are associated with the uranium vein deposits (fig. A10). However, the only district containing mercury of economic significance is the Yellow Pine area (Bailey, 1964) where cinnabar occurs as veins, fracture coatings, and replacements in Precambrian rocks adjacent to the Idaho batholith in ring fractures of the Thunder Mountain caldera (Leonard, chap. H, this volume).

Gold

The location and production of gold mines in the quadrangle are shown on figure A11. The Custer graben (Johnson and McIntyre, 1983) and the Thunder Mountain caldera (Leonard, chap. H, this volume) have produced the bulk of the gold from the area. Gold is present

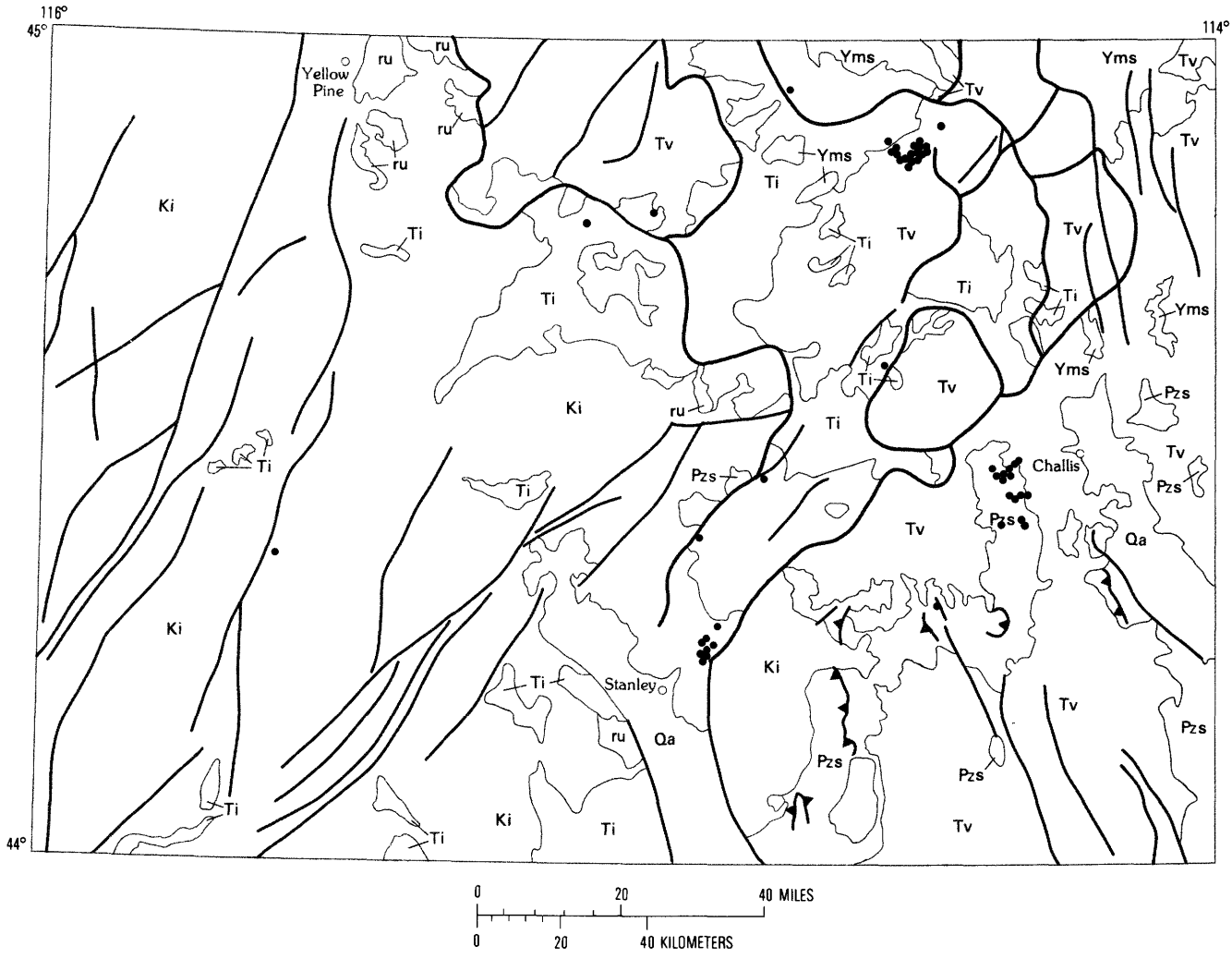

EXPLANATION

Qa	QUATERNARY ALLUVIUM—Includes flood plain, terrace, and alluvial-fan deposits
Ti	TERTIARY INTRUSIVE VOLCANIC ROCKS — Dikes, stocks, and batholiths of dioritic, granitic, or rhyolitic composition
Tv	TERTIARY EXTRUSIVE VOLCANIC ROCKS — Tuffs, lavas, and volcanic sedimentary rocks of rhyolite, rhyodacite, dacite, and andesite
Ki	CRETACEOUS INTRUSIVE ROCKS OF THE IDAHO BATHOLITH — Tonalite, granodiorite, granite, muscovite-biotite granite, and leucocratic granite
Pzs	PALEOZOIC SEDIMENTARY ROCKS — Limestone, dolomite, shale, siltstone, argillite, quartzite, sandstone, and slate
Yms	MIDDLE PROTEROZOIC METAMORPHIC AND SEDIMENTARY ROCKS — Argillite, slate, quartzite, sandstone, siltite, schist, and phyllite
ru	ROCKS OF UNCERTAIN AGE—Argillite, carbonate, quartzite, and phyllite

CONTACT
FAULT
THRUST FAULT — Sawteeth on upper plate
CALDERA BOUNDARY
FLUORSPAR MINE OR PROSPECT

Figure A9. Fluorspar mines and prospects in the Challis quadrangle.

in several types of occurrences in a wide variety of geological settings. The common deposit types (fig. A8) are: (1) gold-silver veins containing subordinate base metals; these occurrences are numerous in the quadrangle, and examples are the Lucky Boy and General Custer mines in the Custer graben, the Yellowjacket mine in the Yellowjacket district, the Mammoth mine in the Grimes Pass district, and the Golden Day mine near Stanley; (2) stockwork veins and

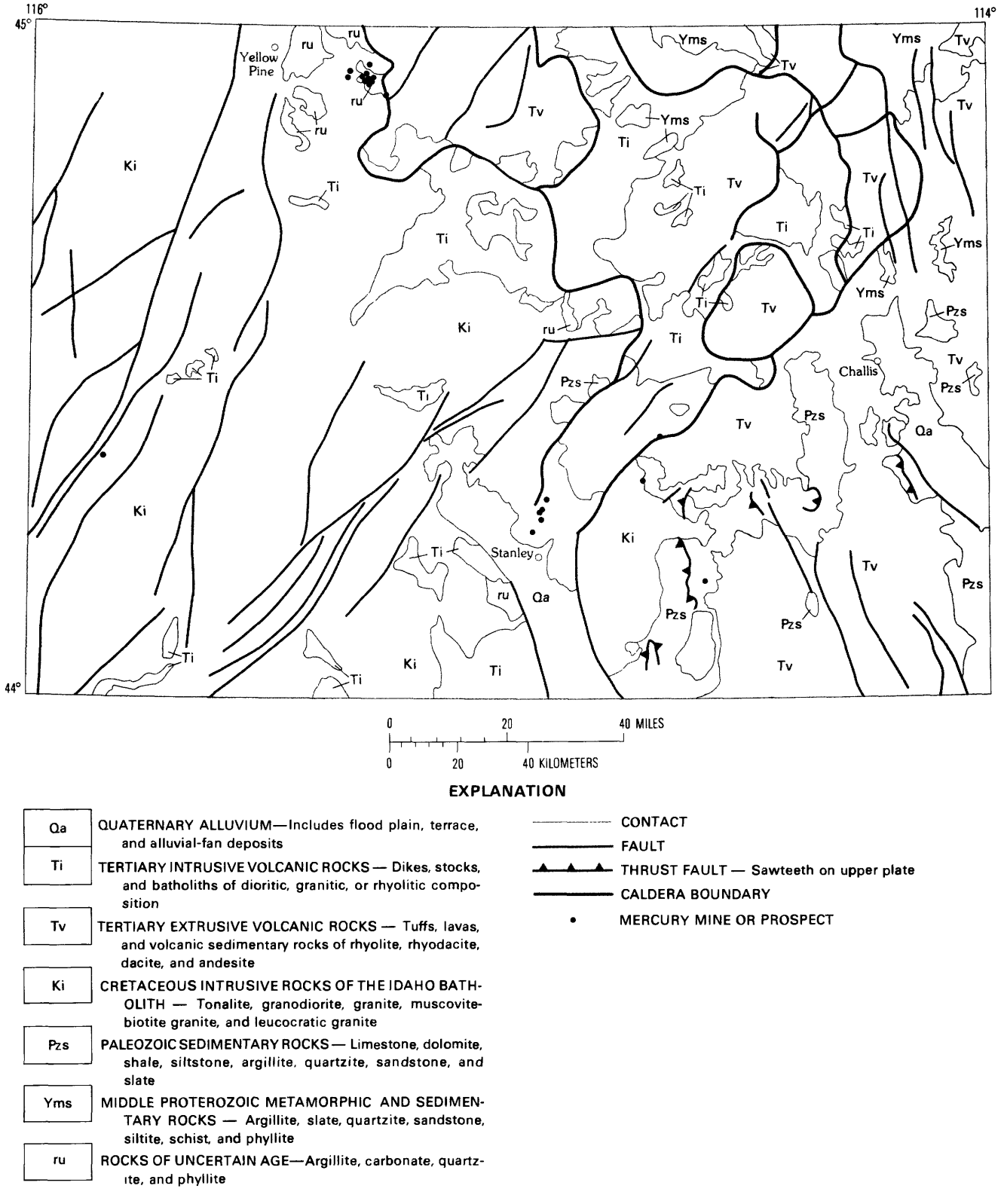

Figure A10. Mercury mines and prospects in the Challis quadrangle.

disseminated gold and silver in high-level rhyolites, such as at the Sunbeam mine in the Custer graben, the Parker Mountain and Snowshoe Creek deposits in the Twin Peaks caldera, and the Singheiser mine in the Panther Creek graben; (3) stratabound gold-silver replacement deposits in volcanic rocks, the best example of which is the Sunnyside mine in the Thunder Mountain caldera; (4) stratabound gold-silver replacement deposits in caldera-

filling sediments, such as at the Dewey mine, also in the Thunder Mountain caldera; (5) vein-replacement deposits in argillized metasedimentary Precambrian rocks, such as the West End deposit in the Yellow Pine district; and (6) gold placer deposits, examples of which are the Yankee Fork placers in the Custer graben, the Loon Creek placers, and the Stanley Creek and Valley Creek placers near Stanley.

Silver

As would be expected, the distribution of silver within the quadrangle strongly resembles that of gold (fig. A12). The main difference is in the relative proportions of the two metals in a given deposit. Like gold, silver occurs in a wide range of deposit types. In addition to the types previously mentioned for gold, two other significant occurrence types for silver are replacement deposits in carbonate rocks containing predominant silver and lead, the best example of which is the Clayton Silver mine; and stratabound syngenetic deposits in argillic rocks, examples of which are the Livingston mine and the vanadium-silver occurrences in the Salmon River assemblage in the Bayhorse district.

Molybdenum

Molybdenum is present in at least five types of occurrences in the Challis quadrangle (figs. A8 and A13). These are: (1) Cretaceous porphyry deposits in granodioritic to granitic rocks at the Thompson Creek mine; (2) Cretaceous porphyry vein stockworks in sedimentary rocks at the Little Boulder Creek deposit; (3) skarn deposits with tungsten in roof pendants and adjacent to the Idaho batholith, such as the Virginia Beth occurrence; (4) Tertiary vein-fracture systems associated with dike swarms, such as the Little Falls deposit; and (5) disseminations and stockworks with gold and silver in high-level rhyolites.

Base metals

Zinc in the quadrangle (fig. A14) occurs in replacements in carbonate rocks, in veins, and in partly remobilized stratabound syngenetic deposits. The remobilized stratabound syngenetic deposits at the Livingston mine and the Hall-Interstate vein were the two largest producing mines.

Lead occurrences are somewhat more scattered than zinc but are strongly associated with the Paleozoic sedimentary rocks (fig. A15). The largest producing mines were the Ramshorn vein deposit in the Bayhorse district, the remobilized stratabound deposit at the Livingston mine, replacement deposits in the Seafoam district, and the Hall-Interstate vein deposit (fig. A8).

Copper occurrences are widely scattered and appear to be associated with the Paleozoic sedimentary rocks and also with the Precambrian sedimentary rocks (fig. A16). The main producing mines were vein deposits in the Bayhorse district and the Hall-Interstate mine, and also vein replacement deposits in the Seafoam district.

METAL PRODUCTION IN RELATION TO GEOLOGIC PROVINCES

The production of gold and silver from the major structural and stratigraphic provinces within the quadrangle is shown on figure A17. Production figures are plotted on a logarithmic scale, and the total amount produced is shown by the value at the top of each column. As can be seen, the Thunder Mountain caldera (TMC, fig. A17) has produced the most gold, followed by the Custer graben (CG), and then roof pendants (RP). The total amount of gold produced from volcanic sources within the Challis volcanic field, the first four columns on figure A17 totaled, is shown by the column labeled TV.

The production of silver shows a somewhat different pattern. Mines within the Paleozoic sedimentary rocks have produced by far the greatest amount of silver. The combined total of the four volcanic provinces, the Panther Creek graben, the Twin Peaks caldera, the Thunder Mountain caldera complex, and the Custer graben, is about 10 times less than the amount produced from the Paleozoic sedimentary rocks.

Production figures thus suggest that gold and lesser amounts of silver are associated with volcanic provinces, and silver with lesser amounts of gold are associated with the Paleozoic sedimentary rocks.

Production data for copper, lead, and zinc from the main geologic provinces in the quadrangle are shown on figure A18. Three patterns are obvious: first, the greatest production by far has come from the Paleozoic sedimentary rocks (PS), by several orders of magnitude; second, the roof pendants (RP) have produced significant amounts of base metals; and third, production of base metals from the volcanic provinces (PCG, TPC, TMC, and CG) is insignificant. The relative proportions of base metals produced from the volcanic provinces is interesting to note. In the Paleozoic rocks, production from greatest to least is lead, zinc, and copper; in the roof pendants the order is zinc, lead, and copper; and in the Precambrian sedimentary and metamorphic rocks the order is copper, lead, and zinc. Copper has been produced from all of the major volcanic provinces except the Twin Peaks caldera, lead from all but the Panther Creek graben and the Twin Peaks caldera, and zinc from all but the Panther Creek graben, Twin Peaks caldera, and Thunder Mountain caldera.

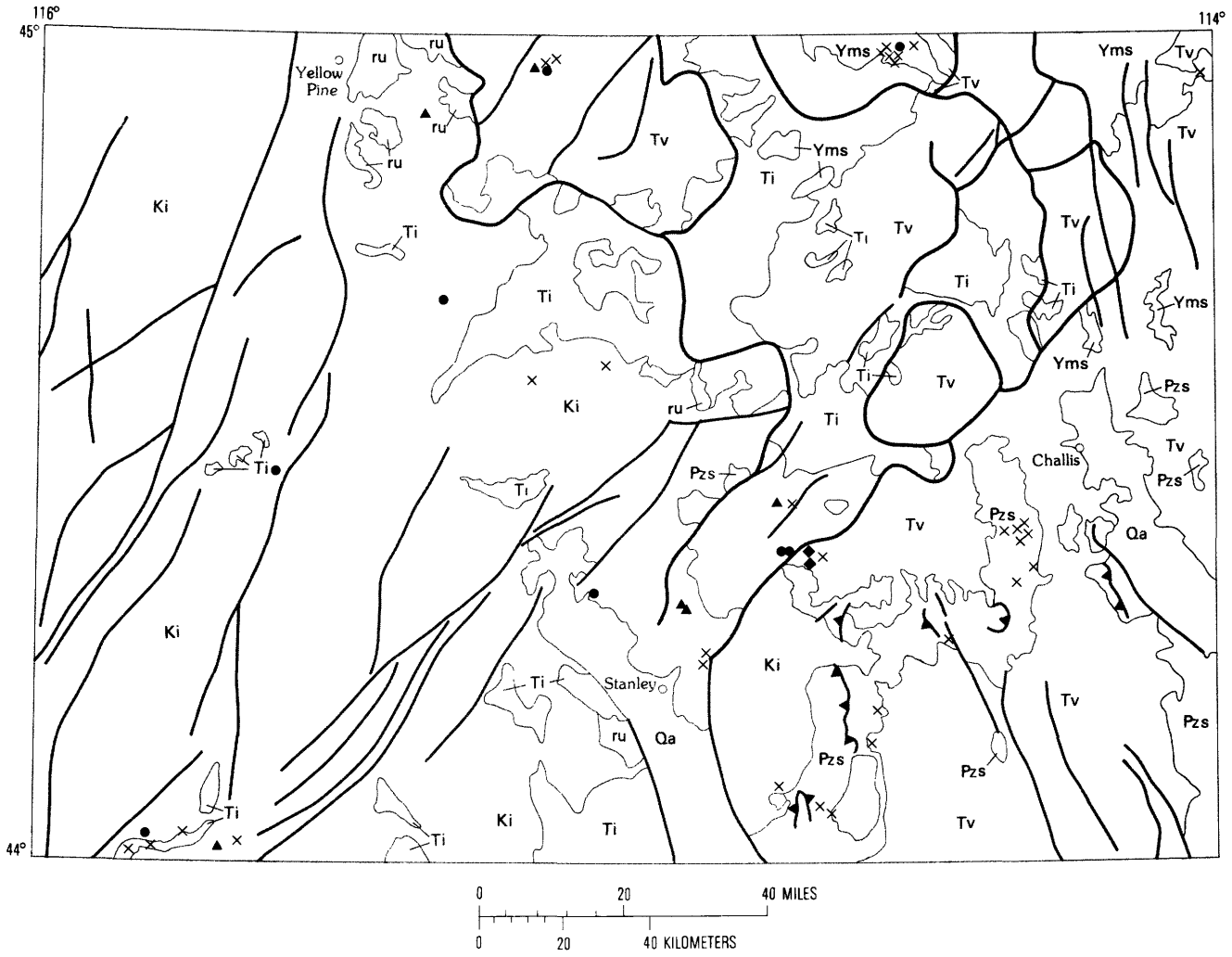

EXPLANATION

Qa	QUATERNARY ALLUVIUM—Includes flood plain, terrace, and alluvial-fan deposits
Ti	TERTIARY INTRUSIVE VOLCANIC ROCKS — Dikes, stocks, and batholiths of dioritic, granitic, or rhyolitic composition
Tv	TERTIARY EXTRUSIVE VOLCANIC ROCKS — Tuffs, lavas, and volcanic sedimentary rocks of rhyolite, rhyodacite, dacite, and andesite
Ki	CRETACEOUS INTRUSIVE ROCKS OF THE IDAHO BATHOLITH — Tonalite, granodiorite, granite, muscovite-biotite granite, and leucocratic granite
Pzs	PALEOZOIC SEDIMENTARY ROCKS — Limestone, dolomite, shale, siltstone, argillite, quartzite, sandstone, and slate
Yms	MIDDLE PROTEROZOIC METAMORPHIC AND SEDIMENTARY ROCKS — Argillite, slate, quartzite, sandstone, siltite, schist, and phyllite
ru	ROCKS OF UNCERTAIN AGE—Argillite, carbonate, quartzite, and phyllite

CONTACT
FAULT
THRUST FAULT — Sawteeth on upper plate
CALDERA BOUNDARY

GOLD MINE SHOWING PRODUCTION IN OUNCES
- ◆ >100,000
- ▲ 10,000-100,000
- ● 1000-10,000
- × <1000

Figure A11. Gold mines and prospects in the Challis quadrangle showing production to 1982.

RESOURCE POTENTIAL OF SELECTED COMMODITIES BASED ON RECENT GEOLOGIC STUDIES

In the following discussion the terms "moderate" and "high" resource potential are used as defined by Taylor and Steven (1983). "A high mineral resource potential is deemed to exist where geologic, geochemical, and geophysical characteristics favorable for resource accumulation are known to be present, or where enough of these characteristics are present to give strong support to genetic models favorable for resource accumulation and

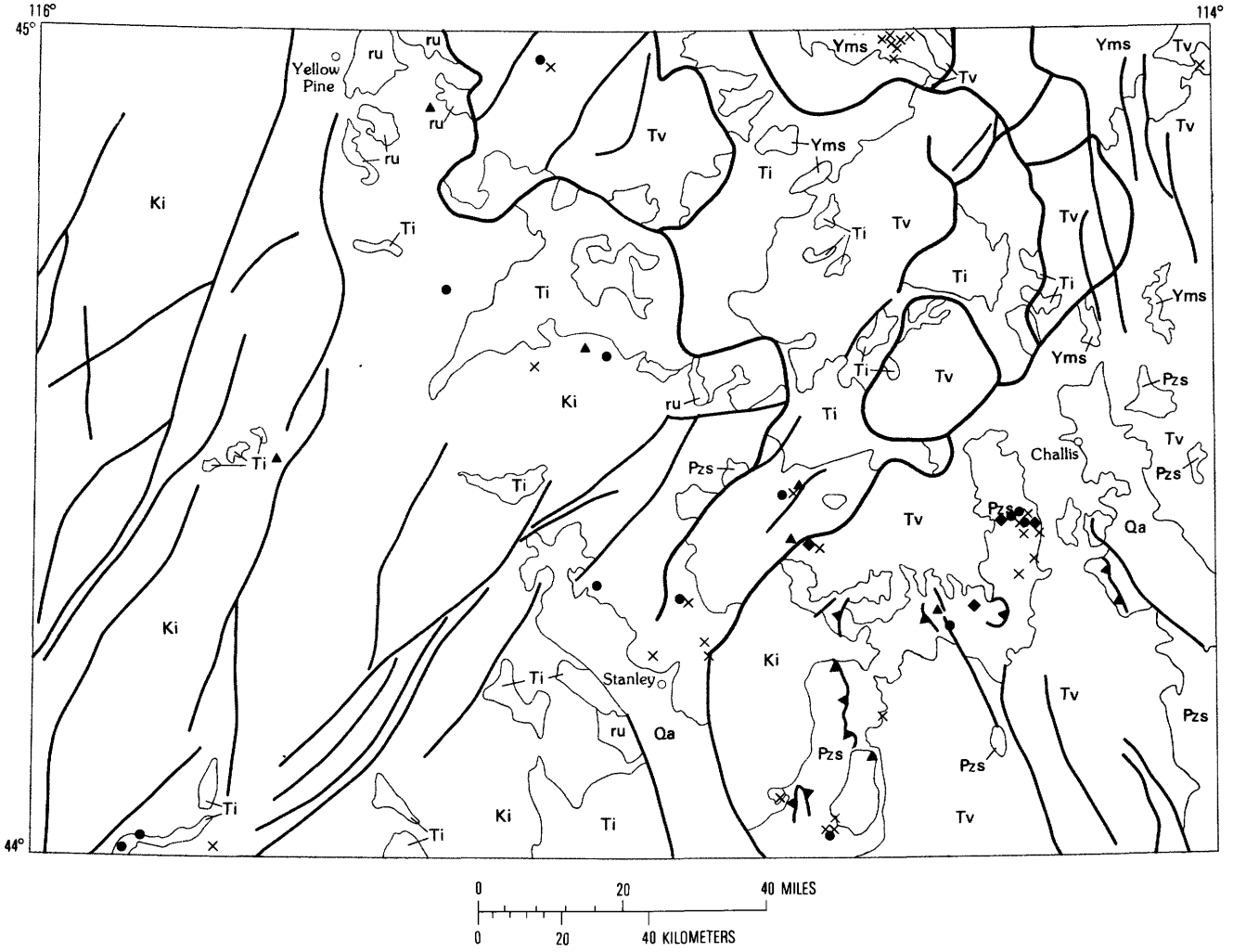

Figure A12. Silver mines and prospects in the Challis quadrangle showing production to 1982.

where evidence shows that mineral concentration—mineralization in the broad sense—has taken place. * * * Moderate mineral resource potential exists where geologic, geochemical, and geophysical characteristics favorable for resource accumulation are known or can reasonably be interpreted to be present but where evidence for mineralization is less clear cut or has not yet been found. A reasonable possibility for the discovery of valuable mineral deposits should exist in all areas rated as having moderate mineral resource potential" (Taylor and Steven, 1983,p. 126).

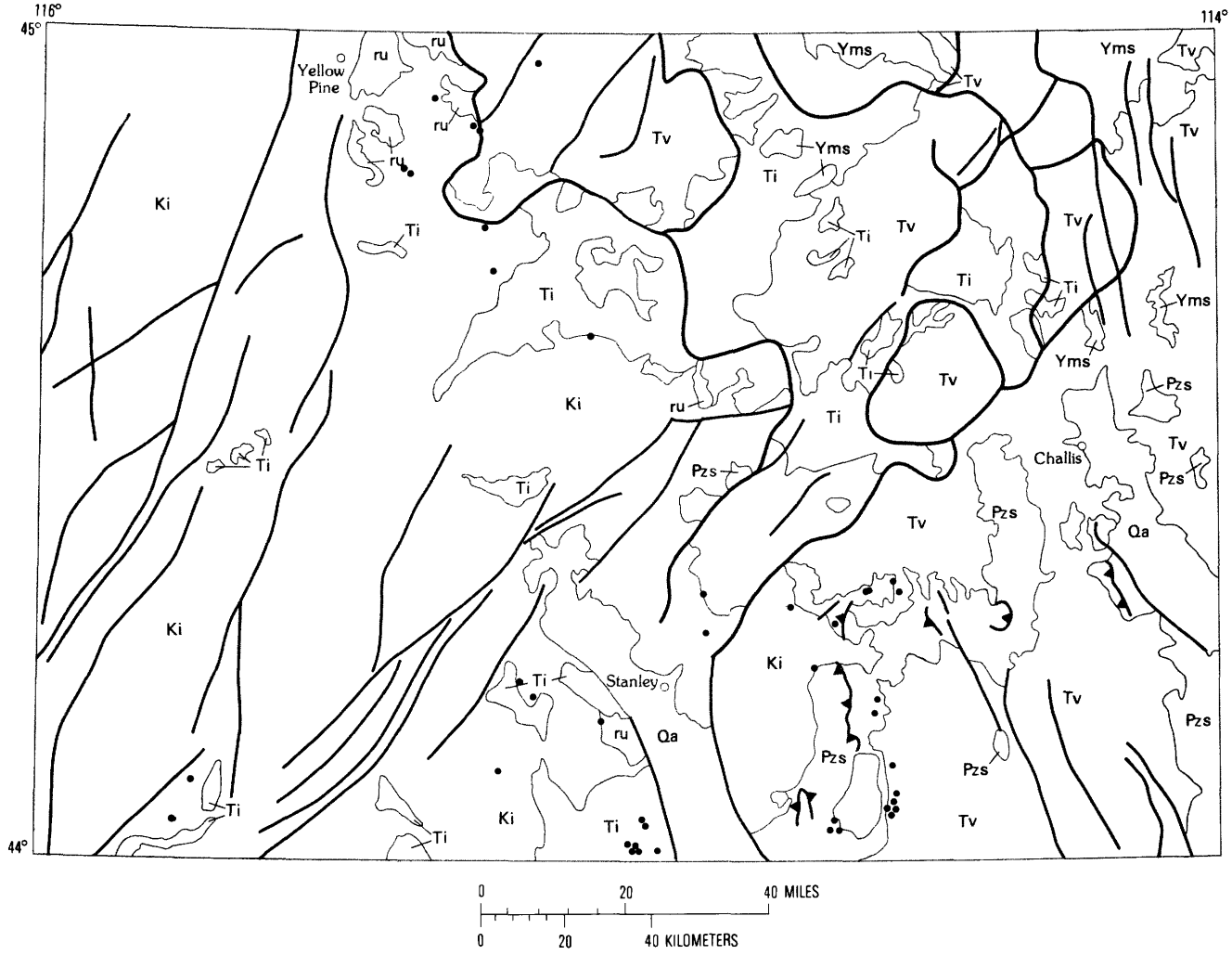

Figure A13. Molybdenum mines and prospects in the Challis quadrangle.

Much of the area along the trans-Challis fault system (fig. A3) has moderate to high resource potential for gold and silver. Gold and silver mines and prospects are closely associated with the fault zone, especially along the southeastern side. Metals associated with the fault zone may be present in the rocks in a wide range of occurrence types, including epithermal gold-silver veins, high-level rhyolites, and disseminated gold-silver stockworks.

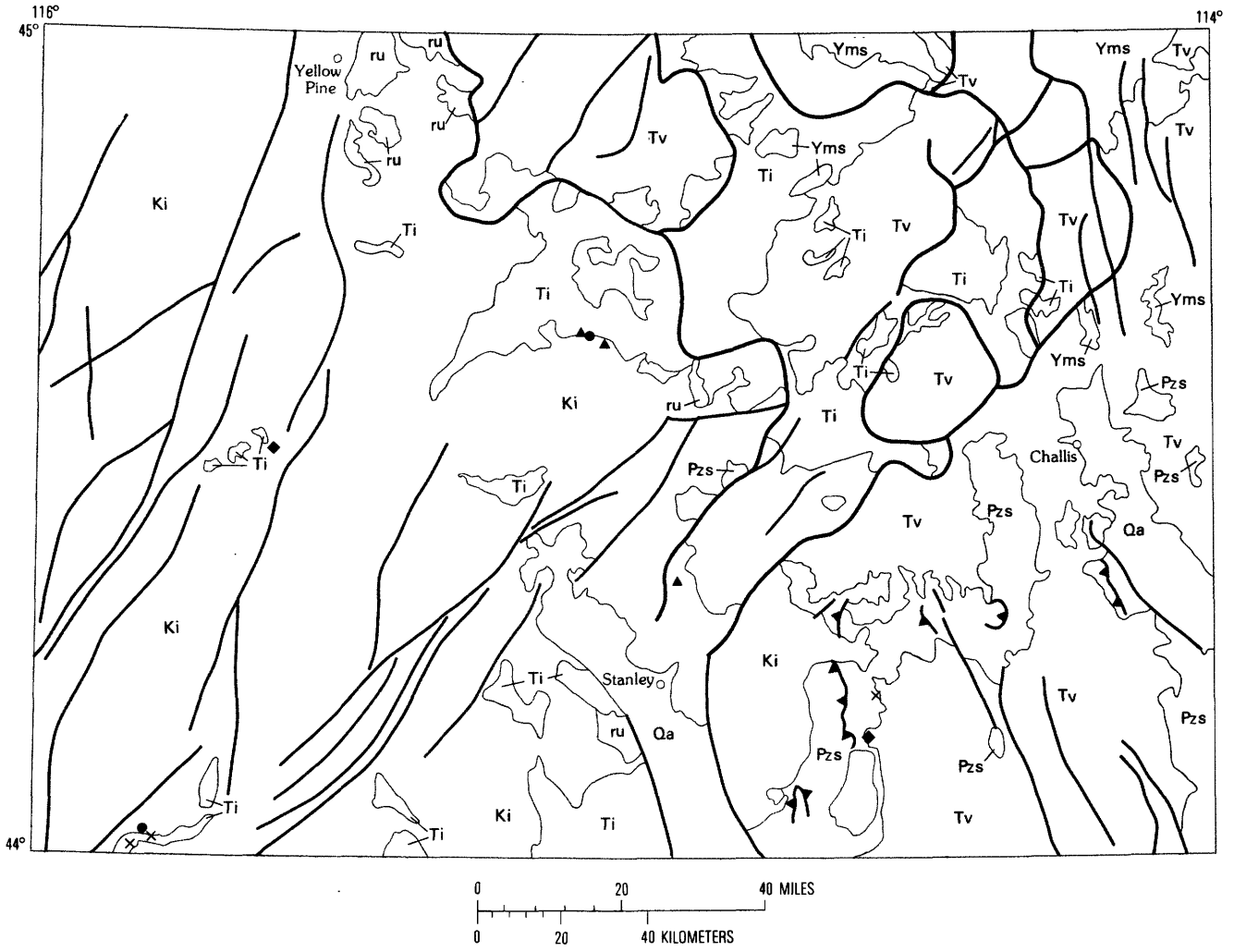

Figure A14. Zinc mines and prospects in the Challis quadrangle showing production to 1982.

Many areas in this zone are covered by forest, particularly in the north along the bounding faults of the Panther Creek graben (figs. A1, A2). Biogeochemical techniques using the wood of Douglas-fir trees (Erdman and others, chap. L, this volume; Leonard and Erdman, 1983) should yield information on the precious-metal potential of that part of the fault zone.

Within the Challis volcanic field, the newly mapped bounding structures of the various calderas must be considered favorable areas for the discovery of additional

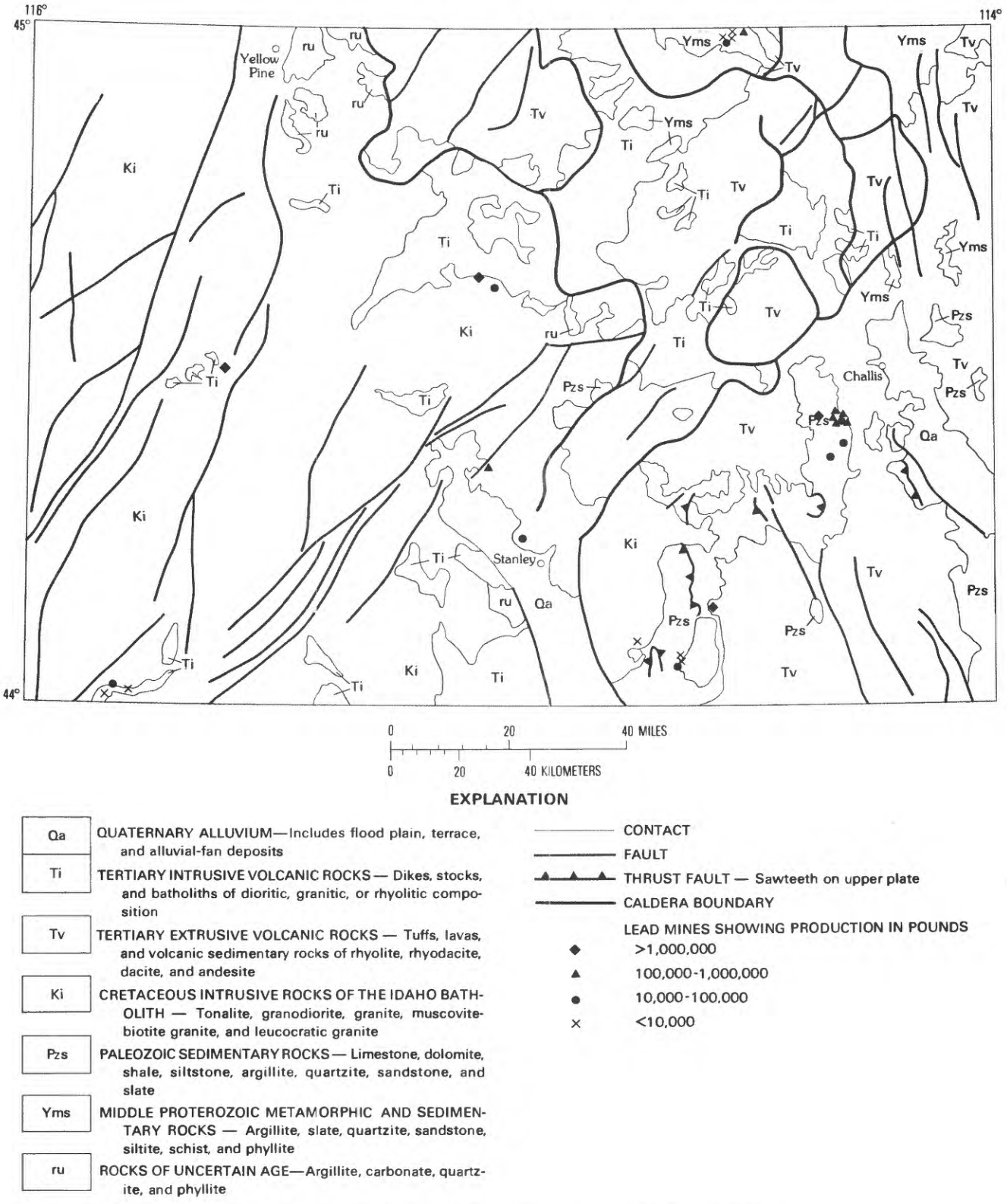

Figure A15. Lead mines and prospects in the Challis quadrangle showing production to 1982.

mineral resources; plumbing systems consisting of faults, fracture zones, joints, and permeable rocks are well developed, and many of these systems have been mineralized. Moderate to high resource potential is assigned to these areas. New mapping (Hardyman, 1981) indicated that the northwestern side of the Twin Peaks caldera is favorable for gold, silver, and molybdenum resources, and the central part contains zeolites along the 12-km length

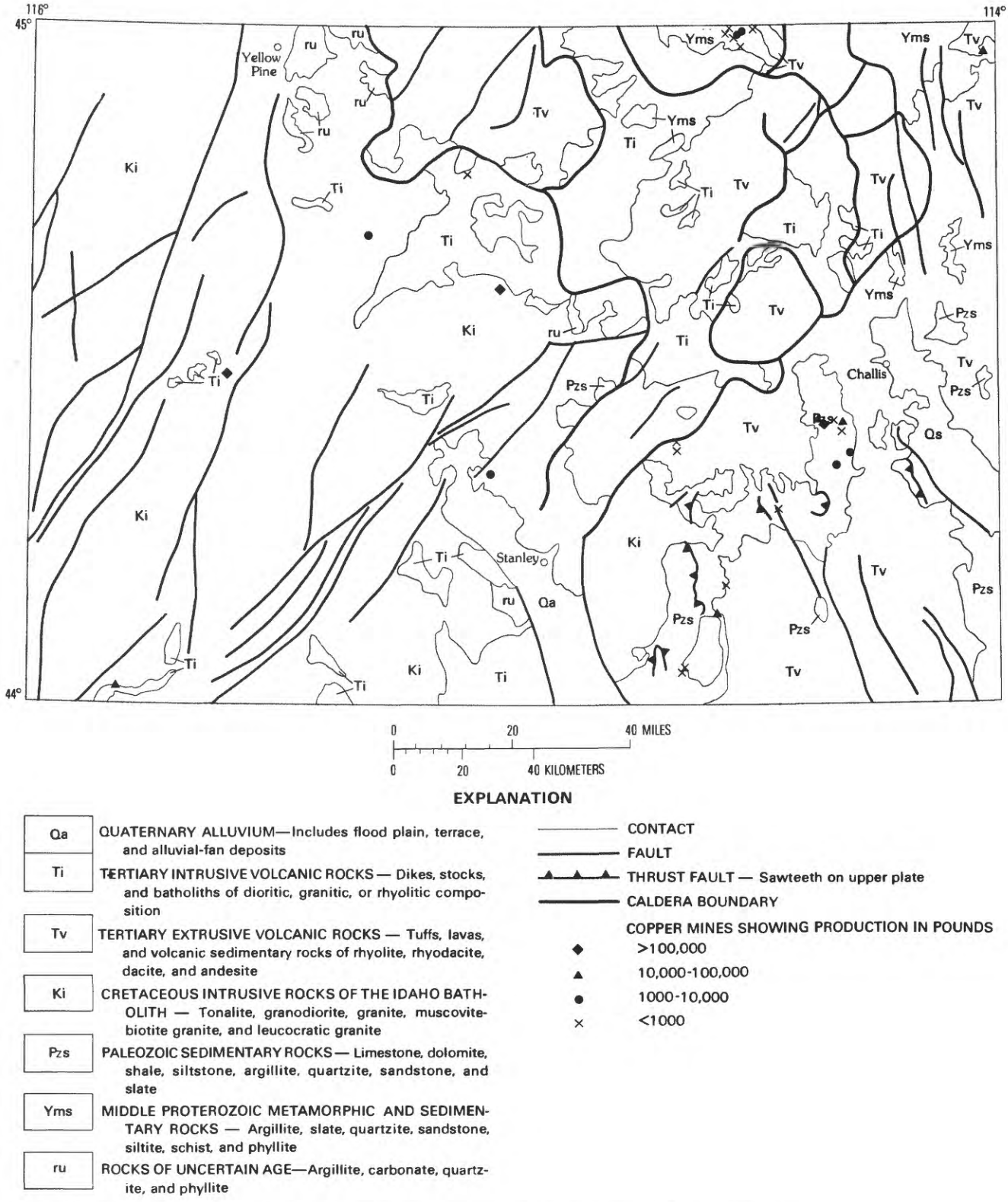

Figure A16. Copper mines and prospects in the Challis quadrangle showing production to 1982.

of the medial fracture zone (Hardyman, chap. G, this volume). The southwestern and western sides of the Thunder Mountain caldera have a high potential for resources of gold, silver, tungsten, mercury, molybdenum, and the rare-earth elements, particularly in silicified and argillized zones (Leonard, chap. H, this volume).

It is interesting to speculate about the roots of the high-level rhyolites. Mapping (fig. A2) showed that these

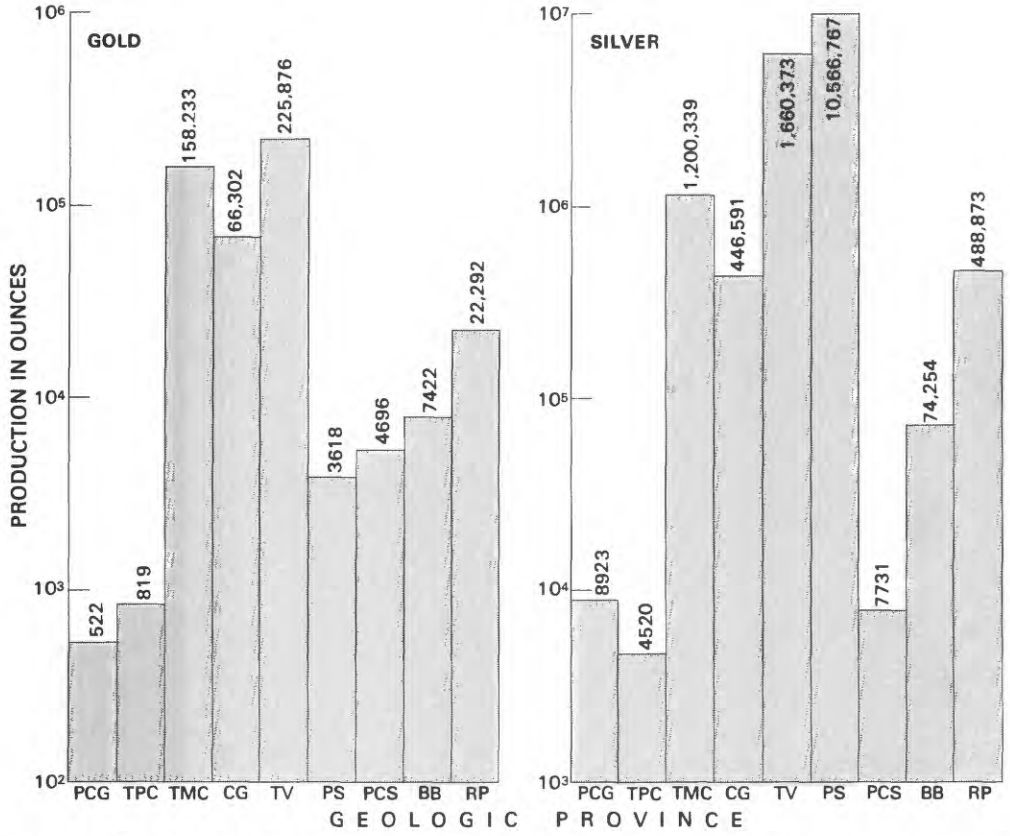

Figure A17. Graph showing the production of gold and silver from the main geologic provinces in the Challis quadrangle. Panther Creek graben (PCG), Twin Peaks caldera (TPC), Thunder Mountain caldera (TMC), Custer graben (CG), Paleozoic sedimentary rocks (PS), Precambrian sedimentary rocks (PCS), Boise Basin dike swarm (BB), roof pendants and skarns (RP), total (TV) from volcanic provinces (PCG+TPC+TMC+CG).

rhyolites (unit Tr) occur within the trans-Challis fault system, suggesting the likelihood of linear feeder systems. All of these high-level rhyolites contain anomalous amounts of molybdenum. Analogy by attribution suggests a comparison with the Little Falls molybdenum deposit (Rostad, 1966) in the Boise Basin dike swarm at the southern end of the trans-Challis fault system (fig. A3). Our assessment model is based on the likelihood of a Little Falls-type molybdenum deposit at depth beneath the high-level rhyolites. This possibility makes the central part of the Van Horn Peak cauldron complex, which contains many high-level rhyolites (Hardyman and Fisher, chap. N, this volume), an area of moderate resource potential for molybdenum.

Sedimentary rocks filling the Thunder Mountain cauldron complex contain gold deposits at the Dewey mine (Leonard, chap. H, this volume). Mapping showed that thick sections of caldera-fill sediments are present near mineralized structures (Fisher, McIntyre, and Johnson, 1983). Moderate resource potential exists for precious-metal deposits in the fill of the Panther Creek graben, Custer graben, Twin Peaks caldera, and the Van Horn Peak cauldron complex (figs. A1, A2).

Roof pendants of metasedimentary rocks along the eastern side of the Idaho batholith are considered to be favorable areas for the occurrence of tungsten deposits as discussed by Cookro (chap. Q, this volume), and the area has a high resource potential.

The greatest resource potential in the quadrangle is within Paleozoic sedimentary rocks. In the Challis-Bayhorse region, horizons of solution breccia are present in the Bayhorse Dolomite (Snyder, 1978; Hobbs, chap. K, this volume). The entire Bayhorse Dolomite is a potential host for breccia-filling fluorspar deposits and has a high resource potential. Elsewhere in the Bayhorse district, fault structures mapped by Hobbs (chaps. D, K, this volume) near the margins of the Bayhorse anticline have a high potential for the occurrence of replacement base- and precious-metal deposits.

Ketner (1983) described mineralized rocks throughout large areas of the western United States that occur near the Ordovician-Silurian boundary. This time interval is represented in the Challis quadrangle by the upper units of the Saturday Mountain Formation, which are mineralized in the Bayhorse-Challis region. These units have a moderate resource potential for base metals.

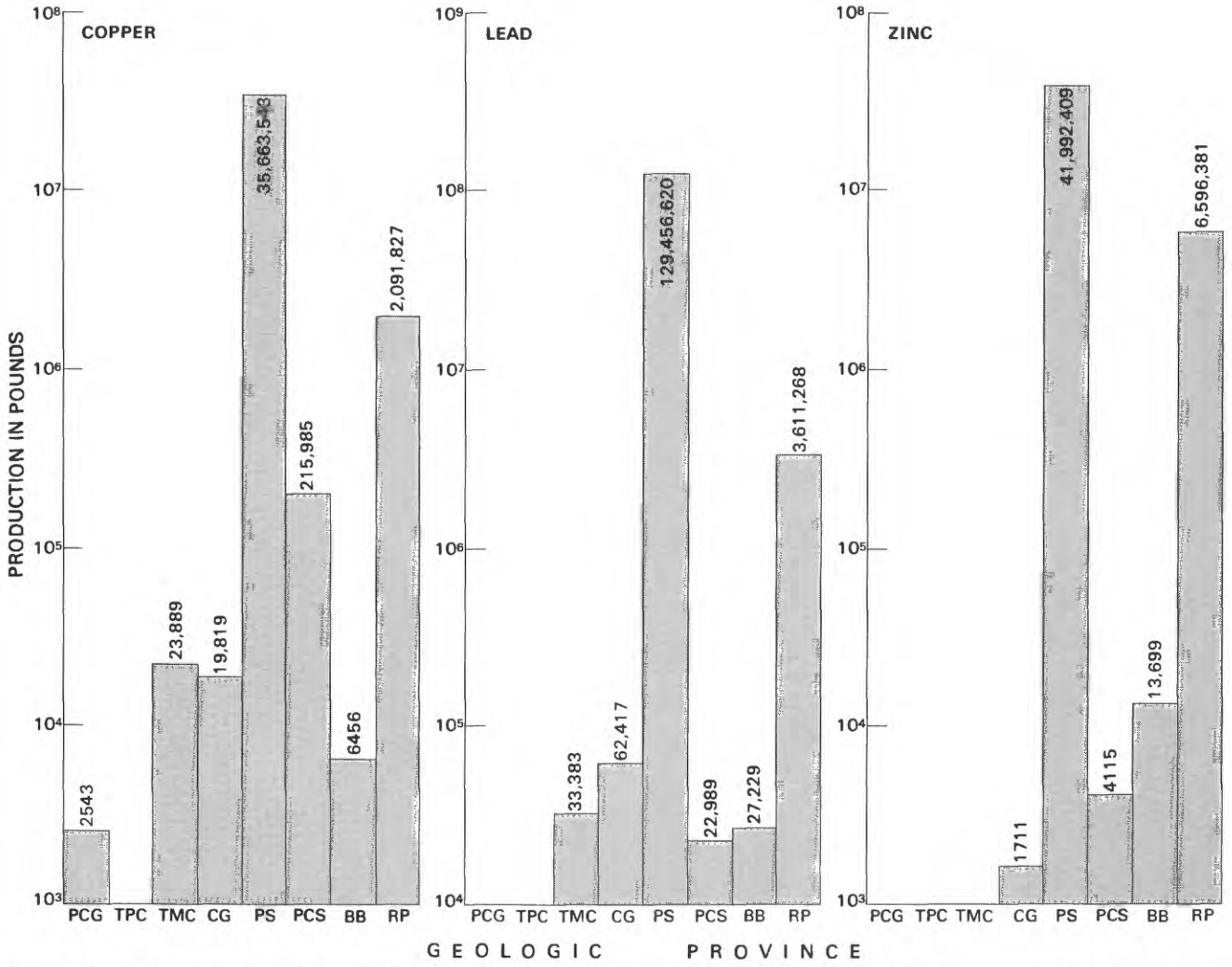

Figure A18. Graph showing the production of copper, lead, and zinc from the main geologic provinces in the Challis quadrangle. Panther Creek graben (PCG), Twin Peaks caldera (TPC), Thunder Mountain caldera (TMC), Custer graben (CG), Paleozoic sedimentary rocks (PS), Precambrian sedimentary rocks (PCS), Boise Basin dike swarm (BB), roof pendants and skarns (RP).

Finally, a high resource potential is assigned to black argillite and micritic limestone beds mapped and described by Hall (chap. J, this volume) in the Devonian Milligen Formation and the Paleozoic Salmon River assemblage. These rocks are particularly favorable for epigenetic vein replacement deposits in areas below regional thrust faults and near Cretaceous and Tertiary stocks. Possible deposit types include lead-silver-zinc vein deposits, lead-zinc-antimony-silver-tin vein deposits similar to Bolivian-type occurrences, skarn tungsten deposits, and porphyry molybdenum stockwork deposits. Stratabound syngenetic deposits of vanadium, silver, zinc, barite, and lead are also present in both the Milligen Formation and the Salmon River assemblage and may contain large resources.

REFERENCES CITED

Anderson, A. L., 1943, The antimony and fluorspar deposits near Meyers Cove, Lemhi County, Idaho: Idaho Bureau of Mines and Geology Pamphlet 62, 20 p.

_____1948, Role of the Idaho batholith during the Laramide orogeny: Economic Geology, v. 43, no. 2, p. 84–99.

Bailey, E. H., 1964, Mercury, *in* Mineral and water resources of Idaho: U.S. Congress, 88th, 2d session, Committee Print, p. 119–123.

Bennett, E. H., 1980, Granitic rocks of Tertiary age in the Idaho batholith and their relation to mineralization: Economic Geology, v. 75, no. 2, p. 278–288.

Callahan, J. E., Cooley, E. F., and Neuerburg, G. J., 1981a, Selected Mo and W concentrations from stream sediments and panned heavy-mineral concentrates, Challis, Idaho 2° quadrangle: U.S. Geological Survey Open-File Report 81-1344, 9 p.

_____1981b, Using the minus 200 mesh fraction in regional stream sediment surveys for Mo-W—results from the Thompson Creek drainage, Idaho [abs.]: Mining Engineering, v. 33, no. 10, p. 1523.

Choate, Raoul, 1962, Geology and ore deposits of the Stanley area: Idaho Bureau of Mines and Geology Pamphlet 126, 122 p.

Cox, D. C., 1954, Fluorspar deposits near Meyers Cove, Lemhi

County, Idaho: U.S. Geological Survey Bulletin 1015-A, 21 p.

Dover, J. H., 1980, Status of the Antler orogeny in central Idaho—clarification and constraints from the Pioneer Mountains, *in* Fouch, T. D., and Magathan, E. R., eds., Paleozoic paleogeography of the west-central United States: Society of Economic Paleontologists and Mineralogists, Rocky Mountain Section, Rocky Mountain paleogeography symposium 1, Denver, Colo., 1980, Proceedings, p. 1-15.

Evans, K. V., 1981, U-Th-Pb zircon geochronology of Proterozoic Y granitic intrusions in the Salmon area, east-central Idaho [abs.]: Geological Society of America Abstracts with Programs, v. 13, no. 4, p. 195.

Fisher, F. S., and May, G. D., 1983, Geochemical characteristics of the metalliferous Salmon River sequence, central Idaho: U.S. Geological Survey Open-File Report 83-670, 28 p.

Fisher, F. S., May, G. D., McIntyre, D. H., and Johnson, F. L., 1983, Mineral resource potential, geologic, and geochemical maps of part of the White Cloud-Boulder Roadless Area, Custer County, Idaho: U.S. Geological Survey Miscellaneous Field Studies Map MF-1580, scale 1:62,500.

Fisher, F. S., McIntyre, D. H., and Johnson, K. M., 1983, Geologic map of the Challis 1°×2° quadrangle, Idaho: U.S. Geological Survey Open-File Report 83-523, 39 p., 2 oversize sheets, scale 1:250,000.

Hall, W. E., Rye, R. O., and Doe, B. R., 1978, Wood River mining district, Idaho—intrusion-related lead-silver deposits derived from country rock source: U.S. Geological Survey Journal of Research, v. 6, no. 5, p. 579-592.

Hardyman, R. F., 1981, Twin Peaks caldera of central Idaho, in Tucker, T. E., ed., Montana Geological Society Field Conference and Symposium Guidebook to southwest Montana: Billings, Mont., Montana Geological Society, p. 317-322.

Hoagland, A. D., 1979, Geology of the Bayhorse fluorite deposit, Custer County, Idaho—A discussion: Economic Geology, v. 74, no. 1, p. 164-165.

Hughes, G. J., Jr., 1982, Basinal setting of the Idaho cobalt belt, Blackbird mining district, Lemhi County, Idaho, *in* The genesis of Rocky Mountain ore deposits—Changes with time and tectonics: Denver Region Exploration Geologists Society Symposium, Denver, Colo., 1982, Proceedings, p. 21-27.

Johnson, K. M., and McIntyre, D. H., 1983, Disseminated gold-silver deposit in a rhyolite dome at the Sunbeam Mine, Custer County, Idaho [abs.]: Geological Society of America Abstracts with Programs, v. 15, no. 5, p. 324.

Ketner, K. B., 1983, Strata-bound, silver-bearing iron, lead, and zinc sulfide deposits in Silurian and Ordovician rocks of allochthonous terranes, Nevada and northern Mexico: U.S. Geological Survey Open-File Report 83-792, 6 p.

Leonard, B. F., and Erdman, J. A., 1983, Preliminary report on geology, geochemistry, geochemical exploration, and biogeochemical exploration of the Red Mountain stockwork, Yellow Pine district, Valley County, Idaho: U.S. Geological Survey Open-File Report 83-151, 49 p.

Mabey, D. R., 1982, Gravity and magnetic features along the eastern margin of the Idaho batholith in central Idaho: Geological Society of America Abstracts with Programs, v. 14, no. 6, p. 320.

Marvin, R. F., Tschanz, C. M., and Mehnert, H. H., 1973, Late Cretaceous age for molybdenite mineralization in Custer County, Idaho: Isochron/West, no. 7, p. 1.

McIntyre, D. H., Ekren, E. B., and Hardyman, R. F., 1982 [1984], Stratigraphic and structural framework of the Challis Volcanics in the eastern half of the Challis 1°×2° quadrangle, Idaho, *in* Bonnichsen, Bill, and Breckenridge, R. M., eds., Cenozoic geology of Idaho: Idaho Bureau of Mines and Geology Bulletin 26, p. 3-22.

McIntyre, D. H., Hobbs, S. W., Marvin, R. F., and Mehnert, H. H., 1976, Late Cretaceous and Eocene ages for hydrothermal alteration and mineralization, Bayhorse district and vicinity, Custer County, Idaho: Isochron/West, no. 16, p. 11-12.

Mitchell, V. E., Strowd, W. B., Hustedde, G. S., and Bennett, E. H., 1981, Mines and prospects of the Challis quadrangle, Idaho: Moscow, Idaho, Idaho Bureau of Mines and Geology, Mines and Prospects Map Series, 47 p.

Rostad, O. H., 1966, Geochemical case history at the Little Falls molybdenite prospect, Boise County, Idaho, in Cameron, E. M., ed., Proceedings, symposium on geochemical prospecting, Ottawa, 1966: Geological Survey of Canada Paper 66-54, p. 249-252.

Schmidt, D. L., and Mackin, J. H., 1970, Quaternary geology of Long and Bear Valleys, west-central Idaho: U.S. Geological Survey Bulletin 1311-A, 22 p.

Shacklette, H. T., and Erdman, J. A., 1982, Uranium in spring water and bryophytes of Basin Creek in central Idaho: Journal of Geochemical Exploration, v. 17, no. 3, p. 221-236.

Skipp, Betty, and Hall, W. E., 1975, Structure and Paleozoic stratigraphy of a complex of thrust plates in the Fish Creek Reservoir area, south-central Idaho: U.S. Geological Survey Journal of Research, v. 3, no. 6, p. 671-689.

Skipp, Betty, Sando, W. J., and Hall, W. E., 1979, The Mississippian and Pennsylvanian (Carboniferous) systems in the United States—Idaho: U.S. Geological Survey Professional Paper 1110-AA, 42 p.

Snyder, K. D., 1978, Geology of the Bayhorse fluorite deposit, Custer County, Idaho: Economic Geology, v. 73, no. 2, p. 207-214.

Taylor, R. B., and Steven, T. A., 1983, Definition of mineral resource potential: Economic Geology, v. 78, no. 6, p. 1268-1270.

NOTE.—THIS COPY IS PART OF THE LIST OF **REFERENCES CITED** IN CHAPTER A AND SHOULD FALL BETWEEN PAGES 26 AND 27.

Tschanz, C. M., Kiilsgaard, T. H., and Seeland, D. A., 1974, Mineral resources of the eastern part of the Sawtooth National Recreation Area, Custer and Blaine Counties, Idaho: U.S. Geological Survey Open-File Report 74–1100, 314 p.

U.S. Bureau of Mines, [1983], Mineral commodity summaries 1983: Washington, D.C., U.S. Government Printing Office, 183 p.

Webring, M. W., and Mabey, D. R., 1981, Principal facts for gravity stations in the Challis, Idaho 1°×2° quadrangle: U.S. Geological Survey OpenFile Report 81–652, 25 p.

Symposium on the Geology and Mineral Deposits of the Challis 1°×2° Quadrangle, Idaho

Chapter B

Plutonic Rocks of Cretaceous Age and Faults in the Atlanta Lobe of the Idaho Batholith, Challis Quadrangle

By THOR H. KIILSGAARD *and* REED S. LEWIS

CONTENTS

FIGURES

TABLES

Abstract

Rocks making up the Atlanta lobe of the Idaho batholith, in the western part of the Challis quadrangle, include tonalite, hornblende-biotite granodiorite, porphyritic granodiorite, biotite granodiorite, muscovite-biotite granite, and leucocratic granite. The rocks were emplaced during the Late Cretaceous.

Tonalite, the oldest rock type, crops out near the western and eastern margins of the batholith. Closely associated with the tonalite are hornblende-biotite granodiorite and porphyritic granodiorite, the latter characterized by unusually large phenocrysts of potassium feldspar. Biotite granodiorite is younger, is the most common rock, and is widely exposed. Muscovite-biotite granite forms the core of the Atlanta lobe and is mineralogically similar to the leucocratic granite, which intrudes the other Cretaceous plutonic rocks.

The Cretaceous plutonic rocks are intensively faulted and intruded by numerous dikes and plutonic rocks of Tertiary age. Principal faults strike north, northwest, and northeast. Northwest-trending faults terminate against the trans-Challis fault system, a major set of northeast-trending faults that extends across the quadrangle and beyond.

INTRODUCTION

The western part of the Challis quadrangle is underlain by the Idaho batholith, an enormous body of granitic rock that underlies most of central Idaho. The batholith consists of two lobes, the northern, Bitterroot, lobe and the southern, Atlanta, lobe, which are separated by a narrow, northwest-trending belt of Precambrian metamorphic rocks, the Salmon River arch (Armstrong, 1975a). Rocks of the Atlanta lobe were emplaced in Late Cretaceous time, were extensively faulted, and were intruded by Tertiary plutonic rocks and swarms of Tertiary dikes.

Although much has been written about various aspects of the Idaho batholith, very little mapping of the rock types that compose the Atlanta lobe (fig. B1) has been done. Schmidt (1964), working in an area extending from near Cascade east to Warm Lake, in the northwestern part of the Challis quadrangle, separated Atlanta lobe rocks into four types. Anderson (1947) separated Tertiary plutonic rocks from older plutonic rocks of the Atlanta lobe in the area south of the South Fork Payette River, in the southwestern corner of the Challis quadrangle. Reid (1963) and Kiilsgaard and others (1970) mapped part of the Sawtooth Range in the south-central part of the Challis quadrangle.

As part of the Challis quadrangle study, we mapped the southwestern quarter of the quadrangle to identify exposed rock types and geologic structures, and to appraise the mineral-resource potential of the area. We also used mapping of other Challis quadrangle workers: Earl Bennett and associates mapped 15-minute quadrangles north of the southwestern quarter of the Challis quadrangle, Wayne Hall mapped southeast of Stanley, and Paul Weis mapped along the western margin of the Challis quadrangle (Fisher and others, 1983).

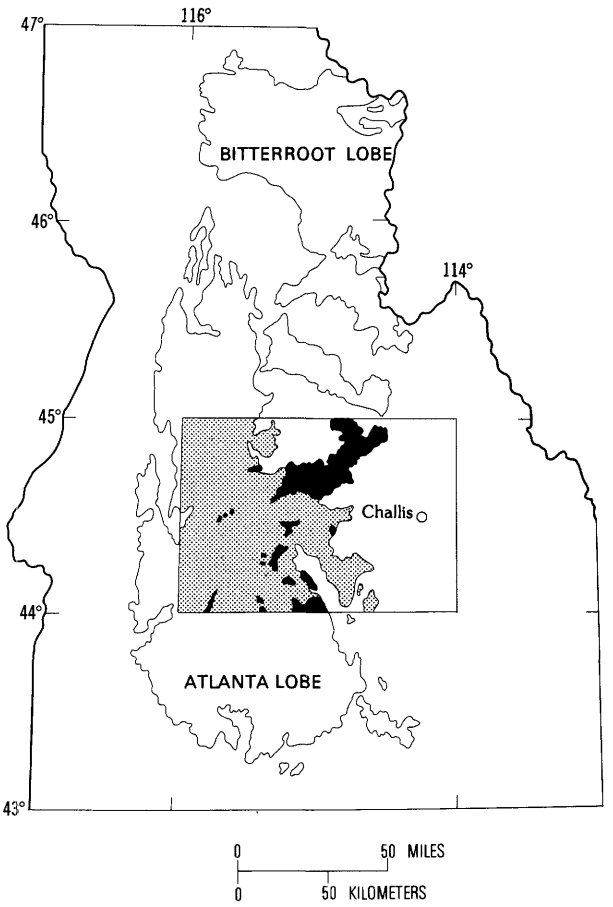

Figure B1. Index map of central Idaho showing location of the Challis quadrangle with respect to the Atlanta lobe of the Idaho batholith. Cretaceous plutonic rocks exposed within the quadrangle are light shaded; Tertiary plutonic rocks are dark shaded.

The part of the Atlanta lobe studied in the Challis quadrangle project consists generally of six rock types. The rock types are tonalite, hornblende-biotite granodiorite, porphyritic granodiorite, biotite granodiorite, muscovite-biotite granite, and leucocratic granite. Batholithic rocks exposed in a small area in the northwestern part of the quadrangle were not separated into specific types and are referred to on the geologic map of the quadrangle as mixed rocks (Fisher and others, 1983).

THE CRETACEOUS ATLANTA LOBE PLUTONIC ROCKS

Lithology

Tonalite

Tonalite grading to granodiorite is exposed along the western edge of the quadrangle and in the central part near the headwaters of Loon Creek (fig. B2). Smaller

exposures of tonalite and granodiorite cap parts of some of the high ridges north and northeast of Deadwood Reservoir and east of Stanley. The rock is gray to dark gray, medium to coarse grained, and equigranular to porphyritic. Andesine is the predominant mineral in the rock. As much as 20 percent biotite gives the rock a dark color and defines a foliation that varies from faint at some localities to intense at others. Variable amounts of hornblende occur in the rock, and yellow-brown sphene as long as 20 mm is common. Shredded flakes of secondary muscovite are in some altered feldspars. Apatite, magnetite, allanite, and zircon are the principal accessory minerals. Modal plots of 12 stained slabs and thin sections of the rock (fig. B3) show a mean composition of 30 percent quartz, 6 percent potassium feldspar, and 64 percent plagioclase.

The quartz diorite gneiss of Donnelly (Schmidt, 1964) is included in the tonalite unit. Other exposures of quartz diorite and gneissic quartz diorite near the western boundary of the Atlanta lobe (Anderson, 1934b, 1952; Moore, 1959; Ross, 1963; Taubeneck, 1971) probably would have been classed as tonalite had the classification of Streckeisen (1973) been used (fig. B3). The gneissic character of tonalitic rocks in marginal facies of the batholith is discussed by Anderson (1942). Hyndman (1983) described the western border zone of the Atlanta lobe as being largely foliated tonalite or trondhjemite, in which steep foliation parallels the inferred country-rock contact.

Field evidence indicates that the tonalite is the oldest of the batholithic rocks. Xenoliths of the foliated tonalitic rock have been found in younger biotite granodiorite at several localities in the western and north-central parts of the quadrangle.

Hornblende-biotite granodiorite

Small, localized exposures of hornblende-biotite granodiorite (fig. B2) are on the high ridges on both sides of the upper reaches of the Deadwood River, and on high ridges to the east. The rock is characterized by hornblende, some of which occurs in such small crystals that it is difficult to recognize in hand specimen. The rock varies from gray to dark gray, depending on the biotite content, which ranges from less than 5 percent to about 20 percent and which defines a weak to strong foliation in the rock. Sphene is abundant and allanite is common. The study of 11 stained slabs and thin sections of the rock show that it has an average modal composition of 27 percent quartz, 20 percent potassium feldspar, and 53 percent plagioclase.

Some exposures of the rock were mapped as tonalite in the field, but subsequent microscopic study of the rock showed it to be granodiorite. Nevertheless, the mineral assemblage, foliation, and general appearance indicate that the rock is closely associated to the tonalite unit.

Porphyritic granodiorite

Although granitic rocks of the Idaho batholith are commonly porphyritic, containing feldspar phenocrysts as long as 15 mm (millimeters), only granodiorite containing unusually large phenocrysts (megacrysts) was mapped as porphyritic. The porphyritic granodiorite is shown as one unit on the geologic map of the Challis quadrangle (Fisher and others, 1983), but it may be subdivided into two varieties (fig. B2).

The most striking and by far the most extensive variety of porphyritic granodiorite is a coarsely porphyritic granitoid rock, characterized by large feldspar megacrysts as long as 10 cm (centimeters), which crops out in a northwest-trending belt that extends more than 125 km (kilometers) across the quadrangle. The rock is dark gray, medium to coarse grained, typically foliated, and contains variable quantities of hornblende. The megacrysts are poikilitic microcline, generally pink but white in some places. They are euhedral in hand specimen; under the microscope the grain boundaries are irregular. Inclusions include anhedral embayed plagioclase and subordinate quartz and biotite. Carlsbad twinning is well developed in the megacrysts and clearly visible in outcrop. Plagioclase is anhedral, has a composition of An 23–37, shows weak normal or reverse zoning, has bent lamellae, and has undergone moderate to extreme sericitization. Epidote locally is present. Quartz is anhedral with well-developed undulatory extinction. The rock contains as much as 15 percent biotite that is pervasively altered to chlorite. Biotite defines the foliation. Hornblende is as much as 8 mm in maximum dimension, and in rare instances has cores of clinopyroxene. Sphene is the most common accessory mineral; other accessories include apatite, allanite, zircon, and opaque minerals.

The foliated, hornblende-bearing, porphyritic granodiorite contains many features of the previously described tonalite and hornblende-biotite granodiorite; it differs mainly in containing microcline megacrysts, the distribution of which are so variable that modal estimates are not consistent (fig. B3). The rock appears to grade into biotite granodiorite and hornblende-biotite granodiorite, but spatially it is mostly associated with the latter rock.

The other variety of porphyritic granodiorite (fig. B2) is light gray, contains less biotite, rarely contains hornblende and then only trace amounts, and the rare foliation, where seen, tends to be weak. The light-gray porphyritic granodiorite crops out chiefly on high ridges in the southwestern part of the quadrangle.

The origin of the microcline megacrysts is controversial. The similarity of megacrysts over large areas and the beltlike distribution and extent of the hornblende-bearing, foliated, porphyritic granodiorite suggests that the megacrysts are of primary origin but formed late in the crystallization sequence. Most evidence, however,

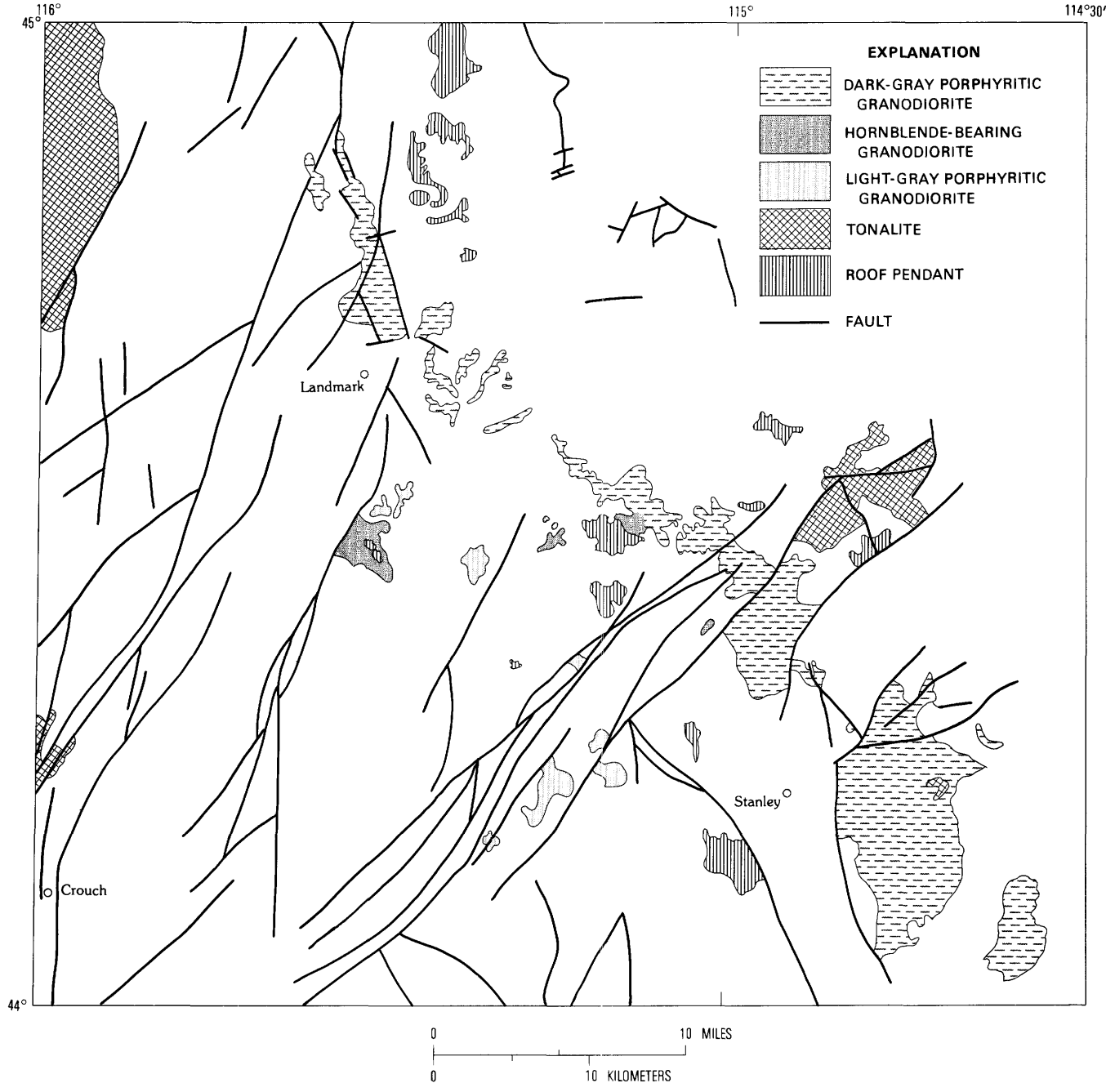

Figure B2. Map of the western part of the Challis quadrangle, showing hornblende-bearing and porphyritic rocks of the Atlanta lobe, and roof pendants.

indicates that they formed from potassium metasomatism. This origin is suggested by their poikilitic texture and embayed inclusions. More convincing evidence is numerous potassium feldspar-rich veinlets that cut the rock and appear to have been a source of potassium-rich fluid for the metasomatism. Megacrysts appear to have grown from the source veinlets and diminish in number away from the veinlets. Some megacrysts have grown across the veinlets, indicating that they grew after formation of the veinlets under subsolidus conditions (Lewis, 1984). Along certain leucocratic granite dikes that have intruded the porphyritic granodiorite, arrays of megacrysts are crowded along the dike contacts (fig. B4). The megacrysts appear to have grown most intensely near the dikes, and their number diminishes sharply away from the dike.

Roof pendants

Isolated roof pendants of metamorphosed sedimentary rocks trend discontinuously northwest across the quadrangle (fig. B2). Generally, they are near the eastern

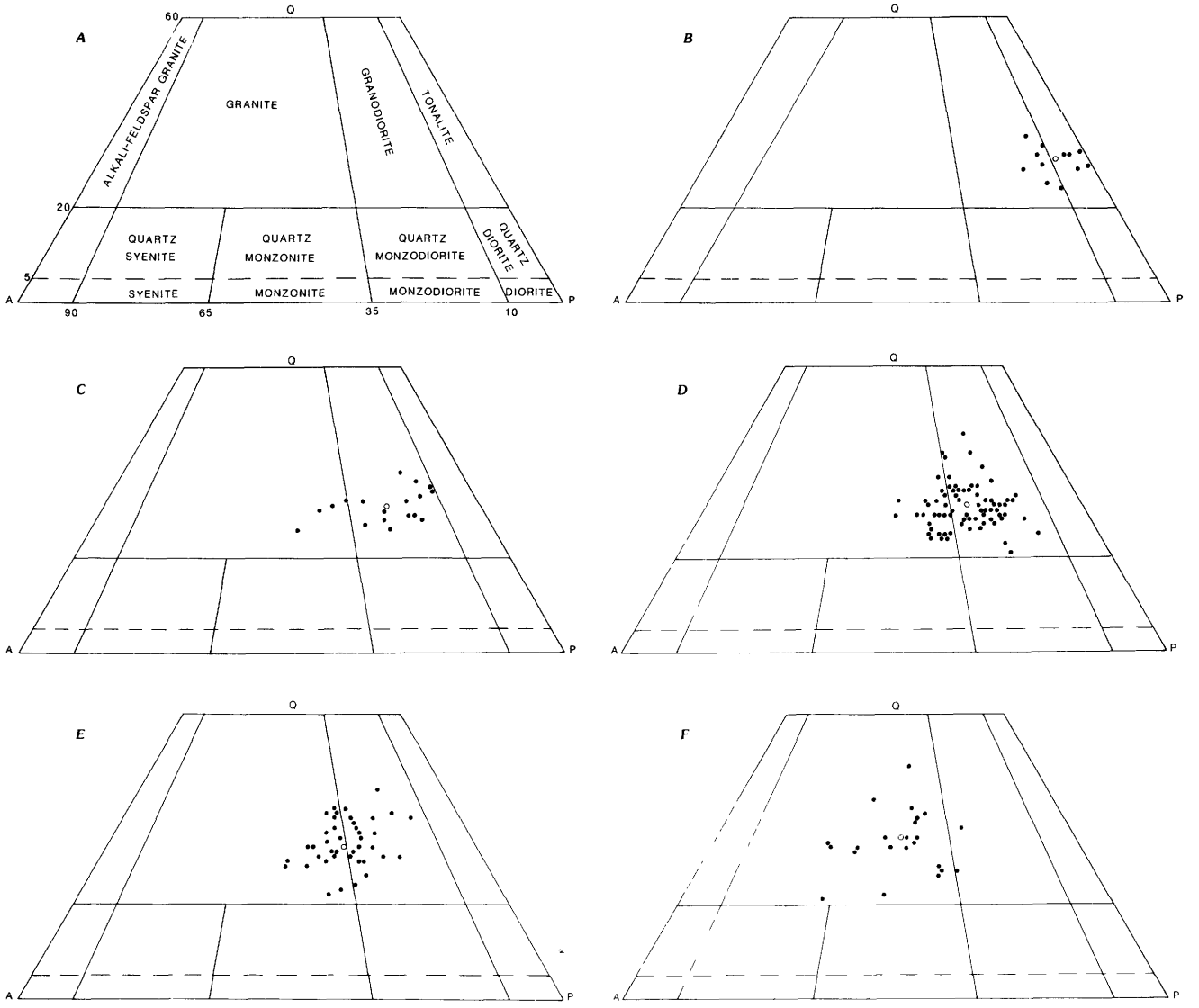

Figure B3. Modal analyses for samples of plutonic rocks of the Atlanta lobe of the Idaho batholith, Challis quadrangle. Analyses normalized to 100 percent quartz (Q), potassium feldspar (A), and plagioclase (P). Open circles show mean values. *A*, rock classification from Streckeisen (1973); *B*, tonalite; *C*, porphyritic granodiorite; *D*, biotite granodiorite; *E*, muscovite-biotite (two-mica) granite; *F*, leucocratic granite.

limits of the Idaho batholith. Many are on ridge tops where they commonly are surrounded by hornblende-biotite granodiorite or by porphyritic granodiorite. Common rock types of the roof pendants include biotite schist, quartzite, carbonate-rich quartzite, quartz-diopside marble, and calc-silicate gneiss. In a few places where foliated granitic rocks could be seen in contact with schist, the foliation of the two rock types is conformable. The conformable contacts and the location of pendants on ridge tops suggest that the roof pendants mark the top or near top of the batholith.

Biotite granodiorite

Biotite granodiorite is the most common rock type of the Atlanta lobe, and it is exposed over a wide area (fig. B5). Included in the unit is the granodiorite of Gold Fork (Schmidt, 1964), the quartz monzonite of Bear Valley (Swanberg and Blackwell, 1973), and part of the rock mapped by Anderson (1947) as quartz monzonite. The rock is light gray, medium to coarse grained, and equigranular to porphyritic. Plagioclase (oligoclase) is the chief component of the rock, with lesser quantities of quartz and potassium feldspar (fig. B3). Biotite averages about 5 percent of the rock, although locally it is more; it is pervasively altered to chlorite. Hornblende and muscovite are present only in trace amounts. Sericite, altered from feldspars, is widespread throughout the rock. Accessory minerals include minute quantities of sphene, allanite, zircon, monazite, and opaque minerals. Foliation is rare in the rock, commonly only near the contacts. The rock weathers readily, and fresh exposures, even on bluff faces, are hard to find. Most of the surface area is covered by grus.

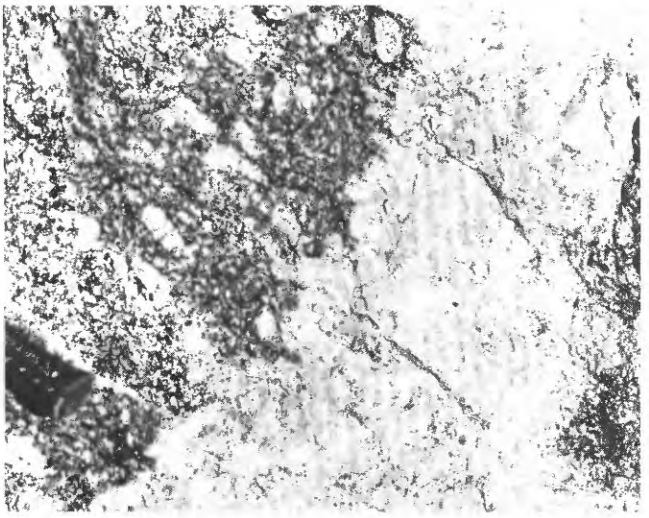

Figure B4. Dike of leucocratic granite cutting porphyritic granodiorite. Note how megacrysts of potassium feldspar appear to have grown out of the dike. Away from the dike, the megacrysts decrease in number. Base of hammer is 4 cm wide. Photograph by Earl Bennett, Idaho Geological Survey.

Field relations indicate that the biotite granodiorite is younger than the tonalite and the hornblende-biotite granodiorite. In the western part of the quadrangle, biotite granodiorite was intruded into older tonalite, and in the 60–90 m (meters)-wide contact zone it has primary foliation as well as xenoliths of tonalite. Xenoliths of hornblende-biotite granodiorite in biotite granodiorite are exposed on the high ridges east and west of the upper reaches of the Deadwood River south of Landmark (fig. B2).

Muscovite-biotite granite

Muscovite is widespread in the Idaho batholith (Larsen and Schmidt, 1958), but in granitic rocks of the Challis quadrangle it occurs principally as secondary muscovite formed from alteration of feldspar minerals. In the western part of the quadrangle, however, there is an irregular, north-trending belt of granite grading to granodiorite that contains notable quantities of primary muscovite. The quartz monzonite of Warm Lake (Schmidt, 1964) is part of this unit. We mapped this rock as muscovite-biotite (two-mica) granite (fig. 5B), using laminated plates or books of muscovite large enough to see in hand specimen as the principal field criterion. We consider this rock to be the core of the Atlanta lobe.

Muscovite-biotite granite is light gray, medium to coarse grained, equigranular to porphyritic rock that consists chiefly of oligoclase, quartz, and potassium feldspar. Modal values show a range in composition of the rock, the mean value within the granite field but very close to the granodiorite field (fig. B3). Muscovite makes up as much as 5 percent of the rock but probably averages about 2 percent in the specimens that were studied. The biotite content averages less than 5 percent. Other characteristics of the rock are local occurrences of small crystals of garnet, the absence of hornblende, and the rare occurrence of sphene. The rock is nonfoliated.

Muscovite-biotite granite is transitional with biotite granodiorite through a zone as wide as 2 km or more. At one locality near the western boundary of the quadrangle, the muscovite-biotite granite has an aphanitic texture in a border zone about 7 m thick at the contact with biotite granodiorite. The texture could have been caused by intrusion into cooler biotite granodiorite. The location of the muscovite-biotite granite in the central part of the batholith (fig. B5) and the transitional contact of the rock with biotite granodiorite also suggests that muscovite-biotite granite is younger.

Leucocratic granite

Leucocratic granite is light gray to nearly white, is fine to medium grained, and has a distinctive anhedral texture. It consists of roughly equal amounts of quartz, plagioclase, and potassium feldspar (fig. B3). The plagioclase (An 25–30) commonly is altered to sericite, as is the potassium feldspar, which is chiefly perthitic microcline. Biotite may constitute as much as 2 percent of the rock and generally is extensively altered to chlorite. Garnets as large as 2 mm in diameter are locally present, as are minute amounts of muscovite. Magnetite is a common accessory mineral, but sphene was found only rarely. Hornblende was not found in the rock.

Leucocratic granite, described as leucocratic quartz monzonite by Reid (1963), as aplite by Cater and others (1973), and as aplitic quartz monzonite by Anderson (1947), occurs as dikes, sill-like masses, and irregular stocks that are resistant to erosion and tend to form high points on ridges. Rubbly weathered scree from the high exposures may be extensive on lower slopes and may give the impression of being derived from larger exposures than actually exist. Exposures of larger masses of the rock are in the southwestern part of the quadrangle on high ridges in upthrown blocks between regional faults. Near Tenmile Creek, west of the Sawtooth Range, the basal contact of a large sill-like mass at least 790 m thick dips east at 6–8° (Kiilsgaard, 1983).

The leucocratic granite intrudes biotite granodiorite, commonly along joints, which indicates that the biotite-granodiorite was solidified prior to intrusion. Leucocratic granite, in turn, is intruded by plutonic rocks of Eocene age. The relation of the leucocratic granite to muscovite-biotite granite is not clear. The two rocks are comparable mineralogically and chemically, differing largely in texture and grain size. Leucocratic granite may represent a more rapidly cooled variety of the muscovite-biotite granite.

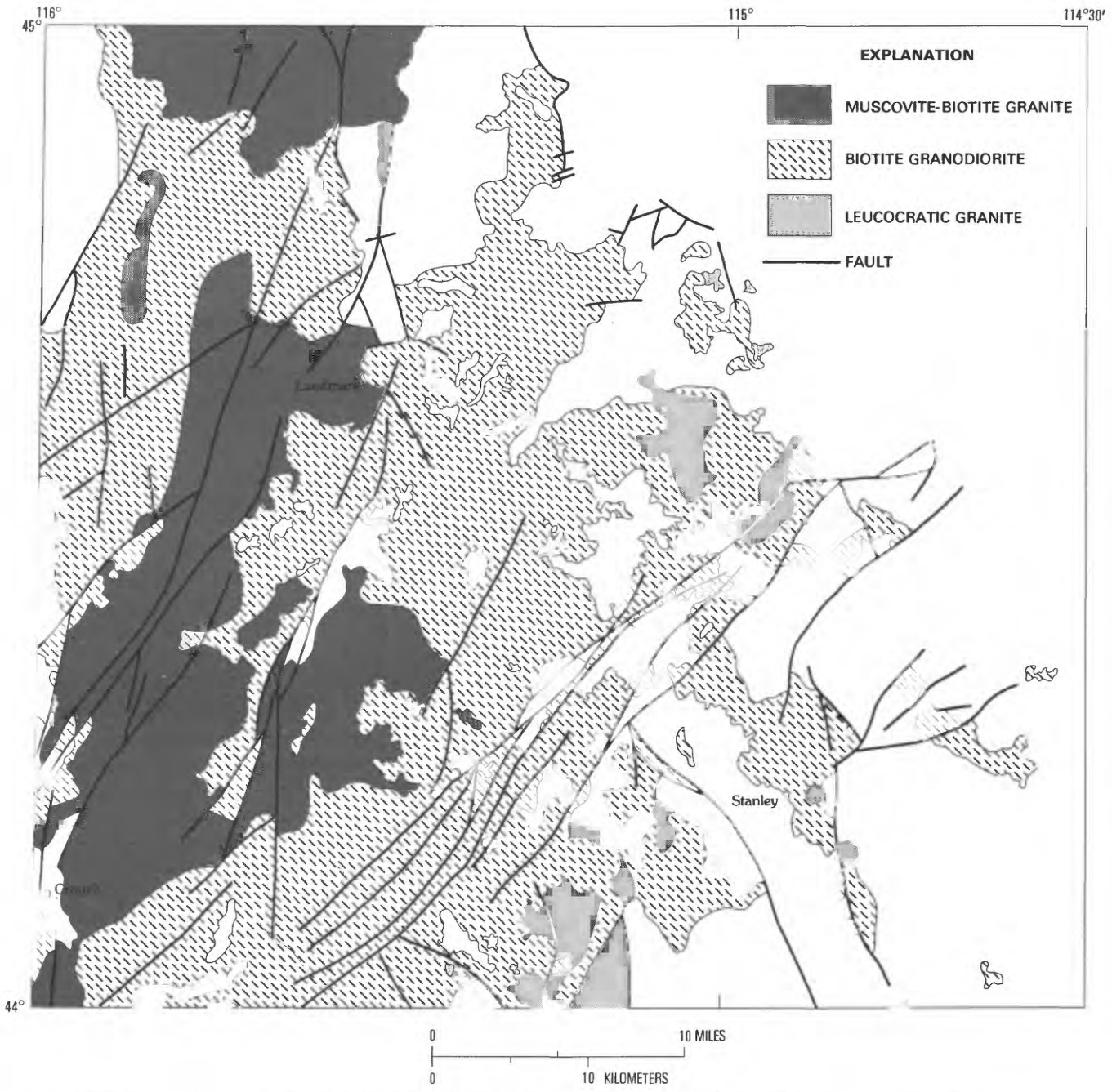

Figure B5. Map of the western part of the Challis quadrangle, showing the more silicic rocks of the Atlanta lobe.

Geochemical composition of Atlanta lobe rocks

Major-element oxide analyses of 65 samples taken across the southwestern quarter of the Challis quadrangle are shown in table B1. The six rock types listed in the table are paired by mineralogical and chemical similarities.

Tonalitic rocks on the west side of the quadrangle are low in SiO_2 and K_2O and high in Al_2O_3, Fe_2O_3, MgO, CaO, TiO_2, and P_2O_5 with respect to leucocratic granite in the east (table B1, figs. B2, B5). The increase in SiO_2 and K_2O content from older tonalite to younger leucocratic granite, the postulated age differences of which are based on field relations, supports the findings of Tilling (1973, 1974) in the Boulder batholith of Montana. SiO_2 and K_2O contents do not increase to the east across the batholith, however, as tonalite and hornblende-bearing porphyritic granodiorite are exposed in eastern parts of the batholith, and the geochemical content of those rocks is comparable to that of similar rocks on the western side (table B1).

Age relations of Atlanta lobe rocks

Radiometric dates obtained from a wide range of plutonic rocks of the Atlanta lobe show a range in age from

Table B1. Mean values of major-element oxides of plutonic rocks of the Atlanta lobe, Challis quadrangle

[Values in weight percent. Analytical determination by X-ray fluorescence. Analysts: J. E. Taggart, J. S. Wahlberg, A. J. Bartel, J. D. Baker, L. L. Jackson, G. R. Mason, D. B. Hatfield, F. E. Lichte, and H. G. Neiman, U.S. Geological Survey. <, less than]

Rock type	No. of Samples	SiO_2	Al_2O_3	[1]Fe_2O_3	MgO	CaO	Na_2O	K_2O	TiO_2	P_2O_5	MnO
Leucocratic granite---	11	75.3	14.0	0.73	0.1	0.78	4.3	4.11	0.05	<0.1	<0.02
Muscovite-biotite granite.	12	73.8	14.6	.92	.3	1.41	3.8	3.47	.10	<.1	.03
Biotite granodiorite.	22	71.9	15.2	1.55	.4	1.91	4.1	3.30	.21	<.1	.02
Light-gray porphyritic granodiorite.	6	71.4	15.3	1.66	.5	2.46	3.95	2.76	.25	.07	.03
Hornblende-biotite granodiorite.	3	66.5	15.5	3.79	1.70	3.98	3.32	2.97	.63	.21	.07
Tonalite----------	11	64.0	16.9	4.40	1.6	4.64	3.7	2.36	.77	.26	.07

[1]Total iron reported as Fe_2O_3.

135 m.y. (million years) (Larsen and others, 1958) to 43 m.y. (McDowell and Kulp, 1969). This spread in reported ages has been narrowed by the efforts of subsequent workers. Armstrong (1975b) pointed out that some of the earlier uranium-lead dates are too high. Geologic mapping has shown that some plutonic rocks previously considered as components of the Atlanta lobe are younger (Reid, 1963; Kiilsgaard and others, 1970). Potassium-argon dating of these younger intrusive rocks show them to be of Eocene age (Armstrong, 1975b; Criss, 1980; Kiilsgaard, 1983; Bennett and Knowles, chap. F, this volume). Vast areas of the Atlanta lobe have been affected by widespread Eocene plutonism that reset the potassium-argon system in older batholithic rocks (McDowell and Kulp, 1969; Criss and others, 1982). Armstrong (1975b) has summarized data on age determinations of Idaho rocks, and Armstrong and others (1977) noted that the Atlanta lobe of the Idaho batholith was emplaced during the culmination of Cretaceous igneous activity about 75 to 100 m.y. ago. The oldest ages have been obtained from rocks along the western and eastern edges of the Atlanta lobe and the youngest ages from rocks in the central part (Armstrong and others, 1977; Criss and others, 1982).

In the Challis quadrangle, Cretaceous plutonic rocks of the Atlanta lobe may be grouped into three categories, each of which appears to have been emplaced at a different time.

1. A batholithic border facies of foliated tonalite grading to hornblende-bearing granodiorite, xenoliths of which are in contiguous biotite granodiorite and on high ridges across the lobe in the west-central part of the quadrangle.
2. A major central part of the batholith that consists of biotite granodiorite in transitional contact with muscovite-biotite granite that forms the core of the batholith. Crosscutting relationships of these two rock types have not been found. The core location, transitional contact, and potassium-argon ages (table B2) suggest that the muscovite-biotite granite may be slightly younger.

Table B2. Potassium-argon ages of Cretaceous plutonic rocks of the Atlanta lobe, Challis quadrangle

[Dated by R. F. Marvin, U.S. Geological Survey; except for four samples dated by R. J. Fleck, U.S. Geological Survey]

Rock type	No. of Samples	Age (m.y.)
Leucocratic granite----------	6	72–64
Muscovite-biotite granite----------	8	75–66
Biotite granodiorite----------	10	82–69
Tonalite and porphyritic granodiorite.	6	73–97

3. Stocks and dikes of leucocratic granite that intrude all older rocks. Leucocratic granite crosscuts pegmatite dikes in biotite granodiorite, which indicates that it was emplaced after crystallization of the biotite granodiorite. Dikes of leucocratic granite along joints in biotite granodiorite also indicate solidification of the latter rock prior to dike intrusion.

The range in age of the rock types (table B2) indicates overlapping time of emplacement, although the time span for the different types is in general agreement with geologic mapping results. Three of the leucocratic granite samples are from hydrothermally altered areas, and biotite from the samples gave ages ranging from 64 to 66 m.y., ages that may be too young due to argon loss. Biotite from the other three leucocratic granite samples gave an age of about 72 m.y., an age that may be more representative of the emplacement age of the rock. Muscovite-biotite pairs in six samples of muscovite-biotite granite gave concordant ages. Only biotite was dated in the 10 biotite granodiorite samples. Biotite also was dated in the six tonalite and porphyritic granodiorite samples.

Zircon from a sample of porphyritic granodiorite taken at milepost 201, U.S. Highway 75 east of Stanley, lat 114°50′ N., long 44°20′ E., was analyzed by Lynn Fischer, U.S. Geological Survey, and the uranium-lead age obtained was 88±6 m.y. This zircon age agrees with a potassium-argon age of 87.7±2.7 m.y. obtained from

hornblende collected at the same locality. Biotite from this locality gave a potassium-argon age of 79.8±2.7 m.y. The zircon age also agrees with a potassium-argon age of 90±3 m.y. obtained from hornblende from quartz diorite collected near Donnelly on the western side of the Idaho batholith (Armstrong, 1975b). Field evidence and radiometric ages indicate that the oldest plutonic rocks are in the western and eastern border zones of the Atlanta lobe.

MAJOR REGIONAL FAULTS IN PLUTONIC ROCKS OF THE CHALLIS QUADRANGLE

The plutonic rocks of the Atlanta lobe are extensively faulted. Displacement along faults commonly cannot be measured because of the absence of horizon markers; thus, some estimates are based on topographic relief. Some regional faults extend across the Challis quadrangle, and appear to have guided emplacement of Tertiary plutonic rocks and dikes. In a general way, the regional faults may be grouped in three sets: northerly trending, northwest trending, and northeast trending.

Faults trending in a northerly direction

A set of major northerly trending faults crosses the western part of the Challis quadrangle (Fisher and others, 1983). Two of these faults cross the upper reaches of Scriver Creek north of Crouch; the western one, the Middle Fork Payette fault, extends north along the Middle Fork Payette River, and the eastern one, the South Fork Salmon fault, extends along the South Fork Salmon River (fig. B6). Surface traces of both faults are clearly displayed on LANDSAT imagery and are shown on the ground surface by alignment of topographic features and local exposures of sheared and crushed rocks. Muscovite-biotite granite has been offset by left-lateral movement along both faults (fig. B5).

The north-trending Boise Ridge fault (fig. B6) was identified by Anderson (1947), the location determined from the scarp along the east side of Boise Ridge and the displacement of well-defined datum planes, including basalt flows of the Miocene Columbia River Group. The fault displacement proposed by Anderson was checked by examining the 110-m-thick exposure of west-dipping basalt that caps Hawley Mountain 2.5 km southwest of the southwestern corner of the Challis quadrangle and west of the fault. Exposures of basalt east of the fault also were examined. Normal magnetic polarity measurements were obtained from most of the basalt test sites on both the eastern and western sides of the fault. Samples of basalt from different exposures on both sides of the fault were analyzed in the laboratory of Peter Hooper, Washington State University, Pullman. Analytical data resemble those of the Weiser Basalt, which overlies the Grande Ronde Basalt of the Columbia River Basalt Group, (Hooper, oral commun., 1985). The Grande Ronde Basalt is no older than 16.5 m.y. (Hooper, 1982). Magnetic polarity and chemical data indicate that the same basalt is on both sides of the fault. Accepting the base of the basalt as a datum plane, measurements show that basalt east of the fault has been downdropped a minimum of 490 m with respect to basalt west of the fault. The age of initial movement along the fault cannot be determined from the data on hand, but displacement of the basalt cannot be older than 16.5 m.y.

The Boise Ridge fault enters Garden Valley east of Crouch and probably extends north along the valley of the Middle Fork Payette River, although near Crouch the fault is concealed by alluvium. North of Crouch, sedimentary rocks of the Payette Formation terminate against the fault. Floral assemblages, collected from the probable upper part of the Payette, are of middle to early late Miocene age (W. C. Rember, University of Idaho, written commun., 1983) or about 13 m.y. old. The sedimentary rocks have been tilted west by fault movement, and as they terminate against the fault, displacement along the fault can be no older than about 13 m.y., a fault-displacement age that is probably the same for the basalt displacement east of Hawley Mountain.

The Deadwood fault zone (fig. B6) is well exposed along the west side of Deadwood River, north from its junction with the South Fork Payette River. To the north, near Deadwood Reservoir, the fault splits into several strands that merge near the Deadwood mine and continue north along Johnson Creek in Deadwood canyon (Fisher and others, 1983). The fault zone has a distinct topographic expression; the west side is upthrown. Foliated hornblende-biotite granodiorite east of the fault zone and near the Deadwood mine is about 500 m lower than similar rock on the high ridge west of the fault, which suggests fault displacement of at least that much.

Northwest-trending faults

Three major northwest-trending faults, Sawtooth, Bear River, and Deer Park (fig. B6), are in the southern part of the Challis quadrangle and terminate against the trans-Challis fault system.

The Sawtooth fault extends more than 60 km along the eastern side of the Sawtooth Range. Throughout most of its projected length, the fault is masked by glacial moraine or alluvium, but it is recognized by the linear front of the range, truncated ridges, the towering rise of the Sawtooth Range above Sawtooth Valley, and a linear gradient in the aeromagnetic pattern (Kiilsgaard and others, 1970, pl. 1; Mabey and Webring, chap. E, this volume, fig. E5). South of the Challis quadrangle, along the western side of the Salmon River, the fault juxtaposes Paleozoic metasedimentary rocks and Eocene Challis

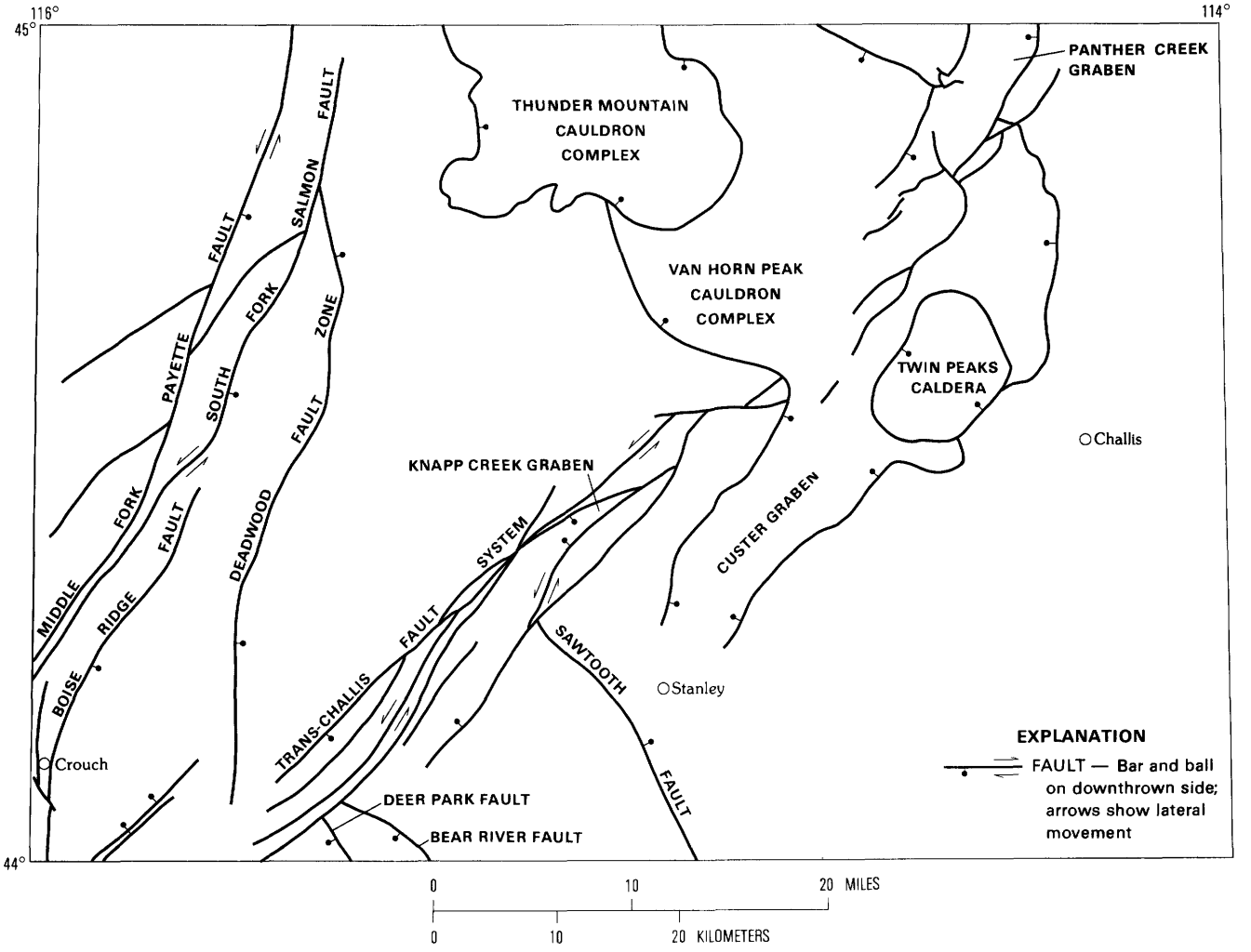

Figure B6. Map of the Challis quadrangle, showing principal faults, grabens, cauldron complexes, and caldera.

Volcanics. Minimum displacement along the fault was estimated by Reid (1963) as 1,200 ft (feet), the upthrown side to the west.

The Bear River fault extends from the North Fork Boise River to the South Fork Payette River, about 22 km (Kiilsgaard, 1983). It is best exposed on the ridge northwest of Bear River, where it forms a broad zone, tens of meters wide, of crushed, sheared, and intensely altered granite of Tertiary age (fig. M3, chap. M, this volume), and southeast of Bear River where Tertiary granite is displaced against biotite granodiorite of the Atlanta lobe. The Bear River fault may be the offset segment of the Montezuma fault, which extends more than 40 km along the western flank of the Sawtooth Range south of the Challis quadrangle. The Montezuma fault was first mapped near Atlanta by Anderson (1939), who estimated vertical displacement along the fault to be as much as 2,000 ft, the downdropped side to the southwest. The main part of the Sawtooth Range was considered by Reid (1963) to be a horst bounded on the west by the Montezuma fault and on the east by the Sawtooth fault. The Montezuma fault has been mapped northwest to the North Fork Boise River, where it may terminate or be offset to the southwest, continuing as the Bear River fault (fig. M3).

The Deer Park fault is generally parallel to the Sawtooth and Bear River-Montezuma faults (figs. M3, B6) and extends at least 40 km southeast of the southern boundary of the Challis quadrangle. Anderson (1934a) traced the fault southeast from the South Fork Payette River chiefly by the displacement of an old summit erosion surface. We do not think that the fault reaches the South Fork Payette River but terminates about 1.5 km southeast of the river against a strand of the trans-Challis fault system (Fisher and others, 1983). Southeast of the southern boundary of the Challis quadrangle, the fault scarp forms steep slopes along the southwestern sides of Goat Mountain and Swanholm Peak. Vertical displacement in that locality, based on topographic relief, is at least 2,600 ft, the downdropped block on the southwestern side (Kiilsgaard, 1983).

A significant aspect of the northwest-trending faults, Sawtooth, Bear River-Montezuma, and Deer Park,

is that although they have strong topographic expression and extend over considerable strike-length distances, they terminate at the trans-Challis fault system. They do not appear to have been truncated and displaced by the trans-Challis fault system, as no evidence of them has been found northwest of the fault system. The Sawtooth Range appears to be a large upthrust block bounded on the east by the Sawtooth fault, on the west by the Montezuma-Bear River faults, and on the northwest by the trans-Challis fault system. The topographic linearity of the northwest-trending faults and the vertical displacement along them suggests that they are deep faults, and initial movement along them may predate the Idaho batholith. Measurable displacement along them, however, postdates the Idaho batholith. Tertiary gravel is displaced along the Montezuma fault, which suggests post-Pleistocene fault movement. Steep gradients along the North Fork Boise River and Bear River across the scarp of the Deer Park fault (fig. M3) also suggest recent fault movement. Movement quite likely has recurred along the faults up to the present time. Recurrence is suggested by displacement along a similar northwest-trending fault during the Idaho earthquake of Oct. 28, 1983. That fault extends along the western base of the Lost River Range, and appears to be a member of the above-described northwest-trending set of faults.

Northeast-trending faults—the trans-Challis fault system

A broad zone of northeast-trending high-angle regional faults crosses the southwestern quarter of the Challis quadrangle and aligns with the Panther Creek graben (fig. B6). Only near the Van Horn Peak cauldron complex (Ekren, chap. C, this volume) is there a break in fault continuity, and even there the Custer graben, Twin Peaks caldera, and part of the Van Horn Peak cauldron complex are parallel to and presumably part of the same tectonic feature. The faults and grabens make up a regional fault system herein named the trans-Challis fault system.

The trans-Challis fault system extends beyond the Challis quadrangle. Faults of the system extend southwest of the southern boundary of the quadrangle to beyond Idaho City (fig. M5), where at least one of the faults passes beneath the Holocene and Pleistocene Snake River Group. The Panther Creek fault, part of the system, has been mapped more than 30 km northeast of the northern boundary; thus the length of the fault system in the Challis quadrangle region is at least 220 km. The fault system is very well aligned and appears to be continuous with the Great Falls lineament, as proposed by O'Neill and Lopez (1983), who projected the lineament northeast from Idaho across Montana. The trans-Challis fault system therefore appears to be part of a regional tectonic feature.

In the southwestern quarter of the Challis quadrangle, the trans-Challis fault system is best exposed in an area about 30 km west-northwest of Stanley, along the upper reaches of Warm Springs Creek and on the divides at the head of Eightmile Creek and the East Fork of Eightmile Creek (Luthy, 1981; Fisher and others, 1983). In that area are several northeast-striking faults characterized by white to tan, nonresistant fault gouge in bleached and altered granitic rocks; these sheared zones commonly are devoid of vegetation. Some zones of bleached and crushed rock are more than 500 m wide, and within them the rocks are so pulverized that few fragments are more than 30 cm in diameter. Rocks in the more intensely sheared zones are so altered that their original composition is difficult to determine. Dike rocks in the sheared zones are not as altered as the granitic host rock, but they generally are broken by faults, which indicates recurrent movement along the fault zones.

Faults of the trans-Challis fault system in the central and northeastern part of the Challis quadrangle are discussed by Bennett and Knowles (chap. F, this volume), McIntyre and Johnson (chap. I, this volume), Hardyman (chap. G, this volume), and Ekren (chap. C, this volume).

Effect of faults on emplacement of Tertiary plutonic rocks and dikes

The trans-Challis fault system has guided emplacement of Tertiary dikes and Tertiary plutonic intrusive rocks. This guidance is particularly evident in the northern part of Boise Basin and along the South Fork Payette River (fig. M5). The dike swarm in Boise Basin trends more or less parallel to major faults of the trans-Challis fault system, although dikes within the swarm strike in various directions. The dikes range from diabase to rhyolite in composition, most are porphyritic, and they range from 0.5 to 60 m thick and to as long as 2 km. A dioritic stock in the northern part of Boise Basin reaches widths of more than 1.5 km and is more than 16 km long (fig. M5). Biotite from a similar plutonic stock within the trans-Challis fault system (fig. M5) gave a potassium-argon age of 49.2 m.y. (Kiilsgaard and Bennett, chap. M, this volume), and zircon from a rhyolite dike at the Little Falls molybdenum deposit (fig. M5) gave a fission-track age of 29.3 m.y. (F. S. Fisher, oral commun., 1983).

Pink granite, intrusive into biotite granodiorite of the Idaho batholith, is exposed along the trans-Challis fault system in an area about 30 km west-northwest of Stanley. The granite is lithologically comparable to Eocene pink granite exposed in the Sawtooth Range and is considered to be of the same age. The exposure of granite is elongated along the trans-Challis trend and is in part fault bounded, but at the northeast and southwest ends, it is displaced along northeast-trending faults. Swarms of rhyolite and rhyodacite dikes, elongated along the trans-Challis system, intrude the pink granite and the older

biotite granodiorite to the southwest and northeast. Near the north end of Copper Mountain, in the Knapp Creek graben (fig. B6), pink granite intrudes overlying intrusive rhyolite in what appears to be an instance where a shallow batholith has intruded its own hypabyssal-equivalent rock. Hornblende from the pink granite gave a potassium-argon age of 45.3±0.4 m.y. (R. J. Fleck, oral commun., 1983). Intrusion of the rhyolite by pink granite is indicated by (1) a chilled zone of fine-grained pink granite as much as 9 m thick beneath the contact; (2) an uneven pink granite-rhyolite contact, with pink granite protruding as much as 30 m into the rhyolite, a small dikelet of pink granite cutting the rhyolite, and foundered blocks of the overlying rhyolite engulfed in the pink granite; (3) the rather flat roof contact, which may be traced along a canyon wall for almost 1 km beneath the overlying rhyolite. The intrusive character of the rhyolite is proven by the way in which it cuts across the bedding of metasedimentary roof pendants and by the low-angle contact it makes with overlying biotite granodiorite of the Atlanta lobe that forms the top of Copper Mountain. Xenoliths of biotite granodiorite are in the intrusive rhyolite.

To the northeast, still within the Knapp Creek graben, the intrusive rhyolite is in unconformable contact with extrusive volcanic rocks ranging from flow-banded rhyolite to rhyolitic lapilli tuff and vitrophyre. The rhyolitic rocks are characterized by phenocrysts of sanidine. Well-developed flow banding is defined by alternating 1–2 mm reddish-white laminations composed of spherulites (Lewis, 1984). A fossilized wood fragment was found in the tuffaceous rocks. Sanidine from the extrusive rhyolite gave a potassium-argon age of 39.0 m.y. (R. J. Fleck, oral commun., 1984).

The extrusive rhyolitic rocks form a northeast-trending ridge about 10 km long, which rises more than 470 m above flanking valley floors, yet extrusive rocks are not found beyond the flanking valleys. There is no surface evidence that suggests a northeast-trending valley that might have been filled by extrusive rocks, the remnants of which account for the present ridge. Instead, the rocks are preserved in the northeast-trending Knapp Creek graben. The graben block apparently has been tilted to the northeast because the volcanic rocks in the northeastern part of the graben give way to the shallow intrusive rhyolite and pink granite exposed to the southwest.

Vertical displacement along the trans-Challis fault system was not measured as there are no horizon markers. There are few topographic breaks along the faults such as the scarps along the northwest-trending faults and some of the north-trending faults. Left-lateral displacement along faults of the trans-Challis system is indicated at several localities. Along the northwestern side of the Knapp Creek graben, Eocene granite appears to be offset 2.9 km (Fisher and others, 1983). Southwest of the Knapp Creek graben, an exposure of Tertiary granite is offset about 800 m by left-lateral displacement along one of the strands of the trans-Challis fault system (Luthy, 1981). Left-lateral movement along a trans-Challis fault south-southwest of the Knapp Creek graben has displaced Tertiary granite about 535 m.

Age of faulting

The age of initial movement along the trans-Challis fault system is obscure, but evidence indicates that adjustment along the system could have recurred from Precambrian to Holocene time. In the southwestern quarter of the Challis quadrangle the indicated timespan of faulting, based on field evidence, is rather short. Fault movement displaced Cretaceous plutonic rocks of the Atlanta lobe and guided emplacement of Eocene granitic rocks and younger dikes. Subsequent movement along the faults displaced the Eocene granitic rocks and the dikes. Many Eocene rhyolites of the Challis Volcanics in the northeastern part of the quadrangle are elongated along the trans-Challis system (Fisher and others, 1983), and their emplacement obviously has been guided by faults of the system. Holocene fault movement has disrupted stream terraces that contain glacial erratics of presumable Pleistocene age. The densest distribution of recent earthquake epicenters in Idaho is in the Challis quadrangle (Roy Breckenridge, Idaho Geological Survey, written commun., 1983), most of them plotting within the trans-Challis fault system.

Near the northern boundary of the Challis quadrangle the Middle Proterozoic Yellowjacket Formation is displaced against Eocene volcanic rocks of the Challis Volcanics in the Panther Creek graben, but about 16 km farther northeast the Panther Creek fault offsets the contact between Yellowjacket Formation and 1.4-b.y. (billion years)-old plutonic rock (Lopez, 1981). At that locality, the Panther Creek fault is marked by tight isoclinal folds in the Yellowjacket Formation, and truncation of them by the 1.4-b.y.-old plutonic rocks indicates Precambrian movement along the fault (J. M. O'Neill and D. A. Lopez, written commun., 1984).

The remarkable linearity of the trans-Challis fault system for at least 220 km in the Challis quadrangle vicinity, the grabens and calderas within the system, and the linearity of intrusive and extrusive rocks along the system all indicate crustal extension and deep faulting and rifting that may have existed before intrusion of the Idaho batholith. Fault-movement evidence now visible in the quadrangle represents recurrent adjustment along faults of the system.

REFERENCES CITED

Anderson, A. L., 1934a, A preliminary report on recent block faulting in Idaho: Northwest Science, v. 8, no. 2, p. 17–28.

_____1934b, Geology of the Pearl-Horseshoe Bend gold belt, Idaho: Idaho Bureau of Mines and Geology Pamphlet 41, 36 p.

_____1939, Geology and ore deposits of the Atlanta district, Elmore County, Idaho: Idaho Bureau of Mines and Geology Pamphlet 49, 71 p.

_____1942, Endomorphism of the Idaho batholith: Geological Society of America Bulletin, v. 53, no. 8, p. 1099–1126.

_____1947, Geology and ore deposits of the Boise Basin, Idaho: U.S. Geological Survey Bulletin 944-C, 319 p.

_____1952, Multiple emplacement of the Idaho batholith: Journal of Geology, v. 60, no. 3, p. 255–265.

Armstrong, R. L., 1975a, Precambrian (1500 m.y. old) rocks of central Idaho—The Salmon River arch and its role in Cordilleran sedimentation and tectonics: American Journal of Science, v. 275-A, p. 437–467.

_____1975b, The geochronometry of Idaho: Isochron/West, no. 14, 51 p.

Armstrong, R. L., Taubeneck, W. H., and Hales, P. O., 1977, Rb-Sr and K-Ar geochronometry of Mesozoic granitic rocks and their Sr isotopic composition, Oregon, Washington, and Idaho; Geological Society of America Bulletin, v. 88, p. 397–411.

Cater, F. W., Pinckney, D. M., Hamilton, W. B., Parker, R. L., Weldin, R. D., Close, T. J., and Zilka, N. T., 1973, Mineral resources of the Idaho Primitive Area and vicinity, Idaho: U.S. Geological Survey Bulletin 1304, 431 p.

Criss, R. E., 1980, An $^{18}O/^{16}O$, D/H and K-Ar study of the southern half of the Idaho batholith: Pasadena, California Institute of Technology Ph.D. dissertation.

Criss, R. E., Lanphere, M. A., and Taylor, H. P., Jr., 1982, Effects of regional uplift, deformation, and meteoric-hydrothermal metamorphism on K-Ar ages of biotites in the southern half of the Idaho batholith: Journal of Geophysical Research, Ser. B, v. 87, no. 8, p. 7029–7046.

Fisher, F. S., McIntyre, D. H., and Johnson, K. M., 1983, Geologic map of the Challis 1°×2° quadrangle, Idaho: U.S. Geological Survey Open-File Report 83–523, 41 p., 2 maps, scale 1:250,000.

Hooper, P. R., 1982, The Columbia River basalts: Science, v. 215, no. 4539, p. 1463–1468.

Hyndman, D. W., 1983, The Idaho batholith and associated plutons, Idaho and western Montana: Geological Society of America Memoir 159, p. 213–240.

Kiilsgaard, T. H., 1983, Geologic map of the Ten Mile West Roadless Area, Boise and Elmore Counties, Idaho: U.S. Geological Survey Miscellaneous Field Studies Map MF-1500-A, scale 1:62, 500.

Kiilsgaard, T. H., Freeman, V. L., and Coffman, J. S., 1970, Mineral resources of the Sawtooth Primitive Area, Idaho: U.S. Geological Survey Bulletin 1319-D, p. D1–D174.

Larsen, E. S., Jr., Gottfried, D., Jaffe, H. W., and Waring, C. L., 1958, Lead-alpha ages of the Mesozoic batholiths of western North America: U.S. Geological Survey Bulletin 1070-B, p. 35–62.

Larsen, E. S., Jr. and Schmidt, R. G., 1958, A reconnaissance of the Idaho batholith and comparison with the southern California batholith: U.S. Geological Survey Bulletin 1070-A, 32 p.

Lewis, R. S., 1984, Geology of the Cape Horn quadrangle, south-central Idaho: University of Washington M.S. thesis, 91 p.

Lopez, D. A., 1981, Stratigraphy of the Yellowjacket Formation of east-central Idaho: U.S. Geological Survey Open-File Report 81–1088, 219 p.

Luthy, S. T., 1981, The petrology of Cretaceous and Tertiary intrusive rocks of the Red Mountain-Bull Trout Point area, Boise, Custer, and Valley Counties, Idaho: Missoula, University of Montana M.A. thesis.

McDowell, F. W., and Kulp, J. L., 1969, Potassium-argon dating of the Idaho batholith: Geological Society of America Bulletin, v. 80, no. 11, p. 2379–2382.

Moore, J. G., 1959, The quartz diorite boundary line in the western United States: Journal of Geology, v. 67, no. 2, p. 198–210.

O'Neill, J. M., and Lopez, D. A., 1983, Great Falls lineament, Idaho and Montana [abs.]: American Association of Petroleum Geologists Bulletin, v. 67, no. 8, p. 1350–1351.

Reid, R. R., 1963, Reconnaissance geology of the Sawtooth Range: Idaho Bureau of Mines and Geology Pamphlet 129, 37 p.

Ross, C. P., 1963, Evolution of ideas relative to the Idaho batholith: Northwest Science, v. 37, no. 2, p. 45–60.

Schmidt, D. L., 1964, Reconnaissance petrographic cross section of the Idaho batholith in Adams and Valley Counties, Idaho: U.S. Geological Survey Bulletin 1181-C, 50 p.

Streckeisen, A. L., 1973, Plutonic rocks—Classification and nomenclature recommended by the IUGS Subcommission on the Systematics of Igneous Rocks: Geotimes, v. 18, p. 26–30.

Swanberg, C. A., and Blackwell, D. D., 1973, Areal distribution and geophysical significance of heat generation in the Idaho batholith and adjacent intrusions in eastern Oregon and western Montana: Geological Society of America Bulletin, v. 84, no. 4, p. 1261–1282.

Taubeneck, W. H., 1971, Idaho batholith and its southern extension: Geological Society of America Bulletin, v. 82, no. 3, p. 1899–1928.

Tilling, R. I., 1973, Boulder batholith, Montana—A product of two contemporaneous but chemically distinct magma series: Geological Society of America Bulletin, v. 84, no. 12, p. 3879–3899.

_____1974, Composition and time relations of plutonic and associated volcanic rocks, Boulder batholith region, Montana: Geological Society of America Bulletin, v. 85, no. 12, p. 1925–1931.

Symposium on the Geology and Mineral Deposits of the Challis 1°×2° Quadrangle, Idaho

Chapter C

Eocene Cauldron-Related Volcanic Events in the Challis Quadrangle

By E. B. EKREN

CONTENTS

FIGURES

TABLES

Abstract

Volcanism started in the Challis quadrangle about 51 m.y. (million years) ago when intermediate-composition lavas were erupted from numerous vents in the eastern and north-central parts of the quadrangle. Succeeding voluminous eruptions of tuff caused two cauldron complexes to form. The easternmost, termed the Van Horn Peak cauldron complex, began with the eruption of the 48.4 m.y.-old rhyodacite tuff of Ellis Creek, following minor activity in the Corral Creek segment. Cauldron formation ended with the eruption of the 45–47 m.y.-old rhyolite tuff of Challis Creek. The north-central complex, termed the Thunder Mountain cauldron complex, also started with the eruption of a rhyodacite tuff about 47–48 m.y. ago and ended with the eruption of a 45–46 m.y.-old rhyolite tuff informally called the Sunnyside rhyolite. The two cauldron complexes lie on the southeastern and northwestern flanks of the granitic Casto pluton and probably reflect the evolution of separate cupolas on the rising magma body that formed the pluton.

INTRODUCTION

This chapter briefly describes the principal volcanic events of Eocene age in the Challis quadrangle, stressing the relationships between the principal ash-flow tuffs and the various cauldrons or cauldron segments that formed as the result of these tuff eruptions. More detailed lithologic descriptions of the volcanic units, especially the rocks that are not associated with cauldrons, are in McIntyre and others (1982) and Fisher and others (1983). Descriptions of the granitic rocks of Eocene age are in the chapter by Bennett and Knowles (chap. F, this volume).

The Challis Volcanics of Eocene age were first named and described by Ross (1933, 1934), who noted the variety of rock types and thick sections of volcanic rocks preserved locally in central Idaho (fig. C1); the concept of calderas was poorly understood at that time. Calderas were first recognized at Thunder Mountain by B. F. Leonard (*in* Cater and others, 1973, p. 45–51). The present study, done under the Conterminous United States Mineral Assessment Program (CUSMAP), has provided a more complete understanding of the Thunder Mountain cauldron complex and led to the recognition of the Van Horn Peak cauldron complex and two volcanic-related graben east of the Thunder Mountain area.

The term "cauldron complex," as used in this chapter, denotes a volcanic terrane within which many related cauldrons occur. Although the cauldrons originally were basin-shaped topographic depressions (calderas) bounded by arcuate faults, subsequent events have greatly modified them.

Prior to deep erosion, the outflow sheets from the calderas probably covered large areas surrounding their sources. Outflow from the Challis volcanic field may have overlapped Eocene volcanic fields in adjacent states (fig. C1), which in turn overlapped extensive fields in southern British Columbia (for example, see Souther, 1970). The area affected by this Eocene volcanic episode was huge, and the volume of volcanic rock extruded was immense. The cause of this volcanic activity, however, is debated. According to Lipman and others (1972) and Lipman (1983), the ultimate cause was the subduction of the Farallon plate beneath the North American continent. Fox (1983), on the other hand, believed that the ultimate cause was intracontinental rifting triggered by collision of the Pacific plate with the North American plates.

Northwest- and northeast-trending faults existed prior to volcanism (McIntyre and others, 1982), as indicated by regional geologic mapping for the CUSMAP study of the Challis quadrangle. More than 1,000 ft (feet) (300 m (meters)) of structural and topographic relief existed along some northwest- and north-striking normal faults in the southeastern part of the quadrangle (D. H. McIntyre, oral commun., 1983; Hays and others, 1978). The rugged topography of the prevolcanic surface was recognized by Ross (1937). Furthermore, along the northern boundary of the quadrangle, several northwest and northeast-striking faults are present that are primarily strike-slip faults; lateral displacements along these faults also largely predate the earliest volcanic activity.

STRATIGRAPHY AND SEQUENCE OF EOCENE VOLCANIC EVENTS

The volcanic rocks are preserved mostly in the eastern half and north-central part of the quadrangle. The preserved remnants in the eastern half are mostly within the Van Horn Peak cauldron complex, the Panther Creek graben, and the Custer graben (fig. C2). In addition, a considerable thickness of intermediate-composition lavas and remnants of outflow tuff sheets are preserved outside of these structures. The volcanic rocks in the north-central part, on the other hand, are preserved only within the Thunder Mountain cauldron complex (fig. C5) and an early segment of the Van Horn Peak cauldron complex that extended into the Thunder Mountain region.

Except for the earliest volcanic eruptions, the two cauldron complexes and their eruptive volcanic centers were independently active, producing a series of distinctive ash-flow tuff sheets.

VAN HORN PEAK CAULDRON COMPLEX AND ADJACENT AREAS

Intermediate-composition and mafic lavas

Volcanic activity started about 51 m.y. ago with the eruption of intermediate and mafic lavas from numerous vents (fig. C2) scattered throughout a large part of the eastern half of the quadrangle (McIntyre and others, 1982).

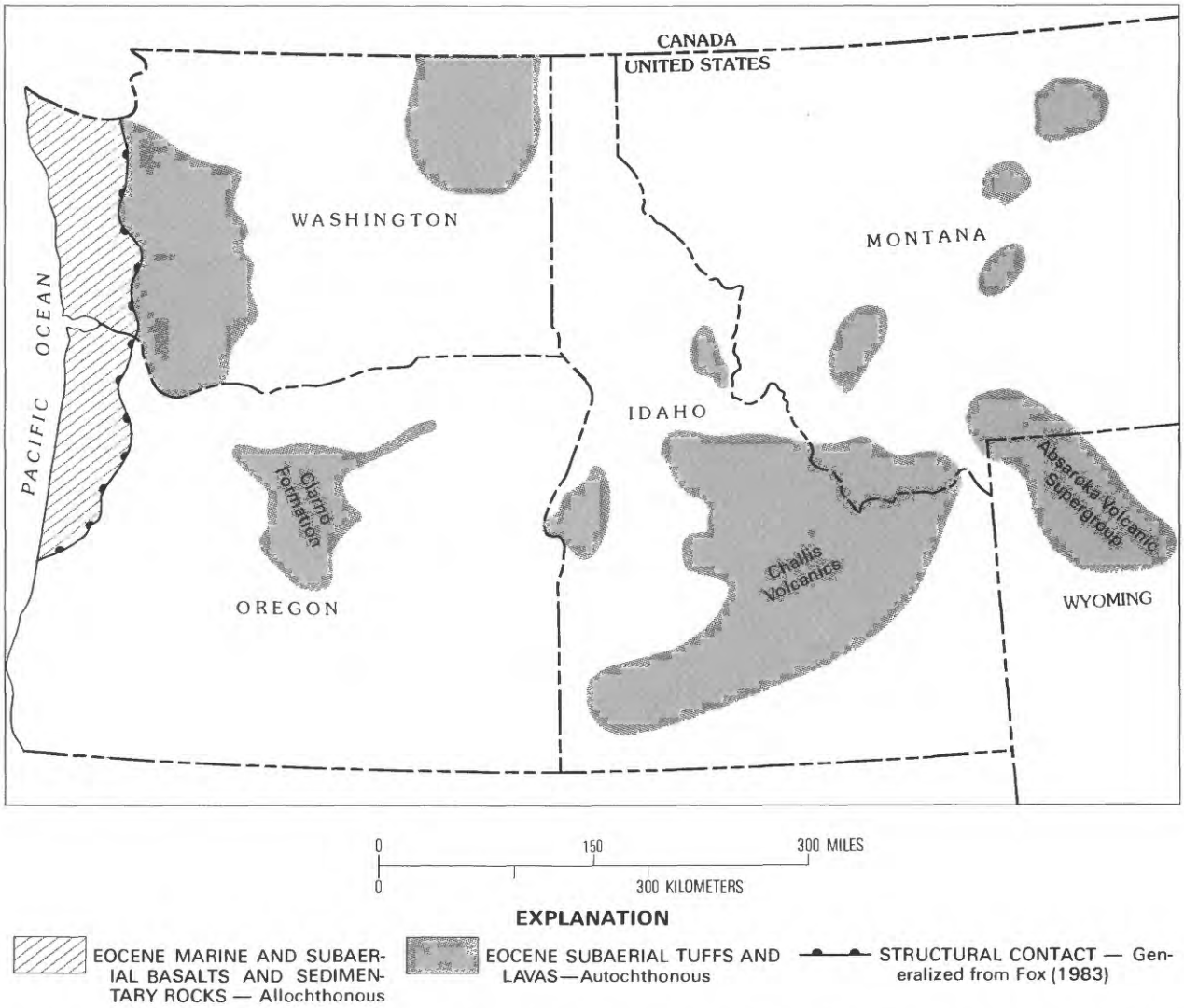

Figure C1. Map of the northwestern United States showing areas within which remnants of volcanic rocks of Eocene age are preserved.

The eruption of these lavas continued for about 2 m.y. and was accompanied by only minor eruptions of tuff. Most of the intermediate lava is dacite and rhyodacite in composition, but the lava sequences commonly contain potassium-rich basalt, andesite, latite, and locally quartz latite.

The dacite and rhyodacite rocks typically contain 30 percent conspicuous phenocrysts (fig. C3) consisting of plagioclase, 3–10 mm long, and various combinations of mafic phenocrysts including biotite, hornblende, clinopyroxene, orthopyroxene, and altered olivine. Quartz phenocrysts are locally present.

The potassium-rich basalt and andesite commonly occur together, and both are rich in K_2O and MgO (McIntyre and others, 1982). They are mostly aphanitic gray rocks that weather brownish gray and black. They commonly contain altered olivine and xenocrystic quartz with reaction rims.

Potassium-rich basalt, andesite, and latite lavas are present in several of the older lava sequences that are about 51 m.y. to about 49 m.y. old. These lavas also form a regionally extensive and volumetrically large younger stratigraphic unit as much as 400 m thick erupted about 48 m.y. ago, after the initial subsidence of the Van Horn Peak cauldron complex. Both the older and younger lavas form tabular flows of considerable areal extent. These flows were obviously less viscous than the dacite and rhyodacite and appear to have been fed from long, narrow dikes and from plugs.

In both stratigraphic horizons the potassium-rich basalt, andesite, and latite flows are megascopically and microscopically very similar. Most flows are brown and reddish brown, weathering gray to black. Most contain only sparse phenocrysts of clinopyroxene that locally are as long as 1 cm. More rarely, they contain hornblende in addition to clinopyroxene and also minor plagioclase.

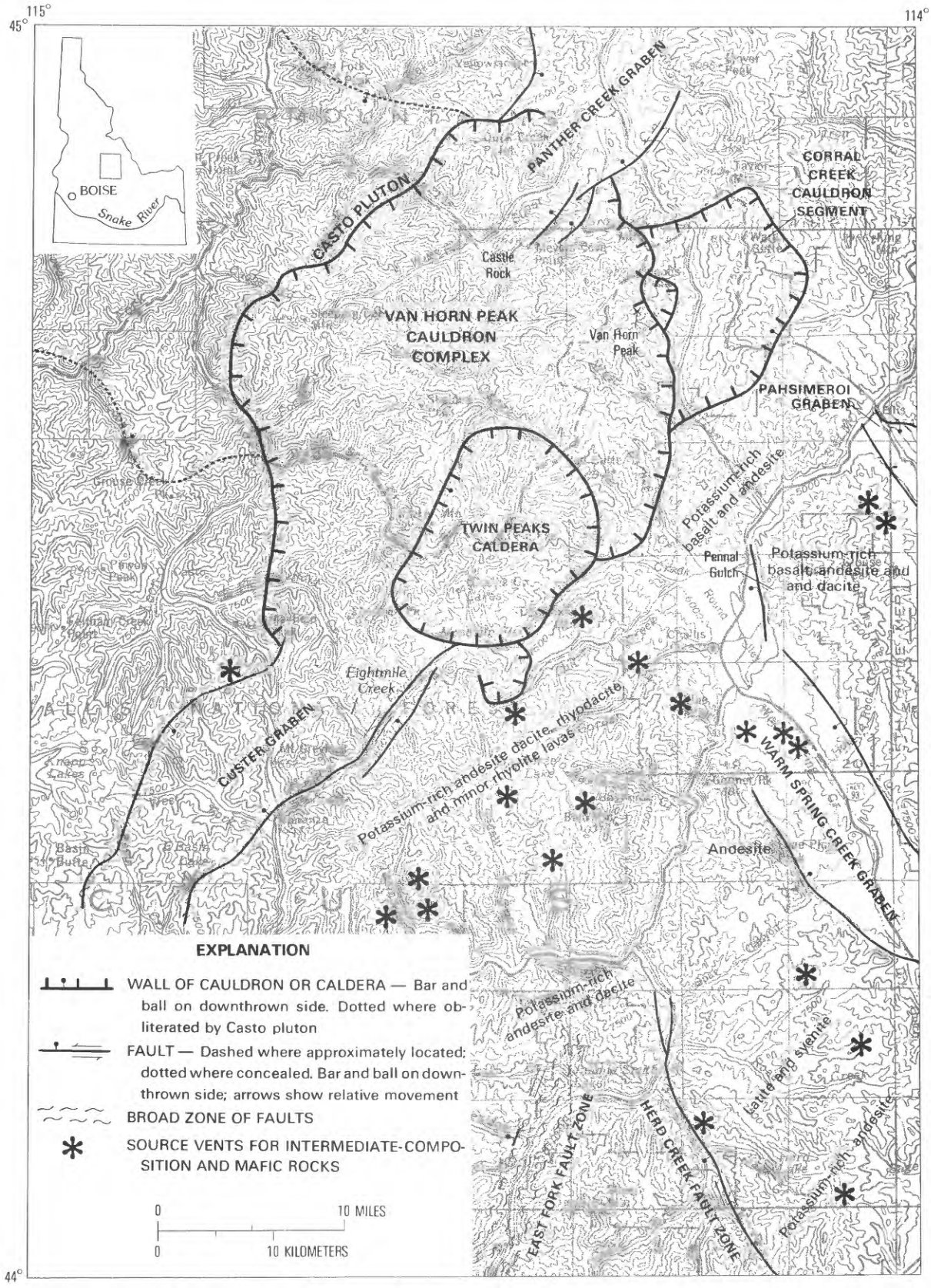

Figure C2. Map of the eastern part of the Challis quadrangle showing vents for intermediate-composition and mafic volcanic rocks and other structural and volcanic features. Predominant volcanic-rock compositions also shown. Generalized from McIntyre and others (1982). Base from U.S. Geological Survey, Idaho state map, 1968, scale 500,000.

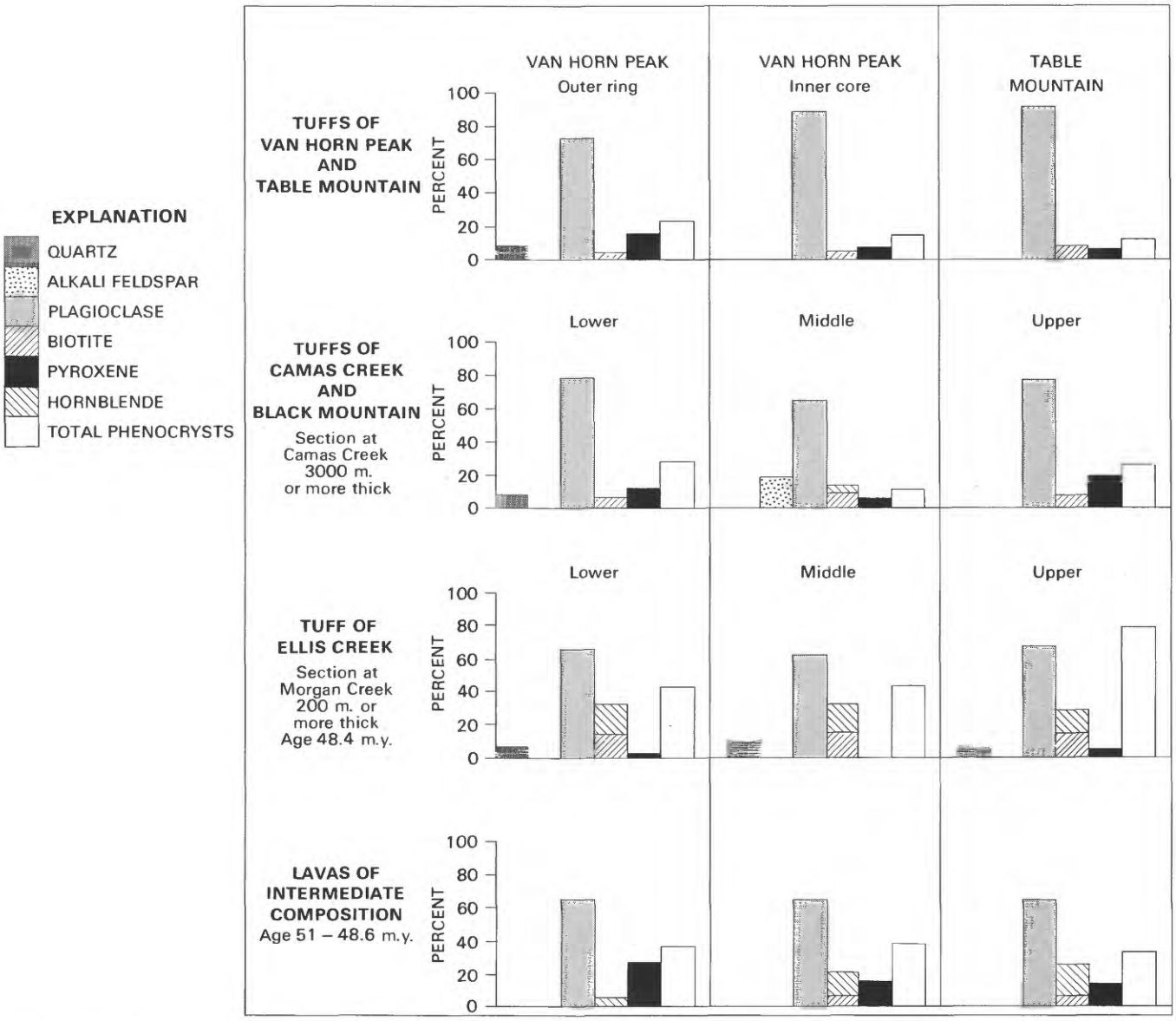

Figure C3. Volume percent of phenocrysts and abundance of six phenocryst mineral components of principal volcanic rocks in the Van Horn Peak cauldron complex, central Idaho.

McIntyre and others (1982) reported that some black glassy latite flows contain conspicuous altered olivine.

Cauldron-related rocks

Tuff of Corral Creek

The first significant ash-flow unit erupted from the Van Horn Peak cauldron complex was a dacite or rhyodacite tuff rich in lithic fragments called the tuff of Corral Creek (table C1). This tuff is intercalated with dacite, latite, and minor potassium-rich andesite flows and is older than the tuff of Ellis Creek, which is associated with the major collapse of the cauldron complex. The tuff of Corral Creek contains as much as 50 percent lithic fragments of dacite and latite. It is generally densely welded and contains about 10 percent phenocrysts of plagioclase, 5 percent phenocrysts of hypersthene, and sparse hornblende. The eruption of this tuff caused the Corral Creek cauldron segment, in the northeastern part of the Van Horn Peak cauldron complex (fig. C4), to collapse along pre-existing northeast- and northwest-striking faults. The collapsed block rapidly filled with mudflows and lava flows of dacite and latite (fig. C5).

Tuff of Ellis Creek

The rhyodacite tuff of Ellis Creek, erupted about 48.4 m.y. ago, was, before erosion, the most voluminous volcanic unit in the Challis quadrangle. Some remnants of the outflow sheet are more than 300 m thick, and the unit is at least 1,500 m thick where preserved within the cauldron complex (figs. C4, C6). Remnants of the unit

Table C1. Major rock units of the Van Horn Peak cauldron complex, Challis quadrangle
[Leaders (---), no K-Ar age]

Unit	Lithology	K-Ar age (m.y.)
Tuff of Challis Creek (caldera forming and filling).	Alkali rhyolite-----	45–46.5
Tuff of Castle Rock (caldera filling).	Rhyolite----------	---
Quartz-biotite tuff (caldera forming).	Rhyolite and quartz latite.	---
Tuff of Table Mountain	Quartz latite and rhyolite.	47.8
Tuffs of Camas Creek and Black Mountain (caldera filling).	Quartz latite and rhyodacite.	---
Tuff of Ellis Creek (caldera forming).	Rhyodacite----------	48.4
Tuff of Corral Creek	Rhyodacite----------	---

are preserved as far as 25–35 km both south and east of the cauldron-complex boundary. The outflow sheet has been eroded from other areas, but if it once extended 30 km in all directions from the cauldron complex, it would have had an original volume on the order of at least 400 km^3 (cubic kilometers). Of course, this figure does not include the uncertain but surely very large volume of tuff trapped within the cauldron complex itself. The eruption of this enormous ash-flow sheet is inferred to have caused collapse of a northwest-trending, roughly elliptical area about 70 km long and 40 km wide (fig. C4). The subsided source area of the cauldron is now in part occupied by the Casto pluton. The intracauldron tuff on both sides of the granite pluton tends to be darker colored than the outflow sheet, because of abundant magnetite dust, and it contains ubiquitous epidote. In some places within the cauldron complex, however, the tuff is virtually the same color as the outflow sheet (fig. C7).

The tuff of Ellis Creek is all rhyodacite. There is no obvious mineralogic change from base to top, although there are more phenocrysts at the top (fig. C3). Pumice is typically darker than the matrix, and the pumice tends to contain larger plagioclase phenocrysts than the matrix. In places the plagioclase in the pumice is as long as 1 cm, whereas the plagioclase in the matrix rarely exceeds 4 or 5 mm. Quartz phenocrysts are sparse but distinctive because they are so strongly resorbed. Biotite is the principal mafic mineral; hornblende is present everywhere and in some exposures is nearly as abundant as biotite (fig. C3). Trace amounts of clinopyroxene were observed in a few thin sections.

Tuff of Eightmile Creek and tuffs of Camas Creek and Black Mountain

Following the eruption of the voluminous tuff of Ellis Creek, a series of eruptions produced ash flows that

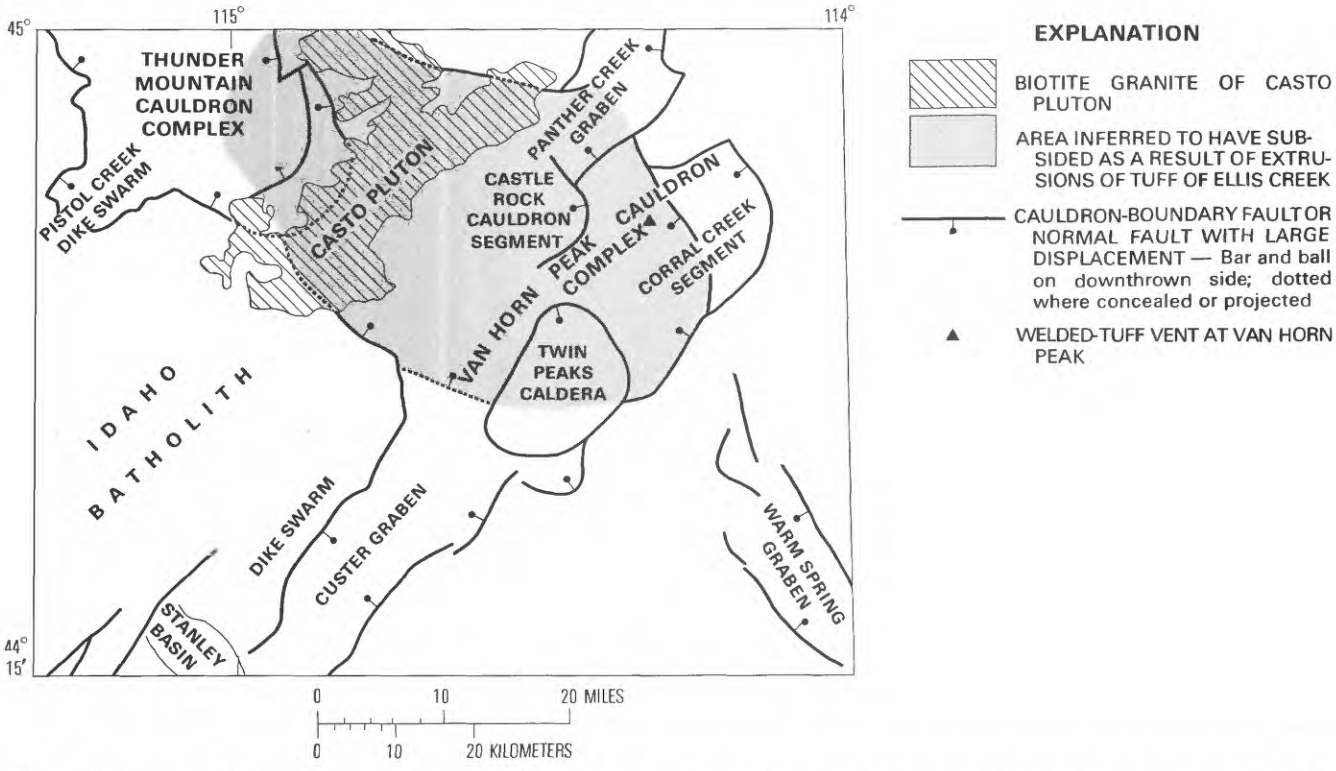

Figure C4. Map of the northeastern part of the Challis quadrangle showing principal structural and volcanic features. Shaded area is inferred cauldron that originated with the voluminous eruptions of the tuff of Ellis Creek.

Figure C5. Mud flow or lahar in Corral Creek cauldron segment. These flows were cold because they engulfed standing trees that are now petrified and show little evidence of charring.

filled the subsiding cauldron complex. The earliest of these is the tuff of Eightmile Creek (McIntyre and others, 1982). This unit is megascopically very similar to the Ellis Creek but contains alkali feldspar, more quartz, and less biotite and hornblende. The tuff of Eightmile Creek is thin in outflow sections where it is generally mapped with other volcanic units, but, in the northern part of the Custer graben (Foster, 1982) (fig. C4) and in the Meyers Cove area (fig. C6) in the north-central part of the Van Horn Peak cauldron complex, it is 600–800 m thick. The large thicknesses in these two localities suggest that an elongate area, extending northward through the northern Custer graben to Meyers Cove and perhaps as far to the north as the northern boundary of the Van Horn Peak cauldron complex, probably subsided during the eruption of the tuff of Eightmile Creek.

The eruption of the tuff of Eightmile Creek was followed, with little or no time lapse, by eruption of the tuffs of Camas Creek and Black Mountain. Where best exposed along Camas Creek and at Black Mountain, the tuffs are intracauldron rocks that consist of several cooling units. The lowest cooling units are megascopically and mineralogically identical to rock in the outer part of the welded-tuff vent at Van Horn Peak (Ekren, 1981). The densely welded parts of the tuffs throughout the Camas Creek-Black Mountain section commonly are black because abundant magnetite dust is distributed throughout the groundmass. Where the rocks are not densely welded, they are not impregnated with magnetite and are various shades of gray. The pumice lapilli are chloritized and are dark green or brownish green, darker than the matrix that encloses them. Modes of samples of the tuffs in the Camas Creek-Black Mountain sequence are similar to the Eightmile Creek, but the phenocrysts are smaller and fewer. In contrast to the tuffs of Ellis and Eightmile Creeks, whose principal mafic mineral is biotite, and hornblende is a secondary mafic constituent, the Camas Creek-Black Mountain sequence contains altered pyroxene as the principal mafite, and biotite and hornblende are secondary.

Tuffs in the Van Horn Peak vent

The Van Horn Peak welded-tuff vent (Ekren, 1981) is a prominent landmark in the Challis area (fig. C8). Two distinct tuff units occur within the cone-shaped vent: the older tuff forms a discontinuous outer ring or rim that is inferred to comprise remnants of an early vent-filling tuff that correlates with the lower tuffs in the Camas Creek-Black Mountain sequence; the younger tuff forms a circular (in plan view) inner core that is about 1.5 km in diameter. This inner core is mineralogically identical to the tuff of Table Mountain (McIntyre and Hobbs, 1978; fig. C3, this chapter) that caps Table Mountain within the Corral Creek segment of the Van Horn Peak cauldron complex (figs. C4, C6). The tuff of the inner core intrudes the outer-ring remnants and also many other country rocks, including the tuff of Eightmile Creek, caldera-filling sedimentary rocks, breccia, and rhyolite. Eutaxitic foliation defined by flattened pumice fragments parallels the flanks of the conical plug and dips consistently inward 60–80° (fig. C8, *A* and *B*). The tuffs in the vent and adjacent rocks are riddled with small intrusive masses of both rhyolitic and intermediate composition.

Quartz-biotite tuff

The eruption of the quartz-biotite tuff (table C1) probably caused the initial collapse of the Castle Rock half-moon or trapdoor cauldron segment (figs. C4, C6). The tuff is thickest within this cauldron segment and appears to have been hottest there. The tuff consists of at least two megascopically indistinguishable cooling units separated by a thin zone of bedded tuff a few meters to possibly as much as 30 m thick. Neither cooling unit was systematically sampled from base to top during this study. Thin sections of samples from widely scattered outcrops show about 30 percent phenocrysts consisting of quartz, alkali feldspar, and plagioclase in subequal amounts, and 4–18 percent biotite and lesser hornblende. The quartz grains commonly are as large as 4 mm (locally as large as 6 mm) and mostly quite smoky. Some of the smoky quartz is optically anomalous, having optic angles as large as 15° or 20°. These anomalous grains are not strained, and they do not show inclusions. The tuff contains allanite as a common accessory mineral.

Evidence of high temperatures near Castle Rock includes extensive flow layering and local thick zones of

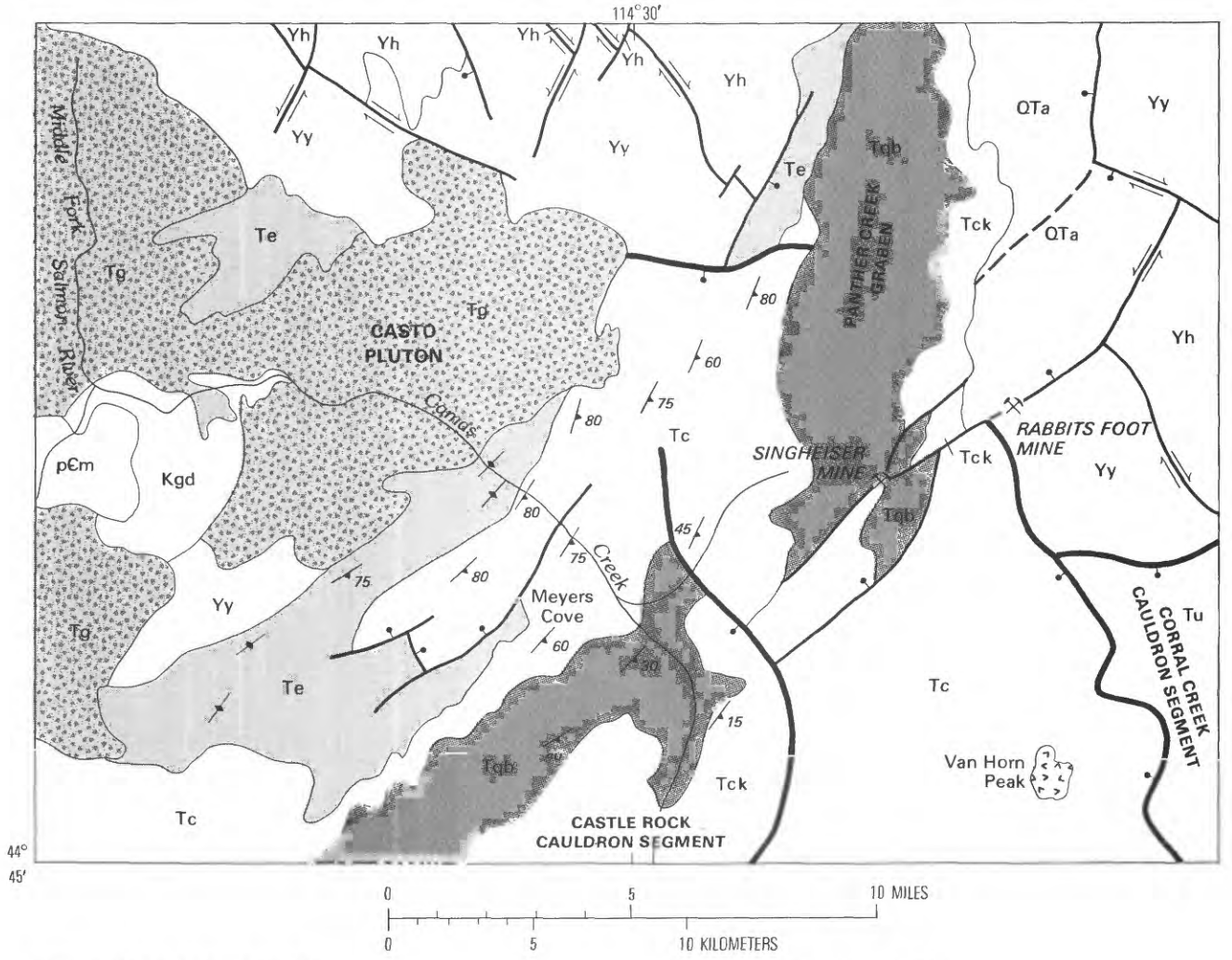

CORRELATION OF MAP UNITS

QTa		QUATERNARY AND TERTIARY
Tck	Eocene	TERTIARY
Tqb	Eocene	TERTIARY
Tg	Eocene	TERTIARY
Tc	Eocene	TERTIARY
Te	Eocene	TERTIARY
Tu	Eocene	TERTIARY
Unconformity		
Kgd		CRETACEOUS
Unconformity		
Yh		MIDDLE PROTEROZOIC
Yy		MIDDLE PROTEROZOIC
p€m		PRECAMBRIAN

DESCRIPTION OF MAP UNITS

QUATERNARY
QTa Alluvium and colluvium filling grabens

EOCENE
Tck Tuff of Castle Rock
Tqb Quartz-biotite tuff and other tuffs younger than tuffs of Camas Creek and Black Mountain
Tg Granite rocks of Castro pluton
Tc Tuffs of Camas Creek and Black Mountain
Te Tuff of Ellis Creek
Tu Volcanic rocks of Corral Creek cauldron segment, undivided

CRETACEOUS
Kgd Grandodiorite

MIDDLE PROTEROZOIC
Yh Hoodoo Quartzite
Yy Yellowjacket Formation

PRECAMBRIAN
p€m Metamorphic rocks

CONTACT — Approximately located

FAULT — Dashed where approximately located. Arrows show relative movement. Bar and ball on downthrown side

CAULDRON-BOUNDARY FAULT — Bar and ball on downthrown side

WELDED-TUFF VENT

STRIKE AND DIP OF FOLIATION IN WELDED TUFF
15 Inclined
Vertical

Figure C6. Generalized geologic map of the Camas Creek area.

Figure C7. The tuff of Ellis Creek. *A*, outflow sheet just east of Salmon River on Highway 93 between Challis and Salmon; the tuff is about 100 m thick in this area, and despite the soft-weathering aspect is densely welded; *B*, densely welded, steeply dipping intracauldron tuff near Camas Creek; note that the pumice lapilli (best seen near compass) are darker than the matrix; a dark aphyric apophysis is visible in upper right.

flow brecciation. These features are similar to those described in the extremely hot ash-flow tuffs of Owyhee County, Idaho, by Ekren and others (1984).

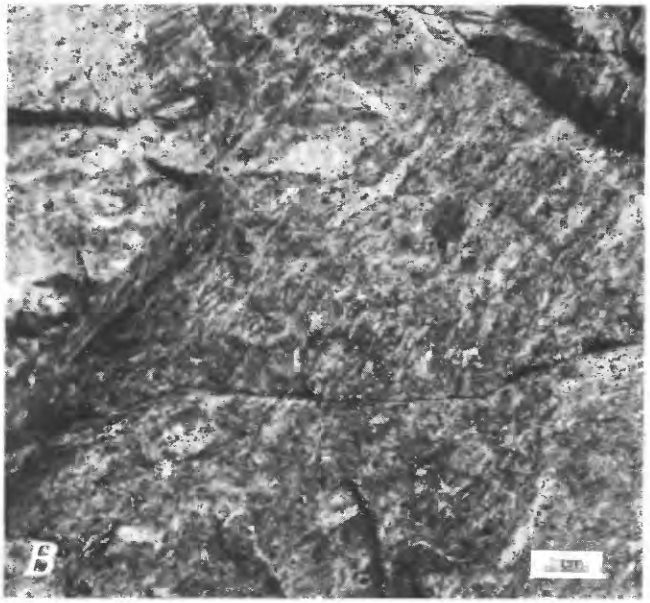

Figure C8. Rocks of the tuff of Van Horn Peak vent. *A*, columnar jointing on the west flank of the vent; foliation within the jointed zone dips about 70° toward the east, central, part of the vent; *B*, flattened pumice (light patches) on the north flank of the vent at the contact with country rock; foliation as defined by the pumice dips 65° toward the central part of the vent.

Tuff of Castle Rock

This sequence of cauldron- and graben-filling tuff (unit Tck, fig. C6) is recognized with certainty only within the Castle Rock cauldron segment and within the Panther Creek graben. Although the rocks are mostly poorly welded, they are almost totally preserved, due to rapid subsidence and subsequent deep burial in both structures. The sequence resembles the tuff of Challis Creek (Hardyman, chap. G, this volume) so closely that it was originally correlated with that tuff (for example, see McIntyre and others, 1982). Both tuff sequences are red or reddish, and both contain predominant alkali feldspar. They differ in two important ways: (1) All of the Castle Rock cooling units are quite rich in small volcanic lithic fragments from base to top, and the Challis Creek cooling units are nearly free of lithic fragments. (2) All of the Castle Rock cooling units contain sparse but ubiquitous flakes of biotite; the Challis Creek cooling units, on the other hand, do not contain enough biotite to be commonly observed either in hand specimen or thin section. Furthermore, the tuff of Castle Rock is generally only partly welded, whereas the tuff of Challis Creek is generally densely welded.

The tuff within the Castle Rock cauldron segment consists of five cooling units with thin interbeds of ashfall tuff; the entire sequence is 630 m thick. It consists of a partly welded to nonwelded, slope-forming cooling unit, rich in lithic fragments, about 190 m thick at the base, that rests on the quartz-biotite tuff. This cooling unit is overlain by a cliff-forming, moderately welded unit about 150 m thick, which is overlain by two thin, partly welded, slope-forming cooling units, rich in lithic fragments, each about 30 m thick. The uppermost cooling unit forms cliffs and is about 230 m thick (fig. C9). These units are less welded northward in the Panther Creek graben where only one unit consistently forms cliffs. Most of the units in the graben are virtually nonwelded and form tepee-shaped monoliths and varicolored hoodoos. Some of these monolith-forming units are glassy and pumice fragments are silky—remarkable preservation for tuffs at least 45 m.y. old. All the units contain 20–30 percent phenocrysts consisting of 15–45 percent quartz; 45–78 percent alkali feldspar; 1–4 percent plagioclase; a trace to 3 percent clinopyroxene, hornblende, and biotite; and trace amounts of accessory allanite as well as ubiquitous zircon and apatite.

Tuff of Challis Creek

The eruption of the tuff of Challis Creek was the final important volcanic event in the Van Horn Peak cauldron complex. Its eruption created the Twin Peaks caldera (fig. C4; Hardyman, 1981, chap. G, this volume). This tuff, as stated previously, is very similar to the tuff of Castle Rock. Hardyman recognized two thick (each 300 m or more) cooling units within the Twin Peaks caldera. The inference that the tuff of Challis Creek is younger than the tuff of Castle Rock is based on the fact that no tuff of Challis Creek is now recognized in either the Castle Rock cauldron or the Panther Creek graben. Surely some remnants of tuff of Challis Creek would have been preserved there if it were the older unit.

Figure C9. Castle Rock, which is made up of two moderately welded, cliff-forming rhyolitic cooling units of the tuff of Castle Rock, separated by two thin, partly welded, slope- and bench-forming cooling units rich in lithic fragments.

THUNDER MOUNTAIN CAULDRON COMPLEX

Mapping of the part of the Thunder Mountain cauldron complex that lies in the Challis 1°×2° quadrangle by Ekren and G. D. May during this study (*in* Fisher and others, 1983) resulted in a somewhat different interpretation and outline of the complex than that deduced earlier by Leonard and Marvin (1982) on the basis of reconnaissance traverses. Nevertheless, there were more important agreements than disagreements.

Ekren and May concluded that the sequence of events in the Thunder Mountain cauldron complex was very similar to that at the Van Horn Peak cauldron complex. The first volcanic activity was the eruption of mostly latite lavas (table C1) and minor intercalated latite tuffs, starting about 49–51 m.y. ago (Leonard and Marvin, 1982). This activity was followed by eruption of tuffs that are characterized by abundant, well-flattened pumice lapilli the size of dimes and quarters. These tuffs have the same kinds of pumice and the same mineralogy as the lower parts of the tuffs of Camas Creek and Black Mountain (table C2). In fact, the sequences of tuffs from the two cauldron complexes may actually interfinger in some localities within each of the cauldron areas; however, interfingering was not proven conclusively during this study. Available chemical data (fig. C10) indicate that the dime- and quarter-lapilli tuff ranges in composition from rhyodacite to rhyolite, a chemical range inferred also for the tuffs of Camas Creek and Black Mountain (McIntyre and others, 1982).

Table C2. Chemical analyses and CIPW norms for volcanic rocks

[Samples collected by B. F. Leonard. Analyses by U.S. Geological Survey analysts: H. F. Phillips, P. L. D. Elmore, K. E. White, E. L. Munson,

Sample No.—	1	2	3	4	5	6	7	8	9
Field No.—	Y-54-582	83L57	AAS-262	L-64-2639	L-62-2150	Y-54-565	L-56-1361	Y-54-597	Y-54-598
Lab No.—	140642	D-256196	D101856	D100631	I-4100	140641	149464	140643	140644
N. latitude—	45°00′28"	45°00′42"	44°58′00"	44°48′12"	45°14′42"	45°01′45"	45°10′40"	45°05′06"	45°04′24"
W. longitude—	115°15′12"	115°15′54"	115°08′00"	115°18′21"	115°15′12"	115°16′30"	115°22′50"	115°21′36"	115°19′45"
Chemical analyses									
SiO_2	57.9	58.0	58.18	58.61	58.72	59.0	61.9	62.6	63.1
Al_2O_3	17.3	17.3	16.20	15.42	14.79	17.5	17.3	16.2	15.5
Fe_2O_3	2.0	1.40	1.71	2.29	1.25	2.1	3.2	2.3	2.0
FeO	3.9	3.85	4.82	3.71	4.77	3.4	2.7	2.6	2.4
MgO	3.0	2.56	3.13	3.74	5.67	2.4	1.4	2.2	2.7
CaO	7.4	6.65	5.52	5.14	5.97	6.2	3.9	4.1	3.6
Na_2O	2.7	2.74	3.43	2.69	2.62	3.1	3.5	3.3	3.5
K_2O	2.2	2.42	3.03	3.38	2.08	2.5	3.2	2.9	3.5
H_2O^+	1.6	1.87	1.08	2.44	2.23	1.8	1.0	2.0	2.0
H_2O^-	.12	.15	.35	.68	.48	.05	.2	.2	.09
TiO_2	.98	.85	.89	.85	.78	.92	.96	.74	.70
P_2O_5	.39	.28	.59	.31	.20	.36	.30	.32	.34
MnO	.11	.09	.11	.11	.12	.11	.09	.09	.07
CO_2	.74	1.56	.1	.44	.15	1.1	<.05	.26	.76
Cl	.04	<.01	.05	.01	.00	.01	.01	.01	.00
F	.01	.06	.13	.07	.05	.04	.10	.00	.03
Sum	100.39	99.78	99.32	99.89	99.88	100.59	99.76	99.82	100.29
CIPW norms									
Q	15.04	19.43	10.33	14.44	13.67	17.20	19.63	20.98	19.87
C		2.45				1.89	2.0	1.49	2.01
or	13.02	14.83	17.90	20.65	12.65	14.74	18.92	17.14	20.70
ab	22.60	24.04	28.92	23.54	22.82	26.22	29.62	27.89	29.62
an	28.71	22.09	19.88	20.70	23.12	21.34	16.58	16.78	10.77
di-wo	.31	.00	1.26	.29	2.11	.00	.00	.00	.00
di-en	7.47	.00	7.76	.19	1.34	5.97	3.48	5.48	6.73
di-fs	4.10	.00	5.36	.08	.63	3.20	.90	1.82	1.73
hy-en	.00	6.61	.00	9.44	13.20	.00	.00	.00	.00
hy-fs	.00	2.39	.00	3.77	6.23	.00	.00	.00	.00
ol-fo	.00	.00	.00	.00	.00	.00	.00	.00	.00
ol-fa	.00	.00	.00	.00	.00	.00	.00	.00	.00
mt	2.90	2.11	2.48	3.43	1.87	3.06	4.63	3.33	2.90
hm	.00	.00	.00	.00	.00	.00	.00	.00	.00
il	1.86	1.67	2.64	1.67	1.53	1.75	1.82	1.41	1.34
ap	.93	.69	1.41	.76	.49	.84	.71	.77	.80
cc	1.68	3.68	.00	1.03	.35	2.50	.00	.59	1.73
Felsic-mafic ratio $(SiO_2+K_2O+Na_2O)/(FeO+Fe_2O_3+MgO+CaO)$									
	3+	4+	4.2	4.3	3.6	4.6	6.1	6.1	6.6

SAMPLE

1. Latite lava: 43 percent phenocrysts consisting of 65 percent plagioclase (0.1–2.0 mm), 21 percent clinopyroxene (0.1–0.5 mm), 13 percent chloritized pyroxene; dense microcrystalline, structureless groundmass.
2. Latite lava: 33 percent phenocrysts consisting of 71 percent plagioclase (0.1–3.0 mm), 22 percent chloritized pyroxene (0.1–0.5 mm), 3 percent oxidized biotite or hornblende, 2 percent quartz, 1.5 percent apatite; dense microcrystalline, structureless groundmass.
3. Latite lava: 60 percent unoriented plagioclase microlites (0.1–0.3 mm), 5 percent altered pyroxene (0.1 mm), 25–30 percent black opaque groundmass.
4. Latite lava: 34 percent phenocrysts consisting of 60 percent plagioclase (0.2–5.0 mm), 23 percent clinopyroxene (0.2–2.5 mm), 17 percent chloritized pyroxene; dense, weakly trachytic groundmass.
5. Latite lava: 36 percent phenocrysts consisting of 42 percent plagioclase (as long as 3.0 mm), 45 percent chloritized pyroxene (glomerocrysts and clots as long as 4 mm), 13 percent clinopyroxene (as long as 4 mm); dense trachytic felty groundmass.
6. Latite intrusion: 64 percent phenocrysts consisting of 80 percent plagioclase (as long as 6.0 mm), 15 percent chloritized pyroxene; 3.7 percent oxidized biotite, 1.5 percent fresh clinopyroxene; microgranular groundmass.
7. Dacite lava: about 20 percent phenocrysts consisting of 70 percent fresh plagioclase (0.1–10.0 mm), and 30 percent chloritized pyroxene; pilotaxitic groundmass.
8. Dacite lava: about 20 percent phenocrysts consisting of 70 percent plagioclase (0.1–5.0 mm), 30 percent mostly chloritized clinopyroxene, trace of biotite; pilotaxitic groundmass.
9. Dacite lava: 19 percent phenocrysts consisting of 57 percent plagioclase (as long as 5 mm), 8.5 percent quartz (as long as 3 mm), 17 percent chloritized, oxidized hornblende, 17 percent chloritized, calcitized pyroxene; pilotaxitic groundmass.

from the Thunder Mountain cauldron complex, Challis quadrangle

C. L. Parker, A. J. Bartel, E. L. Brandt, D. F. Powers, S. M. Berthold, P. W. Scott, and V. C. Smith. N., north; W., west; <, less than]

10	11	12	13	14	15	16	17	18	19	20
83GM105	83GM101	83L69	L-61-229	L-74-7	TM-71-2	Y-54-599	83L64	Y-54-599A	H-54-63	L-61-106
D-256194	D-256193	D-256199	W3559	D103789	D103790	140645	D-256198	140646	140640	H3558
45°03'00"	45°02'48"	45°03'54"	45°02'24"	44°58'54"	44°52'00"	45°03'36"	45°03'00"	45°03'36"	45°03'45"	45°03'30"
115°21'18"	115°20'54"	115°19'27"	115°22'12"	115°05'00"	115°02'00"	115°18'48"	115°21'42"	115°18'48"	115°15'48"	115°24'12"
Chemical analyses										
63.6	63.9	67.2	69.57	71.02	71.59	74.4	74.7	75.1	76.7	76.88
15.4	15.0	14.9	14.94	14.23	14.57	14.0	13.6	14.0	13.6	13.14
1.33	1.34	1.76	1.45	2.09	1.22	1.6	.58	1.1	.91	.24
2.54	2.44	1.56	1.25	.58	.76	1.0	.80	.30	.08	.20
1.65	1.50	1.92	.75	.38	.36	.00	.12	.08	.02	.06
3.77	3.30	2.05	1.03	1.47	1.15	.38	.16	.45	.12	.04
3.30	3.33	3.78	3.86	3.15	3.17	3.7	3.44	3.4	3.1	2.84
3.70	3.72	3.63	4.46	5.15	5.01	5.1	5.02	5.2	5.1	5.27
1.58	1.82	1.43	1.18	.58	1.22	.52	.72	.79	.77	.65
.10	.32	.09	.58	.68	.32	.07	.03	.11	.06	.26
.57	.54	.54	.32	.40	.30	.11	.09	.10	.11	.10
.18	.17	.20	.07	.09	.09	.09	<.05	.07	.01	.01
.06	.06	.05	.05	.04	.04	.03	<.02	.02	.02	.00
1.48	1.78	.05	.12	.00	.00	.27	<.01	<.05	<.05	.00
<.01	<.01	<.01	.01	.00	.00	.02	<.01	.00	.01	.00
.06	.04	.03	.05	.07	.04	.00	.03	.00	.00	.03
99.32	99.26	99.19	99.69	99.93	99.84	101.29	99.29	100.72	100.61	99.72
CIPW norms										
23.58	25.90	25.08	27.53	29.94	31.78	33.33	35.10	34.58	38.94	40.54
3.05	4.15	1.66	2.39	1.03	2.09	2.43	2.25	2.14	2.80	2.75
22.40	22.64	21.97	26.93	30.86	30.13	30.10	30.11	30.72	30.10	31.53
28.61	29.02	32.75	33.37	27.03	27.30	31.14	29.55	28.73	26.22	24.33
8.37	4.13	8.75	3.98	6.80	5.21	.00	.81	1.76	.50	.13
.00	.00	.00	.00	.00	.00	.00	.00	.00	.00	.00
.00	.00	.00	.00	.00	.00	.00	.00	.20	.05	.00
.00	.00	.00	.00	.00	.00	.39	.00	.00	.00	.00
4.21	3.85	4.90	1.91	.96	.91	.00	.30	.00	.00	.15
2.80	2.67	.63	.68	.00	.00	.00	.85	.00	.00	.00
.00	.00	.00	.00	.00	.00	.00	.00	.00	.00	.00
.00	.00	.00	.00	.00	.00	.00	.00	.00	.00	.00
1.98	2.00	2.61	2.15	.85	1.74	2.32	.85	.75	.00	.35
.00	.00	.00	.00	1.53	.04	.00	.00	.59	.91	.00
1.11	1.06	1.05	.62	.77	.58	.21	.17	.19	.21	.19
.44	.41	.49	.17	.22	.22	.20	.00	.17	.00	.02
3.45	4.17	.12	.28	.00	.00	.48	.00	.00	.00	.00
Felsic-mafic ratio $(SiO_2+K_2O+Na_2O)/(FeO+Fe_2O_3+MgO+CaO)$										
7.6	8.3	10.2	17.4	17.5	22.9	27.9	50.1	43.4	75.1	157.4

DESCRIPTIONS

10. Rhyodacite tuff (contains dime- and quarter-size pumice lapilli): about 15 percent phenocrysts consisting of 60 percent plagioclase (0.1–3.0 mm), 10 percent quartz (0.5–2.0 mm), 25 percent altered pyroxene, 5 percent altered hornblende; shards visible in groundmass.
11. Rhyodacite tuff (contains dime- and quarter-size pumice lapilli): about 10-15 percent phenocrysts consisting of 60 percent plagioclase (0.1–3.0 mm), 5 percent quartz (0.5–2.0 mm), 35 percent altered pyroxene, 10 percent altered hornblende(?); shards visible in groundmass.
12. Rhyodacite lava: about 40 percent phenocrysts consisting of 65 percent plagioclase (0.1–8.0 mm), 35 percent oxidized, chloritized biotite and hornblende, possible sparse altered pyroxene; dense trachytic groundmass.
13. Rhyolite tuff (contains dime- and quarter-size pumice lapilli): 11 percent phenocrysts consisting of 46 percent plagioclase (as long as 2 mm), 22 percent alkali feldspar (as long as 3 mm), 9 percent quartz (as long as 2 mm), 11 percent chloritized pyroxene, 7 percent altered hornblende, 5 percent oxidized biotite; considerable epidote in altered feldspar and groundmass.
14. Rhyolite tuff ("lower Sunnyside"): 48 percent phenocrysts consisting of 39 percent alkali feldspar (as long as 4 mm), 28 percent plagioclase (as long as 4 mm), 23 percent quartz (as long as 3 mm), 4.8 percent oxidized biotite, 4.8 percent altered hornblende; probable lower part of a cooling unit.
15. Rhyolite tuff ("lower Sunnyside"): 34 percent phenocrysts consisting of 46 percent plagioclase (as long as 4 mm), 22 percent quartz (as long as 3 mm), 13 percent alkali feldspar (as long as 4 mm), 11 percent chloritized biotite, 5 percent chloritized hornblende, 2 percent possible altered pyroxene; strong propylitic alteration; feldspars albitized and partly replaced by zeolite.

16–20. Rhyolite (buff rhyolite): few phenocrysts; flow laminated, some laminae contain abundant tiny vapor-phase crystals. Rhyolite contains 3-5 percent small (0.5–2.0 mm) feldspar crystals that are principally plagioclase but are so replaced by albite and sericite that they are not easily distinguished from albitized sanidine; all contain sparse altered hornblende and traces of altered biotite; patches of secondary quartz suggests silicification as well as albitization.

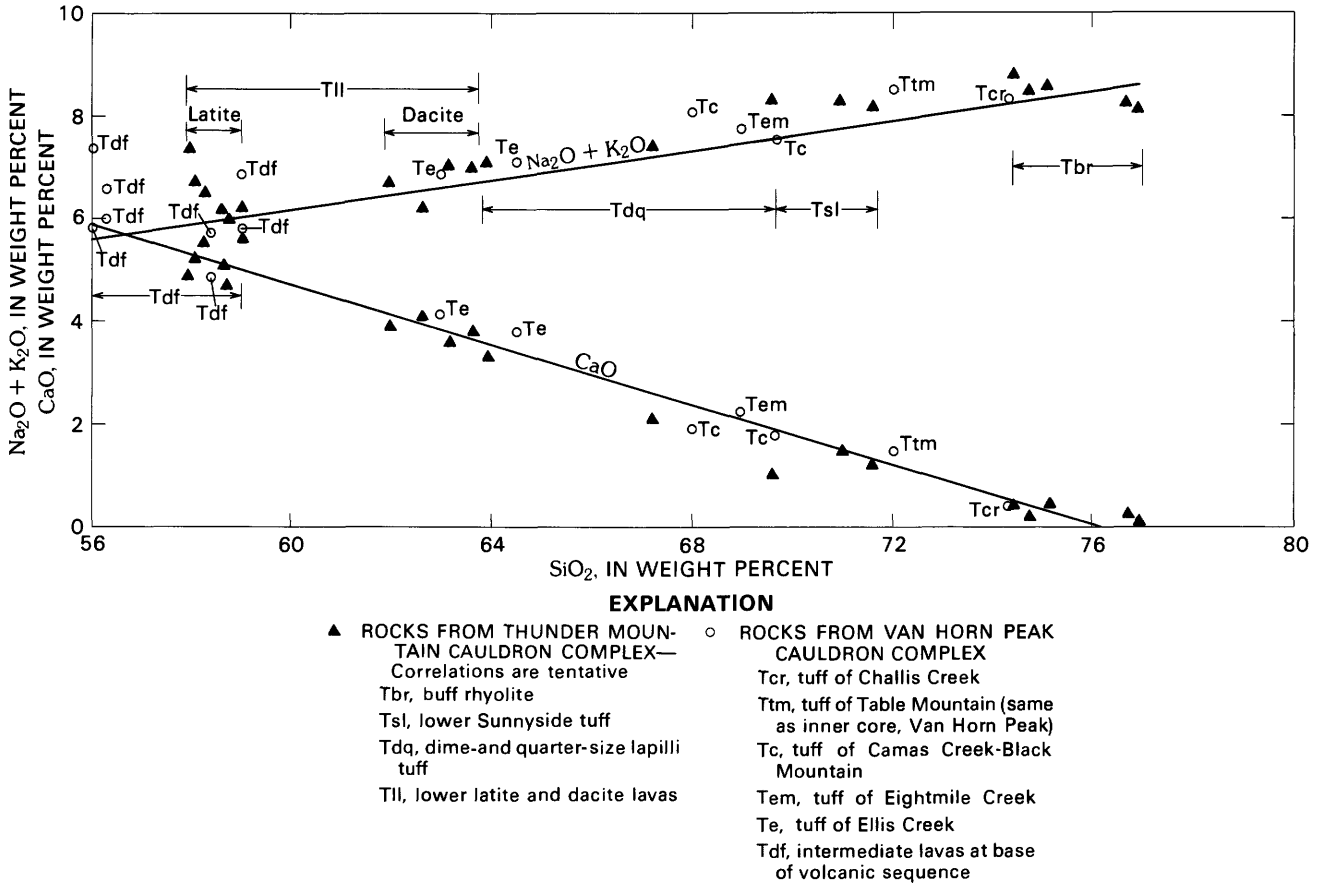

Figure C10. Alkali-lime diagram for analyses of rocks from Thunder Mountain and Van Horn Peak cauldron complexes. Solid squares, rocks from Thunder Mountain cauldron complex; Tbr, buff rhyolite; Tsl, lower Sunnyside tuff; Tdq, dime- and quarter-size lapilli tuff; Tll, lower latite and dacite lavas. Open circles, rocks from Van Horn Peak cauldron complex; Tcr, tuff of Challis Creek; Ttm, tuff of Table Mountain (same as inner core, Van Horn Peak); Tc, tuff of Camas Creek and Black Mountain; Tem, tuff of Eightmile Creek; Te, tuff of Ellis Creek; Tdf, intermediate lavas at the base of the volcanic sequence. Correlations of "lower Sunnyside tuff" are tentative.

The third major event in the Thunder Mountain cauldron complex was the eruption of the "lower Sunnyside tuff[1]," which consists of at least three compositionally zoned cooling units of rhyolite and quartz latite tuff. Each cooling unit grades upward from a rhyolite base, rich in quartz and alkali feldspar, to a quartz latite top, rich in plagioclase and mafic minerals (principally biotite) and low in quartz and alkali feldspar. This is the classic zonation of cauldron-forming tuffs (for example, compare with the Miocene Timber Mountain Tuff of Byers and others (1976), and with Lipman and others (1966). These three units are each 100–300 m thick. They are slightly to moderately hydrothermally altered.

The final major pyroclastic activity in the Thunder Mountain cauldron complex was the emplacement of megabreccia followed by the eruption of "upper Sunnyside tuff." The breccia (at least 100 m thick) was recognized only in the western part of the complex where it consists of large blocks (in places as large as a small house) of "lower Sunnyside tuff" in a matrix of "upper Sunnyside tuff." This unit may have been formed by landsliding concomitant with the early eruptions of "upper Sunnyside tuff" or it may have been extruded as tuff extremely rich in lithic fragments. The "upper Sunnyside tuff" is a multiple-flow compound cooling unit that is the counterpart in the Thunder Mountain cauldron complex of the tuffs of Castle Rock and Challis Creek in the Van Horn Peak cauldron complex. The "upper Sunnyside tuff" is rhyolitic and mostly red, reddish gray, and red brown. It shows no obvious mineralogical zoning except that the basal vitrophyre contains as many as four grains of hornblende and eight grains of pigeonite per thin section, whereas the upper devitrified part of the unit contains only sparse biotite as a mafic constituent. The tuff contains essentially no plagioclase, and the ratio of quartz to alkali feldspar, although variable, does not show any systematic variation from base to top.

[1]This informal unit, with the "upper Sunnyside tuff," comprise the informal Sunnyside rhyolite of Leonard and Marvin (1982).

CHEMICAL COMPOSITION OF THE VOLCANIC ROCKS

Chemical analyses of the principal volcanic rocks in the eastern half of the Challis quadrangle have been published previously by McIntyre and others (1982). Additional analyses of the tuff of Challis Creek and related rhyolite intrusive rocks are presented by Hardyman (chap. G, this volume). Chemical analyses of 20 volcanic rocks from the Thunder Mountain cauldron complex are shown in table C2. The mineralogy and available chemical analyses of rocks from the Van Horn Peak and Thunder Mountain cauldron complexes show that the rocks are a calc-alkaline suite, although a small amount of alkali basalt is present in the eastern part of the quadrangle (McIntyre and others, 1982, table 1). The volcanic rocks have an alkali-lime index (Peacock, 1931) of between 56 and 57 (fig. C10) and fall along the calc-alkaline trends of Ringwood (1974) (fig. C11).

No peralkaline rocks were found, although the composition of some of the intrusive rhyolites of Hardyman (chap. G, this volume) approaches the peralkaline field of Shand (1947). Both Al_2O_3/Na_2O+K_2O and Al_2O_3/Na_2O+K_2O+CaO for those rocks nearly equal unity. The buff rhyolite and related rocks in the Thunder Mountain cauldron complex (table C2, samples 16–20) are alkali rhyolite and extreme alkali rhyolite according to the classification of Young (*in* Segerstrom and Young, 1972) but, nevertheless, are not peralkaline (fig. C12). These rhyolites are inferred to be older than the informal Sunnyside rhyolite (Leonard and Marvin, 1982). Nevertheless, they are richer in silica and alkalis than the "lower Sunnyside tuff" (table C2, samples 14, 15). No chemical analyses are available for the "upper Sunnyside tuff." It contains more quartz and alkali feldspar phenocrysts than the "lower Sunnyside," suggesting that it is richer in silica and alkalis and, therefore, is chemically very similar to the buff rhyolite.

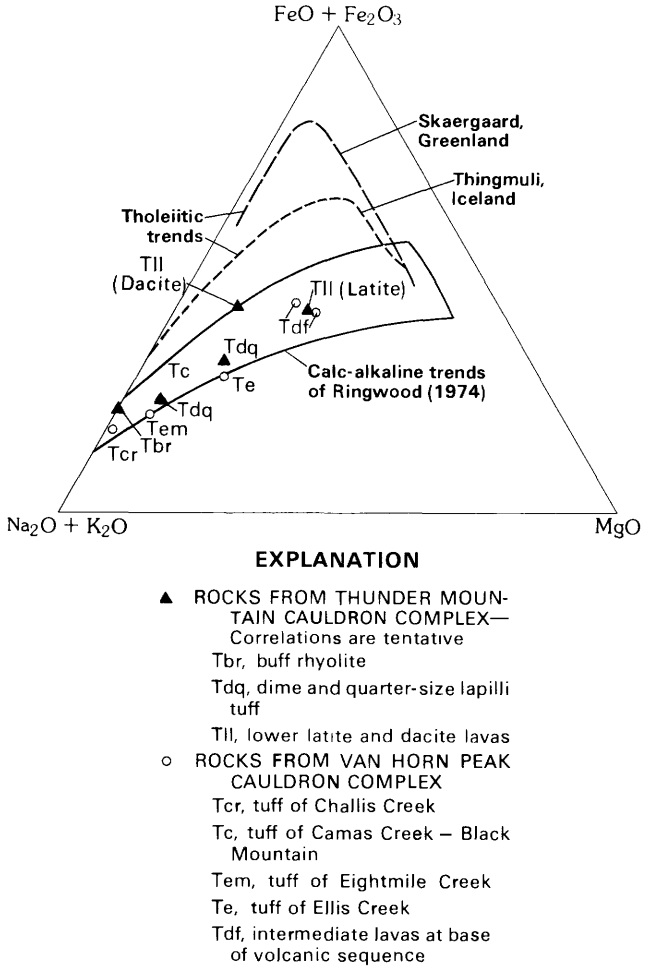

Figure C11. AFM plot of volcanic rocks from the Van Horn Peak and Thunder Mountain cauldron complexes. Tholeiitic trends from Skaergaard, Greenland, and Thingmuli, Iceland, and calc-alkaline trends of Ringwood (1974) are also shown.

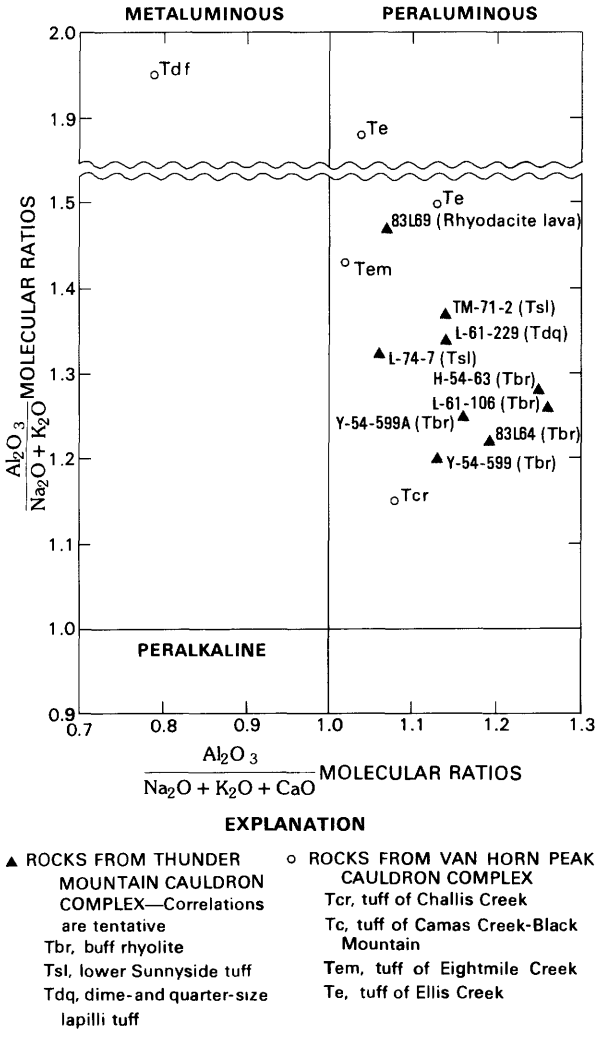

Figure C12. Classification of principal volcanic rocks of the Challis quadrangle using peralkaline-peraluminous-metaluminous divisions of Shand (1947). Modified from Pallister (1982). Sample numbers refer to analyses in table C2.

REFERENCES CITED

Byers, F. M., Jr., Carr, W. J., Orkild, P. P., Quinlivan, W. D., and Sargent, K. A., 1976, Volcanic suites and related cauldrons of Timber Mountain-Oasis Valley caldera complex, southern Nevada: U.S. Geological Survey Professional Paper 919, 70 p.

Cater, F. W., Pinckney, D. M., Hamilton, W. B., Parker, R. L., Weldin, R. D., Close, T. J., and Zilka, N. T., 1973, Mineral resources of the Idaho Primitive Area and vicinity, Idaho: U.S. Geological Survey Bulletin 1304, 431 p.

Ekren, E. B., 1981, Van Horn Peak—a welded tuff vent in central Idaho: Montana Geological Society, Field Conference and Symposium Guidebook to Southwest Montana, p. 311–315.

Ekren, E. B., McIntyre, D. H., and Bennett, E. H., 1984, High-temperature, large-volume, lavalike ash-flow tuffs without calderas in southwestern Idaho: U.S. Geological Survey Professional Paper 1272, 76 p.

Fisher, F. S., McIntyre, D. H., and Johnson, K. M., 1983, Geologic map of the Challis 1°×2° quadrangle, Idaho: U.S. Geological Survey Open-File Report 83–523, 41 p., 2 sheets, scale 1:250,000.

Foster, Fess, 1982, Geologic map of Mount Jordan and vicinity, Custer County, Idaho: U.S. Geological Survey Miscellaneous Field Studies Map MF–1434, scale 1:24,000.

Fox, K. F., Jr., 1983, Melanges and their bearing on Late Mesozoic and Tertiary subduction and interplate translation at the west edge of the North American plate: U.S. Geological Survey Professional Paper 1198, 40 p.

Hardyman, R. F., 1981, Twin Peaks caldera of central Idaho: Montana Geological Society, Field Conference and Symposium Guidebook to Southwest Montana, p. 317–322.

Hays, W. H., McIntyre, D. H., and Hobbs, S. W., 1978, Geologic map of the Lone Pine Peak quadrangle, Custer County, Idaho: U.S. Geological Survey Open-File Report 78–1060, scale 1:62,500.

Leonard, B. F., and Marvin, R. F., 1982 [1984], Temporal evolution of the Thunder Mountain caldera and related features, central Idaho, *in* Bill Bonnichsen and R. M. Breckenridge, eds., Cenozoic geology of Idaho: Idaho Bureau of Mines and Geology Bulletin 26, p. 23–41.

Lipman, P. W., 1983, Tectonic setting of the Mid to Late Tertiary in the Rocky Mountain region—A review, *in* The genesis of Rocky Mountain ore deposits—Changes with time and tectonics: Denver Region Exploration Geologists Society Symposium, Denver, 1982, Proceedings, p. 125–131.

Lipman, P. W., Christiansen, R. L., and O'Connor, J. T., 1966, A compositionally zoned ash-flow sheet in southern Nevada: U.S. Geological Survey Professional Paper 524–F, p. F1–F47.

Lipman, P. W., Prostka, H. J., and Christiansen, R. L., 1972, Early and Middle Cenozoic, Part 1 *of* Cenozoic volcanism and plate-tectonic evolution of the western United States, *in* A discussion on volcanism and the structure of the Earth: Royal Society of London Philosophical Transactions, ser. A, v. 271, no. 1213, p. 217–248.

McIntyre, D. H., Ekren, E. B., and Hardyman, R. F., 1982 [1984], Stratigraphic and structural framework of the Challis Volcanics in the eastern half of the Challis 1°×2° quadrangle, Idaho, *in* Bill Bonnichsen and R. M. Breckenridge, eds., Cenozoic geology of Idaho: Idaho Bureau of Mines and Geology Bulletin 26, p. 3–22.

McIntyre, D. H., and Hobbs, S. W., 1978, Geologic map of the Challis quadrangle, Custer County, Idaho: U.S. Geological Survey Open-File Report 78–1059, scale 1:62,500.

Pallister, J. S., 1982, Reconnaissance geology of the Jabal Al Ilman quadrangle, sheet 18144A, Kingdom of Saudi Arabia: Saudi Arabian Deputy Ministry for Mineral Resources Open-File Report USGS–OF–02–90, 61 p.

Peacock, M. A., 1931, Classification of igneous rock series: Journal of Geology, v. 39, no. 1, p. 54–67.

Ringwood, A. E., 1974, The petrological evolution of island arc systems: Geological Society of London Journal, v. 130, pt. 3, p. 183–204.

Ross, C. P., 1933, The Thunder Mountain mining district, Custer and Camas Counties, Idaho: Idaho Bureau of Mines and Geology Pamphlet 33, 26 p.

_____1934, Geology and ore deposits of the Casto quadrangle, Idaho: U.S. Geological Survey Bulletin 854, 135 p.

_____1937, Geology and ore deposits of the Bayhorse region, Custer County, Idaho: U.S. Geological Survey Bulletin 877, 161 p.

Segerstrom, Kenneth, and Young, E. J., 1972 [1973], General geology of the Hahns Peak and Farwell Mountain quadrangles, Routt County, Colorado, *with a discussion of* Upper Triassic and pre-Morrison Jurassic rocks, by G. N. Pipiringos: U.S. Geological Survey Bulletin 1349, 63 p.

Shand, S. J., 1947, Eruptive rocks, their genesis, composition, classification, and their relation to ore deposits, *with a chapter on* Meteorites (2d ed.): New York, John Wiley, 444 p.

Souther, J. G., 1970, Volcanism and its relationship to recent crustal movements in the Canadian Cordillera: Canadian Journal of Earth Sciences, v. 7, no. 2, pt. 2, p. 553–568.

Symposium on the Geology and Mineral Deposits of the Challis 1°×2° Quadrangle, Idaho

Chapter D

Precambrian and Paleozoic Sedimentary Terranes in the Bayhorse Area of the Challis Quadrangle

By S. WARREN HOBBS

CONTENTS

FIGURES

Abstract

Limited outcrops of pre-Tertiary sedimentary rocks of Proterozoic to Permian age are exposed mainly in the eastern half of the Challis quadrangle, in the Bayhorse region, and extend south into the Wood River region. They provide the only information on the early sedimentary history and structural complexity of a great stack of allochthonous terranes. These rocks indicate a long and varied sedimentary record from the Early Proterozoic through the Paleozoic. Sedimentation was interrupted by regional folding and faulting in the Cambrian and Ordovician and was followed by extensive early Mesozoic folding, by extensive middle and late Mesozoic west-to-east thrust faulting, and by late Mesozoic normal faulting. The Idaho batholith intruded and engulfed the allochthonous sedimentary sequences in the mid-to-Late Cretaceous, and the Challis Volcanics blanketed the region in Eocene time.

The Bayhorse region contains six fault-bounded structural-stratigraphic terranes, each of which is made up of a sedimentary sequence that differs significantly from that of adjacent terranes. Four of the six terranes include stratigraphic units older than Middle Ordovician that have not been definitely correlated with rocks beyond the Bayhorse area, but Middle Ordovician and younger units of three terranes are widespread far to the east and south.

The physical properties, stratigraphic succession, and composition of the rocks in each terrane have profoundly influenced the origin and localization of ore deposits. The Salmon River lineament, a major northeast-trending fault or fault zone, separates two of the terranes, and may have regional significance for the distribution of mineral occurrences.

INTRODUCTION

The Bayhorse region in central Custer County, Idaho, includes the rugged Salmon River Mountains highland in its western part and the northern part of the east-central Idaho Basin and Range Province to the east. More than 35,000 ft (feet) of predominantly marine strata of Paleozoic age or older occur within the area. These strata were folded and thrust faulted during the late Paleozoic and early Mesozoic by northeasterly directed compressional forces and were subsequently cut by steep normal faults during the late Mesozoic and Tertiary. A major north-northeast-trending structural break, called the Salmon River lineament, divides the area with significant differences in lithology and structure on each side.

The pre-Tertiary sedimentary rocks now exposed in the Challis 1°×2° quadrangle are but bits and pieces of a once very extensive and locally very thick stratigraphic record that was largely destroyed in the western half of the quadrangle by the Cretaceous Idaho batholith and was extensively buried in the eastern half by the Eocene Challis Volcanics. These sedimentary rocks, or their metamorphosed equivalents, are exposed over less than 15 percent of the Challis quadrangle, and their distribution and general ages are shown on figure D1. The areas shown as Precambrian contain Middle Proterozoic rocks but include some that are probably older and certainly some that grade into the Late Proterozoic and maybe even the early Paleozoic. Cambrian to Devonian strata include a great diversity of rocks of various ages and facies that are discussed in more detail later in this chapter. The Mississippian through Permian strata make up two general groups, one along the southern part of the eastern border of the Challis 1°×2° quadrangle that represents the predominantly carbonate cratonic facies and one farther west in the drainage basin of the mainstem Salmon River that comprises western continental margin-deep sea black-shale facies. These groups are juxtaposed by extensive thrust faulting. The Mesozoic and Tertiary plutonic rocks make up the mid- to Late Cretaceous Idaho batholith and the Eocene plutons and dike swarms that together largely engulf the main mass of the sedimentary rocks in the western half of the Challis 1°×2° quadrangle. Only scattered roof pendants of the sedimentary rocks remain in this area. Eocene Challis Volcanics, and Quaternary deposits of great variety, bury extensive areas of both the sedimentary rocks and the batholith.

The sedimentary rocks of the Challis 1°×2° quadrangle and adjoining areas are of specific interest because of the close relation of the stratigraphic units to evaluation of the mineral resource potential of the quadrangle. Of equal importance are the physical characteristics and the composition of the sedimentary section—porosity, permeability, carbonate content, geochemistry, and other factors that can be directly related to known ore deposits and, consequently, are factors to be used in locating deposits as yet unknown. Structure is also intimately related to the origin and localization of ore deposits, and only by careful geologic mapping can we hope to understand the sedimentary and structural history. And most exciting is the mounting documentation that points to the origin of many ore deposits by the remobilization of metals from sedimentary source rock and their concentration in favorable structural settings. Details of some of the source rocks are described by Hall (chap. J, this volume).

TERRANES OF MIDDLE PROTEROZOIC AND PALEOZOIC ROCKS

The Bayhorse area has been divided into five units that are here termed structural-stratigraphic terranes, for purposes of stratigraphic and structural description and analysis (fig. D2). These terranes are generally bounded by major faults, have consistent internal structural styles, and consist of rocks that differ in significant ways from those of other terranes. Although each terrane is an integral part of the geologic patchwork that is the whole area, each shows a locally unique combination of geologic features that raises serious and as yet unresolved problems in relating one terrane to another and in the possible

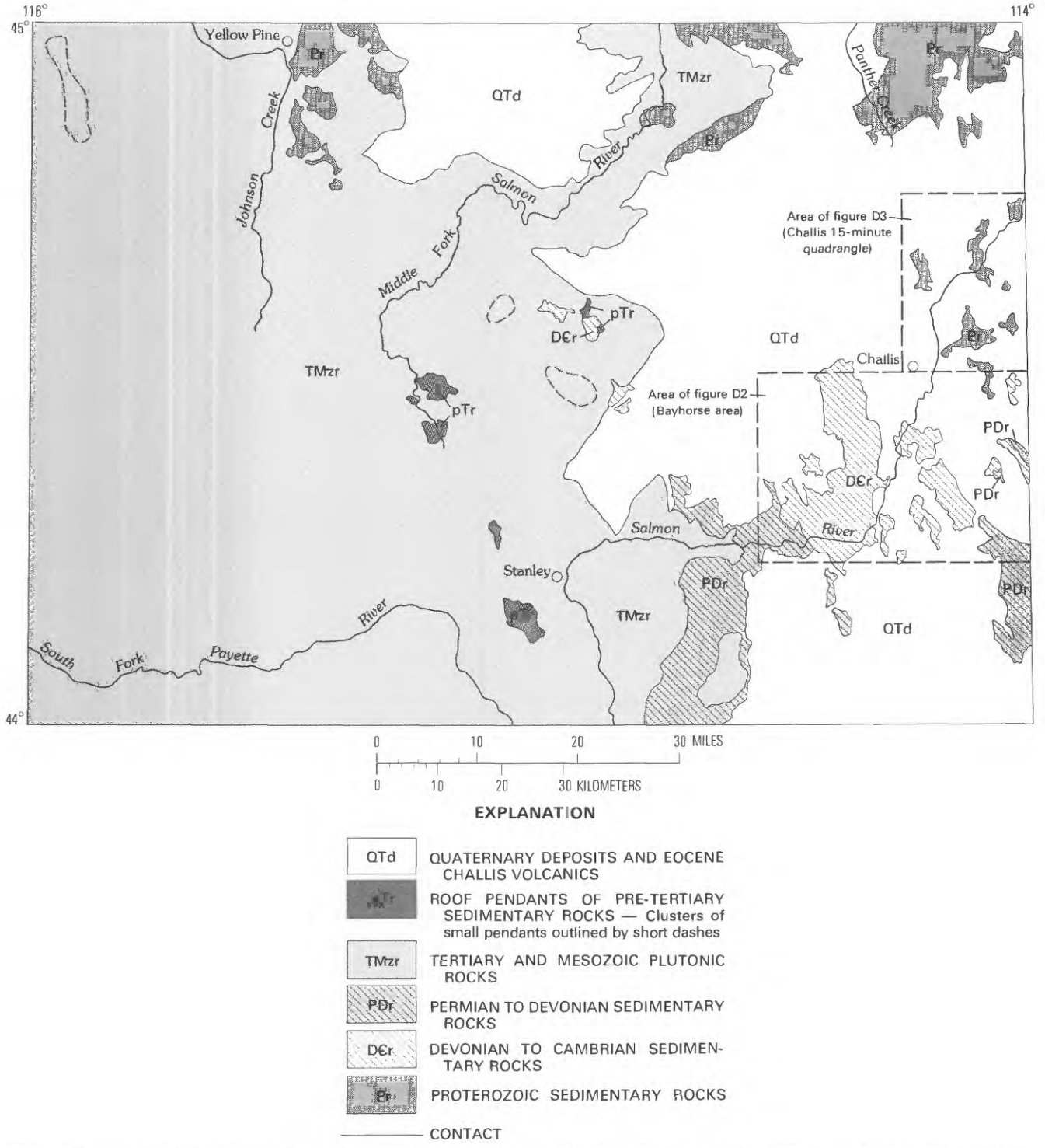

Figure D1. Map showing outcrop areas of pre-Tertiary sedimentary rocks and Cretaceous-Tertiary plutonic rocks in the Challis 1°×2° quadrangle.

correlation of the geology with that of areas outside the Bayhorse region.

The original geographic and stratigraphic relations between some of these terranes have not been accurately determined, but by describing and delimiting the components of each terrane our present knowledge will be defined and the remaining problems outlined. The following discussion of the terranes emphasizes the major elements of the structure and stratigraphy of each.

Terrane A

This terrane comprises rocks of Proterozoic age that are best exposed in the Challis 15-minute quadrangle to the

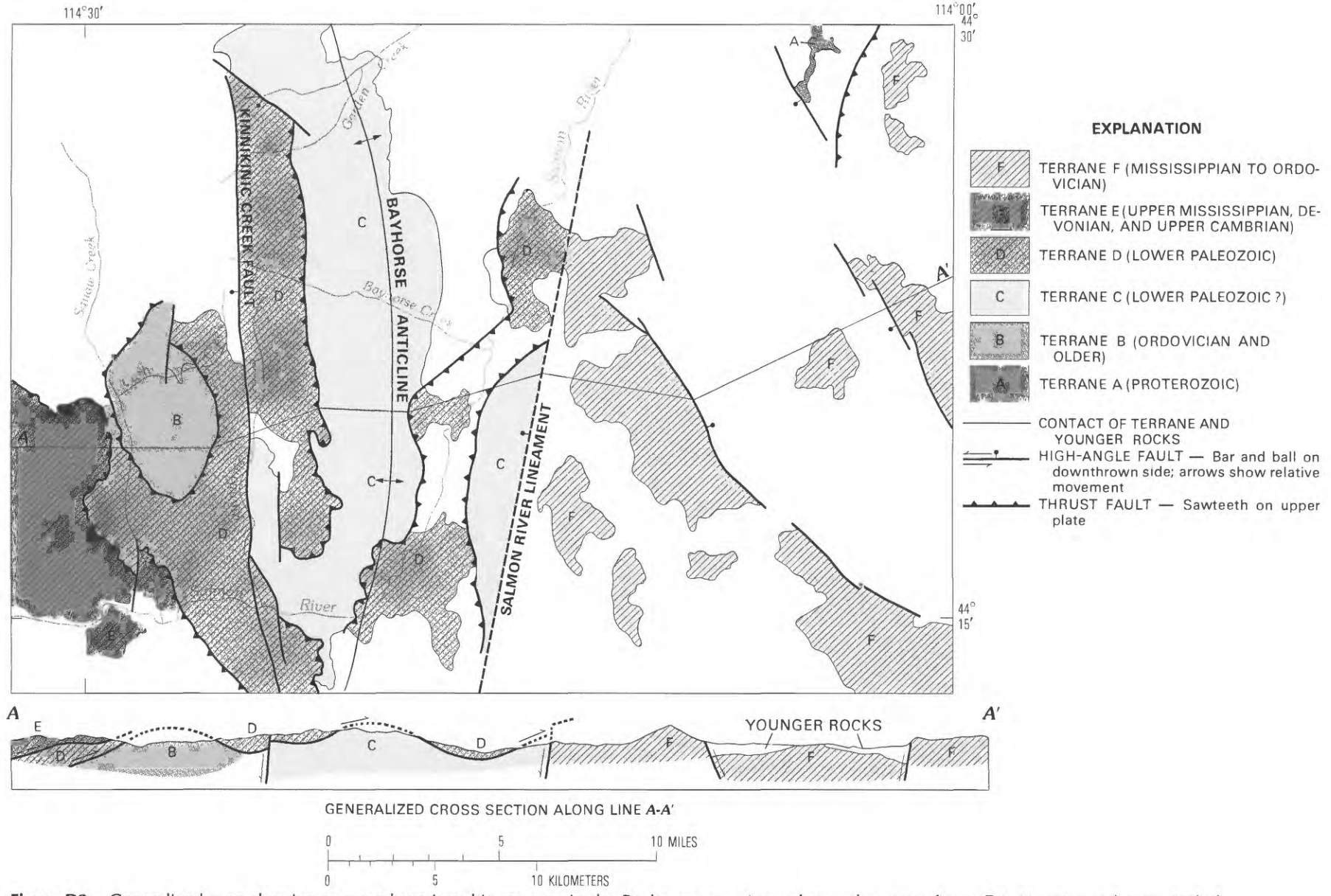

Figure D2. Generalized map showing structural-stratigraphic terranes in the Bayhorse area. Area of map shown on figure D1. Unpatterned areas include Eocene volcanic rocks.

north of the Bayhorse area (McIntyre and Hobbs, 1978) and across the northern edge of the Challis 1°×2° quadrangle (figs. D1, D3). Those rocks across the northern edge of the 1°×2° quadrangle are, for the most part, the Yellowjacket Formation, which is the lowest and most widespread recognized formation in the Middle Proterozoic in central Idaho. Yellowjacket strata that consist of more than 10,000 ft of argillite, siltite, and fine-grained sandstone are discussed in more detail by Modreski (chap. R, this volume). These rocks are of interest because of the stratabound cobalt deposits within them in the Blackbird district just north of the Challis 1°×2° quadrangle boundary. Related cobalt-bearing sulfide deposits are in the northeastern corner of the Challis 1°×2° quadrangle.

Within the Challis 15-minute quadrangle, segments of younger Proterozoic units are exposed (fig. D3). The oldest of these is the Apple Creek Formation, which is a thin-bedded, well-laminated, medium-greenish-gray to grayish-red-purple siltstone containing irregular streaks and lenses of light-gray, pinkish to pale-brown, fine-grained sandstone cemented by ferrodolomite. No exposures of the overlying Gunsight Formation are within this area. The Swauger Formation is mainly pinkish-purple to nearly white, medium- to coarse-grained, slightly feldspathic quartzite at least 10,000 ft thick. Beds range from 1–6 ft thick but generally are 3–5 ft, and many show prominent cross-lamination. Ripple marks are well developed in places. Both the Apple Creek and Swauger Formations are widely distributed in the Lemhi Range east of the Challis 1°×2° quadrangle (Ruppel and others, 1975; Ruppel, 1980). The Swauger Formation is overlain by the Lawson Creek Formation, which is the youngest known unit of the Middle Proterozoic in this part of Idaho (Hobbs, 1980). This unit grades upward from massive quartzite of the Swauger through a transition zone into a red-purple, thin-bedded siltstone-argillite sequence that is more than 4,000 ft thick. The top is concealed by Challis Volcanics.

Scattered exposures in the southern part of the Challis 15-minute quadrangle are a heterogeneous mixture of green phyllite; argillite; siltstone; massive- to

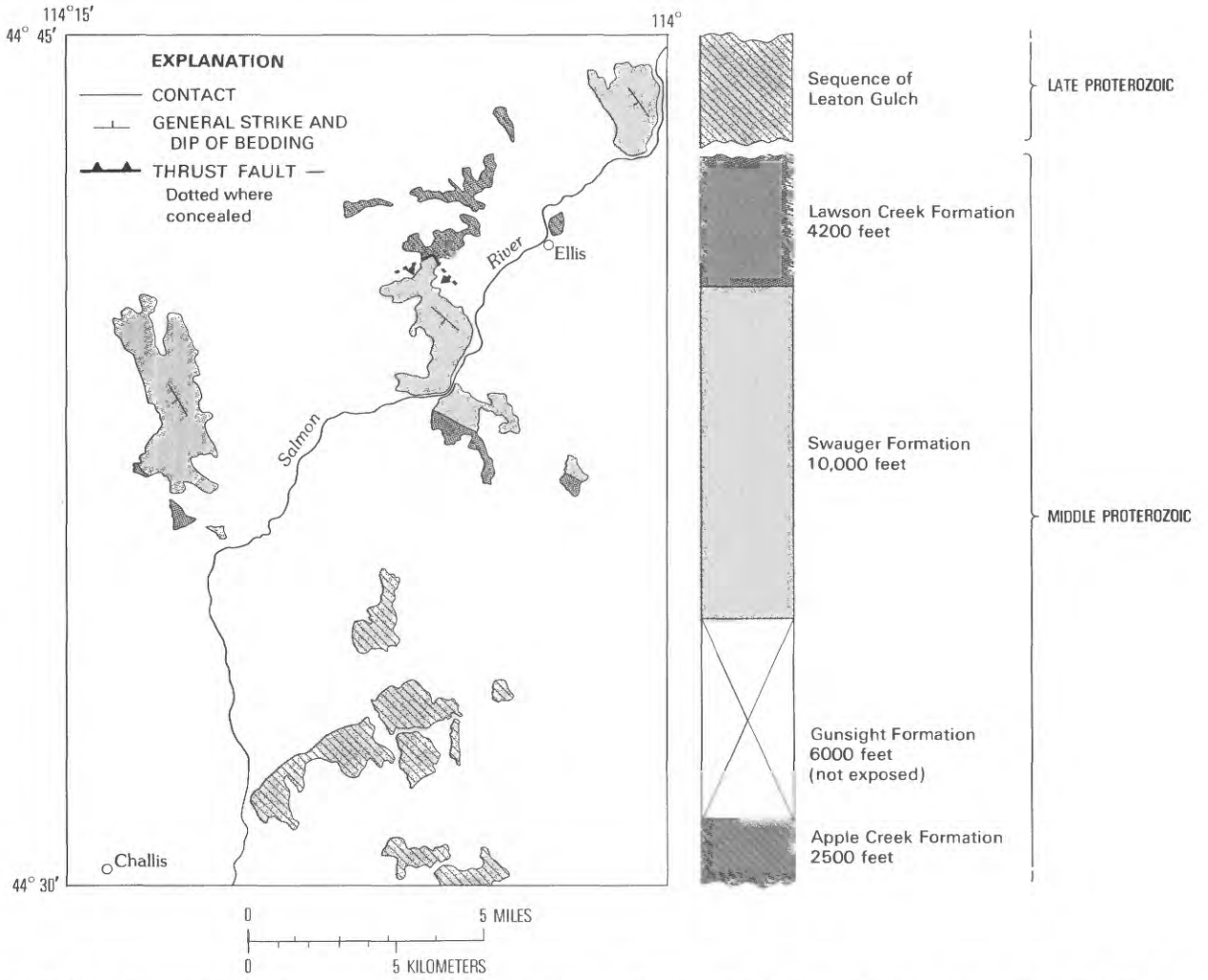

Figure D3. Generalized columnar section and geologic map showing distribution of Proterozoic rocks in the Challis 15-minute quadrangle.

thin-bedded, white to pink quartzite with some breccia and conglomerate; and local layers of pure, massive, crystalline dolomite. These strata, called informally the sequence of Leaton Gulch, are of equivocal age but are probably Late Proterozoic and could likely include some Early Cambrian. They may be related to comparable strata in the southern part of the Lemhi Range to the southeast (McCandless, 1982).

Terrane B

Terrane B consists of less than 0.5 sq mi (square mile) of exposed strata of Ordovician and Middle Cambrian age and older(?) within a window in a major thrust sheet on upper Squaw Creek in the western part of the Bayhorse area (fig. D2). The sequence comprises more than 2,500 ft of strata. The upper unit is a medium- to thick-bedded, sandy and silty, light-colored dolomite at least 500 ft thick, whose age, based on poorly preserved fossils, is most probably Ordovician. The dolomite rests disconformably on a sequence of strata that consists of: (1) an upper red and green shale and siltstone unit of unknown thickness that contains unequivocal basal Middle Cambrian fossils; (2) 1,300 ft of clean, medium-bedded, slightly feldspathic, medium-pinkish-gray quartzite named the Lower or Middle Cambrian Cash Creek Quartzite; (3) a very distinctive carbonate zone, about 600 ft thick, that includes massive dolomite at the top and thinly laminated, calcareous siltstone in the lower 500 ft; and (4) a basal, very massive, cross-laminated white quartzite, the quartzite of Boundary Creek, more than 400 ft thick whose base is covered (Hobbs and others, 1968). The total sequence in terrane B is known only from this one area of outcrop, and nothing comparable has been identified in eastern Idaho. The nearest possible correlatives are some of the units described by McCandless (1982) in the southern Lemhi Range.

Several diverse structural features are important elements of terrane B: (1) the terrane is bounded at the top by a major thrust fault that brings quartzites of terrane D over the Ordovician carbonate of terrane B; (2) within terrane B the unconformity between the Ordovician carbonate and the lower Middle Cambrian siltstone documents uplift, steep faulting, and planation of the Cambrian section before deposition of the Ordovician carbonate; and (3) the base of the quartzite of Boundary Creek is not exposed, but the lowest outcrops show much brecciation that may relate to a thrust fault not far below.

Anticlinal folding followed the major thrusting of terrane D over terrane B and produced the present configuration in which the thrust plate is folded nearly parallel to the bedding. The possible extension of this fold, and the strata within it, beyond the known exposures is uncertain because of masking by overlying allochthons and the Challis Volcanics.

Terrane C

Terrane C consists of a block of undated strata of probable Early Ordovician and Late Cambrian age that includes four lithologic units and forms the core of the massive Bayhorse anticline that trends north across the entire Bayhorse area (fig. D2). Numerous mines and mineral occurrences of the central Bayhorse mining district are within this anticline. Strata that make up this structure form a generally concordant sequence that is more than 5,000 ft thick and comprises the Ramshorn Slate (Ordovician?), Bayhorse Dolomite (Ordovician?), and Garden Creek Phyllite (Cambrian?) of C. P. Ross (1934), and the informally named lower dolomite of Bayhorse Creek that was discovered by D. P. Wheeler (Umont Mining, Inc., oral commun., 1964).

The basal unit is massive dolomite that is barely exposed in the narrow valley of Bayhorse Creek, but which is known from drill-hole data to be underlain at a depth of about 200 ft by an intrusive porphyry. Overlying the dolomite is the Garden Creek Phyllite, a black, carbonaceous, internally folded argillaceous rock having well-developed axial-plane cleavage and whose original thickness can only be estimated at about 750 ft. Narrow quartz veins that cut this unit have yielded small amounts of lead, zinc, and silver. Its upper part grades into the thin-bedded impure black limestone of the basal Bayhorse Dolomite that overlies the Garden Creek.

The Bayhorse Dolomite is of indeterminate original thickness. Its upper contact is an erosional disconformity or low-angle unconformity, and the unit ranges from several hundred to more than 1,200 ft thick. The lower one-half to two-thirds is thin- to medium-bedded, dark-gray impure limestone; the upper part is massive, medium- to thick-bedded, cream-colored dolomite. At least two intervals near the top contain several thin-bedded, platy siltstone beds, silty dolomite, and dolomitic siltstone. Oolitic (pisolitic) zones, where they have been preserved, are distinctive marker horizons in the upper part of the section. In many places the dolomite, at its contact with the overlying Ramshorn Slate, is marked by collapse breccias, cavern fillings, and other features related to a karst topography that was developed during the interval of exposure before deposition of the Ramshorn. The structural and stratigraphic significance of this break in the depositional record is unknown, but this paleokarst horizon was very important in the localization of mineral deposits.

The uppermost unit of terrane C is the Ramshorn Slate. This unit is predominantly a thin-bedded, characteristically laminated argillite, siltstone, and sandy siltstone containing thin sandstone and pebble conglomerate near the top. Near Bayhorse and Garden Creeks a very thick, massive pebble and cobble channel conglomerate at the base marks a major stream valley that crossed the old eroded surface. This basal conglomerate, locally more

than 400 ft thick, feathers out to the north and south in to sandy facies of the basal Ramshorn.

Most of the Ramshorn Slate has a very well developed slaty or axial-plane cleavage that gives the rock a deceptively simple structural grain or false bedding. The real bedding in the slate is deformed into irregular wavy folds and locally well-developed isoclinal drag folds, all of which are cut by the pervasive axial-plane cleavage. The complex internal structure of the unit precludes accurate measurement of thickness, but it probably totals at least 2,400 ft.

No part of terrane C is definitely dated, but small shell fragments from several localities in the Bayhorse Dolomite strongly suggest an early Paleozoic age, and this evidence, together with general stratigraphic considerations, makes an age of Early Ordovician or Late Cambrian for all of the section most probable. Furthermore, none of the four formations that make up terrane C has been conclusively identified outside of the Bayhorse area, although Baldwin (1951), Ross (1937, 1947), and McCandless (1982) suggested possible correlations of certain units in the Lost River Range and the southern part of the Lemhi Range with the Ramshorn Slate, Bayhorse Dolomite, and Garden Creek Phyllite.

Terrane D

Rocks of terrane D, although including units that differ widely in lithology and age, make up a generally conformable sequence of a major allochthon whose upper contact is with the thrust sheet of terrane E, and whose lower contact, wherever seen, is with terrane B or the Ramshorn Slate of terrane C.

Two contrasting groups of strata are within terrane D: a lower, undated thick quartzite sequence, and an upper, well-dated Ordovician carbonate-quartzite sequence. The lower quartzite of this terrane comprises more than 3,000 ft of heterogeneous, predominantly quartzitic strata that are parts of at least two and possibly more separate stratigraphic sequences that have been juxtaposed during the complex structural history of the area. The most prominent, thickest, and most widespread member is the Ordovician Clayton Mine Quartzite (Hobbs and others, 1968) that can be traced or correlated with a fair degree of certainty from its type section near Clayton over much of the western half of the Bayhorse area (fig. D2).

Most of the Clayton Mine Quartzite is composed of poorly sorted, coarse- to medium-grained feldspathic quartzite that includes conglomerate layers, pebbly quartzite in the upper part, and a few thin, discontinuous dolomite layers near the base. Several siltstone intervals and scattered shale partings are distributed in the lower part of the section. Many of the thick quartzite layers are cross-laminated. The color of these rocks ranges from light gray, light yellowish orange, or light pink in the western part to reddish gray, red, and purple to the east. Most of the quartzite is medium to thin bedded with some interbeds of siltstone. Feldspar is abundant, and much of it is very coarse. This quartzite sequence is underlain by the major thrust fault that overlies terranes B and C.

Two other quartzite units that are included in terrane B are probably related to the Clayton Mine Quartzite. One of these units is a quartzite sequence on upper Cash Creek, east of terrane B, that has many of the attributes of the Clayton Mine Quartzite but has pronounced differences in lithology and structure that preclude definite correlation. Most of the quartzite is thin to medium bedded with thin interbeds of siltstone and one siltstone interval at least 300 ft thick. Feldspar is abundant, and much of it is very coarse. This quartzite unit is underlain by a major thrust fault that is folded into a broad antiform; the quartzite rests on Ordovician carbonate at the exposures in upper Cash Creek and on Middle Cambrian shale at the exposures west of Squaw Creek.

A quartzite unit that is more questionably correlated with the Clayton Mine Quartzite is a sequence that is informally called the siltstone, sandy siltstone, and quartzite of the Rob Roy mine area. These strata along Kinnikinic Creek near the Clayton Silver mine make up a thick, heterogeneous sequence of various quartzite and siltstone layers and, in its lower half, scattered beds of pure dolomite.

The Clayton Mine Quartzite has been identified beyond the Bayhorse area only in the central Pioneer Mountains about 40 mi (miles) to the south-southwest. Possibly the Proterozoic Wilbert Formation, as described in the southern Lemhi Range by Ruppel and others (1975) and as further described by McCandless (1982), may correlate with some facies of the Clayton Mine Quartzite, but direct evidence is lacking.

A disconformity separates the Clayton Mine Quartzite from the overlying Ella Dolomite and represents an unknown time interval. It is marked by a sharp, drastic change in depositional regimes and by an apparent low-angle unconformity.

The Middle Ordovician Ella Dolomite, the Middle Ordovician Kinnikinic Quartzite, and the Middle Ordovician and younger (possibly lowermost Silurian) Saturday Mountain Formation lie above the disconformity (Hobbs and others, 1968). The Ella Dolomite is a massive, medium- to thick-bedded, laminated dolomite at least 700 ft thick. The Kinnikinic is a fine-grained, pure, well-indurated quartzite, and the Saturday Mountain comprises more than 3,000 ft of impure dolomite and limestone with some thick zones of black shale and a few quartzite beds. These are all well-dated formations whose type localities are within the Bayhorse area (Ross, 1937; Hobbs and others, 1968). Both the Saturday Mountain Formation and the Kinnikinic Quartzite correlate with units far to the east and south of the Bayhorse area. Scattered roof

pendants of metamorphosed calcareous and quartzitic rocks in the Idaho batholith to the west and south of the Bayhorse area are considered to be detached parts of these formations.

The allochthon that consists of the D terrane is folded in general conformity with the major folds of the underlying B and C terranes. In detail, however, the strata within the allochthon are locally very intensely folded and deformed. The allochthon appears to terminate eastward at the Salmon River lineament, and this boundary may represent an uplifted block against which the allochthon stalled or over which it rode. However, no extension of this thrust plate has been identified east of the lineament.

Terrane E

Rocks that make up terrane E, in the southwestern corner of the Clayton 7 1/2-minute quadrangle, are but a very small part of an extensive allochthon of stratigraphically and tectonically complex strata that has been transported for an unknown distance from the west to its present position where it overlies the Ordovician units of terrane D (fig. D2). These strata, described by Nilsen (1977) as the Salmon River sequence and redesignated the Salmon River assemblage in this chapter, consist of generally dark-gray to nearly black argillite, calcareous siltstone, siltstone, turbidite, and lesser amounts of fine-grained quartzite with some relatively pure limestone. Much of the assemblage in the Bayhorse area is thin to medium bedded and consists of interlaminated siliceous-facies argillite, siltstone, fine-grained sandstone, and local limestone turbidites. Small-scale current structures, sole markings, and local contortion produced by syndepositional slumping are abundant. Farther to the west and south the allochthon includes less sand and silt and more laminated siliceous-facies black argillite with interlayered calcareous siltstone and local fine-grained quartzite. Most of the beds dip steeply to the west, and many have internal structures that indicate that tops are to the east. The structure within the allochthon, however, is very complex, and the great apparent thickness that is exposed westward from the Bayhorse area can most reasonably be explained by isoclinal folding, thrust faulting, and the attendant duplication of section that has not everywhere been recognized. The western edge of the allochthon is intruded by the Idaho batholith, overlapped by higher thrust plates of Pennsylvanian and Permian strata, or covered by Challis Volcanics (Hall, chap. J, this volume).

Although the strata of terrane E have much in common with the Lower Mississippian Copper Basin Formation of Ross (1962a), they include lithologies and faunas that contrast quite significantly in some places with those of the Copper Basin Formation. The Late Mississippian age of the Salmon River sequence (Nilsen, 1977) was based on two collections of fossils derived from float material discovered at two localities. One of these faunas was in a single, semirounded float block that was collected in Deerspring Gulch, an informally named drainage on the northern side of the Salmon River opposite the mouth of Slate Creek, near the southern edge of the Thompson Creek 7 1/2 minute quadrangle. This material (USGS loc. no. 24408-PC) was examined by J. T. Dutro, Jr., in consultation with W. J. Sando, who reported (written commun., 1971) that "This collection is Mississippian in age, most probably middle or Late Mississippian. The large fragment of the spiriferoid brachiopod, Anthracospirifer, is most useful because that genus is now known to range from late Early Mississippian to Middle Pennsylvanian. Other elements of the fauna, though not diagnostic, are compatible with the Mississippian age assignment."

Conodonts from the same material were studied by J. W. Huddle (written commun., 1971) who reported that several diagnostic species "* * * occur with Apatognathus in the upper part of the St. Louis Limestone in the Mississippi Valley. This collection could be as old as late St. Louis time or as young as early Chesterian time." An abundant calcareous Formaniferal fauna was reported by Betty Skipp (written commun., 1972) to be "* * * a middle Visean (late Meramecian) fauna which represents F.Z. 13-15 of the Mamet Foraminiferal zonation. These zones are present in the St. Louis and Ste. Genevieve Limestones of the midcontinent region; the fauna is typical of the lower part of the Scott Peak Formation of south-central Idaho (Mamet and others, 1971)." Although the stratigraphic section on the ridge above this specimen locality contains widely scattered carbonate beds in the predominantly argillite-siltite sequence, no fossils were found in place. The closest known fossil-bearing carbonate section of comparable age is the Scott Peak Formation, a part of terrane F where exposed in the southeastern corner of the Bayhorse area (fig. D2).

Material from a second faunal locality, in the lower part of Mill Creek near the northern boundary of the Livingston Creek 7 1/2-minute quadrangle, comprises a large angular float block that contains an abundant megafauna (USGS loc. no. 27036-PC). This block, found about 1 mi southeast of the Deerspring Gulch locality, is roughly at the same stratigraphic horizon and of similar age. It has also been reported on by J. T. Dutro, Jr. (written commun., 1979), who stated, "The excellent silicified fossils are identifiable as an assemblage characteristic of Upper Mississippian strata in the northern Rocky Mountains. The assemblage is of probable late, but not latest, Chesterian age, approximately a correlative of Mamet Foraminiferal Zone 18. Beds of about this age occur also in the Surrett Canyon Formation of Idaho, the Horseshoe Shale Member of the Amsden Formation of Wyoming, and the Big Snowy Group of central Montana. The most diagnostic species is *Anthracospirifer shawi shawi* Gordon, which occurs in Zone 18 equivalents in Wyoming

(Gordon, 1975)." No similar material has been found in undisturbed outcrops anywhere else in terrane E.

Subsequent sampling of several well-defined carbonate and calcareous sandstone and siltstone horizons at five localities within the predominantly siltstone and calcareous siltstone parts of terrane E has produced conodonts whose ages range from Late Cambrian to Late Devonian. Two of these localities have been collected from by F. G. Poole, W. E. Hall, and S. W. Hobbs in the lower reaches of Thompson Creek in the Thompson Creek 7 1/2-minute quadrangle. The first locality (USGS loc. no. 11020-SD), on the west bank of Thompson Creek about 2 mi above its mouth, was reported by J. E. Repetski to contain conodonts of Late Devonian age. Material from the second locality, about 0.5 mi south of the first and on the same side of Thompson Creek, includes three samples, two of which were collected by Poole and Hall (USGS loc. nos. 9851-CO and 9852-CO), and the third by Hobbs (USGS loc. no. 9618-CO). Conodonts from these three collections were studied by J. E. Repetski, who reported that two were of Late Cambrian age and the third "Most likely latest Cambrian to earliest Ordovician." Samples from outcrops in a roadcut on State Scenic Route 75 about 1.1 mi west of the mouth of Thompson Creek were collected by F. G. Poole (USGS loc. nos. 10736-SD and 10737-SD) and examined by A. G. Harris, who reported them to be Middle Devonian. The remaining two known localities are in the lower valleys of Sheephead Creek and Last Chance Creek, which are west-side tributaries to Slate Creek about 4 mi and 5 mi, respectively, above its junction with the Salmon River, and in the west-central part of the Livingston Creek quadrangle. The sample from Sheephead Creek was collected by Poole and Hall (USGS loc. no. 11021-SD) from detrital limestone float blocks on the north side of the valley and less than 0.5 mi above its junction with Slate Creek, and reported by J. E. Repetski to have an age of "Middle Ordovician to Middle Devonian". Similar material from the north side of Last Chance Creek about 1,000 ft above its junction with Slate Creek was reported by Repetski to be Late Devonian.

Several aspects of the terrane E allochthon, including the widely different ages of strata, the documented structural complexity, and the variations in lithologic character, make the use of the term "sequence" inappropriate, as applied to these strata. It is here proposed that the strata that make up terrane E be called the Salmon River assemblage. No connotation as to origin is implied.

Terrane F

All the Paleozoic strata east of the Salmon River lineament (fig. D2) are included in this terrane, which is but a small part of the very extensive east-central Idaho Basin and Range Province. In the Bayhorse area the strata are largely of middle and late Paleozoic age, are predominantly carbonate, and represent parts of the stratigraphic sections that are mostly absent in the terranes to the west. The stratigraphic section exposed here is an extension of the stratigraphy studied in the Lost River Range by Ross (1947) and Mapel and others (1965), and across southeastern Idaho and southwestern Montana by numerous other workers.

The Kinnikinic Quartzite of Ordovician age is the oldest unit in terrane F, and both it and the overlying Saturday Mountain Formation consist of significantly different facies and thicknesses than those described in terranes west of the lineament. In terrane F, the Saturday Mountain Formation grades stratigraphically upward into rocks that are equivalent to the Roberts Mountains Formation of Nevada. Succeeding strata make up the predominantly carbonate succession of the upper Paleozoic eastern facies that includes the Silurian Laketown Dolomite, the Devonian Beartooth Butte Formation, Grand View Dolomite, Jefferson Dolomite, and Three Forks Formation, and the Mississippian McGowan Creek, Middle Canyon, and Scott Peak Formations.

The structural pattern of terrane F, although containing many elements of the prevailing patterns in terranes B, C, and D, is dominated by an extensional regime of post-Eocene age that produced well-developed block-fault ranges with wide intermontane basins. The N.-30° W. regional trend of the basins and ranges and internal structures in the major fault blocks is distinctly different from the predominantly northern trends of fold axes and steep faults of the other terranes to the west.

THE SALMON RIVER LINEAMENT

A major fault or fault zone that I have called the Salmon River lineament marks the boundary between terrane F and terranes C and D, just west of it (fig. D2). This structure merits special attention in a description of the geology of the Bayhorse area because it stands out as a consistent, linear structural and stratigraphic boundary. Although poorly exposed and ill defined, the pronounced differences in structural trends, deformation, and stratigraphic facies across the lineament are strong evidence for its possible regional significance. It can be clearly identified only in the north-central part of the map area (fig. D2) where a north-northeast-trending zone of very complex faulting that separates terrane D from terrane F is present. The structure is buried by Challis Volcanics and Quaternary deposits to the north and south.

Of the three main differences that distinguish the geology on one side of the lineament from that on the other, the stratigraphic record is the most compelling. The heterogeneous Ordovician and older lithologies to the west contrast markedly with the very thick and predominantly carbonate Ordovician, Silurian, Devonian, and

Mississippian sections that predominate east of the lineament. The Saturday Mountain Formation and the Kinnikinic Quartzite, however, are present as a part of the stratigraphic section on both sides, and notable facies changes within these units across the boundary are further cogent evidence of the structural significance of this break. West of the lineament the Kinnikinic Quartzite, although folded and faulted, is estimated to be 500 to 800 ft thick. It contains partings and interbeds of black shale and siltstone, anomalous irregularities of bedding and grain size, and impurities that impart an uncharacteristic dark color to much of the unit. Kinnikinic Quartzite east of the lineament is significantly thicker, more massive, and very pure.

The Saturday Mountain Formation on opposite sides of the lineament shows an even more striking contrast both in composition and in thickness. The western facies consists of a thick heterogeneous section of massive dolomite, sandy dolomite, silty limestone, calcareous siltstone, black shale, and a few beds of dolomitic quartzite. The total thickness of the western facies of the Saturday Mountain Formation near Squaw Creek is estimated to be about 3,000 ft. The eastern facies that spans the same age range consists of a continuous section of relatively pure, medium- to thin-bedded dolomite that is less than 1,000 ft thick.

Although the regional significance of the Salmon River lineament remains obscure, these substantial facies changes, which occur within a distance of a few miles, together with compelling evidence for tectonic shortening and structural discontinuities across the structure, indicate that the Salmon River lineament is a major tectonic feature. One notable aspect of the feature is the near absence of ore deposits east of this line in the Bayhorse area, as well as throughout the entire Lost River Range from Challis to Arco; this absence contrasts sharply with the numerous mines and prospects to the west.

SUMMARY

The six terranes as described above include strata of widely diverse source areas, environments of deposition, and, to some extent, structural style. Terranes A, B, and C have no exposed basal thrust faults, but work in many of the surrounding areas provided strong evidence that all rocks in central Idaho from Middle Proterozoic through Permian have been thrust from the west as a series of imbricate allochthons, and that the resulting structural pattern in the Bayhorse area has been further complicated by younger steep normal faults and the enigmatic Salmon River lineament. These various structural-stratigraphic terranes that have a complex geologic history and varied composition and that have been invaded by a series of igneous rocks of several ages provide a prime environment for the generation and localization of ore deposits, not only in the Bayhorse area, but throughout central Idaho.

REFERENCES CITED

Baldwin, E. M., 1951, Faulting in the Lost River Range of Idaho: American Journal of Science, v. 249, no. 12, p. 884–902.

Gordon, Mackenzie, Jr., 1975 [1976], Brachiopoda of the Amsden Formation (Mississippian and Pennsylvanian) of Wyoming: U.S. Geological Survey Professional Paper 848-D, p. D1–D86, 13 pls.

Hobbs, S. W., 1980, The Lawson Creek Formation of Middle Proterozoic age in east-central Idaho: U.S. Geological Survey Bulletin 1482-E, 12 p.

Hobbs, S. W., Hays, W. H., and Ross, R. J., Jr., 1968, The Kinnikinic Quartzite of central Idaho—redefinition and subdivision: U.S. Geological Survey Bulletin 1254-J, p. J1–J22.

Mamet, B. L., Skipp, Betty, and Sando, W. J., 1971, Biostratigraphy of upper Mississippian and associated Carboniferous rocks in south-central Idaho: American Association of Petroleum Geologists Bulletin, v. 55, no. 1, p. 20–33.

Mapel, W. J., Read, W. H., and Smith, R. K., 1965, Geologic map and sections of the Doublespring quadrangle, Custer and Lemhi Counties, Idaho: U.S. Geological Survey Geologic Quadrangle Map GQ-464, scale 1:62,500.

McCandless, D. O., 1982, A re-evaluation of Cambrian through Middle Ordovician stratigraphy of the southern Lemhi Range: University Park, Pa., The Pennsylvania State University, M.S. thesis, 157 p.

McIntyre, D. H., and Hobbs, S. W., 1978, Geologic map of the Challis quadrangle, Custer County, Idaho: U.S. Geological Survey Open-File Report 78-1059, scale 1:62,500.

Nilsen, T. H., 1977, Paleogeography of Mississippian turbidites in south-central Idaho, *in* Stewart, J. H., Stevens, C. H., and Fritsche, A. E., eds., Paleozoic paleogeography of the western United States: Society of Economic Paleontologists and Mineralogists, Pacific Section, Pacific Coast Paleogeography Symposium 1, p. 275–299.

Ross, C. P., 1934, Correlation and interpretation of Paleozoic stratigraphy in south-central Idaho: Geological Society of America Bulletin, v. 45, no. 5, p. 937–1000.

_____1937, Geology and ore deposits of the Bayhorse region, Custer County, Idaho: U.S. Geological Survey Bulletin 877, 161 p.

_____1947, Geology of the Borah Peak quadrangle, Idaho: Geological Society of America Bulletin, v. 58, no. 12, p. 1085–1160.

_____1962a, Stratified rocks in south-central Idaho: Idaho Bureau of Mines and Geology Pamphlet 125, 126 p.

_____1962b, Upper Paleozoic rocks in central Idaho: American Association of Petroleum Geologists Bulletin, v. 46, no. 3, p. 384–387.

Ruppel, E. T., 1980, Geologic map of the Patterson quadrangle, Lemhi County, Idaho: U.S. Geological Survey Geologic Quadrangle Map GQ-1529, scale 1:62,500.

Ruppel, E. T., Ross, R. J., Jr., and Schleicher, David, 1975, Precambrian Z and lower Ordovician rocks in east-central Idaho, *in* Precambrian and lower Ordovician rocks in east-central Idaho: U.S. Geological Survey Professional Paper 889-B, p. 25–34.

Symposium on the Geology and Mineral Deposits of the Challis 1°×2° Quadrangle, Idaho

Chapter E

Regional Geophysical Studies in the Challis Quadrangle

By DON R. MABEY *and* MICHAEL W. WEBRING

CONTENTS

FIGURES

Abstract

Regional aeromagnetic and gravity data in the Challis quadrangle can be used to define several crustal blocks with distinctive lithologies and different geologic histories. The geophysical data confirm the general outlines of the Thunder Mountain and Van Horn Peak cauldron complexes. The part of the Idaho batholith that occurs within the quadrangle is a low-density mass that is weakly magnetic. The buried parts of Eocene intrusive masses appear more extensive than the parts exposed at the surface. A regional magnetic high in the northeastern corner of the quadrangle is produced by magnetite-rich zones in Precambrian sedimentary rocks. The high average topographic altitude of the quadrangle is an isostatic response to a mass deficiency at depth.

INTRODUCTION

The Challis quadrangle contains examples of most of the major geologic structures of the northern Rocky Mountains: a large Cretaceous batholith, Tertiary igneous intrusive bodies in a variety of sizes and shapes, Tertiary volcanic fields, including large caldera complexes, Paleozoic sedimentary rocks juxtaposed by major overthrusts, Precambrian sedimentary and metamorphic rocks, basin-and-range structures, and an active seismic zone.

The U.S. Geological Survey compiled and interpreted regional gravity and aeromagnetic maps of the quadrangle as part of the CUSMAP (Conterminous United States Mineral Assessment Program) study of the Challis 1°×2° quadrangle. Geophysical data were available from several earlier studies. Gravity data had been obtained in earlier surveys by the Geological Survey (unpub. data) primarily in the intermontane valleys and along roads. The U.S. Department of Defense had obtained data using an approximate 15-km (kilometer) grid for the entire quadrangle. As part of the CUSMAP study, the data from these earlier surveys were merged into a single data set. Additional gravity stations were established to complete an approximate minimum 5-km grid over the quadrangle (Webring, 1981). The data were reduced to the Bouguer anomaly using a density factor of 2.67 g/cm^3 (grams per cubic centimeter) and computer-calculated terrain corrections to a distance of 167 km from each station. The Bouguer anomaly values for nearly all stations are considered to be accurate to within 1 mGal (milligal).

The aeromagnetic coverage is based primarily on earlier surveys by and for the Geological Survey, having flight lines 1.6 and 3.2 km (1 and 2 miles) apart and flight levels 2,740 and 3,650 m (meters) (9,000 and 12,000 feet) above sea level. One additional survey was flown in the southeastern part of the quadrangle to complete the coverage. The data from the several surveys were adjusted to a common datum using the International Geophysical Reference Field of 1975 and analytically continued to 3,650 m.

Davis (*in* Cater and others, 1973) has qualitatively analyzed the aeromagnetic field in the north-central section of the quadrangle as part of the Idaho Primitive Area study. In addition to the aeromagnetic data presented in this report, data are available from the U.S. Department of Energy's NURE (National Uranium Resource Evaluation) program. Flight lines for these data are 9.66 km (6 miles) apart and about 122 m (400 feet) above the land surface. The NURE data are useful in detailed analysis along the flight lines.

PHYSICAL PROPERTIES OF THE ROCKS

Most of the rocks in the Challis quadrangle can be divided into six groups based on density and magnetization. The most dense rocks, averaging about 2.7 g/cm^3, are of Precambrian age. Paleozoic sedimentary rocks have a lower average density, about 2.6 g/cm^3. The granodiorite and two-mica granite that make up the main mass of the Idaho batholith in the Challis quadrangle are 2.58 g/cm^3. Tonalite and related rocks in the western margin of the Idaho batholith are more dense, averaging about 2.67 g/cm^3. The larger Tertiary intrusive bodies are of two densities: the granite of the Sawtooth batholith averages about 2.56 g/cm^3, but the Tertiary diorite is more dense, about 2.7 g/cm^3. The Tertiary volcanic rocks and the Cenozoic sedimentary rocks are the least dense; the volcanic rocks range widely in density and magnetization. The Cenozoic and pre-Cretaceous rocks are generally weakly magnetic, but Precambrian sedimentary rocks locally contain magnetite-rich zones that are very strongly magnetic. Most of the rocks of the Idaho batholith are weakly to moderately magnetic. The Tertiary intrusive rocks are more strongly magnetic than the Idaho batholith. Some of the Tertiary volcanic rocks are very strongly magnetic, and remanent magnetization, both normal and reverse, is commonly greater than induced magnetization.

GRAVITY AND MAGNETIC FEATURES IN THE CHALLIS QUADRANGLE

The regional anomalies in the Challis quadrangle are related to the geographic setting of the quadrangle. Although the highest point in Idaho, Mount Borah, is about 24 km east of the quadrangle, the quadrangle has the highest average topography in Idaho. The quadrangle is largely within a broad regional Bouguer gravity low centered over central Idaho (fig. E1). Excluding low Bouguer anomaly values in a local gravity low over Lemhi Valley east of the quadrangle, which reflect very thick basin fill, the Bouguer anomaly values in the Challis quadrangle are the lowest in the northwestern United States. The Bouguer anomaly, both regionally and within the

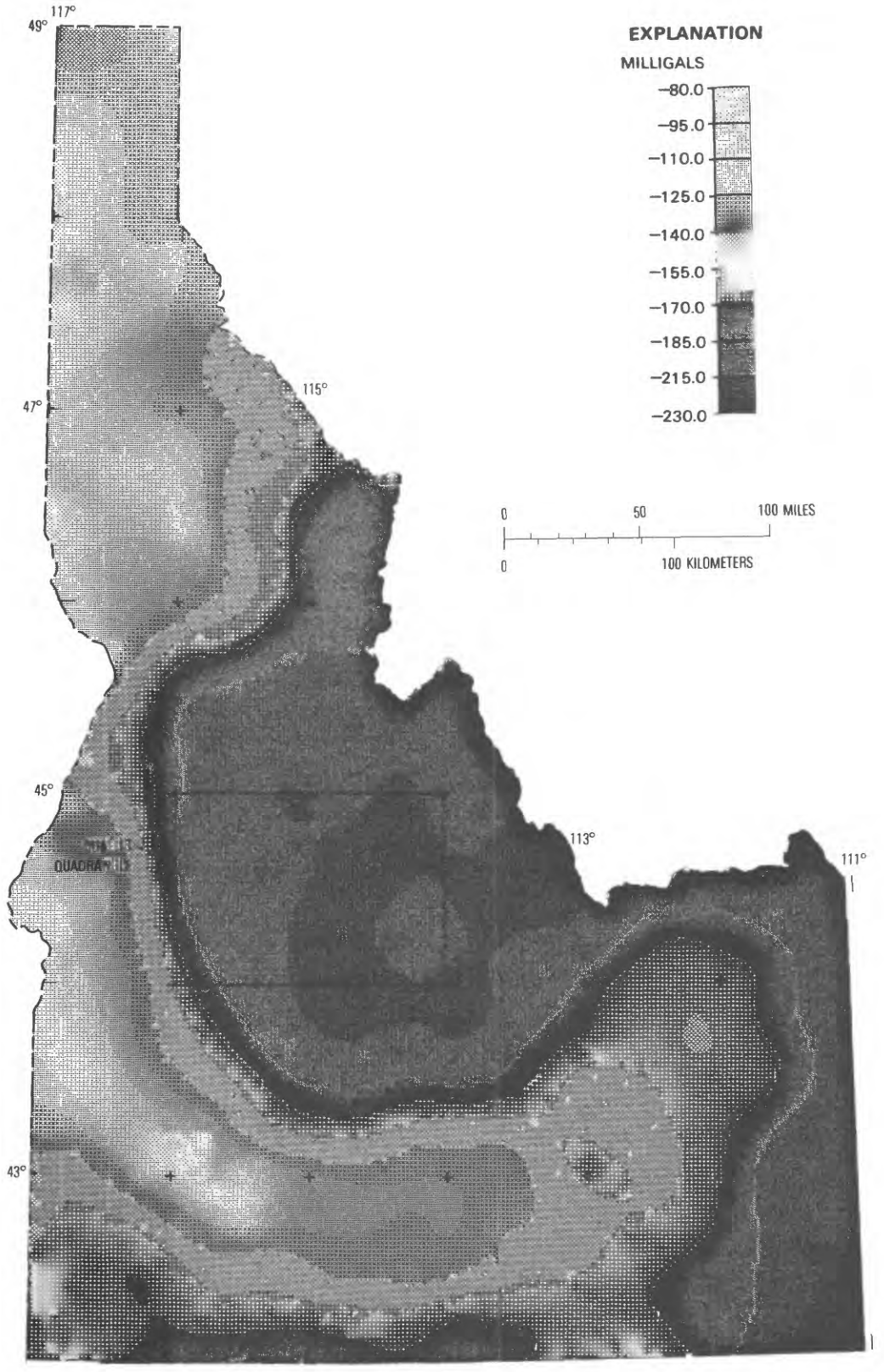

Figure E1. Regional gravity contour map of Idaho. Wavelengths shorter than 64 km removed during processing of data.

Challis quadrangle, shows a strong inverse correlation with regional elevation; the Bouguer anomaly values decrease toward the highest topography in the Challis quadrangle. This broad gravity low reflects the approximate isostatic balance of the region, as a negative-mass anomaly underlies and supports the high topography. Much of this

regional negative-mass anomaly likely results from a thickened crust under central Idaho. Superimposed on this broad regional low are more local anomalies that reflect mass anomalies in the upper crust.

The local anomalies and departures from a calculated isostatic anomaly can be best identified if the broad regional field is removed. The regional field can be derived in several ways. One way is to correct the free-air anomaly value for each station for the gravity effect of a layer of rock having a thickness equal to the difference between the altitude of the station and the average altitude over an area around the station. The residual anomaly shown in figure E2 was generated using a 64-km averaging radius. The resulting value is about equal to the free-air anomaly that would be measured at a station at the average altitude and corrects the free-air anomaly for the strong dependence on the altitude of the individual stations. The resulting anomaly is a form of isostatic anomaly called the average free-air or Faye anomaly (Mabey, 1966). On the residual-gravity anomaly map of the region (fig. E2), the values in eastern Idaho are generally more positive than those to the west, and the major gravity high in the eastern part of the Challis quadrangle is a prominent regional feature. With values near zero, the area of the Idaho batholith appears to be more nearly consistent with the residual anomaly than the area to the east and was chosen to represent the residual gravity anomaly from which the interpreted cross sections (figs. E6–E8) were derived.

The complete Bouguer anomaly map of the Challis quadrangle (fig. E3) shows the strong inverse correlation with regional elevation; the trough of lowest values is over the Sawtooth batholith in the south and over the Van Horn Peak cauldron complex in the north. The residual gravity anomaly (fig. E4), from which the correlation with regional altitude is largely removed, better illustrates the local gravity anomalies. Gravity lows are produced by the low-density sedimentary rocks underlying the intermontane valleys. The largest low is over the Sawtooth Valley with a smaller low over Round Valley. Large gravity lows are over the Van Horn Peak and Thunder Mountain cauldron complexes. Gravity highs and lows are over the Cretaceous and Tertiary plutons. The largest is the low over the Idaho batholith. The crest of the large north-trending gravity high in the southeastern part of the quadrangle approximately coincides with the Bayhorse anticline in Paleozoic sedimentary rocks (Hobbs, chap. D, this volume).

The residual magnetic field (fig. E5) shows a broad low over the Idaho batholith. Most of the local highs within this low reflect Tertiary intrusions. In the west the older phases of the batholith are marked by increased magnetic intensity. The Sawtooth batholith and the Casto pluton both produce large magnetic highs. Several areas of Tertiary volcanic rocks produce positive or negative anomalies depending on the direction of remanent magnetization. A very large magnetic high occurs over volcanic rock at the southeastern edge of the Van Horn Peak cauldron complex. An extensive magnetic high occurs in the area of the Bayhorse anticline. The magnetic high in the northeastern corner of the quadrangle is part of a 110-km-long high trending northwest across Precambrian quartzite and phyllite. This regional anomaly trends toward the Blackbird cobalt mine a few kilometers north of the quadrangle but terminates short of the mine.

Several linear or nearly linear features are apparent on the gravity and magnetic maps (figs. E2–E5). The clearest feature, here called the Yankee Fork lineament (fig. E3), is one of a series of northeast-trending lineaments in eastern Idaho; the most prominent is the eastern Snake River Plain. The Yankee Fork lineament forms the northern limit of abundant Paleozoic rock and the southeastern limit of the Van Horn Peak cauldron complex; it approximately coincides with the trans-Challis fault system (Kiilsgaard and Lewis, chap. B, this volume). Another less well defined lineament is here called the Mayfield lineament (fig. E3). These two lineaments appear to define blocks of crust having contrasting physical properties that have responded differently to the regional stress affecting central Idaho.

GRAVITY AND MAGNETIC PROFILES

The major regional gravity and magnetic anomalies in the Challis quadrangle are shown by three profiles (figs. E4–E8); two that trend generally east across the quadrangle and one that trends southeast across the Van Horn Peak cauldron complex. Structural cross sections shown with the profiles (figs. E6–E8) were produced by a Marquardt (1963) nonlinear inversion technique operating on both the gravity and magnetic data (Webring, 1985).

At the western end of the northern east-west profile (*A–A′*, fig. E6), both the Bouguer and average free-air gravity anomalies increase westward toward the border phases of the Idaho batholith. The Thunder Mountain cauldron complex is indicated by a gravity low and strong magnetic relief over part of the complex. Gravity and magnetic highs occur over the Casto pluton; these highs match the higher density and susceptibility of the rocks, measured from a limited number of samples, compared to the Idaho batholith. The gravity low over the Panther Creek graben indicates subsurface structure that correlates well with the structure inferred from the surface geology. The magnetic high at the eastern end of the profile is over the magnetite-rich zone in the Precambrian sedimentary rocks.

Profile *B–B′* crosses the Van Horn Peak cauldron complex (fig. E7). It shows anomalies over the Thunder Mountain cauldron complex and the Casto pluton that are similar to profile *A–A′*. The broad gravity low over the Van Horn Peak cauldron complex (fig. E4) contains

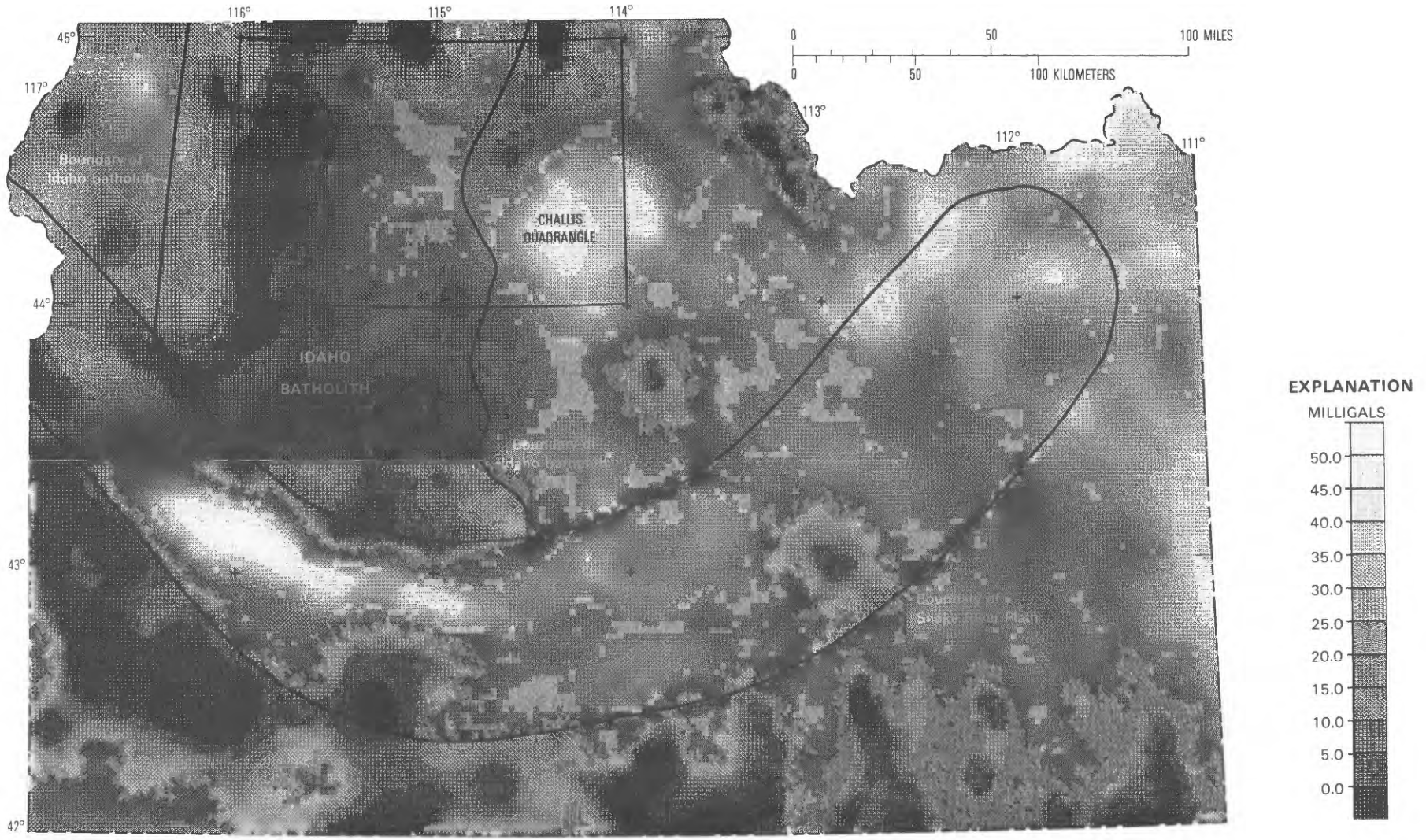

Figure E2. Residual gravity anomaly map of southern Idaho.

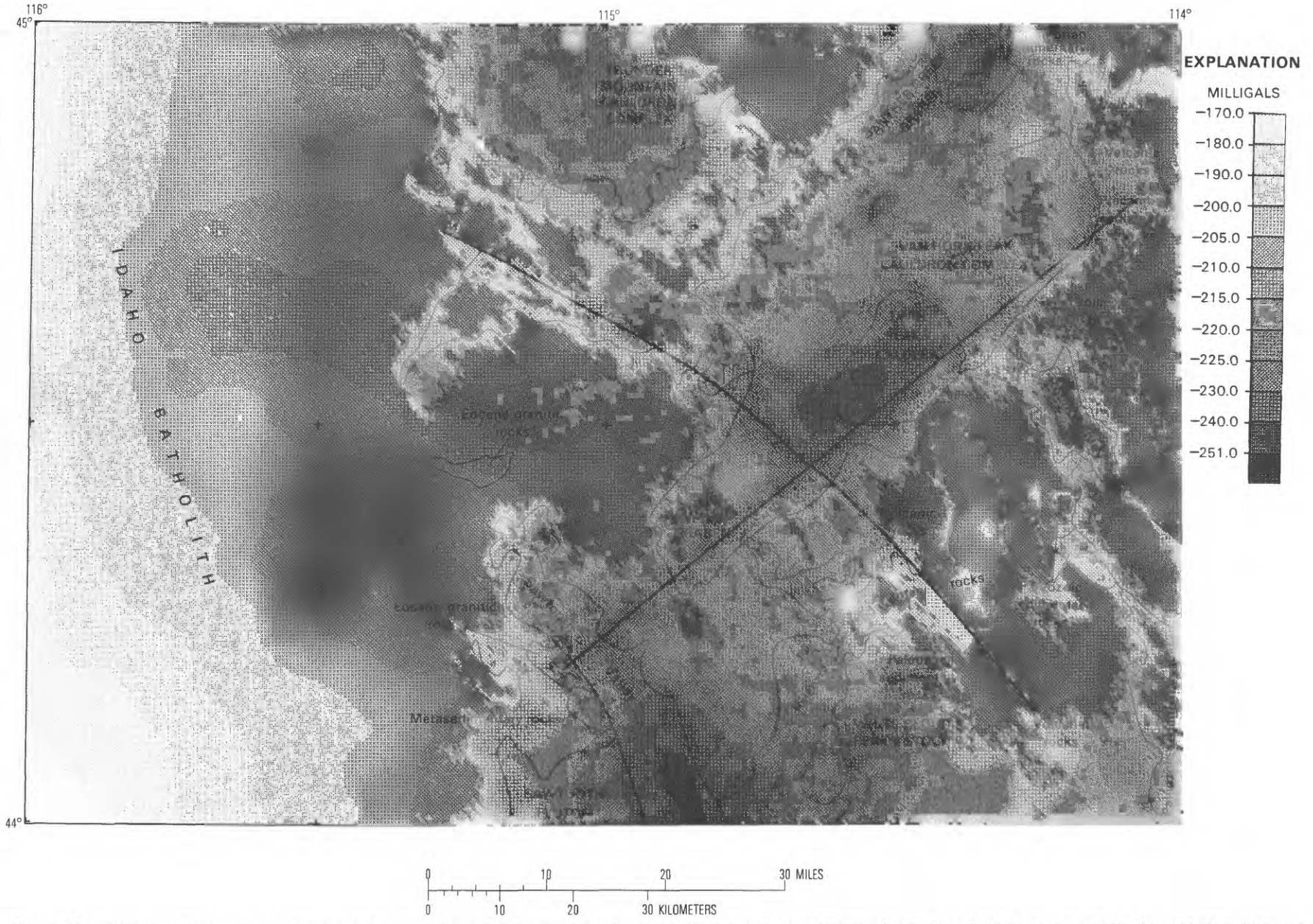

Figure E3. Complete Bouguer gravity anomaly map of the Challis quadrangle. Reduction density is 2.67 g/cm^3. ML, Mayfield lineament; YFL, Yankee Fork lineament.

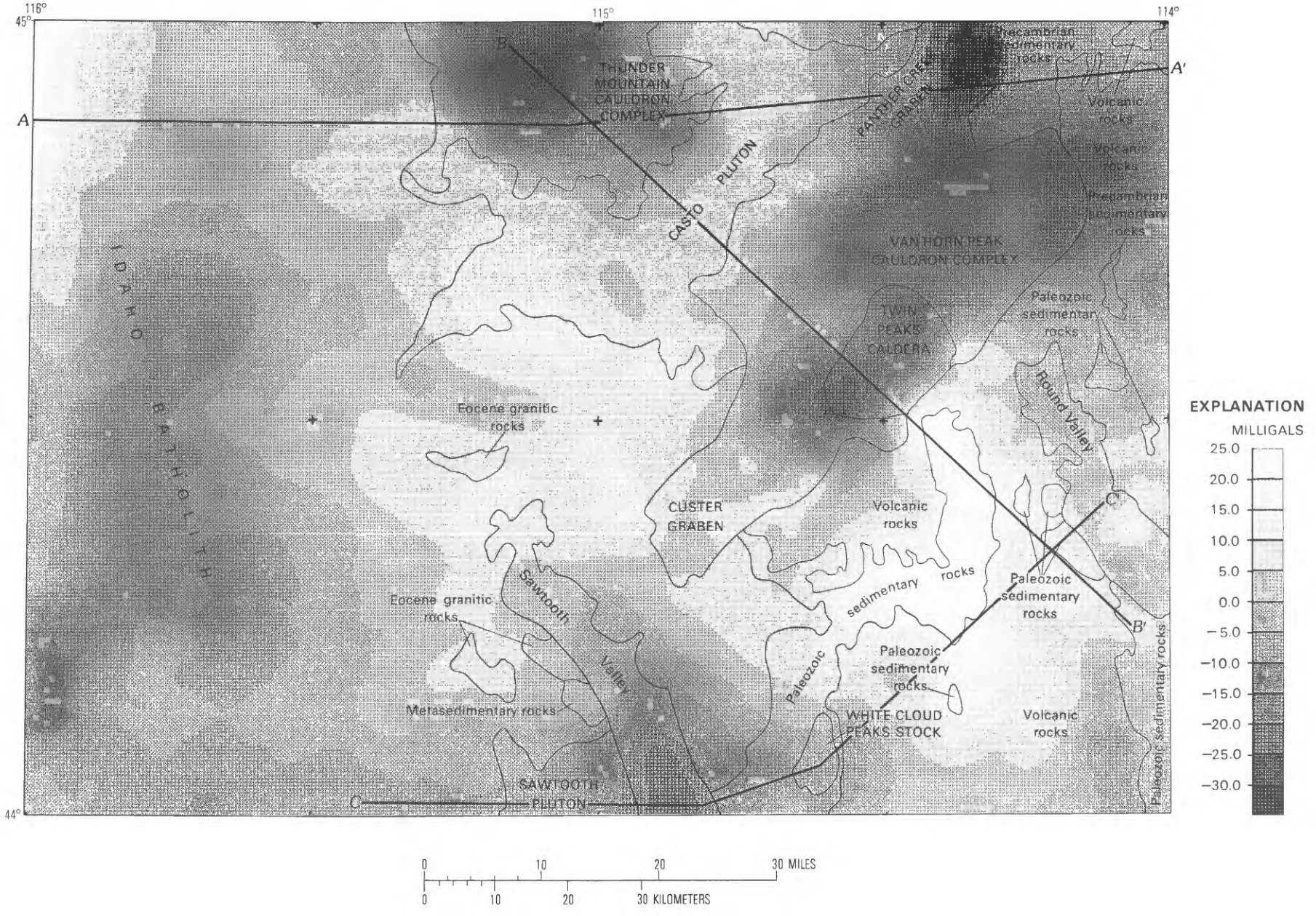

Figure E4. Residual gravity anomaly map of the Challis quadrangle, showing lines of profiles shown in figures E6–E8.

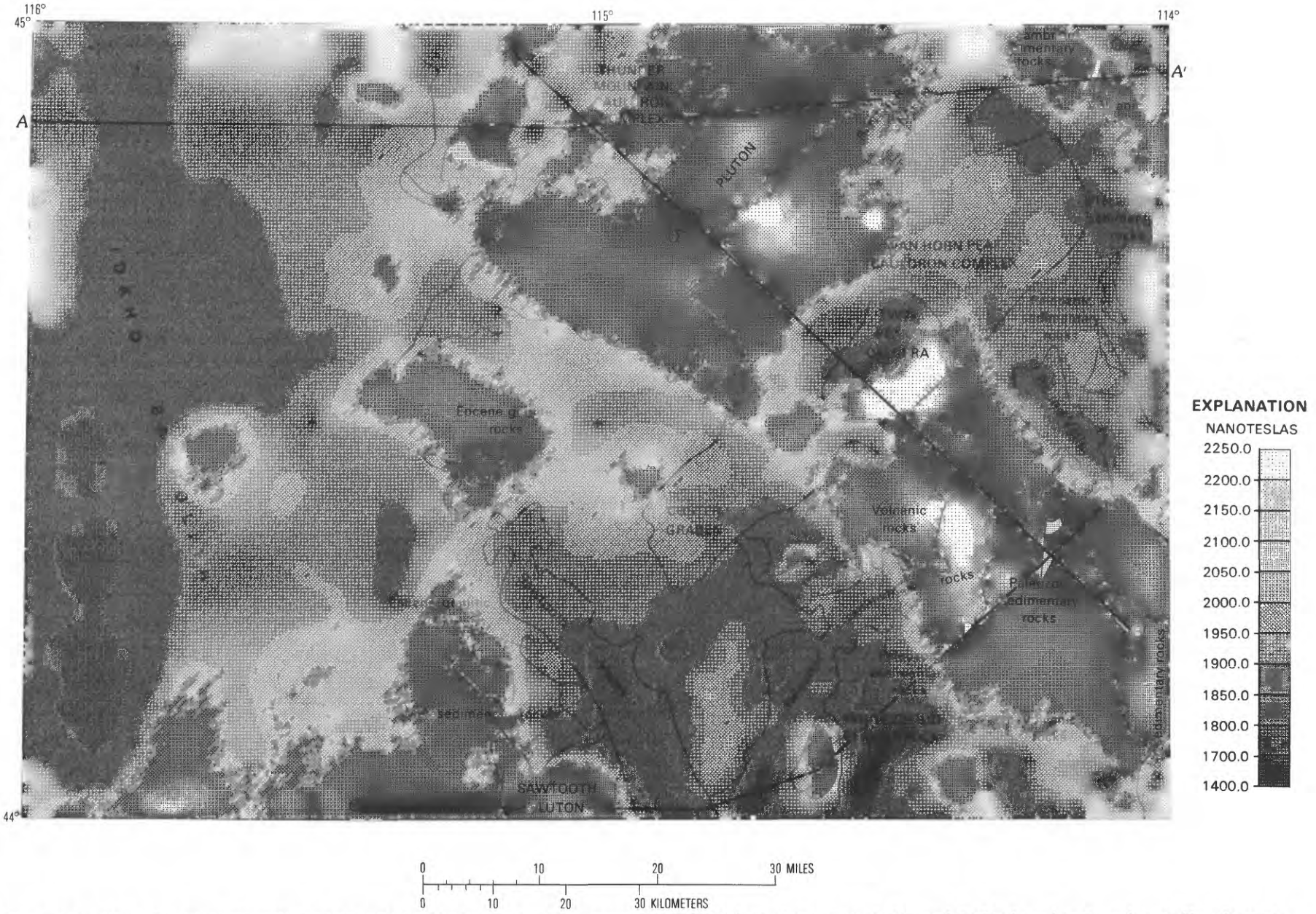

Figure E5. Map of residual magnetic anomaly of the Challis quadrangle measured at 12,000 feet. Lines *A–A′*, *B–B′*, and *C–C′* show locations for profiles shown in figures E6–E8.

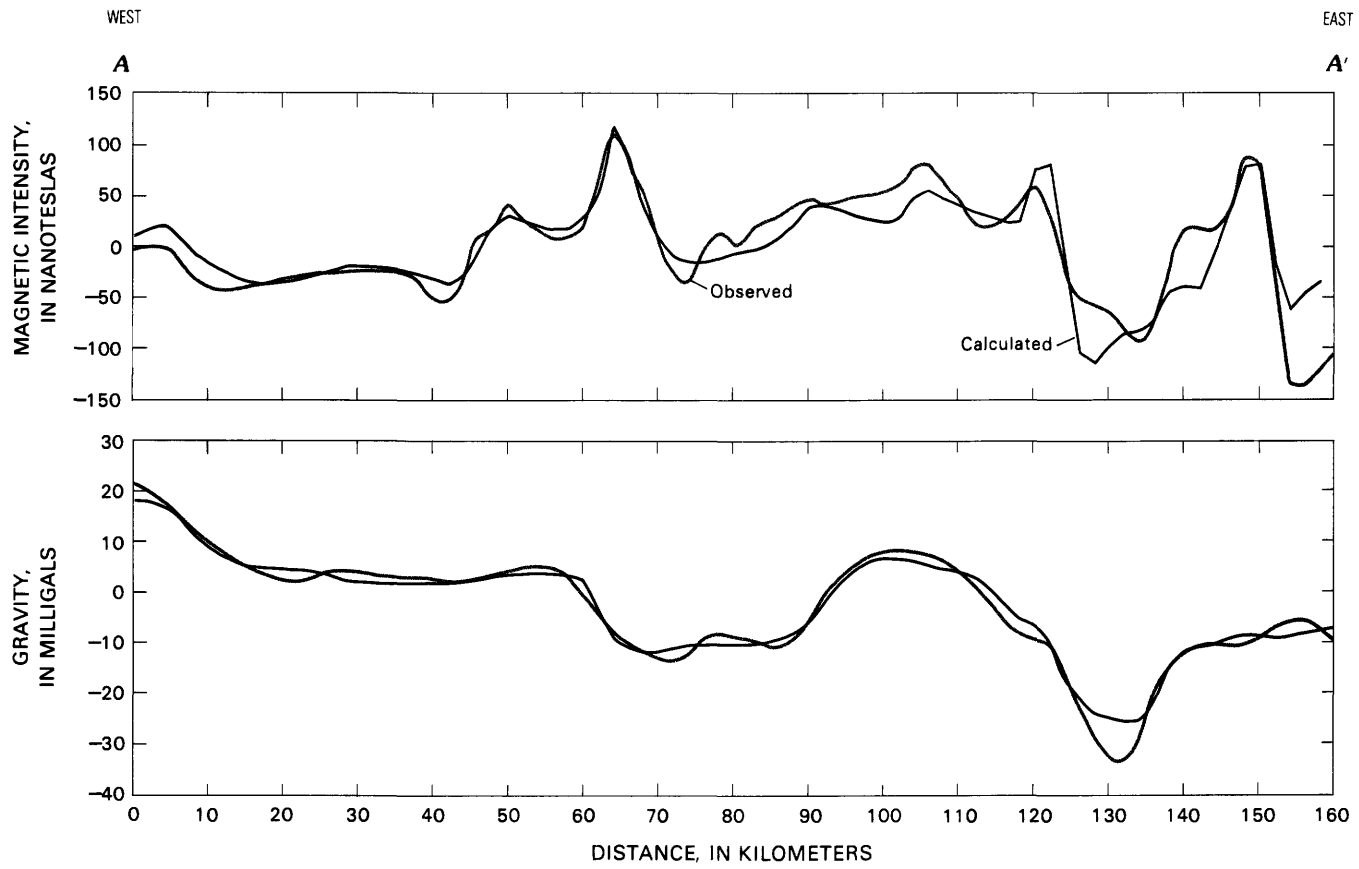

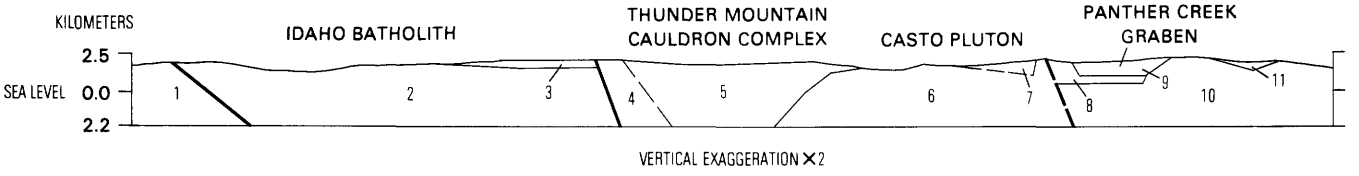

Figure E6. Profiles of magnetic and gravity data, and model showing variations in physical properties of rocks along line *A–A'*, Challis quadrangle. Line of profiles shown in figures E4 and E5. Dashed lines indicate poorly resolved boundaries.

an interior low on the southeast, over the Twin Peaks caldera. This anomaly is caused partly by the low-density fill in the cauldron complex but may also be caused partly by underlying low-density intrusive bodies. The highest amplitude magnetic anomaly in the Challis quadrangle lies near the southeastern edge of the Twin Peaks caldera. The anomaly can be produced by a tabular, steeply dipping mass that is modeled as a ring-fracture intrusive body.

Profile *C–C'* (fig. E8) shows a magnetic high over the Sawtooth batholith. Modeling of this anomaly indicates that part of the Sawtooth batholith is downfaulted under Sawtooth Valley. The gravity and magnetic lows that coincide approximately with the valley appear to reflect both the low-density basin fill and a weak reverse magnetization of the Sawtooth batholith. East of Sawtooth Valley, at 110 km from the western end of

Body no.	Density (gm/cm^3)	Magnetic susceptibility ($cgsx10^{-3}$)	Rock characteristics
1	2.66	1.0	Idaho batholith; tonalite.
2	2.55	.5	Idaho batholith; granodiorite.
3	2.70	3.8	Precambrian metasedimentary rocks.
4	2.46	2.2	Thunder Mountain cauldron complex; volcanic rocks more magnetic than no. 5.
5	2.46	1.19	Thunder Mountain cauldron complex; volcanic rocks.
6	2.58	1.81	Casto pluton; granitic rocks.
7	2.32	.04	Van Horn Peak cauldron complex; volcanic rocks.
8	2.23	1.10	Panther Creek graben; lower layer rocks of unknown composition.
9	2.13	-.77	Panther Creek; volcanic rocks of upper layer.
10	2.60	3.0	Precambrian metasedimentary rocks; same as no. 3 at surface; unknown at depth.
11	2.48	-1.0	Volcanic rocks.

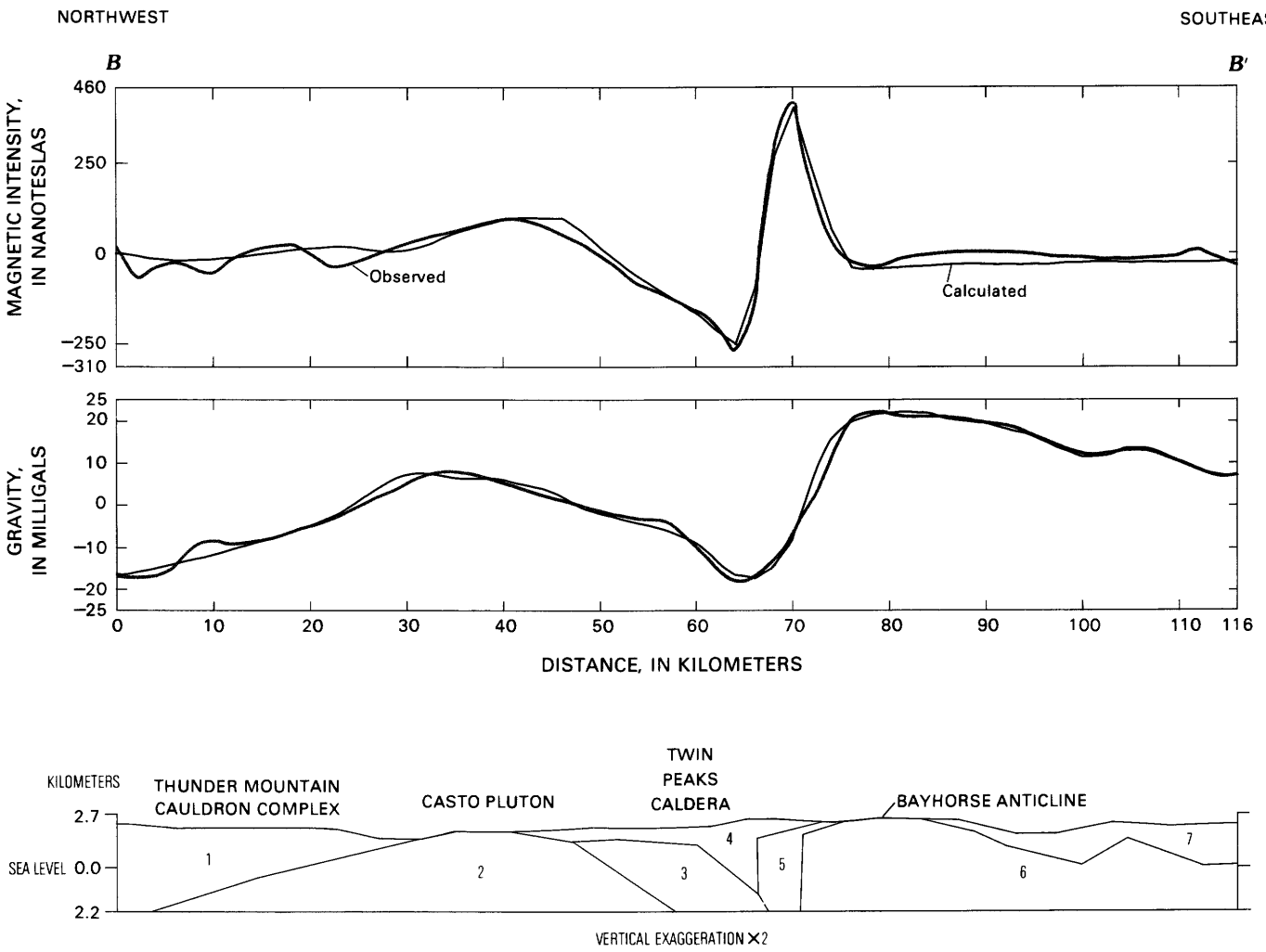

Figure E7. Profiles of magnetic and gravity data, and model showing variations in physical properties of rocks along line *B–B'*, Challis quadrangle. Line of profiles shown in figures E4 and E5. Dashed line indicates poorly resolved boundary.

profile *C-C'* (fig. E8), a prominent magnetic high occurs over the White Cloud Peaks stock. The large magnetic low over the adjoining outcrop of Eocene volcanic rocks indicates reverse remanent magnetization. Gravity and magnetic highs coincide approximately with the Bayhorse anticline where it is intersected by the profile. The gravity high is offset slightly to the west and the magnetic high to the east. The axis of the gravity high closely follows the axis of the anticline, but the magnetic high does not. The eastern edge of the gravity high coincides approximately with the Salmon River lineament of Hobbs (chap. D, this volume).

Body no.	Density (gm/cm^3)	Magnetic susceptibility ($cgs \times 10^{-3}$)	Rock characteristics
1	2.47	1.18	Thunder Mountain cauldron complex; volcanic rocks.
2	2.56	1.89	Casto pluton; granitic rocks.
3	2.50	-.56	Twin Peaks caldera; weak reverse remanent magnetization.
4	2.35	-1.10	Twin Peaks caldera; surface layer, reverse remanent magnetization.
5	2.39	4.7	Twin Peaks caldera; ring-fracture intrusion, highly magnetic.
6	2.67	.1	Bayhorse anticline; Paleozoic sedimentary rocks.
7	2.45	.1	Combination of alluvial valley fill and volcanic rocks.

CONCLUSIONS

The regional gravity and magnetic data for the Challis quadrangle indicate that the part of the Idaho batholith in the quadrangle is a low-density mass and is relatively weakly magnetic. Eocene intrusive masses appear to be more extensive in the subsurface than at the ground surface. The geophysical data generally confirm the structures defined by surface mapping of the Thunder Mountain and Van Horn Peak cauldron complexes. A regional magnetic high in the northeastern corner of the quadrangle is produced by magnetite-rich zones in Precambrian sedimentary rocks. The high average topographic altitude of the quadrangle is an isostatic response to a mass deficiency at depth.

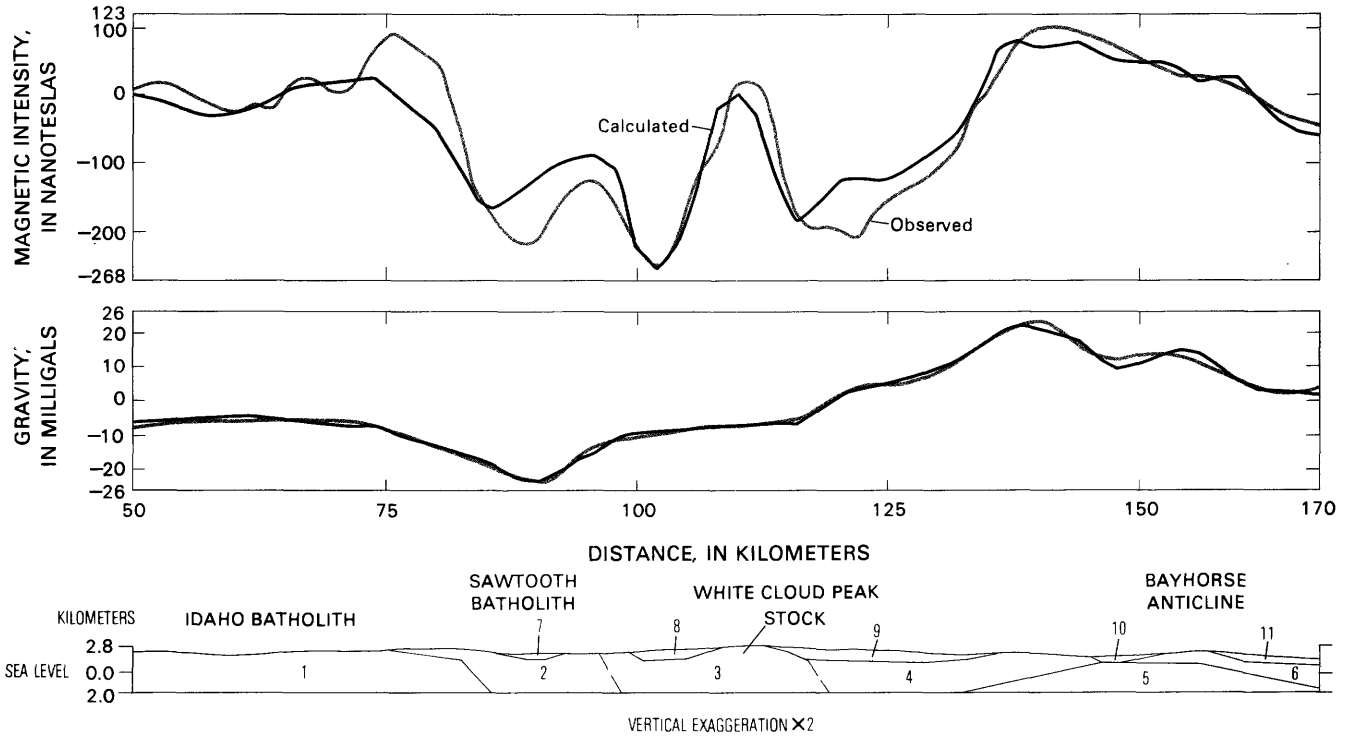

Figure E8. Profiles of magnetic and gravity data, and model showing variations in physical properties of rocks along line C–C', Challis quadrangle. Line of profiles shown in figures E4 and E5. Dashed lines indicate poorly resolved boundaries.

The geophysical data can be used to define several blocks of crust within the Challis quadrangle. These blocks appear to have distinctive lithologies and different geologic histories.

The regional geophysical data can be used to develop exploration strategies and to identify broad targets for more intensive exploration. For example, the magnetic and gravity anomalies can be used to infer the location and three-dimensional geometry of some of the large intrusive bodies that are related to mineral occurrences, and subtle magnetic lows appear to indicate areas of alteration.

Body no.	Density (gm/cm^3)	Magnetic susceptibility ($cgs \times 10^{-3}$)	Rock characteristics
1	2.55	1.5	Idaho batholith; granodiorite.
2	2.46	-.2	Sawtooth batholith; granite.
3	2.55	.1	White Cloud Peaks stock; granodiorite.
4	2.74	.1	Bayhorse anticline; Paleozoic sedimentary rocks.
5	2.67	2.2	Bayhorse anticline; Precambrian metasedimentary rocks.
6	2.68	.1	Paleozoic sedimentary rocks.
7	2.10	.1	Alluvial fill in Sawtooth Valley.
8	2.52	-3.2	Combination of Paleozoic sedimentary rocks and Tertiary volcanic rocks.
9	2.31	-4.0	Volcanic rocks.
10	2.41	.5	Volcanic rocks.
11	2.27	2.4	Alluvial valley fill.

REFERENCES CITED

Cater, F. W., Pinckney, D. M., Hamilton, W. B., Parker, R. L., Weldin, R. D., Close, T. J., Zilka, N. T., 1973, Mineral resources of the Idaho Primitive Area and vicinity, Idaho, *with a section on* Aeromagnetic interpretation, by W. E. Davis: U.S. Geological Survey Bulletin 1304, 431 p.

Mabey, D. R., 1966, Relation between gravity anomalies and regional topography in Nevada and the eastern Snake River Plain, Idaho: U.S. Geological Survey Professional Paper 550-B, p. B108-B110.

Marquardt, D. W., 1963, An algorithm for least-squares estimation of nonlinear parameters: Journal of the Society of Industrial and Applied Mathematics, v. 11, no. 2, p. 431-441.

Webring, M. W., 1985, SAKI—A FORTRAN program for generalized linear inversion of gravity and magnetic profiles: U.S. Geological Survey Open-File Report 85-122, 104 p.

Webring, M. W., and Mabey, D. R., 1981, Principal facts for gravity stations in the Challis 1°×2° quadrangle, Idaho: U.S. Geological Survey Open-File Report 81-652, 24 p., 1 sheet, scale 1:250,000.

Symposium on the Geology and Mineral Deposits of the Challis 1°×2° Quadrangle, Idaho

Chapter F

Tertiary Plutons and Related Rocks in Central Idaho

By EARL H. BENNETT[1] *and* CHARLES R. KNOWLES[1]

CONTENTS

FIGURES

TABLES

[1]Idaho Geological Survey, Moscow, Idaho 83843

Abstract

The Tertiary plutonic rocks in the Challis quadrangle are a bimodal suite consisting of 42- to 45-m.y. (million years)-old epizonal granite and 45- to 50-m.y.-old quartz monzodiorite. Both rock types are best exposed in the central one-third of the quadrangle. Each plutonic type has an associated hypabyssal intrusive equivalent, which collectively are known as the Idaho porphyry belt, and other dike swarms. Areal distribution and similarity of rock type suggest that each of the hypabyssal units has a volcanic equivalent that is part of the Eocene Challis Volcanics.

The Tertiary granite and quartz monzodiorite complexes are generally found near each other. These rocks have many of the characteristics of anorogenic (A-type) granite and are probably genetically related to intracontinental rifting or extension.

Many of the intrusive rocks in the north-central and eastern parts of the map area are along major northeast-trending faults that are related to Eocene extension. One of these structures is named the trans-Challis fault system. The system extends across Idaho and possibly Montana. Major northwest-trending basin-and-range structures in the southern Atlanta lobe terminate against the trans-Challis fault system. The system and similar northeast-trending structures are complicated by regional uplift that has been more extensive in the western part of the Idaho batholith, where plutonic rocks of Cretaceous are forming the core of the Atlanta lobe are exposed.

The Tertiary plutons, including the Sawtooth batholith and others in the Hailey 1°×2° quadrangle, south of the Challis quadrangle, are exposed in a series of rhomboid-shaped fault blocks formed by the intersection of major northwest- and northeast-trending faults. The northwest-trending faults are basin-and-range structures that produced a series of horsts and grabens. Erosion of the horst blocks has exposed the Tertiary plutons; grabens contain older plutonic units of the Idaho batholith.

INTRODUCTION

Geologic mapping and related laboratory studies conducted as part of the Challis 1°×2° quadrangle CUSMAP (Conterminous United States Mineral Assessment Program) project have produced new information about the plutonic, hypabyssal, and volcanic rocks of Tertiary age in central Idaho. The bimodality of the plutonic suite and the close relationship between the plutonic rocks and equivalent hypabyssal and volcanic units is a major finding of the study (table F1).

Acknowledgments.—The following University of Idaho students assisted in the field work for this study: W. B. Strowd, R. S. Lewis, M. J. Barber, E. A. Kaufman, D. J. Shiveler, Ted Cammarata, P. C. Rogers, T. M. Scanlan, and D. A. Cockrum.

PREVIOUS WORK

The pioneering study in the Challis quadrangle was of the Casto 30-minute quadrangle by C. P. Ross (1934). He mapped and named the Casto pluton (fig. F1, area 12) and several diorite bodies (fig. F1, areas D, F). He also described and subdivided the Challis Volcanics and the Casto Volcanics. Cater and others (1973) mapped part of the diorite along the Rapid River (fig. F1, area H) and noted that the Casto Volcanics are probably altered units of the Challis Volcanics; he abandoned the name "Casto Volcanics."

Olson (1968) first described the Idaho porphyry belt, a series of hypabyssal dikes that extends from the Boise Basin to the Casto quadrangle. Hyndman and others (1977) recognized that the dike swarm appeared to truncate northwest-trending basin-and-range structures in eastern Idaho. The Sawtooth batholith (fig. F1, area 26) was mapped by Reid (1963). Tschanz and others (1974) described Tertiary units in the Sawtooth National Recreation Area (fig. F1, areas 32, 33, Q, R).

Studies that were made of the Tertiary plutonic rocks in general include those by Anderson (1952) and Ross (1928, 1963). Armstrong (1975) published numerous age dates on the Tertiary plutonic rocks and interpreted these dates. Swanberg and Blackwell (1973) summarized the state of knowledge about the Idaho batholith and noted the high radioactivity associated with the Tertiary granite. Also, they first described and named the Twin Springs pluton (fig. F1, area 29). Bennett (1980a) described the Tertiary granite in Idaho and noted the similarities between numerous individual granite bodies. Criss (1981) and Criss and Taylor (1983) interpreted oxygen isotope data and age dates in the Tertiary granite in the Atlanta lobe of the Idaho batholith.

LITHOLOGY OF THE PLUTONS AND RELATED ROCKS

The Tertiary plutonic rocks in central Idaho are a bimodal suite of granite and quartz monzodiorite, as indicated by the modes and norms calculated from studies of samples of the rocks in the Challis quadrangle (fig. F2). This bimodality is similar to other Tertiary igneous systems in the western United States (Lipman and others, 1972). Rock names used are from the IUGS (International Union of Geological Sciences) classification (Streckeisen, 1976).

In many places the monzodiorite bodies are intimately mixed with numerous hypabyssal rhyodacite-dacite bodies. These mixed rocks are called monzodiorite in

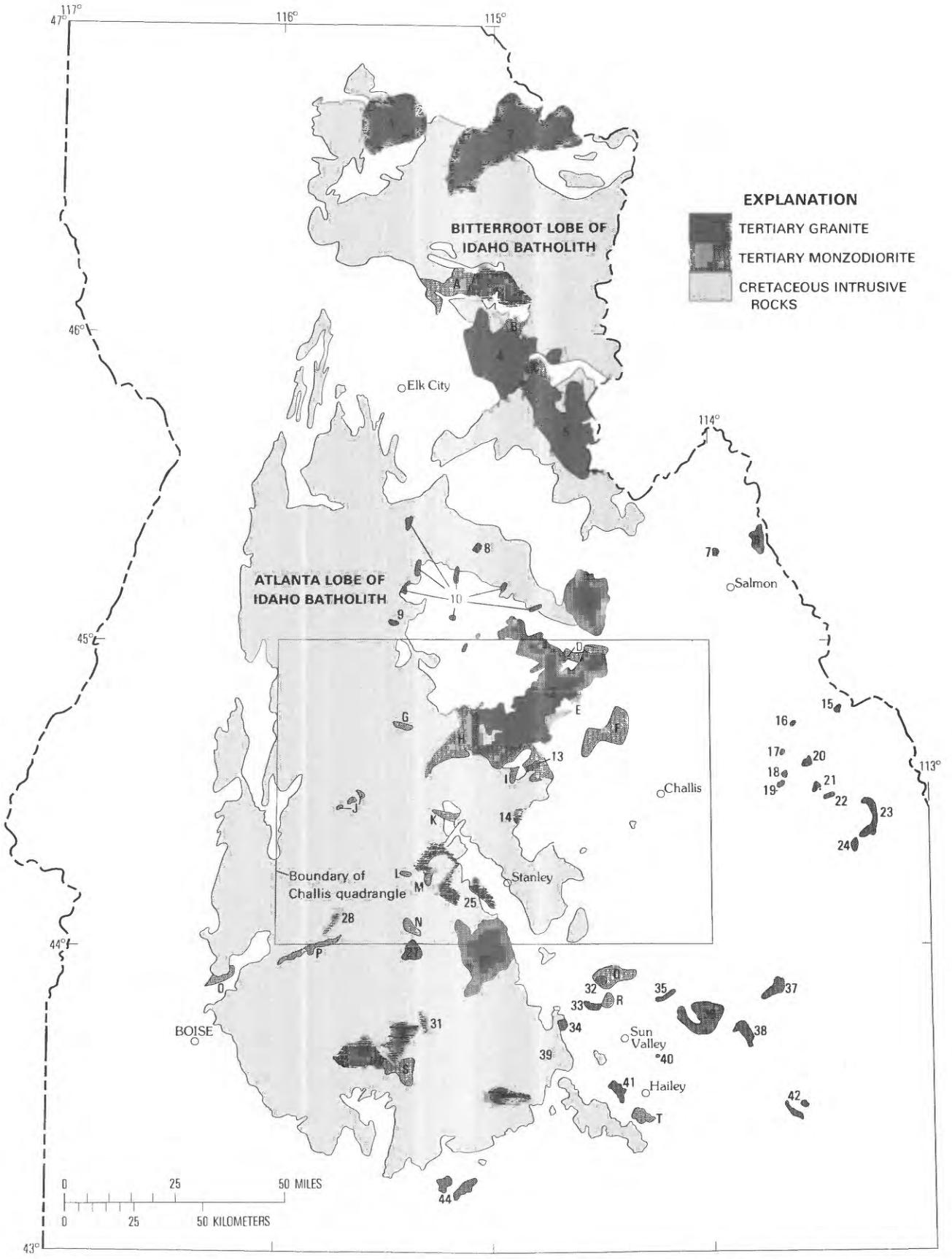

Figure F1. Map and table showing location of Tertiary and Cretaceous plutonic rocks. Modified from Bennett (1980a).

Tertiary granite plutons in Idaho
[Do., ditto]

Map No.	Name	Age and dating method	Reference
1	Bungalow stock	43 m.y., K-Ar	Hietanen (1969).
2	Lolo batholith	Age unknown	Nold (1974).
3	Whistling Pig pluton	51 m.y., K-Ar (hornblende)	Toth (1983); Greenwood and Morrison (1973).
4	Running Creek pluton	49 m.y., K-Ar	Toth and others (1983); Greenwood and Morrison (1973).
5	Painted Rocks pluton (Painted Lake stock?).	Age unknown	Toth and others (1983); Fisk (1969).
6	Carmen stock	----do.	Ruppel (1978).
7	Bobcat Gulch	49 m.y., K-Ar	Bunning and Burnet (1981).
8	Whimstick Creek stock	Age unknown	Bennett (unpub. data).
9	Logan Creek stock	38 m.y., K-Ar	B. F. Leonard, U.S. Geological Survey, written commun., 1979.
10	Small unnamed stocks in Idaho Primitive Area.	Age unknown	Cater and others (1973).
11	Crags pluton	44-48 m.y., K-Ar	Cater and others (1975).
12	Casto batholith	43 m.y., K-Ar	Cater and others (1973); Ross (1934).
13	Casto batholith, Tincup outlier.	Age unknown	Ross (1934).
14	Knapp Peak stock	----do.	Fisher and others (1983).
15	Little Eightmile stock	----do.	Ruppel (1978).
16	Alder Creek stock	----do.	Do.
17	Falls Creek stock	----do.	Do.
18	North Fork stock	----do.	Do.
19	Ima stock (concealed)	48 m.y., K-Ar	Ora Rostad, AMAX Corp., written commun., 1978.
20	Blue Jay stock	51 m.y., K-Ar	Ruppel (1978).
21	Park Fork stock	Age unknown	Do.
22	Big Timber stock	----do.	Do.
23	Gilmore stock	49 m.y., K-Ar (dike)	Do.
24	Sawmill Canyon stock	Age unknown	Do.
25	North Sawtooth batholith	----do.	Fisher and others (1983).
26	Sawtooth batholith	45 m.y. (about), K-Ar	Fisher and others (1983); Kiilsgaard and others (1970); Reid (1963).
27	Sawtooth batholith (Tenmile).	43.6 m.y., K-Ar	Kiilsgaard (1983).
28	Unnamed pluton	Age unknown	Fisher and others (1983).
29	Twin Springs pluton	38-39 m.y., K-Ar	Swanberg and Blackwell (1973); Criss (1981).
30	Dismal Swamp stock	44 m.y., K-Ar	Bennett (1980a); Criss (1981).
31	Steel Mountain stock	Age unknown	Bennett (1980a).
32	Ibex Canyon stock	----do.	Tschanz and others (1974).
33	Boulder stock	----do.	Do.
34	Prairie Creek stock	----do.	C. M. Tschanz, U.S. Geological Survey, written commun., 1979.
35	Summit Creek stock	----do.	Dover and others, (1976).
36	Pioneer Mountain stock	45 m.y., K-Ar	Do.
37	Mackay stock	40-50 m.y., zircon	Nelson and Ross (1968).
38	Lake Creek pluton	48 m.y., K-Ar	Paull and others (1972).
39	Shaw Mountain stock	Age unknown	C. M. Tschanz, U.S. Geological Survey, written commun., 1979.
40	Possible stock beneath Triumph mine.	----do.	Hall and others (1978).
41	Clarendon Hot Springs stock.	----do.	Bennett (unpub. data).
42	Possible Tertiary intrusion in Lava Creek mining district.	----do.	Ross (1931); Anderson (1929).
43	Soldier Mountain stock	----do.	Bennett (unpub. data).
44	Hall Gulch stock	----do.	R. F. Delong (University of Idaho, unpub. data).

Figure F1 Continued.

this chapter. Numerous rhyolite dikes in the Challis map area are believed to be related to the Tertiary granitic intrusions.

In general, the monzodiorite and the granite plutons are closely associated spatially. The Casto pluton, for example, is ringed by several monzodiorites (fig. F1, areas D, E, F, H, I). The granite plutons and diorite are very similar in age also (fig. F1, table), and they may possibly be comagmatic. The ages of the three monzodiorites in the Bitterroot lobe of the Idaho batholith (fig. F1, areas A, B, C) are highly speculative as there are no dates available for these units, but they are lithologically similar to the Tertiary diorites in the Atlanta lobe (Toth, 1983). As noted, each plutonic rock type has a hypabyssal

Tertiary monzodiorite-dacite-rhyodacite complexes and plutons in Idaho
[Do., ditto]

Map No.	Name	Age and dating method	Reference
A	Unnamed monzodiorite	Age unknown	Toth and others (1983).
B	do.	do.	Do.
C	do.	do.	Do.
D	do.	do.	Ross (1934); Fisher and others (1983).
E	do.	do.	Fisher and others (1983).
F	do.	do.	Do.
G	Lake Mountain stock	do.	Do.
H	Monzodiorite along the Rapid River.	do.	Do.
I	Monzodiorite at Pinyon Peak.	do.	Bennett (unpub. data).
J	Monzodiorite at Monumental Peak.	47.2 m.y., K-Ar	Robert Fleck, written commun., 1983.
K	Diorite at Cape Horn Lakes.	47.1 m.y., K-Ar	Fisher and others (1983); Armstrong (1975); Olson (1968); Lewis (1984).
L	Unnamed monzodiorite	Age unknown	Fisher and others (1983).
M	do.	do.	Do.
N	Diorite at Jackson Peak	46-50 m.y., K-Ar	Do.
O	Diorite at Horseshoe Bend.	Age unknown	Anderson (1934).
P	Diorite of Boise Basin	44-48 m.y., K-Ar	Fisher and others (1983); Anderson (1947); Olson (1968); Percious and others (1967).
Q	Diorite of Ibex Canyon	Age unknown	Tschanz and others (1974).
R	Diorite of Silver Peak	do.	Do.
S	Diorite of Trinity Mountain.	44 m.y., K-Ar	Bennett (1980a); Criss (1981).
T	Quartz diorite of Hailey	do.	Hall and others (1974).

Figure F1 Continued.

equivalent (granite-rhyolite, monzodiorite-rhyodacite to dacite). Each type also has volcanic equivalents that are described later.

Monzodiorite and related rocks

Typical monzodiorite in the Challis quadrangle is coarse-grained, hornblende-bearing, quartz monzodiorite that contains mafic restite inclusions in places. A good example of this rock type is exposed at Jackson Peak (fig. F1, area N). Similar occurrences are at Monumental Peak (area J), Lake Mountain (area G), below Pinyon Peak (area I), and at Cape Horn Lakes (area K). These monzodiorite plutons, although generally distinctive in the field, can be confused with tonalite of Cretaceous age in the quadrangle (Kiilsgaard and Lewis, chap B, this volume), as in the Loon Creek area, where both occur. The monzodiorite and tonalite can generally be distinguished in thin section, because plagioclase zoning in the older tonalite is simple, whereas plagioclase zoning in the Tertiary monzodiorite is quite complex (Lewis, 1984).

The diorites within the Challis quadrangle are typified by the large body along Rapid River (fig. F1, area H). The diorite of Rapid River consists of small monzodiorite stocks and thousands of rhyodacite-dacite dikes, which intrude the older rocks of the Idaho batholith.

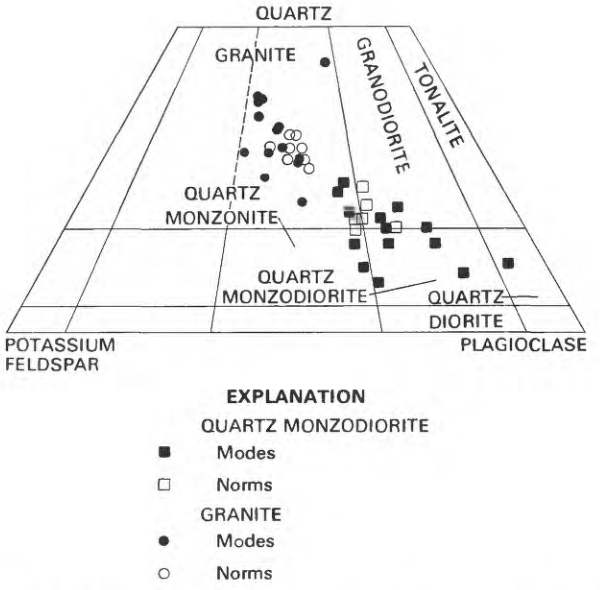

Figure F2. Classification diagram showing composition of samples from several Tertiary granite plutons and diorite complexes, Atlanta lobe of the Idaho batholith, central Idaho. Composition determined from modes and norms of samples. Classification diagram from Streckeisen (1976).

These exposures are probably equal in size to the Sawtooth batholith. Rapid River and the Middle Fork of the Salmon River dissect the diorite, and the best exposures of it are

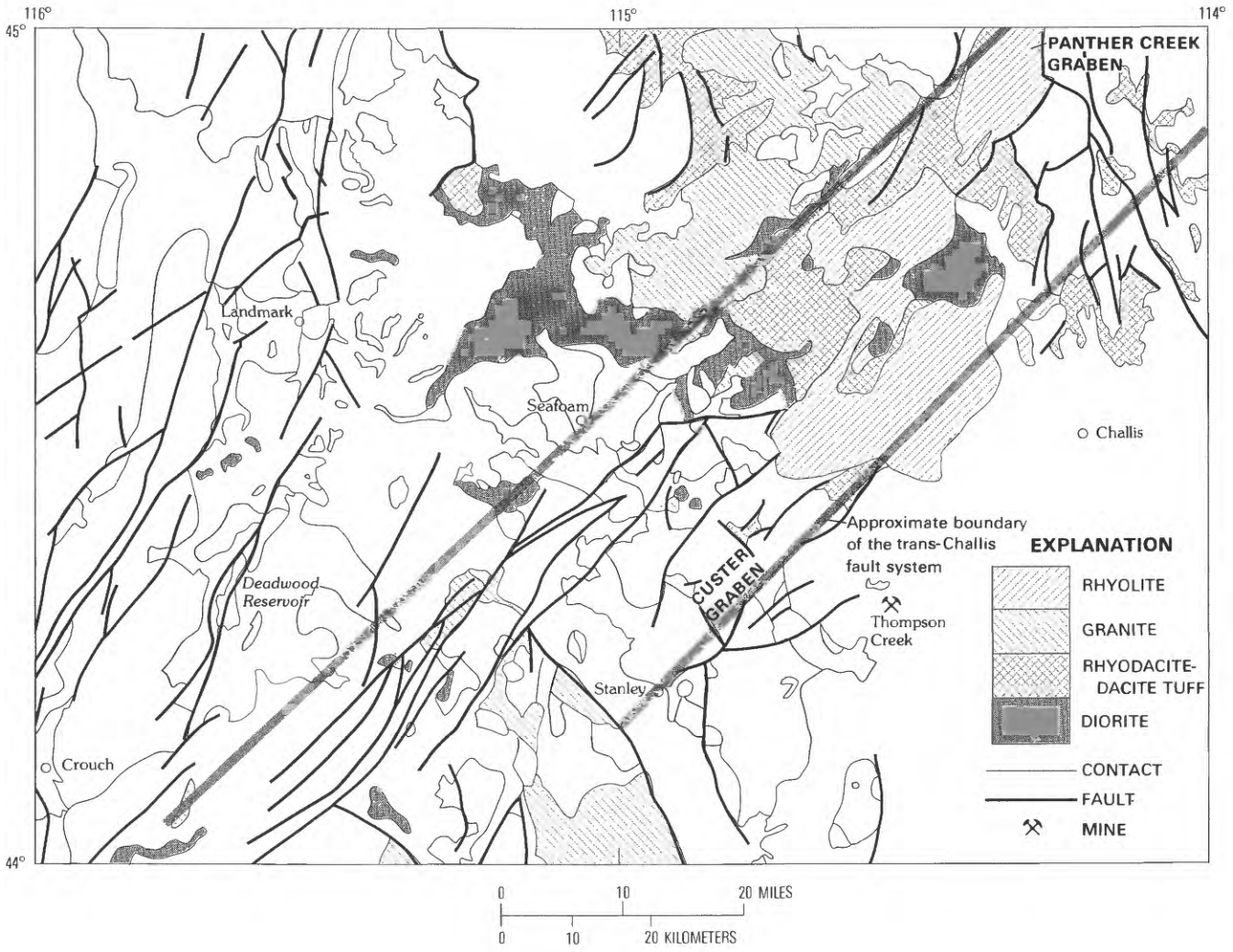

Figure F3. Map showing the trans-Challis fault system and Tertiary plutonic and volcanic units. Units not described are shown on figure A2 (chap. A).

along the river valleys. The Middle Fork of the Salmon River at Indian Creek makes a U-shaped bend, following the contact between the diorite and older batholithic rocks to the north (Fisher, chap. A, fig. A2, this volume).

The rhyodacite-dacite dikes in the diorite of Rapid River are good examples of hypabyssal equivalents of the monzodiorite bodies in the Challis quadrangle. The dikes generally consist of fine-grained, gray to green rock that is porphyritic in places. Phenocrysts where present consist of hornblende, biotite, and plagioclase in varying proportions. These dikes are widespread throughout the batholith and, with rhyolite dikes that are the hypabyssal equivalent of the granite, make up most of the Tertiary dike swarms in the Atlanta lobe.

The probable volcanic equivalents of the plutonic (monzodiorite) and hypabyssal (rhyodacite-dacite) units are the tuff of Ellis Creek, the tuff of Eightmile Creek, and the tuffs of Camas Creek and Black Mountain (formerly called the Casto Volcanics) (table F1; Ekren, chap. C, this volume). The map patterns of these units closely conform to the geologic map pattern of the Casto Volcanics as shown by Ross (1934). The composition and age of these volcanic rocks are similar to the diorite stocks and dikes, and they are spatially related.

Granite and related rocks

Tertiary granite in the Idaho batholith is more widespread than monzogranite or diorite and is present in the central part of the Challis quadrangle (fig. F1). However, lack of recognition of diorite in the field may have resulted in mapping of less diorite than is actually present.

Most of the Tertiary granite plutons in Idaho have the following characteristics, based on studies by Bennett (1980a) and Criss and Taylor (1983). These are similar to the characteristics of anorogenic granites as described by Loiselle and Wones (1979), Collins and others (1982), White and Chappell (1983), and Anderson (1983).

Table F1. Tentative correlation of plutonic, hypabyssal, and volcanic rocks of Tertiary age in the Challis quadrangle, Idaho
[Based in part on McIntyre and others (1982), Ekren (chap. C, this volume), and Hardyman (chap. G, this volume)].

Plutonic unit	Hypabyssal unit	Volcanic unit
Pink granite----------	Rhyolite dikes----------	Rhyolite flows and tuffs; includes rocks related to the Twin Peaks caldera. Explosive origin (Hardyman, chap. G, this volume).
Monzodiorite----------	Dacite-rhyodacite dikes (green and gray).	Tuff of Eightmile Creek, tuff of Ellis Creek, tuffs of Camas Creek and Black Mountain; centered on Van Horn Peak cauldron complex. Explosive origin (Ekren, chap. C, this volume).
Unknown----------	Rhyodacite-andesite sills	Dacite, andesite, rhyodacite; mostly flows from localized vents. Nonexplosive origin (McIntyre and others, 1982).

- A major component of the granite is potassium feldspar, which imparts a distinctive pink color to the rocks.
- The composition is in the granite field of the IUGS classification system (fig. F2).
- Most granite has vertical jointing that results in rugged topography such as on the Sawtooth batholith (fig. F1, area 26).
- Miarolitic cavities indicate epizonal emplacement (probably within a few kilometers or less of the surface).
- Most rocks average two to three times more uranium, thorium, and potassium-40 than the Cretaceous Idaho batholith, as measured with a gamma-ray spectrometer. Smoky quartz crystals that line miarolitic cavities are a product of this high radioactivity. Many areas of granite are clearly delineated on the National Uranium Resource Evaluation (NURE) airborne gamma-ray spectrometry surveys in Idaho.
- Most granite has a high content of large-cation elements, including tin, tungsten, uranium, thorium, molybdenum, and other elements such as niobium, zirconium, some lead, zinc, and beryllium. Beryl crystals were found in the Sawtooth batholith, the Dismal Swamp stock, and the Crags pluton (fig. F1), according to Reid (1963) and Pattee and others (1968). Anomalous amounts of these elements are common in stream-sediment samples collected from Tertiary granite terranes (Kiilsgaard and others, 1970; Cater and others, 1979; Coxe and Toth, 1983; Kiilsgaard, 1983a).
- Microprobe analyses for fluorine in biotite from selected Tertiary granite and Cretaceous plutonic rocks (table F2) show a high fluorine content in the Tertiary granite. High fluorine indicates that these rocks formed from dry melts that were able to rise to within a few kilometers of the Earth's surface before crystallizing. Fluorite and topaz occur in miarolitic cavities in the Sawtooth batholith and other Tertiary granite plutons.
- Analyses of biotite show high iron-magnesium ratios (table F2). Biotite in the Tertiary granite is much closer in composition to annite, the iron-rich end member of the biotite series, than to phlogopite, the magnesium-rich end member. Biotite in the Knapp Peak stock (fig. F1, area 14) is almost pure annite.

The high iron content may contribute to the positive aeromagnetic expression of the Tertiary granite. Fayalite, the iron-rich end member of the olivine series, occurs as inclusions in the Sawtooth batholith and the Knapp Peak stock.

- Perthitic potassium feldspar seen in thin section indicates that the granite has, in part, hypersolvus texture. Well-developed intergrowths of myrmekite and granophyric textures are common. Some phases of the Tertiary granite plutons contain two kinds of feldspar and no indication of hypersolvus texture. In others, large perthitic potassium feldspar grains are in a finer grained groundmass of plagioclase and quartz, indicating quenching of the magma by release of volatiles. In general, textures indicate high-temperature crystallization complicated by quenching.
- Oxygen isotope studies indicate that large hot-water convective systems composed of meteoric water, rather than magmatic water (based on oxygen and hydrogen isotope studies), circulated around the Tertiary granite bodies (Criss and Taylor, 1983).
- The Tertiary granite in Idaho is slightly peraluminous by Shand's (1927) classification, having A/CNK (aluminum/alkali) ratios of greater than 1.0 (table F3). The granite is probably alkali-calcic to calc-alkaline according to Peacock's (1931) classification, although this classification is difficult to apply as the Tertiary granite does not form a differentiated suite. The Reynolds and Keith (1982) scheme classifies peraluminous granite as alkaline or subalkaline using K_2OCaO/SiO_2 or CaO/SiO_2 variation diagrams. The boundary between the two fields approximates the calc alkalic-alkali calcic boundary of Peacock (1931). Idaho Tertiary granite plots in the alkaline field on both variation diagrams.

Whole-rock chemical analyses (table F3) show that the Tertiary granite contains less Al_2O_3, MgO, and CaO; more K_2O and SiO_2; and about the same Na_2O as the Cretaceous granite and Australian S- and I-type granitoid rocks (table F3). This composition is probably typical of anorogenic granite worldwide as indicated by the similarity to the average composition of Australian A-type granite.

- Preliminary data indicate that the Tertiary granite is lower in strontium and higher in rubidium than Cretaceous granitic rocks (table F4).

Table F2. Microprobe analyses of iron, magnesium, fluorine, and chlorine in biotite samples from Tertiary and Cretaceous intrusive rocks and stoichiometric annite and phlogopite
[Values in percent; leaders (--), amounts less than 0.1 percent detection limit]

Sample source	Fe	Mg	F	Cl
Sawtooth batholith (Tertiary)----------	17.1	3.8	3.7	--
Twin Springs pluton (Tertiary)---------	12.9	8.3	4.2	--
Crags pluton (Tertiary)----------	21.6	3.5	1.7	--
Knapp Peak stock (Tertiary)----------	29.0	.1	1.2	0.43
Annite (stoichiometric)----------	33.9	.0	--	--
Phlogopite (stoichiometric)----------	.0	18.3	--	--
Diorite of Rapid River (Tertiary)------	16.5	6.9	.4	--
Two-mica granite (Cretaceous)----------	19.8	2.8	.7	--
Granodiorite (Cretaceous)----------	18.7	4.8	.9	.41
Pat Hughes (Thompson Creek) stock (Cretaceous).	14.7	6.2	1.0	--
White Cloud stock (Cretaceous)---------	14.6	7.9	1.2	--

The hypabyssal equivalent of the granite is numerous rhyolite dikes. These dikes are throughout the Challis map area but are concentrated in the trans-Challis fault system.

The Knapp Peak stock (fig. F1, area 14) is interesting because it contains features of both granite and rhyolite. Most of the stock is very fine grained and in places looks like rhyolite. Its upper part, however, is typical Tertiary granite. The fine-grained part of the stock is similar to other rhyolite plugs and stocks that intrude faults in the trans-Challis fault system (fig. F4). These intrusive bodies, in turn, connect to rhyolite flows that are part of the Challis Volcanics (Hardyman, chap. G, this volume). Also on Copper Mountain at the north end of the Sawtooth batholith, granite becomes intrusive rhyolite through a short distance (Kiilsgaard and Bennett, chap. M, this volume). The intrusive rhyolite is overlain by rhyolite flows between Beaver and Knapp Creeks, in the Knapp Creek graben (fig. A2). The graben is also within the trans-Challis fault system.

Other volcanic rocks

Major units of the Challis Volcanics, including the tuff of Ellis Creek, the tuffs of Camas Creek and Black Mountain (formerly called the Casto Volcanics), and rhyolite in the trans-Challis fault zone, are related to the diorite stocks and dikes and granite plutons. The lower units of the Challis Volcanics, dacite, rhyodacite, and andesite, do not appear to be related to the bimodal Tertiary plutonic rocks. These rocks are called the rhyodacite-andesite unit in this chapter. Ekren (chap. C, this volume) describes the rhyodacite-andesite unit and identifies numerous small volcanic centers for these rocks. These rocks are mostly flows and are not related to explosive volcanism, as are the volcanic rocks that are related to the bimodal plutonic rocks. The rhyodacite-andesite unit has a different composition and covers a much broader area than the other units of the Challis Volcanics. The rhyodacite-andesite unit has not been related to any major plutonic bodies.

Table F3. Whole-rock chemical analyses of samples
[Leaders (---), no data; A/CNK,

	1	2	3	4	5	6	7	8	9	10
SiO_2-----	75.22	77.11	74.83	75.20	73.31	73.22	77.33	75.69	75.88	76.30
Al_2O_3----	13.07	12.54	13.50	12.90	13.50	14.17	12.75	13.01	13.22	12.81
Fe_2O_3----	.67	.21	.47	1.55	.89	.96	.35	.24	.27	.23
FeO------	.79	.25	.53	---	1.04	.91	.41	.28	.24	.20
MgO------	.25	.24	.12	.20	.20	.30	.26	.23	.27	.10
CaO------	.69	.35	.63	.55	.57	1.30	.13	.49	.21	.24
Na_2O-----	3.54	3.78	3.46	3.34	3.14	3.42	3.58	3.50	4.15	3.89
K_2O------	4.70	4.52	4.93	5.02	5.01	5.20	4.87	5.01	4.99	4.71
TiO_2-----	.15	.09	.04	.14	.24	.24	.10	.04	.09	.05
P_2O_5-----	.07	.06	.05	.10	.05	.08	.02	.03	.04	.01
MnO------	.03	.05	.02	.02	.06	.04	.02	.02	.05	.03
A/CNK-----	1.19	1.07	1.06	1.08	1.17	1.12	1.12	1.08	1.05	1.07

SAMPLE

1. Sawtooth batholith, average of nine analyses.
2. Dismal Swamp stock, average of two analyses.
3. Granite of Cape Horn Lakes (Lewis, 1984), average of six analyses.
4. Running Creek pluton (Coxe and Toth, 1983), average of 52 analyses.
5. Whistling Pig pluton, (W. E. Motzer, University of Idaho, written commun., 1985), average of 12 analyses.
6. Painted Rock pluton, northern part (W. E. Motzer, University of Idaho, written commun., 1985), average of six analyses.
7. Lolo batholith, one analysis.
8. Bungalow stock, one analysis.
9. Twin Springs pluton, two analyses.
10. Steel Mountain stock, one analysis.

In the Loon Creek area the rhyodacite-andesite rocks are the extrusive equivalent of andesite sills and dikes. Hundreds of sills intrude roof pendants of Paleozoic rocks and fill joints in batholithic rocks just west of the General, a 10,300-ft (foot)-high peak west of Mayfield Creek. These sills and a vent complex described by Foster (1982) probably fed rhyodacite-andesite flows south of the General in the Mt. Jordan area.

STRUCTURAL SETTING OF THE TERTIARY PLUTONS

Several Tertiary plutons and related units are within the trans-Challis fault system, a major structural feature that crosses the Challis quadrangle. South of this northeast-trending fault system, Tertiary granite is exposed in upthrown blocks between major northwest-trending basin-and-range faults.

The trans-Challis fault system and related features

The trans-Challis fault system is a major northeast-trending structural zone that crosses the Challis quadrangle (figs. A2, F4–F6; chaps. B, M). A northeast-trending structural zone was first suggested by Hyndman and others (1977), who recognized that the Idaho porphyry belt appears to truncate northwest-trending basin-and-range mountains like the Beaverhead Mountains and Lemhi and Lost River Ranges in eastern Idaho. The fault zone was delineated by mapping done as part of the CUSMAP study. The fault zone includes the Custer graben, the Panther Creek graben, and the Knapp Creek graben (figs. A2, F6). Confinement of rhyolitic volcanic rocks to the Custer graben is apparent. The rhyodacite-andesite volcanic units, Paleozoic rocks, and underlying batholithic rocks are exposed in upthrown fault blocks near the margins of the trans-Challis fault system.

The trans-Challis fault system is a southwestern extension of the Great Falls lineament, a major structural zone that trends northeast across central Idaho, from the Panther Creek area in the northeast corner of the Challis quadrangle to the Canadian border and perhaps beyond. O'Neill and others (1982) and O'Neill and Lopez (1983) described the lineament and showed that it passes just west of the Boulder batholith in Montana (fig. F5). The lineament is not only a significant regional structure but also largely controlled emplacement of Tertiary plutonic and volcanic rocks and related mineralization (Kiilsgaard and Bennett, chap. M, this volume).

The tuffs of Camas Creek and Black Mountain and the tuff of Ellis Creek, related to the monzodiorite complexes, and eruptive centers in the Van Horn Peak cauldron complex (Ekren, chap. C, this volume), are mostly confined to the trans-Challis fault system. Likewise, many rhyolite intrusions and related rhyolitic volcanic rocks, including the Twin Peaks caldera (Hardyman, chap. G, this volume), are in this fault system.

from Tertiary plutons in Idaho and comparative rocks
alumina-alkali ratio]

11	12	13	14	15	16	17	18	19	20
73.74	75.22	73.60	67.98	69.08	70.42	72.00	65.57	70.13	59.30
14.17	13.39	12.69	14.49	14.30	15.44	15.30	15.27	15.36	18.30
1.13	.49	.99	1.27	.73	.92	1.35	1.61	1.05	1.62
1.29	.56	1.72	2.57	3.23	1.42	---	2.35	1.21	4.71
.73	.22	.33	1.75	1.82	.87	.43	2.12	1.13	5.53
.95	.25	1.09	3.78	2.49	2.56	1.80	3.22	2.76	7.70
3.72	3.37	3.54	2.95	2.20	3.70	4.01	3.81	3.87	3.34
4.85	5.27	4.51	3.05	3.63	3.19	3.80	3.84	3.75	3.14
.27	.09	.33	.45	.55	.39	.17	.62	.36	.91
.08	.01	.09	.11	.13	.13	.08	.22	.15	.38
.05	.03	.06	.08	.06	.04	.03	.07	.05	.12
1.08	1.14	1.03	0.97	1.25	1.09	1.07	0.94	1.00	0.80

DESCRIPTIONS

11. Mackay stock, one analysis.
12. Crags pluton, one analysis.
13. A-type granite (White and Chappell, 1983), average of 31 analyses.
14. I-type granite (White and Chappell, 1983), average of 532 analyses.
15. S-type granite (White and Chappell, 1983), average of 316 analyses.
16. Granodiorite of Atlanta lobe, average of 45 analyses.
17. Granodiorite of Bitterroot lobe (Cox and Toth, 1983), average of 69 analyses.
18. Diorite of Jackson Peak, average of four samples.
19. Diorite of Trinity Mountain, one analysis.
20. Diorite of Cape Horn Lakes (Lewis, 1984), average of six analyses.

Table F4. Values of rubidium and strontium in samples of plutonic rocks in the Challis quadrangle and the Bitterroot lobe of the Idaho batholith

[Values are in parts per million. Challis quadrangle data is preliminary, from Robert Fleck (U.S. Geological Survey, written commun., 1983); Bitterroot lobe data is from Hyndman (1984); Do., ditto]

Sample	Rubidium	Strontium
Tertiary granite:		
Sawtooth batholith (Tenmile)-------	167.7	83.9
Do.----------	143.2	345.0
Red Mountain stock (near Knapp Peak stock).	160.0	129.0
Sawtooth batholith (near Stanley Lake).	154.0	133.0
Atlanta lobe rocks (average):		
Granodiorite (7 samples)----------	74.1 (36-154)[1]	803.0 (610-1,517)[1]
Two-mica granite (1 sample)-------	80.2	785.0
Leucogranite (2 samples)----------	86.3	750.0
Bitterroot lobe rocks (average):		
Granodiorite (12 samples)---------	83.1 (66-99)[1]	896.9 (583-1,080)[1]

[1]Range of values in samples.

West of the trans-Challis fault system are many Tertiary intrusive bodies. A broad area of northeast-trending dike swarms, including the Pistol Creek swarm, together form the Idaho porphyry belt. This name should perhaps be used only for the area west of the fault system, as there are numerous other dike swarms throughout the southern part of the Atlanta lobe, outside of the Idaho porphyry belt. The Thunder Mountain cauldron complex (fig. A2), the Casto batholith (fig. F1, area 12), the diorite of Rapid River (fig. F1, area H), and other related intrusive bodies are also just west of the fault system. The Idaho porphyry belt and the Tertiary intrusions represent a deeper zone of exposure than that in the fault system, because the two-mica granite core of the Atlanta lobe west of the fault system has been uplifted relative to the fault system (Kiilsgaard and Lewis, chap. B, this volume).

Regional structural elements in central Idaho include lineaments parallel to the trans-Challis fault system bounding the northern side of the eastern Snake River Plain (Mabey and Webring, chap. E, this volume) and extending from Sun Valley, Idaho, to just north of Dillon, Mont., and beyond. The Sun Valley-Dillon lineament may have formed the straight eastern side of the Boulder batholith (Ruppel, 1982).

Northwest-trending structures

Well-known northwest-trending structures in the Challis quadrangle include the faults bordering the Beaverhead Mountains and the Lemhi and Lost River ranges (Ruppel, 1982). As noted, these faults abruptly terminate at the trans-Challis fault system. In addition, other faults parallel to these major ranges cut through the southern Atlanta lobe, to the west. They include the Sawtooth, Montezuma, Deer Park, Trinity Mountain, Boise Front, and several unnamed faults (fig. F5). These faults produced a series of horsts and grabens in the Atlanta lobe rocks similar to the basin-and-range type horsts and grabens to the east. These faults also terminate against the trans-Challis fault system; for example, the Deer Park fault ends abruptly at the South Fork of the Payette River (Kiilsgaard, 1983b). The Tertiary granite and monzodiorite are exposed in horsts between the northwest-trending faults. Intervening grabens contain older batholithic rocks that were mineralized during the Tertiary (Kiilsgaard and Bennett, chap. M, this volume).

The intersection of northwest-trending basin-and-range structures and northeast-trending Eocene extensional structures may be important loci for earthquake activity. The intersection of the Sun Valley-Dillon lineament and the Lost River Range fault marks the epicenter of the magnitude-7.2 earthquake of Oct. 28, 1983, just north of Mackay, Idaho.

The simple horst and graben structure in the Atlanta lobe could be related to either basin and range extension or to a scheme of block faulting, along basement-rock-cored block faults proposed by Ruppel (1982). We believe that exposures of Tertiary rocks in the southern Atlanta lobe are a result of possible Precambrian structures reactivated during basin-and-range extension. In the southern part of the Atlanta lobe, the simple horst-and-graben structure is complicated by a series of poorly exposed northeast-trending fault segments that parallel the trans-Challis fault system. The Atlanta dike swarm that lies just north of Atlanta, Idaho, may be in one of these fault zones, as may the Middle Fork of the Boise River. The southern end of the Sawtooth batholith may be truncated by one of these zones (fig. F7). The northeast-trending faults combined with the northwest-trending faults that produced the horst-and-graben structure have broken the southern Atlanta lobe into rhomboid-shaped blocks that have moved up and down relative to each other. The Sawtooth batholith is the most elevated block, and Atlanta Hill is the most downthrown block recognized so far.

Although the northwest-trending faults have not been observed in the western part of the Atlanta lobe in the Challis quadrangle, and in places terminate against the trans-Challis fault system, they may possibly have extended farther to the northwest at one time. Altered porphyritic granodiorite trends northwest across the Atlanta lobe (fig. F5; Kiilsgaard and Lewis, chap. B, this volume). These rocks may be related to ancestral northwest-trending basement faults. Traces of most of the northwest-trending faults in the western half of the quadrangle may have been destroyed by the uplift of the Atlanta lobe and related faulting, such as the Deadwood fault, plus the development of the trans-Challis fault system and related volcanic activity.

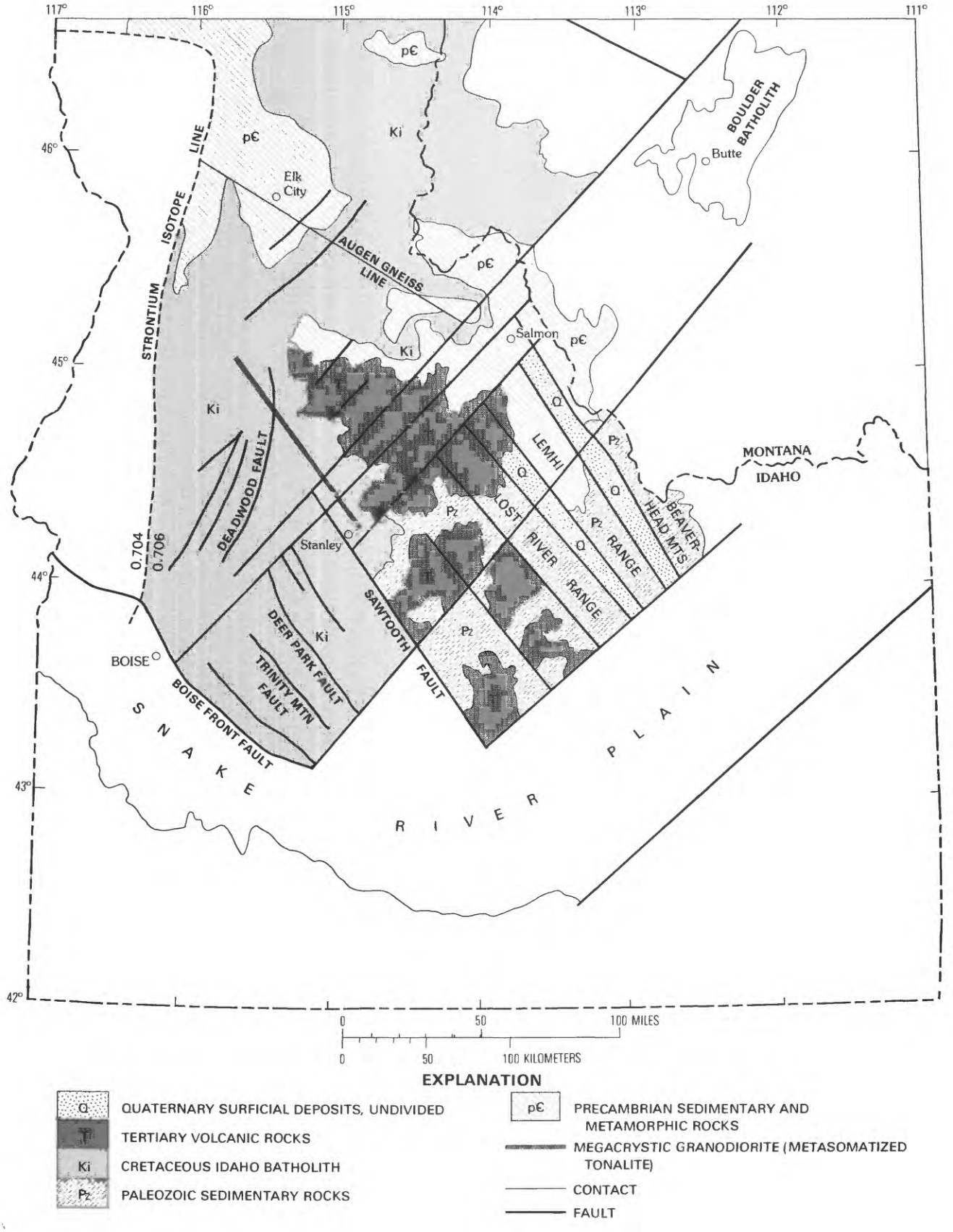

Figure F4. Map showing selected structural features in central Idaho and western Montana. Strontium isotope line from Armstrong and others (1977).

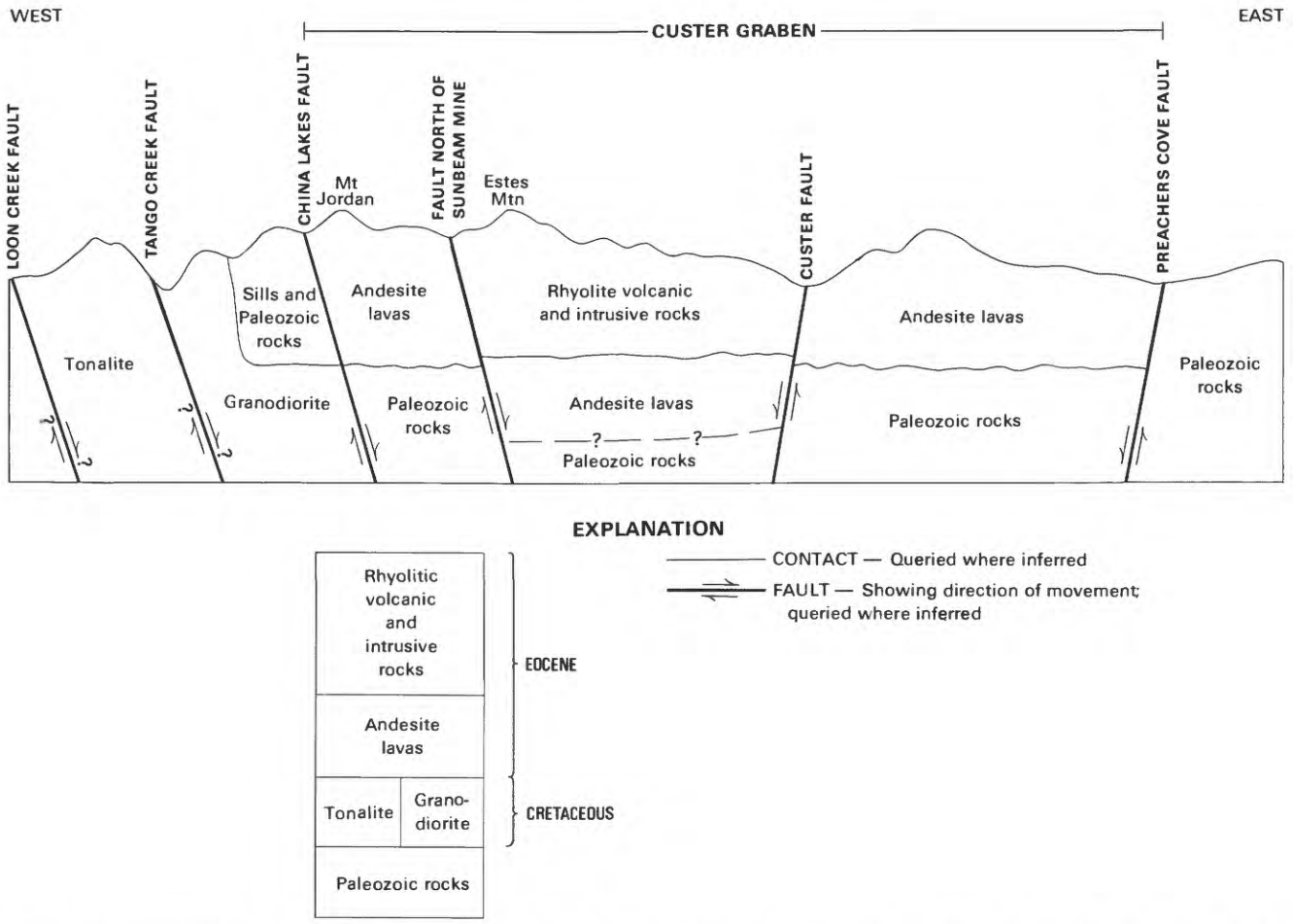

Figure F5. Generalized cross section of the trans-Challis fault system from Loon Creek to east of the Salmon River, Challis quadrangle. Horizontal scale about 1:250,000; no vertical scale.

ANOROGENIC ORIGIN OF THE TERTIARY PLUTONIC ROCKS

The bimodal Tertiary plutonic rocks in the Challis quadrangle are similar to anorogenic suites in other parts of the world. The main characteristics of A-type, anorogenic granite are very similar to the characteristics of the Tertiary granite, listed previously in this chapter. Loiselle and Wones (1979) described the characteristics of A-type or anorogenic granite. More recently, Collins and others (1982) and White and Chappell (1983) described anorogenic granite in Australia, compared it to other A-type granite in the world, and contrasted the A-type with the more familiar orogenic S- and I-type granite. Anderson (1983) summarized the characteristics of Proterozoic anorogenic granite.

The source and genesis of anorogenic granite are debated. Collins and others (1982) and Loiselle and Wones (1979) believed that the magmas from which anorogenic granite was formed came from a granulite terrane from which an earlier magma had been produced. The magma that formed the Cretaceous Idaho batholith must have had a major crustal component because the core of the batholith consists of S-type, two-mica granite (Kiilsgaard and Lewis, chap. B, this volume). Anderson (1983) suggested an alternative source for anorogenic granitic magmas, fusion of the lower crust containing I-type granite. All these authors agreed that these bimodal rocks formed by some type of continental extensional force, perhaps related to intracontinental rifting.

The diorite stocks and dikes, the other half of the anorogenic suite, are the more mafic analog of the granite. The origin of the diorite is not clear, although bimodal volcanism, generally producing basalt and rhyolite, is widely recognized as an important result of basin-and-range extension that postdates the Eocene plutonic-volcanic activity in Idaho. The diorite was probably formed from hybrid magmas as described by Hamilton (1981), "Arc magmas generated at depths near 100 kilometers by dehydration of subducting slabs are olivine rich mela-basalts, but the magmas that reach the surface in mature continental magmatic arcs have an average composition near that of rhyodacite. Depth-varying fractionations and equilibrations profoundly modify the initial

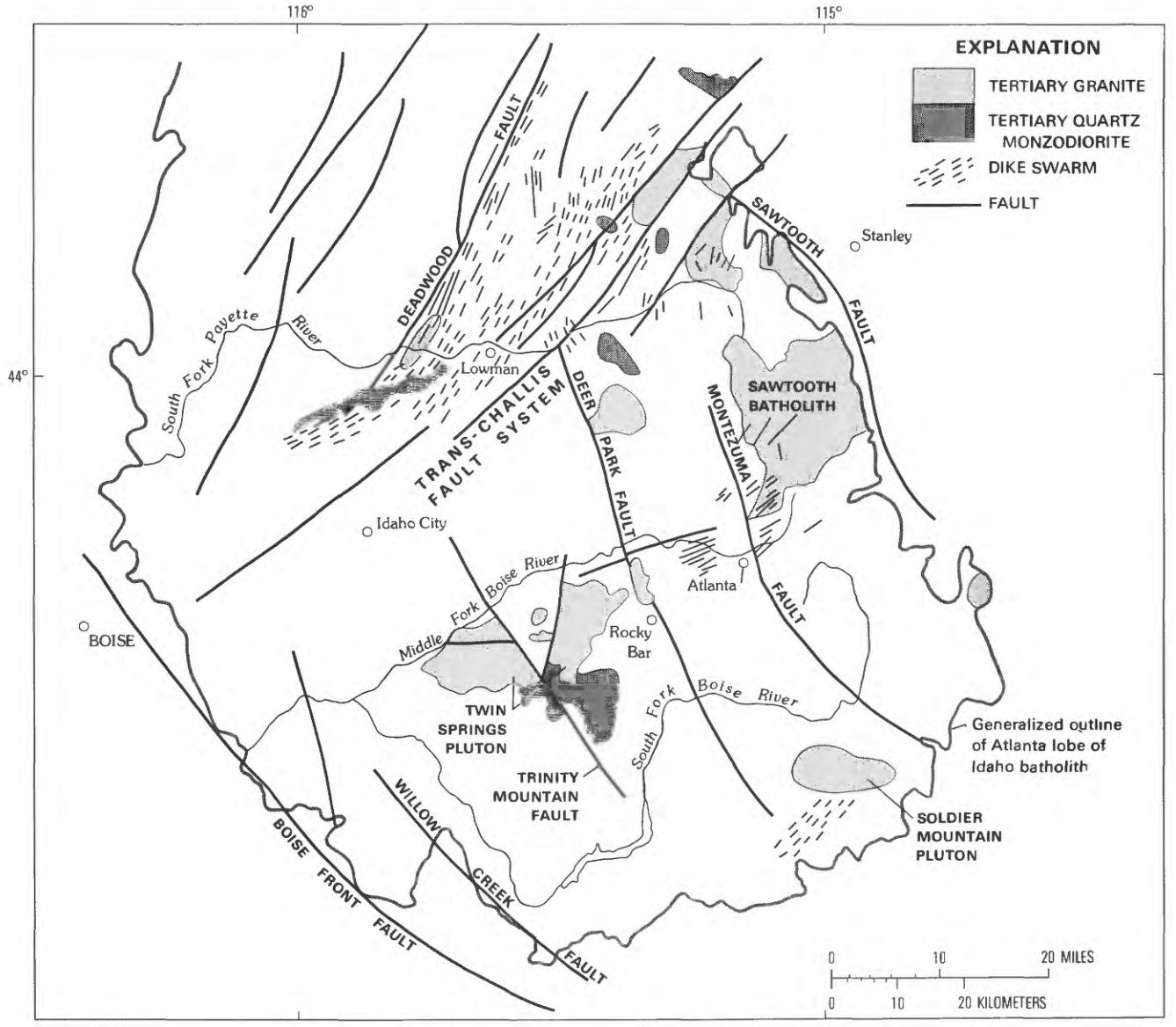

Figure F6. Simplified geologic map of the southern Atlanta lobe of the Idaho batholith. Modified from Bennett (1980b).

magmas." The diorite complexes in Idaho may be contaminated mafic magmas generated during extension. These magmas provided heat to melt the lower crust, forming anorogenic granite.

REFERENCES CITED

Anderson, A. L., 1929, Geology and ore deposits of the Lava Creek district, Idaho: Idaho Bureau of Mines and Geology Pamphlet 32, 70 p.

_____1934, Geology of the Pearl-Horseshoe Bend gold belt, Idaho: Idaho Bureau of Mines and Geology Pamphlet 41, 36 p.

_____1947, Geology and ore deposits of Boise basin, Idaho: U.S. Geological Survey Bulletin 944-C, p. 113–319.

_____1952, Multiple emplacement of the Idaho batholith: Journal of Geology, v. 60, no. 3, p. 255–265.

Anderson, J. L., 1983, Proterozoic anorogenic granite plutonism of North America: Geological Society of America Memoir 161, p. 133–154.

Armstrong, R. L., 1975, The geochronometry of Idaho: Isochron/West, no. 14, p. 1–50.

Armstrong, R. L., Taubeneck, W. H., and Hales, P. O., 1977, Rb-Sr and K-Ar geochronometry of Mesozoic granitic rocks and their Sr isotopic composition, Oregon, Washington, and Idaho: Geological Society of America Bulletin, v. 88, p. 397–411.

Bennett, E. H., 1980a, Granitic-rocks of Tertiary age in the Idaho batholith and their relation to mineralization: Economic Geology, v. 75, no. 2, p. 278–288.

_____1980b, Reconnaissance geology and geochemistry of the Trinity Mountain-Steel Mountain area, Elmore County, Idaho: Idaho Bureau of Mines and Geology Open-File Report 80–11, 56 p.

Bunning, B. B., and Burnet, F. W., 1981, Copper-molybdenum mineralization in the Bobcat Gulch porphyry system, Lemhi County, Idaho: Northwest Mining Association, annual meeting, 1981, Spokane, Wash.

Cater, F. W., Pinckney, D. M., Hamilton, W. B., Parker, R. L., Weldin, R. D., Close, T. J., and Zilka, N. T., 1973, Mineral resources of the Idaho Primitive Area and vicinity, Idaho: U.S. Geological Survey Bulletin 1304, 431 p.

Cater, F. W., Pinckney, D. M., and Stotelmeyer, R. B., 1975, Mineral resources of the Clear Creek-Upper Big Creek study area, contiguous to the Idaho Primitive Area, Lemhi County, Idaho: U.S. Geological Survey Bulletin 1391-C, 41 p.

Collins, W. J., Beams, S. D., White, A. J. R., and Chappell, B. W., 1982, Nature and origin of A-type granites with particular reference to southeastern Australia: Contributions to Mineralogy and Petrology, v. 80, no. 2, p. 189–200.

Coxe, B. W., and Toth, M. I., 1983, Geochemical maps of the Selway-Bitterroot Wilderness, Idaho County, Idaho, and Missoula and Ravalli Counties, Montana: U.S. Geological Survey Miscellaneous Field Studies Map MF-1495-C, scale 1:125,000.

Criss, R. E., 1981, An $^{18}O/^{16}O$, D/H and K-Ar study of the southern half of the Idaho batholith: Pasadena, California Institute of Technology Ph.D. thesis, 401 p.

Criss, R. E., and Taylor, H. P., Jr., 1983, An $^{18}O/^{16}O$ and D/H study of Tertiary hydrothermal systems in the southern half of the Idaho batholith: Geological Society of America Bulletin, v. 94, no. 5, p. 640–663.

Dover, J. H., Hall, W. E., Hobbs, S. W., Tschanz, C. M., Batchelder, J. N., and Simons, F. S., 1976, Geologic map of the Pioneer Mountains region, Blaine and Custer Counties, Idaho: U.S. Geological Survey Open-File Report 76-75, scale 1:62,500.

EG&G Geometrics, 1979, Aerial gamma ray and magnetic survey, Idaho project, Hailey quadrangle of Idaho—final report: U.S. Department of Energy Open-file Report GJBX-1080, 731 p.

Fisher, F. S., McIntyre, D. H., and Johnson, K. M., 1983, Geologic map of the Challis 1°×2° quadrangle, Idaho: U.S. Geological Survey Open-File Report 83-523, 41 p., 2 maps, scale 1:250,000.

Fisk, H. G., 1969 [1970], Painted Rocks Lake area, southern Ravalli County, Montana: Montana Bureau of Mines and Geology Special Publication 47, 1 sheet.

Foster, Fess, 1982, Geologic map of Mt. Jordan and vicinity, Custer County, Idaho: U.S. Geological Survey Miscellaneous Field Studies Map MF-1434.

Greenwood, W. R., and Morrison, D. A., 1973, Reconnaissance geology of the Selway-Bitterroot Wilderness area: Idaho Bureau of Mines and Geology Pamphlet 154, 30 p.

Hall, W. E., Batchelder, J. N., and Douglass, R. C., 1974, Stratigraphic section of the Wood River Formation, Blaine County, Idaho: U.S. Geological Survey Journal of Research, v. 2, no. 1, p. 89–95.

Hall, W. E., Rye, R. O., and Doe, B. R., 1978, Wood River mining district, Idaho—Intrusion-related lead-silver deposits derived from country rock source: U.S. Geological Survey Journal of Research, v. 6, no. 5, p. 579–592.

Hamilton, Warren, 1981, Crustal evolution by arc magmatism, *in* The origin and evolution of the Earth's continental crust: Royal Society of London Philosophical Transactions, ser. A, v. 301, no. 1461, p. 279–291.

Hietanen, Anna, 1969, Distribution of Fe and Mg between garnet, staurolite, and biotite in aluminum-rich schist in various metamorphic zones north of the Idaho batholith: American Journal of Science, v. 267, p. 422–456.

Hyndman, D. W., 1984, A petrographic and chemical section through the northern Idaho batholith: Journal of Geology, v. 92, p. 83–102.

Hyndman, D. W., Badley, Ruth, and Rebal, Donald, 1977, Northeast-trending early Tertiary dike swarm in central Idaho and western Montana [abs.]: Geological Society of America Abstracts with Programs, v. 9, no. 6, p. 734.

Kiilsgaard, T. H., 1983a, Geochemical map of the Ten Mile West Roadless Area, Boise and Elmore Counties, Idaho: U.S. Geological Survey Miscellaneous Field Studies Map MF-1500-B, scale 1:62,500.

_____1983b, Geologic map of the Ten Mile West Roadless Area, Boise and Elmore Counties, Idaho: U.S. Geological Survey Miscellaneous Field Studies Map MF-1500-A, scale 1:62,5000.

Kiilsgaard, T. H., Freeman, V. L., and Coffman, J. S., 1970, Mineral resources of the Sawtooth Primitive Area, Idaho: U.S. Geological Survey Bulletin 1319-D, 174 p.

Lewis, R. S., 1984, Geology of the Cape Horn Lakes quadrangle, south-central Idaho: Seattle, University of Washington M.S. thesis, 90 p.

Lipman, P. W., Prostka, H. J., and Christiansen, R. L., 1972, Cenozoic volcanism and plate-tectonic evolution of the western United States. Part I, Early and middle Cenozoic: Royal Society of London Philosophical Transactions, v. 271-A, p. 217–248.

Loiselle, M. C., and Wones, D. R., 1979, Characteristics and origin of anorogenic granites [abs]: Geological Society of America Abstracts with Programs, v. 11, no. 7, p. 468.

McIntyre, D. H., Ekren, E. B., and Hardyman, R. F., 1982, Stratigraphic and structural frameworks of the Challis Volcanics in the eastern half of the Challis 1°×2° quadrangle, Idaho, *in* Bonnichsen, Bill, and Breckenridge, R. M., eds., Cenozoic geology of Idaho: Idaho Bureau of Mines and Geology Bulletin 26, p. 3–22.

Nelson, W. H., and Ross, C. P., 1968, Geology of part of the Alder Creek mining district, Custer County, Idaho: U.S. Geological Survey Bulletin 1252-A, p. 1–30.

Nold, J. L., 1974, Geology of the northeastern border zone of the Idaho batholith: Northwest Geology, v. 3, p. 47–52.

Olson, H. J., 1968, The geology and tectonics of the Idaho porphyry belt from the Boise basin to the Casto quadrangle: University of Arizona Ph.D. thesis, 154 p.

O'Neill, J. M., and Lopez, D. A., 1983, Great Falls lineament, Idaho and Montana [abs.]: American Association of Petroleum Geologists Bulletin, v. 67, no. 8, p. 1350–1351.

O'Neill, J. M., Lopez, D. A., and Desmarais, N. R., 1982, Recurrent movement along and characteristics of, northeast-trending faults in part of east-central Idaho and west-central Montana [abs.]: Geological Society of America Abstracts with Programs, v. 14, no. 6, p. 345.

Pattee, E. C., Van Noy, R. M., and Weldin, R. D., 1968, Beryllium resources of Idaho, Washington, Montana, and Oregon: U.S. Bureau of Mines Report of Investigation 7148, 169 p.

Paull, R. A., Wolbrink, M. A., Volkman, R. G., and Grover, R. L., 1972, Stratigraphy of the Copper Basin Group, Pioneer Mountains, south-central Idaho: American Association of Petroleum Geologists Bulletin, v. 56, no. 8, p. 1370–1401.

Peacock, M. A., 1931, Classification of igneous rock series: Journal of Geology, v. 39, no. 1, p. 54–67.

Percious, J. K., Damon, P. E., and Olson, H. J., 1967, Radiometric dating of Idaho batholith porphyries: U.S. Atomic Energy Commission Annual Progress Report, No. C00–689–76, Appendix A-X, p. 1–6.

Reid, R. R., 1963, Reconnaissance geology of the Sawtooth Range: Idaho Bureau of Mines and Geology Pamphlet 129, 37 p.

Reynolds, S. J., and Keith, S. B., 1982, Geochemistry and mineral potential of peraluminous granitoids, *in* Arizona Bureau of Geology and Mineral Technology, Field Notes, v. 12, no. 4, p. 4–6.

Ross, C. P., 1928, Mesozoic and Tertiary granitic rocks in Idaho: Journal of Geology, v. 36, no. 8, p. 673–693.

_____1931, A classification of the lode deposits of south-central Idaho: Economic Geology, v. 26, no. 2, p. 169–185.

_____1934, Geology and ore deposits of the Casto quadrangle, Idaho: U.S. Geological Survey Bulletin 854, 135 p.

_____1963, Evolution of ideas pertaining to the Idaho batholith: Northwest Science, v. 37, p. 45–63.

Ruppel, E. T., 1978, Medicine Lodge thrust system, east-central Idaho and southwest Montana: U.S. Geological Survey Professional Paper 1031, 23 p.

_____1982, Cenozoic block uplifts in east-central Idaho and southwest Montana: U.S. Geological Survey Professional Paper 1224, 24 p.

Shand, S. J., 1927, The eruptive rocks: New York, Wiley, 488 p.

Streckeisen, A. L., 1976, To each plutonic rock its proper name: Earth Science Review, v. 12, p. 1–33.

Swanberg, C. A., and Blackwell, B. D., 1973, Areal distribution and geophysical significance of heat generation in the Idaho batholith and adjacent intrusions in eastern Oregon and western Montana: Geological Society of America Bulletin, v. 84, no. 4, p. 1261–1282.

Toth, M. I., 1983, Reconnaissance geologic map of the Selway-Bitterroot Wilderness, Idaho County, Idaho, and Missoula and Ravalli Counties, Montana: U.S. Geological Survey Miscellaneous Field Studies Map MF-1495-B, scale 1:125,000.

Toth, M. I., Coxe, B. W., Zilka, N. T., and Hamilton, M. M., 1983, Mineral resource potential map of the Selway-Bitterroot Wilderness, Idaho County, Idaho, and Missoula and Ravalli Counties, Montana: U.S. Geological Survey Miscellaneous Field Studies Map MF-1495-A, scale 1:125,000.

Tschanz, C. M., Kiilsgaard, T. H., Seeland, D. A., Van Noy, R. M., Ridenour, James, Zilka, N. T., Federspiel, F. E., Evans, R. K., Tuchek, E. T., and McMahan, A. B., 1974, Mineral resources of the eastern part of the Sawtooth National Recreation Area, Custer and Blaine Counties, Idaho, *with sections on* Aeromagnetic survey and tentative interpretation, by D. R. Mabey and C. M. Tschanz, *and* Electromagnetic surveys, by F. C. Frischknecht: U.S. Geological Survey open-file report, 2 v., 648 p.

White, A. J. R., and Chappell, B. W., 1983, Granitoid types and their distribution in the Lachlan Fold Belt, southeastern Australia: Geological Society of America Memoir 159, p. 21–34.

Symposium on the Geology and Mineral Deposits of the Challis 1°×2° Quadrangle, Idaho

Chapter G

The Twin Peaks Caldera and Associated Ore Deposits

By R. F. HARDYMAN

CONTENTS

FIGURES

TABLE

Abstract

The Twin Peaks caldera formed about 45 m.y. ago with the eruption of large volumes of ash-flow tuff that formed an extensive outflow sheet and ponded within the collapse structure to a thickness of more than several hundred meters. Following this initial caldera-forming cycle, additional collapse took place in the northern half of the structure, concomitant with renewed eruption of ash-flow tuff. An extensive megabreccia, consisting of caldera-wall slump debris, is intercalated with this tuff, and together these rocks have buried much of the collapsed northern structural block. The youngest magmatic event to affect the caldera was the emplacement of many rhyolite intrusions within the failed northern structural block and along the northern ring-fracture system.

Hydrothermal activity was localized along the caldera ring-fracture system and within the northern structural block. Rocks of the southern structural block of the caldera, however, were little affected by hydrothermal solutions. Hydrothermal solutions have zeolitically altered an extensive zone of intracaldera rocks separating the two structural blocks of the caldera. In addition, hydrothermal solutions, that may in part be temporally related to intrusive rhyolites in the northern structural block, have altered some of these intrusions. Precious-metal deposits have been mined from the Parker Mountain district on the western margin of the caldera.

INTRODUCTION

The Twin Peaks caldera, approximately 13 km (kilometers) northwest of Challis, Idaho, is a Valles-size caldera with dimensions of 20 by 14 km. It formed about 45 m.y. ago with the eruption of approximately 320 km^3 (cubic kilometers) of alkali-rhyolite ash-flow tuff, the tuff of Challis Creek. It is the youngest recognized collapse structure of the Van Horn Peak cauldron complex, which was the source area for most of the pyroclastic rocks of the Challis volcanic field in the eastern half of the Challis quadrangle.

The caldera was first recognized through geologic mapping in 1979 as part of the CUSMAP (Conterminous United States Mineral Assessment Program) study of the Challis quadrangle. A brief description of the caldera and the intracaldera pyroclastic rocks, together with an interpretation of its collapse history, has been presented elsewhere (Hardyman, 1981, 1983). This chapter reviews the structural setting of the caldera and discusses the precious-metal mineral deposits and hydrothermally altered rock associated with the caldera.

GEOLOGIC SETTING

The Twin Peaks caldera is a roughly elliptical collapse structure, about 20 km in longest dimension, which lies at the northeastern end of the Custer graben and along the southern margin of the Van Horn Peak cauldron complex (fig. G1). These structures lie within a regionally extensive, northeast-trending zone of normal faults, grabens, and caldera segments of the Van Horn Peak cauldron complex that collectively are elements of the trans-Challis fault system (Kiilsgaard and Lewis, chap. B, this volume; Fisher, chap. A, this volume, fig. A1). The fairly linear southern margin, and especially the northern margin of the caldera may have formed by collapse along pre-existing northeast-trending faults in the pre-Tertiary basement rocks (Hardyman, 1981, p. 322).

The caldera is approximately centered on Twin Peaks, two similar glaciated peaks more than 10,300 ft (feet) (3,139 meters) in elevation (lat 44°36'N., long 114°27'W.) that were carved from intracaldera ash-flow tuff. The tuffs of Challis Creek are the youngest pyroclastic rocks of the Challis Volcanics in this region and cap many of the high peaks near the caldera to the north and west. Erosional remnants of the tuff of Challis Creek are preserved on the crest of the Pahsimeroi Mountains, about 24 km east of the Twin Peaks caldera, and remnants have been identified as far as 40 km southeast of the caldera along the Salmon River (McIntyre and others, 1982) and as far as 20 km west of the caldera.

Extreme and abrupt thickness changes of the rhyolite tuffs of Challis Creek, together with arcuate faults that juxtapose very dissimilar ash-flow tuffs and other volcanic rocks, define the caldera margins (Fisher and others, 1983). In addition, intermediate to silicic intrusive rocks and localized deposits of caldera-wall slump debris clearly delineate the caldera margins. Older rhyodacitic lavas and intrusions, for the most part, bound the caldera on the south and east, and older pyroclastic rocks of the Van Horn Peak cauldron complex bound the caldera on the west and north. Pre-Tertiary basement rocks are exposed about 5 km east of the caldera and about 2 km south. Plutonic rocks of the Idaho batholith crop out about 10 km west of the western margin of the caldera.

STRUCTURAL ELEMENTS OF THE CALDERA

The Twin Peaks caldera is divisible into three parts: (1) an earliest collapse segment at the southwestern end; (2) a southeastern structural block; and (3) a northwestern structural block. Together these structural elements record a complex history of collapse and concomitant volcanism. Geologic relations just west of the southwestern margin of the caldera proper suggest a collapse segment that I interpret to record the earliest subsidence of the Twin Peaks caldera. The southeastern and northwestern structural blocks within the caldera are separated by a northeast-trending line along the northern flanks of Twin Peaks.

Earliest Collapse Segment

A 10-mGal (milligal) negative gravity anomaly is associated with the Twin Peaks caldera and is one part

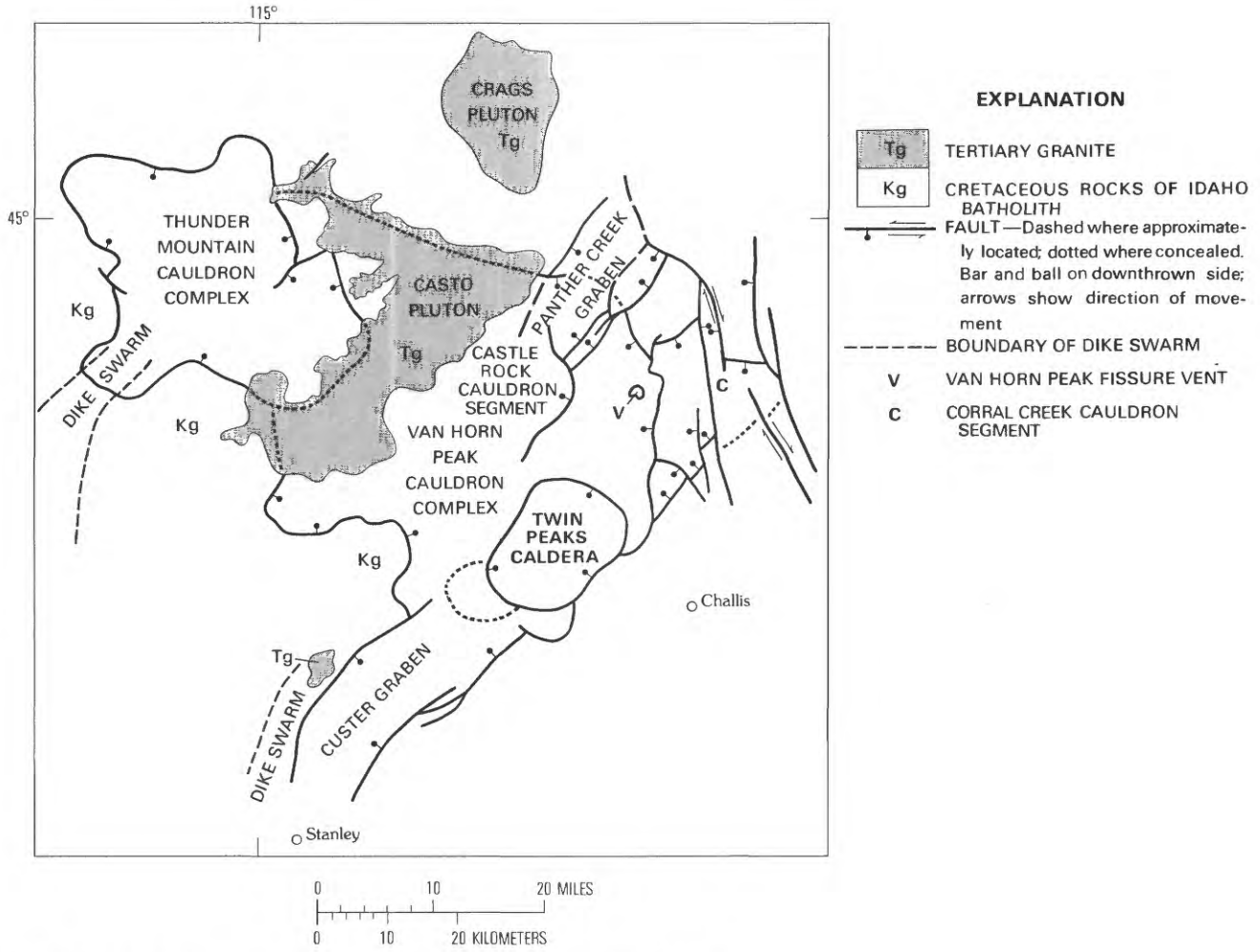

Figure G1. Structure map of the central part of the Challis quadrangle.

of a peanut-shaped gravity-anomaly pattern having an 18-mGal low centered near the western margin of the caldera (fig. G2; Mabey and Webring, chap. E, this volume). The 18-mGal gravity low coincides with an area containing exposures of rhyolitic ash-flow tuff and overlying volcaniclastic sedimentary rocks that are intruded by younger rhyolites. The moderately welded rhyolite ash-flow tuff is at least 215 m (meters) thick and grades upward into air-fall tuff. These rocks are similar in modes to the tuffs of Challis Creek and certainly are products of the same magmas that produced the tuffs of the Twin Peaks caldera. The ash-flow to air-fall tuff section in this 18-mGal gravity-low area is overlain by at least 120 m of coarse pebble conglomerate and volcaniclastic sandstone. Clasts of pyroclastic rocks of older units in the Challis volcanic field occur in these sedimentary rocks, but clasts of densely welded tuff of Challis Creek from the Twin Peaks caldera, which presumably once formed an outflow sheet in this area, are absent.

Details of the stratigraphic relations between rocks of these exposures and intracaldera tuffs just to the east are obscure due to intrusive rhyolites that pervade the rocks in this area. The above relations, however, suggest that the rhyolite ash-flow tuff and overlying sedimentary rocks infill an early collapse segment of the Twin Peaks caldera and that continued eruption of tuffs of Challis Creek and subsequent caldera collapse shifted slightly to the east-northeast.

Southeastern Structural Block

The southeastern half of the Twin Peaks caldera is a simple intact structural block composed of two major intracaldera-filling ash-flow-tuff cooling units (map units Tcr_1 and Tcr_3, fig. G3) that total at least 800 m in thickness. The lower cooling unit is 500 m thick, and the upper cooling unit (the top of which has been removed by erosion) is at least 310 m thick. At least two thin ash flows and discontinuous epiclastic sedimentary rocks separate the two thick cooling units. These cooling-break tuffs and sedimentary rocks are about 33 m thick.

Rocks of the two thick cooling units are very similar petrographically and in hand specimen, and collectively

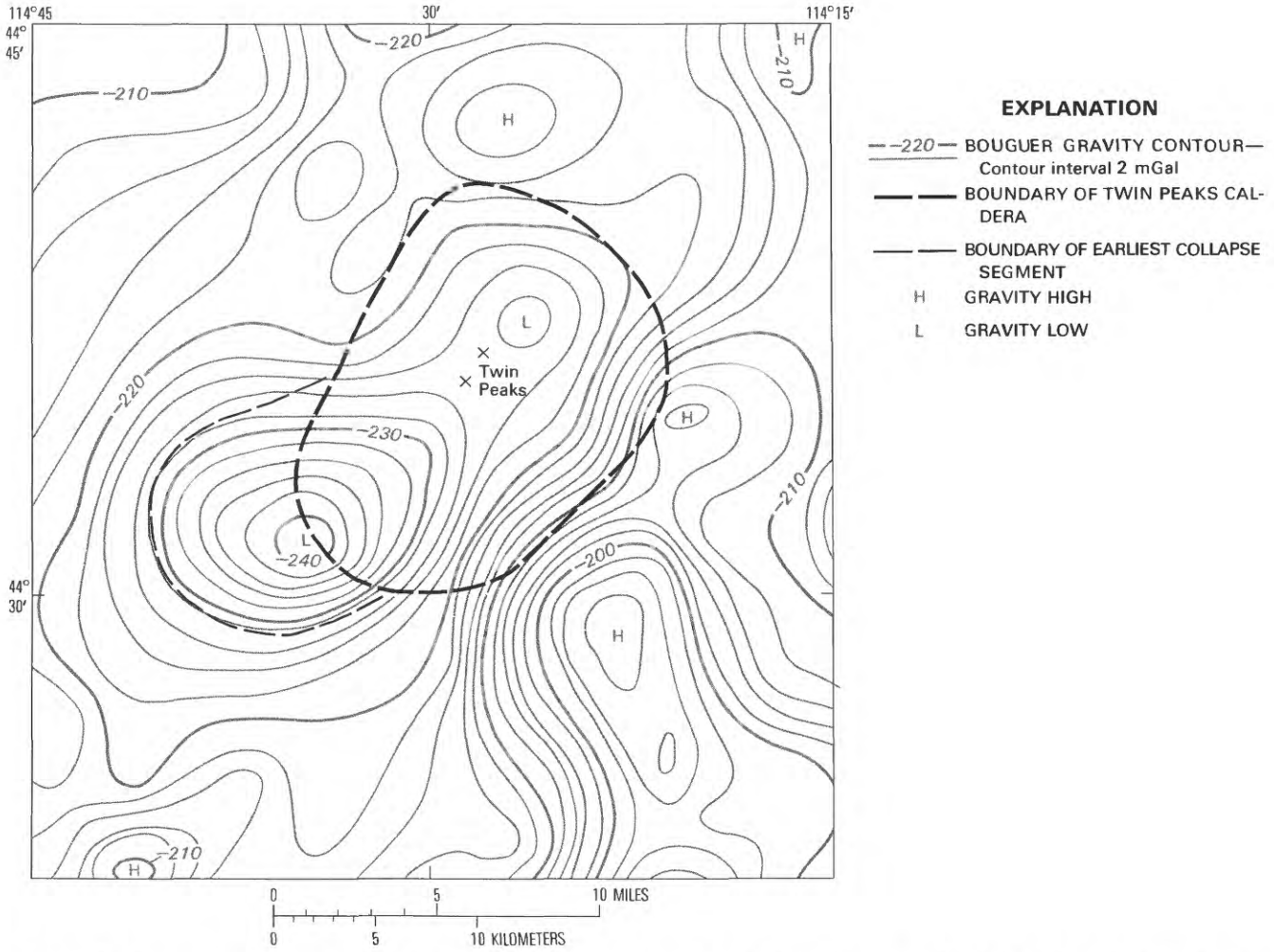

Figure G2. Bouguer gravity map of the Twin Peaks area, Challis quadrangle. From Mabey and Webring (chap. E, this volume).

with the cooling break tuffs, they compose the intracauldron tuff of Challis Creek. These tuffs contain abundant phenocrysts of sanidine and quartz and only minor plagioclase (fig. G4). The tuff of Challis Creek is distinctive in its paucity of plagioclase and near lack of any ferromagnesian minerals, especially biotite. Clinopyroxene is preserved in vitrophyres, and pseudomorphs are observable in devitrified tuff, but biotite is rare. Chemically, the rocks of the tuff of Challis Creek, as their modes suggest, are alkali rhyolites (table G1).

The tuffs in the southeastern half of the caldera dip gently 10–20° south-southeast and are little disrupted by faulting (fig. G5). This half of the caldera apparently represents the intact part of the caldera fill that was little affected by subsequent renewed collapse and explosive volcanism.

Northwestern Structural Block

In contrast to the structurally simple southeastern half of the caldera, geologic relationships in the northwestern half are complex and record additional pyroclastic volcanism and associated structural collapse. Much of the northern half of the caldera is filled with ash-flow tuff and megabreccia deposited during further collapse of the northern block (fig. G3). Collapse of this structural block, which probably resembled the present southeastern half of the caldera, was apparently piecemeal and catastrophic, leaving nearly the entire northern margin of the caldera exposed as a topographic wall. Collapse of this wall during continued eruption of pyroclastic material resulted in a megabreccia deposit intermixed with ash-flow tuff (unit Tsd, fig. G5). Ash-flow eruptions during collapse of the north wall probably issued from a major medial fracture (now buried) and perhaps from around foundering segments of the original northern half of the infilled caldera. Preliminary petrography of the ash-flow tuff (unit Tcrm, fig. G4) enclosing megabreccia blocks indicates that plagioclase is significantly more abundant in this megabreccia tuff than in the major intracaldera tuff cooling units.

The megabreccia deposit is exposed over an area of about 29 km² (square kilometers) and contains an

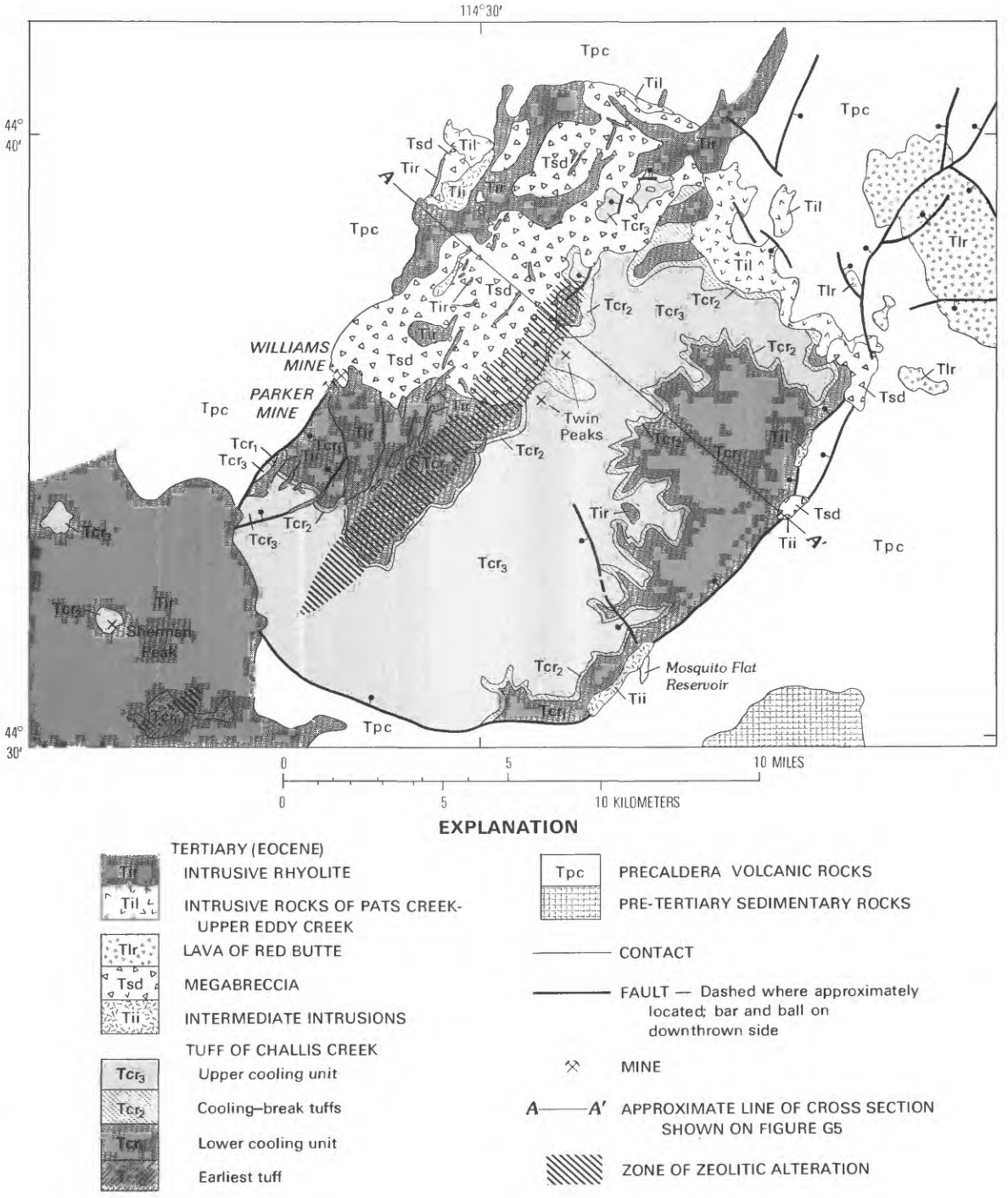

Figure G3. Generalized geologic map of the Eocene Twin Peaks caldera.

estimated 24 km³ of material ranging from bedded, coarse-grained talus to unsorted boulder- and block-dominated debris (Hardyman, 1983). Megabreccia blocks range from cobble to house size (more than 65 meters in length) and include intermediate lava, rhyolite, and nearly all of the older pyroclastic units of the Van Horn Peak cauldron complex that are exposed just north of the caldera. Blocks of tuff of Challis Creek are also abundant in this deposit. The megabreccia unit laps against and locally over both cooling units of the tuff of Challis Creek that form the escarpment marking the northern boundary of the southeastern caldera block.

ASSOCIATED HYDROTHERMALLY ALTERED ROCKS

Hydrothermally altered rocks associated with the Twin Peaks caldera occur along the southern ring-fracture system, along the medial zone marking the boundary

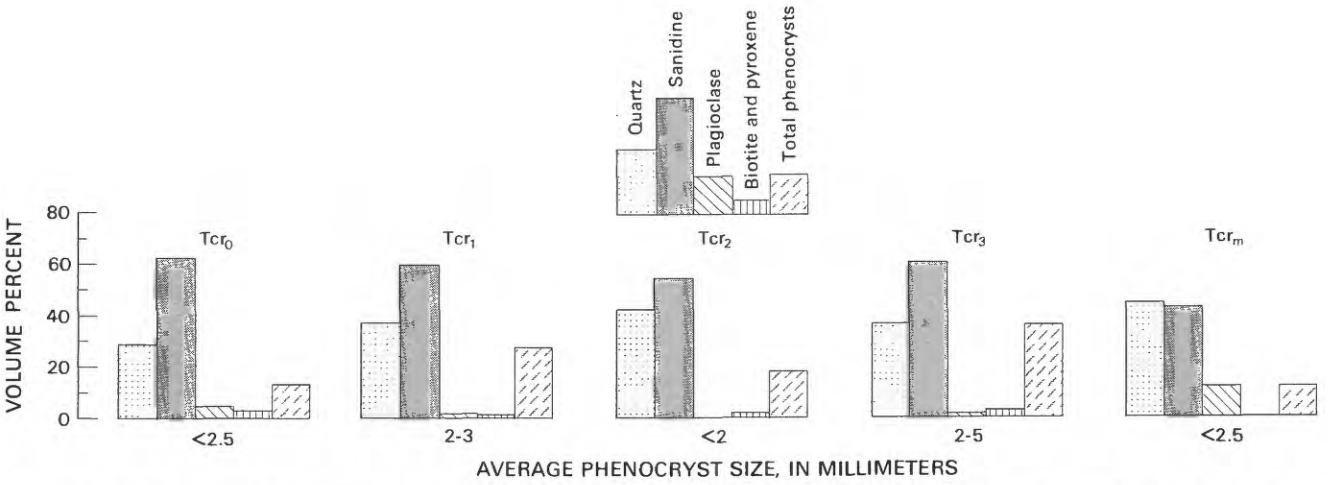

Figure G4. Average modal phenocryst abundances of intracaldera tuffs of the Twin Peaks caldera. Tcr_0, tuff of earliest collapse segment; Tcr_1, lower cooling unit, tuff of Challis Creek; Tcr_2, cooling break tuffs; Tcr_3, upper cooling unit, tuff of Challis Creek; Tcr_m, megabreccia-matrix tuff.

Table G1. Average values of nine chemical analyses and CIPW normative values of intracaldera tuffs of Challis Creek, Challis quadrangle.

Chemical analyses		Normative values	
SiO_2	75.33	q	38.11
Al_2O_3	12.08	c	1.04
Fe_2O_3	1.43	or	30.85
FeO	.18	ab	26.68
MgO	.08	an	1.32
CaO	.26	hy-en	.20
Na_2O	3.08	mt	.24
K_2O	5.10	hm	1.30
H_2O^+	.51	il	.25
H_2O^-	.47		
TiO_2	.13		
P_2O_5	.00		
MnO	.01		
CO_2	.00		
Sum	98.66		

between the two intracaldera structural blocks, and associated with rhyolitic intrusions that occur primarily within the northern half of the caldera (fig. G3). Rocks of the southeastern structural block are generally unaltered, except along the southern ring fracture, but hydrothermal alteration has been locally pervasive within the structurally more disrupted northwestern half of the caldera.

Alteration Along The Southern Ring Fracture

The southern and southeastern margin of the caldera coincides with Challis Creek from near Pats Creek (shown on the Twin Peaks 15-minute quadrangle topographic map) southwest and west to above Mosquito Flat. West of Mosquito Flat the caldera margin is defined by a fault that trends across the ridge just north of Summit Rock, near Mill Creek Summit, and extends into the uppermost Yankee Fork drainage. This fault juxtaposes densely welded tuff of Challis Creek on the north against older tuffs and rhyolite lavas on the south. Below Mosquito Flat, tuff of Challis Creek forms the canyon walls on the north side of Challis Creek, and older rhyodacitic lavas and intrusions are exposed on the south side of the creek. Intermediate-composition intrusive rocks occur locally along this part of the caldera ring fracture. These rocks are propylitically altered and contain disseminated pyrite. Plagioclase and ferromagnesian minerals are altered to calcite and chlorite.

One small porphyry intrusion, containing distinctive plagioclase phenocrysts as long as 6 cm, and exposed on Challis Creek road about 6.4 km northeast of Mosquito Flat Reservoir, is highly sheared and has quartz-sericite alteration. This rock contains narrow quartz-carbonate-limonite veinlets. This intrusion is partly buried by caldera-wall slump debris that is locally exposed along the southeastern margin of the caldera (fig. G3). Rocks of this caldera-wall slump debris are also altered to a carbonate-clay assemblage.

Intrusive rocks along the northeastern margin of the caldera (unit Til, fig. G3) cut tuff of Challis Creek, but this intrusion and adjacent tuffs are little altered. A similar pluglike intrusive mass along the north margin of the caldera contains abundant gas cavities containing rosettes of gypsum and minor calcite.

Intracaldera tuffs of the southeastern structural block are essentially unaltered except for one zone of weak, zeolitically altered tuff exposed on the upland erosion surface about 5 km north of Mosquito Flat Reservoir (fig. G3). Here the altered tuff adjoins a small dikelike plug of intrusive rhyolite (unit Tir), which is the only rhyolite intrusion that has been observed within the southeastern half of the caldera.

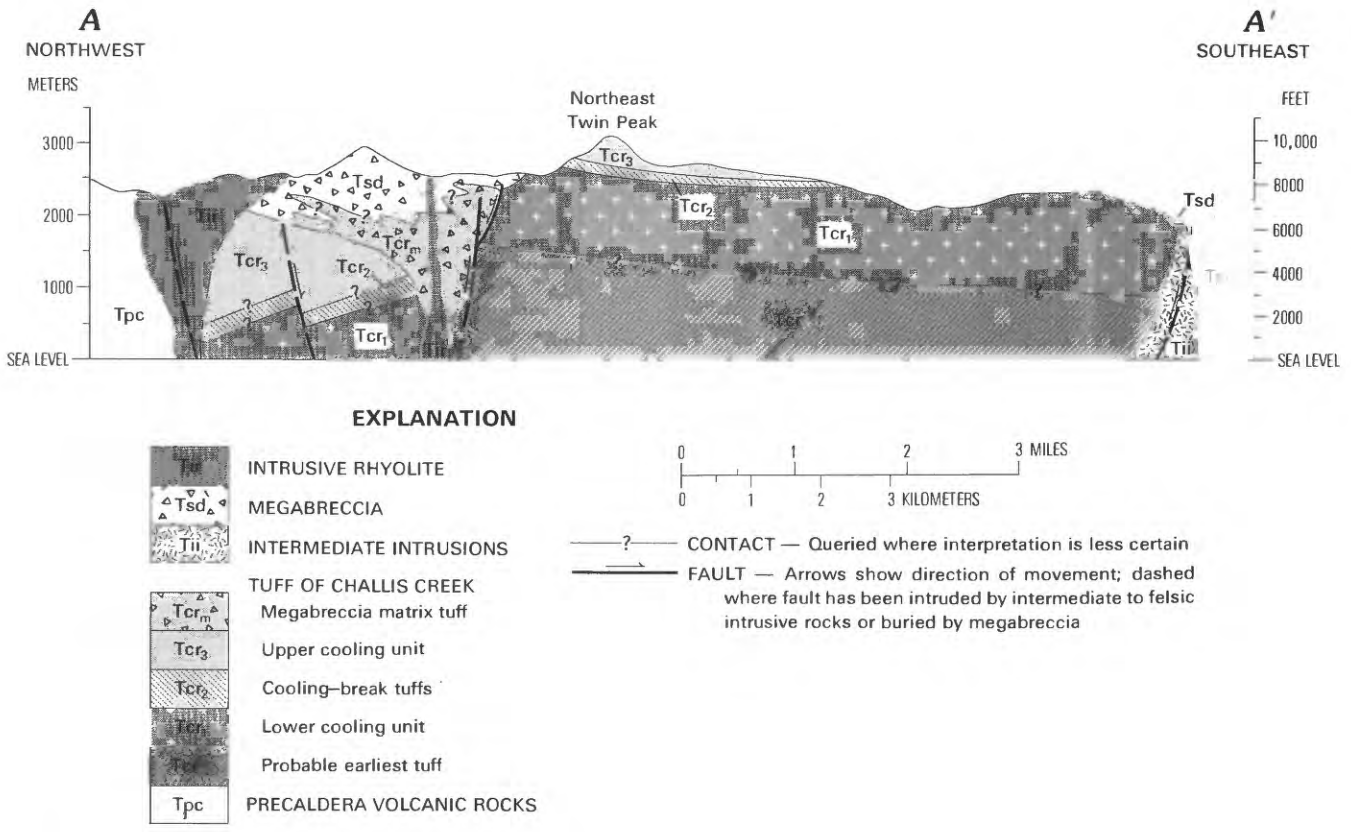

Figure G5. Diagrammatic cross section across the Tertiary Twin Peaks caldera. Line of section shown on figure G3.

Medial Zeolite Zone

An extensive northeast-trending zone of zeolitic altered volcanic rocks coincides with the medial line that separates the two structural blocks of the Twin Peaks caldera (fig. G3). Zeolitized rocks in this zone include ash-flow tuff of the lower cooling unit of the tuff of Challis Creek, megabreccia matrix tuff, and some megabreccia blocks within the megabreccia deposit. Zeolites are visible petrographically in most samples from this zone and replace glass shards and pumice fragments. X-ray analysis of samples collected across and along strike of this zone shows mordenite and clinoptilolite. Zeolitically altered rocks are easily recognized in outcrop because they are bleached to pale green or buff and generally do not support vegetation; this lack of vegetation is probably the result of nutrient deficiencies in these altered rocks (fig. G6). Locally within this zone, pyrite-bearing, limonitically stained, northeast-trending rhyolite dikes cut the zeolitized rock. The zone of zeolitized rock extends at least 12,000 m along strike and is locally at least 1,000 m wide. Patches of zeolitized rock occur sporadically along strike to the southwestern caldera margin, and zeolitized rock occurs outside the caldera in tuffs within the earliest collapse segment.

The amount of zeolitized tuff indicates that large volumes of hydrothermal fluids permeated the rocks along this zone. Presumably a medial fault or faults, now mostly buried and marking the southern boundary of the foundered northwestern half of the caldera, served as conduits for these low-temperature hydrothermal waters.

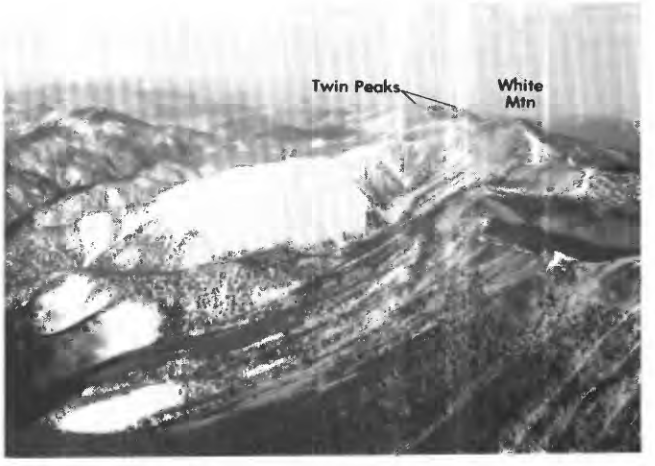

Figure G6. Zeolitized ash-flow tuff of Challis Creek (light-colored, treeless outcrops) along medial structural boundary within the Twin Peaks caldera. View to the northwest along strike of the zeolite zone from near the southwestern margin of the caldera.

Altered Intrusive Rhyolites in the Northwestern Structural Block

Intrusive rhyolites that postdate caldera collapse are abundant in the northwestern half of the caldera where they crosscut intracaldera tuff of Challis Creek and the megabreccia deposit (fig. G3). The ring fracture along the northern margin of the caldera served as the conduit for emplacement of some of the rhyolites, but they are not restricted to the ring-fracture zone. The northeastern trend of many of the linear dikes within this half of the caldera probably indicates northeast-trending structures in the precaldera basement rocks.

The rhyolites are similar in appearance and mineralogy to intrusive rhyolites found elsewhere in the Van Horn Peak cauldron complex and adjacent Custer and Panther Creek grabens (Hardyman and Fisher, chap. N, this volume). These rocks are aphyric to porphyritic and generally contain sanidine or sanidine and quartz.

Many of the rhyolite dikes are stained by limonite and contain disseminated pyrite. Alteration of these dikes and other rhyolite masses ranges from argillic to quartz sericitic and locally strongly silicic. In some intrusive bodies, the rhyolite is brecciated. Brecciation may occur along intrusive contacts or may occur as isolated breccia bodies within massive rhyolite. One such breccia body, within the intrusive rhyolite mass (unit Tir) along the northern ring fracture (fig. G3), resembles a hydrothermal or explosion breccia. Fragments in this breccia are monolithologic and consist of angular rhyolite fragments set in a matrix of finer grained breccia. Quartz-lined cavities occur in the breccia matrix, and hairline quartz veins crosscut fragments and the breccia matrix. Commonly, breccias, such as this example, are weakly to strongly altered, are limonitically stained, and contain pyrite.

ASSOCIATED ORE DEPOSITS

The only known mineral deposits associated with the Twin Peaks caldera occur along the northwestern margin near Parker Mountain. Gold-silver deposits were intermittently mined at the Parker mine and adjacent Williams mine from about 1905 to 1926 (Ross, 1934). Total reported production from these mines is 819 ounces of gold and 4,520 ounces of silver (A. Leszcykowski, U.S. Bureau of Mines, written commun., 1983). Brief descriptions of these mines were reported by Umpleby (1913) and Ross (1934).

Precious metals were produced at the Parker mine (Parker Mountain mine of Ross, 1934, p. 127) from vein quartz and silicified volcanic rock in a shear zone 3–5 ft wide that I interpret to be associated with the ring-fracture system along this segment of the caldera margin. At the Williams property, about 500 m to the north-northeast along the ring-fracture zone, ore was mined from silicified breccia that contains fragments of petrified wood, fine-grained tuffaceous sediment, and dark carbonaceous material (fig. G7). These fragments are interpreted to come from surficial deposits accumulated in depressions along the caldera ring-fracture zone at the time of caldera-wall collapse and accumulation of the megabreccia deposit.

The Parker and Williams mines are both near the northwestern contact of a large rhyolite intrusive mass that extends inward from the caldera margin (unit Tir, fig. G3). My interpretation of the geology at these deposits is shown in figure G8. Aphyric to porphyritic rhyolite was emplaced along the ring fracture and intruded megabreccia. Precious-metal-bearing fluids ascended along this conduit and along associated sympathetic fractures, silicifying and mineralizing older tuffs (and possibly caldera-related tuffs) at the Parker mine, and silicifying breccia, of similar collapse origin as the megabreccia deposit, at the Williams property. I do not interpret the breccia exposed at the surface at the Williams property to be an intrusive breccia,

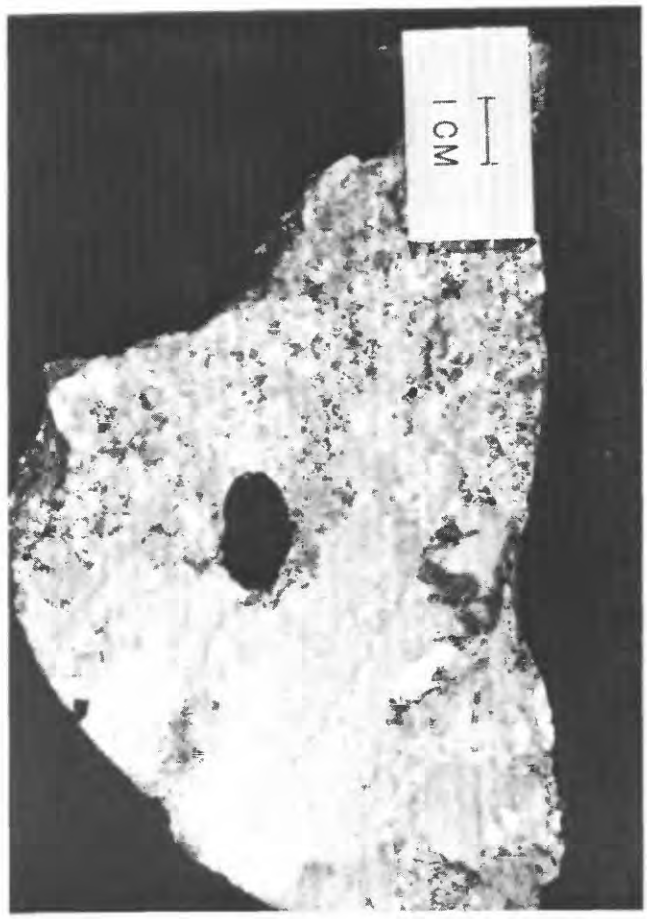

Figure G7. Altered fine-grained volcanic breccia collected at the ground surface near the Williams mine on the northwestern side of the Twin Peaks caldera. Light-colored fragments are very fine grained tuffaceous rock; dark fragment is carbonaceous material. Note subtle layering of the breccia.

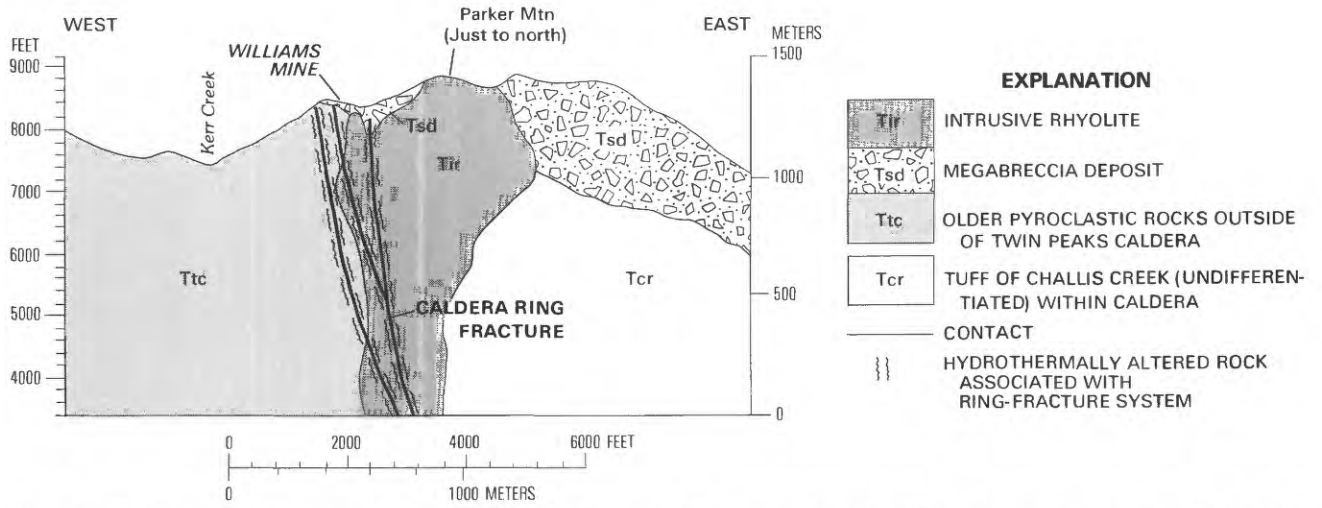

Figure G8. Diagrammatic cross section of geologic relations of Tertiary rocks at the Williams and Parker mines, Twin Peaks caldera. Line of section is through the Williams mine; the Parker mine is toward the reader from the section and along the zone of sympathetic fractures associated with the caldera ring fracture.

although narrow veins of hydrothermal breccia probably occur along fractures in the underlying intrusive rhyolite.

CONCLUSIONS

Subsequent to the initial caldera-forming volcanism, the northern half of the Twin Peaks caldera failed along structures, now mostly buried, into which postcollapse intrusive rhyolites were emplaced. Many of these rhyolites intruded to near-surface levels, and some contain spatially associated hydrothermal- or explosion-breccia bodies.

The structural disruption of the northern half of the caldera provided the most favorably prepared ground for the circulation of hydrothermal fluids. These fluids extensively altered the intracaldera tuffs along a northeast-trending medial zone through the caldera and locally altered intrusive rhyolites and tuffs elsewhere in the northern structural block. Hydrothermal activity along the western ring-fracture zone produced precious-metal deposits at the Parker and Williams mines. The northern half of the caldera has the most potential for mineral deposits.

REFERENCES CITED

Fisher, F. S., McIntyre, D. H., and Johnson, K. M., 1983, Geologic map of the Challis 1°×2° quadrangle, Idaho: U.S. Geological Survey Open-File Report 83–523, 41 p., 2 maps, scale 1:250,000.

Hardyman, R. F., 1981, Twin Peaks caldera of central Idaho, *in* Tucker, T. E., and others, Guidebook to southwest Montana: Montana Geological Society, Field Conference and Symposium, p. 317–322.

_____1983, Multiple collapse of the Twin Peaks caldera, Challis volcanic field, Idaho: Geological Society of America Abstracts with Programs 1983, v. 15, no. 5, p. 433 [combined Cordilleran-Rocky Mountain section meeting].

McIntyre, D. H., Ekren, E. B., and Hardyman, R. F., 1982 [1984], Stratigraphic and structural framework of the Challis Volcanics in the eastern half of the Challis 1°×2° quadrangle, Idaho; *in* Bonnichsen, Bill, and Breckenridge, R. M., eds., Cenozoic geology of Idaho: Idaho Bureau of Mines and Geology Bulletin v. 26, p. 3–22.

Ross, C. P., 1934, Geology and ore deposits of the Casto quadrangle, Idaho: U.S. Geological Survey Bulletin 854, p. 127–130.

Umpleby, J. B., 1913, Geology and ore deposits of Lemhi County, Idaho: U.S. Geological Survey Bulletin 528, 182 p.

Symposium on the Geology and Mineral Deposits of the Challis 1°×2° Quadrangle, Idaho

Chapter H

Ore Deposits Related to the Thunder Mountain Caldera Complex

By B. F. LEONARD

Abstract

Mined deposits of gold, silver, mercury, antimony, and tungsten are structurally related to subsidence of the Eocene caldera complex and to superposed regional strain shown by north-striking right-lateral shear zones and northeast-striking extension fractures. Gold deposits of the Thunder Mountain mining district are in the pyroclastic and volcaniclastic filling of Challis Volcanics in the central, youngest caldera. All the other mined deposits are outside the youngest caldera, within or close to silicified zones that cut plutonic and metamorphic rocks of the Idaho batholith. The extra-caldera deposits are near the intersection of discontinuous ring and radial fractures of the subsided complex. Ring fractures at ⅓, ½, ⅔, ⅚, and ⅞ of the 30-km radius of the cauldron (superstructure bounding the caldera complex) are favored loci for the extra-caldera deposits, most of which are xenothermal, virtually lacking in regional zoning of metals, and derived from metal sources only broadly referable to Tertiary magmatic processes. The distribution of many prospects fits the hypothesis that relates extra-caldera mined deposits primarily to large subsidence structures and superposed shear zones. Though cauldron subsidence (about 47 m.y. ago) and regional strain (superposed about 44 m.y. ago) are datable events, and though extensive silicification is by inference not older than about 44 m.y., the age of metallization remains uncertain. Interpretation of the Eocene structures and the mineral deposits within them is further complicated by widespread block faulting that has affected rocks of Miocene and Holocene age. Despite these uncertainties and complexities, the relations of large structures of Eocene age, together with local patterns of wallrock alteration, help narrow the search for concealed ore deposits related to the caldera complex.

Symposium on the Geology and Mineral Deposits of the Challis 1°×2° Quadrangle, Idaho

Chapter I

Epithermal Gold-Silver Mineralization Related to Volcanic Subsidence in the Custer Graben, Custer County, Idaho

By D. H. McINTYRE *and* K. M. JOHNSON

CONTENTS

FIGURES

Abstract

The Custer graben is a 13-by-32 km (kilometer) northeast-trending volcano-tectonic graben in the Challis volcanic field in central Idaho. The Yankee Fork mining district, within the graben, has produced in excess of $12,000,000 in gold, silver, copper, lead, and zinc since the early 1880's.

Four major rock types are present within the graben: Paleozoic sedimentary rocks and Tertiary andesite, pyroclastic rocks, and rhyolite. Graben subsidence began about 48 m.y. (million years) ago with the eruption of the tuff of Eightmile Creek. Hydrothermal alteration and epithermal mineralization took place about 45 m.y. ago in parts of the graben where there was both silicic intrusive activity and persistent fault movement.

The andesites, pyroclastic rocks, and rhyolites are hosts for vein and disseminated mineral deposits. Ores are localized along a few discrete northeast- and northwest-trending fracture zones. Hypogene alteration consisted of pervasive propylitization and silicification followed by less extensive oxidation. Ore minerals are electrum, native gold and silver, chalcopyrite, and various sulfosalt minerals in a gangue of pyrite and fine-grained quartz.

Volcano-tectonic subsidence features are good exploration targets because young high-level mineral deposits are preserved in this environment. The Custer graben was an important host for epithermal mineral deposits because it had a favorable combination of source rocks, hydrothermal fluids, and suitably permeable host rocks. The processes that formed the mineral deposits were genetically related to structural and intrusive events accompanying the development of the graben.

INTRODUCTION

The Custer graben is a major northeast-trending volcano-tectonic depression in the Challis volcanic field in the east-central part of the Challis quadrangle (fig. A1, chap. A, this volume). It is part of the trans-Challis fault system (Bennett and Knowles, chap. F, and Kiilsgaard and Lewis, chap. B, this volume). The graben is an Eocene structural feature that has little modern-day topographic expression. The part of the graben southwest of the Yankee Fork mining district has been outlined by Choate (1962) and Siems and others (1979); within and northeast of the mining district it has been mapped by McIntyre (unpub. data, 1975–82) and by Foster (1982). The Yankee Fork mining district, most of which is within the graben, has produced more than $12,000,000 in gold and silver since the 1880's (Anderson, 1949; Koschmann and Bergendahl, 1968). Most of this production was from mines along or near major faults and fractures within the graben and near the graben margin.

STRATIGRAPHY

The oldest rocks that occur in and near the Custer graben are dark-gray siltite, argillite, quartzite, and limestone of the Lower Permian Grand Prize Formation (Hall, chap. J, this volume). These rocks are intruded by granitic rocks of the Cretaceous Idaho batholith (fig. I1). The Grand Prize Formation and granitic rocks of the Idaho batholith are the two principal rock types that underlie volcanic rocks within the Custer graben. The exposures of Grand Prize Formation within the graben in the Yankee Fork mining district and the local occurrence of Grand Prize clasts in a breccia pipe that crosscuts rocks of the graben fill suggest that much of the graben in and northeast of the mining district is underlain by rocks of this unit. The part of the Custer graben southwest of the mining district is underlain chiefly by rocks of the Idaho batholith.

The oldest volcanic rocks in and around the Custer graben are andesite lavas and associated pyroclastic rocks that were emplaced about 50 m.y. ago, prior to graben formation. These rocks were erupted from several centers, two of which are within the area of figure I1, one near Mt. Jordan (Foster, 1982) and the other east of Mt. Greylock. The total thickness of andesite lavas exceeds 1 km (fig. I2).

Initial subsidence of the Custer graben accompanied eruption of a quartz latitic ash-flow tuff, the tuff of Eightmile Creek, which is in part as old as about 48 m.y. Continued graben subsidence trapped a sequence more than 300 m thick of quartz latitic to rhyolitic pyroclastic rocks and minor rhyolite lava that were derived from a variety of sources. This sequence is no younger than about 47 m.y.

Patterns of deposition within the graben were influenced by the irregular topography on the underlying andesite and by different subsidence rates of the various fault-bounded blocks within the graben. Subaqueous deposition occurred in blocks bounded by faults having most rapid or most frequently recurrent movement. The most significant fault blocks of this kind are those in the Sunbeam mine-Estes Mountain-Loon Creek Summit area (fig. I1). Movement on these faults persisted during and after the time of mineralization in this area; the faults were important ore controls. Elsewhere in the graben, deposition was wholly subaerial.

Four kinds of Tertiary intrusive rocks are within and near the Custer graben. Andesite intrusions occur in the vent areas from which the andesite lavas were erupted. A granodiorite-quartz monzonite stock is southeast of Custer. Exposures there are of the roof zone of the stock; small dikes and plugs, an aeromagnetic high, and the distribution of altered rocks indicate a buried extension of this stock at least 3 km west of the area where it crops out. Many dikes, domes, and irregular masses of rhyolite occur throughout the graben. The stock southeast of Custer and some of the rhyolite masses have genetically related ore deposits. An irregular mass of intermediate composition intrudes the rhyolite southwest of the Sunbeam mine (fig. I1). It was emplaced following ore deposition.

Foster (1982) suggested that some of these late intermediate-composition intrusions may have fed a lava field that once buried the rocks now exposed. Some such

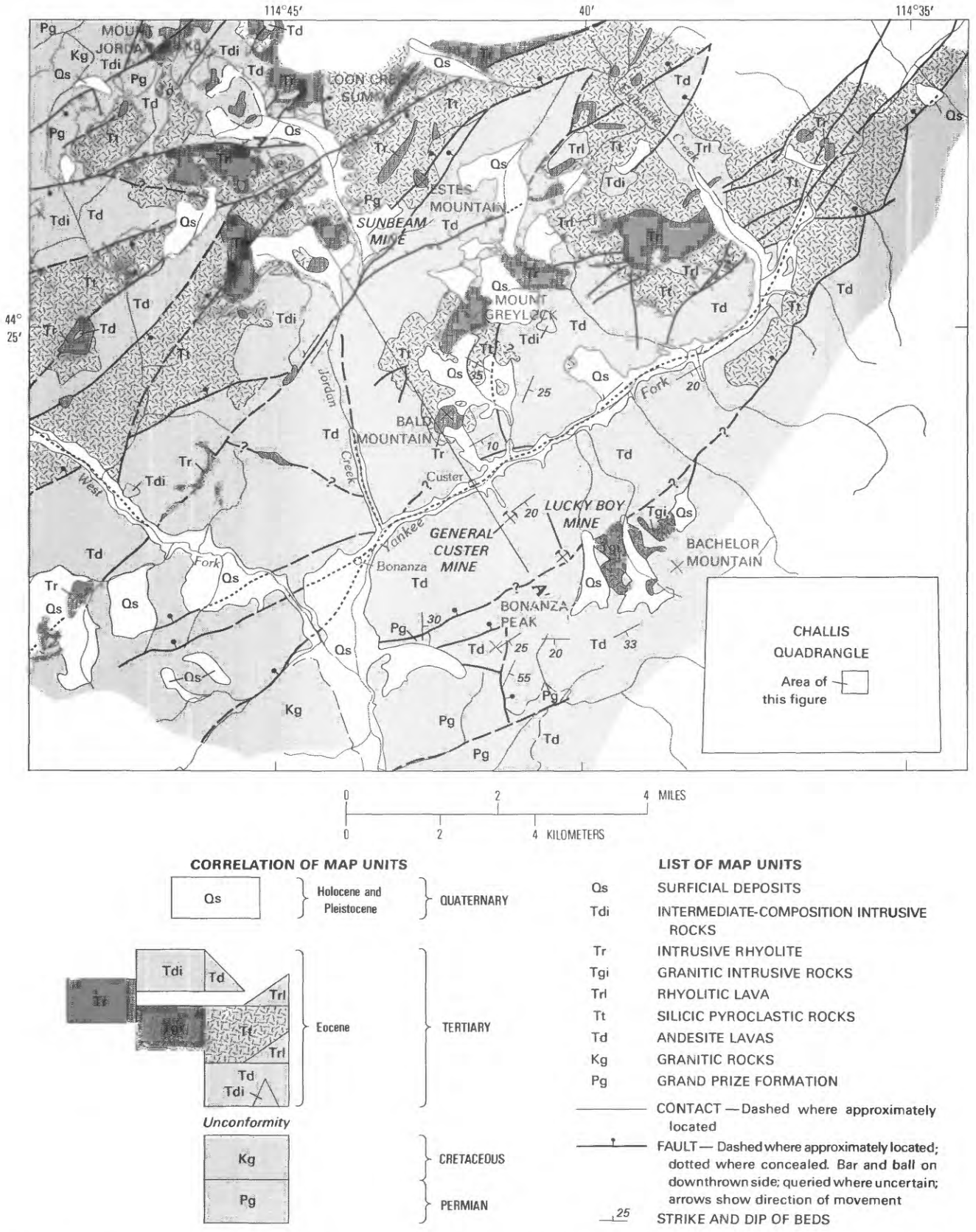

Figure I1. Geologic map of the part of the Custer graben that includes the Yankee Fork mining district. Faults that bound the graben are near Mt. Jordan on the northwest, and north of Bonanza Peak on the southeast. Section *A–A′* is shown on figure I2. Generalized from D. H. McIntyre (unpub. data, 1975–82) and Foster (1982).

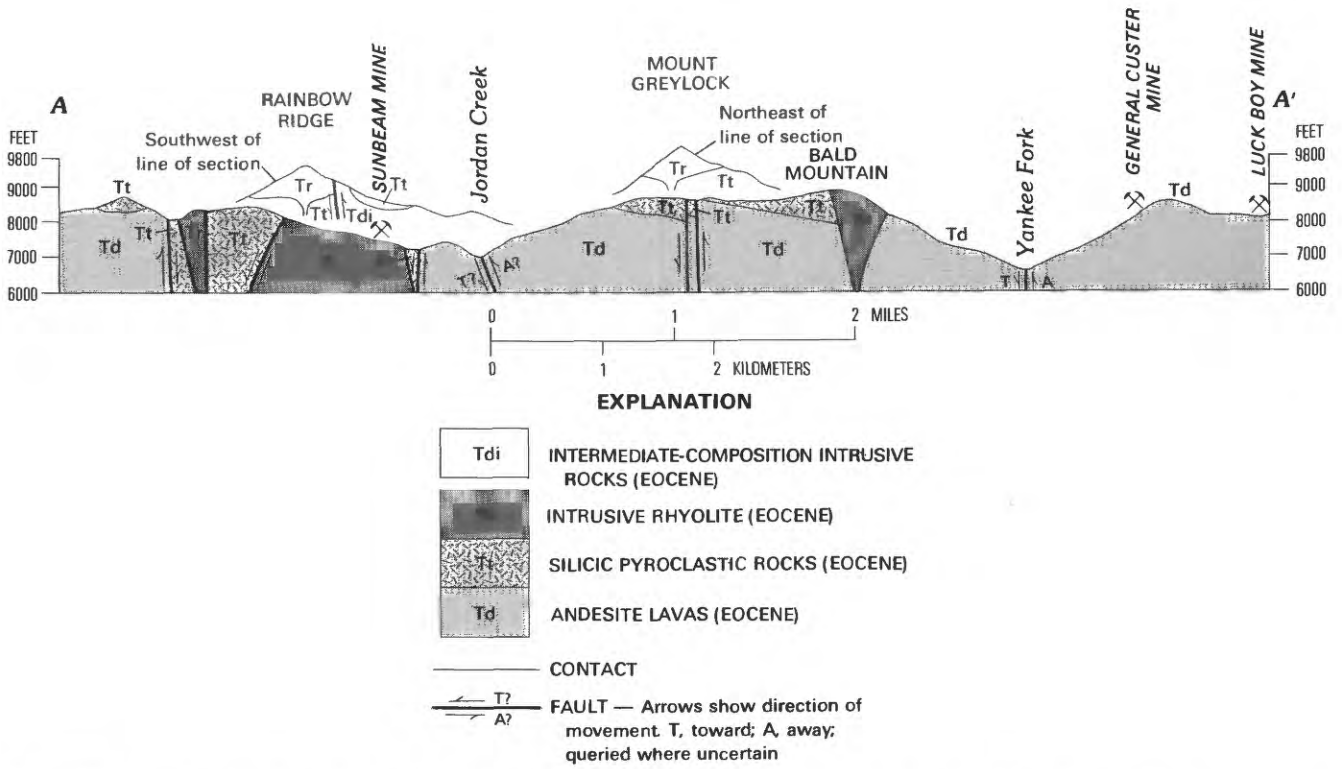

Figure 12. Cross section through part of the Custer graben, along line *A–A'* (fig. 11). Rainbow Ridge is an informal name used in this report for the ridge formed by a rhyolite dome west of the Sunbeam mine.

cover appears necessary to account for the preservation of the currently exposed graben fill (fig. 12).

The ages of the intrusive rocks within the graben are only incompletely known. Zircon from hydrothermally altered rhyolite at the Sunbeam mine gave a fission-track age of 45.8±2.3 m.y. This is an age for the hydrothermal alteration, which presumably is not significantly younger than the intrusion. A potassium-argon age of 47.4±1.8 m.y. has been obtained for biotite from the rhyolite dome at Mt. Greylock. Age analysis of this sample is not yet complete, so this result should be considered provisional (R. F. Marvin, oral commun., 1984).

STRUCTURE

The most prominent structures within the graben are northeast-trending faults that parallel the graben margins. Most of the faults have a predominant dip-slip component. Some also have a measurable strike-slip component; about 2 km of left-lateral strike-slip displacement is demonstrable along the northeast-trending fault that follows the Yankee Fork near Custer. About 0.4 km of dip-slip displacement (down to the northwest) also occurred along this fault. These displacements postdate the mineralization. The fault now is the most obvious one near the southeastern margin of the Custer graben. Farther southeast is another northeast-trending fault that juxtaposes andesitic lava and the Grand Prize Formation. This fault is the outermost in the fault zone at the southeastern margin of the graben.

Comparable displacements, both dip slip and strike slip, may have taken place along the fault zone at the northwestern margin of the graben as well as along faults within the graben fill. Detailed mapping at the Sunbeam mine shows lateral and vertical fault displacements of tens of meters on minor faults subsidiary to nearby major fault zones. Movement on both major and minor faults began before and continued after mineralization at the Sunbeam mine (McIntyre and Johnson, 1983).

MINERALIZATION AND ALTERATION

Mineralization in the Yankee Fork mining district resulted in high-grade gold-silver veins and associated chimneylike deposits, disseminated gold-silver deposits, and gold-silver veins having relatively high base-metal contents. Anomalous concentrations of gold, silver, copper, and molybdenum were found in stream-sediment geochemical surveys (McDanal and others, 1984). The deposits occur within andesite, silicic tuff, and rhyolite and are localized along northeast- and northwest-trending fractures.

The deposits are concentrated in two areas, the Sunbeam mine-Estes Mountain area and the Charles

Dickens-Lucky Boy mines area (fig. I3). Both areas are surrounded by broad haloes of propylitic alteration. The rocks near the deposits commonly are intensely altered to clay minerals and quartz. Supergene leaching caused by weathering of pyrite adds to the bleached appearance of rocks exposed near the ore deposits.

The rocks in large zones encompassing the two mineralized areas are characterized by depletion of oxygen-18 (^{18}O). Ratios of ^{18}O to ^{16}O are lowest near clusters of ore deposits and increase systematically away from the deposits; the areas affected are larger than those having strong visible alteration (Criss and others, 1985). The ^{18}O depletion occurred during alteration and mineralization when the rocks interacted with meteoric-hydrothermal fluids of moderate temperature and low ^{18}O content that were circulating around shallow-level silicic intrusions (Criss and others, 1985).

Most of the early-day production in the district came from the high-grade gold-silver veins. Typically, as at the General Custer and Sunbeam mines, the ore minerals in these veins are so fine grained as to make identification of ore minerals difficult or impossible, although bunches of coarse-grained gold and silver-bearing minerals were found in the early-day operations at some of the mines (Anderson, 1949). The gangue most commonly is fine-grained quartz, generally white but often gray, blue, or bluish gray because of the finely disseminated, dark metallic minerals it contains. One exception is the Lucky Boy mine, where the gangue is about half calcite and half quartz. Pyrite is ubiquitous and often is the only identifiable metallic mineral in the veins. Anderson (1949) identified under the microscope pyrite, chalcopyrite, sphalerite, tetrahedrite, arsenopyrite, enargite, galena, stephanite, miargyrite, pyrargyrite, argentite, aguilarite, gold, and electrum.

The largest producing mine in the Yankee Fork district (fig. I4) was the General Custer mine, where erosion stripped most of the hanging wall from a northwest-trending vein, vastly reducing mining costs. The vein filling at the General Custer is fine-grained quartz in which the ore minerals occur as dark-colored blotches. The gold was largely free, and silver occurred as native silver, argentite, and cerargyrite. The ore is reported to have contained 80 to 90 ounces of silver for each ounce of gold (Anderson, 1949).

Production from other properties in the district was small compared to that from the General Custer mine. Other mines in the district reporting much more silver than gold include the Lucky Boy, McFadden, and a host of small producers. The Montana and Sunbeam produced more gold than silver. Sunbeam ore is said to have had a gold-silver ratio of 2.5 to 1 (Lockard and Rice, 1971).

A broad zone of disseminated gold and silver surrounds the high-grade veins at the Sunbeam mine. The host rocks are variably argillized and silicified rhyolite and

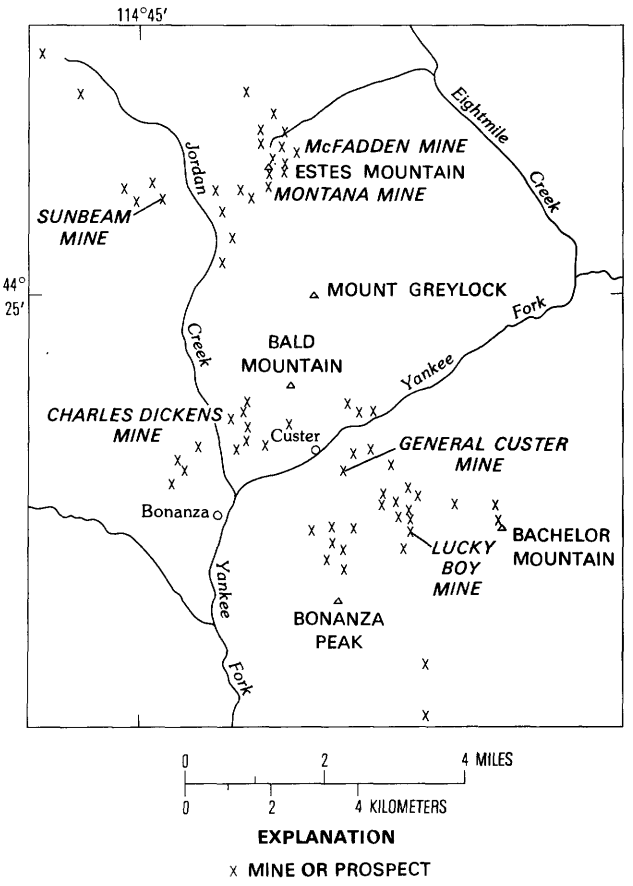

Figure I3. Map showing principal mines and prospects, Yankee Fork mining district, Custer graben.

silicic tuff. A similarly altered zone in andesite surrounds the General Custer vein. The zone is controlled in part by many small faults known from mining exploration in the area but not shown on figure I1. Both deposits were being explored in 1983.

The principal gold-silver-base metal occurrence in the district is at the Charles Dickens mine (fig. I3). The Dickens produced more silver than gold; only minor amounts of copper, lead, and zinc were produced. The base metals occur in chalcopyrite, covellite, galena, and sphalerite. The veins rich in base metals may have been deposited at greater depth than those containing only gold and silver.

ORE GENESIS

Exceptionally long-lived movement along two northeast-trending fault zones, one in the Sunbeam mine-Estes Mountain area and the other in the Charles Dickens-Lucky Boy mines area, was a controlling factor for ore localization within the Custer graben. Movement on these faults began with initial graben subsidence, and, as noted above, locally influenced depositional environments within the graben. These and other fault zones within the graben localized intrusion of rhyolite and the granodiorite-quartz

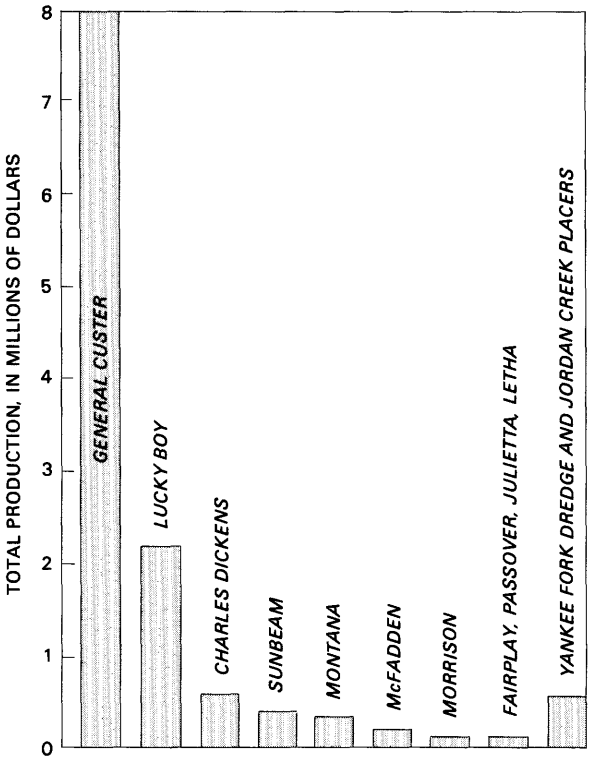

Figure 14. Value of total production of precious metals from mines during 1882 to 1959 in the Yankee Fork mining district, Custer graben.

monzonite stock. Continued fault movement and repeated renewal of fracture permeability in these fault zones permitted establishment of extensive, long-lived hydrothermal convection cells within each fault zone. Hydrothermal convection was driven by heat from the silicic intrusions. These processes continued long enough to permit formation of ore-grade deposits. Cooling of the silicic intrusions brought hydrothermal circulation to an end. Fault movement continued after hydrothermal circulation and ore deposition had ceased.

The source of the metal ions is not known with certainty. The Grand Prize Formation, which underlies the graben within the mining district, is a likely source for base metals and silver because, elsewhere in the region, it is known to be intrinsically rich in these metals (Hall, chap. J, this volume). The contribution of the silicic magmas to the metal content of the ore deposits in the graben is not known.

ORE PRESERVATION

Graben subsidence and further burial after ore deposition helped protect the deposits from erosion, which probably has continued with little interruption from late Eocene to the present. As indicated above, the area may have been covered by a blanket of lavas of intermediate composition. How thick or how extensive these or other postmineralization cover rocks may have been is speculative because no trace of them now remains.

There is some evidence that not all the deposits originally formed have been preserved. At Mount Jordan, at the northwestern margin of the graben, there is an occurrence of anomalous copper and other base metals in the volcanic rocks (Foster and Cooley, 1982). This occurrence may represent a lower level of a hydrothermal system that deposited precious metals at a higher level, now removed by erosion. Vertical zonation, with base metals below precious metals, occurs within the graben at Estes Mountain.

Not all the precious metals from eroded lode deposits escaped the area. Rich placer deposits in Quaternary gravels along Jordan Creek and Yankee Fork were mined extensively before 1952 (Choate, 1952). Several small-scale placer operations were underway in 1983.

CONCLUSIONS

The Custer graben contains epithermal ore deposits because of a combination of favorable characteristics. Paleozoic sedimentary rocks that form the basement beneath the mining district are a potentially rich source of a variety of metals. Rhyolite and granodiorite-quartz monzonite magmas also may have been sources for metals. The heat that accompanied intrusion of these silicic magmas drove extensive hydrothermal circulation systems in which meteoric water was the predominant component. Faults that remained active during and after graben formation provided pathways for the fluids and sites for ore deposition. In parts of the graben where there was little faulting or no silicic intrusive activity, there also are no known ore deposits and few prospects.

Another critical factor for the presence of epithermal ore deposits is preservation. This is one of the major reasons why Tertiary volcano-tectonic subsidence structures are good exploration targets. Subsidence and infilling of a graben or caldera preserves ore deposits that have been formed within them. Otherwise, epithermal deposits, especially those as old as Eocene, would long since have been lost to erosion, which is probably what happened to deposits that formed in areas adjoining the graben margin but on the upthrown side of the graben-bounding faults.

REFERENCES CITED

Anderson, A. L., 1949, Silver-gold deposits of the Yankee Fork district, Custer County, Idaho: Idaho Bureau of Mines and Geology Pamphlet 83, 37 p.

Choate, Raoul, 1962, Geology and ore deposits of the Stanley area [Idaho]: Idaho Bureau of Mines and Geology Pamphlet 126, 121 p.

Criss, R. E., Champion, D. E., and McIntyre, D. H., 1985, Oxygen isotope, aeromagnetic, and gravity anomalies associated with hydrothermally altered zones in the Yankee Fork mining district, Custer County, Idaho: Economic Geology, v. 80, no. 5, p. 1277–1296.

Foster, Fess, 1982, Geologic map of Mt. Jordan and vicinity, Custer County, Idaho: U.S. Geological Survey Miscellaneous Field Studies Map MF-1434.

Foster, Fess, and Cooley, E. F., 1982, Semiquantitative spectrographic analyses of rocks from the Mt. Jordan vicinity, Custer County, Idaho: U.S. Geological Survey Open-File Report 82–467, 13 p.

Koschmann, A. H., and Bergendahl, M. H., 1968, Principal gold-producing districts of the United States: U.S. Geological Survey Professional Paper 610, 283 p.

Lockard, D. W., and Rice, W. L., 1971, Preliminary investigation of a low-grade gold deposit in Custer County, Idaho: U.S. Bureau of Mines Open-File Report 5–71, 40 p.

McDanal, S. K., Cooley, E. F., and Callahan, J. E., 1984, Analytical results of stream-sediment and nonmagnetic heavy-mineral-concentrate samples with sample locality map from portions of the Challis 1°×2° quadrangle, Idaho: U.S. Geological Survey Open-File Report 84–0634, 389 p.

McIntyre, D. H., and Johnson, K. M., 1983, Geologic map of part of the Sunbeam mine area, Custer County, Idaho: U.S. Geological Survey Open-File Report 83–329, [scale 1:2,400].

Siems, P. L., Albers, D. F., Malloy, R. W., Mitchell, V. E., and Perley, P. C., 1979, Uranium potential and geology of the Challis Volcanics of the Basin Creek-Yankee Fork area, Custer County, Idaho: U.S. Department of Energy Report GJBX-33(79), 200 p.

Symposium on the Geology and Mineral Deposits of the Challis 1°×2° Quadrangle, Idaho

Chapter J

Stratigraphy of and Mineral Deposits in Middle and Upper Paleozoic Rocks of the Black-Shale Mineral Belt, Central Idaho

By WAYNE E. HALL

CONTENTS

FIGURES

TABLES

Abstract

A belt of highly mineralized, black, siliceous-facies sedimentary rocks of Late Cambrian to Permian age crops out on the eastern side of the Idaho batholith in central Idaho. All of the Paleozoic rocks are allochthonous and occur in imbricated structural plates separated by regional thrust faults. The structural plates are stacked, younger formations over older, in most places. The value of past production of metals from this belt is $65 million; a conservative estimate of the total known resources is $6 billion. The most intensely mineralized zones are in black argillite and micritic limestone beds of the Milligen Formation (Devonian) and the Salmon River assemblage (Upper Mississippian, Upper Devonian, and Upper Cambrian) and the Dollarhide Formation (Permian) below regional thrust faults near biotite granodiorite stocks of Cretaceous age.

Mineral resources include: (1) many small to moderate-size, high-grade lead-silver-zinc vein deposits; (2) an area containing tin associated with lead-silver vein deposits in the Galena and Boulder Basin districts; (3) skarn tungsten veins; (4) two large molybdenum stockwork deposits; and (5) stratabound deposits of zinc, barite, vanadium, and possibly lead and silver. As much as 6 weight percent tin occurs in ore at Boulder Basin in a mineralogic and chemical assemblage (Pb-Zn-Sb-Ag-Au-Sn-Se) similar to Bolivian-type tin deposits. These deposits occur in limy sandstone of the Pennsylvanian and Permian Wood River Formation near Eocene hypabyssal intrusive bodies; all other lead-silver vein deposits are in black argillite sequences near Cretaceous stocks.

The black shale beds contain and probably are the source of metals for the vein deposits. Also, some of the productive deposits are stratabound and are syngenetic. Recent mining activity has concentrated on exploration for the stratabound syngenetic deposits in the black-shale mineral belt and on development and bringing into production the Thompson Creek molybdenum stockwork deposit.

INTRODUCTION

A belt of highly mineralized, black siliceous-facies sedimentary rocks, 145 km (kilometers) long in a north-northwest direction and 15 to 45 km wide, of Late Cambrian to Permian age crops out on the eastern side of the Idaho batholith, from the Salmon River in the south-central part of the Challis quadrangle south to Bellevue, Idaho, in the Hailey quadrangle (fig. J1). This area is called the central Idaho black-shale mineral belt in this report. The belt extends east to the Bayhorse district, which is discussed by Hobbs (chaps. D and K, this volume). This chapter presents a preliminary overview of the stratigraphy, structure, and ore deposits of the belt.

The value of past production of metals, mostly lead and silver, from the central Idaho black-shale mineral belt is $65 million; a conservative estimate of the total known resources, most of which are in two molybdenum stockwork deposits, is $6 billion. Mining districts within the belt include, from north to south, the Slate Creek, Little and Big Boulder Creeks, Germania Creek, Fourth of July Creek, East Fork, Galena, Boulder Basin, Carrietown, Triumph-Parker mineral belt, and Wood River (fig. J2).

Most of the production from the black-shale mineral belt was from lead-silver deposits mined during the late 19th century and World War II. Early descriptions of the geology and ore deposits were by Anderson and others (1950), Ross (1937), Umpleby (1915), and Umpleby and others (1930). Recently, the geology of the black-shale mineral belt has been reinterpreted; all the fine-grained, carbonaceous Paleozoic formations are now recognized to be allochthonous, and many of the ore deposits are syngenetic. A partial listing of recent references includes: Dover (1969, 1981), Hall and Czamanske (1972), and Hall and others (1978, 1984).

The geology of the central Idaho black-shale mineral belt (figs. J3 and J4) was mapped by the author in the south-central part of the Challis quadrangle south of the Salmon River and in the Wood River area, and by S. W. Hobbs north of the Salmon River (Fisher and others, 1983; Hobbs and others, 1975). The geology (fig. J1) in both the northern and southern parts of the belt is simplified from detailed mapping. The geology in the central part of the belt, in the Galena and Boulder Basin mining districts, is based on only three east-west traverses made to trace the Paleozoic formations and thrust faults between the areas of detailed mapping. Many Tertiary porphyry intrusions in the Paleozoic rocks were not mapped in making these traverses.

GEOLOGY

The sedimentary rocks in the central Idaho black-shale mineral belt are predominantly black, fine-grained, siliceous-facies argillite, siltite, limy sandstone, shale, and siltstone of Late Cambrian to Permian age. All of the Paleozoic rocks are allochthonous and occur in imbricated structural plates separated by major thrust faults. The structural plates are stacked with predominantly younger Paleozoic sequences over older ones. All of the formations are tectono-stratigraphic units. Different names are applied to essentially coeval rock units on separate thrust plates if the lithology, internal structures, degree of sorting and roundness of clasts, and composition of clasts make each unit lithologically distinctive. The Paleozoic rocks are intruded by granitic plutons of Late Cretaceous and Eocene age and by dikes and sills of porphyritic dacite and rhyodacite and rhyolite of Eocene age. Thick sequences of the Eocene Challis Volcanics unconformably overlie the Paleozoic and Cretaceous rocks.

Sedimentary Rocks

Ordovician to Devonian Rocks, Undivided

The undivided Ordovician to Devonian rocks (fig. J3, map unit DSOu) include the Phi Kappa (Ordovician)

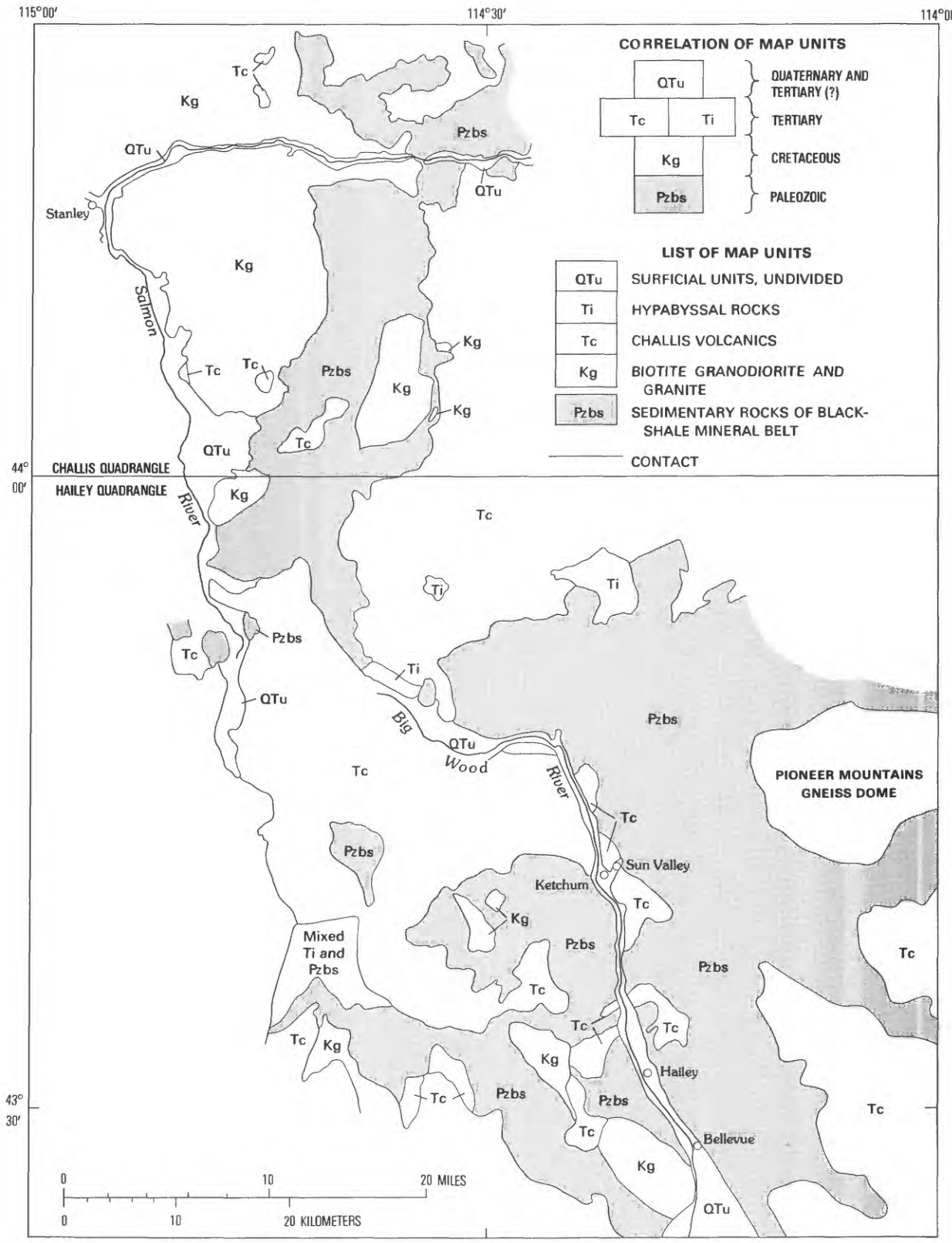

Figure J1. Simplified geologic map of the black-shale mineral belt, central Idaho.

and Trail Creek (Silurian) Formations, which were originally named by Umpleby and others (1930) and were described and redefined by Dover and others (1980), and an unnamed Silurian and Devonian unit described by Dover (1981, p. 34). Dover showed that the Phi Kappa and Trail Creek Formations consist of an intricately

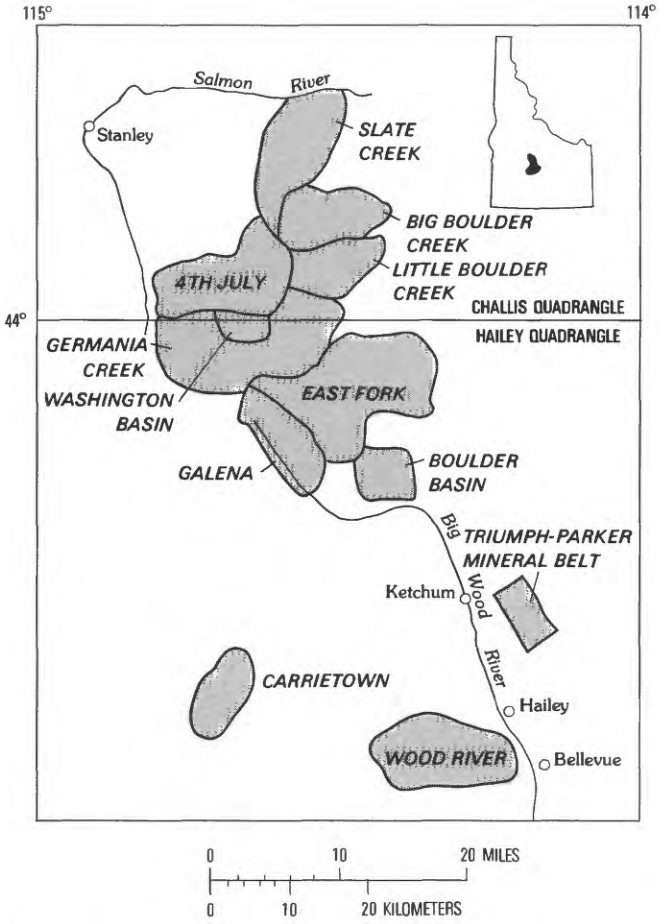

Figure J2. Index map showing the study area and mining districts in the black-shale mineral belt, central Idaho.

imbricated series of thrust slices that are composed of black argillite and shale imbricated with thrust slices of metasiltstone, fine-grained quartzite, and siliceous mudstone. Much of the shale and mudstone is finely laminated and contains internal structures such as scour, crossbedding, and convolutions, indicating deposition of these transitional deposits on a slope, which is interpreted from facies models to have been near the continental margin.

Milligen Formation

The Devonian Milligen Formation (fig. J4, map unit Dm) crops out in a northwest-trending belt about 50 km long and 11 km wide in the Wood River area. The formation consists of interbedded dark-gray to black siliceous argillite, siltite, and micritic limestone but includes minor dolomitic siltstone, quartzite, and granule conglomerate in the upper part. The formation is divided into two informal members—a lower member at least 900 m (meters) thick of dark siliceous argillite and an upper member as much as 300 m thick that is much less argillitic and more heterogeneous in lithology (Sandberg and others, 1975). The lower unit is a deep-water siliceous oceanic facies, and the upper unit was deposited during uplift that presaged the Antler orogeny. A more complete description of the lithology and metamorphic grade of the Milligen is given in Sandberg and others (1975).

Copper Basin Formation

The Mississippian Copper Basin Formation (fig. J4, map unit Mc) crops out along the eastern side of the study area, mostly on the north side of the Pioneer Mountains gneiss dome. The Copper Basin is a deep-sea fan turbidite sequence at least 3,000 m thick that was deposited in a foreland basin between the Antler highland on the west and the craton to the east (Nilsen, 1977). The formation consists of dark-gray argillite and siltite in the lower part, thinly bedded, fine-grained limestone turbidites in the middle, and siliceous pebble conglomerate and quartzite in the upper part.

Salmon River Assemblage

The Salmon River assemblage (fig. J3, map unit P_Zsr) was named informally by Nilsen (1977) for a sequence composed of limestone turbidites interbedded with dark-gray argillite, siltite, shale, and fine-grained quartzite. The assemblage is well exposed along the Salmon River in the northern part of the study area (fig. J3). It is intensely deformed, so the thickness is difficult to measure, but it is estimated to be more than 2,000 m thick.

The Salmon River assemblage is a tectonostratigraphic mixture of Late Cambrian, Late Devonian, and Late Mississippian fine-grained, carbonaceous rocks. The fossil reports indicating the mixture of ages in the Salmon River assemblage are given in Hobbs (chap. D, this volume). Late Cambrian fauna have been identified from silty, carbonaceous limestone interbedded with argillite on the eastern margin of the Salmon River allochthon on the western side of Thompson Creek (fig. J3). The limestone is interpreted by Hobbs and Hall to be a tectonic slice at the base of the allochthon. Conodonts of Late Devonian age have been identified by Repetski (*in* Hobbs, chap. D, this volume) from samples of carbonaceous limestone that were collected by F. G. Poole and George Desborough and by Poole and Hall between tributary canyons on the west side of Slate Creek on the southwest to Thompson Creek on the northeast (fig. J3). The limestone is interbedded throughout a large part of the stratigraphic thickness of the assemblage. Two specimens of float from the same terrane as the collections of Poole and Hall contained a megafauna that is Late Mississippian (Hobbs, chap. D, this volume). This part of the Salmon River assemblage, consisting of graded, fine-grained carbonaceous rocks, was deposited on a slope, probably near the edge of the continental slope. The Salmon River assemblage rocks are weakly metamorphosed and have a fracture cleavage that is almost parallel

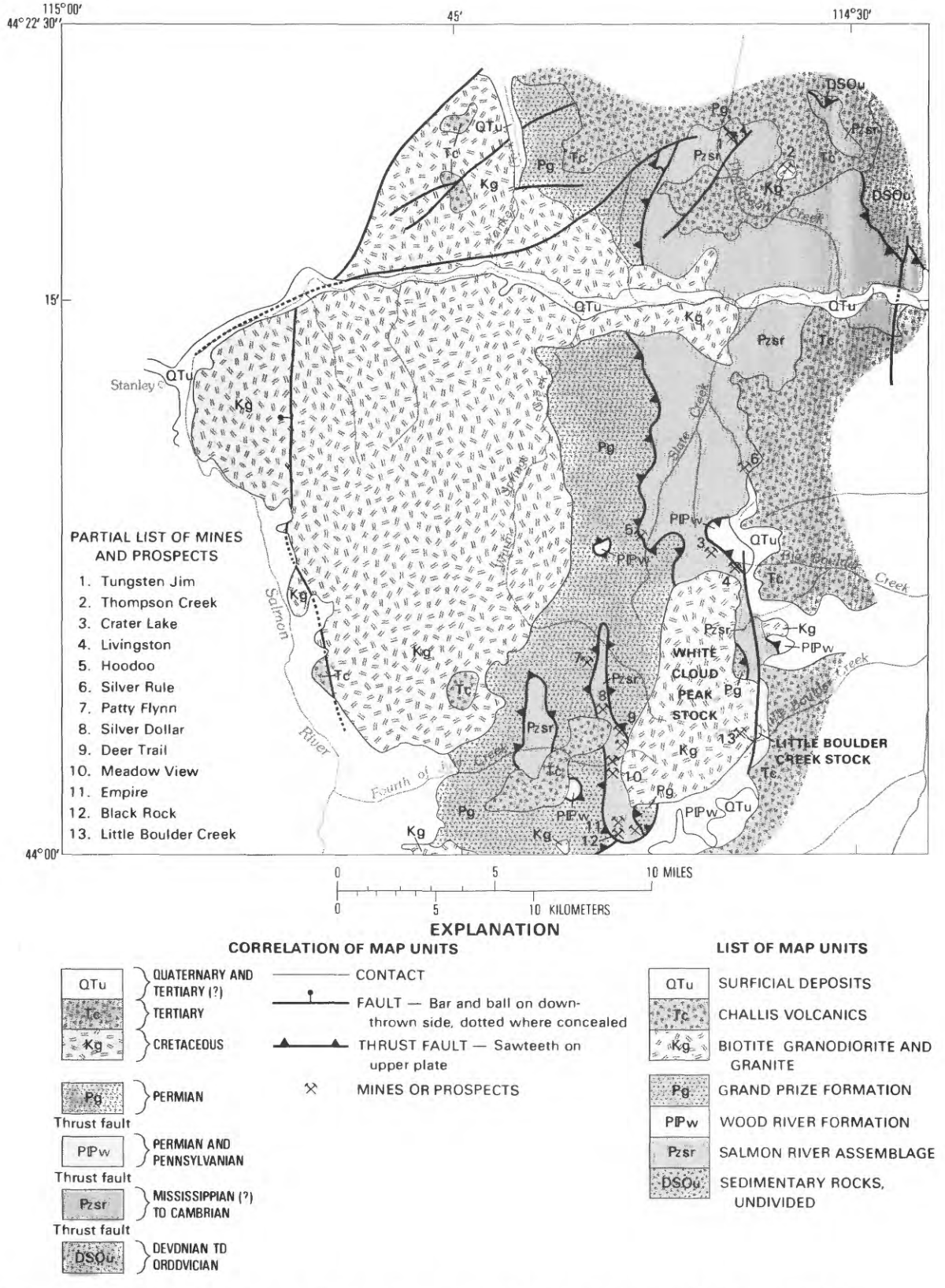

Figure J3. Simplified geologic map of the northern part of the black-shale mineral belt, central Idaho.

to bedding. They differ from the Milligen Formation, which has a penetrative shear cleavage that is at a large angle to bedding, has a much higher metamorphic grade, and has a phyllitic sheen.

Wood River Formation

The Pennsylvanian-Permian Wood River Formation (figs. J3 and J4, map unit IPw) crops out in a northwest-

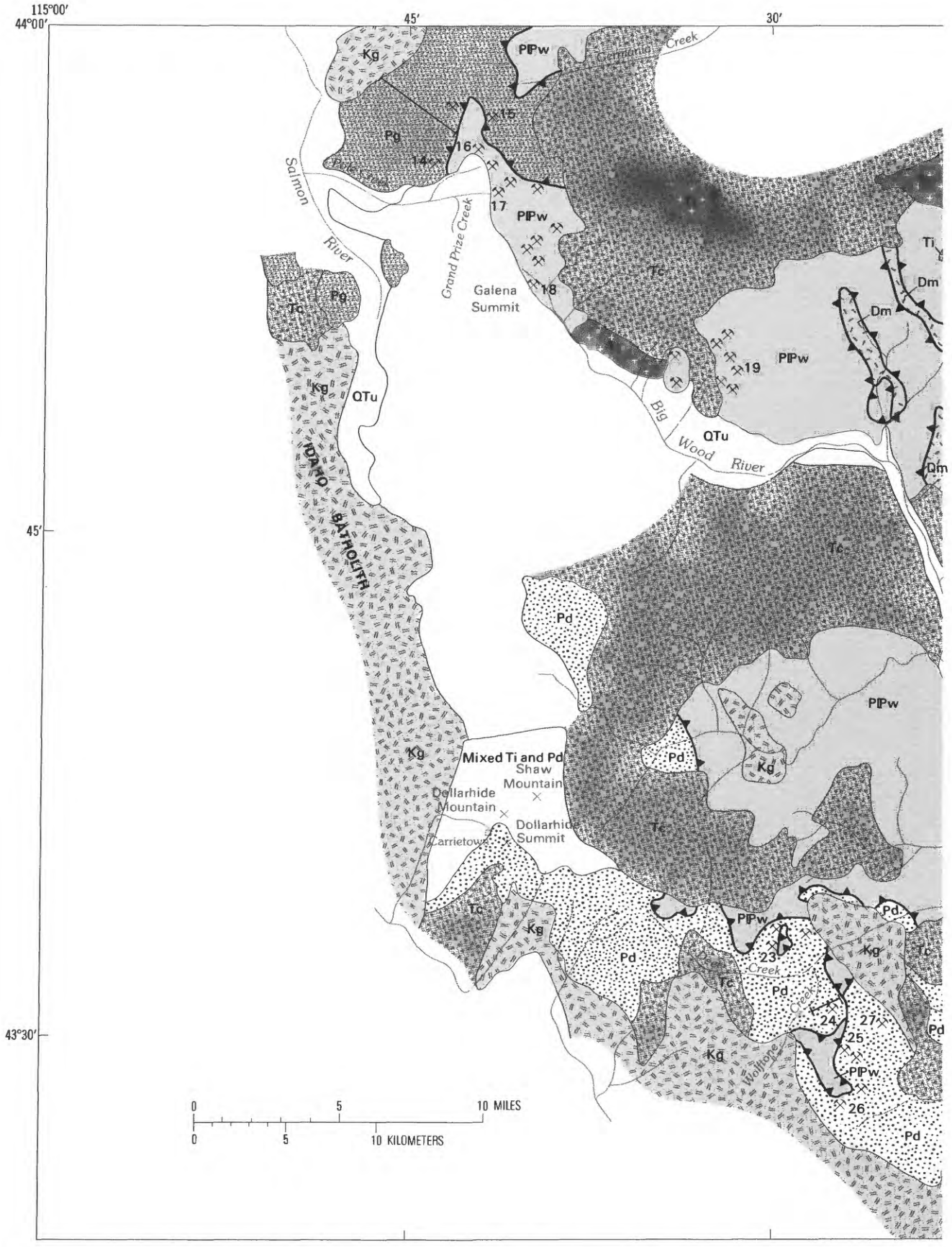

Figure J4. Simplified geologic map of the southern part of the black-shale mineral belt, central Idaho.

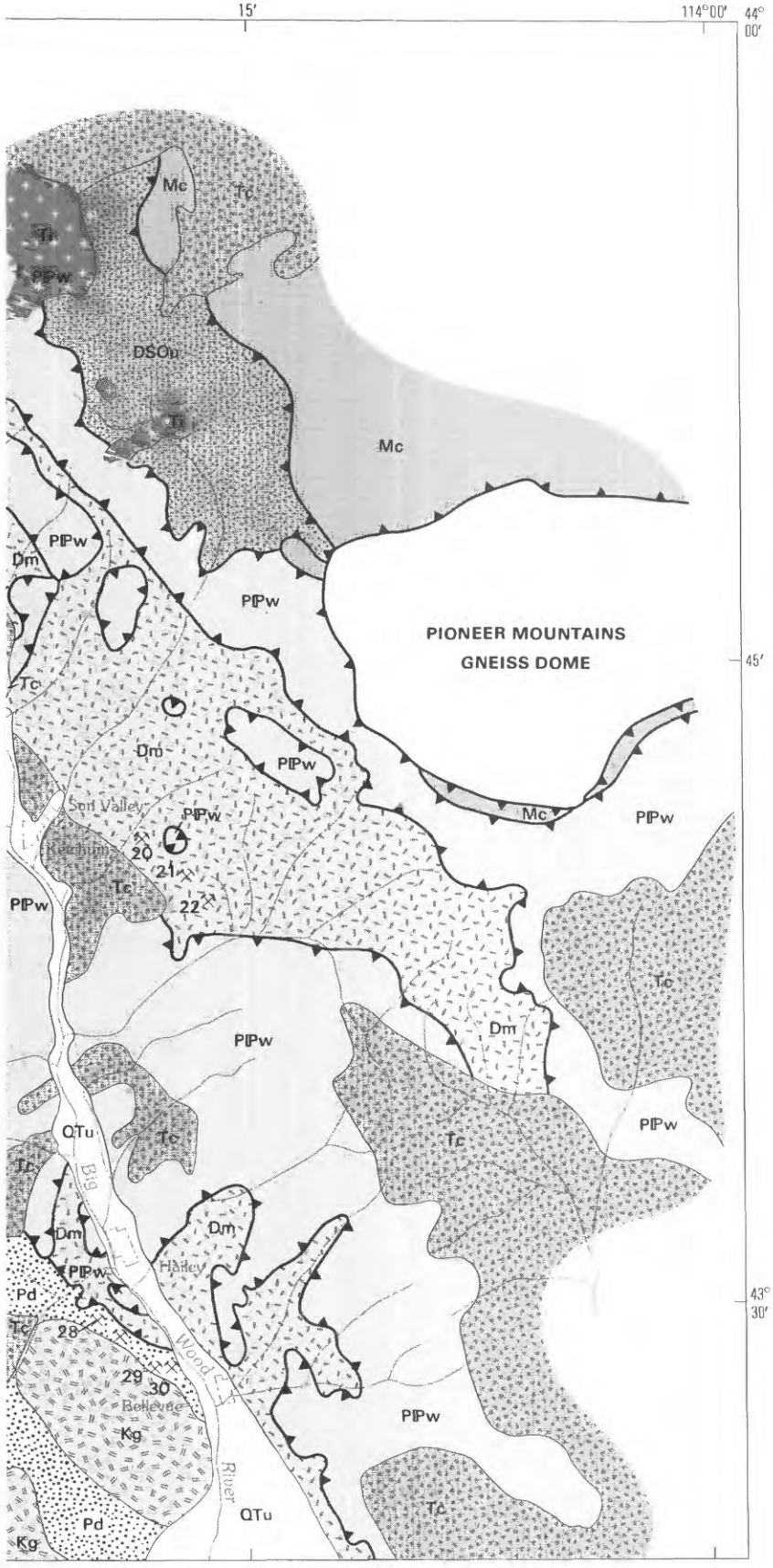

CORRELATION OF MAP UNITS

QTu	QUATERNARY AND TERTIARY (?)
Tc, Ti	TERTIARY
Kg	CRETACEOUS
Pd	PERMIAN
Thrust fault	
Pg	PERMIAN
Thrust fault	
PPw	PERMIAN AND PENNSYLVANIAN
Thrust fault	
Mc	MISSISSIPPIAN
Dm	DEVONIAN
Thrust fault	
DSOu	DEVONIAN TO ORDOVICIAN

LIST OF MAP UNITS

QTu	SURFICIAL DEPOSITS, UNDIVIDED
Ti	HYPABYSSAL INTRUSIVE ROCKS
Tc	CHALLIS VOLCANICS
Kg	BIOTITE GRANODIORITE AND GRANITE
Pd	DOLLARHIDE FORMATION
Pg	GRAND PRIZE FORMATION
PPw	WOOD RIVER FORMATION
Mc	COPPER BASIN FORMATION
Dm	MILLIGEN FORMATION
DSOu	SEDIMENTARY ROCKS, UNDIVIDED

CONTACT

THRUST FAULT — Sawteeth on upper plate

MEASURED SECTION

MINES AND PROSPECTS

PARTIAL LIST OF MINES AND PROSPECTS

14. Peace of Mine
15. Pole Group
16. Darlin
17. Stoneboat
18. Black Carbonate
19. Golden Glow
20. Independence
21. Triumph
22. North Star
23. Deer Creek barite
24. Red Cloud
25. Red Elephant
26. Liberty Gem
27. Eureka
28. Snoose
29. Minnie Moore
30. Silver Star Queen

Figure J4. Continued.

trending belt 100 km long and 40 km wide throughout the Wood River area north to White Cloud Peaks. The formation is about 3,000 m thick. It consists of a basal siliceous conglomerate as thick as 120 m, and thick sequences of fine-grained, light-gray, limy sandstone and interbedded fine-grained quartzite and silty limestone. The formation was subdivided into seven units by Hall and others (1974). It ranges in age from Middle Pennsylvanian (Desmoinesian) to Early Permian (Wolfcampian and Leonardian?).

Dollarhide Formation

Dollarhide Formation (Permian; fig. J4, map unit Pd) is the name given herein for a sequence of interbedded, dark-gray carbonaceous limestone, siltite, fine-grained quartzite, sandstone, and minor granule conglomerate that is exposed along the ridge between Dollarhide Summit and Dollarhide Mountain in the Dollarhide Mountain 7 1/2-minute quadrangle, 32 km west of Ketchum; this is the type locality for the formation. The Dollarhide Formation, formerly mapped as part of the Wood River Formation, crops out over an area of about 100 sq km (square kilometers). It was intruded by the Idaho batholith.

The formation is characterized by highly carbonaceous limestone, fine-grained limy sandstone, siltstone, and siltite that is banded dark-gray and brown in layers 1 to 4 cm (centimeters) thick. Graded bedding and convolute structures are common. The limestone, siltstone, and siltite of the Dollarhide Formation are more poorly sorted and have less rounded and larger sand grains than Wood River Formation limy sandstone and quartzite of the same age.

A partial section of Dollarhide Formation 653 m thick was measured on the eastern side of Wolftone Creek in the Mahoney Butte 7 1/2 minute quadrangle, 12 km west of Hailey, in sec. 8, T. 2 N., R. 17 E., on the north side of the Red Cloud mine (fig. J4). This was selected as a reference locality because it contains the only fossils that have been found in the Dollarhide Formation.

Measured partial section of Dollarhide Formation

[Measured by W. E. Hall on ridge north of Red Cloud mine in sec. 8, T. 2 N., R. 17 E.]

Thrust-fault contact with overlying Wood River Formation unit 5

Dollarhide Formation:	Thickness (meters)
Limestone, silty, gray, carbonaceous, fine-grained	22
Siltite, dark-gray, carbonaceous; and quartzite, gray, fine-grained	15
Limestone, gray, fine-grained, carbonaceous, thin-bedded	15

Measured partial section of Dollarhide Formation—Continued

Dollarhide Formation:—Continued	Thickness (meters)
Quartzite, light- to dark-gray, fine-grained; and siltite, gray, carbonaceous	191
Siltstone, limy, dark-gray, carbonaceous; and quartzite, fine-grained; shattered	27
Quartzite, gray, fine- to medium-grained, cross bedded; and siltstone, limy, gray	15
Siltstone, limy, gray; and quartzite, medium-gray, fine-grained, carbonaceous; beds 15–30 cm thick	92
Limestone, silty, gray, carbonaceous; and siltite, gray, thin-bedded	15
Siltite, gray, carbonaceous; some parts limy; beds 15–30 cm thick; graded bedding	22
Siltstone, limy, gray; and siltite, gray, laminated; beds 1–2 cm thick	53
Sandstone, limy, gray, grain size 1–2 mm (millimeters); and siltite, gray, shattered	15
Limestone, silty, gray, laminated; beds 1–2 cm thick	7
Sandstone, limy, gray, medium-grained; and siltstone, limy, gray; convolute structures in fine-grained siliceous beds; graded beds, 5–15 cm thick	7
Limestone, silty, gray, carbonaceous; and siltstone, limy, gray on fresh surfaces, weathers dark brown; beds 10–20 cm thick; graded beds	53
Siltstone, gray, limy; and limestone, silty; contains abundant fusulinids (collection P-134); age is Early Permian (R. C. Douglass, written commun., 1978)	7
Total thickness incomplete Dollarhide Formation	653

Base not exposed

R. C. Douglass (written commun., 1978) reported the following on the age of fusulinids collected in Wolftone Creek in the lowest unit of the measured section: "Collection P-134, Blaine County, Idaho * * * the fusulinids present have had most of the gross structures destroyed. Again the carbonaceous matter in the wall of the outer volution displays the detailed structure of the keriotheca beautifully. The wall structure indicates a Late Pennsylvanian to Permian age. The critical gross structures are not preserved, but one section includes an oblique equatorial that suggests highly arched chambers characteristic of the Early Permian *Pseudofusulina*. I cannot make a positive statement about the age of this material, but the odds are now better that this is Early Permian rather than Late Pennsylvanian. In any event, I would show this unit as more likely Early Permian."

Grand Prize Formation

Grand Prize Formation (figs. J3 and J4, map unit Pg) is the name given herein for a thick sequence of interbedded light- to medium-gray limy siltstone; fine-grained

quartzite; dark-gray, banded siltite; and medium- to dark-gray, carbonaceous, silty to sandy limestone that is well exposed in the Horton Peak 7½-minute quadrangle, Custer County, on the northern side of Pole Creek at the confluence with Grand Prize Creek; this is the type locality for the formation. The formation was previously mapped as part of the Wood River Formation by Ross (1937) and Tschanz and others (1974), but it overlies the Wood River Formation in thrust-fault contact and is lithologically distinct from the Wood River Formation. It crops out over an area of 800 sq km from 2 km north of Galena Summit north to the Yankee Fork of the Salmon River.

The formation is divided into four informal units at the type locality on the north slope of Pole Creek canyon at the confluence with Grand Prize Creek, 6.4 km south of the southern boundary of the Challis quadrangle.

Measured partial section of Grand Prize Formation
[Section measured by W. E. Hall]

	Thickness (meters)
Top not exposed	
Grand Prize Formation:	
4. Siltite, dark-gray, banded, weathers dark red and reddish brown; and limestone, silty, fine-grained, gray and bluish-gray, crossbedded, contains soft-sediment deformation	150
3. Siltstone, limy, gray, banded, medium- to thick-bedded, in part contact metamorphosed and bleached to light-gray hornfels and calc-hornfels; and dark-gray carbonaceous siltite, banded, crossbedded, contains convolute structures	580
2. Limestone, silty, bluish-gray, fine-grained; contains abundant fossil debris but no diagnostic fossils for age determination	30
1. Siltite, carbonaceous, dark-gray, prominently banded, limy in upper part; limestone, gray, sandy, abundant crossbedding and convolute structures in lower part	690
Total thickness units 1–4, Grand Prize Formation	1,450

The age of the Grand Prize Formation is Early Permian (Leonardian), and it could be as old as Early Permian (Wolfcampian) or Pennsylvanian. C. M. Tschanz collected a sample from the base of the type locality at the confluence of Grand Prize and Pole Creeks from which two conodonts were separated. B. R. Wardlaw (written commun., 1979) identified the conodonts as *Neogondolella idahoensis* (Youngquist, Hawley, and Miller)-2, and said: "*Neogondolella idahoensis* indicates a Leonardian-Roadian age (middle-upper Leonardian of U.S. Geological Survey usage). This age is equivalent to the uppermost part of the Pequop Formation, the Kaibab and Grandeur Formations, and the lower part of the Meade Peak Phosphatic Shale Member of the Phosphoria Formation in southern Idaho, Utah, and Nevada."

A sample of limestone of the Grand Prize Formation was collected by S. W. Hobbs from the SunBeam 7½-minute quadrangle, Custer County, on the east side of Peach Creek (lat 44°17′43″ N.; long 114°38′27″ W.). The sample was processed for conodont extraction and examined by A. G. Harris (written commun., 1981), who reported:

10 Pa elements of *Adetognathus* sp.
6 Pa elements of *Hindeodus* cf. *H. Minutus* (Ellison)
9 Pa elements of *Idiognathodus* sp.
2 M elements
2 Pb elements
31 indeterminate bar, blade, and platform fragments.

These conodonts are poorly preserved, stretched, corroded, and mostly incomplete, so that species determination is uncertain to impossible. Nonetheless, the species that these specimens probably represent are long-ranging common elements of shelf faunas in the Pennsylvanian through earliest Permian (late Morrowan to late Wolfcampian).

Plutonic Rocks

The Paleozoic rocks are intruded by many plutons of biotite granodiorite and biotite granite of Cretaceous age, and by small Eocene hypabyssal biotite granite plutons and dacite, rhyodacite, and rhyolite dikes and sills (figs. J3 and J4). Two molybdenum stockwork deposits are associated with the Cretaceous calc-alkaline Thompson Creek biotite granodiorite-biotite granite stock and the White Cloud Peaks and Little Boulder Creek biotite granodiorite stocks (fig. J3). Many of the lead-silver-zinc vein deposits are localized near small plutons of Cretaceous biotite granodiorite. Most of these plutons are sills or laccoliths that intruded into and along the brecciated zones of thrust faults, and most vein deposits are localized in steep shear zones below the thrusts. At the Livingston mine and in the Galena and Boulder Basin districts, the vein deposits are localized next to dikes and sills of Eocene rhyolite, rhyodacite, and dacite porphyry.

Structure

All of the Paleozoic formations are allochthonous and are separated by regional thrust faults. The central Idaho black-shale mineral belt (figs. J3 and J4) can be described as two separate, imbricated stacks of thrust plates. The northern stack, which includes the Salmon River sequence and Grand Prize Formation, is herein called the Boulder Mountains stack. It extends from the Galena district north to the Tungsten Jim mine (fig. J3), and east from the study area into the western Bayhorse district (Hobbs, chap. D, this volume). The southern stack is called the Pioneer Mountains stack. It extends south and southeast from the Boulder Basin. The only allochthon that transcends both stacks is the Wood River

allochthon, which extends north along the southeastern margin of the Boulder Mountains. The allochthons have all been thrust to the east or northeast for distances that range from a few kilometers to as much as 200 km.

Boulder Mountains Stack

The Boulder Mountains stack includes three allochthonous sequences of late Paleozoic age in the Boulder Mountains (figs. J3 and J4). The structurally lowest unit is the Salmon River assemblage of Late Cambrian, Late Devonian, and Late Mississippian age. The base of the Salmon River assemblage is a thrust fault that brought it over Devonian and older rocks (fig. J3) (Hobbs and others, 1975). The Wood River Formation overlies the southeastern part of the Salmon River assemblage south of the Livingston mine. The Grand Prize Formation structurally overlies both of the above units and was thrust 450 m upward and toward the northeast over the topographically high Salmon River assemblage. This relation is well exposed on the north slope of Washington basin, where the thrust fault is exposed in the basin floor rising eastward to the basin rim. This upward and eastward transport of the Grand Prize Formation over the Salmon River assemblage caused intense brecciation, forming a tectonic breccia as much as 300 m thick. This zone of breccia follows the thrust fault and locally cuts across bedding in both the overlying and underlying allochthons. This tectonic breccia is what Thomasson (1959) called Hailey Conglomerate Member of the Wood River Formation in his measured sections in the Boulder Mountains, at Slate Creek and Fourth of July Creek; it has been described by Winsor (1981, p. 25).

Both the Salmon River assemblage and the Grand Prize Formation are highly deformed into tight isoclinal folds; axial planes of the folds are steep and are truncated by the thrust faults separating the two allochthons. This truncation indicates that folding was prior to or during early stages of thrusting.

Pioneer Mountains Stack

The Copper Basin Formation is the structurally lowest element in the Pioneer Mountains stack of thrust plates in the study area (fig. J4). It crops out only along the eastern edge of the study area north of the Pioneer Mountains gneiss dome, and it extends to the east into Copper Basin where it has been described by Paull and others (1972), Skipp and Hall (1975), and Nilsen (1977).

The Copper Basin Formation is structurally overlain by undivided Devonian, Silurian, and Ordovician rocks (fig. J4, map unit DSOu), which are an imbricated complex of thrust slices shown in figures J3 and J4 as a single tectono-stratigraphic unit. This Devonian-to-Ordovician unit is interpreted to be structurally overlain by the Milligen Formation, which is widespread through the Wood River area and is the favorable host rock for ore deposits in the Wood River lead-silver district (fig. J2). The Milligen Formation is highly deformed, with axial planes of tight folds nearly horizontal, and the dark-gray Milligen argillite beds have a shear cleavage with oriented sericite that cuts across bedding and gives the rock a phyllitic sheen. This cleavage, phyllitic sheen, and internal deformation is unique to the Milligen. The author believes that these features formed during tectonic transport of the Milligen during the Antler orogeny, possibly while being obducted across a subduction zone, in the latest Devonian and Mississippian. Davis (1984) described microstructures in the Milligen that he interprets formed during the Antler orogeny.

The Milligen is overlain in thrust-fault contact by the Wood River Formation. The Wood River Formation is deformed into broad, open folds and is much less metamorphosed than the Milligen. As much as 1,500 m of the Wood River Formation have been cut out in the troughs of synclines by the Wood River thrust fault at the base of the allochthon.

In the western part of the Pioneer Mountains stack, near the Red Cloud mine and west of Bellevue at the Silver Star Queen mine, the Milligen Formation structurally overlies the Dollarhide Formation, and the Dollarhide Formation is the host rock for the lead-silver deposits west of the Wood River. The Dollarhide Formation is only weakly metamorphosed. The Dollarhide Formation is overlain in thrust-fault contact by the Wood River Formation near the Deer Creek barite deposit (fig. J4, no. 23).

ORE DEPOSITS

The central Idaho black-shale mineral belt is a highly mineralized area containing deposits of antimony, barite, lead, molybdenum, silver, tin, tungsten, vanadium, and zinc. Mines that have a recorded production or have had extensive exploration work are shown in figures J3 and J4. The most favorable hosts for ore are the carbonaceous black argillite and micritic limestone of the Devonian Milligen Formation, carbonaceous argillite, siltite, and silty limestone of the Upper Cambrian, Upper Devonian, and Upper Mississippian Salmon River assemblage, and the carbonaceous micritic limestone and siltite of the Dollarhide Formation near granitic plutons of Cretaceous or Eocene age. They contain abundant high-grade lead-silver-zinc vein deposits, tungsten skarn deposits, and syngenetic deposits of barite, sphalerite, and vanadium. The Wood River Formation is unfavorable for ore deposits in the Bellevue-Hailey-Sun Valley area (fig. J4) but contains many small lead-silver-zinc-tin veins in the Galena and Boulder Basin districts. The lead-silver-zinc vein deposits and the syngenetic deposits are

discussed here; the tungsten skarn deposits are discussed by Cookro (chap. Q, this volume).

Lead-Silver-Zinc Vein Deposits

Most of the past mining in the central Idaho black-shale mineral belt has been from lead-silver-zinc vein deposits (figs. J3 and J4). Vein deposits in the Dollarhide Formation are present in the Wood River district near Bellevue and Hailey and on the west side of Dollarhide Summit (fig. J2); in the Milligen Formation in the Triumph-Independence mine area (fig. J4, nos. 20, 21) east of Sun Valley; in the Wood River Formation in the Galena and Boulder Basin districts; and in the Salmon River assemblage in the Boulder Mountains. The following conditions are common to all the vein deposits:

1. The host rock is black shale.
2. The veins lie under but close to regional thrust faults, especially where the thrust faults are arched or domed, as, for example, at the Triumph mine (fig. J4, no. 21).
3. The veins are close to contacts of granitic intrusive rocks, predominantly of Cretaceous but also of Eocene age.
4. The most productive deposits have a siderite-quartz gangue rather than a calcite-quartz gangue.

These lead-silver veins have a regional mineralogical zoning pattern. In the southern part of the black-shale belt near Hailey and Bellevue, the principal sulfide minerals are galena, bournonite ($PbCuSbS_3$), sphalerite, and pyrite (Hall and Czamanske, 1972). Siderite is the principal gangue mineral; calcite and quartz are present but less abundant. The galena is argentiferous; for each percent of lead, the ore averages 1.25 ounces silver per ton. The galena was analyzed by electron microprobe by G. K. Czamanske (Hall and Czamanske, 1972) and contains abundant antimony and silver and small amounts of copper, iron, manganese, selenium, and tin. Seven purified mineral separates of galena contained 2,100 to 5,000 ppm (about 65–150 oz) silver and 3,100 to 4,700 ppm antimony. About one-half of the antimony and silver is in solid solution in the galena; the rest is present in minute inclusions, predominantly as diaphorite ($Pb_2Sb_3Ag_3S_8$) (Hall and Czamanske, 1972).

Emission spectrographic analyses of the lead-silver ore from the Galena and Boulder Basin districts in the central part of the black-shale mineral belt indicate that the ore contains lead, silver, gold, antimony, tin, zinc, copper, and selenium. Ore minerals are galena, stannite, zincian stannite, cassiterite, tellurian canfieldite, and sphalerite (B. F. Leonard, written commun., 1973, *in* Tschanz and others, 1974). Silver-bearing tetrahedrite and a silver telluride mineral were identified by Robert Felder and Robert Oscarson (written commun., 1984). These silver-tin-lead vein deposits resemble the productive tin-silver deposits of Bolivia in many respects. The veins are narrow (a few centimeters to 2 m wide), steeply dipping lenticular structures in the Wood River Formation and are closely associated with rhyodacite and dacite porphyry dikes and sills of Tertiary age. Tschanz and others (1974) recognized the widespread occurrence of tin in these lead-silver veins through a systematic regional geochemical sampling program. Analyses of 92 mineralized rock samples from dumps and in place within this belt contained from 0.05 to 6 percent tin (Tschanz and others, 1974). Semiquantitative spectrographic analyses of two grab samples taken from dumps in the Boulder Basin district are given in table J1. The samples contain abundant silver, gold, antimony, tin, and selenium as well as lead, zinc, and copper. These two samples apparently are representative of some shoots of high-grade ore that was mined from small ore bodies in the Boulder Basin district. Umpleby (1915), who visited the district in 1912, reported ore shoots that averaged 360 ounces of silver and 3 ounces of gold per ton.

Table J1. Semiquantitative emission spectrographic analyses of two samples of lead-silver-tin sulfide ore from mine dumps in the Boulder Basin mining district, Blaine County, Idaho

[>, more than; ~, about; NA, not analyzed for]

Element	Sample 1		Sample 2	
	(ppm)	(oz/ton)	(ppm)	(oz/ton)
Ag---	5,000	~160	15,000	~500
As---	1,000	NA	3,000	NA
Au---	20	~0.6	200	~6
Cu---	20,000	NA	>20,000	NA
Pb---	>100,000	NA	>50,000	NA
Sb---	20,000	NA	>50,000	NA
Sn---	300	NA	15,000	NA
Se---	NA	NA	3,100	NA

The localities of all mineralized rock samples collected by Tschanz and others (1974) that contained more than 0.05 percent tin are shown in figure J5*A*. Anomalous concentrations of tin occur in a north-trending belt 50 km long and 5 km wide that extends from the Boulder Basin district to the Big Boulder Creek district.

The greatest concentrations of deposits containing anomalous tin are in the Galena and Boulder Basin districts. The mineralogy and resource potential of the deposits in the Boulder Basin district are currently being investigated. Preliminary mineralogical studies indicate that the tin is present in stannite; silver is present in tetrahedrite and a small amount of silver telluride. The localities of mineralized rock samples containing anomalous concentrations of lead (more than 14,500 ppm), silver (more than 100 ppm), and antimony (more than 3,000 ppm) are shown in figures J5*B*, J5*C*, and J5*D*, respectively. Lead, silver, tin, and antimony occur together throughout the northern half of the black-shale mineral belt (figs. J3, J4, J5).

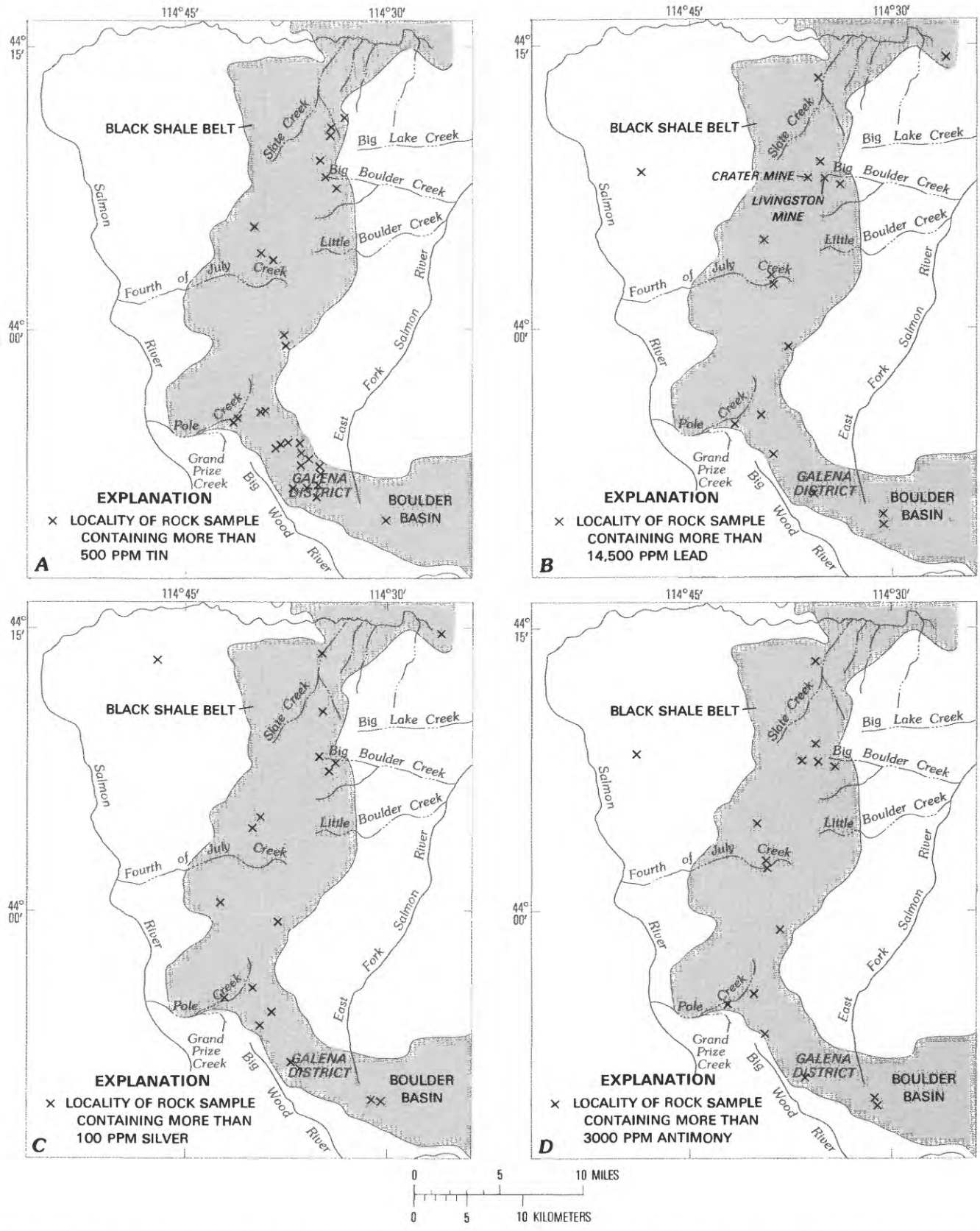

Figure J5. Maps showing localities of rock samples containing anomalous amounts of selected metals, black-shale mineral belt, central Idaho.

In the northern part of the black-shale mineral belt, at the Livingston and Crater mines, the principal ore mineral is jamesonite ($Pb_4FeSb_6S_{14}$), which is present from surface outcrop to the deepest mine workings, which are 580 m below the ground surface at the Livingston mine (Kiilsgaard, 1949). Galena, sphalerite, chalcopyrite, pyrite, pyrrhotite, and arsenopyrite are also common sulfide minerals in the ore. The ore has a ratio of about 1 oz silver to 2 percent lead, but the mode of occurrence of silver in the ore is not known. The ore also contains a trace of gold (Kiilsgaard, 1949).

Molybdenum Stockwork Deposits

Most of the value of the known mineral resources in the central Idaho black-shale mineral belt is from two large, extensively explored molybdenum stockwork deposits. The molybdenum stockwork deposit at Thompson Creek is in a biotite granodiorite and biotite granite stock of Late Cretaceous age that intruded the Salmon River assemblage (Hall and others, 1984). This mine began operation in August 1983. The Little Boulder Creek deposit in the White Cloud Peaks is a molybdenum stockwork in contact-metamorphosed limy sandstone of unit 6 of the Wood River Formation on the east side of the Little Boulder Creek stock (fig. J3). The deposit contains scheelite as well as molybdenite. As one of the molybdenum deposits has been described in detail elsewhere (Hall and others, 1984), they are not described here.

Stratabound Deposits

Much mineral exploration in central Idaho during the past decade has been concentrated on the potential for stratabound syngenetic ore bodies in the Paleozoic black shale and argillite beds, using the Selwyn basin in western Canada as a model (Carne and Cathro, 1982). A geochemical study of the concentration and distribution of metals in the Salmon River assemblage was made by Fisher and May (1983). They found that the elements most consistently anomalous include silver, barium, copper, molybdenum, vanadium, and zinc, as compared to average values for black shale in the United States determined by Vine and Tourtelot (1970) (table J2).

The samples of Fisher and May (1983) showed that highly carbonaceous bands in the Salmon River assemblage contain as much as 10,000 ppm vanadium, and the assemblage may be a possible future resource for vanadium. A similar study was made of the Milligen and Phi Kappa Formations in the Boulder and Pioneer Mountains by Simons (1981). He found that these formations contained anomalous amounts of metals but in concentrations lower than those of the Salmon River assemblage; the values were about the same as for the average of black shales of the United States as given in Vine and Tourtelot (1970).

Table J2. Anomalous concentrations of selected elements in samples from the Salmon River assemblage, central Idaho.

[<, less than; >, more than; ⩾, more than or equal to]

Element	Range of concentration (ppm)	Threshold values for anomalous concentrations Vine and Tourtelot (1970) (ppm)	Percent of anomalous samples
Ag---	1-15	⩾5	7
Ba---	20-5,000	⩾3,000	9
Cu---	10-7,000	⩾100	25
Mo---	<5-100	⩾50	11
V----	30-10,000	⩾1,000	26
Zn---	<200->10,000	⩾200	28

Most of the ore deposits that have been mined, which are principally epigenetic lead-silver-zinc vein deposits, occur only in the black-shale sequences. The veins are localized close to contacts with granitic stocks of Cretaceous and Eocene age just below regional thrust faults. Hall and others (1978) showed that the hydrothermal fluid that deposited the ore in the Wood River area was mainly of meteoric origin and that the sulfur and lead had a shallow, crustal source. They showed that the geology, isotope, and fluid-inclusion data are consistent with an environment of hydrothermal systems of predominant meteoric water in faulted and shattered Paleozoic rocks near granitic stocks. This environment permitted deep circulation of hydrothermal fluids, which dissolved the metals and sulfur from the Paleozoic black shale and deposited ore in favorable beds and shear zones under regional thrust faults. The thrust faults form structural traps for the ore fluids.

It is now generally recognized that not only are the black shales hosts and probable sources of metals for the vein deposits, but some of the productive deposits are stratabound and are probably of syngenetic origin. These deposits include the zinc and barite ore bodies at the Hoodoo mine, some stratabound zinc ore bodies at the Triumph mine, and the barite deposits at Deer Creek, 10 km west-northwest of Hailey (fig. J4). These deposits contain very fine grained stratabound ore similar in texture to that at known syngenetic deposits. All the deposits are close to plutonic bodies, and the ore is partly recrystallized and locally remobilized. This contact metamorphism makes identification of original sedimentary textures and structures difficult in many places.

Stratabound lead-zinc ore at the Triumph mine (fig. J6) was originally called "complex bedded ore high in zinc" by Kiilsgaard (*in* Anderson and others, 1950) and was considered to have formed as the replacement of a favorable limestone bed. It is reinterpreted now by Kiilsgaard and the author as syngenetic sphalerite ore. The largest shoot of stratabound zinc ore was 200 m along strike, 2 to 15 m thick, extended 50 m down dip, and

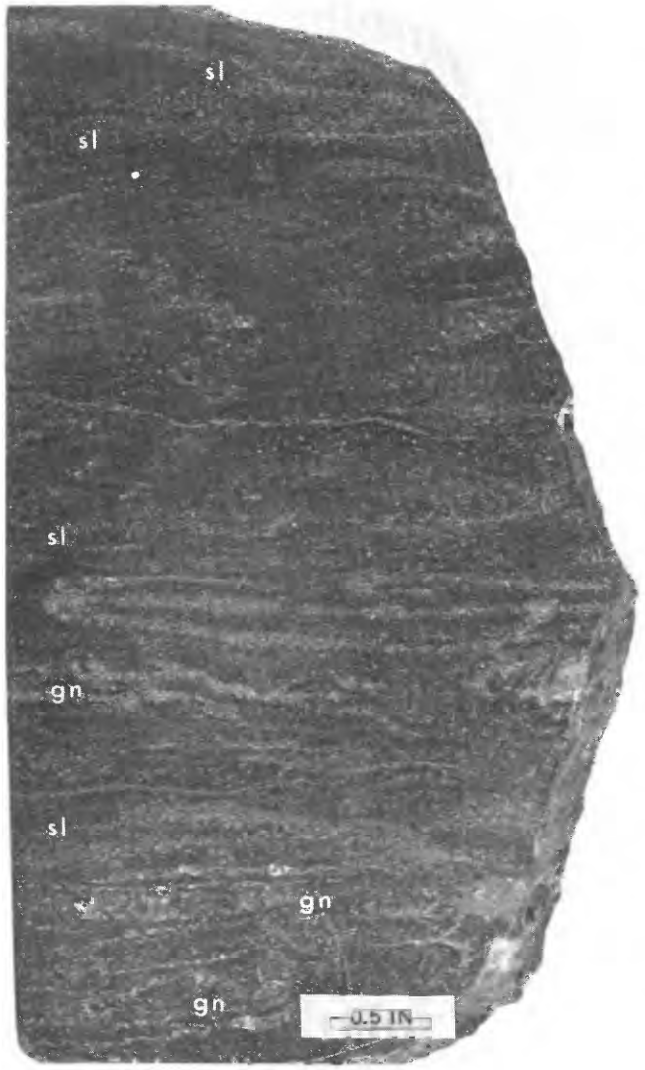

Figure J6. Polished slab of stratabound zinc-lead-silver ore from the Triumph mine, central Idaho. The ore contains disseminated grains of sphalerite, galena, pyrite, and arsenopyrite concentrated along bedding in a micritic limestone of the Milligen Formation (Devonian). Pyrite is finely disseminated throughout the rock, and arsenopyrite was identified by microscopic examination of the ore. gn, galena; sl, sphalerite.

averaged 5.9 percent lead, 13 percent zinc, and 6.5 ounces of silver per ton (Kiilsgaard, *in* Anderson and others, 1950, p. 50).

The ore from the Triumph mine shown in figure J6 is a fine-grained, thinly bedded, dark-gray, carbonacous, micritic, silty limestone containing minute grains of sphalerite, galena, arsenopyrite, and pyrite disseminated along the bedding. The grain size of the micritic limestone is 0.05 to 0.1 mm. The limestone is locally recrystallized into veinlets and lenses that are mostly parallel to bedding. The sulfide minerals occur as disseminated, anhedral grains concentrated in specific beds and are in part recrystallized and remobilized into minute pods or veinlets. The recrystallization and mobilization of the sulfide minerals are due to an inferred underlying granitic stock that has metamorphosed micritic limestone to tremolite-bearing limestone and calc-hornfels, and argillite to hornfels in the mine area.

The existence of stratabound syngenetic lead-silver ore is more nebulous. The lead-silver ore is more coarse grained than the syngenetic sphalerite ore, and much of it obviously crosscuts bedding. At the Livingston mine, most of the ore has come from the Livingston vein, which strikes about west and dips 28–44° N. The vein is parallel to bedding of the host Salmon River assemblage and lies a short distance below the thrust-fault contact with the overlying Wood River Formation (fig. J3). High-grade lead-silver ore shoots are localized close to the intersections of Eocene rhyolite porphyry dikes with the stratabound Livingston vein (Kiilsgaard, 1949). Kiilsgaard resampled the Livingston vein in 1983 on the 1,800–, 2,000–, 2,200–, and 2,400–ft (foot) levels. The samples collected on the 1,800–, 2,000–, and 2,200–ft levels were all from an ore shoot that is parallel to bedding. On the 2,400–ft level, galena was collected from veinlets cutting the rhyolite porphyry Blumenthal dike (T. H. Kiilsgaard, written commun., 1984).

Ore from the Livingston vein (fig. J7) consists of highly deformed black, siliceous argillite with bedded sphalerite, pyrite, and minor galena and jamesonite, which are interpreted to be syngenetic sulfide minerals that were deposited with the black argillite. The syngenetic sulfide ore and black-shale host rock were subsequently shattered and displaced by steep, north-striking faults (Kiilsgaard, 1949). The shattering probably also was related to intrusion of rhyolite porphyry dikes adjacent to the Livingston

Figure J7. Polished slab of jamesonite ore from the 2,200–ft level of the Livingston mine, central Idaho. The ore contains fine-grained pyrite, sphalerite, jamesonite, and galena disseminated along bedding in tightly folded and shattered siliceous argillite (a) of the Salmon River assemblage (Paleozoic). The folded, mineralized argillite is part of the Livingston vein near a rhyolite porphyry dike. The fractures and matrix between argillite clasts are filled with pods and lenses of jamesonite (b), galena (c), and sphalerite (d) that have been remobilized from the mineralized argillite.

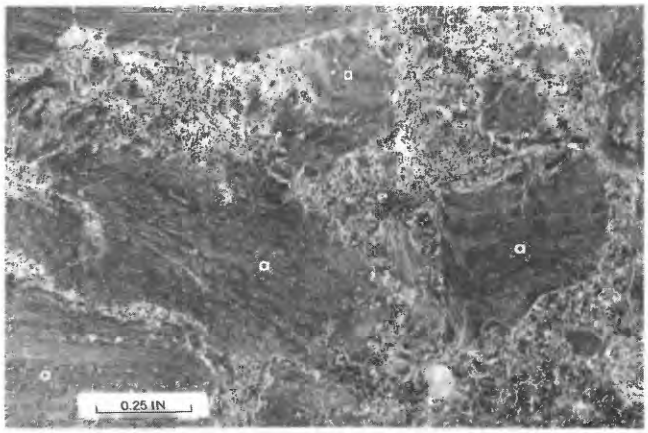

vein. At the time of intrusion of the dikes, the lead-silver minerals were locally remobilized, forming crosscutting veinlets and filling or replacing the matrix between the shattered argillite fragments (fig. J7). The remobilized lead-silver minerals formed some of the highest-grade ore bodies at the intersections of the rhyolite dikes and the Livingston vein. Brecciation continued after intrusion of the rhyolite porphyry dikes, and veinlets of galena cut rhyolite. Fluid-inclusion and isotopic evidence for a syngenetic origin of the stratabound ore is given by Howe and Hall (chap. P, this volume).

REFERENCES CITED

Anderson, A. L., Kiilsgaard, T. H., and Fryklund, V. C., Jr., 1950, Detailed geology of certain areas in the Mineral Hill and Warm Springs mining districts, Blaine County, Idaho: Idaho Bureau of Mines and Geology Pamphlet 90, 73 p.

Carne, R. C., and Cathro, R. J., 1982, Sedimentary exhalative (sedex) zinc-lead-silver deposits, northern Canadian Cordillera: Canadian Institute of Mining Bulletin 75, p. 66–78.

Davis, Steven, 1984, Antler orogenic microstructures in the Devonian Milligen Formation, Pioneer Mountains, central Idaho: Geological Society of America Abstracts with Programs v. 16, no. 4, p. 220.

Dover, J. H., 1969, Bedrock geology of the Pioneer Mountains, Blaine and Custer Counties, central Idaho: Idaho Bureau of Mines and Geology Pamphlet 142, 61 p.

_____1981, Geology of the Boulder-Pioneer Wilderness Study Area, Blaine and Custer Counties, Idaho, chap. A *of* U.S. Geological Survey and U.S. Bureau of Mines, Mineral resources of the Boulder-Pioneer Wilderness Study Area, Blaine and Custer Counties, Idaho: U.S. Geological Survey Bulletin 1497-A, p. 1–75.

Dover, J. H., Berry, W. B. N., and Ross, R. J., Jr., 1980, Ordovician and Silurian Phi Kappa and Trail Creek Formations, Pioneer Mountains, central Idaho—Stratigraphic and structural revisions, and new data on graptolite faunas: U.S. Geological Survey Professional Paper 1090, 54 p.

Fisher, F. S., and May, G. D., 1983, Geochemical characteristics of the metalliferous Salmon River sequence, central Idaho: U.S. Geological Survey Open-File Report 83-670, 30 p.

Fisher, F. S., McIntyre, D. H., and Johnson, K. M., 1983, Geologic map of the Challis 1°×2° quadrangle, Idaho: U.S. Geological Survey Open-File Report 83-523, 41 p., 2 maps, scale 1:250,000.

Hall, W. E., Batchelder, J. N., and Douglass, R. C., 1974, Stratigraphic section of the Wood River Formation, Blaine County, Idaho: U.S. Geological Survey Journal of Research, v. 2, no. 1, p. 89–95.

Hall, W. E., and Czamanske, G. K., 1972, Mineralogy and trace element content of the Wood River lead-silver district, Blaine County, Idaho: Economic Geology, v. 67, no. 3, p. 350–361.

Hall, W. E., Rye, R. O., and Doe, B. R., 1978, Wood River mining district, Idaho—intrusion-related lead-silver deposits derived from country rock source: U.S. Geological Survey Journal of Research, v. 6, no. 5, p. 579–592.

Hall, W. E., Schmidt, E. A., Howe, S. S., and Broch, M. J., 1984, The Thompson Creek, Idaho porphyry molybdenum deposit—an example of a fluorine-deficient molybdenum granodiorite system: Sixth Quadrennial International Association on the Genesis of Ore Deposits, Tbilisi, USSR, 1982, Proceedings; E. Schweizerbart'sche Verlagsbuchhandlung, Stuttgart, v. 1, p. 349–358.

Hobbs, S. W., Hays, W. H., and McIntyre, D. H., 1975, Geologic map of the Clayton quadrangle, Custer County, Idaho: U.S. Geological Survey Open-File Report 75-76, 23 p., 1 map, scale 1:62,500.

Kiilsgaard, T. H., 1949, The geology and ore deposits of the Boulder Creek mining district, Custer County, Idaho: Idaho Bureau of Mines and Geology Pamphlet 88, 28 p.

Nilsen, T. H., 1977, Paleogeography of Mississippian turbidites in south-central Idaho, *in* Pacific Coast Paleogeography Symposium, 1st, Bakersfield, Calif., 1977, Paleozoic paleogeography of the western United States: Los Angeles, Society of Economic Paleontologists and Mineralogists, Pacific Section, p. 275–299.

Paull, R. A., Wolbrink, M. A., Volkmann, R. G., and Grover, R. L., 1972, Stratigraphy of the Copper Basin Group, Pioneer Mountains, south-central Idaho: American Association of Petroleum Geologists Bulletin, v. 56, no. 8, p. 1370–1401.

Ross, C. P., 1937, Geology and ore deposits of the Bayhorse region, Custer County, Idaho: U.S. Geological Survey Bulletin 877, 161 p.

Sandberg, C. A., Hall, W. E., Batchelder, J. N., and Axelsen, Claus, 1975, Stratigraphy, conodont dating, and paleotectonic interpretation of the type Milligen Formation (Devonian), Wood River area, Idaho: U.S. Geological Survey Journal of Research, v. 3, no. 6, p. 707–720.

Simons, F. S., 1981, A geological and geochemical evaluation of the mineral resources of the Boulder-Pioneer Wilderness Study Area, Blaine and Custer Counties, Idaho, chap. C *of* U.S. Geological Survey and U.S. Bureau of Mines, Mineral resources of the Boulder-Pioneer Wilderness Study Area, Blaine and Custer Counties, Idaho: U.S. Geological Survey Bulletin 1497-C, p. 87–180.

Skipp, Betty, and Hall, W. E., 1975, Structure and Paleozoic stratigraphy of a complex of thrust plates in the Fish Creek Reservoir area, south-central Idaho: U.S. Geological Survey Journal of Research, v. 3, no. 6, p. 671–689.

Thomasson, M. R., 1959, Late Paleozoic stratigraphy and paleotectonics of central and eastern Idaho: Madison, University of Wisconsin Ph. D. thesis, 244 p.

Tschanz, C. M., Kiilsgaard, T. H., Seeland, D. A., Van Noy, R. M., Ridenour, J., Zilka, N. T., Federspiel, F. E., Evans, R. K., Tuchek, E. T., and McMahan, A. B., 1974, Mineral resources of the eastern part of the Sawtooth National Recreation Area, Custer and Blaine Counties, Idaho: U.S. Geological Survey Open-file report, 2 v., 648 p.

Umpleby, J. B., 1915, Ore deposits in the Sawtooth quadrangle, Blaine and Custer Counties, Idaho: U.S. Geological Survey Bulletin 580, p. 221–249.

Umpleby, J. B., Westgate, L. G., and Ross, C. P., 1930, Geology and ore deposits of the Wood River region, Idaho: U.S. Geological Survey Bulletin 814, 250 p.

Vine, J. D., and Tourtelot, E. B., 1970, Geochemistry of black shale deposits—a summary report: Economic Geology, v. 65, no. 3, p. 253–272.

Winsor, H. C., 1981, The paleogeography and paleoenvironments of the Middle Pennsylvanian part of the Wood River Formation in south-central Idaho: San Jose, Calif., San Jose State University M.S. thesis, 81 p.

Symposium on the Geology and Mineral Deposits of the Challis 1°×2° Quadrangle, Idaho

Chapter K

Structural and Stratigraphic Controls of Ore Deposits in the Bayhorse Area, Idaho

By S. WARREN HOBBS

CONTENTS

FIGURES

Abstract

Major mineral commodities produced from the Bayhorse region include lead, zinc, silver, gold, molybdenum, tungsten, and fluorspar. Mineral commodities of unknown potential include tin, copper, vanadium, uranium, and barite.

Three factors dominate the placement of ore deposits in this region: (1) the sedimentary sections—their depositional history, composition, physical characteristics, and general chemical composition; (2) the structural evolution of the area and the resulting pattern of folds and faults; and (3) the associated intrusive rocks that supplied some of the ore-forming elements but mainly supplied energy to mobilize hydrothermal fluids throughout the stratigraphic section.

Deposition of most of the fluorite and some of the lead-zinc-silver minerals in occurrences that flank the Bayhorse anticline was largely controlled by an extensive zone of solution, brecciation, and collapse structures that makes up a paleokarst horizon developed beneath an ancient erosion surface cut on Bayhorse Dolomite, which is now capped by the impervious Ramshorn Slate. Steep faults that intersect this zone were channels for ore solutions from some subjacent source into a porous, reactive environment of deposition. Similar steep faults that cut other carbonate units at the Clayton Silver mine and mines on Squaw Creek also have been channels to replacement ore bodies of considerable size. At the Ramshorn and Skylark mines, steep faults in the Ramshorn Slate controlled the location of sulfide-bearing quartz-siderite veins that are in places controlled by bedding as well.

Intrusive rocks served both as the source of mineralizing solutions in contact-metamorphic aureoles and, more significantly, as the source of energy to circulate connate and meteoric waters that mobilized sparse syngenetic metals and carried them to favorable sites of deposition.

INTRODUCTION

The Bayhorse area in the east-central part of the Challis quadrangle (fig. D1, Hobbs, chap. D, this volume) is a small, economically important area in which a variety of mineral deposits and occurrences have been mined or are known. The earliest recorded mineral discovery in the Bayhorse area was in 1887 at the Riverview mine on Bayhorse Creek. Other discoveries followed quickly, and by 1900 most of the major deposits in the area had been developed. Continued interest in mineral deposits led to geological investigations by many workers, from the earlier studies of Umpleby (1913), Ross (1937), Anderson (1954), and others, to the more recent work of the U.S. Geological Survey (Hays and others, 1978; Hobbs, 1980; Hobbs and others, 1975; McIntyre and Hobbs, 1978; McIntyre and others, 1982), Idaho Bureau of Mines and Geology, and many students, and the very detailed and concentrated exploration activities of numerous geologists with mining companies.

The major mineral commodities of the Bayhorse area and environs include lead, zinc, silver, tungsten, gold, molybdenum, and fluorspar. Secondary commodities that are known either within the Bayhorse area or nearby, and that may have potential for future mining development include tin, copper, barite, uranium, and vanadium.

Two periods of mineralization, one related to the middle Late Cretaceous Idaho batholith and the other to the Eocene Challis Volcanics and their coeval granitic plutons, were recognized by Ross (1931) during his early studies of the Bayhorse area and adjacent areas. More recent studies have identified ore deposits related to other periods of mineralizing activity. Accumulating evidence indicates that the mineralizing processes and the plumbing systems that controlled the localization and deposition of ore deposits were active for a long time.

Many of the basic concepts of ore genesis and control of ore deposition in central Idaho are presented by Hall (chap. J, this volume). This chapter (K) expands these concepts, emphasizing the localization of ore deposits in the Bayhorse area and describing several modes of occurrence that have been recognized in this mining district that could serve as guides for future discovery of mineral deposits.

Three factors that seem to control the location of ore deposits in central Idaho are:

1. The sequence of sedimentary rocks; its depositional history, composition, physical characteristics, strata-bound and syngenetic ore-mineral content, and minor-element chemical composition.
2. The structural features; the pattern of folds and faults that resulted from a long history of deformation.
3. The intrusive rocks; the possible source of certain ore elements and the source of energy for the movement of metal-bearing fluids through the country rock.

One or more of these factors has influenced the localization of the major ore deposits in the Bayhorse area.

MINERAL DEPOSITS NEAR THE RAMSHORN SLATE-BAYHORSE DOLOMITE CONTACT

One of the stratigraphic terranes that comprise the basic geologic elements of the Bayhorse area (Hobbs, chap. D, this volume) includes terrane C, a sequence of lower Paleozoic strata that is folded into a major north-trending anticline in the central part of the area (fig. K1). This sequence is composed of the Ramshorn Slate at the top, underlain by the Bayhorse Dolomite, both of Ordovician(?) age, the Cambrian(?) Garden Creek Phyllite, and a lower dolomite also of Cambrian(?) age (fig. K2*A*). The stratigraphy and sedimentary history that is illustrated by these strata influenced the localization of deposits of lead, zinc, and fluorspar in the Bayhorse area. Several major mines and numerous prospects are in the Bayhorse Dolomite along and near its contact with the overlying Ramshorn Slate. This contact is a major erosional disconformity, and an unknown thickness of

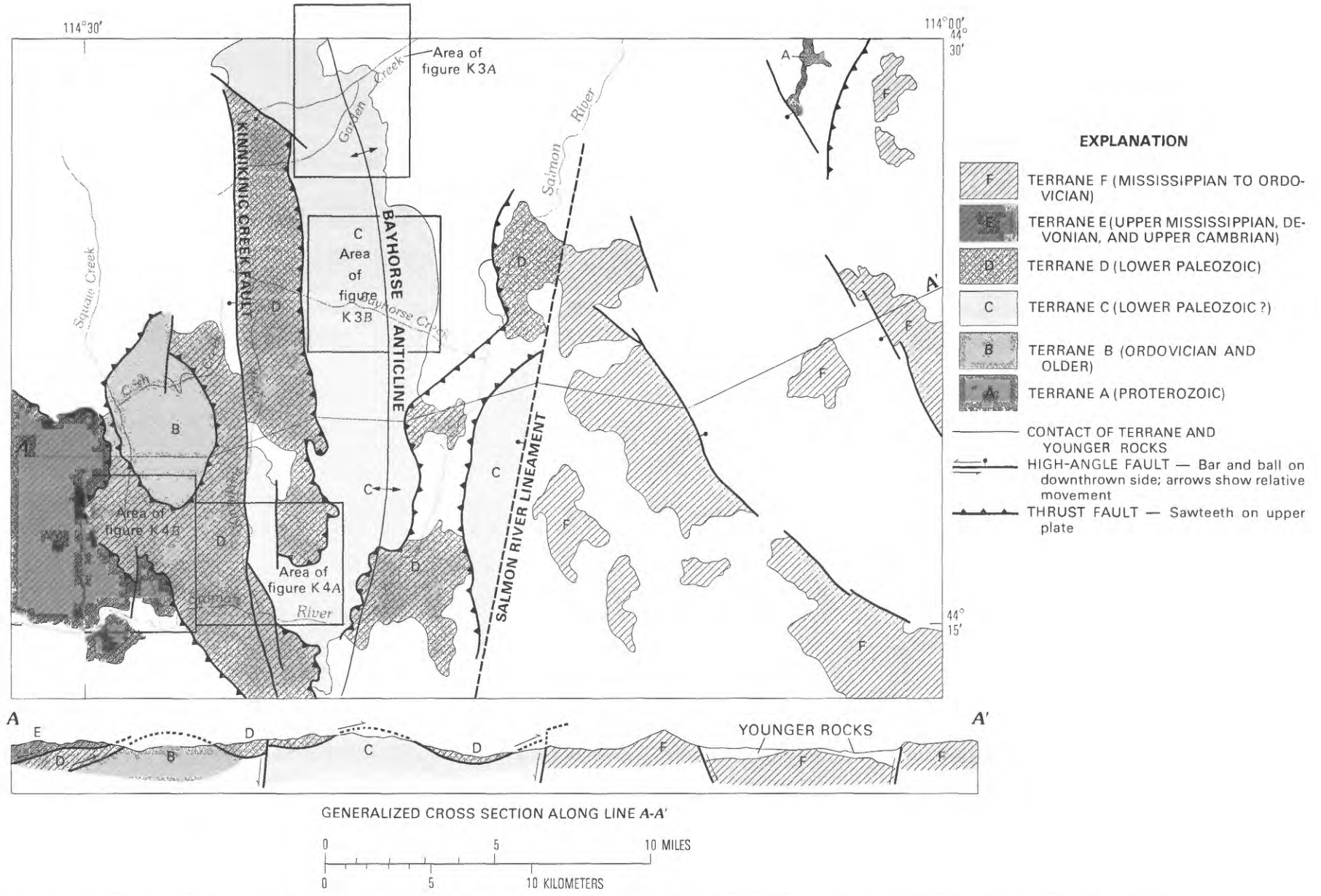

Figure K1. Generalized map and cross section showing structural-stratigraphic terranes in the Bayhorse area, and the location of figures K3 and K4.

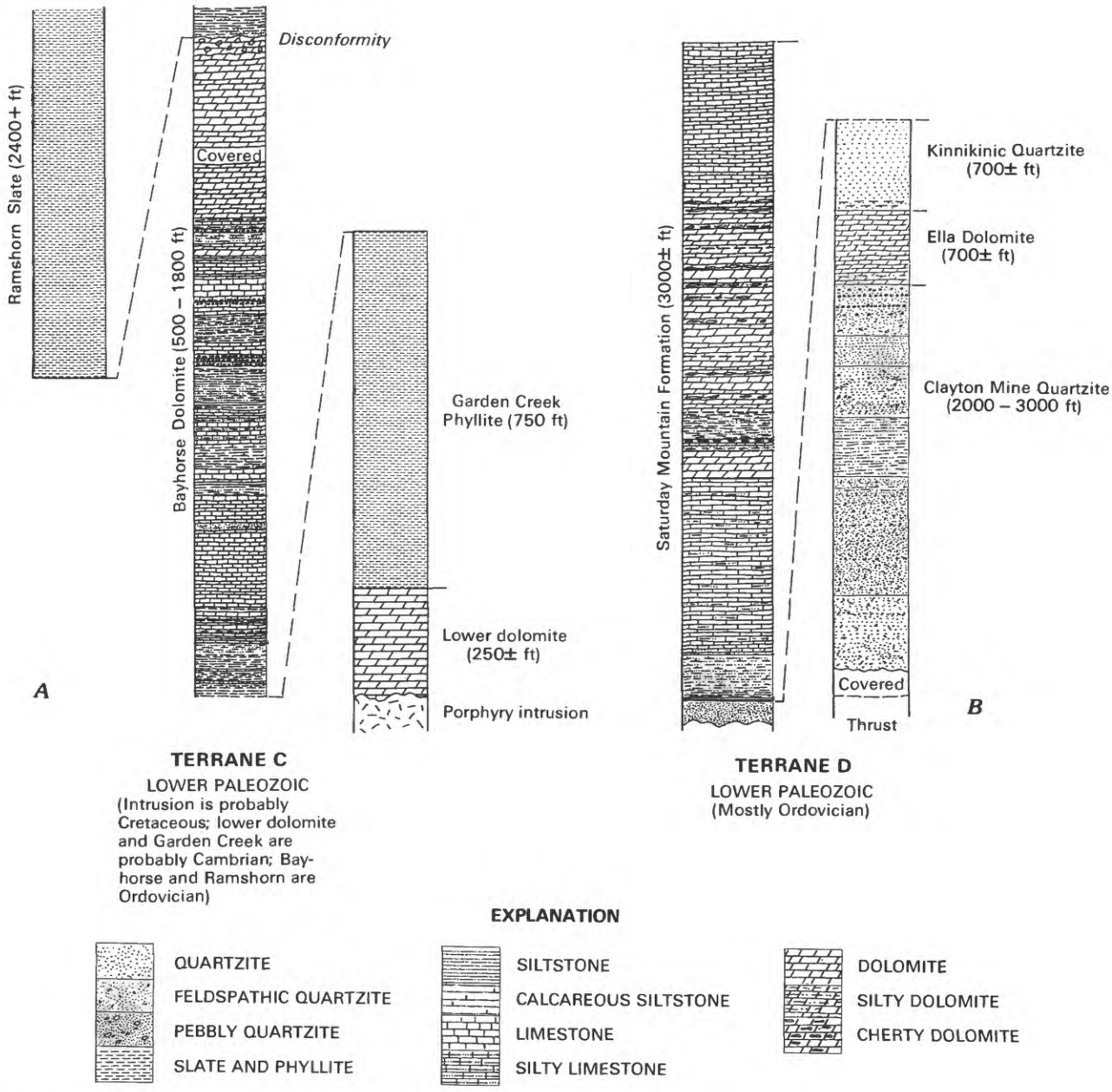

Figure K2. Columnar sections of terranes C and D, Bayhorse area.

Bayhorse Dolomite was eroded before the Ramshorn Slate was deposited. The wide thickness range of the Bayhorse Dolomite (500–1,500 ft (feet)) reflects this erosional event, as does the drastic change in depositional regime in Ramshorn time that produced the Ramshorn siltstone, sandstone, and locally a very thick basal conglomerate.

Beneath this contact, the Bayhorse Dolomite shows very striking evidence of this disconformity and prolonged exposure to extensive weathering. Different parts of the dolomite are present below the Ramshorn at different places; nearly everywhere the carbonate strata show deep weathering that consists of carbonate dissolution and local accumulation of residual sand and clay, brecciated and silicified carbonate, and local cavern filling of transported material. At least one breccia pipe, possibly a solution-collapse feature, has been recognized, but its origin is as yet unproved. Part of this disturbed zone at the contact is most certainly related to the Ordovician erosion that produced the disconformity and to the development of what is now a paleokarst horizon; the zone appears to have been modified and probably enlarged by deformation during folding.

The geologic evolution of terrane C as described above has produced an extensive stratigraphically and structurally controlled permeable zone that is capped by a thick, impermeable slate sequence (Ramshorn Slate). The zone was a channel for subsequent circulating hydrothermal waters that probably modified the channel by solution and further brecciation. These or subsequent hydrothermal fluids introduced the ore-forming elements

that were precipitated to form the ore deposits in or near this permeable horizon. Generally north-trending, steeply dipping faults and fractures have served as channels that fed mineralizing solutions into the brecciated paleokarst zone. In some places these same fractures and solutions have localized vein-filling or replacement ore deposits of several types at other stratigraphic horizons.

Many mines and prospects, mostly for fluorspar but some for lead and silver, are localized along or near the Bayhorse Dolomite-Ramshorn Slate contact in the northern part of the Bayhorse anticline (fig. K3*A*). The fluorspar prospect on Mill Creek (fig. K3*A*) on the west limb of the Bayhorse anticline at its north end is in weathered and brecciated zones of the Bayhorse Dolomite at or very near the contact with overlying Ramshorn Slate. At this place, the disconformity between these two units has been cut into the dolomite to the level of one of several pisolite horizons that have become, in part, host rocks for the sparse fluorspar deposits that have so far been discovered here. On the east limb of the anticline about 2 mi (miles) to the southeast, the Chalspar No. 1 vein is in a steeply dipping fault zone in Bayhorse Dolomite whose relation to the disconformity is unknown. This fault and its vein material may have been a channel that fed ore-bearing fluids into parts of the paleokarst horizon that have been removed by erosion here. The Chalspar No. 2 and No. 5 prospects on the west limb of the anticline are in brecciated zones related to both stratabound breccias and to steeply dipping shear and fault zones that parallel the major fold axis and that offset the contact between the Bayhorse Dolomite and the Ramshorn Slate. Although the geologic relations are not completely clear, the combined effects of both of these ore controls certainly contributed to the concentration of fluorspar at these two locations. At the Westspar and Troxspar localities, fluorspar and some minor sulfide minerals are in brecciated dolomite close below the basal conglomerate of the Ramshorn Slate on opposite sides of the Bayhorse anticline. As with the other deposits, the brecciated and mineralized rock along or near the disconformity strongly suggests a genetic relationship. At the Keystone Mountain property on the gently south-plunging nose of the Bayhorse anticline, the disconformity is alternately exposed and covered for more than 6,000 ft across the axis of the fold and well down both flanks. Brecciation, silicification, and fluorspar occur along most of this distance either at the contact or in a horizon several hundred feet below the contact. Some sulfide minerals on the lower part of the east limb are probably related to the same structural setting.

The main Bayhorse mining district (fig. K3*B*) is on the Bayhorse anticline just south of the area of figure K3*A*. The district has the same stratigraphic and structural setting that the northern district has. The Pacific mine ore body is near the crest of the anticline, within a highly brecciated zone in the Bayhorse Dolomite, and below the contact of the dolomite with a small patch of nearly flat lying Ramshorn Slate. This major deposit contains both base metals and fluorspar that were probably deposited in two separate metallogenic episodes (Snyder, 1978). Several hundred feet of essentially undisturbed dolomite separates the main ore bodies of the Pacific mine from the Ramshorn contact, and the dolomite adjacent to the contact is less mineralized and brecciated than at the mine. The development of breccia at two levels within the dolomite below the Ramshorn contact may have resulted from a complex event involving the disconformity, stratigraphy, structure, and compositional differences of the carbonate strata, all of which could have controlled the rate of solution and brecciation.

The Beardsley and Riverview deposits are on the east flank of the Bayhorse anticline where the dolomite dips from gently eastward to vertical, but both are near the disconformity and undoubtedly were controlled by the character of the weathered horizon. Several small occurrences of base metals to the south are in comparable structural settings (fig. K3*B*). One of these, the Turtle mine, is barely exposed in a very small erosional window of Bayhorse Dolomite within an extensive area of the overlying Ramshorn Slate. All of the mines and prospects described above and shown on figure K3 are very close to the disconformity, which was probably critical to their origin.

Mineralizing solutions that followed the near-bedding-plane brecciated and porous zones related to the disconformity were undoubtedly channeled along the steeply dipping, north-trending normal faults that postdate thrusting and folding. Examples of these faults are the major steep faults that bracket the deposits at Keystone Mountain and the Bayhorse district (fig. K3). The Beardsley mine in the Bayhorse district (fig. K3*B*) reportedly includes replacement deposits in the dolomite (below the breccia zone described above) that could be related to the adjacent steep fault that is, itself, mineralized in places.

The control of ore deposition by the north-trending anticline and faults is more obvious at the well-known silver-bearing veins in Ramshorn Slate at the Ramshorn and Skylark mines on upper Bayhorse Creek (fig. K3*B*). These veins, consisting of galena and tetrahedrite in a quartz-siderite-crushed slate gangue, are in complex north-trending shear and fault zones that are controlled in part by the west-dipping slaty cleavage of the Ramshorn Slate. Relation of these veins to the small Juliette stock to the south is suggested by a potassium-argon age of the stock of 98.1 m.y. (million years) and of sericite from a selvage along the Skylark veins of 95.1 m.y. (McIntyre and others, 1976; recalculated using currently accepted constants).

MINERAL DEPOSITS IN TERRANE D

Terrane D (Hobbs, chap. D, this volume) includes a stratigraphic sequence consisting of two quartzite units and two carbonate units (fig. K2*B*). These units are best

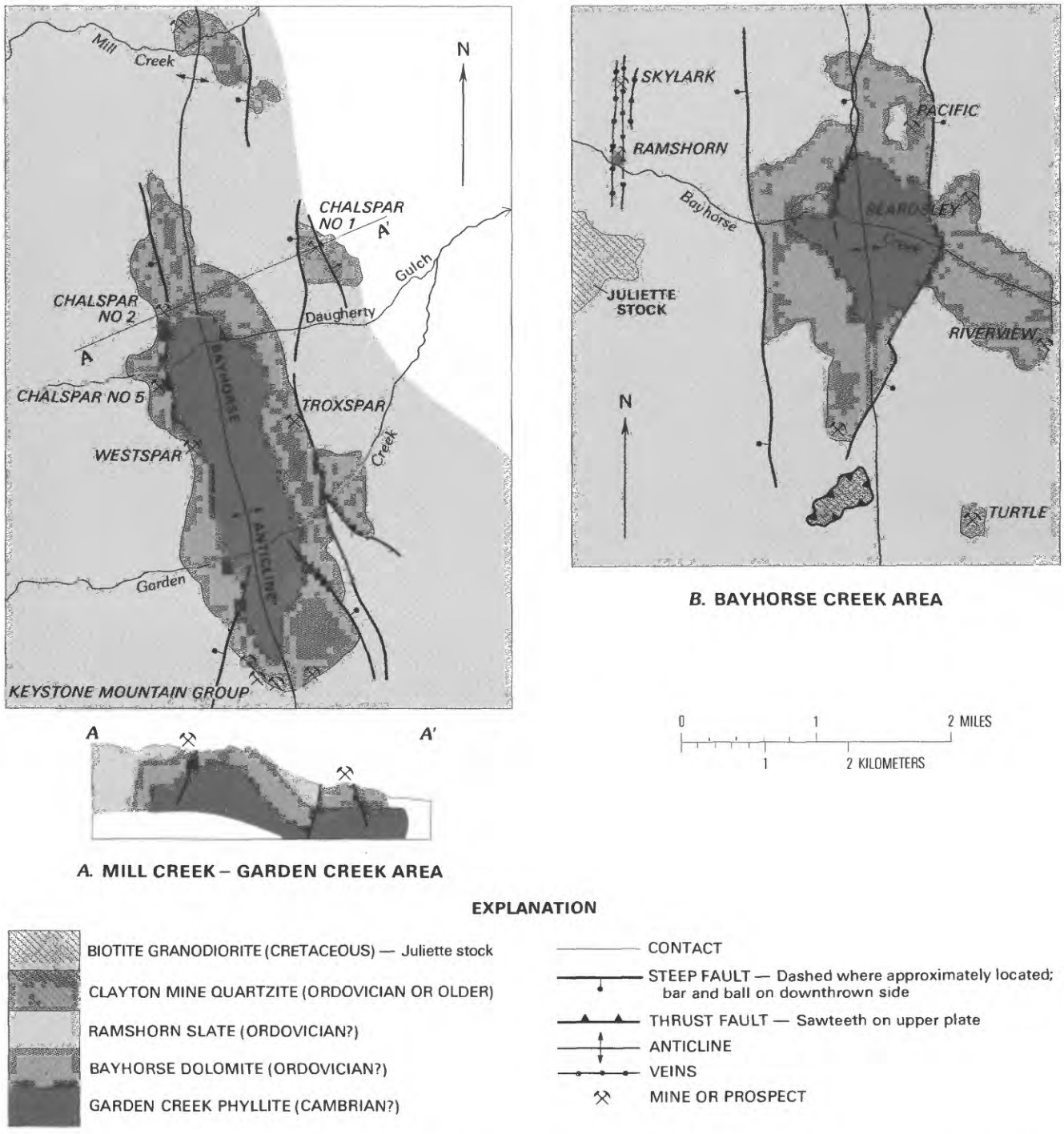

Figure K3. Geologic maps of the Mill Creek-Garden Creek and Bayhorse Creek areas. Location of maps shown on figure K1.

exposed in the western half of the Bayhorse area and especially in the valleys of Squaw and Kinnikinic Creeks. As in terrane C, the major stratigraphic control of ore deposits is the reactive carbonate units, which, in this area, are the Ordovician Ella Dolomite and the Ordovician Saturday Mountain Formation. The major structural controls are both earlier low-angle thrust faults and later steeply dipping normal faults. The sequence in terrane D contains no notable disconformities such as the one that controls ore deposition in terrane C.

At the Clayton Silver mine on Kinnikinic Creek (fig. K4*A*), a relatively small block of Ordovician Ella Dolomite, bounded by two steep normal faults and capped by a flat thrust fault, contains a replacement ore body of lead, zinc, and silver that has been mined for many years. The steep boundary faults were the channels for

hydrothermal solutions, and the structurally disturbed and reactive dolomite was an ideal location for deposition of ore. Although the effect of the overlying thrust plate cannot be documented, it probably had some control over the containment of the hydrothermal solutions.

The Red Bird and Dryden mines (fig. K4*B*) are at opposite ends of a major fault or series of faults that parallel the general course of Squaw Creek. Both mines have replacement ore bodies in carbonates of the Saturday Mountain Formation. Analyses of soil samples taken along traverses perpendicular to the fault between the Red Bird and Dryden deposits showed anomalous amounts of lead and zinc, indicating that the fault was a channel for mineralizing solutions along much of its length. The South Butte property is along a side fault that splits from this major fault zone and cuts carbonate beds that could be either Saturday Mountain Formation or Ella Dolomite. Several other deposits on the west side of Squaw Creek are along or near other steeply dipping faults. An intriguing common factor of all these deposits in the western part of this area is their proximity to an overlying thrust plate or to the projection of such a plate. These relations could well have important genetic implications, as proposed by Hall (chap. J, this volume), who has documented in areas to the south and west of the Bayhorse area that the intersection of steeply dipping normal faults and younger low-angle thrust faults provides an ideal environment for the formation of ore deposits.

RELATIONSHIP OF MINERAL DEPOSITS TO INTRUSIVE ROCKS

Intrusive rocks of several ages were undoubtedly involved directly or indirectly in the origin of many of the ore deposits. The contact of the main body of the mid-Cretaceous Idaho batholith is a few miles to the west of the Bayhorse area (fig. D1), and minor offshoots and outliers occur within the Bayhorse area. Small Tertiary intrusive bodies related to the Challis Volcanics are scattered through the area and may underlie some parts of it at shallow depth. The control that these plutonic rocks

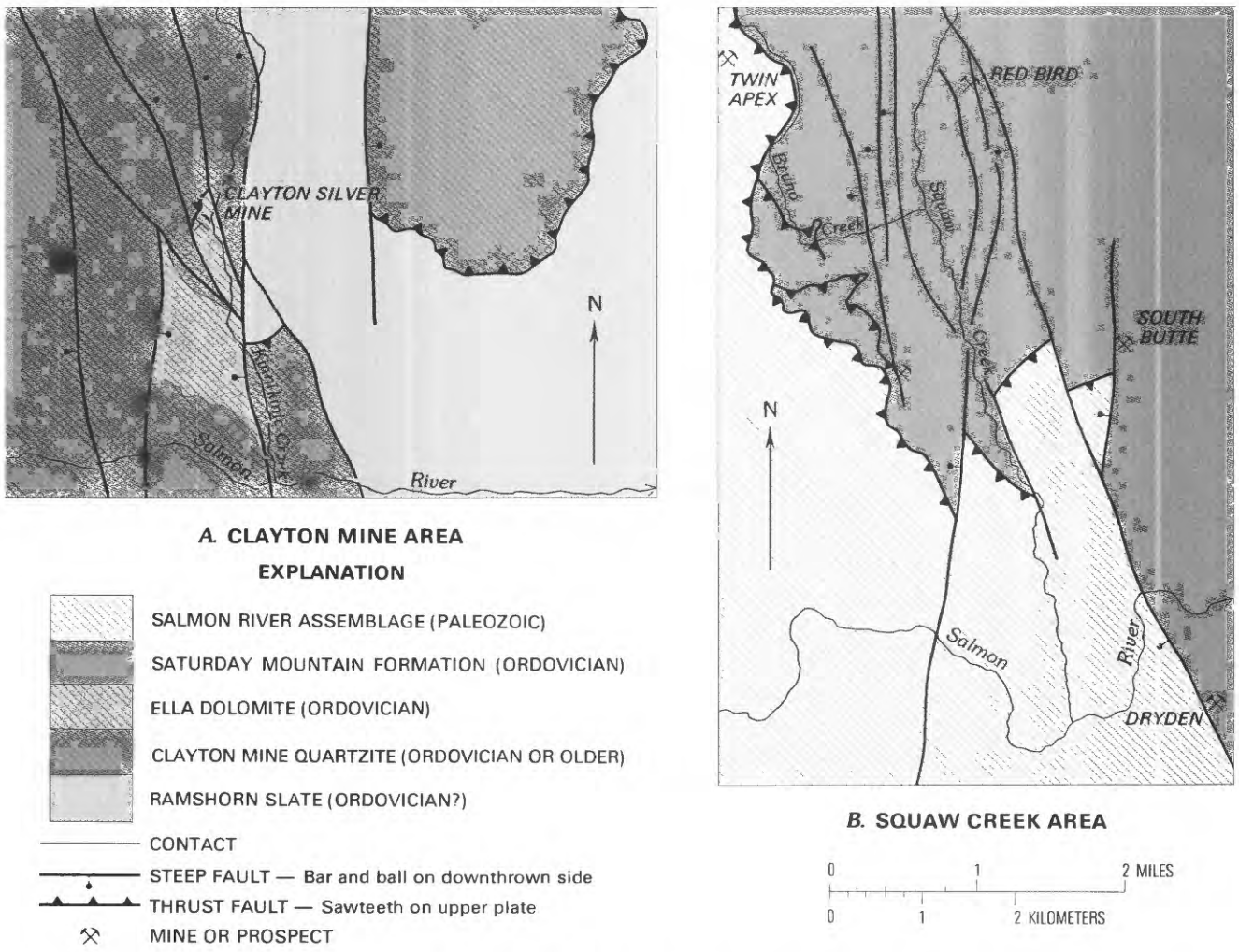

Figure K4. Geologic maps of the Clayton Silver mine and Squaw Creek areas. Locations of maps shown on figure K1.

have on ore deposits relates in large part to the stratigraphy and structure with which they react or interact.

The direct contact of the batholith with carbonate rocks in the Lower Permian Grand Prize Formation, which is slightly west of the Bayhorse area, resulted in one productive scheelite-bearing skarn deposit and several prospects. These deposits and many others are discussed by Cookro (chap. Q, this volume). These same plutonic rocks elsewhere possibly supplied magmatic fluids and gases that followed structures of various kinds and transported metals into favorable sites of deposition. Furthermore, it is becoming increasingly apparent (Hall, chap. J, this volume) that igneous rocks provided the energy to activate connate and meteoric waters that permeate crustal rocks, leach the entrapped metals, and carry these elements to sites of deposition. Such sedimentary source rocks, good examples of which are in the Challis quadrangle, could well be the ultimate stratigraphic control on the formation of ore deposits.

REFERENCES CITED

Anderson, A. L., 1954, A preliminary report on the fluorspar mineralization near Challis, Custer County, Idaho: Idaho Bureau of Mines and Geology Pamphlet 101, 12 p.

Hays, W. H., McIntyre, D. H., and Hobbs, S. W., 1978, Geologic map of the Lone Pine Peak quadrangle, Custer County, Idaho: U.S. Geological Survey Open-File Report 78–1060, scale 1:62,500.

Hobbs, S. W., 1980, The Lawson Creek Formation of Middle Proterozoic age in east-central Idaho: U.S. Geological Survey Bulletin 1482–E, p. 1–12.

Hobbs, S. W., Hays, W. H., and McIntyre, D. H., 1975, Geologic map of the Clayton quadrangle, Custer County, Idaho: U.S. Geological Survey Open-File Report 75–76, 23 p., 1 map, scale 1:62,500.

McIntyre, D. H., Hobbs, S. W., Marvin, R. F., and Mehnert, H. H., 1976, Late Cretaceous and Eocene ages for hydrothermal alteration and mineralization, Bayhorse district and vicinity, Custer County, Idaho: Isochron/West, no. 16, p. 11–12.

McIntyre, D. H., Ekren, E. B., and Hardyman, R. F., 1982, Stratigraphic and structural framework of the Challis Volcanics in the eastern half of the Challis 1°×2° quadrangle, *in* Bill Bonnichsen and R. M. Breckenridge, eds., Cenozoic geology of Idaho: Idaho Bureau of Mines and Geology Bulletin 26, p. 3–22.

McIntyre D. H., and Hobbs, S. W., 1978, Geologic map of the Challis quadrangle, Custer County, Idaho: U.S. Geological Survey Open-File Report 78–1059, scale 1:62,500.

Ross, C. P., 1931, A classification of the lode deposits of south-central Idaho: Economic Geology, v. 26, no. 2, p. 169–185.

_____1937, Geology and ore deposits of the Bayhorse region, Custer County, Idaho: U.S. Geological Survey Bulletin 877, 161 p.

Snyder, K. D., 1978, Geology of the Bayhorse fluorite deposit, Custer County, Idaho: Economic Geology, v. 73, no. 2, p. 207–214.

Umpleby, J. B., 1913, Some ore deposits in northwestern Custer County, Idaho: U.S. Geological Survey Bulletin 539, 104 p.

Symposium on the Geology and Mineral Deposits of the Challis 1°×2° Quadrangle, Idaho

Chapter L

A Case for Plants in Exploration—Gold in Douglas-Fir at the Red Mountain Stockwork, Yellow Pine District, Idaho

By J. A. ERDMAN, B. F. LEONARD, *and* D. M. McKOWN

CONTENTS

FIGURES

Abstract

Exploration targets for concealed deposits of gold, molybdenum, and tungsten exist outside the Red Mountain stockwork, based on evidence from this study. The targets are new and, to a considerable degree, unexpected from other surface evidence. The biogeochemical anomalies that help define the targets are extensive, and the deposits that might be sought are presumably of low grade.

Red Mountain, which lies on the western edge of the ring-fracture zone of the Eocene Quartz Creek cauldron (Leonard and Marvin, 1982), has been prospected for gold and silver for at least 50 years. A biogeochemical study was conducted in 1980–81 in an attempt to better assess the mineral potential of the stockwork area. Bedrock contacts are concealed by colluvium, glacial deposits, and forest cover. Soil and plant samples were collected on 200-yd (yard) centers of a sampling grid over an area of 3,600 ft (feet) by 8,400 ft. The wood of douglas-fir (*Pseudotsuga menziesii*) and the leaves of beargrass (*Xerophyllum tenax*) were used because they concentrate gold and molybdenum, respectively. Results of the soil sampling were insignificant, although they did indicate a tungsten anomaly south of the stockwork. Analysis of ashed wood by instrumental neutron activation yielded gold values of 0.07–14.2 ppm (parts per million) and revealed two distinct gold populations. More important, the highly anomalous samples (more than 4 ppm) are concentrated in the southern quarter of the sample grid in an area that has no anomalous gold in the sampled soils, has not been prospected for gold, and lies within inclusion-bearing granodiorite, not stockwork. Beargrass samples, which typically contain 20 ppm molybdenum, contained less than 5 to more than 500 ppm. A belt of localities of samples containing above-median values of molybdenum transects some part of every geologic unit except the quartz body at the summit of Red Mountain. The great extent and the continuity of this belt require some comparably extensive bedrock source of the molybdenum. The location, shape, and molybdenum content of the bedrock source remain conjectural, but the source must be large. Subsequent geomagnetic traverses confirmed the belt configuration.

INTRODUCTION

Biogeochemical studies were conducted in 1980–81 in an attempt to better assess the mineral resource potential of the Red Mountain stockwork area. The Red Mountain stockwork is 3.5 mi (miles) north-northeast of Yellow Pine, a small settlement near the northwestern corner of the Challis quadrangle. Red Mountain, so called from the reddish-brown color of its soil, is an informal name in local use for the land mass between Quartz Ridge and the forks of Quartz and Vein Creeks (fig. L1). The stockwork has been prospected for gold and silver for at least half a century with little success. Recently, however, the area has received renewed interest by several claim holders, in large measure owing to our geochemical studies.

Acknowledgments.—J. G. Brophy, William Lynch, and D. K. Swanson served as field assistants in 1979–81. Spectrographers L. A. Bradley, E. F. Cooley, and M. J. Malcolm, chemist J. G. Crock and his associates, and plant analysts Thelma Harms and Clara Papp provided the analytical data essential to this report. Mary Lou Tompkins processed the analytical data for computer treatment. A. T. Miesch introduced us to the Gapmap program used for part of the statistical analysis. All the workers listed above are or were members of the U.S. Geological Survey. C. W. Erdman and Eleanor Leonard helped with surveying and sample collecting.

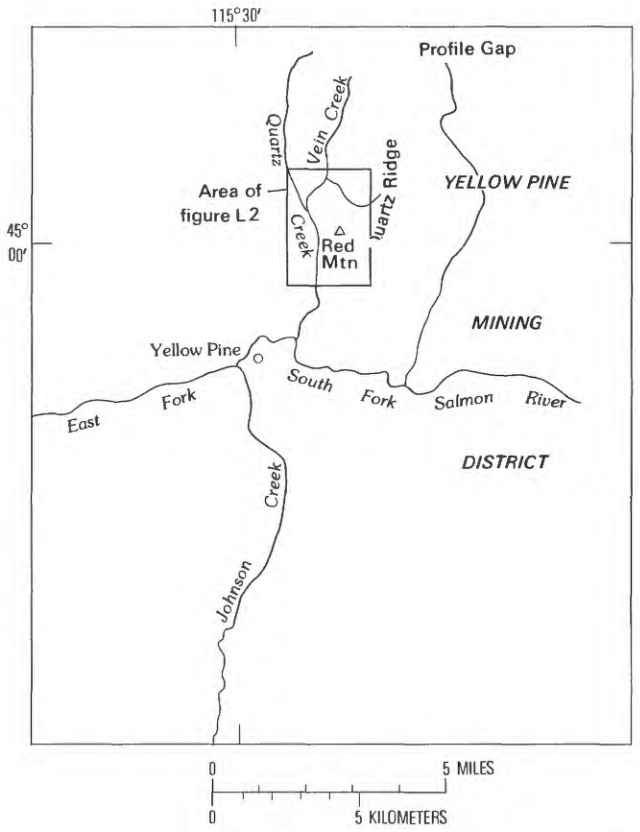

Figure L1. Index map of Red Mountain and vicinity, Yellow Pine mining district. From U.S. Geological Survey, Challis and Elk City quadrangles, 1:250,000.

GEOLOGIC SETTING

The Red Mountain stockwork is a geologic anomaly in the region for the following reasons: (1) it is a fine-scale stockwork, instead of a system of subparallel quartz veins with sporadic apophyses; (2) it is cut by small radial dikes, rather than by a few large dikes or by dike swarms; (3) it is locally dissected by radial faults; (4) it contains molybdenite, rarely seen in the Yellow Pine gold-mining district (Koschmann and Bergendahl, 1968), as well as scheelite and stibnite, which are common ore minerals in the district; (5) it contains sparsely disseminated pyrrhotite in addition to ubiquitous pyrite and arsenopyrite; and (6) its envelope of clay-mineral alteration is by far the largest

known in the region. Because the stockwork is geologically anomalous, it is the kind of feature that exploration geologists are always looking for—and hoping to find ore bearing.

The stockwork is near the western margin of the Quartz Creek cauldron (fig. L2), the very large Eocene subsidence feature that contains the Cougar Basin and Thunder Mountain calderas of Challis Volcanics (Leonard and Marvin, 1982). At the latitude of Red Mountain, north-striking ring fractures and attendant silicified zones of the cauldron appear to be offset along an ill-defined, east-trending zone that is partly occupied by the Red Mountain stockwork. The Johnson Creek-Quartz Creek silicified zone cannot be traced farther northward up Quartz Creek, and the Profile-Smith Creek silicified zone, passing through Profile Summit (Profile Gap), cannot be traced farther southward down Quartz Ridge. During subsidence of the Quartz Creek cauldron, it is reasonable to suppose that the mechanical energy ordinarily released along radial or other faults linking discontinuous ring fractures may have accumulated at the site now occupied by the stockwork. The Red Mountain block, severely strained, yielded partly by internal deformation and partly by intense crackling. Later, the silica-bearing solutions that produced the quartz veins and lodes of the great ring-fracture-controlled silicified zones penetrated the crackled ground of the Red Mountain block and formed the stockwork.

Because contacts of the rock units at Red Mountain are concealed at the surface by colluvium or locally by other Quaternary deposits, Leonard mapped the contacts by float. Details of the geology and ore minerals observed at Red Mountain are given in Leonard and Erdman (1983). For this report the geology (fig. L3) has been simplified from unpublished mapping of Leonard as follows:

1. Undifferentiated Quaternary deposits (unit Qs, fig. L3).

2. A virtually barren quartz body on the summit of Red Mountain, the Summit quartz body (unit Tsq, fig. L3).

3. A quartz stockwork surrounding the quartz body and underlying the upper slopes of the mountain (unit Tst, fig. L3). This stockwork contains quartz veins and veinlets, commonly intersecting, and replacement aggregates of quartz. It locally contains relics of granite.

4. A small, isolated part of a silicified zone, within granite, exposed low on the northwestern flank of Red Mountain (unit Tsz, fig. L3). The north end of the Quartz Creek silicified zone, here consisting of minor quartz veins, veinlets, and replacement patches in granite or in the mixed-rock unit, is poorly exposed southwest of Red Mountain.

5. A Cretaceous granite surrounding most of the stockwork and underlying the lower slopes (unit Kig, fig. L3). This unit is variably deformed, locally argillized, and sporadically replaced by muscovite and quartz.

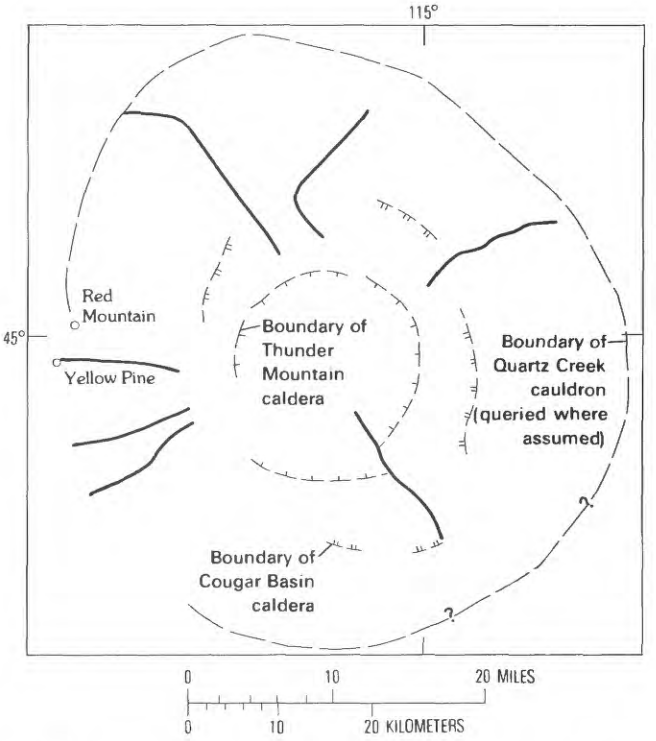

Figure L2. Generalized structure map of the Thunder Mountain caldera complex, Challis quadrangle. Heavy lines, faults. From Leonard and Marvin (1982).

6. A biotite-muscovite granodiorite of the Idaho batholith exposed at the northern edge of the area (unit Kigd, fig. L3). The unit is similar to the regional batholithic rock type; it is porphyritic to subporphyritic and is generally little altered.

7. A mixed-rock unit at the southeastern corner of the study area (unit Kim, fig. L3). It is a mass of granodiorite and alaskite of the Idaho batholith suite, here containing sparse inclusions of quartzite, biotite schist, and amphibolite of the Middle Proterozoic Yellowjacket Formation.

Taken as a whole, the following features suggest that a Tertiary intrusion is concealed beneath Red Mountain: (1) the presence of radial dikes and faults; (2) the presence and gross shape of map units Tsq, Tst, and Kig (fig. L3); (3) the drainage pattern; (4) the zonal distribution of clay minerals in soil; (5) the subelliptical shape of the molybdenum anomaly in beargrass, described below; and (6) the crudely oval pattern of magnetic anomalies. The gold anomaly, described below, is in the area underlain, for the most part, by the inclusion-bearing granodiorite (unit Kim, fig. L3), not the stockwork.

VEGETATION AND SOILS

The study area is characterized by fairly rugged terrain that ranges from 6,000 ft at Quartz Creek on the

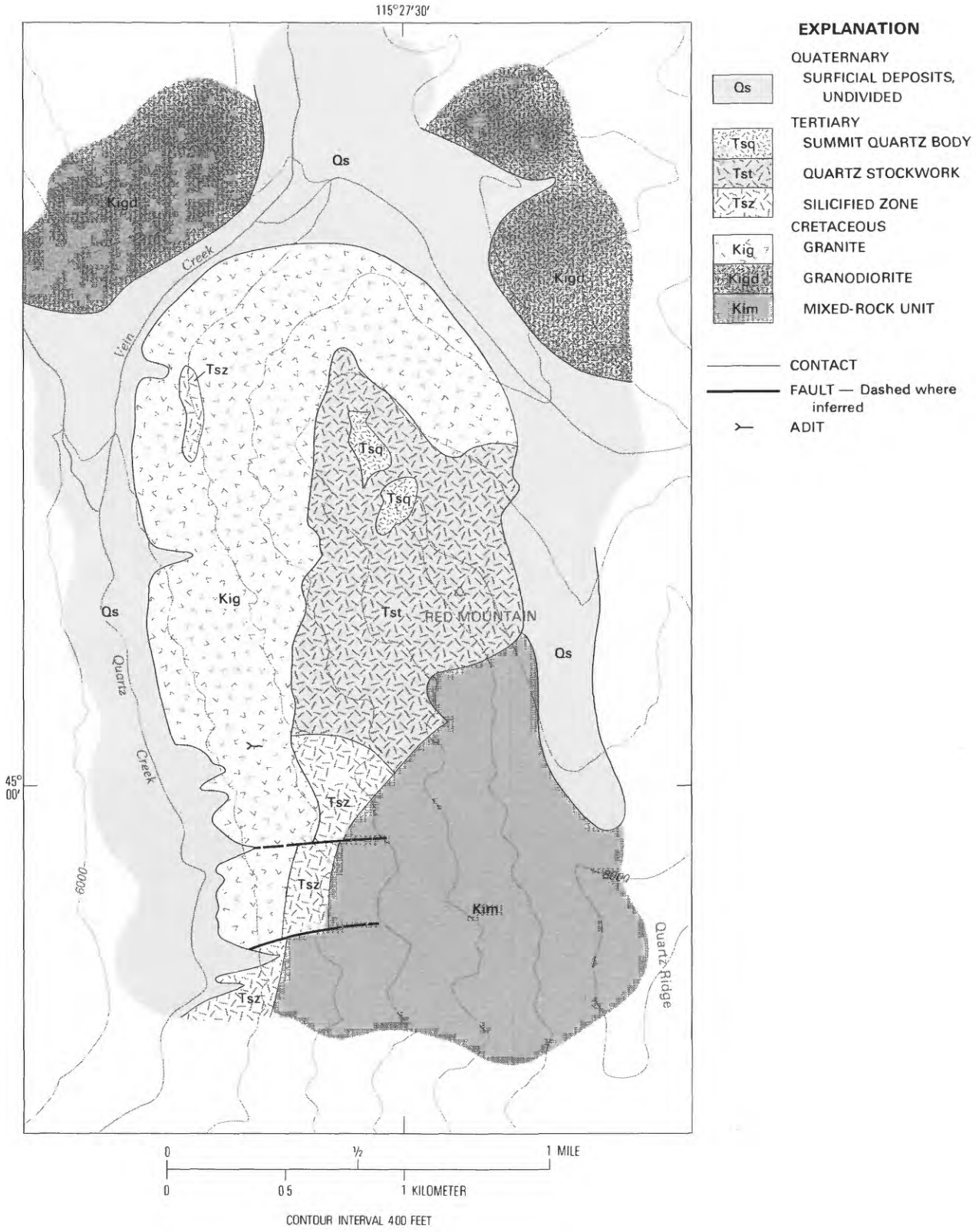

Figure L3. Generalized geologic map of the Red Mountain stockwork area. Base from U.S. Geological Survey, 1:24,000, Yellow Pine and Profile Gap quadrangles.

western edge to about 8,000 ft at Quartz Ridge on the east (fig. L1).

The forest zone is mainly upper montane and is dominated by douglas-fir (*Pseudotsuga menziesii* [Mirbel] Franco), although lodgepole pine (*Pinus contorta* Dougl.) and limber pine (*P. flexilis* James) are locally common. At higher elevations and on the slopes with northern exposures, elements of the subalpine forest, engelmann

spruce (*Picea engelmannii* Parry) and subalpine fir (*Abies lasiocarpa* [Hook.] Nutt.), either partly or totally replace the douglas-fir. Douglas-fir is also absent along many of the streams; these areas are ideal habitats for blue spruce (*Picea pungens* Engelm.). The proximity of the sampling grid to the riparian and subalpine zones, therefore, leaves several gaps in the plant-sampling design, described below.

The forest understory consists of many species of small trees or shrubs, such as aspen (*Populus tremuloides* Michx.), alder (*Alnus* sp.), chokecherry (*Prunus virginiana* L.), and serviceberry (*Amelanchier alnifolia* Nutt.). Common ground-cover species are beargrass (*Xerophyllum tenax* [Pursh] Nutt.), grouseberry (*Vaccinium scoparium* Leiberg), and elk sedge (*Carex geyeri* Boott), plus a fairly rich assemblage of other herbaceous plants.

The soils of the Red Mountain area are mainly residual or very nearly so. Most of the clay minerals in soil developed on bedrock reflect the hypogene alteration of the parent bedrock. The clay minerals in soil of the study area (Leonard and Erdman, 1983) are distinctively zoned. The sericite and kaolinite zones are crudely central to the stockwork, and the montmorillonite and chlorite zones are peripheral.

FIELD METHODS

A gridded sampling design with centers 200 yds apart was used in collecting soil and vegetation samples from the stockwork area in 1980. Based on the initial analytical results, the sample grid was extended in 1981 to the south and east, for a total of 124 localities. Even the extended grid did not enclose the area of anomalous samples.

A soil sample, weighing 0.5–1 kg (kilogram), was taken at each grid intercept at a depth of 4–8 in. (inches) after the site was scraped free of forest litter or plant growth. The sample was screened to minus 10 mesh, mixed, and split into two parts, one for chemical analysis and the other for clay studies. Organic debris that passed the stainless-steel screen was later floated off with water in the laboratory.

Douglas-fir was selected as the main sampling medium for the biogeochemical survey for two reasons. First, although it does not grow everywhere in the study area, it is more common than the several other species of conifer that occur there. And second, ". . . wherever douglas-fir occurs it affords an excellent biogeochemical tool" (Warren, 1980, p. 361). Warren and Delavault (1950) were the first to report a gold content in douglas-fir, 0.65 ppm, in the ash of "fresh new growth" from a mineralized area in British Columbia.

Results from a biogeochemical survey in 1979 of many mineral prospects in the Challis quadrangle (Erdman, unpub. data) pointed to douglas-fir as a likely concentrator of gold, specifically its wood tissue. In a study of the Empire gold district in Colorado, Curtin and others (1968) concluded that gold is most concentrated in tree roots. However, in our judgment, wood from the tree trunk is more easily sampled than is that from the roots. Our results do not agree with those of Khotamov and others (1966), who found gold most concentrated in the leaves of plants.

We selected a medium-size douglas-fir tree (about 18 inches in trunk diameter) that was closest to each sample point at the grid intercept. Some trees were not close to the intercept and soil-sample pit, but all of the sampled trees were within 100 ft of the grid point. In some places, the only tree available for sampling was either somewhat smaller or, more commonly, considerably larger than moderate size.

About 50 g (grams) of wood were extracted from the trunk using a brace and bit. This amount filled a small cloth sample bag and provided sufficient ash for analyses by emission spectroscopy and neutron activation. The ash yield of wood is 0.1–0.3 percent, so most samples yielded, at minimum, 50 mg (milligrams) of ash.

Two types of wood can be clearly recognized when coring, a commonly thin zone of almost white sapwood and an interior zone of red heartwood. We sampled the sapwood, each sample requiring about six borings, on the average.

Analytical precision was estimated from analyses of duplicate samples taken from nine trees scattered throughout the 1980 study area. Separate bags were filled from alternate sapwood borings. We found the reproducibility of analytical results to be satisfactory for the purposes of this study.

In addition to sampling douglas-fir mainly for its gold content, we also sampled two kinds of herbaceous plants, beargrass and elk sedge, because of their ability to concentrate molybdenum. Molybdenum is often a pathfinder element in gold occurrences and is of special interest at Red Mountain because molybdenite occurs there. Beargrass, a member of the lily family, is a large, clump-forming herb common to the area; samples of the leaves were collected from 96 of the grid-sample locations. The samples were taken from three to five mature, healthy plants within 100 ft of the soil-sample pit and grid intercept, and the samples of leaves from the individual plants were combined into one sample weighing several hundred grams. Eighteen samples of elk sedge, each sample a composite of leaves of three or more plants near the soil-sample pit, were collected along the three southernmost traverse lines where beargrass was absent (14 locations) or where beargrass and elk sedge were collectible as paired samples (4 locations). Based on the small number of paired samples from a restricted area, elk sedge may be the better concentrator of molybdenum, but beargrass is more quickly recognized, identified, and collected.

ANALYTICAL METHODS

The minus-10-mesh fraction of the soil samples was pulverized, then analyzed for 40 elements by semiquantitative emission spectroscopy and for gold, mercury, tungsten, arsenic, and antimony by special methods: atomic absorption for gold and mercury, inductively coupled plasma for tungsten, and hydride generation-atomic absorption for arsenic and antimony.

The plant samples were first oven dried at 40°C (Celsius), then pulverized to pass a 1.3-mm (millimeter) sieve in a Wiley[1] mill, and finally ashed in a muffle furnace having controls that permitted a slow increase in temperature to a maximum of 500°C. The heating and cooling cycle was 24 hours. Small aliquots of ash (about 10 mg) were submitted for analysis of 29 elements by semiquantitative emission spectroscopy.

Gold determinations were made on samples of about 30–40 mg by neutron-activation analysis, a technique considered to be ideal for samples of small mass and containing low element concentrations (Warren, 1980; Brooks and others, 1981; Hoffman and Brooker, 1982). Instrumental neutron-activation analysis provides a relatively convenient, precise measurement of low-level gold in ashed plant samples. In the analysis of the sapwood of douglas-fir, the method yielded a detection limit of about 0.008 ppm gold in the ash, which corresponds to 0.05 ppb (parts per billion) in the dried raw wood. Based on replicate measurement of a single sample, the precision was within 10 percent at the 0.1-ppm level. Briefly, the technique is:

Aliquots of 30–40 mg of wood ash were weighed into precleaned 2/5-dram polyvial irradiation containers. Elemental standards were prepared by weighing similar volume aliquots of U.S. Geological Survey gold-quartz standard GQS-1 (Millard and others, 1969) and by evaporating aliquots of a multielement standard solution containing gold, arsenic, and antimony onto Specpure SiO_2. Samples and standards were simultaneously irradiated in the U.S. Geological Survey Triga reactor (at Denver) for 8 hours at 5×10^{12} neutrons per square centimeter per second. Irradiated sample vials were cleaned externally with water and loaded into appropriate automatic sample-changer vials (2-dram polyvials) for counting. Data were acquired automatically from a system consisting of multiple germanium (lithium) detectors with sample changers coupled to a Nuclear Data ND-6620 computer-based multichannel analyzer. Samples and standards were successively counted for 20 minutes each after a decay period of 4–6 days, and a direct comparison of sample and standard peak area was made after appropriate normalization for differences in decay time and dead time.

Tungsten was determined colorimetrically (Quin and Brooks, 1972) in samples of ashed beargrass leaves. The molybdenum content determined by semiquantitative emission spectroscopy was confirmed colorimetrically on a representative suite of these samples.

[1]Trade names used in this chapter are for descriptive purposes only and do not imply endorsement by the U.S. Geological Survey.

RESULTS OF ANALYSES

Metal anomalies in soils sampled from the study area are mostly subtle and not extensive, although the samples did indicate a tungsten anomaly south of the stockwork. The only gold anomaly, 1.1 ppm, was in a sample from a site on the stockwork. Gold concentrations in most soil samples were less than 0.05 ppm. Specifics of the soil results are given in Leonard and Erdman (1983, p. 21–29).

In contrast to the metals in soil, the metals in plant ash showed anomalies so strong and associated areas of above-median values so large that Red Mountain would be an attractive area for exploration even if the local geology were unknown. Few of the metal anomalies in plants are in samples from the stockwork. Rather, they are from geologically puzzling terrane—the valley fill of Quartz Creek and the inclusion-bearing granodiorite. The anomalies are consistent with the inference of a concealed elliptical feature that may be hoodlike and may contain more than one mineralized zone.

Gold distribution

Gold concentrations in the ash of douglas-fir sapwood ranged from 0.07 to 14.2 ppm, more than two orders of magnitude. More important, the highly anomalous samples (containing more than 4 ppm) were concentrated in the southern part of the sampling grid (fig. L4) where no anomalous gold was found in the soils. This area has not been prospected for gold and is underlain by inclusion-bearing granodiorite, not stockwork.

The mean of the gold values is 0.85 ppm, and the standard deviation is 1.72. Because the frequency distribution is strongly skewed (skewness, 5.2), we plotted the frequency distribution on a log scale and transformed the data to logarithms to compute the geometric means (fig. L5). The histogram (fig. L5) shows a bimodal distribution, which suggests the presence of two populations. This possibility was tested by using a statistic recently proposed by Miesch (1981). The statistic is a standardized gap which, if significant, can be taken as the separation between two geochemical populations. The results indicate a significant gap (fig. L5) whose probability of occurrence if no anomaly were present is 0.086 (confidence level, 91.4 percent). The gold values for 53 of the 114 samples are to the right of the gap (fig. L5), whose center is at 0.35 ppm. Therefore, two populations of approximately equal size are indicated, the upper one being anomalous.

Another measure of the remarkably high concentrations of gold in the anomalous sample population at

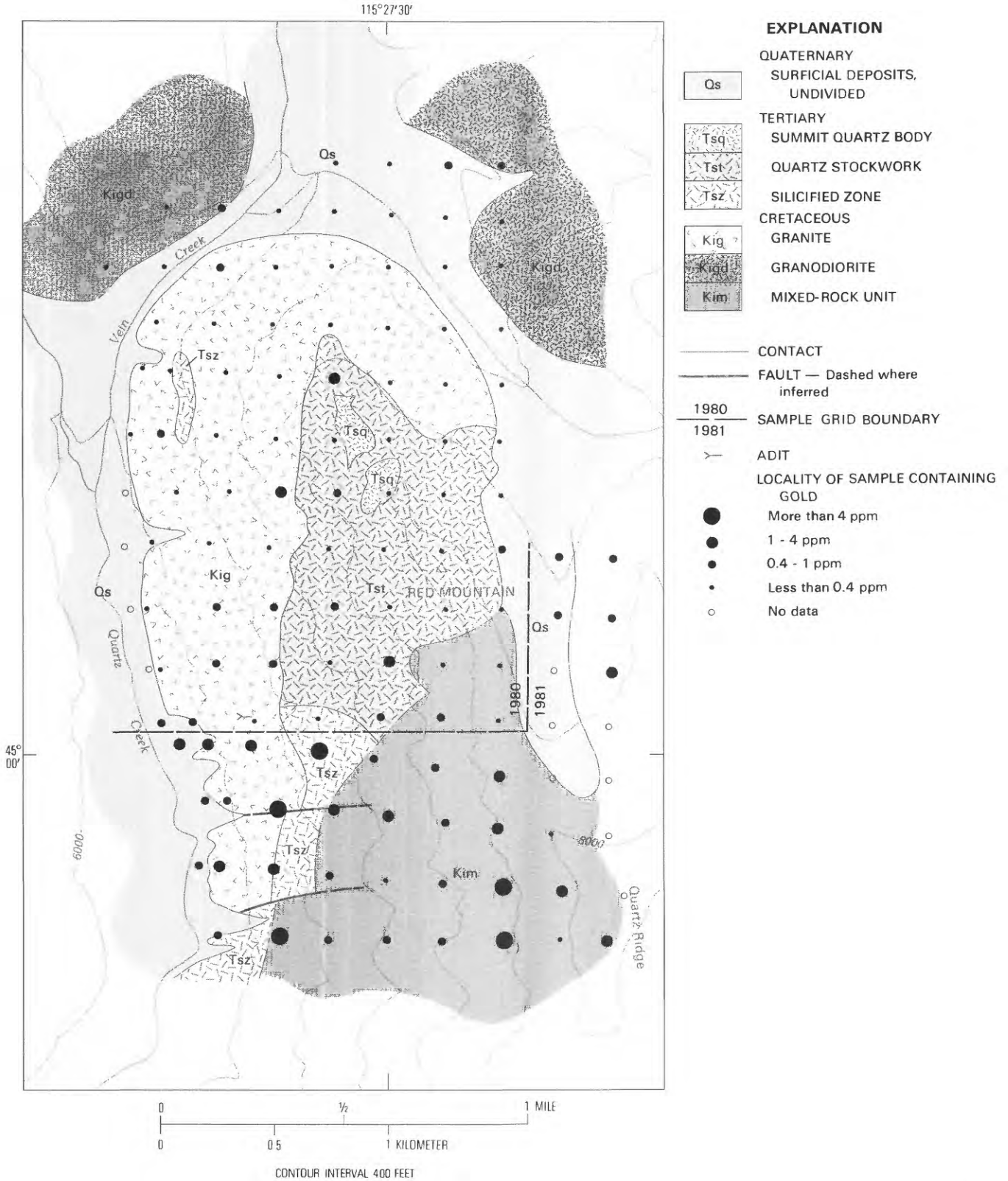

Figure L4. Map showing sample localities and concentrations of gold in the ash of douglas-fir wood, Red Mountain area. The threshold between background and anomalous concentrations is 0.4 ppm.

Red Mountain is the gold in a suite of 20 samples of douglas-fir wood from the Basin Creek watershed, which is northeast of Stanley but in an area of no known gold mineralization. There the gold concentrations ranged from 0.04 to 0.31 ppm, which correspond with the statement by Shacklette and others (1970, p. 2) that the amounts of gold in plant ash are usually much smaller than 1 ppm.

The only reasonable conclusion we can reach is that gold levels are unusually high in the southern quarter of the sampled area. Lakin and others (1974) stated, "The

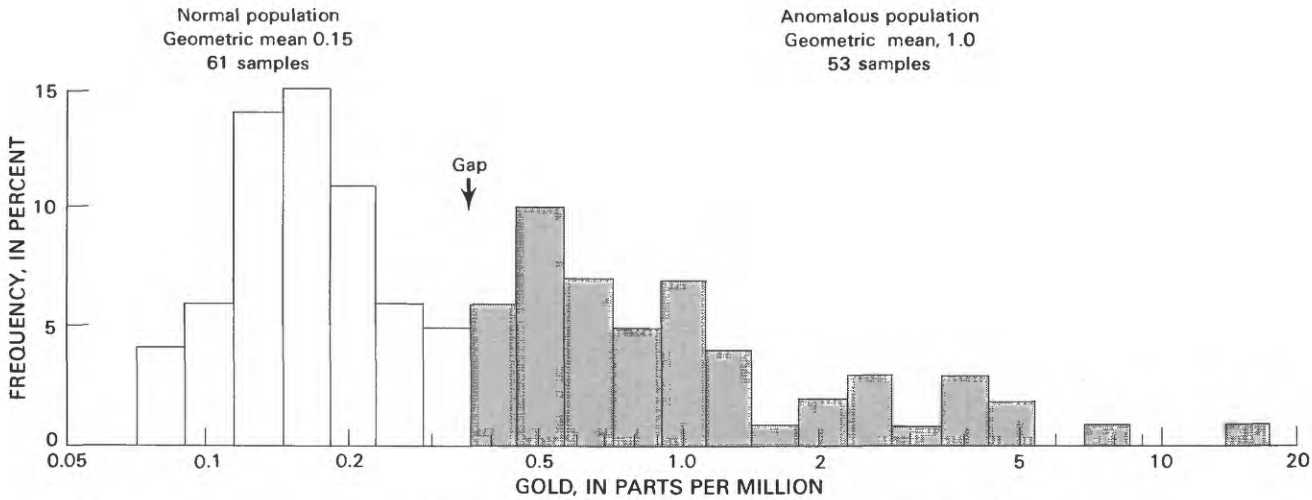

Figure L5. Histogram of gold in the ash of douglas-fir wood, showing two populations, Red Mountain area.

relative insolubility of gold drastically limits the portion of the total gold under the plant that is available to the plant roots." Therefore, we would expect to find such unusual concentrations of gold in plants only in an area where gold is relatively abundant. The high concentrations observed in the ash of douglas-fir wood, but not in soil from the same sample sites and those nearby, suggest that the root system of the trees has taken up gold from a source deeper than that which commonly contributes gold to the soil.

Molybdenum distribution

Biogeochemical sampling for possible polymetallic occurrences may require the use of more than one type of plant. We sampled douglas-fir mainly for its ability to concentrate gold, but we sampled beargrass, and to a limited extent elk sedge, because of their ability to concentrate molybdenum.

Molybdenum concentrations in beargrass sampled from the Challis quadrangle in 1979 were less than 5 to 20 ppm; these were in areas that were considered unmineralized for molybdenum.

The molybdenum content of 96 samples of ashed beargrass leaves from the study area ranged from less than 5 to more than 500 ppm; that of 18 samples of elk sedge leaves ranged from 5 to 100 ppm. The 50th and 95th percentiles were the same from both plants, 20 and 100 ppm, respectively.

Normal concentrations of molybdenum in elk sedge appear to be about 20 ppm, based on 27 samples collected from nine prospects or mines that represented various kinds of mineral deposits in the region. Anomalous concentrations of 100 to 200 ppm were observed in samples from the Sunnyside gold mine in the Thunder Mountain mining district, the new Thompson Creek mine (a world-class molybdenum deposit), and several tungsten occurrences.

With few exceptions, all above-median values were from samples in a belt that extends around the western side of the grid area and is peripheral to the exposed stockwork (fig. L6). We were unable to close off the anomaly by means of the sampling design that we used.

The belt of above-median values of molybdenum in beargrass and elk sedge transects some part of every geologic map unit in the area except the summit quartz body (unit Tsq, fig. L3). Much of the belt is on Quaternary deposits, either alluvial, glacial, or colluvial, and is therefore most difficult to interpret.

We can draw one inference with assurance; the great extent and the continuity of the belt of above-median molybdenum values in beargrass and sedge requires some comparably extensive bedrock source of molybdenum. The location, shape, and molybdenum content of the bedrock source remain conjectural, but the source must be large.

Tungsten distribution

In his book on biogeochemical exploration for mineral deposits, Kovalevskii (1979, p. 87) stated, "The most important indicators of molybdenum and tungsten deposits are the elements themselves." Yet very little is known of the absorption of tungsten by plants (Kovalevskiy, 1966). Quin and Brooks (1974) reported that even though soil sampling was generally satisfactory, tree-trunk sampling was effective in locating extensions of known scheelite-bearing reefs in New Zealand.

Previous studies by Leonard (in press) on the response of beargrass to tungsten occurrences encouraged us to submit our samples for analysis by colorimetry. At Red Mountain, the tungsten anomaly in beargrass is clearly subtle; ashed leaves of beargrass contain less than 1 to 2 ppm tungsten. Nevertheless, at this low level the areal distribution of the 1- and 2 ppm values shows a pattern generally resembling that of the major belt of above-median values of molybdenum in beargrass (fig. L7).

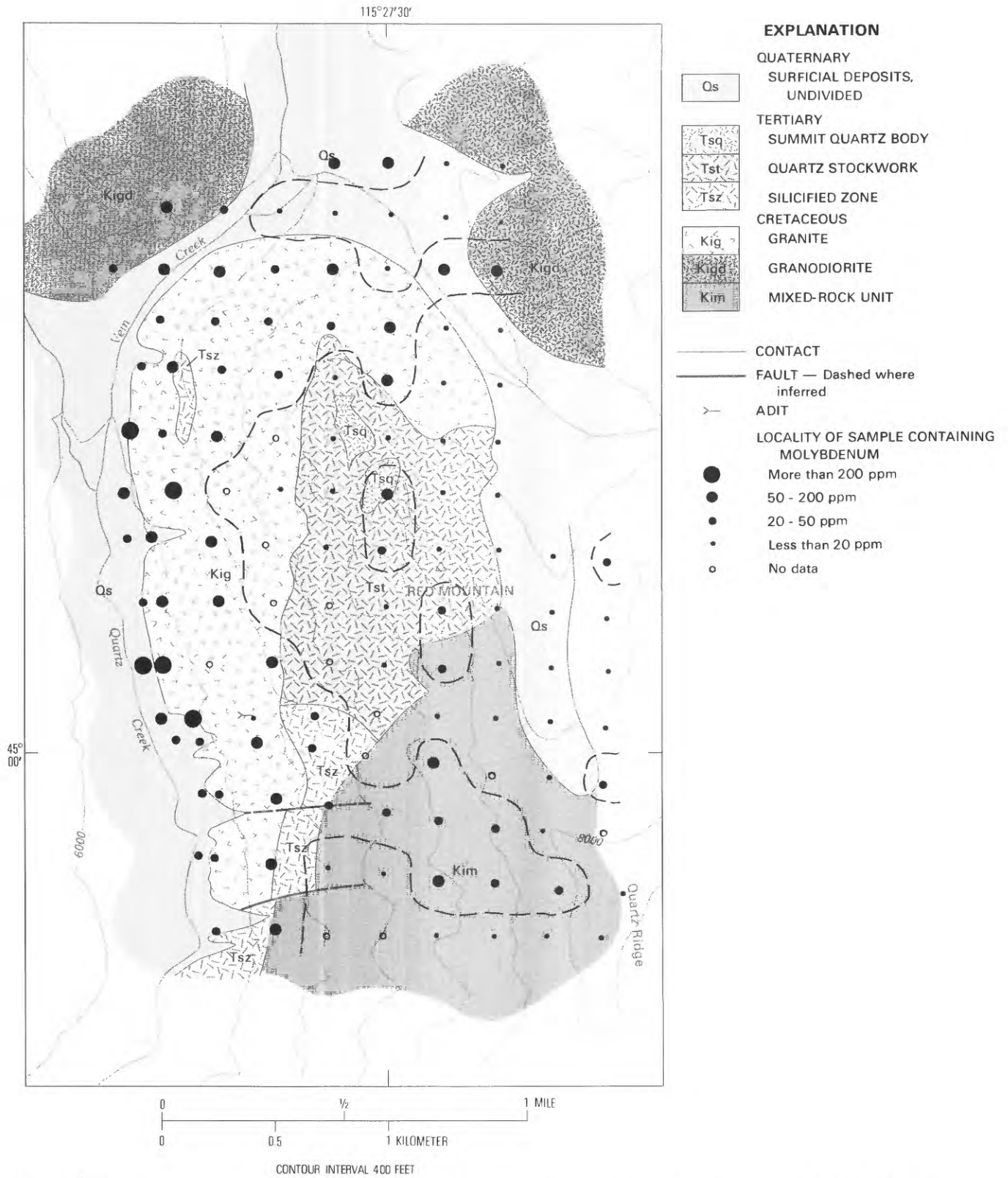

Figure L6. Map showing sample localities and concentrations of molybdenum in the ash of beargrass and elk sedge, Red Mountain area. Isopleths (dashed lines) enclose localities of samples having values above the median (20 ppm).

GEOMAGNETIC ANOMALIES

The biogeochemical data provide evidence of an apparent subsurface structure that was not obvious from detailed surface mapping. It is discordant with the bedrock structure. A subsequent packborne geomagnetic survey tended to confirm this conclusion.

An aeromagnetic map of part of the Elk City 1°×2° quadrangle (U.S. Geological Survey (1972), contour interval 20 gammas), shows a distinct crowding of contours

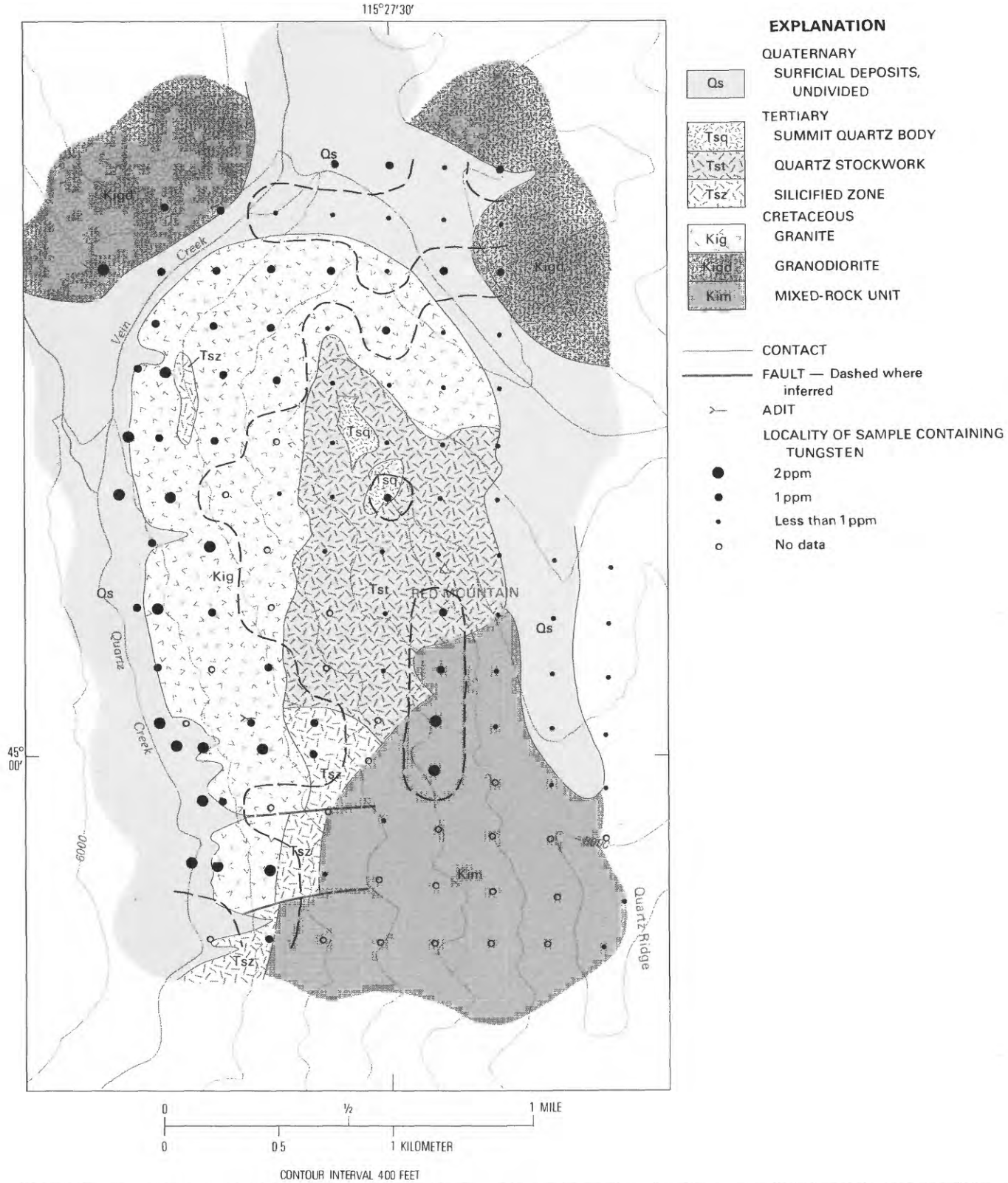

Figure L7. Map showing sample localities and concentrations of tungsten in the ash of beargrass, Red Mountain area. Isopleths (dashed lines) enclose localities of samples containing detectable tungsten.

in the Red Mountain area but no isolated magnetic high or low. Therefore, in making a ground survey by precession magnetometer, we did not expect to learn much about the gross structure of the area. We did hope that a ground survey would show the distribution of disseminated ferromagnetic pyrrhotite within stockwork or granite, and that the pattern of its distribution would be useful in interpreting local structures. We found, instead, that Red Mountain itself is an area of uninterpretable magnetic noise, that magnetic anomalies having some continuity are present north, west,

Figure L8. Map showing traces of geomagnetic anomalies, Red Mountain area. Centerlines of magnetic anomalies indicate surface traces of sharply defined increases (or decreases) of magnetic intensity measured on the ground with a portable magnetometer. Gamma values indicate heights (depths) of the peaks above (below) background level.

and south of the mountain, and that the northern and southern anomalies are discordant to the rock structure as mapped. More detailed work would be required to choose between near-surface alteration and deep-seated structure as the probable cause of these magnetic anomalies.

Details of the packborne magnetometer survey and of the specific anomalies are described in Leonard and Erdman (1983). Collectively, the magnetic anomalies of the Red

Mountain area show the features of an oval (fig. L8). Its major axis is nearly north-south, its north end is flattened, its south end is tapered, its west side is rectilinear, and its east side is barely sketched. The mappable part of the oval resembles the shape of the curved belt of above-median values of molybdenum in beargrass, and the two features are superposed along the western and southern sides of the grid.

Our best guess is that the sources of the magnetic anomalies are somehow related to wallrock alteration attendant on mineralization. The anomalies discordantly overprint the east-trending part of the belt of above-median values of molybdenum in beargrass and the swatch of high values of gold in douglas-fir, but they are confined to these biogeochemical domains.

CONCLUSIONS

Evidence obtained from this study indicates possible exploration targets for concealed deposits of gold, molybdenum, and tungsten at Red Mountain. The targets are new, the biogeochemical anomalies that help define the targets are extensive, and the deposits that might be sought are presumably of low grade but perhaps large.

The distribution of metals in plants, of clay minerals in soil, and of low-intensity magnetic anomalies at the limits of the sampling grid strongly suggest that the subsurface structure of the area is different from the structure that can be mapped. The subsurface structure may be hoodlike, relatively flat or gently undulating beneath the exposed quartz stockwork, but draped downward and covered by Quaternary deposits along Vein Creek and Quartz Creek.

Several of the targets would be unsuspected if our study did not show that plants concentrate gold, molybdenum, and tungsten. The advantages of sampling plants in lieu of or as a complement to sampling soils are especially clear in searching for gold. Two of these advantages are the circumvention of the particle sparsity effect (Harris, 1982) and the ability of plants to extract elements from a large volume of soil and underlying weathered bedrock.

REFERENCES CITED

Brooks, R. R., Holzbecher, J., and Ryan, D. E., 1981, Horsetails (*Equisetum*) as indirect indicators of gold mineralization: Journal of Geochemical Exploration, v. 16, p. 21–26.

Curtin, G. C., Lakin, H. W., Neuerburg, G. J., and Hubert, A. E., 1968, Utilization of humus-rich forest soil (mull) in geochemical exploration for gold: U.S. Geological Survey Circular 562, 11 p.

Harris, J. F., 1982, Sampling and analytical requirements for effective use of geochemistry in exploration for gold, *in* Levinson, A. A., ed., Precious metals in the northern Cordillera: Association of Exploration Geochemists Symposium, Vancouver 1981, Proceedings, p. 5367.

Hoffman, E. L., and Brooker, E. J., 1982, The determination of gold by neutron activation analysis, *in* Levinson, A. A., ed., Precious metals in the northern Cordillera: Association of Exploration Geochemists Symposium, Vancouver 1981, Proceedings, p. 69–77.

Khotamov, Sh., Lobanov, E. M., and Kist, A. A., 1966, [The problem of the concentration of gold in organs of plants from ore districts]: Akademiya Nauk Tadzhikskoy SSR Doklady, v. 9, no. 11, p. 27–30 (in Russian).

Koschmann, A. H., and Bergendahl, M. H., 1968, Principal gold-producing districts of the Unted States: U.S. Geological Survey Professional Paper 610, 283 p.

Kovalevskii, A. L., 1979, Biogeochemical exploration for mineral deposits: New Delhi, Amerind Publishing Company Pvt. Ltd.; also available from National Technical Information Service, Springfield, Va., 22170, as Report TT 76–52029; 136 p.

Kovalevskiy, A. L., 1966, Biogeochemistry of tungsten in plants: Geochemistry International, v. 3, p. 555–562.

Lakin, H. W., Curtin, G. C., and Hubert, A. E., 1974, Geochemistry of gold in the weathering cycle: U.S. Geological Survey Bulletin 1330, 80 p.

Leonard, B. F., in press, The Golden Gate tungsten deposit and metal anomalies in nearby soils and plants, Yellow Pine district, Valley County, Idaho: U.S. Geological Survey Open-File Report 83–835.

Leonard, B. F., and Erdman, J. A., 1983, Preliminary report on geology, geochemical exploration, and biogeochemical exploration of the Red Mountain stockwork, Yellow Pine district, Valley County, Idaho: U.S. Geological Survey Open-File Report 83–151, 49 p.

Leonard, B. F., and Marvin, R. F., 1982 [1984], Temporal evolution of the Thunder Mountain caldera and related features, central Idaho, *in* Bonnichsen, Bill, and Breckenridge, R. M., eds., The Cenozoic of Idaho: Idaho Bureau of Mines and Geology Bulletin 26, p. 23–41.

Miesch, A. T., 1981, Estimation of the geochemical threshold and its statistical significance: Journal of Geochemical Exploration, v. 16, p. 49–76.

Millard, H. T., Jr., Marinenko, John, and McLane, J. E., 1969, Establishment of gold-quartz standard GQS-1: U.S. Geological Survey Circular 598, 6 p.

Quin, B. F., and Brooks, R. R., 1972, The rapid determination of tungsten in soils, stream sediments, rocks and vegetation: Analytica Chimica Acta, v. 58, p. 301–309.

_____1974, Tungsten concentrations in plants and soils as a means of detecting scheelite bearing ore bodies in New Zealand: Plant and Soil, v. 41, p. 177–188.

Shacklette, H. T., Lakin, H. W., Hubert, A. E., and Curtin, G. C., 1970, Absorption of gold by plants: U.S. Geological Survey Bulletin 1314–B, 23 p.

U.S. Geological Survey, 1972, Aeromagnetic map of part of the Elk City 1° by 2° quadrangle, Idaho-Montana: U.S. Geological Survey Geophysical Investigations Map GP-841, scale 1:250,000.

Warren, H. V., 1980, Biogeochemistry, trace elements, and mineral exploration, *in* Davies, B. E., ed., Applied soil trace elements: New York, Wiley, p. 353–380.

Warren, H. V., and Delavault, R. E., 1950, Gold and silver content of some trees and horsetails in British Columbia: Geological Society of America Bulletin, v. 61, p. 123–128.

Symposium on the Geology and Mineral Deposits of the Challis 1°×2° Quadrangle, Idaho

Chapter M

Mineral Deposits in the Southern Part of the Atlanta Lobe of the Idaho Batholith and their Genetic Relation to Tertiary Intrusive Rocks and to Faults

By THOR H. KIILSGAARD *and* EARL H. BENNETT[1]

CONTENTS

[1]Idaho Geological Survey, Moscow, Idaho.

FIGURES

Abstract

Most mineral deposits in the Atlanta lobe of the Idaho batholith are genetically related to Tertiary intrusive rocks; regional faults have controlled location of the deposits. Pink granite of the Sawtooth batholith, in the Sawtooth Wilderness, about 45 m.y. (million years) old, contains more beryllium, uranium, fluorine, and molybdenum than does rock of the Idaho batholith. Gold-silver vein deposits along the western side of the Sawtooth batholith are concentrated in hydrothermally altered rocks of the Idaho batholith on the downthrown side of the Montezuma fault. Many of the veins follow or crosscut Tertiary dikes.

Pink granite of the Sawtooth batholith and nearby dioritic rocks about 47 m.y. old crop out in the Ten Mile West Roadless Area, as do swarms of associated dikes. Geochemical sampling shows silver, gold, and molybdenum concentrated near the intrusive Tertiary rocks along northwest-trending faults that cross the area.

A major northeast-trending fault system controls the location of vein deposits in the Boise Basin. Tertiary plutonic rocks and dikes have intruded along the faults, and the veins cut both the Tertiary plutonic rocks and the dikes. Two molybdenum deposits in the area occur in and along rhyolitic dikes, and a fission-track date from zircon taken from rhyolite at one of the deposits gives a date of 29.3±1.7 m.y. Veinlets containing molybdenite cut the rhyolite and are younger. The mineralization probably relates to waning phases of the Tertiary plutonic activity. Mineral deposits in Tertiary rocks also occur along northeast-trending faults and grabens in the northeastern part of the Challis quadrangle.

INTRODUCTION

Most mineral deposits in the Atlanta lobe of the Idaho batholith are genetically related to intrusive rocks of Tertiary age and are structurally controlled by regional faults. Granitic rocks of the Atlanta lobe of the Idaho batholith (fig. A2, chap A; and fig. B1, chap. B, this volume), now considered to be Cretaceous in age, and principal faults in the western part of the Challis quadrangle are described by Kiilsgaard and Lewis (chap. B, this volume), and Tertiary intrusive rocks of Eocene age are described by Bennett and Knowles (chap. F, this volume). The epigenetic character of mineral deposits in Tertiary intrusive rocks was first recognized by Lindgren (1898) in a description of mineral deposits near Boise Basin, Idaho. Anderson (1951) believed that mineral deposits in the southern part of the Idaho batholith were not genetically related to the batholith but were associated with early Tertiary igneous activity. Characteristics of the Tertiary intrusive rocks and their relation to mineral deposits have been discussed by Bennett (1980).

Four areas in or near the Challis quadrangle, in which mineral deposits, Tertiary intrusive rocks, and faults are present, are discussed in this chapter. The areas are: the Sawtooth Wilderness, the Ten Mile West Roadless Area, the Boise Basin, and a northeast-trending belt, the trans-Challis fault system, that extends across the Challis quadrangle (fig. M1).

SAWTOOTH WILDERNESS

Geology

The Sawtooth Wilderness, formerly called the Sawtooth Primitive Area, covers most of the Sawtooth Range southwest of Stanley (fig. M1). The most conspicuous rock type in the range is pink granite identified by Reid (1963, p. 8) as making up the Sawtooth batholith. The granite is distinguished by coarse granitoid texture and abundant perthitic potassium feldspar, which gives the rock its characteristic pink color. Biotite from three samples of the rock, analyzed by the potassium-argon method, gave ages of 43.7, 44.1, and 44.4 m.y., respectively (Armstrong, 1975); these ages were recalculated to 44.9, 45.7, and 45.6 m.y., using the decay constants of Steiger and Jaeger (1977), and identify the rock as Tertiary (Eocene). The pink granite intrudes rocks of the Idaho batholith, which are principally granodiorite. Both the younger Sawtooth batholith and the older Idaho batholith are intruded by innumerable dikes that range from diabase to rhyolite in composition. The more common dikes range from 1.5 to 15 m (meters) in thickness and from a few hundred meters to more than 1 km (kilometer) in length. Structurally, the Sawtooth Range is a large horst, bounded on the northeastern side by the Sawtooth fault and on the southwestern side by the Montezuma fault (fig. M2).

Anomalous metal concentrations in pink granite of the Sawtooth batholith

Pink granite of the Sawtooth batholith contains more anomalous concentrations of metals than do rocks

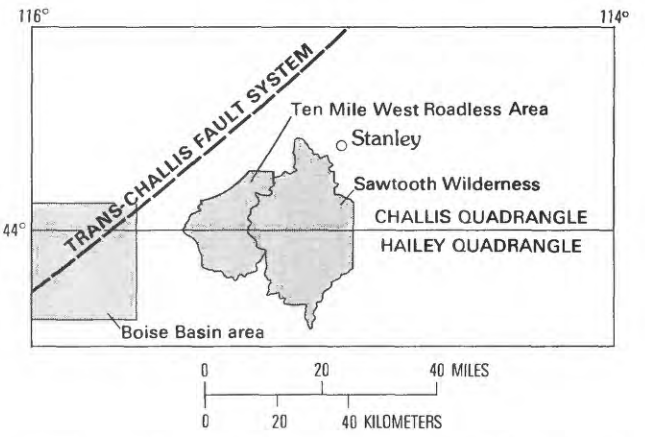

Figure M1. Index map showing the location of the Sawtooth Wilderness, Ten Mile West Roadless Area, and Boise Basin, and the approximate trace of the trans-Challis fault system, Idaho.

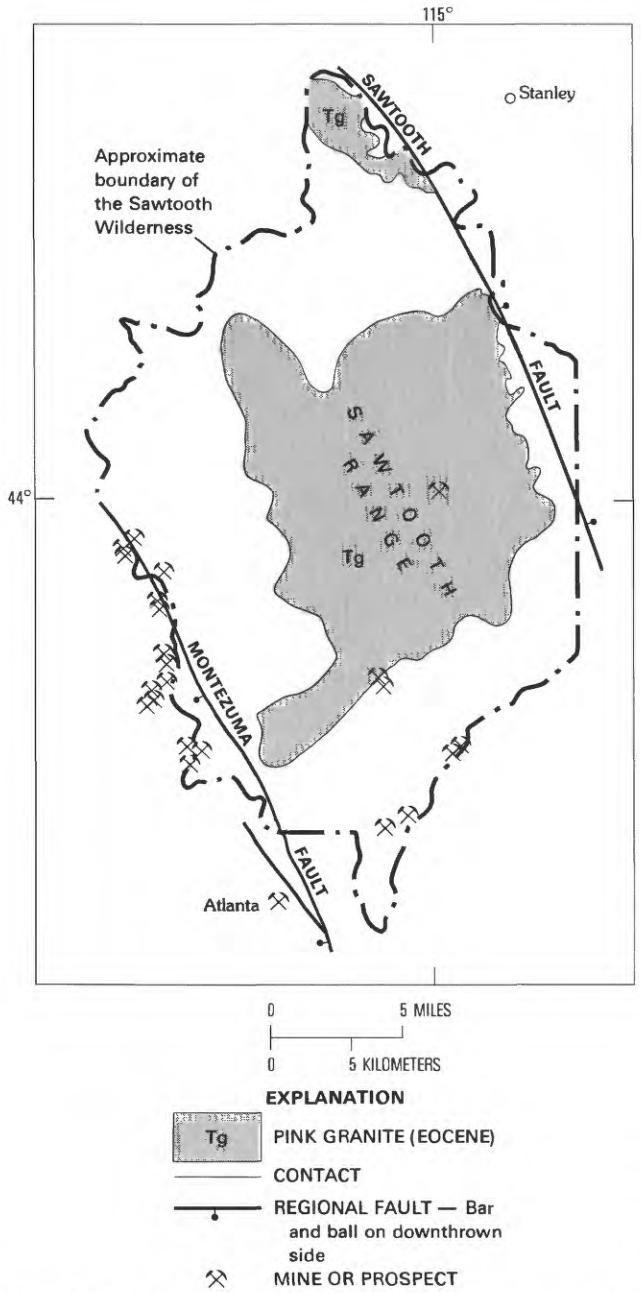

Figure M2. Map of the Sawtooth Wilderness showing major geologic features, and mines and prospects.

of the Idaho batholith. This conclusion is based on an appraisal of the mineral resoures of the former Sawtooth Primitive Area (Kiilsgaard and others, 1970) during which more than 1,100 samples of stream sediments, rocks, and mineralized deposits were collected and analyzed.

Beryllium is distinctly anomalous in rocks of the Sawtooth batholith, as determined by analyses of rock and stream-sediment samples (Kiilsgaard and others, 1970, fig. 9). The median beryllium content of unaltered granitic rocks of the Sawtooth batholith is 6 ppm (parts per million), in contrast to a median content of 1 ppm beryllium in rocks of the Idaho batholith.

Molybdenum is concentrated in pink granite of the Sawtooth batholith. Forty-three samples of altered granite, taken largely from northeast-trending altered zones, ranged from 2 to 1,500 ppm molybdenum but averaged 122 ppm. In contrast, 49 samples of altered granitic rock of the Idaho batholith contained an average of 13 ppm molybdenum (Kiilsgaard and others, 1970, table 1, pls. 1, 2). Samples from obviously mineralized localities, of both types of rock, were excluded from the comparison. The clustered distribution of molybdenum in the Sawtooth granite batholith is readily apparent (Kiilsgaard and others, 1970, fig. 8). Other mineralized localities shown in that figure as outside of the Sawtooth batholith are chiefly quartz veins that are explored by various prospect workings and are known to contain minor quantities of molybdenite. None of the large altered zones of Sawtooth granite batholith have been explored sufficiently to determine whether they contain molybdenum deposits of commercial significance.

Uranium also is concentrated in the pink granite of the Sawtooth batholith. Uranium content of 10 samples of the rock ranged from 10 to 190 ppm. The pink granite consistently has been found to be two to three times more radioactive than rocks of the Idaho batholith. Sediment samples from streams that drain areas underlain by pink granite of the Sawtooth batholith, particularly samples rich in organic debris, contained appreciable uranium. Stream-sediment samples that contained 100 ppm or more uranium were collected from a large area in the southern part of the Sawtooth batholith (Kiilsgaard and others, 1970, table 4, fig. 10). Despite the widespread, anomalously high uranium content in stream-sediment and rock samples, no concentrated deposits of uranium were found in rocks of the area.

High background values in uranium, molybdenum, and beryllium are characteristic of anorogenic granite (A-type) worldwide. The Sawtooth batholith and other similar granitic plutons in Idaho are believed to consist of anorogenic granite and are described by Bennett and Knowles (chap. F, this volume).

Gold-silver deposits and their relation to the Montezuma fault

A conspicuous geologic feature near the western border of the Sawtooth Wilderness is the concentration of gold-silver deposits along the Montezuma fault, chiefly along the western side of the fault in the downthrown block (fig. M2). The largest and most productive of these deposits is the Atlanta lode, which was discovered in 1864 and was worked intermittently through several mines until the early 1950's. For several years, the Atlanta lode was the largest producer of gold in Idaho.

The gold-silver deposits along the Montezuma fault have many common characteristics. They are quartz veins

from which gold has been the most valuable metal produced, most of which was native gold mined from the oxidized zone near the surface. Ballard (1928, p. 17) described auriferous pyrite at deeper levels of mines in the Atlanta lode, where the grade of ore was lower and where silver sulfide minerals also were produced, as were minor quantities of lead-zinc minerals. Native gold in the oxidized zone probably resulted from oxidation of the auriferous pyrite and other gold-bearing sulfide minerals. Although more valuable, gold has been exceeded by silver in total weight of metal produced. Anderson (1939, p. 23) noted that in early bonanza deposits in the Atlanta district, the ratio of silver to gold by weight was as much as 200 to 1. Granitic host rock of the gold-silver deposits is hydrothermally altered, with extensive sericite developed from feldspar minerals. Even away from the deposits, the country rock shows the effects of strong hydrothermal alteration. The quartz veins commonly extend along the walls of Tertiary dikes. Fragments of dike rock are found in some quartz veins; some mineralized quartz veins cut across the dikes, but in other places dikes cut across the veins. Parallel quartz veins have been found along both walls of an intervening dike, much like two pieces of bread on either side of a slice of salami in a sandwich. The spatial relationship of the veins and dikes indicates that both were deposited more or less contemporaneously. Comparable dikes intrude the Sawtooth batholith and therefore are younger, which indicates that veins associated with such dikes also are younger than the batholithic rocks.

Gold-silver deposits along the Montezuma fault are structurally controlled by the fault (fig. M2). The extent, linearity, and amount of displacement along the fault indicate that it is a deep fault that originated before the mineral deposits. Downward displacement of the western, hanging-wall, block of the fault created fractures in the block that made it more permeable, both to intruding dikes and mineralizing solutions. Field evidence, however, suggests recurrent movement along the fault after mineral deposition. Anderson (1939, p. 17) observed that the Montezuma fault cut and displaced the Atlanta lode. Gravel of possible Pleistocene age caps the ridge northwest of Atlanta in the downdropped block of the Montezuma fault. Rock types in the gravel are the same as those that crop out east of the fault, in the uplifted horst, but similar gravel was not found in that area, which suggests that rapid erosion has stripped the gravel from the uplifted terrane and that movement along the fault is Pleistocene or younger. Erosion also may account for the scarcity of vein outcrops in the uplifted block east of the Montezuma fault.

Recurrent movement along preexisting faults in central Idaho may be more commonplace than has been previously assumed. An excellent example of such movement is that associated with the earthquake of Oct. 28, 1983, which occurred on a fault along the western front of the Lost River Range just southeast of the Challis quadrangle. That fault appears to be of the same pattern as the Montezuma fault. It strikes northwest, dips southwest, and is marked by an ancestral crushed and sheared zone. During the October 1983 earthquake, terrane along the western side of the fault dropped as much as 3.5 m. Multiple fractures formed in the downdropped block, extending at various angles away from the main fault. Fractures in the downdropped block of the Montezuma fault, some of which subsequently were mineralized, may have formed from similar recurrent fault movement.

TEN MILE WEST ROADLESS AREA

Geology

The Ten Mile West Roadless Area adjoins the western side of the Sawtooth Wilderness (fig. M1). The geology of the two areas is similar. Granitic rocks of the Idaho batholith underlie most of the roadless area. The batholithic rock is intruded by dioritic rocks and by pink granite, both of Tertiary age. All of the plutonic rocks are intruded by Tertiary dikes, and all rocks are displaced along northwest-trending faults (Kiilsgaard, 1983a). The largest exposure of dioritic rocks is along the ridge leading southeast from Jackson Peak (unit Tdc, fig. M3). The rocks are dark, are characterized by abundant hornblende, biotite, and magnetite, and range from quartz monzodiorite to granite in composition, although porphyritic granodiorite is the more common rock type. Biotite from two samples of the porphyritic granodiorite, from near Jackson Peak, gave potassium-argon ages that averaged 46.7 m.y.; hornblende from the two samples averaged 49.3 m.y. (R. J. Fleck, written commun., 1981). The granodiorite thus is Eocene in age.

Pink granite in the roadless area is identical to pink granite of the Sawtooth Wilderness. Parts of two samples of the rock from exposures northeast of Goat Mountain gave whole-rock rubidium-strontium ages of 43.6 m.y. (R. J. Fleck, written commun., 1983), which agree with previously mentioned dates for the Sawtooth batholith and which indicate that the pink granite is slightly younger than the dioritic rocks.

Innumerable dikes that range from diabase to rhyolite in composition intrude the plutonic rocks. Most of the dikes are porphyritic. Rhyolite and quartz latite are the more common dike types, and they tend to cluster near and show a close affinity to the Tertiary pink granite. Rhyolite dikes, like the pink granite, tend to be more radioactive than other dikes. By contrast, the more dacitic dikes tend to be near or in line with exposures of the dioritic intrusive rocks and probably represent offshoots from those intrusions.

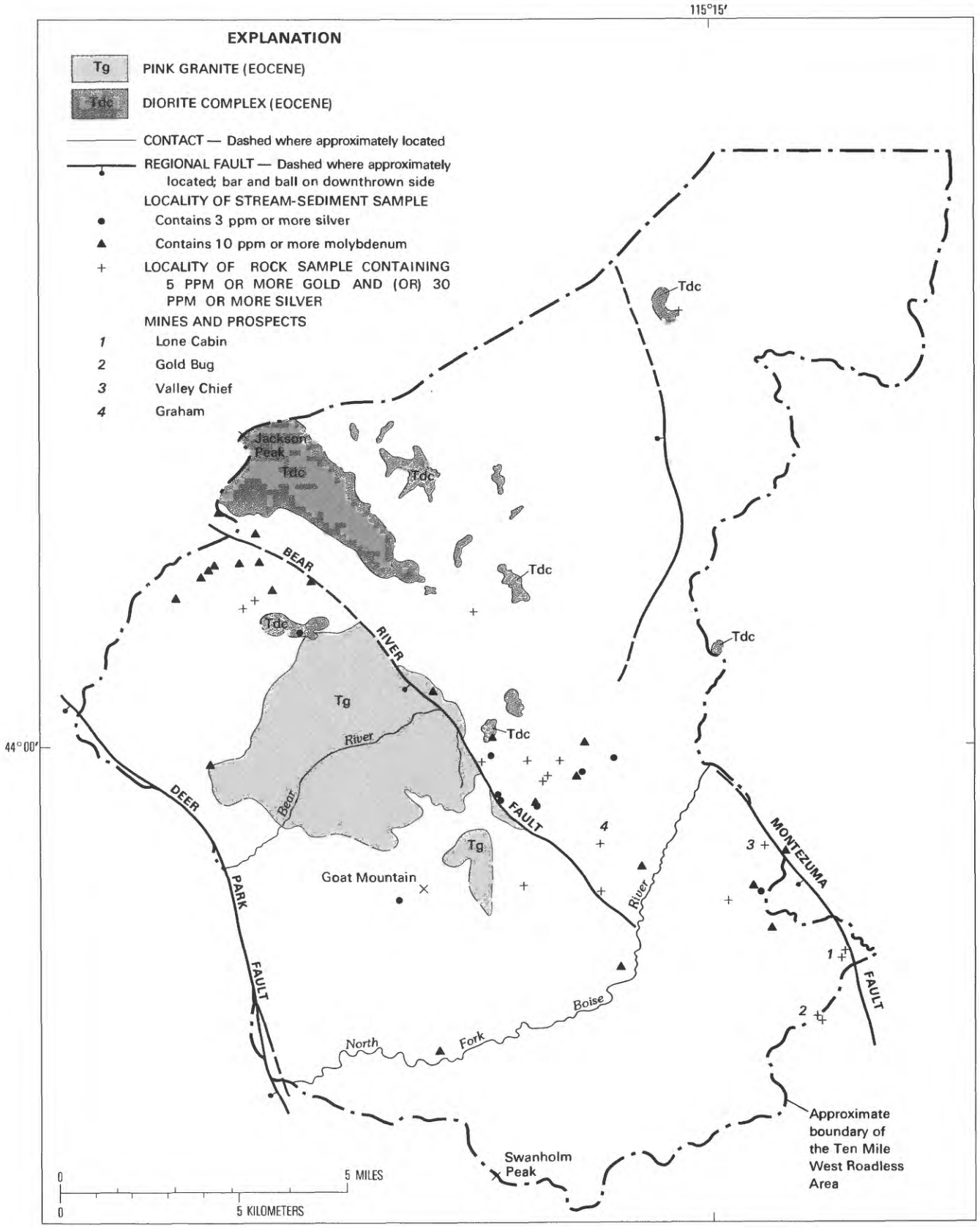

Figure M3. Simplified geologic map of the Ten Mile West Roadless Area, showing sample localities.

The Montezuma fault was traced from the Sawtooth Wilderness northwest to the North Fork Boise River (fig. M3). It may continue to the northwest or may be offset to the southwest by an inferred northeast-trending fault and then continue northwest as the Bear River fault (Kiilsgaard, 1983a). The southwest side of the roadless area is bounded by the Deer Park fault, the western side of which is downdropped like the Montezuma fault.

The age of initial movement along the northwest-trending faults is uncertain. The Bear River fault trends parallel to the largest exposure of dioritic rocks, which suggests that the fault or a parallel companion fault could have guided intrusion of those rocks. The pink granite also is exposed along the Bear River fault, but it is not clear if this location reflects intrusive guidance by the fault, as the fault has displaced pink granite northeast of Goat Mountain. Exposure of the pink granite could result from uplift between the Deer Park and Bear River faults and resulting accelerated erosion. Elsewhere in the area, the displacement of Quaternary gravel along faults indicates recent fault movement, as does the rapid downcutting of streams across fault scarps.

Geochemical analyses

A total of 584 rock and stream-sediment samples from the Ten Mile West Roadless Area were collected and analyzed. Stream-sediment samples that contained detectable silver (0.5 ppm), as determined by semiquantitative spectrographic analysis, came from many localities (Kiilsgaard, 1982), but stream-sediment samples that contained 3 ppm or more silver were largely from sites near the pink Tertiary granite and along the Bear River and Montezuma faults. Many stream-sediment samples also contained concentrations of molybdenum, and some samples that contained 10 ppm or more molybdenum were from streams that drain areas that also yielded higher values in silver. Sediments of some streams draining the northwestern part of the roadless area are enriched only in molybdenum (Kiilsgaard, 1983b).

Mineral deposits related to faults

Mineral deposits in the roadless area are concentrated in hydrothermally altered rocks along the western side of the Montezuma fault and on both sides of the Bear River fault (Kiilsgaard and others, 1983). The Lone Cabin prospect, just west of the Montezuma fault (fig. M3), consists of four adits, all caved, and several pits and trenches that explore a vein over a strike length of more than 305 m. Of eight samples taken at the property in 1966, the richest one, a selected sample from a dump, contained 3.5 oz (ounce) gold per ton (Kiilsgaard and others, 1970, p. D75). Twelve samples taken at the prospect in 1981 contained none to 0.80 oz gold and none to 0.90 oz silver per ton (Kiilsgaard and others, 1983, p. 8).

The Gold Bug prospect (fig. M3) also is west of the Montezuma fault. The prospect has been explored by an adit and several pits and trenches. Of 18 samples taken of iron-stained and altered granitic rock at the prospect, the richest sample contained 3.20 oz gold per ton (Kiilsgaard and others, 1983, p. 5).

The Valley Chief prospect (fig. M3) is another mineralized locality near the Montezuma fault. Two adits at the prospect, both caved at the portal, explore a vein whose outcrop may be traced for about 550 m. The richest of ten samples of vein outcrop and dump material contained 14.6 oz silver per ton (Kiilsgaard and others, 1983, p. 8).

The Graham mine (fig. M3) is on the east side of the Bear River fault. It consists of several adits that explore quartz veins and dikes, samples from which yielded low values in silver and gold. Northwest-striking quartz veins that cross the ridge between Big and Little Silver Creeks north of the Graham mine also are on the Graham property, and samples from these veins and from adjoining hydrothermally altered granitic rock contained as much as 43 ppm gold and ranged from 15 to 120 ppm silver (Kiilsgaard, 1983b, fig. 4). Some stream-sediment samples from tributaries both downstream and upstream from the quartz veins were enriched in silver and molybdenum.

Mineral resource potential

A northwest-trending belt that has a potential for resources of one or more of the metals gold, silver, molybdenum, lead, and zinc crosses the Ten Mile West Roadless Area. The belt is about 4.8 km wide and is structurally controlled by the Montezuma and Bear River faults (Kiilsgaard and others, 1983). In addition to the faults, the concept of a mineralized belt is supported by widespread hydrothermally altered granitic rocks, mineralized lode deposits, the pattern of stream-sediment samples that contained anomalously high metal content, some of which may indicate undiscovered mineral deposits, and by identified placer-gold deposits. The clustering of dikes and the location of intrusive plutonic rocks of Tertiary age at and near the mineralized localities also are distinguishing marks of the belt. Altered granitic rocks of the Idaho batholith along the Bear River fault may be underlain at shallow depth by Tertiary intrusive rocks, an observation supported by alteration features and by geophysical studies (Mabey, in press).

At the Graham mine (fig. M3), a mineralized quartz vein cuts across a rhyolite dike, which indicates that the vein is younger than the dike. If the dike is related to a nearby exposure of pink granite of Tertiary age, as is likely, both the dike and the vein can reasonably be assumed to be genetically related to the Tertiary plutonic activity.

MINERAL-DEPOSIT RELATIONSHIP TO THE MONTEZUMA AND BEAR RIVER FAULTS, SAWTOOTH WILDERNESS AND TEN MILE WEST ROADLESS AREA

The spatial relationship of mineral deposits to the Montezuma and Bear River faults along the western side of the Sawtooth Wilderness and across the Ten Mile West Roadless Area is shown in figure M4. Most of the deposits are in downthrown blocks of the faults, in or near fractures created by movement along the faults. Hydrothermal alteration of rocks in and near the mineralized localities is pervasive, part of a regional alteration feature that resulted from Tertiary plutonic activity (Criss and Taylor, 1983). Mineral assemblages and characteristics of the gold-silver veins indicate that they are epithermal and may not extend to great depths. The crosscutting relationship of veins and some of the dikes suggests that mineralization occurred during waning stages of Tertiary plutonic activity. The belt along the western side of the Montezuma fault and along both sides of the Bear River fault has a potential for mineral resources.

BOISE BASIN AREA

The northern part of the Boise Basin area extends into the Challis quadrangle (fig. M1). Placer gold was discovered in Boise Basin in 1862, and lode deposits were discovered soon thereafter. One of the lode deposits, the Gold Hill mine, was located in 1863 and was worked almost continuously from its discovery until 1938 (Anderson, 1947, p. 176). The total amount of gold produced from the basin is disputed because of incomplete early-day records, the difficulty of separating gold production of Boise Basin from production of other localities in Boise County, and because some of the gold that was mined was not reported. From recorded production statistics, a total of about 2,891,000 ounces of gold was produced from Boise Basin, of which about 74 percent came from placer deposits. The accumulated output makes Boise Basin the largest gold-producing district in Idaho and one of the larger gold-producing districts in the United States.

Geology

Boise Basin is underlain by granitic rocks of the Idaho batholith that have been intruded by Tertiary stocks and dikes. More or less parallel northeast-trending faults, members of the trans-Challis fault system, cross Boise Basin and appear to have guided emplacement of the dikes and possibly the stocks as well. Gold-bearing quartz veins crop out in the district, the more productive of which trend more or less parallel to Tertiary dikes. Some of the quartz veins extend along dike walls, some are within dikes, but some veins are cut by dikes. Erosion of the veins has produced the placer deposits of the basin.

A northeast-trending belt of dikes and stocks intrudes the Idaho batholith in the northern part of the Boise Basin (fig. M5). Lindgren (1898) and Ballard (1924) first described the rocks, but Ross (1934, p. 250) first classed the intrusives as Tertiary (Miocene). Anderson (1947) mapped the area, identified different types of dikes, and separated the dikes from the stocks. He identified diorite, granodiorite, and quartz-hornblende-biotite monzonite porphyry as common rock types of the stocks and noted that the largest of the stocks was more than 1 mile wide and more than 10 miles long. Rocks of the large stock are similar to those of the dioritic complex mapped in the Ten Mile Roadless Area and are characterized by phenocrysts of zoned andesine, hornblende, fresh biotite, and magnetite in a pinkish-gray matrix that consists chiefly of potassium feldspar. Biotite from a somewhat similar rock exposed in a stock that is crossed by the South Fork Payette River (fig. M5) gave a potassium-argon age of 48 m.y. (Percious and others, 1967), but a recalculated age, using the decay constants of Steiger and Jaeger (1977) showed the rock to be 49.2 ± 1.4 m.y. old. Dacite porphyry and rhyolite porphyry are the more common types of dike rock; rhyolite porphyry is particularly common along the western side of the northeast-striking dike swarm. Many of the dacitic dikes are similar in composition to the Tertiary stocks and appear to be offshoots of those larger masses.

The dikes and stocks are aligned along the trans-Challis fault system, which extends northeast across the Boise Basin. The westernmost fault of the system projects into the vicinity of Quartzburg, where Ballard (1924, p. 53) described a broad zone of shearing 0.5 mile or more wide, which is believed to be part of the system. Large, more-or-less parallel, northeast-trending faults occur near Pioneerville, Centerville, and Idaho City (fig. M5), and some of them are mentioned by Lindgren (1898, p. 667) and Anderson (1947, p. 168). All of the faults are southwestern extensions of the broad trans-Challis fault system described by Kiilsgaard and Lewis (chap. B, this volume).

Mineral Deposits

Veins at 78 mines and prospects in the Boise Basin are shown in figure M5. Anderson (1947, p. 180–191) divided these veins into two groups, early Tertiary gold-quartz deposits, most of which occupy fissure and fracture zones trending west-northwest, and Miocene gold deposits confined to the belt of porphyry dikes. Ballard (1924, p. 40–42) described the relation of quartz veins to dikes and regional shearing and noted that the more productive lode deposits form at the intersections of shear zones and rhyolite dikes. In mines that Ballard examined,

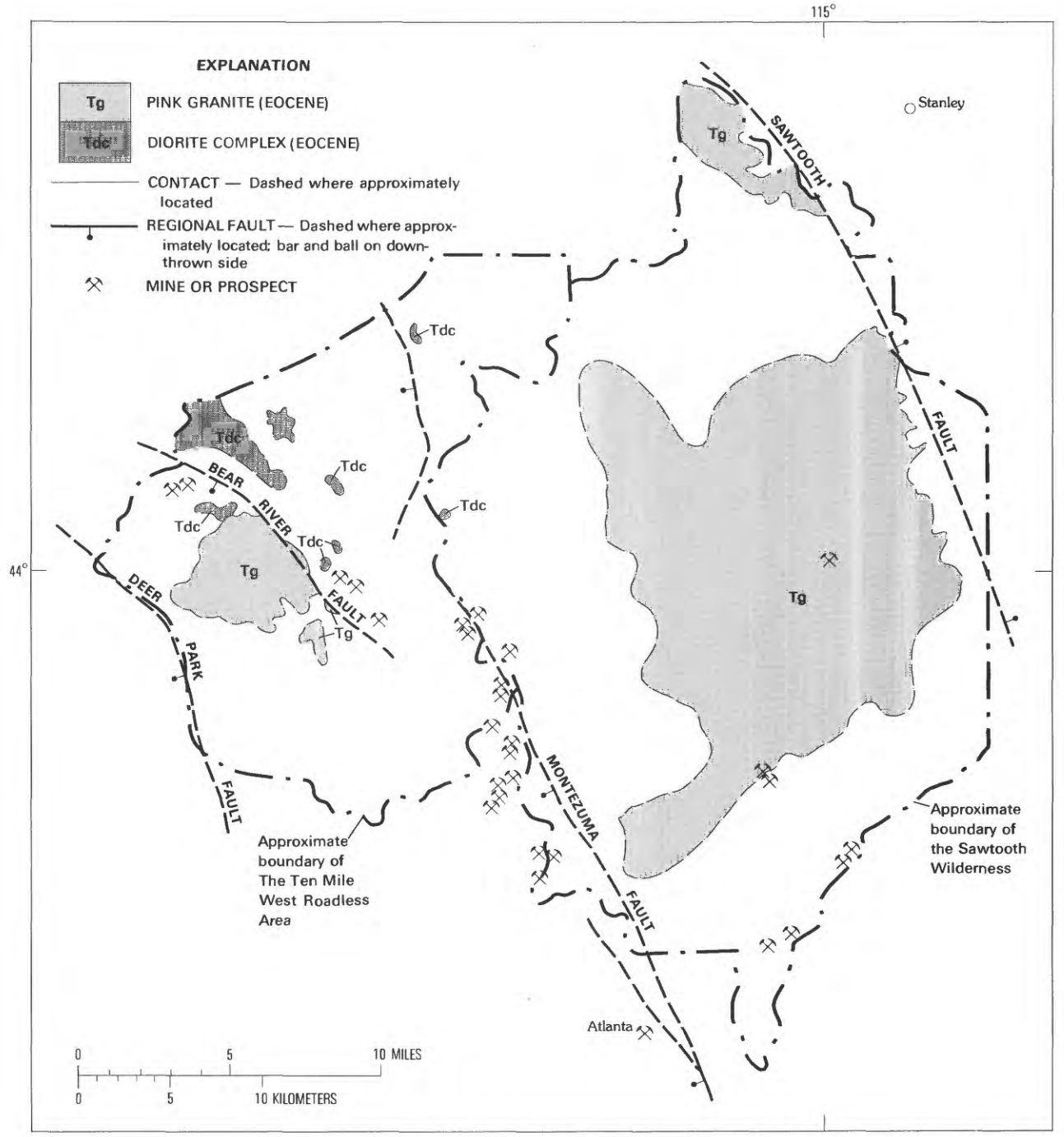

Figure M4. Map of the Sawtooth Wilderness and Ten Mile West Roadless Area, showing location of mines and prospects with respect to the Montezuma and Bear River faults.

the shear zones were well defined within hydrothermally altered granitic rock, but at the more brittle, acidic dikes, the shearing tended to become countless seams and fractures, all of which made the dike rock more permeable to subsequent mineralizing solutions (Ballard, 1924, p. 42). Ore bodies mined in the rhyolitic dikes tended to pinch out in the enclosing granitic rock. Some ore bodies in rhyolitic dikes were found to be cut by still younger rhyolite dikes, which indicates a close relationship between the age of mineralization and the age of dike intrusion.

Gold was the principal metal mined from the Boise Basin lode deposits, but minor amounts of other metals also were produced. Deposits of lead-bismuth sulfides were found along the Quartzburg mineral zone as far northeast as Mineral Hill, according to Ballard (1924, p. 47), as was argentiferous galena, and lesser amounts of

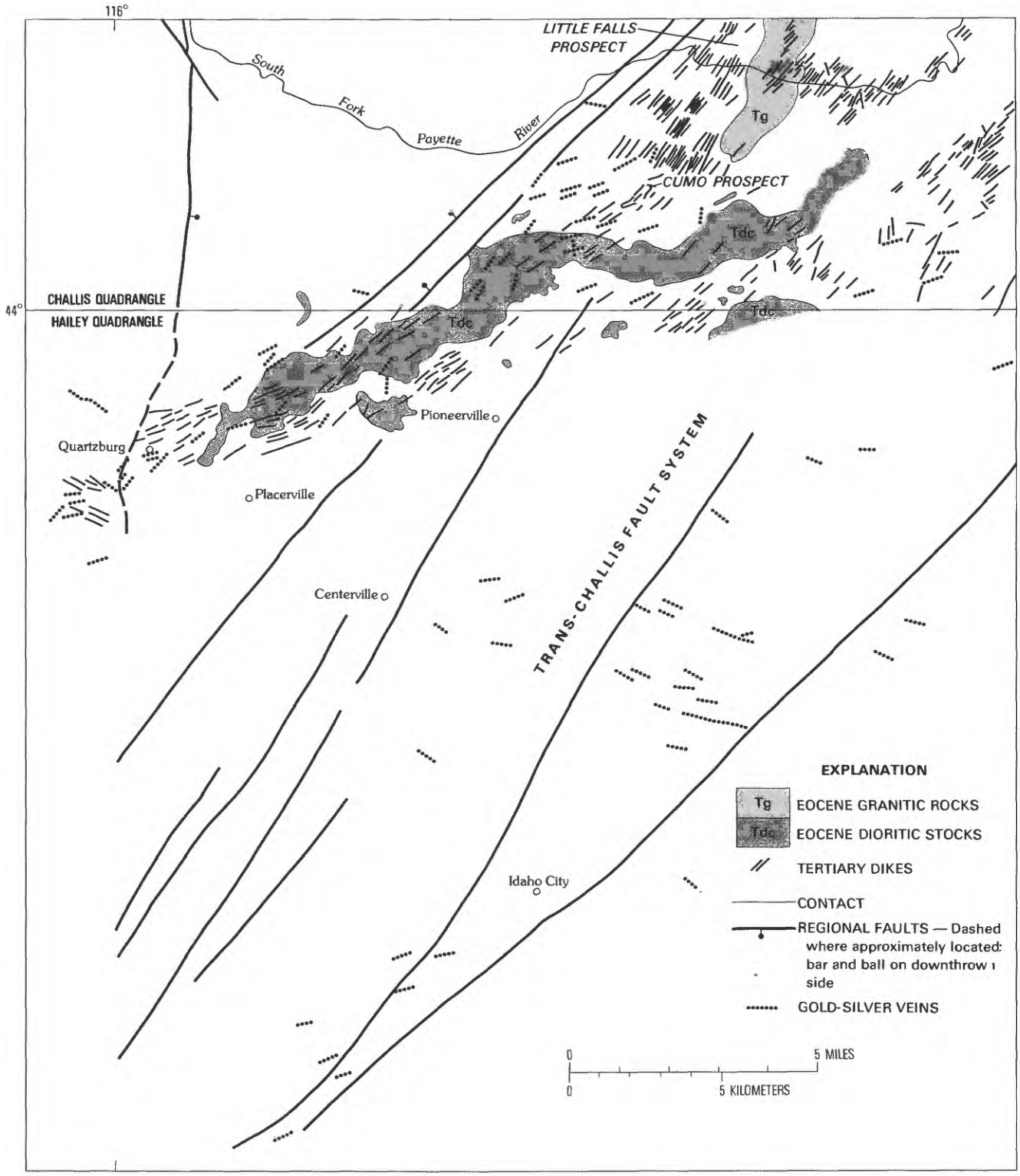

Figure M5. Map of Boise Basin showing location and strike of gold-silver veins with respect to regional faults of the trans-Challis fault system, stocks of dioritic rocks, granitic rocks, and Tertiary dikes. Modified from Anderson (1947).

sphalerite, chalcopyrite, and tetrahedrite. Anderson (1947, p. 191) noted that at several deposits silver was the most valuable metal.

The Cumo deposit was explored for molybdenum in the late 1970's and early 1980's by AMAX Corp. At that property, veinlets and disseminations of molybdenite occur in rhyolitic dikes, although at least one rhyolite dike cuts across the mineralized body. The Little Falls prospect

(fig. M5) on the South Fork Payette River is another molybdenum deposit at which stockwork veinlets of molybdenite cut across rhyolite dikes. Zircon from a rhyolite dike at the Little Falls deposit gave a fission-track age of 29.3±1.7 m.y (F. S. Fisher, oral commun., 1983).

Accumulated field evidence indicates that vein deposits of the Boise Basin are in fractures related to regional northeast-trending faults. The mineralized deposits are in dikes but in some places are cut by dikes, thereby indicating a close genetic relationship. If the zircon dating at the Little Falls deposit may be taken as a measure, the deposits are younger than 29 m.y., or no older than Miocene, an age proposed by Ballard (1924, p. 41).

GOLD-SILVER DEPOSITS ALONG OR NEAR THE TRANS-CHALLIS FAULT SYSTEM

The broad zone of northeast-trending regional faults described by Kiilsgaard and Lewis (chap. B, this volume) as the trans-Challis fault system, a name proposed by Earl Bennett, exerts a control on the location of many gold-silver deposits within or near the Challis quadrangle (fig. M6). The previously described Boise Basin deposits are within the fault system. The Banner mine (fig. M6, no. 28), east of the Boise Basin district and within the trans-Challis fault system, produced silver ore valued at about $3,000,000. Anderson and Rasor (1934, p. 372) described the northeast-striking Banner veins as accompanied by porphyry dikes. They noted that one of the veins passes through a rhyolite dike, but a lamprophyre dike is in a fissure with the Banner vein and is altered but not mineralized. The unmineralized character of the lamprophyre dike indicates that it was intruded shortly after vein formation, soon enough to be altered by thermal solutions passing through the mineralized zones. Granodiorite host rock near the Banner veins is intensely altered and thoroughly sericitized.

The Miller Mountain gold mine (fig. M6, no. 23) in sec. 17, T. 9 N., R. 8 E., about 8 km northeast of Lowman, was the only lode mine producing gold in the southwestern quarter of the Challis quadrangle in 1978–80. A limited tonnage of ore was being mined by A. W. Josue, Lowman, Idaho, and was processed through a small stamp mill. The mineralized material was highly altered granodiorite of the Idaho batholith in which pyrite was the only sulfide mineral seen. The mineralized zone extends along the hanging wall of an andesite dike that strikes N. 80° E., and fault gouge on the dike hanging wall suggests that a fault older than the dike guided emplacement of the dike and the gold mineralization. A prospect 1.2 km west appears to be the strike extension of the Miller Mountain gold deposit.

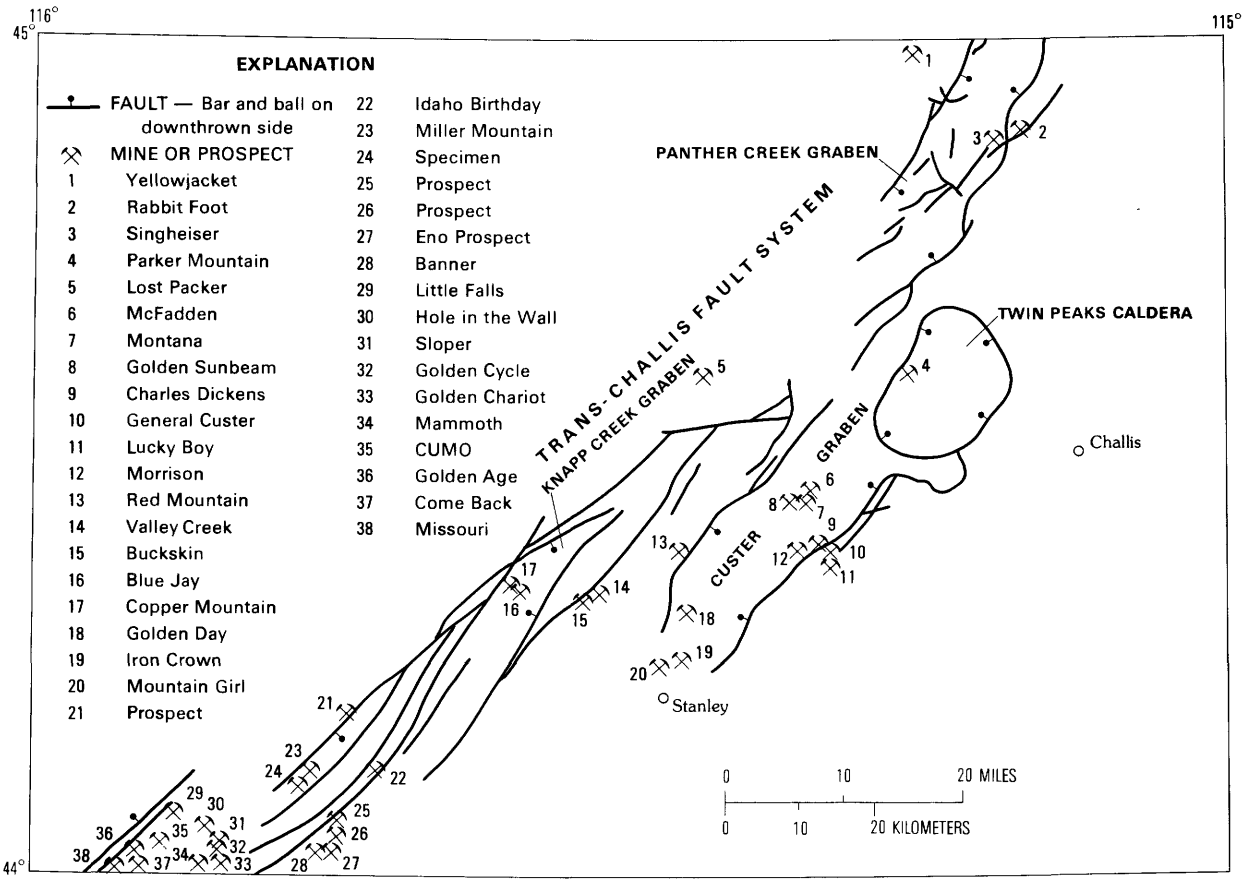

Figure M6. Map showing the location of mines and prospects with respect to the trans-Challis fault system, Challis quadrangle.

The Specimen gold mine (fig. M6, no. 24), about 2.4 km southwest of the Miller Mountain gold mine, is in highly altered granodiorite of the Idaho batholith. An abandoned mill at the mine site processed gold ore from the mine, but the amount of gold produced is not known, and the mine workings were inaccessible in 1979.

The Branson mine, formerly known as the Idaho Birthday mine (fig. M6, no. 22), is south of the mouth of Eightmile Creek, about 19 km east of Lowman. Gold production from the mine reportedly was stopped in 1942 by War Production Board Order L-208, and the mine has been nonproductive since that time. At least three more-or-less parallel quartz veins crop out at the mine. The veins have been explored by several short adits, the northern one about 366 m higher in elevation than the southern one. A gold-bearing vein at an altitude of 1,585 m is intersected by three andesite dikes and is offset by two parallel northeast-trending faults. Pyrite was the only sulfide mineral seen in the faulted vein, two samples from which contained 7 and 5 ppm gold, respectively. A vein intersected in the No. 8 adit, at altitude 1,451 m, strikes N. 53° E., dips 64° NW., and follows the hanging wall of a large northeast-trending fault. The Branson mine is between two major strands of the trans-Challis fault system, one of which extends along Eightmile Creek and the other along East Fork Eightmile Creek. Adjustment along these faults appears to have created fractures in the granodiorite that subsequently were mineralized.

The Lost Packer gold-copper deposit (fig. M6, no. 5) is near the trans-Challis fault system. Umpleby (1913, p. 42–45) described the northeast-striking Lost Packer vein as having been explored for about 2,000 ft (feet) along strike and 1,000 ft along dip. The vein follows a well-defined fault, and it cuts across what Umpleby classed as granite dikes but which currently are recognized as Tertiary dikes, similar in characteristics to those in Boise Basin and elsewhere along the trans-Challis fault system. The vein-dike-fault relationship at the Lost Packer mine is similar to other relationships along the trans-Challis fault system.

Several productive gold-silver mines are in the Custer graben, a structure considered to be part of the trans-Challis fault system. Some of these deposits are described by McIntyre and Johnson (chap. I, this volume) and others by Umpleby (1913, p. 80–90) and Anderson (1949, p. 21–27). Gold-silver deposits in the Twin Peaks caldera, northeast of the Custer graben, are described by Hardyman (chap. G, this volume).

The Singheiser, Rabbit Foot, and Yellowjacket gold deposits (fig. M6, nos. 3, 2, and 1) in the northeastern part of the Challis quadrangle are within or near the trans-Challis fault system. The Leesburg gold district, which is about 31 km northeast of the Challis quadrangle, is directly on strike with the Panther Creek graben (fig. M6), and the gold-bearing veins in the district, like those previously discussed, are within the probable northeastern continuation of the trans-Challis fault system.

Gold-silver deposits from Boise Basin to Leesburg occur within or near the trans-Challis fault system. Most of the deposits have similar characteristics. They are Tertiary in age and either follow or cut across Tertiary dikes or other intrusive bodies. The mineralized deposits occupy fissures that are related to regional faults. Gold and silver are the metals of principal value in the deposits. These features suggest that the gold-silver deposits are products of mineralizing activity that was regionally controlled by adjustment along the trans-Challis fault system.

REFERENCES CITED

Anderson, H. L., 1939, Geology and ore deposits of the Atlanta district, Elmore County, Idaho: Idaho Bureau of Mines and Geology Pamphlet 49, 71 p.

_____1947, Geology and ore deposits of Boise Basin, Idaho: U.S. Geological Survey Bulletin 944–C, 319 p.

_____1949, Silver-gold deposits of the Yankee Fork district, Custer County, Idaho: Idaho Bureau of Mines and Geology Pamphlet 83, 37 p.

_____1951, Metallogenic epochs in Idaho: Economic Geology, v. 46, no. 6, p. 592–607.

Anderson, A. L., and Rasor, A. C., 1934, Silver mineralization in the Banner district, Boise County, Idaho: Economic Geology, v. 29, no. 4, p. 371–387.

Armstrong, R. L., 1975, The geochronometry of Idaho: Isochron/West, no. 14, 51 p.

Ballard, S. M., 1924, Geology and gold resources of the Boise Basin, Boise County, Idaho: Idaho Bureau of Mines and Geology Bulletin 9, 103 p.

_____1928, Geology and ore deposits of the Rocky Bar quadrangle: Idaho Bureau of Mines and Geology Pamphlet 26, 41 p.

Bennett, E. H., 1980, Granitic rocks of Tertiary age in the Idaho batholith and their relation to mineralization: Economic Geology, v. 75, no. 2, p. 278–288.

Criss, R. E., and Taylor, H. P., Jr., 1983, An $^{18}O/^{16}O$ and D/H study of Tertiary hydrothermal systems in the southern half of the Idaho batholith: Geological Society of America Bulletin, v. 94, no. 5, p. 640–663.

Fisher, F. S., McIntyre, D. H., and Johnson, K. M., 1983, Geologic map of the Challis 1°×2° quadrangle, Idaho: U.S. Geological Survey Open-File Report 83–523, 41 p., 2 maps, scale 1:250,000.

Kiilsgaard, T. H., 1982, Analytical determinations from samples taken in the Ten Mile West Roadless Area, Boise and Elmore Counties, Idaho: U.S. Geological Survey Open-File Report 82–1099, 34 p.

_____1983a, Geologic map of the Ten Mile West Roadless Area, Boise and Elmore Counties, Idaho: U.S. Geological Survey Miscellaneous Field Studies Map MF-1500–A, scale 1:62,500.

_____1983b, Geochemical map of the Ten Mile West Roadless Area, Boise and Elmore Counties, Idaho: U.S. Geological Survey Miscellaneous Field Studies Map MF-1500–B, scale 1:62,500.

Kiilsgaard, T. H., Benham, J. R., and Avery, D. W., 1983, Mineral resource potential map of the Ten Mile West Roadless Area, Boise and Elmore Counties, Idaho: U.S. Geological Survey Miscellaneous Field Studies Map MF-1500-C, scale 1:62,500.

Kiilsgaard, T. H., Freeman, V. L., and Coffman, J. S., 1970, Mineral resources of the Sawtooth Primitive Area, Idaho: U.S. Geological Survey Bulletin 1319-D, 174 p.

Lindgren, Waldemar, 1898, The mining districts of the Idaho basin and the Boise Ridge, Idaho: U.S. Geological Survey Eighteenth Annual Report, pt. 3, p. 617-719.

Mabey, D. R., in press, Gravity and magnetic anomalies in the Ten Mile West Roadless Area, Boise and Elmore Counties, Idaho: U.S. Geological Survey Miscellaneous Field Studies Map MF-1500-D.

Percious, J. K., Damon, P. E., and Olson, H. J., 1967, Radiometric dating of Idaho batholith porphyries: U.S. Atomic Energy Commission Annual Progress Report No. C00-689-76, Appendix A-X.

Reid, R. R., 1963, Reconnaissance geology of the Sawtooth Range: Idaho Bureau of Mines and Geology Pamphlet 129, 37 p.

Ross, C. P., 1934, Some lode deposits in the northwestern part of the Boise Basin, Idaho: U.S. Geological Survey Bulletin 846-D, p. 239-277.

Steiger, R. H., and Jaeger, E., compilers, 1977, Subcommission on geochronology—Convention on the use of decay constants in geo- and cosmochronology: Earth and Planetary Science Letters, v. 36, no. 3, p. 359-362.

Umpleby, J. B., 1913, Some ore deposits in northwestern Custer County, Idaho: U.S. Geological Survey Bulletin 539, 104 p.

Symposium on the Geology and Mineral Deposits of the Challis 1°×2° Quadrangle, Idaho

Chapter N

Rhyolite Intrusions and Associated Mineral Deposits in the Challis Volcanic Field, Challis Quadrangle

By R. F. HARDYMAN *and* FREDERICK S. FISHER

CONTENTS

FIGURES

TABLE

Abstract

Intrusion and local extrusion of rhyolite magma within the Van Horn Peak cauldron complex and associated Custer and Panther Creek grabens spanned the entire time (about 48 to 45 m.y. (million years)) of pyroclastic volcanism within the Challis volcanic field. The intrusive rhyolite bodies are similar in chemical composition to many of the Tertiary granite bodies in the Challis quadrangle and to the youngest ash-flow tuffs of the volcanic field, which they intrude. The rhyolites were emplaced at high crustal levels within the volcanic pile and occur primarily as a belt of intrusive bodies that coincide with the regionally extensive, northeast-trending trans-Challis fault system. This system includes a series of subparallel high-angle faults that extends northeast from the Idaho batholith terrane in the southwestern part of the Challis quadrangle to the Van Horn Peak cauldron complex in the northeast. The Custer and Panther Creek grabens, extending southwest and northeast, respectively, from the cauldron complex, are also part of the trans-Challis fault system. Dikes, small pods and pipelike bodies of rhyolite, and multiple intrusive rhyolitic complexes are scattered through the grabens, and this belt of rhyolites extends across the cauldron complex between these two structures.

Locally, rhyolites within the Custer and Panther Creek grabens and the rhyolite belt of the cauldron complex are hydrothermally altered and mineralized. Alteration of these rocks ranges from weakly argillic through moderately strongly quartz sericitic, to strongly silicic. Disseminated pyrite locally is common in unfaulted altered rhyolite, and fine-grained granular pyrite locally is concentrated along structures in some faulted rhyolite bodies. Fluorite, calcite, and quartz are common in vugs and veins in brecciated rhyolite and in altered country rock.

Epithermal precious-metal mineral occurrences are spatially associated with several rhyolite bodies within the rhyolite belt. The known precious-metal occurrences include deposits at the Rabbit Foot and Singheiser mines in the Panther Creek graben and deposits and prospects in the Custer graben, including those at Estes Mountain, the Sunbeam mine, and Red Mountain. No precious-metal deposits or prospects were known within or associated with rhyolites of the rhyolite belt within the Van Horn Peak cauldron complex between the Panther Creek and Custer grabens. Reconnaissance geologic mapping and geochemical sampling of rhyolites in this intracauldron region, however, indicate that some of these rhyolites may have potential for spatially related epithermal mineral deposits.

INTRODUCTION

Intrusive rhyolitic rocks are locally abundant within the Challis quadrangle. They are particularly numerous within the volcanotectonic structures of the eastern part of the quadrangle where the thickest accumulations of pyroclastic rocks of the Challis volcanic field occur. Rhyolites are present within the Custer graben (fig. N1) (McIntyre and Johnson, chap. I, this volume) and within the Panther Creek graben in the northeastern part of the quadrangle. Precious-metal deposits spatially associated with some of the rhyolites within these two areas have been exploited in the past, and mineral exploration in these areas continues to the present. Geologic mapping in the Van Horn Peak cauldron complex and the Twin Peaks caldera has delineated a belt of previously unrecognized intrusive rhyolite bodies that lies between the Custer and Panther Creek grabens. This chapter summarizes the preliminary results of studies of chemical composition, petrography, and field characteristics of these rhyolitic rocks, along with preliminary studies of local hydrothermal alteration and mineralization. Field relationships and alteration and mineralization of rhyolites in the Twin Peaks caldera are further discussed by Hardyman (chap. G, this volume).

STRUCTURAL SETTING

Rhyolitic rocks that postdate cauldron-related pyroclastic rocks of the Challis volcanic field crop out in a northeast-trending belt that extends from the Stanley Basin area to the south, northeastward to near the northeastern corner of the Challis quadrangle (fig. N1). This so-called rhyolite belt conforms to a regional northeast-trending series of faults named the trans-Challis fault system (Kiilsgaard and Lewis, chap. B, this volume). Dike rocks of similar rhyolitic compositions intrude Idaho batholith rocks along this fault zone southwest from the Stanley Basin and, southwest of the Challis quadrangle, trend into the Boise Basin dike swarm that extends northeast from the western Snake River Plain.

Rhyolites northeast of Stanley Basin occur as narrow dikes and small plugs and domes (less than 2.5 sq km (square kilometers)) scattered throughout the northeast-trending Custer graben, across the Van Horn Peak cauldron complex, and into the Panther Creek graben. One large rhyolitic complex is exposed over an area of approximately 129 sq km in the upper East Fork Mayfield Creek region (fig. N1). This areally extensive unit, the rhyolitic complex of East Fork Mayfield Creek, is at the triple juncture of the Custer graben, the Van Horn Peak cauldron complex boundary, and the Twin Peaks caldera ring fracture, and it almost completely engulfs the area interpreted to be the earliest collapse segment of the Twin Peaks caldera.

AGES

Intrusion and local extrusion of rhyolite magma occurred during the entire time (about 48–45 m.y.) of caldera-forming pyroclastic eruptions within the Challis volcanic field. Within the Custer graben-Van Horn Peak cauldron complex-Panther Creek graben area, rhyolite flows in the northeastern part of the Custer graben predate the tuff of Eightmile Creek (46.9±1.6 m.y., McIntyre and others, 1982) and mark an early episode of rhyolitic magmatism. These flows, the rhyolite flows of Mill Creek

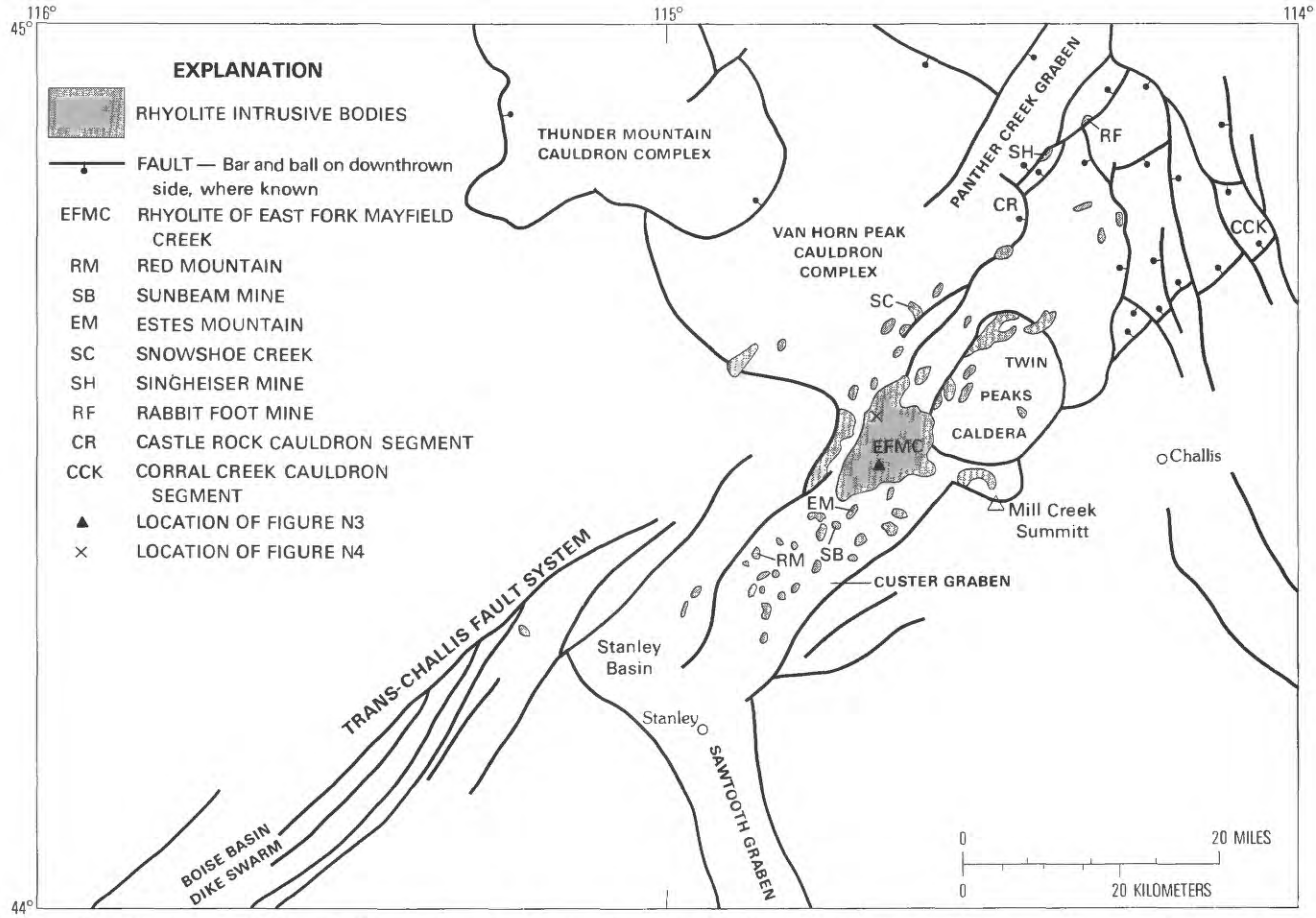

Figure N1. Index map of the Challis quadrangle showing the trans-Challis fault system, cauldron complexes, grabens, and outcrops of the principal intrusions of the rhyolite belt.

Summit (Hobbs and others, 1975), are dated at 48.5±1.2 m.y. (Marvin and Dobson, 1979, p. 17).

A rhyolite flow or possible sill that correlates with a younger generation of rhyolites within the Custer graben and is exposed on upper Tenmile Creek about 10 km west of Mill Creek Summit yielded a date of 46.5±1.7 m.y. (R. F. Marvin, written commun., 1984). In this same area a rhyolite dike cuts an intrusive rhyodacite body dated at 46.0±1.7 m.y. (R.F. Marvin, written commun., 1983). Rhyolites elsewhere in the Custer graben, such as at Mt. Greylock and the Sunbeam mine, are 45–47 m.y. (McIntyre and Johnson, chap. I, this volume). The youngest rhyolite intrusion associated with the rhyolite of Red Mountain in the southwestern part of the Custer graben is 39.1±2.0 m.y. (C. W. Naeser, written commun., 1982).

At least two discrete intrusive events can be demonstrated by field relations within the rhyolitic complex of East Fork Mayfield Creek. This rhyolitic complex is composed of multiple rhyolite intrusions that in part must be younger than about 45 m.y., as rhyolite intrudes outflow tuff of the tuff of Challis Creek. Likewise, rhyolite dikes and plugs to the northeast in the Van Horn Peak cauldron complex intrude all of the intracauldron ash-flow-tuff units, including the youngest tuff, the tuff of Challis Creek. Intrusive rhyolite is abundant in the northern half of the Twin Peaks caldera (the youngest caldera of the Van Horn Peak cauldron complex), and here, too, these rocks postdate the tuff of Challis Creek and younger caldera-wall slump-debris deposits.

COMPOSITIONS

The intrusive rhyolites of this study are mostly porphyritic-aphanitic rocks containing generally less than 10 percent phenocrysts of sanidine and quartz. Sanidine phenocrysts are as large as 1 cm (centimeter) in places, but phenocrysts are typically less than 2 mm (millimeters) in size. Some rhyolites contain phenocrysts of sanidine only, some contain sanidine and minor plagioclase only, and a few dike rocks contain sanidine, quartz, and minor plagioclase and biotite. Augite is present in some places, especially in some vitrophyric rhyolites, but hornblende is conspicuously rare. Aphyric varieties of rhyolite, containing only traces of phenocrystic sanidine and (or) quartz, are locally common. Within some intrusions and along some intrusion contacts, aphyric rhyolite grades into phenocryst-bearing rhyolite.

Major-element-oxide analyses of selected samples of intrusive rhyolites, primarily from the northeastern end of the Custer graben and the East Fork Mayfield Creek are shown in table N1. Regardless of their phenocryst

Table N1. Analyses of intrusive rhyolites of

[Major-element analyses by X-ray spectroscopy by A. J. Bartel, K. Stewart, J. E. Taggart, J. W. Baker, J. S. Wahlberg; FeO, H_2O^+,

Analysis No.-	1	2	3	4	5	6	7	8	9	10
Field No.-----	RH-CH-845	RH-CH-848	RH-CH-851	RH-CH-867	RH-CH-881	RH-CH-886	RH-CH-891	RH-CH-894	RH-CH-901	RH-CH-927
Lab No.------	D-245296	D-245297	D-245298	D-245304	D-245310	D-245313	D-245314	D-245316	D-247772	D-247778
N. latitude--	44°32′	44°31′	44°31′	44°29′30"	44°35′	44°35′30"	44°30′	44°30′	44°29′	44°30′
W. longitude-	114°39′	114°39′50"	114°40′	114°31′30"	114°42′30"	14°40′	114°37′30"	114°37′	114°39′	114°42′30"
Major oxides (weight percent)										
SiO_2----------	78.80	76.90	76.20	78.90	75.20	72.60	73.90	79.20	77.90	80.50
Al_2O_3----------	10.20	12.40	12.70	10.70	12.50	14.00	13.20	10.10	11.10	10.30
Fe_2O_3----------	1.44	.91	1.41	.83	1.21	1.17	1.34	1.39	1.32	1.25
FeO----------	.04	.54	.09	.09	.11	.08	.12	.03	.12	.10
MgO----------	.00	.00	.00	.14	.22	.10	.00	.00	.00	.00
CaO----------	.17	.13	.16	.53	.25	.81	.40	.07	.13	.07
Na_2O----------	2.85	3.71	3.81	2.46	2.57	3.74	3.83	3.24	3.53	3.30
K_2O----------	4.43	4.74	4.72	4.29	5.16	5.05	5.29	4.00	4.56	4.17
H_2O^+----------	.48	.56	.41	.83	.95	.44	.49	.46	.22	.45
H_2O^-----------	.36	.10	.05	.10	.32	.15	.00	.08	.20	.10
TiO_2----------	.09	.09	.08	.08	.10	.23	.17	.07	.10	.10
P_2O_5----------	.00	.00	.00	.00	.00	.00	.00	.00	.00	.00
MnO----------	.00	.00	.00	.00	.00	.00	.00	.00	.00	.00
CO_2----------	.00	.00	.00	.00	.04	.00	.00	.00	.00	.00
Sum------	98.86	100.08	99.63	98.95	98.63	98.37	98.74	98.64	99.18	100.34
CIPW norms (weight percent; calculated using major oxide analyses normalized to 100 percent H_2O free)										
q----------	45.83	37.08	35.93	47.78	40.83	30.35	31.08	45.78	40.14	45.29
c----------	.42	.94	1.04	1.07	2.39	.93	.45	.32	.12	.23
or----------	26.72	28.17	28.13	25.86	31.32	30.56	31.83	24.10	27.28	24.69
ab----------	24.61	31.58	32.51	21.24	22.34	32.41	33.00	27.96	30.24	27.98
an----------	.86	.65	.80	2.68	1.01	4.12	2.02	.35	.65	.35
di-wo----------	.00	.00	.00	.00	.00	.00	.00	.00	.00	.00
di-en----------	.00	.00	.00	.00	.00	.00	.00	.00	.00	.00
di-fs----------	.00	.00	.00	.00	.00	.00	.00	.00	.00	.00
hy-en----------	.00	.00	.00	.36	.56	.26	.00	.00	.00	.00
hy-fs----------	.00	.09	.00	.00	.00	.00	.00	.00	.00	.00
ol-fo----------	.00	.00	.00	.00	.00	.00	.00	.00	.00	.00
ol-fa----------	.00	.00	.00	.00	.00	.00	.00	.00	.00	.00
mt----------	.00	1.33	.06	.06	.07	.00	.00	.00	.10	.03
hm----------	1.47	.00	1.38	.81	1.20	1.20	1.36	1.42	1.27	1.23
il----------	.09	.17	.15	.16	.20	.17	.26	.06	.19	.19
ap----------	.00	.00	.00	.00	.00	.00	.00	.00	.00	.00
cc----------	.00	.00	.00	.00	.09	.00	.00	.00	.00	.00
Phenocryst mineralogy.	s,q	s,q	s	Aphyric	s,p, b(altered) h(trace, altered).	s,q,p, b (trace).	s, py (trace).	s,q	s,q	s,q

SAMPLE

1. Autobrecciated porphyritic rhyolite, rhyolitic complex of East Fork Mayfield Creek; west of Sherman Peak.
2. Microvesicular porphyritic rhyolite, rhyolitic complex of East Fork Mayfield Creek; west of Sherman Peak; quartz-lined flattened gas cavities.
3. Porphyritic intrusive rhyolite, rhyolitic complex of East Fork Mayfield Creek; contains numerous diktytaxiticlike cavities; East Fork Mayfield Creek.
4. Aphyric rhyolite intrusion; junction of McKay Creek and Yankee Fork, northeastern part of Custer graben.
5. Porphyritic intrusive rhyolite, locally autobrecciated and spherulitic, some hairline quartz veinlets, clay-chlorite alteration; Ibex Creek.
6. Porphyritic intrusive rhyolite; south of Mid Cottonwood Point lookout.
7. Faintly flow-foliated, porphyritic intrusive rhyolite with minor miarolitic cavities; Twelvemile Creek, northeastern part of Custer graben.
8. Spherulitic, locally autobrecciated porphyritic intrusive rhyolite with opal-lined gas cavities; ridge east of Twelvemile Creek, northeastern part of Custer graben.
9. Crystal-poor, porphyritic rhyolite lava or possible sill with autobrecciated base; ridge between Tenmile and Eightmile Creeks; northeastern part of Custer graben This rhyolite dated at 46.5±1.7 Ma (see text).
10. Massive, locally flow-laminated or autobrecciated, porphyritic rhyolite, silicified, with tridymite and opal in matrix; rhyolitic complex of East Fork Mayfield Creek, uppermost East Fork Mayfield Creek.

of the Van Horn Peak cauldron complex area.

H_2O^-, CO_2 analyses by H. G. Nieman and G. Mason. s, sanidine; q, quartz; p, plagioclase; b, biotite; h, hornblende; py, pyroxene]

11	12	13	14	15	16	17	18	19	20
RH-CH-931	RH-CH-932	RH-CH-932A	RH-CH-933	RH-CH-955	RH-CH-958	RH-CH-960	RH-CH-2035	RH-CH-885	
D-247779	D-247780	D-247781	D-247782	D-247786	D-247788	D-247789	D-254774	D-245312	
44°28′30″	44°29′	44°29′	44°29′	44°38′	44°38′	44°38′	44°45′	44°34′	
114°41′30″	114°41′30″	114°41′30″	114°41′30″	114°49′	114°53′	114°53′	114°45′	114°42′30″	
Major oxides (weight percent)									
80.10	75.80	72.00	70.90	74.80	69.00	74.20	74.60	75.30	75.33
10.30	11.90	11.80	12.20	12.40	12.50	13.80	12.90	12.40	12.08
.19	1.81	.67	1.41	1.47	1.38	.57	.55	1.54	1.43
.12	.18	.90	.40	.03	.34	.13	.74	.49	.18
.00	.12	.10	.19	.00	.11	.10	.24	.00	.08
.12	.07	.39	.72	.29	.72	.59	.78	.13	.26
2.50	3.88	2.76	2.10	3.36	3.03	3.18	3.13	3.65	3.08
5.14	4.90	5.82	4.44	5.41	5.11	6.26	5.24	4.83	5.10
.68	.44	4.20	5.42	.47	4.40	.49	.29	.60	.51
.00	.03	.16	1.14	.04	1.99	.06	.03	.03	.47
.10	.13	.12	.12	.15	.20	.10	.14	.14	.13
.00	.00	.00	.00	.00	.00	.00	.06	.00	.00
.00	.00	.00	.03	.00	.03	.00	.00	.00	.01
.00	.00	.00	.00	.00	.00	.00	.00	.01	.00
99.25	99.26	98.92	99.07	98.42	98.81	99.48	98.70	99.12	98.66
CIPW norms (weight percent; calculated using major oxide analyses normalized to 100 percent H_2O free)									
46.29	34.57	34.14	43.10	34.70	32.58	30.66	34.74	35.88	38.11
.41	.09	.27	2.84	.50	.73	.73	.82	.97	1.04
30.81	29.31	36.37	28.36	32.69	32.67	37.39	31.47	28.98	30.85
21.46	33.23	24.70	19.21	29.07	27.74	27.20	26.92	31.36	26.68
.60	.35	2.05	3.86	1.47	3.86	2.96	3.53	.59	1.32
.00	.00	.00	.00	.00	.00	.00	.00	.00	.00
.00	.00	.00	.00	.00	.00	.00	.00	.00	.00
.00	.00	.00	.00	.00	.00	.00	.00	.00	.00
.00	.30	.26	.51	.00	.30	.25	.61	.00	.20
.00	.00	.95	.00	.00	.00	.00	.68	.00	.00
.00	.00	.00	.00	.00	.00	.00	.00	.00	.00
.00	.00	.00	.00	.00	.00	.00	.00	.00	.00
.10	.21	1.03	1.12	.00	.66	.13	.81	1.19	.24
.12	1.69	.00	.75	1.50	1.03	.49	.00	.74	1.30
.19	.25	.24	.25	.06	.41	.19	.27	.27	.25
.00	.00	.00	.00	.00	.00	.00	.14	.00	.00
.00	.00	.00	.00	.00	.00	.00	.00	.02	.00
s,q	s,q	Aphyric	s,q	s	s, p(trace), py(altered).	s,p b(oxidized).	Not available.	s,q	s,q

DESCRIPTIONS

11. Massive and locally flow-banded intrusive rhyolite, silicified; rhyolitic complex of East Fork Mayfield Creek; uppermost East Fork Mayfield Creek.
12. Younger porphyritic rhyolite dike, vertically flow laminated with stretched vesicles, vitrophyric at margins; rhyolitic complex of East Fork Mayfield Creek, uppermost East Fork Mayfield Creek.
13. Vitrophyre of 12 above.
14. Older, glassy to perlitic, porphyritic rhyolite intruded by 12 and 13 above.
15. Flow-laminated, porphyritic rhyolite grading to vitrophyric autobrecciated rhyolite; ridge east of Grouse Creek Peak.
16. Glassy and perlitic, flow-laminated porphyritic rhyolite; west of Grouse Creek Peak.
17. Devitrified porphyritic rhyolite, vitrophyric along intrusive contact; northeast of Pinyon Peak.
18. Pink granite (Casto pluton-type granite); near Falconberry Ranch on Loon Creek.
19. Quartz porphyry intrusion with quartz, sanidine, and altered ferromagnesian phenocrysts in a granophyric matrix; Ibex Creek.
20. Tuff of Challis Creek (unit Tcr, fig. N9); average of 9 analyses of intracaldera tuffs of Twin Peaks caldera.

mineralogy, these rocks are all high-potassium rhyolites (fig. N2, table N1). Likewise, using the felsic-mafic ratio ($SiO_2+K_2O+Na_2O/FeO+Fe_2O_3+MgO+CaO$) of Segerstrom and Young (1972), these rocks are alkali or extreme alkali rhyolites.

In addition to the seventeen rhyolite analyses, chemical analyses of a granite sample from the Casto pluton and of intracaldera tuff samples from the Twin Peaks caldera are shown in table N1. These rocks are also classified as high-potassium rhyolite (granite) or alkali rhyolite (granite). An average of 10 analyses of Tertiary granite of the Sawtooth Range (E. H. Bennett, Idaho Geological Survey, unpub. data and written commun., 1983), together with the analyses of table N1, are plotted on figure N2. The plotted intrusive rhyolite compositions show considerable scatter in this diagram, but, eliminating the analyses of vitrophyric or perlitic rhyolite samples and analyses of the obviously silicified and probably silicified samples (although not obvious in hand specimen or thin section), they cluster about the plotted compositions of the Tertiary granite samples and the pyroclastic-rock samples from the Twin Peaks caldera. These similarities in composition are probably to be expected because many of these intrusive rhyolites are undoubtedly high-level equivalents of the Tertiary granite. Some intrusions may also represent residual rhyolitic magma emplaced after the explosive eruptions that formed the Twin Peaks caldera.

FIELD CHARACTERISTICS

Rhyolite bodies within the northeast-trending rhyolite belt appear to be intrusive, for the most part. Rarely can unequivocal flow origins be demonstrated by field relations. These rocks typically form linear dikes several meters wide or irregular pods and pipelike intrusive bodies. In outcrop these rocks are commonly massive to flow laminated. Steep to vertical flow foliation is common, and where flow folds are observed, their axial planes are invariably near vertical. Columnar joints, where developed, are typically subhorizontal. Contacts with older volcanic rocks are discordant and steep. Linear northeast-trending dikes and strings of dikelike bodies can be shown locally to have been emplaced along pre-existing faults, and not uncommonly postemplacement faulting has displaced the rhyolites.

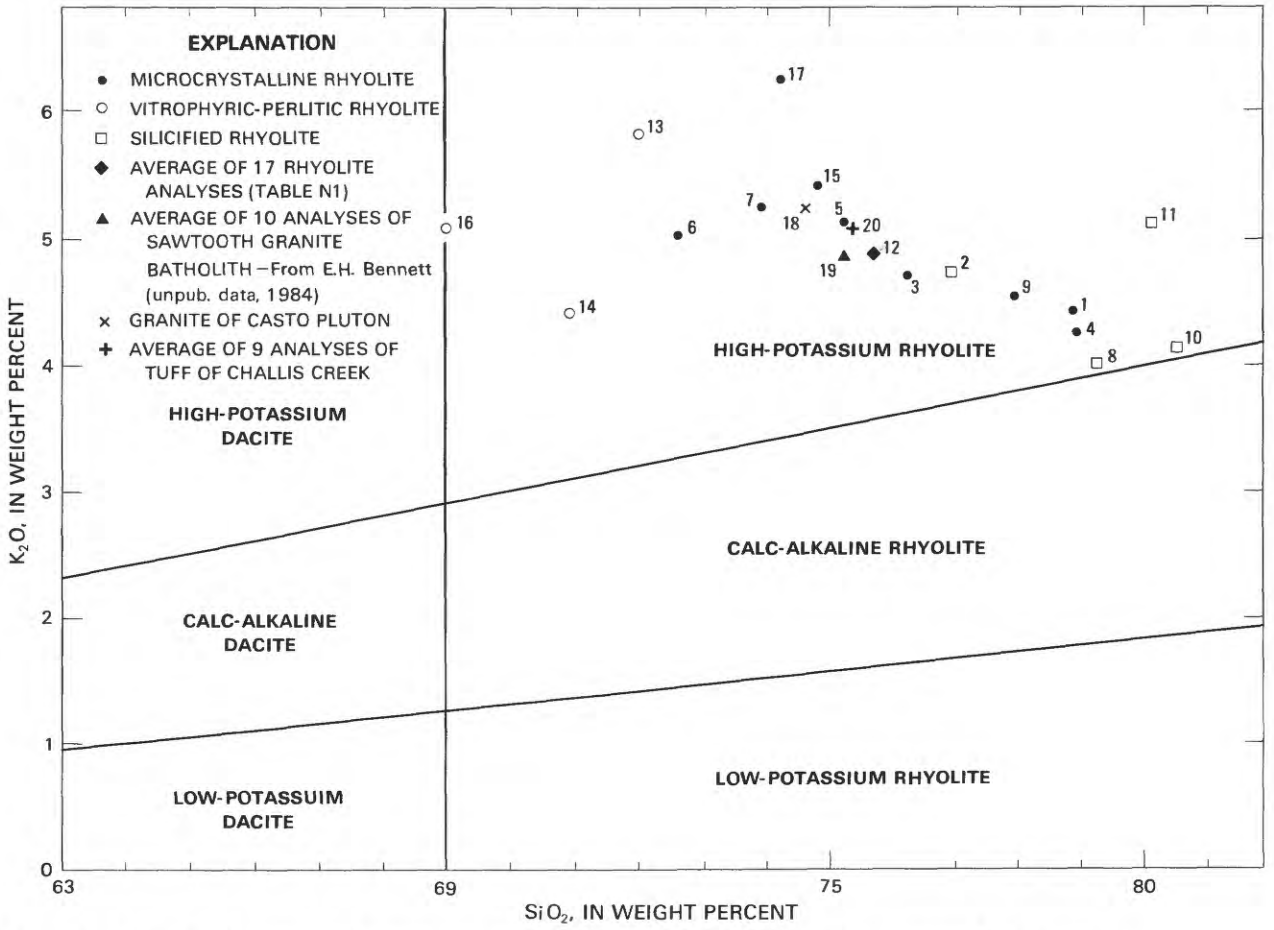

Figure N2. SiO_2-K_2O variation diagram showing classification of rhyolite samples analyzed for this study.

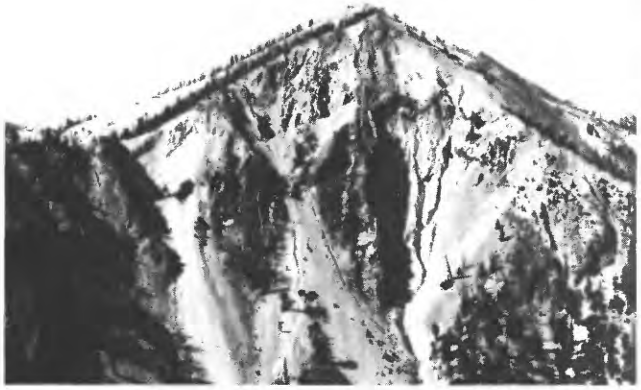

Figure N3. Younger porphyritic rhyolite intrusive bodies (dark outcrops) cutting older devitrified to perlitic rhyolite. Ridge between upper East Fork Mayfield Creek and Yankee Fork drainage. View to the west.

Figure N4. Glassy to perlitic rhyolite (dark outcrops, left foreground) in part intrusive into bedded coarse epiclastic sediments. Rhyolite of East Fork Mayfield Creek near Ibex Creek. View to the southeast.

In some areas, especially in the large rhyolitic complex of East Fork Mayfield Creek, the rhyolite consists of multiple intrusive bodies. At least two intrusive events can be identified in exposures within the rhyolitic complex of East Fork Mayfield Creek in the ridge separating the upper East Fork Mayfield Creek from the Yankee Fork drainage. In this locality (fig. N3), narrow dikes and irregular bodies of light-gray, reddish-brown-weathering porphyritic rhyolite intrude an earlier, buff-devitrified to gray-perlitic phase of intrusive rhyolite.

The younger rhyolite phase (analysis 12, table N1) is locally vitrophyric (analysis 13, table N1) at contacts with the older perlitic rhyolite (analysis 14, table N1). Away from its contacts, the younger phase shows vertical flow lamination and local autobrecciation and contains stretched gas cavities, some infilled with amorphous silica. The older rhyolite intrusive phase might be the eroded core of a bulbous dome that may have breached the surface.

Intrusive rhyolites in other localities within the rhyolitic complex of East Fork Mayfield Creek may have breached the ground surface, as suggested by local lenses of coarse epiclastic sediments, possibly representing dome-apron deposits, isolated within intrusive rhyolite and adjacent to bulbous rhyolite intrusions. One such example, exposed southeast of the junction of Ibex Creek and East Fork Mayfield Creek (locality of fig. N4 on fig. N1), consists of bedded, coarse-grained, tuffaceous sandstone grading up into coarse sedimentary breccia containing abundant porphyritic rhyolite pumice lapilli. Lenses of pyroclastic rhyolite, thin beds of cryptocrystalline silica, and thin rhyolite lava flows or sills are interbedded in this sedimentary section. These sedimentary rocks dip moderately to steeply away from a vitrophyric to perlitic, porphyritic rhyolite plug that in part intrudes the sedimentary rocks (fig. N4).

Other patches of coarse volcaniclastic sediments isolated within the rhyolitic complex of East Fork Mayfield Creek are not apparently related to the intrusive rhyolites but correlate with sedimentary rocks overlying the tuff of Challis Creek that infills the earliest collapse segment of the Twin Peaks caldera (Hardyman, chap. G, this volume).

FABRICS AND INTERNAL TEXTURES

Although they are generally massive or flow laminated, the intrusive rhyolites show a wide variety of fabrics in outcrop. Autobrecciated rhyolite is common, especially along intrusive contacts, but pods or pipelike bodies and irregular zones of breccia occur isolated within massive to flow-laminated rhyolite. Monolithologic autobreccia clasts range in size from less than 1 cm to 25 cm (fig. N5*A*). Some breccias contain as much as 40 percent rounded to subangular fragments (ranging in size from less than 3 mm to about 0.3 m) cemented by interstitial rhyolite or, locally, amorphous silica (fig. N5*B*).

Other intrusive rhyolite breccias, containing rounded aphyric or porphyritic rhyolite fragments in a phenocryst-bearing matrix, resemble pebble dikes (fig. N6).

Some pipelike breccia pods are perlitic to devitrified and are locally frothy and lithophysal and grade outward into rock that is like tuff breccia along their intrusive contacts. Some rhyolite breccias are pervasively silicified, and drusy cavities, some with infillings of later amorphous silica, are common, regardless of other textures or fabrics present. Miarolitic cavities, irregular diktytaxiticlike cavities, hairline quartz veinlets, and vein breccias are commonly present in massive to flow-laminated rhyolite bodies and in breccias.

Groundmass textures in the rhyolitic rocks are as varied as their macroscopic fabrics. Textures range from glassy or perlitic to microcrystalline, where grain sizes

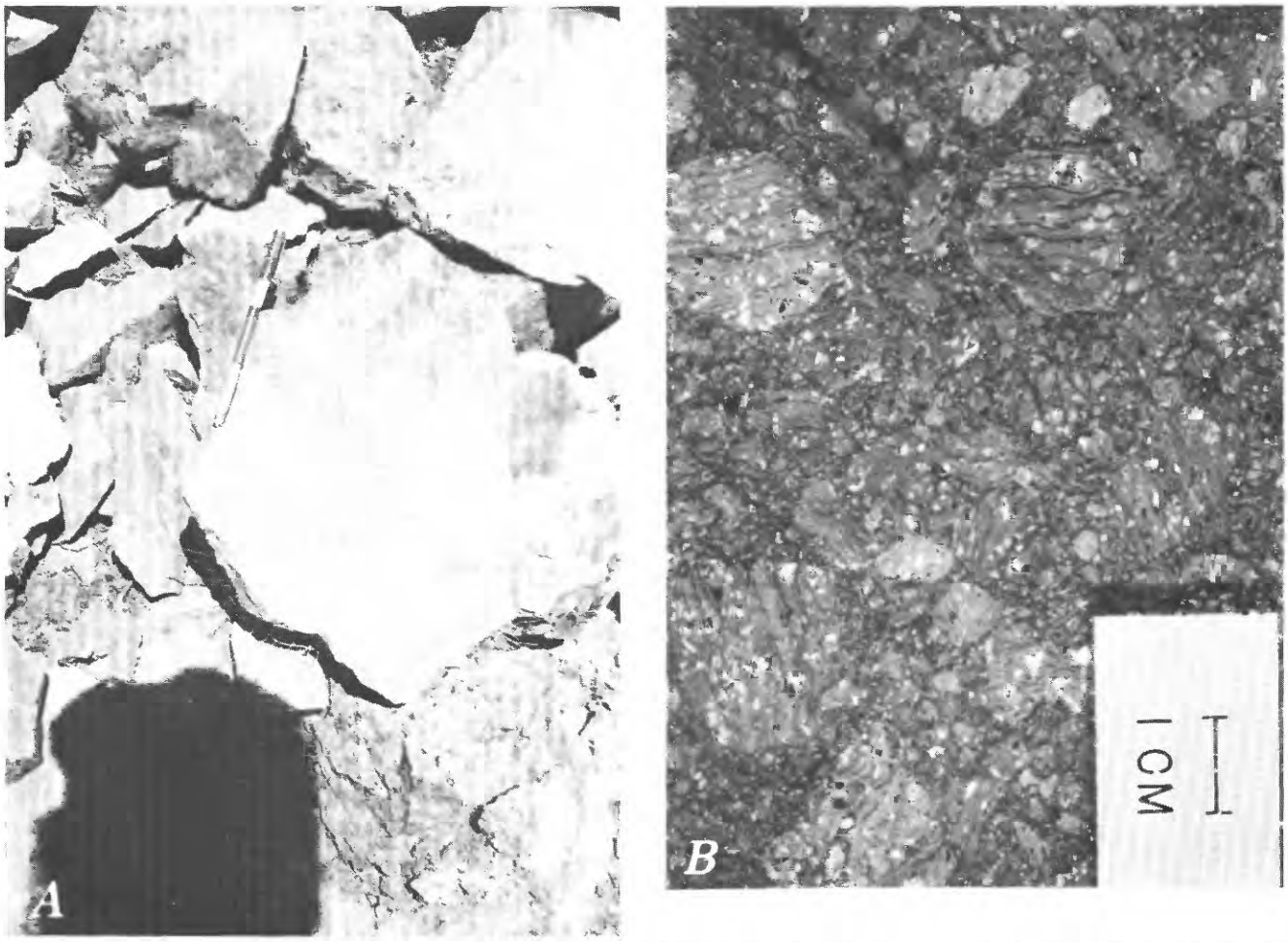

Figure N5. Breccia fabrics in rhyolites of the Challis volcanic field. *A*, brecciated rhyolite containing angular rhyolite clasts as large as 25 cm with interstitial devitrified rhyolite matrix or locally amorphous silica matrix. Pencil is 14 cm long. *B*, rhyolite breccia containing abundant rounded to subrounded, flow-laminated, porphyritic rhyolite clasts in a matrix of the same rhyolite.

rarely exceed 0.2 mm. Microcrystalline textures are locally pilotaxitic to felted, but allotriomorphic granular and typically blotchy or snowflake textures prevail (fig. N7). Micrographic to micromyrmekitic textures (fig. N8) commonly dominate the groundmass; spherulitic devitrification textures are also common.

ALTERATION AND MINERALIZATION

Rhyolites in the rhyolite belt are varicolored, in gray to light brown or pinkish red. Where hydrothermally altered, these rocks are bleached and weakly to intensely stained by limonite or hematite. Alteration of these rocks ranges from weakly argillic through moderately strongly quartz-sericitic to locally strongly silicic. Disseminated pyrite (as much as 2 percent observed) is locally common in unfaulted altered rhyolite, and fine-grained granular pyrite is locally concentrated along structures in some faulted rhyolite bodies. Fluorite as disseminated grains, replacements, veins, and open-space fillings in brecciated rhyolite and in altered country rock is locally common. Calcite, gypsum, or quartz commonly fills open spaces in brecciated altered rhyolite and in veins.

Epithermal precious-metal mineralization has affected several rhyolite bodies throughout the rhyolite belt. Known mineral occurrences include deposits at the Rabbit Foot mine (116 oz Au, 136 oz Ag, reported production) and Singheiser mine (317 oz Au, 8,415 oz Ag, reported production), in the Panther Creek graben; and deposits or prospects in the Custer graben, including those at Red Mountain, the Sunbeam mine, and Estes Mountain (McIntyre and Johnson, chap. I, this volume).

The Snowshoe Creek area, about 6 km northwest of the Twin Peaks caldera (fig. N1), is one example of a favorable location for rhyolite-associated mineralization that lies within the area of the Van Horn Peak cauldron complex. In this area (fig. N9) dikes and plugs of rhyolite and rhyolite breccia intrude intracaldera pyroclastic rocks related to the Van Horn Peak cauldron complex that are unconformably overlain by outflow ash-flow tuff from the Twin Peaks caldera.

Northeast-trending faults displace the pyroclastic rocks, and in part rhyolite appears to intrude at least one

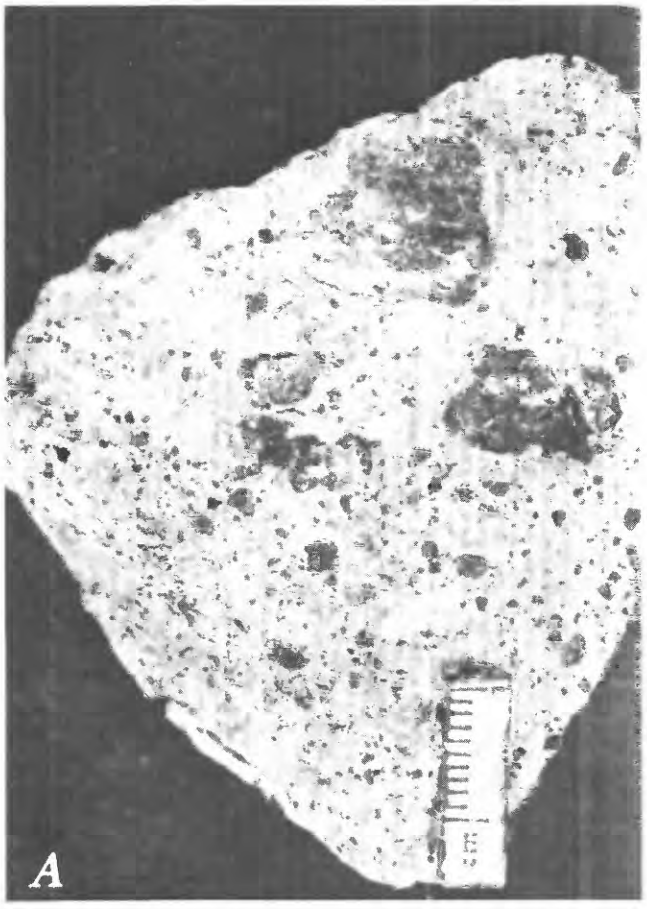

Figure N6. Intrusive rhyolite breccia resembling a pebble dike, Challis quadrangle. *A*, rounded, devitrified to glassy, porphyritic rhyolite fragments in a breccia matrix containing quartz and sanidine phenocrysts. *B*, photomicrograph of thin section from the hand specimen in *A*.

of these structures. Locally, the rhyolite and older pyroclastic rocks are moderately to strongly argillized and sericitically altered. Brecciated rock along structures is silicified and contains fluorite, calcite, and quartz in open vugs and veins. Disseminated pyrite is present along faults and in rhyolite and adjacent pyroclastic rocks. Stockwork hairline quartz veinlets are common in the rhyolites and in the country rock.

Sixty rock-chip samples were collected for geochemical study from 50 localities in the Snowshoe Creek area (fig. N10). Anomalous values of arsenic (5–2,000 ppm), molybdenum (7–700 ppm), and silver (0.5–10 ppm) were obtained from some samples (fig. N10). In addition, one sample contained 0.05 ppm gold and another contained 2,000 ppm lead. Trace amounts of beryllium (1–10 ppm), antimony (1–18 ppm), zirconium (50–500 ppm), lanthanum (20–150 ppm), niobium (20–100 ppm), and barium (50–2,000 ppm) were also present in some samples.

The intrusive rhyolite in the Snowshoe Creek area is only one example of rhyolite that may have potential for spatially associated precious-metal deposits. Other rhyolites (some intrusions are too small to show on fig. N1)

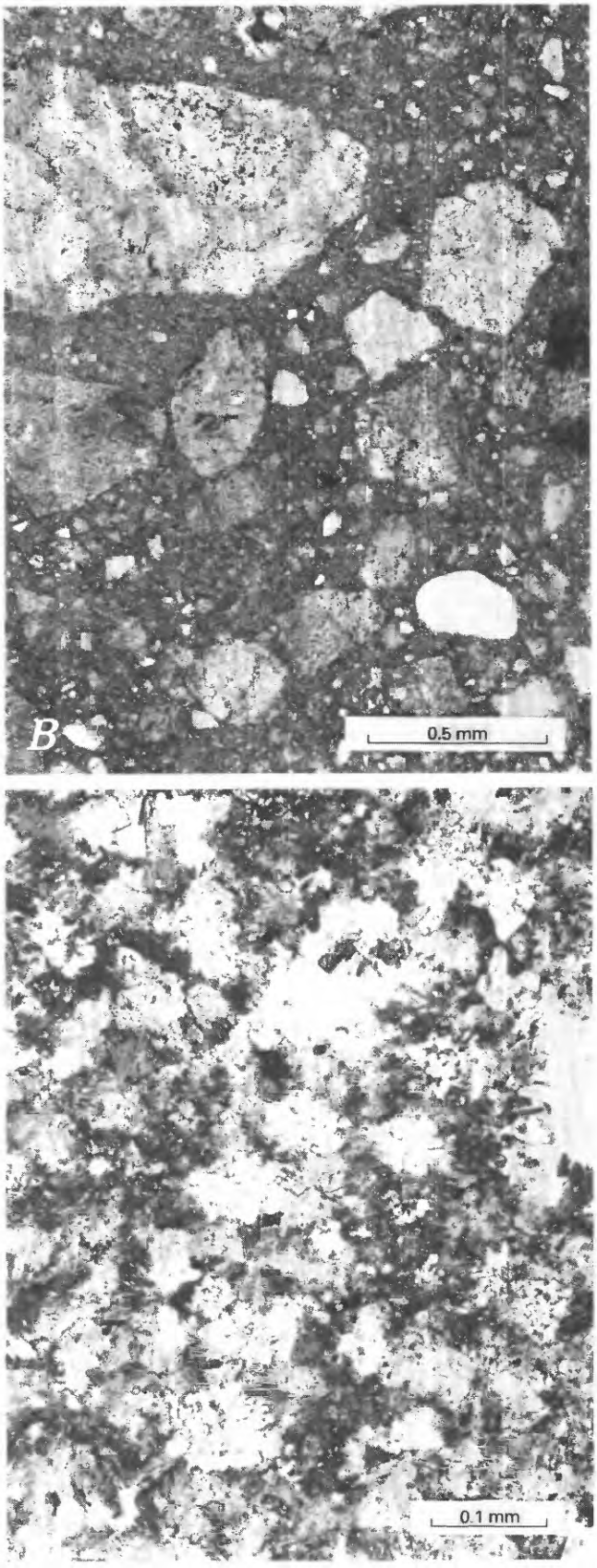

Figure N7. Photomicrograph of blotchy or snowflake-textured microcrystalline matrix of porphyritic rhyolite, Challis volcanic field.

Figure N8. Photomicrograph of micromyrmekitic texture in matrix of porphyritic rhyolite intrusive body, Challis volcanic field.

within the area of the Van Horn Peak cauldron complex, including the East Fork Mayfield Creek multiple intrusion, are altered and have associated structures that are similar to the Snowshoe Creek area and to rhyolites in the Panther Creek and Custer grabens.

CONCLUSIONS

Intrusive and minor extrusive rocks of rhyolitic composition that postdate cauldron-related pyroclastic rocks of the Challis volcanic field crop out in a northeast-trending belt that is essentially coincident with the trans-Challis fault system. Rhyolites within this belt are aphyric to porphyritic and have textures and field relations that indicate emplacement at shallow levels of the crust. Some of the intrusive rhyolites appear to have breached the surface and formed flow-dome complexes.

Hydrothermal alteration has affected some of the high-level rhyolite bodies within the Van Horn Peak cauldron complex, and rhyolite breccias are common. The presence of favorable permeable zones in these rhyolites combined with the presence of hydrothermally altered rock suggests that these rhyolites are favorable targets for mineral exploration. Preliminary investigation of the Snowshoe Creek area indicates that this is a favorable prospect for precious-metal deposits spatially associated with intrusive rhyolite.

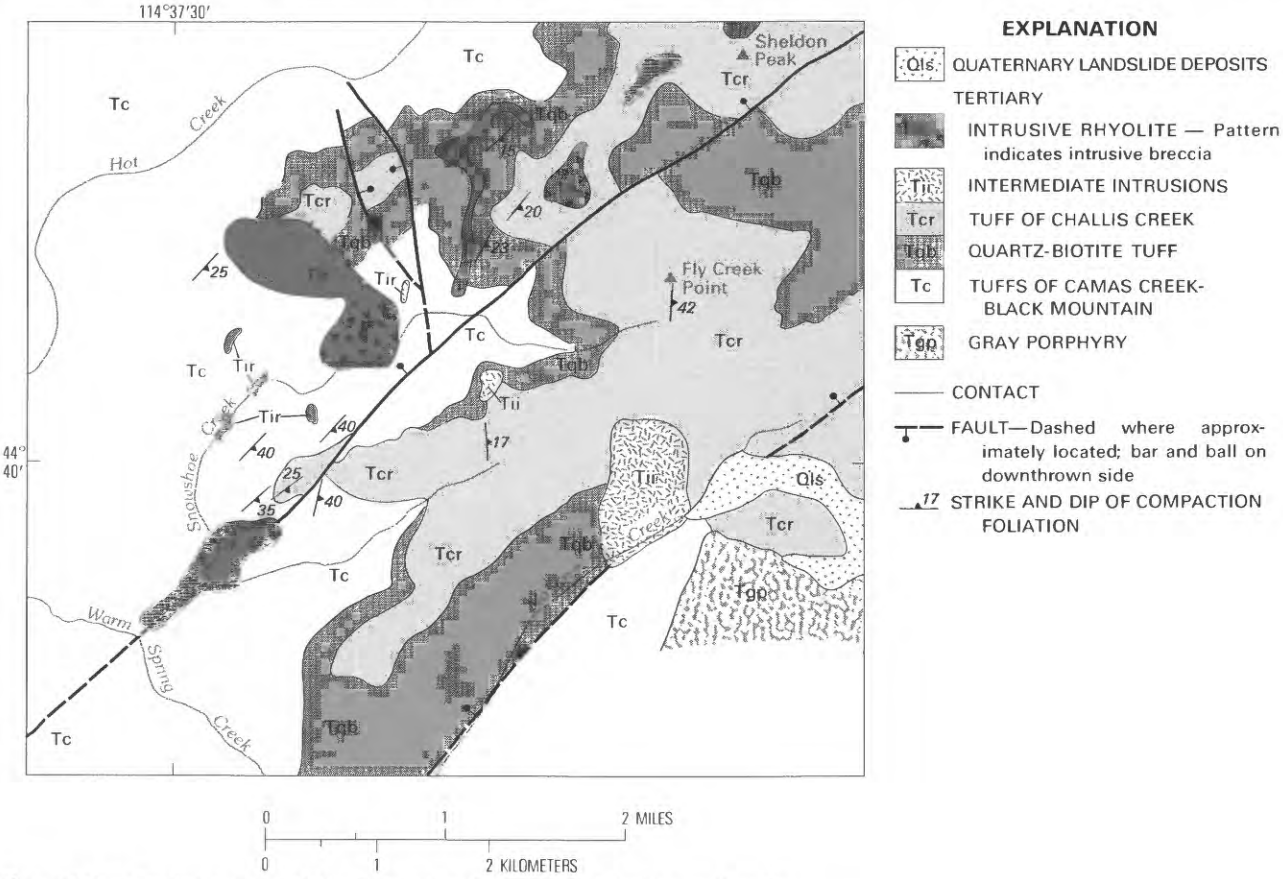

Figure N9. Geologic map of the Snowshoe Creek area, Challis quadrangle.

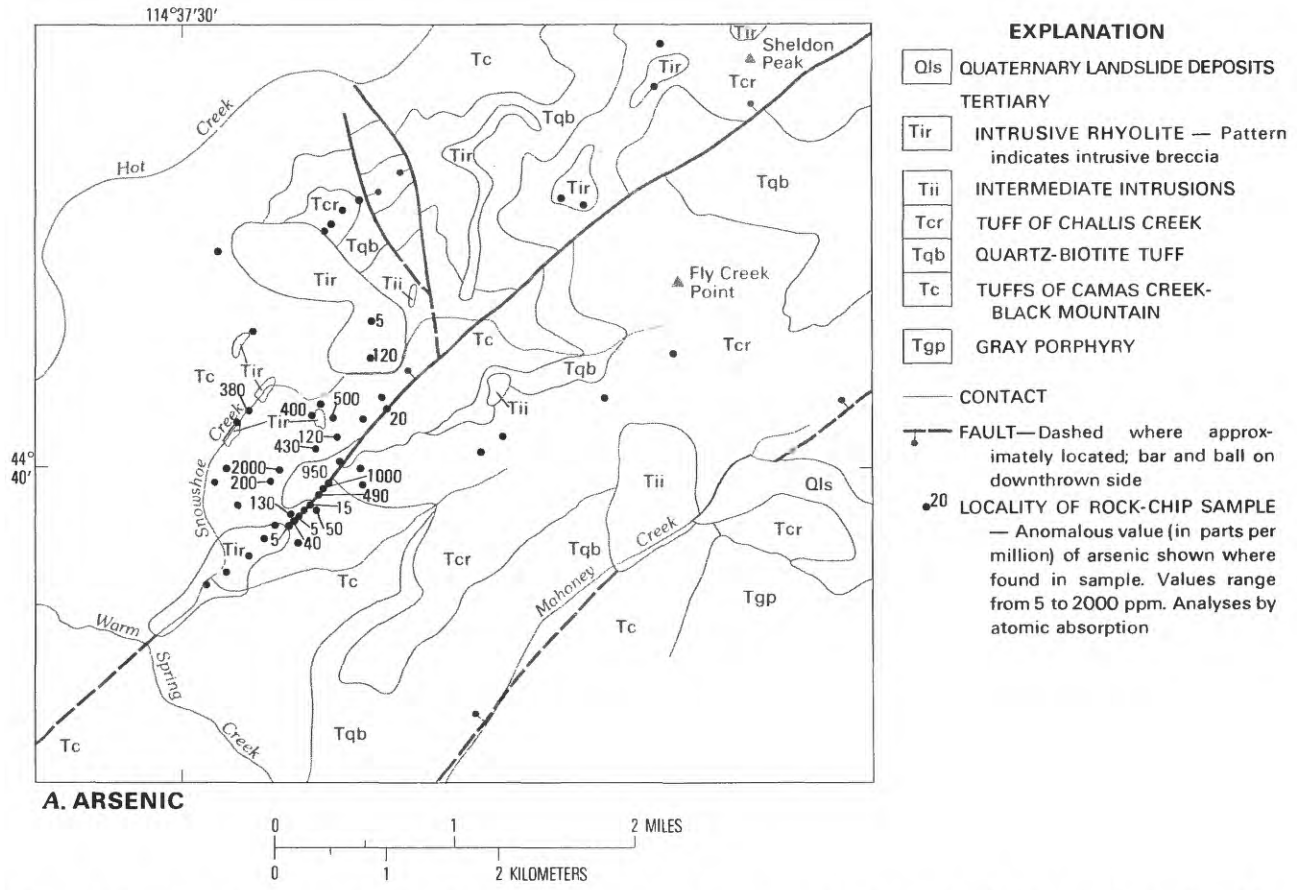

Figure N10. Maps of the Snowshoe Creek area, Challis quadrangle, showing localities of rock-chip samples analyzed for arsenic, gold, silver, and molybdenum.

REFERENCES CITED

Ewart, A., 1979, A review of the mineralogy and chemistry of Tertiary-Recent dacitic, latitic, rhyolitic, and related salic volcanic rocks, *in* Barker, F., ed., Trondhjemites, dacites, and related rocks: Amsterdam, Elsevier, p. 13–121.

Hobbs, S. W., Hays, W. H., and McIntyre, D. H., 1975, Geologic map of the Clayton quadrangle, Custer County, Idaho: U.S. Geological Survey Open-File Report 75–76, 23 p., 1 pl., scale 1:62,500.

Marvin, R. F., and Dobson, S. W., 1979, Radiometric ages—compilation B, U.S. Geological Survey: Isochron/West, no. 26, 32 p.

McIntyre, D. H., Ekren, E. B., and Hardyman, R. F., 1982 [1984], Stratigraphic and structural framework of the Challis Volcanics in the eastern half of the Challis 1°×2° quadrangle, Idaho, *in* Bonnichsen, Bill, and Breckenridge, R. M., eds., Cenozoic geology of Idaho: Idaho Bureau of Mines and Geology Bulletin 26, p. 3–22.

Segerstrom, Kenneth, and Young, E. J., 1972 [1973], General geology of the Hahns Peak and Farwell Mountain quadrangles, Routt County, Colorado, *with a discussion of* Upper Triassic and pre-Morrison Jurassic rocks, by G. N. Pipiringos: U.S. Geological Survey Bulletin 1349, 63 p.

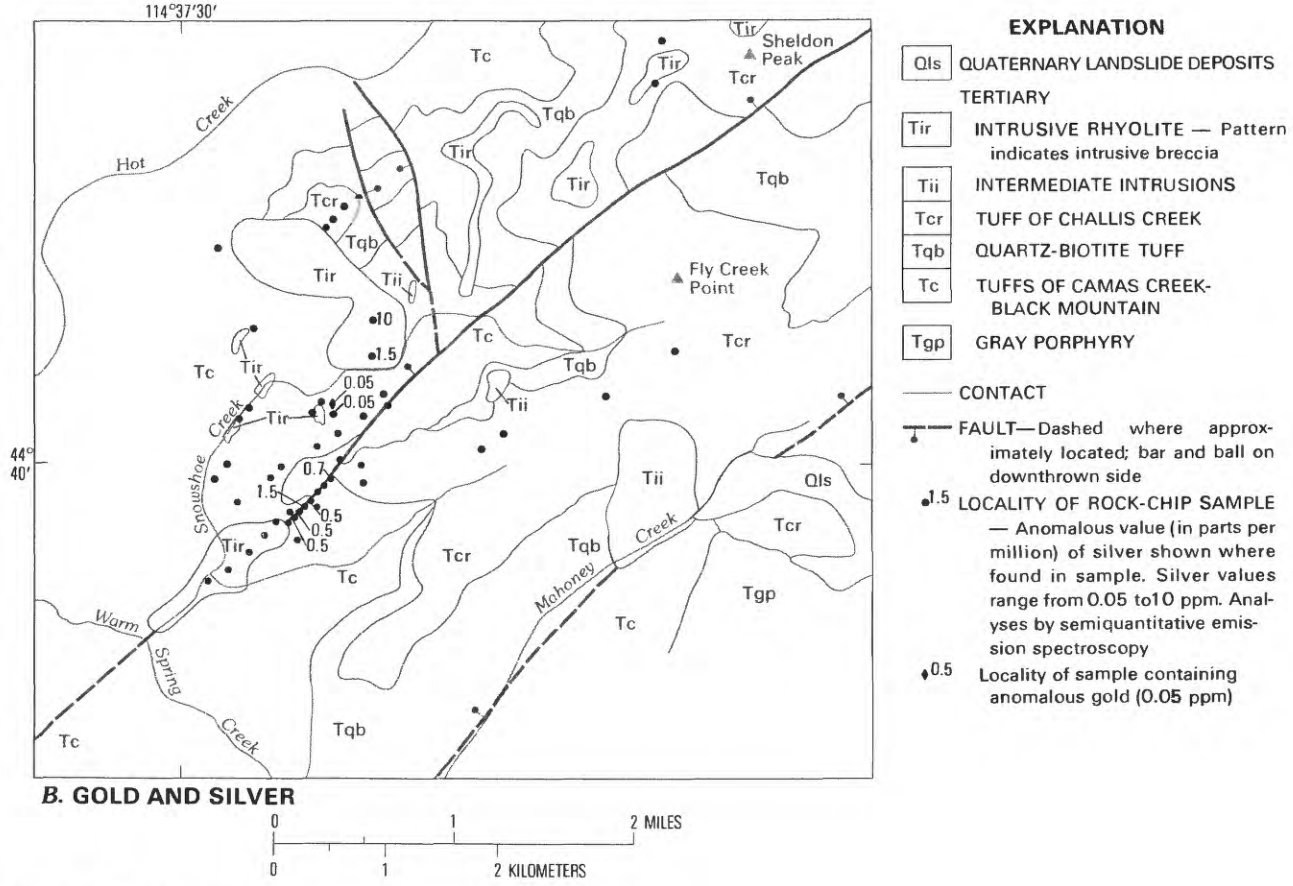

Figure N10. Continued.

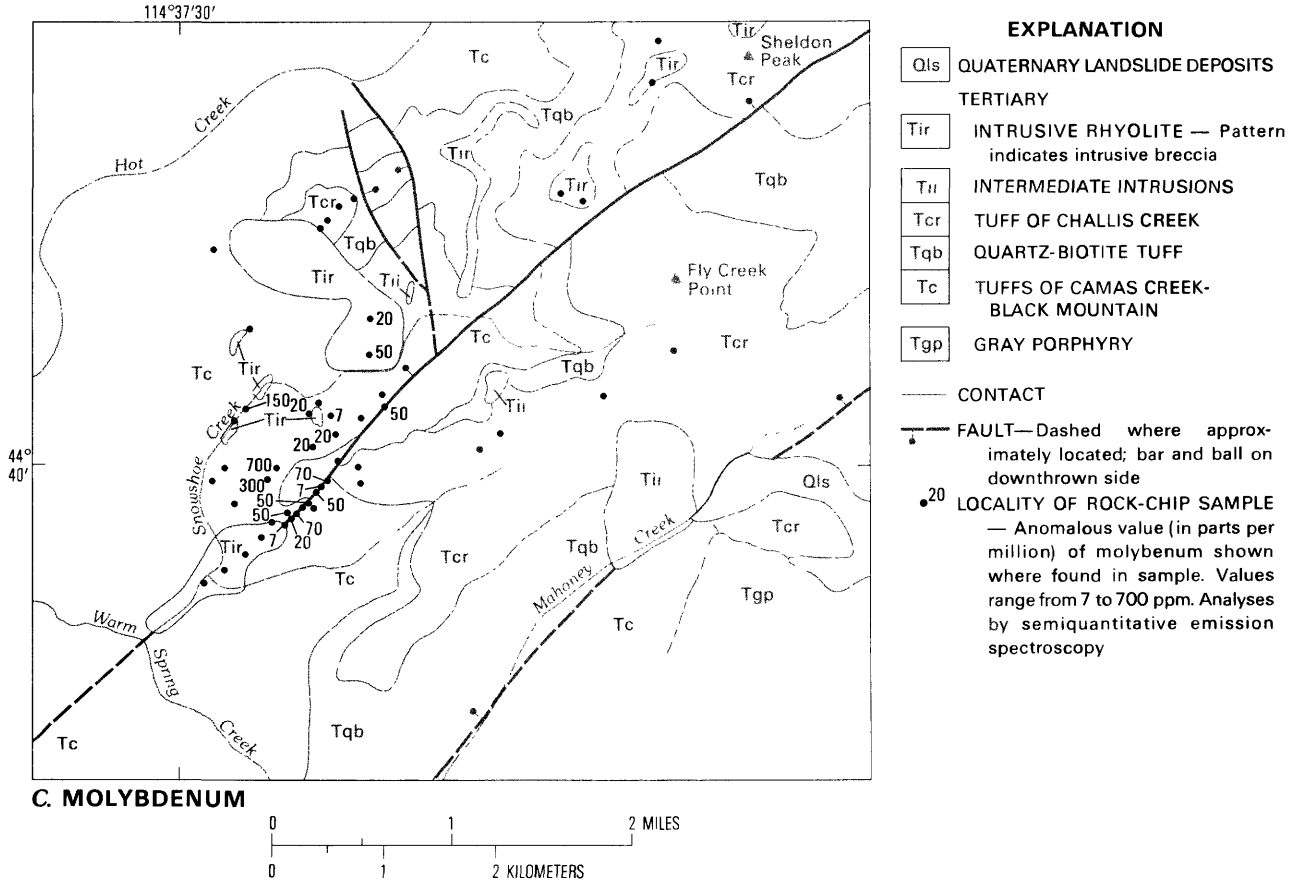

Figure N10. Continued.

Symposium on the Geology and Mineral Deposits of the Challis 1°×2° Quadrangle, Idaho

Chapter O

Lead-Isotope Characteristics of Ore Systems in Central Idaho

By BRUCE R. DOE *and* M. H. DELEVAUX

Abstract

About 60 new lead-isotope analyses were made on ore mineral, igneous-rock, and shale samples from central Idaho. The analyses were made to test the use of lead-isotope studies in mineral-resource evaluation of Cretaceous and Tertiary magmatothermal deposits.

The lead-isotope pattern is complex, but the analyses can be separated into two groups, A and B. Group A analyses have many values of $^{206}Pb/^{204}Pb$ more than or equal to 18.0, but some values exceed 21. All Group B analyses have values of 18.5 or more, and most are between 19 and 20. For Group A and B analyses that have similar values of $^{206}Pb/^{204}Pb$, $^{208}Pb/^{204}Pb$ values of Group A analyses are greater than Group B analyses. Tin granites can be in either Group A or B and cannot be distinguished from molybdenum deposits by lead isotope ratios.

Group A values are similar to those from samples from the Rocky Mountains; Group B values resemble those from the Great Basin. Large molybdenum deposits generally have lower values of $^{206}Pb/^{204}Pb$, but values are in both isotopic groups. For example, Group A values were found in samples from the Thompson Creek deposit, and Group B values were found in samples from the White Cloud deposit. Analyses from the Clayton Silver mine are also in Group A, but $^{206}Pb/^{204}Pb$ here range between 18 and 19.

Group B analyses are from samples from a horn-shaped band opening to the east along the boundary between the Challis and Hailey quadrangles. Group A galena samples are from areas of positive gravity anomalies, where the gravity is not dominated by volcanic rocks, indicating relatively shallow Precambrian crystalline basement. Their lead-isotope apparent age is 1,620±100 m.y. Group B samples are from areas that do not have positive gravity anomalies, indicating that the crystalline basement is deep or absent. The primary source of these lead isotopes seems to be material deep under the Great Basin, rather than shallow Paleozoic or Middle Proterozoic Belt Supergroup rocks.

Symposium on the Geology and Mineral Deposits of the Challis 1°×2° Quadrangle, Idaho

Chapter P

Light-Stable-Isotope Characteristics of Ore Systems in Central Idaho

By STEPHEN S. HOWE *and* WAYNE E. HALL

CONTENTS

Abstract

Light stable isotopes in mineral deposits and their host rocks were investigated to place constraints on the sources of water and sulfur in hydrothermal systems of central Idaho. Analyses of inclusion fluids extracted from crushed sulfide and gangue minerals from Cretaceous porphyry and vein deposits give δD values of -130±25 per mil, indicating the presence of meteoric water. Meteoric water, which continued to predominate in hydrothermal systems around Tertiary plutons within the Idaho batholith, created zones extremely depleted in deuterium and ^{18}O in areas larger than 15,000 km^2 (square kilometers) through water-rock interactions. The $\delta^{34}S$ values of sulfide minerals from most of the Cretaceous and Tertiary mineral deposits are quite high, generally from +4 to +13 per mil; several samples from deposits considered to be of syngenetic or remobilized-syngenetic origin have $\delta^{34}S$ values as high as +23 per mil. No correlation between commodity and sulfur-isotopic composition exists. Mineral deposits in black shale, however, generally have $\delta^{34}S$ values higher than those in carbonate rocks, quartzite, or granite. Although many of the mining districts are isotopically inhomogeneous, individual deposits commonly have very similar sulfur-isotopic compositions.

These isotopic data support a model in which meteoric water, set into convective circulation by heat from granitic intrusions, leached ^{34}S-enriched sulfur from crustal sources, such as syngenetic sulfide minerals in sedimentary rocks, evaporite deposits, or pre-Cretaceous sulfide deposits. The sulfur then mixed locally in varying proportions with ^{34}S-depleted sulfur from the magmatic reservoirs of adjacent plutons. This hybrid sulfur was then homogenized isotopically before reaching the sites of ore deposition.

INTRODUCTION

An objective of the CUSMAP (Conterminous United States Mineral Assessment Program) study of the Challis quadrangle was to develop models for the formation of a variety of mineral deposits that occur within the quadrangle. The origin of metals, water, and sulfur in the hydrothermal systems of the deposits is of paramount importance in the formulation of these models. This chapter summarizes the hydrogen- and oxygen-isotope data from earlier studies by Hall and others (1978, 1984) and Criss and Taylor (1983) and their conclusions concerning the source of water in certain hydrothermal systems. It also contains a tabulation of all of the sulfur-isotope data available to 1984 and a preliminary interpretation of the source of sulfur in 45 pre-Cretaceous, Cretaceous, and Tertiary mineral deposits in the Challis quadrangle and in parts of the adjoining Hailey and Elk City 1°×2° quadrangles (fig. P1, table P1). The deposits include lead-zinc-silver-tin-antimony-bismuth veins and breccia filling, molybdenum stockworks, lead-zinc-silver and barite stratabound deposits, and cobalt-copper stratabound and vein deposits. We have concentrated our discussion on mineral deposits within the extensive black-shale belt east of the Idaho batholith (Hall, chap. J, this volume) due to the interest of the mining industry in this terrane.

Table P1. Localities sampled for study of sulfur isotopes, Elk City, Challis, and Hailey 1°×2° quadrangles

[do., ditto; leaders (---), unknown, unnamed, or undefined mining district]

Loc. No. (fig. P1)	Name	Mining district	County
	Elk City quadrangle		
1	Blackbird mine	Blackbird	Lemhi
	Challis quadrangle		
2	Quartz Creek prospect	Yellowpine	Valley
3	Seafoam Lake prospect	Seafoam	Custer
4	Little Falls prospect	Grimes Pass	Boise
5	Carlson Gulch mine	---do.	Do.
6	Comeback mine	---do.	Do.
7	Ramshorn mine	Bayhorse	Custer
8	Beardsley Gulch mine	---do.	Do.
9	Pacific mine	---do.	Do.
10	Rattlesnake Creek prospect.	---do.	Do.
11	Buckskin mine	---do.	Do.
12	Thompson Creek mine	---do.	Do.
13	Rob Roy mine	---do.	Do.
14	Dryden mine	---do.	Do.
15	Roadcut between Buckskin and Thompson Creek mines.	---do.	Do.
16	Hoodoo mine	Boulder Creek	Custer
17	Livingston mine	---do.	Do.
18	Willow Lake prospect	---do.	Do.
19	Little Boulder Creek prospect	---do.	Do.
20	Silver Dollar prospect	East Fork	Do.
	Hailey quadrangle		
21	Unnamed prospect	Galena	Blaine
22	---do.	Boulder Basin	Do.
23	Golden Glow mine	---do.	Do.
24	Webfoot mine	Vienna	Do.
25	GAF prospect	--	Camas
26	Rooks Creek prospect	Boyle Mountain	Blaine
27	Unnamed prospect	---do.	Do.
28	Upper prospect	Carrietown	Camas
29	Unnamed dump	---do.	Do.
30	Horn Silver mine	---do.	Do.
31	Carrie Leonard mine	---do.	Do.
32	Panther Gulch prospect	--	Blaine
33	Red Cloud mine	Wolftone	Do.
34	Deer Creek mine	Wood River	Do.
35	Eureka mine	---do.	Do.
36	Liberty Gem mine	---do.	Do.
37	Treasure Vault mine	---do.	Do.
38	Silver Star Queen mine	Wood River	Blaine
39	Minnie Moore mine	---do.	Do.
40	Dennison mine	---do.	Do.
41	North Star mine	---do.	Do.
42	Triumph mine	---do.	Do.
43	Independence mine	---do.	Do.
44	Trail Creek prospect	---do.	Do.
45	Lake Creek-Trail Creek prospect.	---do.	Do.

Acknowledgments.—J. N. Batchelder, W. J. Pickthorn, and L. D. White assisted various phases of the study, in the laboratory of J. R. O'Neil, U.S. Geological Survey, Menlo Park, Calif.

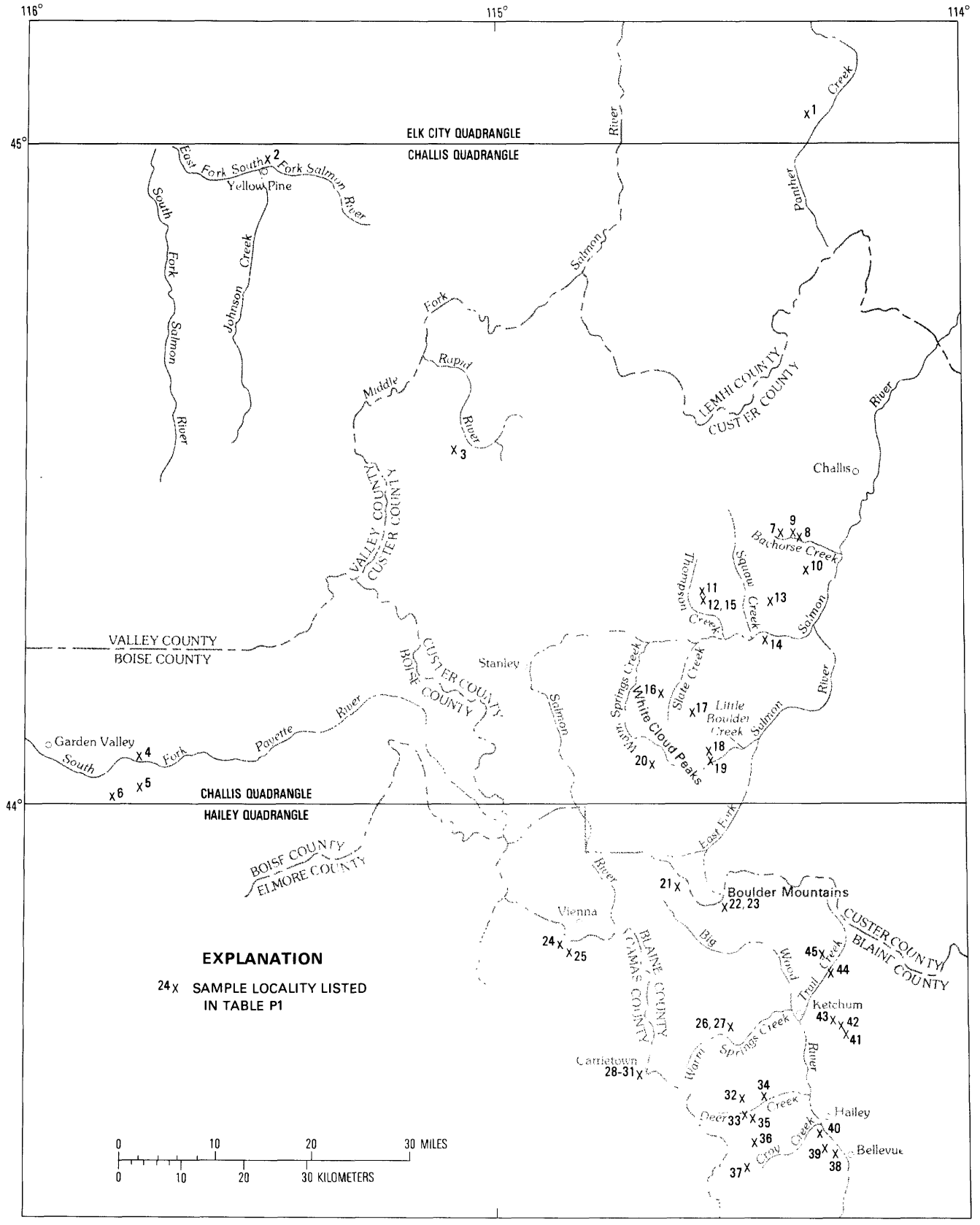

Figure P1. Localities of samples collected for sulfur-isotope study in the Elk City, Challis, and Hailey 1°×2° quadrangles. A description of the localities is in table P1.

ANALYTICAL TECHNIQUES

Sulfide and gangue minerals were crushed in evacuated stainless-steel tubes to liberate inclusion fluids. The water in these fluids was reacted with uranium at 700°C (Celsius), and the evolved hydrogen was collected on charcoal in glass sample bottles, similar to the method of Friedman (1953). Water released from hydrous silicates decomposed at 1,300°C by an RF induction furnace (Godfrey, 1962) was reacted in the same manner.

Quartz and feldspar were powdered and reacted with BrF_5 or ClF_3 at 600°C for 16 hours in nickel reaction tubes heated by electric resistance furnaces, using the methods of Clayton and Mayeda (1963) and Borthwick and Harmon (1982). The liberated oxygen was converted to CO_2 by a heated carbon rod. Siderite was reacted with H_3PO_4 at 50°C for 6 days to evolve CO_2 (McCrea, 1950). The CO_2 was collected in glass sample bottles.

Powdered sulfide minerals were mixed with excess Cu_2O and placed in silica tubes. The tubes were heated at 1,150°C for 10 minutes in a resistance furnace. The SO_2 generated was purified of O_2, CO_2, and H_2O by vacuum distillation and then collected in glass bottles or 6-mm glass tubes.

The hydrogen-, oxygen-, and sulfur-isotopic compositions of the collected H_2, CO_2, and SO_2 were analyzed using three different mass spectrometers. The hydrogen- and oxygen-isotopic compositions are reported in the standard δ notation as per mil deviations from SMOW (Standard Mean Ocean Water), and the sulfur-isotopic compositions are reported as per mil deviations from CDT (Canon Diablo Troilite). The precision of the analyses is ± 1 per mil for δD and ± 0.1 per mil for $\delta^{18}O$ and $\delta^{34}S$.

SOURCE OF WATER IN THE HYDROTHERMAL SYSTEMS

The most direct evidence concerning the source of water in the hydrothermal systems of two types of mineral deposits in central Idaho comes from the hydrogen-isotopic compositions of inclusion fluids extracted from sulfide and gangue minerals from the Cretaceous Thompson Creek stockwork molybdenum deposit and the Cretaceous Wood River lead-zinc-silver vein deposits (localities 12 and 34–45, fig. P1). Samples of minerals thought to have been deposited during main ore-formation episodes were identified after measurements of the homogenization temperatures and salinities of fluid inclusions were made (Hall and others, 1978, 1984). Highly depleted D (deuterium) compositions of -130 ± 25 per mil and -115 ± 5 per mil for samples from the molybdenum and lead-zinc-silver deposits, respectively (table P2), indicate that the ore fluids in these deposits were derived predominantly from meteoric water (Taylor, 1979). A δD value of -58 per mil for water in hydrothermal white mica that formed during the earliest period of potassic alteration at the Thompson Creek deposit (Hall and others, 1984) suggests that magmatic water was present initially in the hydrothermal system of this deposit.

Table P2. Hydrogen-isotope analyses of water in white mica and in fluid inclusions in sulfide and gangue minerals, and oxygen-isotope analyses of quartz and siderite, from central Idaho

[Values in per mil; $\delta^{18}O_{H_2O}$ values for quartz calculated from Matsuhisa and others (1979) and for siderite from Becker and Clayton (1976), with T=280°C and T=270°C for Thompson Creek and Wood River deposits, respectively, from fluid-inclusion homogenization temperatures (Hall and others, 1978, 1984); do., ditto; leaders (---), no analyses or calculations]

Sample No.	Mineral	δD_{H_2O}	$\delta^{18}O$ mineral	Calculated $\delta^{18}O_{H_2O}$ at T
	Thompson Creek deposit			
SWH-152-----	White mica-----	-58	--	--
S-27-747----	Quartz--------	--	11.2	3.6
S-27-770----	---do.--------	-108	10.7	3.1
S-27-789----	---do.--------	-121	10.9	3.3
WH-81-5-----	---do.--------	-126	--	--
WH-81-6-----	Galena--------	-108	--	--
S-51-13-----	Quartz--------	-155	--	--
S-64-12-----	---do.--------	-144	--	--
S-73-9------	---do.--------	-135	--	--
S-73-11-----	---do.--------	-138	--	--
S-89-2------	---do.--------	-123	--	--
S-94-11-----	---do.--------	-123	--	--
	Wood River deposit			
WH-70-8A----	Galena and sphalerite.	-110	--	--
WH-70-13B---	Siderite------	--	14.8	7.8
WH-70-15----	---do.--------	-120	13.3	6.3
WH-70-16----	Galena and sphalerite.	-120	--	--
A-36--------	Quartz--------	-115	16.4	8.4
A-227-------	---do.--------	-116	--	--

Oxygen isotopes commonly help indicate the extent to which hydrothermal fluids have undergone isotopic exchange with surrounding country rocks. Quartz from the Thompson Creek stockwork deposit has a $\delta^{18}O$ value of $+11.0\pm0.3$ per mil, whereas quartz and siderite from the Wood River deposits have $\delta^{18}O$ values of $+14.9\pm1.6$ per mil (table P2). The calculated oxygen-isotopic compositions of the water that deposited these gangue minerals are about +3.3 and +7.5 per mil, respectively. For the Thompson Creek deposit, a $\delta^{18}O$ value of +3.3 per mil for the water is that of a fluid in approximate isotopic equilibrium with granitic rocks. However, the heavier $\delta^{18}O$ values for the fluids that deposited the Wood River ores suggest that the fluids had partly exchanged ^{18}O with ^{18}O-enriched shale host rocks[1].

Meteoric water continued to dominate hydrothermal systems during the Tertiary. Huge zones, areas larger

[1]Two analyses of the host rock, the Devonian Milligen Formation, gave high $\delta^{18}O$ values of +18.8 and +20.7 per mill (Hall and others, 1978).

than 15,000 square kilometers extremely depleted in D and ^{18}O, developed around Tertiary plutons within the Idaho batholith due to water-rock interactions. Criss and Taylor (1983) showed the distribution of ^{18}O values for coexisting quartz and feldspar from rocks of the Atlanta lobe of the Idaho batholith (fig. P2). Feldspar is much more susceptible to isotopic exchange during hydrothermal alteration than is quartz (Taylor, 1979; Cole and others, 1983). The strongly skewed $\delta^{18}O$ values for the feldspar clearly show the pronounced depletion in ^{18}O due to interactions with meteoric water. Deuterium in biotite and ^{18}O in feldspar are also extremely depleted in altered rocks of the Atlanta lobe (fig. P3; Criss and Taylor, 1983). Only repeated circulation of low-D, low-^{18}O meteoric water through these rocks could lower the δD and $\delta^{18}O$ values so greatly. Criss and Taylor (1983) suggested that many epithermal gold-silver deposits related to Tertiary plutonism within the Idaho batholith are associated with these altered rocks and that low-^{18}O halos may be useful targets for mineral exploration.

SOURCE OF SULFUR IN THE HYDROTHERMAL SYSTEMS

The sulfur-isotopic compositions of the deposits sampled are generally enriched in ^{34}S (fig. P4; appendix). Although the values range from 3.5 to +22.9 per mil, most are between +4 and +13 per mil. Four sulfide-mineral samples and one sulfate-mineral sample from pre-Cretaceous deposits considered to be syngenetic or remobilized syngenetic, as discussed by Hall (chap. J, this volume), have values of +11.3, +11.3, +13.2, +15.6, and +22.9 per mil.

Within most individual deposits, the order of enrichment of ^{34}S in coexisting epigenetic sulfide minerals is galena<bournonite<sphalerite<pyrite<molybdenite, precisely the fractionation trend expected for deposition under conditions of isotopic equilibrium, even though few of the minerals were deposited contemporaneously. For this reason, we hoped that isotopic fractionation between two coexisting sulfide minerals could be used to calculate geologically reasonable pressure-independent temperatures of mineralization. Sulfide pairs (table P3; appendix) from several lead-zinc-silver vein deposits apparently did precipitate at geologically reasonable temperatures of 191° to 375°C, which, for the Wood River deposits, match fluid-inclusion homogenization temperatures fairly closely (Hall and others, 1978).

Rye and Ohmoto (1974) have shown that similar types of deposits commonly have somewhat different sulfur-isotopic compositions, and that for some deposits these differences are a result of incorporating sulfur from different sources in the deposit. The absence of correlation between commodity or type of deposit and sulfur-isotopic composition is also true for most of the deposits examined in central Idaho (appendix). Some deposits are relatively enriched in ^{34}S, such as the Thompson Creek stockwork molybdenum deposit (average $\delta^{34}S$ is +10.6 per mil), and the Livingston lead-zinc-silver vein deposit, (average $\delta^{34}S$ is +11.9 per mil). Also, some deposits are relatively depleted in ^{34}S, such as the Little Boulder Creek stockwork molybdenum deposit, (average $\delta^{34}S$ is +6.4 per mil) and the Dryden lead-zinc-zilver vein deposit (average $\delta^{34}S$ is +5.0 per mil).

When the $\delta^{34}S$ values are grouped by lithology of the host rocks for the deposits (fig. P5), an interesting distinction is seen. Deposits within the Ordovician(?) Ramshorn Slate, the Devonian Milligen Formation, and the Cambrian to Mississippian Salmon River assemblage[2], all predominantly black shale, have $\delta^{34}S$ values averaging 6

[2]Formations described in detail by Hobbs (chap. D, this volume) and by Hall (chap. J, this volume).

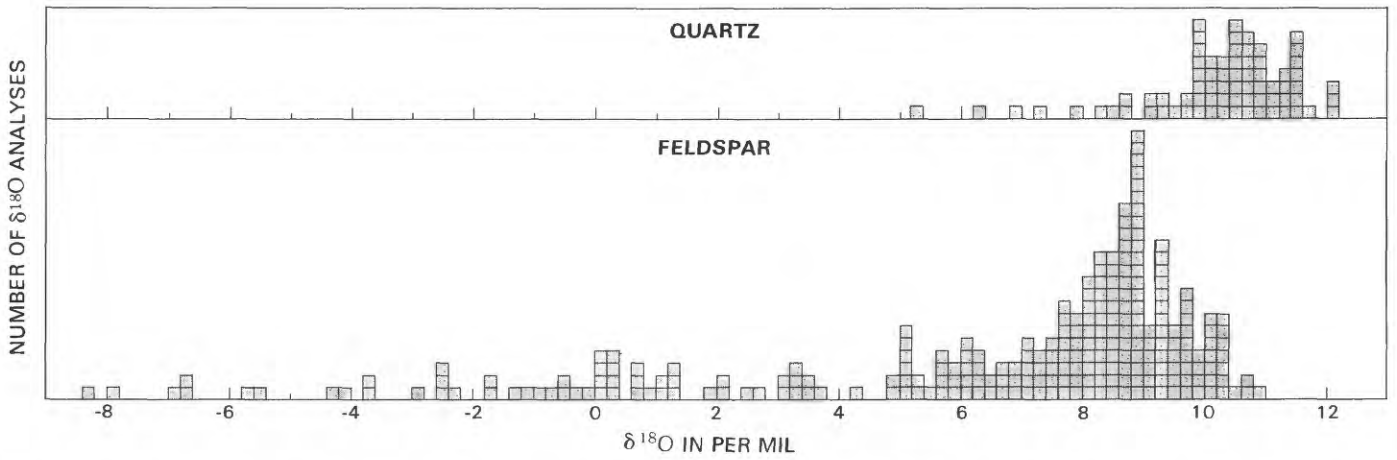

Figure P2. Distribution of $\delta^{18}O$ values of samples coexisting quartz and feldspar from rocks of the Atlanta lobe of the Idaho batholith. From Criss and Taylor (1983).

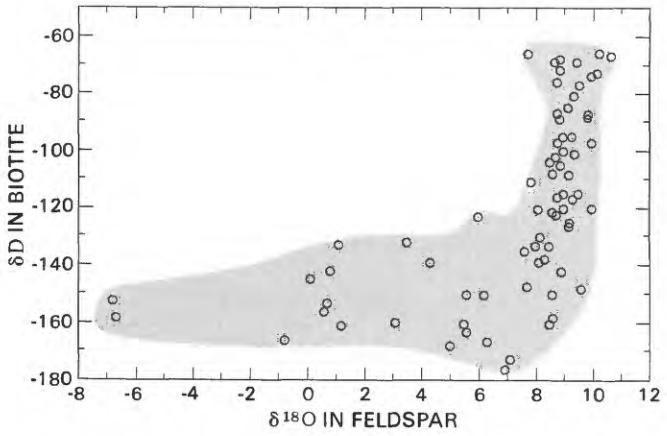

Figure P3. Graph of δD values of samples of biotite (with or without chlorite) plotted against the $\delta^{18}O$ values of coexisting feldspar in altered rocks of the Atlanta lobe of the Idaho batholith. Original composition for δD was about −65 to −75 per mil, and for $\delta^{18}O$, +8 to +11 per mil. From Criss and Taylor (1983).

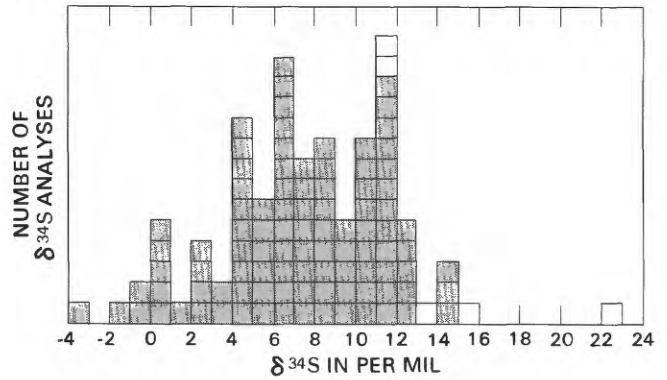

Figure P4. Distribution of $\delta^{34}S$ values of 100 sulfide-mineral samples and one sulfate-mineral sample. Unpatterned areas show samples considered to be of syngenetic or remobilized-syngenetic origin.

Table P3. Comparison of sulfide-pair and fluid-inclusion geothermometry of ore samples from central Idaho

[Sulfide-pair temperatures calculated from appropriate fractionation equations of Ohmoto and Rye (1979), ±45°C due to uncertainties in the fractionation equations and in the analyses of the sulfur-isotopic compositions of the sulfides. Fluid-inclusion temperatures are homogenization temperatures from Hall and others (1978). Leaders (--), no analyses]

Deposit or district	Sulfide-pair temperature (°C)	Fluid-inclusion temperature (°C)
Little Boulder Creek----	322	--
Boulder Basin----------	284	--
Webfoot----------	355	--
Carrietown----------	375, 269	--
Wood River----------	191-291	270±30

per mil greater or heavier than those deposits within carbonate rocks, quartzite, and granite. This gap of 6 per mil appears to cause the bimodal nature of the distribution of all of the $\delta^{34}S$ data (fig. P4). The $\delta^{34}S$ values for deposits in Precambrian metasedimentary rocks fall in between. Although analyses of shales barren of ore are needed, the data suggest that the large positive $\delta^{34}S$

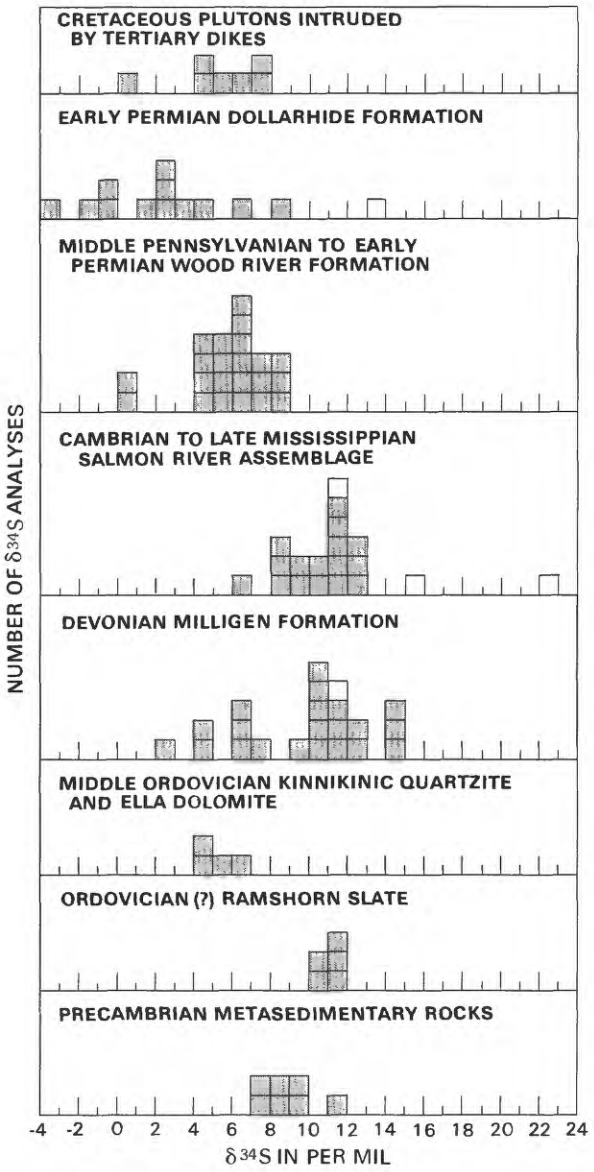

Figure P5. Distribution of $\delta^{34}S$ values in samples of sulfide and sulfate minerals from host rocks of many ages and lithologies. Unpatterned areas show samples considered to be of syngenetic or remobilized-syngenetic origin.

values for the deposits in the black shale reflect the ^{34}S-enriched sulfur-isotopic composition of the black shale itself. Seawater sulfate is the only source of sulfur that has contained such highly ^{34}S-enriched sulfur throughout geologic time (fig. P6; Claypool and others, 1980).

Some of this seawater sulfate was reduced to H_2S in the depositional environments of the black shales. Syngenetic-diagenetic sulfides, disseminated within the sediments or concentrated in lenses, likely had heavy sulfur-isotopic compositions that reflected the isotopic composition of the original sulfate. Disseminated pyrite is known from shale in the Challis and Hailey quadrangles, but no sulfur-isotopic analyses of this pyrite have been made. However, sedimentary pyrite from similar lower Paleozoic host rocks in central Nevada have heavy

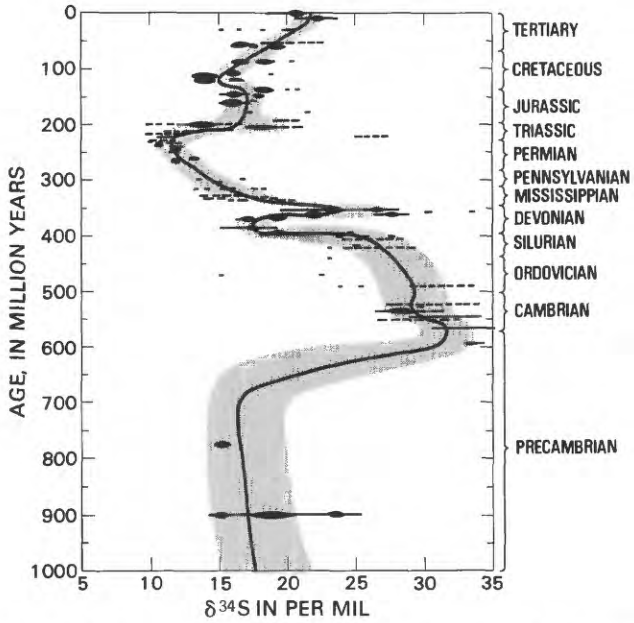

Figure P6. Variation with time in the $\delta^{34}S$ of sulfate in seawater. Dashed lines show the range of relatively few analyses. The heavy line is the best estimate for $\delta^{34}S$ of sulfate mineral in equilibrium with the world ocean surface sulfate of that date. The shaded area is the estimate of the uncertainly of this curve. From Claypool and others (1980).

$\delta^{34}S$ values, as much as +12 per mil (Rye and others, 1974). As noted earlier, sulfide lenses from syngenetic deposits have $\delta^{34}S$ values of +11 to +23 per mil. The seawater sulfate that was not reduced to H_2S may have been incorporated into evaporites and lenses of barite. Although there is no evidence of evaporites in the Challis and Hailey quadrangles, they were deposited on the cratonic shelf to the east. The single sulfate analysis is of a sample of stratabound barite from the Deer Creek deposit (fig. P1, no. 34; table P1) in the Early Permian Dollarhide Formation. Its $\delta^{34}S$ value of +13.2 per mil is nearly identical to that of Permian seawater sulfate (Claypool and others, 1980).

The relative depletion of ^{34}S in the deposits within carbonate rocks and quartzite probably indicates contributions of sulfur from sources more depleted of ^{34}S. These sources may be the carbonate and quartzite themselves, or they may be more deep seated, possibly magmatic, sources, which would typically have lighter sulfur-isotopic compositions (Ohmoto and Rye, 1979). Note the correspondence between the $\delta^{34}S$ values (fig. P5) of the deposits within the carbonate and quartzite, and those of the deposits within granite. Intermediate sulfur-isotopic compositions probably resulted from mixing of seawater sulfate with magmatic sulfur.

The $\delta^{34}S$ values trend lower as the age of the host rock decreases from Late Mississippian to Pennsylvanian to Early Permian (fig. P5). This trend is very similar to that of $\delta^{34}S$ values along the seawater sulfate curve (fig. P6) during this same period. This correspondence may indicate the decrease in $\delta^{34}S$ for seawater sulfate during the upper Paleozoic.

Some mining districts are isotopically inhomogeneous, although individual deposits within them commonly have very similar sulfur-isotopic compositions (table P4). This relationship suggests that the sulfur was homogenized isotopically before it was incorporated into individual deposits.

Table P4. Comparison of the homogeneity in sulfur-isotopic compositions of samples from selected districts and deposits
[Values in per mil]

District	Range in $\delta^{34}S$	Deposit	Range in $\delta^{34}S$
Bayhorse	18.7	Ramshorn	1.4
Boulder Creek	15.4	Livingston	1.5

CONCLUSIONS

Our preliminary interpretation of isotopic data from central Idaho indicates the following model. Cretaceous and Tertiary hydrothermal systems in central Idaho were dominated by meteoric water set into convective circulation by heat from granitic intrusions. Most of the sulfur in the mineral deposits associated with such systems was ^{34}S-enriched sulfur leached from shallow sedimentary sources, such as syngenetic-diagenetic sulfide minerals in sedimentary rocks, evaporite deposits, or pre-Cretaceous sulfide deposits. The sulfur then mixed locally in varying proportions with ^{34}S depleted sulfur from the magmatic reservoirs of adjacent plutons. This hybrid sulfur was then homogenized isotopically before reaching the sites of ore deposition. This model suggests that a wide variety of undiscovered mineral deposits may exist in central Idaho because of the large reservoir of sulfur available to the hydrothermal fluids. The most favorable targets appear to be those areas where granitic stocks intrude the extensive black-shale belt in the region.

REFERENCES CITED

Becker, R. H., and Clayton, R. N., 1976, Oxygen isotope study of a Precambrian banded iron-formation, Hamersley Range, western Australia: Geochimica et Cosmochimica Acta, v. 40, p. 1153–1165.

Borthwick, James, and Harmon, R. S., 1982, A note regarding ClF_3 as an alternative to BrF_5 for oxygen isotope analysis: Geochimica et Cosmochimica Acta, v. 46, p. 1665–1668.

Claypool, G. E., Holser, W. T., Kaplan, I. R., Sakai, Hitoshi, and Zak, Israel, 1980, The age curves of sulfur and oxygen isotopes in marine sulfate and their mutual interpretation: Chemical Geology, v. 28, p. 199–260.

Clayton, R. N., and Mayeda, T. K., 1963, The use of bromine pentafluoride in the extraction of oxygen from oxides and silicates for isotopic analysis: Geochimica et Cosmochimica Acta, v. 27, p. 43–52.

Cole, D. R., Ohmoto, Hiroshi, and Lasaga, A. C., 1983, Isotopic exchange in mineral-fluid systems. I. Theoretical evaluation of oxygen isotopic exchange accompanying surface reactions and diffusion: Geochimica et Cosmochimica Acta, v. 47, p. 1681–1693.

Criss, R. E., and Taylor, H. P., Jr., 1983, An $^{18}O/^{16}O$ and D/H study of Tertiary hydrothermal systems in the southern half of the Idaho batholith: Geological Society of America Bulletin, v. 94, p. 640–663.

Friedman, I. I., 1953, Deuterium content of natural water and other substances: Geochimica et Cosmochimica Acta, v. 4, p. 89–103.

Godfrey, J. D., 1962, The deuterium content of hydrous minerals from the east-central Sierra Nevada and Yosemite National Park: Geochimica et Cosmochimica Acta, v. 26, p. 1215–1245.

Hall, W. E., Rye, R. O., and Doe, B. R., 1978, Wood River mining district, Idaho—intrusion-related lead-silver deposits derived from country rock source: U.S. Geological Survey Journal of Research, v. 6, p. 579–592.

Hall, W. E., Schmidt, E. A., Howe, S. S., and Broch, M. J., 1984, The Thompson Creek, Idaho, porphyry molybdenum deposit—an example of a fluorine-deficient molybdenum granodiorite system, *in* Janelidze, T. V., and Tvalchrelidze, A. G., eds., Proceedings: Sixth Quadrennial International Association on the Genesis of Ore Deposits, Tbilisi, USSR 1982: E. Schweizerbart'sche Verlagsbuchhandlung, Stuttgart, v. 1, p. 349–357.

Matsuhisa, Yukihiro, Goldsmith, J. R., and Clayton, R. N., 1979, Oxygen isotopic fractionation in the system quartz-albite-anorthite-water: Geochimica et Cosmochimica Acta, v. 43, p. 1131–1140.

McCrea, J. M., 1950, On the isotopic chemistry of carbonates and a paleotemperature scale: Journal of Chemical Physics, v. 18, p. 849–857.

Ohmoto, Hiroshi, and Rye, R. O., 1979, Isotopes of sulfur and carbon, *in* Barnes, H. L., ed., Geochemistry of hydrothermal ore deposits, 2d ed.: New York, John Wiley and Sons, p. 509–567.

Rye, R. O., Doe, B. R., and Wells, J. D., 1974, Stable isotope and lead isotope study of the Cortez, Nevada, gold deposit and surrounding area: U.S. Geological Survey Journal of Research, v. 2, p. 13–23.

Rye, R. O., and Ohmoto, Hiroshi, 1974, Sulfur and carbon isotopes and ore genesis—a review: Economic Geology, v. 69, p. 826–842.

Taylor, H. P., Jr., 1979, Oxygen and hydrogen isotope relationships in hydrothermal mineral deposits, *in* Barnes, H. L., ed., Geochemistry of hydrothermal ore deposits, 2d ed.: New York, John Wiley and Sons, p. 236–277.

APPENDIX

Sulfur-isotope analyses of 100 sulfide-mineral samples and one sulfate-mineral sample, and sulfide-pair temperatures of mineralization, from 45 deposits in the Elk City, Challis, and Hailey 1°×2° quadrangles

[$\delta^{34}S$ values in per mil; $\Delta^{34}S = \delta^{34}S_a - \delta^{34}S_b$; temperatures in °C calculated from appropriate fractionation equations of Ohmoto and Rye (1979), ±45°C due to uncertainties in the fractionation equations and analyses of the sulfur-isotopic compositions of the sulfides. do., ditto; leaders (---), no calculations]

Sample No.	Location	Mineral	$\delta^{34}S$	$\Delta^{34}S$	Temperature
	Elk City quadrangle				
MB3-------	Blackbird mine, Blackbird district, Lemhi County	Chalcopyrite----	7.3	---	---
MB8-------	---do.----------	Cobaltite-------	8.1	---	---
	Challis quadrangle				
QC-138-82-	Quartz Creek prospect, Yellowpine district, Valley County.	Sphalerite------	9.1	---	---
QC-170-82-	---do.----------	---do.----------	11.0	---	---
QC-187-82A	---do.----------	---do.----------	9.0	---	---
QC-187-82B	---do.----------	---do.----------	8.9	---	---
F154------	Seafoam Lake prospect, Seafoam district, Custer County.	Galena----------	7.0	---	---
CT2-78----	Little Falls prospect, Grimes Pass district, Boise County.	Molybdenite-----	5.5	---	---
D9S3------	---do.----------	---do.----------	7.5	---	---
T117------	---do.----------	---do.----------	4.1	---	---
F112------	Carlson Gulch mine, Grimes Pass district, Boise County.	Galena----------	6.7	---	---
F107------	Comeback mine, Grimes Pass district, Boise County--	---do.----------	.8	---	---
79T22M----	Ramshorn mine, Bayhorse district, Custer County----	Tetrahedrite----	11.5	---	---
79T23M----	---do.----------	Galena----------	10.1	---	---
79T24M----	---do.----------	Chalcopyrite----	11.3	---	---
T108------	Beardsley Gulch mine, Bayhorse district, Custer County.	Galena----------	11.4	---	---
D6S1------	Pacific mine, Bayhorse district, Custer County-----	---do.----------	10.1	---	---
SWH52-76--	Rattlesnake Creek prospect, Bayhorse district, Custer County.	---do.----------	4.2	---	---
Buckskin--	Buckskin mine, Bayhorse district, Custer County----	---do.----------	6.8	---	---
SWH152-76-	Thompson Creek mine, Bayhorse district, Custer County.	Molybdenite-----	11.4	---	---
CT3-78----	---do.----------	Pyrite----------	9.6	---	---
CT4-78----	---do.----------	---do.----------	9.9	---	---
CT4-78----	---do.----------	Arsenopyrite(?)-	10.4	---	---
S-27-747--	---do.----------	Molybdenite-----	11.3	---	---
S-27-747--	---do.----------	Pyrite----------	12.1	---	---
S-27-770--	---do.----------	Molybdenite-----	10.3	---	---
S-27-789--	---do.----------	---do.----------	11.9	---	---
S-76-895--	---do.----------	Galena----------	8.7	---	---
NN1-551---	---do.----------	Sphalerite------	22.9*	---	---
NN1-951---	---do.----------	Pyrite----------	11.3*	---	---
SWH120-79-	Rob Roy mine, Bayhorse district, Custer County-----	Galena----------	6.6	---	---
SWH154-76-	Dryden mine, Bayhorse district, Custer County------	Galena, coarse--	5.4	---	---
SWH154-76-	---do.----------	Galena, steel---	4.6	---	---
Buckskin drill road.	Roadcut between Buckskin and Thompson Creek mines, Bayhorse district, Custer County.	Galena----------	8.7	---	---
D863A-----	Hoodoo mine, Boulder Creek district, Custer County-	Sphalerite------	15.6*	---	---
T135L-1---	Livingston mine, Boulder Creek district, Custer County.	---do.----------	12.5	---	---
T135L-1---	---do.----------	Jamesonite(?)---	11.4	---	---
80T2------	---do.----------	Galena+minor jamesonite.	11.1	---	---
80T2B-----	---do.----------	Sphalerite------	12.6	---	---
R558------	Willow Lake prospect, Boulder Creek district, Custer County.	Molybdenite-----	8.2	---	---
D851------	Little Boulder Creek prospect, Boulder Creek district, Custer County.	---do.----------	8.7	---	---
D851-1----	---do.----------	---do.----------	6.1	---	---
W190------	---do.----------	Pyrite----------	5.7	---	---
W312A-----	---do.----------	Galena----------	4.0	2.04	322
W312B-----	---do.----------	Sphalerite, black	6.0	---	---
W312C-----	---do.----------	Galena----------	0.2	---	---
W313A-----	---do.----------	Pyrite----------	5.1	---	---
W313B-----	---do.----------	Sphalerite, red-	5.9	---	---
W313C-----	---do.----------	Arsenopyrite----	7.0	---	---
W313C-----	---do.----------	Sphalerite, black	6.4	---	---
CT1-78----	---do.----------	Molybdenite-----	8.6	---	---
T70-------	Silver Dollar prospect, East Fork district, Custer County.	Pyrite----------	8.3	---	---

APPENDIX—Continued.

Sulfur-isotope analyses of 100 sulfide-mineral samples and one sulfate-mineral sample, and sulfide-pair temperatures of mineralization, from 45 deposits in the Elk City, Challis, and Hailey 1°×2° quadrangles

[$\delta^{34}S$ values in per mil; $\Delta^{34}S = \delta^{34}S_a - \delta^{34}S_b$; temperatures in °C calculated from appropriate fractionation equations of Ohmoto and Rye (1979), ±45°C due to uncertainties in the fractionation equations and analyses of the sulfur-isotopic compositions of the sulfides. do., ditto; leaders (---), no calculations]

Sample no.	Location	Mineral	$\delta^{34}S$	$\Delta^{34}S$	Temperature
	Hailey quadrangle				
79T565M---	Unnamed prospect, Galena district, Blaine County	Galena----------	7.6	---	---
D807A-----	Unnamed prospect, Boulder Basin district, Blaine County.	---do.----------	4.5	3.29	284
D807B-----	----do.----------	Pyrite----------	7.8	---	---
D807D-----	----do.----------	Stannite--------	6.2	---	---
79T580M---	Golden Glow mine, Boulder Basin district, Blaine County.	Galena----------	6.8	---	---
T302M-----	Webfoot mine, Vienna district, Blaine County-------	---do.----------	4.2	1.83	355
T302M-----	----do.----------	Sphalerite------	6.0	---	---
76T31-----	GAF prospect, south of Vienna district, Camas County	Galena----------	0.2	---	---
76T31-----	----do.----------	Sphalerite------	0.3	---	---
E758B-----	Rooks Creek prospect, Boyle Mountain district, Blaine County.	Galena----------	4.7	---	---
T49M------	Unnamed prospect, Boyle Mountain district, Blaine County.	---do.----------	5.0	---	---
T9T10M----	Upper prospect, Carrietown district, Camas County--	---do.----------	2.8	---	---
79T10AM---	----do.----------	Molybdenite-----	3.4	---	---
79T10AM---	----do.----------	Sphalerite------	6.2	---	---
D784------	Dump, Carrietown district, Camas County----------	Galena----------	-0.4	2.43	375
D784------	----do.----------	Pyrite----------	2.0	---	---
E880-1----	Horn Silver mine, Carrietown district, Camas County	---do.----------	4.3	---	---
T81M------	----do.----------	Galena----------	1.2	---	---
T68M------	Carrie Leonard mine, Carrietown district, Camas County.	---do.----------	-0.1	2.46	269
T68M------	----do.----------	Sphalerite------	2.4	---	---
E786------	Panther Gulch prospect, Blaine County----------	Galena----------	8.8	---	---
E684------	Red Cloud mine, Wolftone district, Blaine County---	---do.----------	-1.0	---	---
E684A-----	----do.----------	Sphalerite------	-3.5	---	---
D831A-----	Deer Creek mine, Wood River district, Blaine County	Barite----------	13.2*	---	---
WH-70-13B-	Eureka mine, Wood River district, Blaine County-----	Galena----------	6.3	---	---
A-176-----	Liberty Gem mine, Wood River district, Blaine County	---do.----------	2.2	2.17	243
A-176-----	----do.----------	Chalcopyrite----	4.4	---	---
A-176-----	----do.----------	Pyrite----------	4.3	---	---
A-227-----	Treasure Vault mine, Wood River district, Blaine County.	Galena----------	4.0	3.20	291
A-227-----	----do.----------	Pyrite----------	7.2	---	---
WH-70-6---	Silver Star Queen mine, Wood River district, Blaine County.	Galena----------	10.8	---	---
WH-70-6---	----do.----------	Bournonite------	12.6	---	---
WH-70-7---	----do.----------	Galena----------	11.2	---	---
WH-70-7---	----do.----------	Bournonite------	12.6	---	---
WH-70-11--	----do.----------	Galena----------	12.0	2.66	248
WH-70-11--	----do.----------	Sphalerite------	14.6	---	---
WH-70-16--	----do.----------	Galena----------	10.7	3.36	191
WH-70-16--	----do.----------	Sphalerite------	14.0	---	---
WH-70-17--	Silver Star Queen mine, Wood River district, Blaine County.	Galena----------	11.0	3.11	209
WH-70-17--	----do.----------	Sphalerite------	14.1	---	---
A-36------	----do.----------	Galena----------	10.8	---	---
A-43------	Minnie Moore mine, Wood River district, Blaine County.	---do.----------	6.1	---	---
WH-70-12--	Dennison mine, Wood River district, Blaine County--	---do.----------	10.9	---	---
WH-74-2B--	North Star mine, Wood River district, Blaine County	---do.----------	7.2	2.29	289
WH-74-2B--	----do.----------	Sphalerite------	9.5	---	---
S47H------	Triumph mine, Wood River district, Blaine County---	---do.----------	11.3*	---	---
WH-74-1B--	Independence mine, Wood River district, Blaine County.	Galena----------	11.4	---	---
D247------	Trail Creek prospect, Wood River district, Blaine County.	---do.----------	6.7	---	---
T597M-----	Leke Creek-Trail Creek prospect, Wood River district, Blaine County.	---do.----------	0.4	---	---

* Analyeis of eample from deposit thought to be of syngenetic or remobilized-syngenetic origin.

Symposium on the Geology and Mineral Deposits of the Challis 1°×2° Quadrangle, Idaho

Chapter Q

Depositional Controls of Breccia-Fill and Skarn Tungsten Deposits in the Challis Quadrangle

By THERESA M. COOKRO

CONTENTS

FIGURES

Abstract

Breccia-fill and skarn tungsten deposits within the Challis quadrangle have been mined for tungsten, antimony, gold, and silver. The Yellow Pine mine, with characteristic breccia-fill textures, produced 800,000 units of WO_3, 100,000 ounces of gold, and 600,000 ounces of silver. The ore had an average grade of 1.6 percent WO_3. The Springfield mine, a skarn deposit, produced 6,000 units of WO_3 from an unknown grade of ore. Knowledge of several of the recognized depositional controls can be used in exploration for new deposits.

The breccia-fill deposits are within the Idaho batholith and localized where regional shear zones trending north to N. 20° E. intersect local faults trending N. 30°–60° E. that branch from the main shear zone. The mineralized fracture fillings reveal continued brecciation of the rock throughout the time of metal deposition. The breccia was mineralized in three stages which produced: early dissemination of arsenopyrite in the batholith, then quartz-scheelite veins, and later stibnite veins. The three stages are not distinct but grade into one another. The veins are fillings in either extensional fractures or between the breccia clasts of the batholith, or in cavities resulting from the dissolution of feldspar grains. Where the quartz-scheelite veins are in contact with carbonate inclusions in the batholith, replacement textures are prominent. The precious-metal history of these deposits is uncertain. Gold may have been deposited continually throughout the three stages of mineralization, and some silver is reported in stibnite, a late-forming mineral.

Skarn deposits formed at the contact of Upper Cretaceous biotite granodiorite plutons with carbonate-rich Paleozoic and possibly Precambrian metasedimentary rocks. The granodiorite related to the skarn is typical of plutons of the Idaho batholith and White Cloud stock and not typical of the younger Tertiary intrusive rocks. The skarn deposits in the south-central part of the quadrangle are structurally just below thrust faults that are cut by the Idaho batholith. Scheelite in the skarns occurs along bedding planes, within high-angle fault zones, as disseminations, and locally associated with pyrrhotite-bearing veins and replacement sulfide minerals.

INTRODUCTION

The Challis quadrangle contains about 50 tungsten mines and prospects (fig. Q1) that can be grouped into at least three types of occurrences: breccia-fill, skarn, and stockwork. Breccia-fill deposits are within north-striking regional shear zones in the Idaho batholith where minor faults branch from the main shear zones. The granodiorite of the batholith locally contains metasedimentary inclusions; remobilized calcite from these inclusions is common in the breccia-fill deposits. Scheelite is more concentrated where quartz veins containing scheelite are in contact with the carbonate, especially the remobilized calcite. The Yellow Pine and Quartz Creek mines are breccia-fill deposits with carbonate-rich metasedimentary inclusions. The Yellow Pine mine produced tungsten, antimony, gold, and silver (Cooper, 1951), and the Quartz Creek mine sporadically produced tungsten until 1982. Gold, silver, arsenic, mercury, and antimony have been found in several of the deposits, and manganese oxides are ubiquitous.

Skarn deposits are abundant within the Challis quadrangle, and several have produced small amounts of tungsten. The tungsten skarns are at the contact of carbonate-rich Paleozoic and possibly Precambrian metasedimentary rocks with the Idaho batholith. Thrust faults are structurally just above most of the deposits; higher grades of ore are associated with steep faults within the deposits. The skarns are characterized by diopside-hedenbergite, garnet, scheelite, quartz, and feldspar. The sulfide-mineral content of the deposits varies but pyrrhotite is very common. The Springfield, Tungsten Jim, and Meadowview mines, the Emma and Flintstone groups, and an occurrence in Hennessy Meadows are examples of tungsten skarns.

The Red Mountain occurrence, north of the town of Yellow Pine, and the Little Boulder Creek deposit in the White Cloud Peaks are two stockwork deposits with associated tungsten. They were described by Leonard (1983) and Cavanaugh (1979), respectively. The stockwork-type deposit is not discussed in this chapter. Judging from the mining history of the quadrangle, the breccia-fill and skarn deposits (fig. Q2) have the best potential for future discovery and development of tungsten resources.

BRECCIA-FILL DEPOSITS

The breccia-fill deposits are within a major north- to northeast-trending system of shear zones in the Idaho batholith. The shear zones are several kilometers wide and extend approximately from northeast of Garden Valley through the Yellow Pine area and north of the quadrangle. The shear zones are prominent features of the western one-fourth of the Challis quadrangle. The deposits are in fault breccias where more local faults striking N. 30°–60° E. branch from the north-striking shear zones. In the brecciated areas of granodiorite, the rock is vuggy and highly silicified.

The north- to northeast-trending shear zones are shown on the geologic map of the Challis quadrangle (Fisher and others, 1983) in two ways:

1. In the northwestern part of the quadrangle the shear zones are mapped as unit Tsi, which, according to B. F. Leonard (written commun., 1984) is "Silicified zones in granitic rocks of the Idaho batholith. Silicified zones are related to ring fractures of the Thunder Mountain cauldron complex and to attendant superposed north-striking shear zones." In some regions the batholithic rocks were replaced almost completely by silica considered by Leonard to be Tertiary in age.

2. Elsewhere on the map the regional shear zones are shown as prominent north-striking faults. The north-striking faults in the batholithic terrane are zones of intense shearing and silicification.

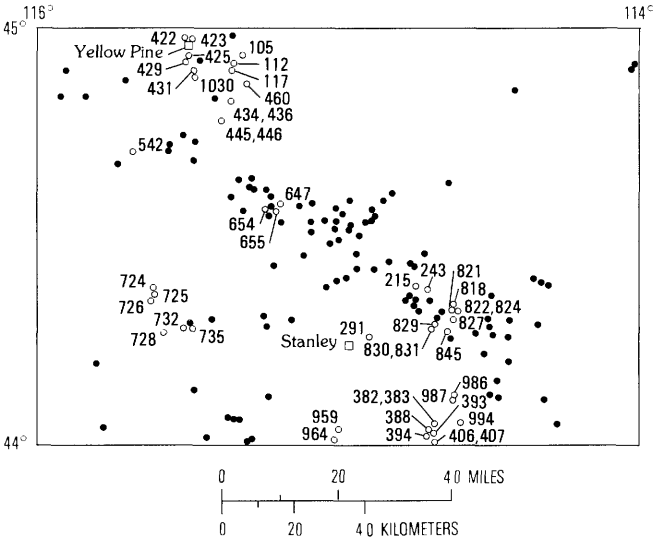

MINES AND PROSPECTS

105	Peterson prospect	654	Muskeg Creek
112	Yellow Pine mine	647	Chuck Creek
117	Sulfide No. 10 prospect	655	Soldier Creek
215	Bonanza mine	724	Horsefly prospect
243	McClure prospect	725	Merry Blue prospect
291	McClure No. 4	726	Wilson Creek
382	Fourth of July deposit	728	White Hawk Meadows
383	Deer Trail mine	732	White Hawk Mountain
388	Red Robin No. 3 prospect	735	BE&L
393	Meadowview prospect	818	Scheelite Nellie, Nelvinny
394	Washington Peak mine		Nos. 1 - 4
406	Reconstruction vein	821	Tungsten Jim mine
407	Washington Basin deposit-Empire	822	Buckskin claims
		824	Greyhound Ridge
422	Warner Gold (W group)	827	Salmon River Scheelite
423	Quartz Creek, Cinnabar	829	Peach Creek No. 2
425	Golden Gate occurrence	830	Patricia Ann occurrence
429	Johnson Creek area	831	Peach Creek W claims
431	Emma group	845	Flintstone Group
434	Copper Mountian prospect	959	Cramer Lakes prospect
436	Big Chief Scheelite	964	Hidden Lake prospect
445	Old Faithful Group mine	986	Sheelite occurrence
446	Springfield mine	987	McClure No. 6 claim
460	Mule Train claims	994	Boulder Creek Prospect
542	Tungsten Point	1030	Hennessy Meadows occurrence

Figure Q1. Map showing localities of tungsten mines and prospects (open circles) and stream-sediment samples containing more than 50 ppm tungsten (solid circles), Challis quadrangle. Modified from Mitchell and others (1981) and Callahan and others (1981), respectively.

Whether or not the regional shear zones are mapped as silicified zones or regional faults, they are broad areas of shearing that contain large amounts of secondary quartz. The silica enrichment of the batholith is especially present where local faults branch off the north-trending shear zones. These intersections commonly form a topographic bulge or mound and contain breccia-fill tungsten deposits. The intersecting faults may be second-order faults that formed in dilated zones, similar to the structure at the Henderson 2 mine in Quebec (Guha and others, 1983).

The Idaho batholith, consisting mostly of biotite granodiorite, is strongly altered and brecciated in the regions of shearing. It is vuggy and appears finer grained than other parts of the batholith due to the influx of fine-grained secondary silica; it contains secondary feldspar veins and sericite is common. The alteration of biotite to

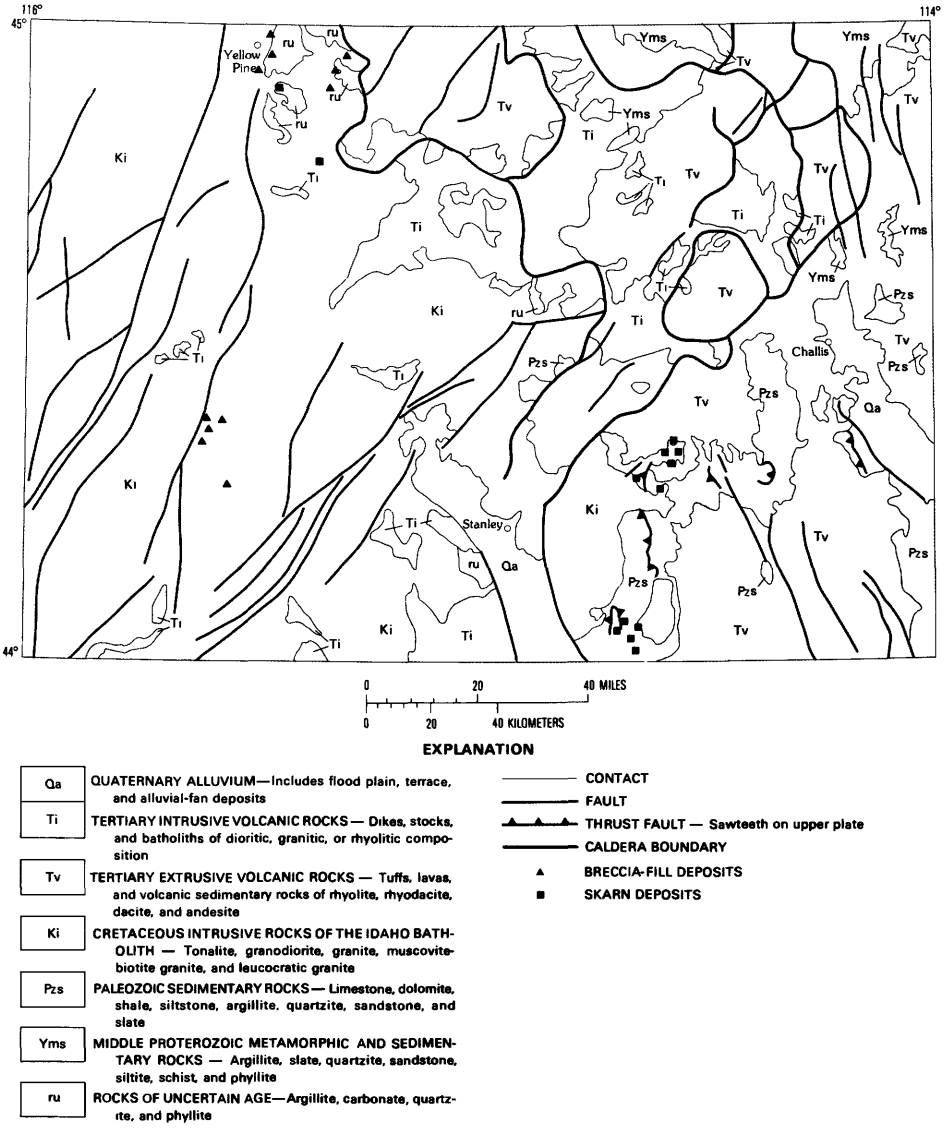

Figure Q2. Map showing locations of breccia-fill and skarn deposits in the Challis quadrangle. Each symbol represents one or more tungsten occurrences or mines. Modified from Fisher (fig. A2, chap. A, this volume).

chlorite and fine-grained oxide minerals, and of feldspars to clay gives the normally speckled granodiorite a uniform light-brown to cream-colored appearance. The primary igneous texture was gradationally lost due to silicification. The batholith contained roof pendants and large inclusions of Paleozoic and Precambrian metasedimentary rocks that were incorporated in the breccia of the shear zones. Remobilized calcite forms veins and broken blocks in the breccia, probably having originated from those inclusions or roof pendants of carbonate metasedimentary rocks within the batholith before brecciation. The remobilized calcite is often extensively replaced by scheelite.

The breccia is both clast and matrix supported; the matrix-supported breccia has higher grades of tungsten. The breccia clasts are not sorted, and the size of the fragments is highly variable. Variations in structure of the breccias can be seen in samples from the Quartz Creek, Yellow Pine, and Golden Gate mines. The intense silicification tends to mask the fragmental structure of the breccias, and in many samples only ultraviolet light shows the brecciated texture, with scheelite and quartz filling in between and outlining the breccia fragments (figs. Q3–Q5). At the Quartz Creek mine the batholith has been mostly crackled, meaning the rock is broken but with only slight rotation of clasts. The Yellow Pine mine has more strongly rotated clasts, but in many places these can be pieced back together in a jigsaw-puzzle fashion. Breccia at the Golden Gate mine is more chaotic and has randomly oriented clasts.

Vugs in areas of silicified batholithic rocks range widely in size, depending on their origin. Several processes formed the vugs: (1) extensional fracturing provided open spaces that range from about 0.3 to 1 m long and that may be partly or wholly filled by secondary materials;

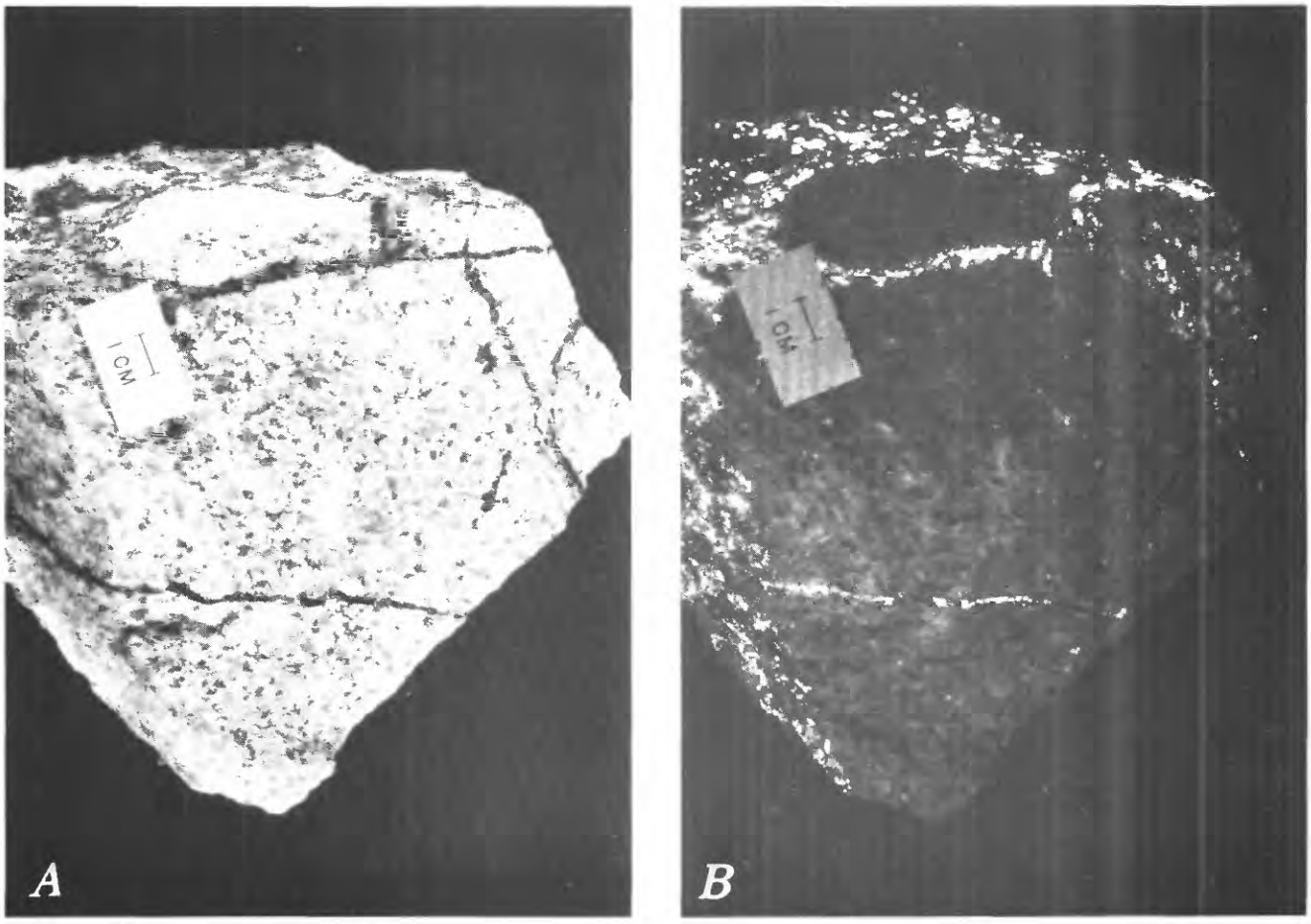

Figure Q3. Sample of tungsten ore from Quartz Creek mine, Challis quadrangle. *A*, sample in ordinary light showing crackle breccia with infillings of remobilized calcite, quartz, and scheelite. *B*, sample in ultraviolet light showing fluorescing scheelite.

(2) leaching of feldspar grains (especially potassium feldspar megacrysts) formed smaller cavities, averaging 5–10 mm across, that later were filled; and (3) leaching of materials between breccia clasts formed vugs of variable sizes that now contain quartz and scheelite.

Cooper (1951) recognized three stages of mineralization at the Yellow Pine mine that could have been partly true for other breccia-fill deposits: (1) dissemination of arsenopyrite and gold; (2) formation of scheelite-quartz veins; and (3) formation of stibnite-silver veins. Cooper favored a replacement origin for most of the scheelite, although he recognized that the scheelite was most abundant in material between rock fragments or breccia clasts. I think that the primary mechanism for introduction of scheelite was in quartz that filled openings within the breccia. Where quartz-scheelite veins are in contact with carbonate rocks or remobilized calcite, scheelite deposits developed by replacement of the carbonate.

At the Quartz Creek mine, Petersen (1984) also found similar evidence for the three stages of mineralization. Gold at Quartz Creek may have been deposited throughout all the stages. In addition to the gold in arsenopyrite at Quartz Creek, Petersen found gold within a late-stage stibnite vein. At least two generations of both scheelite-quartz and stibnite veins show evidence of continued fracturing during mineralization.

Three types of scheelite occurrences are in the breccia-fill deposits: (1) quartz-scheelite veins, (2) replacement of carbonate clasts and remobilized vein carbonate, and (3) fine, powdery coatings on manganese oxides. At the contacts of quartz-scheelite veins and carbonate-rich clasts, some euhedral to subhedral scheelite crystals replace carbonate on the margins of the clasts. At the contacts of quartz-scheelite veins and remobilized calcite, there is massive replacement of calcite with scheelite. The replacement crystals of scheelite commonly have better defined crystal form and are larger than the scheelite crystals in the quartz veins. In some places tiny clay-size crystals of scheelite have formed on the manganese oxides within vugs and on fracture surfaces.

SKARN DEPOSITS

The tungsten-bearing skarn deposits are dark green to light gray, medium to coarse grained, granoblastic, and

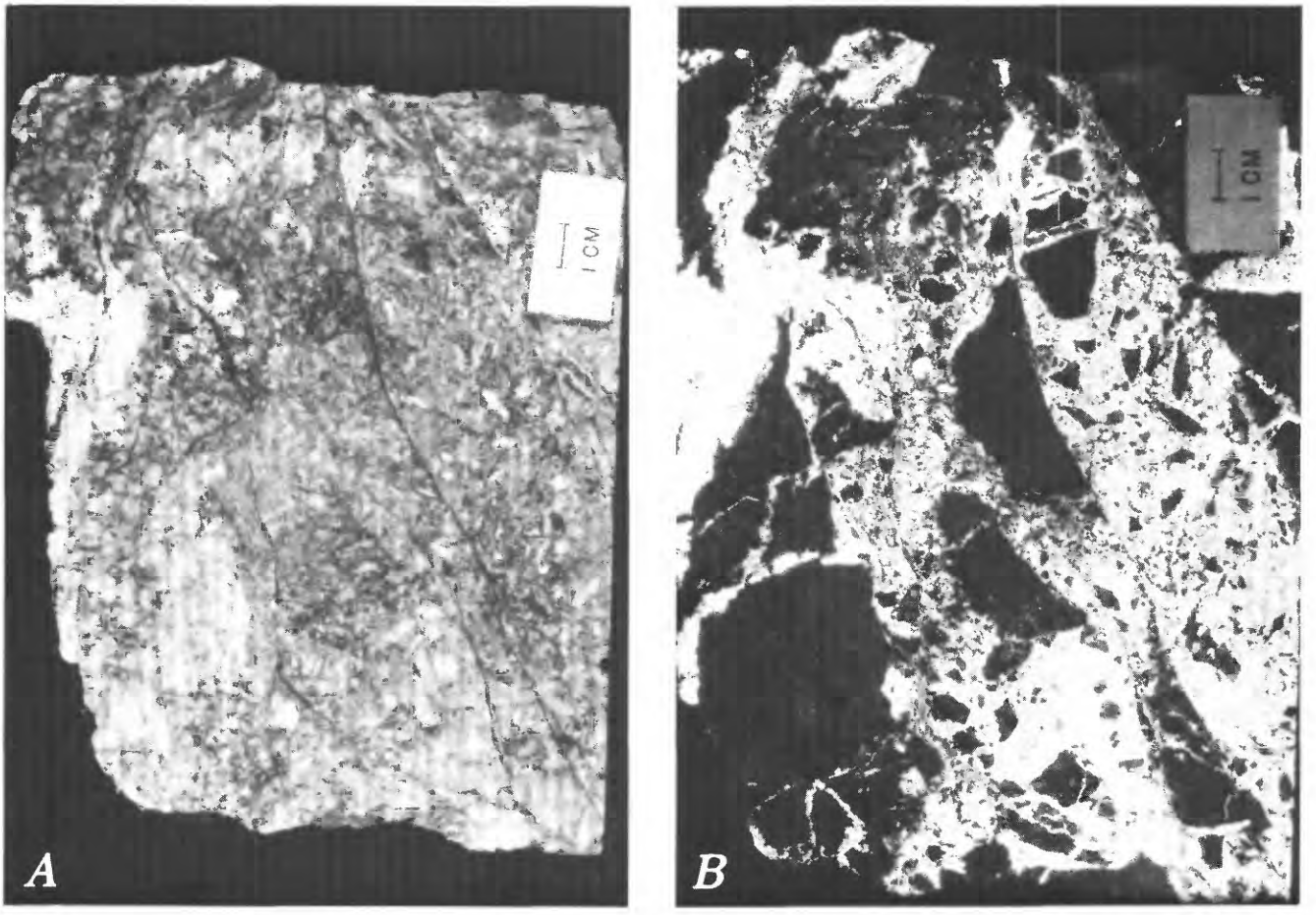

Figure Q4. Sample of tungsten ore from the Yellow Pine mine, Challis quadrangle. *A*, in ordinary light. *B*, in ultraviolet light, showing fluorescing scheelite. Breccia fragments (black) can be seen more clearly in ultraviolet light than in ordinary light.

slightly foliated. Minerals are xenoblastic and include diopside-hedenbergite, plagioclase, quartz, potassium feldspar, biotite, sphene, calcite, garnet, chlorite, epidote, and sericite. Scheelite is the tungsten-bearing mineral. Pyrrhotite, pyrite, arsenopyrite, chalcopyrite, sphalerite, magnetite, ilmenite, galena, jamesonite, stannite, gold, bismuth, and bismuthinite also may be present. Scheelite occurs as disseminations throughout the skarn; it is also controlled by bedding planes and fracture zones. The pyrrhotite-rich zones of sulfide-bearing veins and replacement deposits commonly contain scheelite.

The skarn deposits are in carbonate-bearing beds of Paleozoic and Precambrian metasedimentary rocks where they are in contact with Cretaceous plutons. In the south-central part of the Challis quadrangle the principal Paleozoic host-rock units are the Salmon River assemblage (Mississippian to Cambrian), the Grand Prize Formation (Permian), and the Wood River Formation (Pennsylvanian and Permian) (fig. Q6). A detailed description of these rocks is given by Hall (chap. J, this volume). Because of its small scale, figure Q6 shows skarn deposits as occurring within the batholith or volcanic rocks. Those deposits are either in roof pendants of the batholith or in erosional windows in the volcanics where Paleozoic rocks are exposed. In the northwestern part of the quadrangle the skarns are in Precambrian metasedimentary rocks mapped by B. F. Leonard (unpub. mapping, 1982). The specific Precambrian metasedimentary units are uncertain.

Tungsten skarns in the south-central part of the quadrangle are structurally just below thrust faults that are cut by the Upper Cretaceous Idaho batholith. The thrust faults seem to have controlled late-phase intrusions of the batholith (W. E. Hall, oral commun., 1982). Breccias within high-angle fault zones commonly have greater amounts of scheelite than unfaulted areas. Also, some mine raises follow the steep faults, suggesting former high-grade ore pockets along them. The high-angle faults are not necessarily related to thrust zones.

At the contact with the metasedimentary rocks, the Cretaceous intrusive rocks, including the Idaho batholith and the White Cloud stock, range in composition from

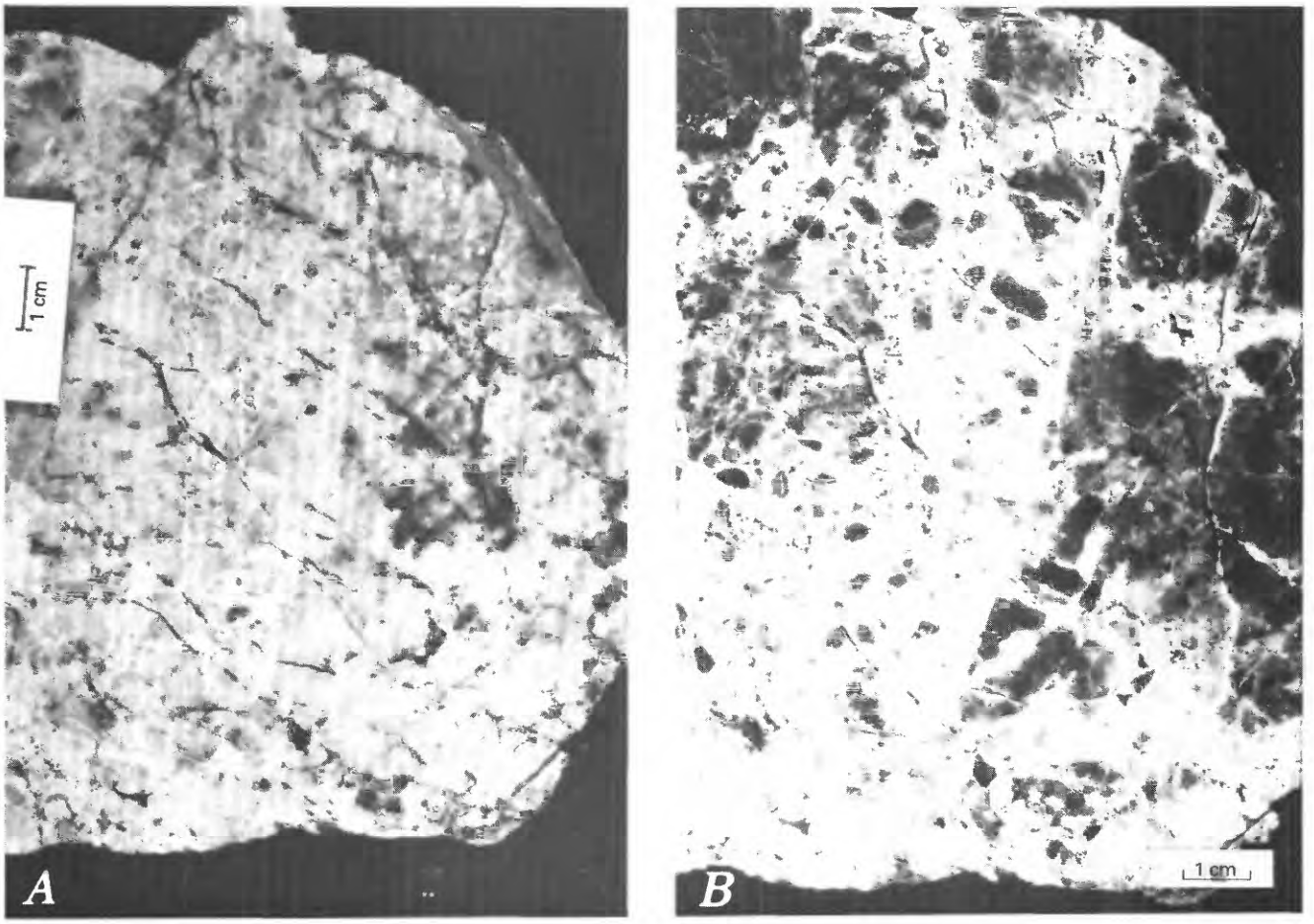

Figure Q5. Sample of tungsten ore from the Golden Gate mine, Challis quadrangle. Brecciation at this mine is extremely difficult to see in hand sample. *A*, in ordinary light. *B*, in ultraviolet light, which shows the breccia clasts not seen in ordinary light.

granite to granodiorite. Biotite within the intrusive bodies near the skarn is often completely altered to a mixture of chlorite and oxide minerals. Most of the tungsten-bearing skarns are heavily chloritized. The Cretaceous intrusions locally contain potassium feldspar veins in contact with potassium feldspar megacrysts. The 1–3 cm long megacrysts are porphyroblasts that incorporate minerals formed earlier such as biotite, quartz, and primary feldspars. In a few areas metasomatism seems to have enhanced the ore grade.

Skarns in the central part of the Challis quadrangle are the Tungsten Jim mine (fig. Q7), the Meadowview prospect, and the Flintstone claim group on Beaver Creek. In the northwestern part of the quadrangle the Springfield mine produced 6,000 units of WO_3 from ore of unknown grade (Cater and others, 1973). Other skarn deposits are the Hennessy Meadows occurrence and the Emma group. See figures Q1 and Q6 for location of deposits.

REFERENCES CITED

Cater, F. W., Pinckney, D. M., Hamilton, W. B., Parker, R. L., Weldin, R. D., Close, T. J., and Zilka, N. T., 1973, Mineral resources of the Idaho Primitive Area and vicinity, Idaho, *with a section on the* Thunder Mountain district, by B. F. Leonard *and a section on* Aeromagnetic interpretation, by W. E. Davis: U.S. Geological Survey Bulletin 1304, 431 p.

Callahan, J. E., Cooley, E. F., and Neuerburg, G. J., 1981, Selected Mo and W assays from stream-sediment samples and panned heavy-mineral concentrates, Challis, Idaho 2° topographic quadrangle: U.S. Geological Survey Open-File Report 81–1344, 13 p.

Cavanaugh, Patrick, 1979, Geology of the Little Boulder Creek (White Cloud) molybdenum deposit, Custer County, Idaho: Missoula, University of Montana Ph.D. dissertation, 100 p.

Cooper, J. R., 1951, Geology of the tungsten, antimony and gold deposits near Stibnite, Idaho: U.S. Geological Survey Bulletin 969–F, p. 151–197.

Fisher, F. S., McIntyre, D. H., and Johnson, K. M., 1983, Geologic map of the Challis 1°×2° quadrangle, Idaho: U.S. Geological Survey Open-File Report 83–523, 39 p., 2 maps, scale 1:250,000 (also available from the Idaho Bureau of Mines and Geology).

Guha, Jayanta, Archamibault, G., and Leroy, J., 1983, A correlation between the evolution of mineralizing fluids and the geomechanical development of a shear zone as illustrated by the Henderson 2 mine, Quebec [Canada]: Economic Geology, v. 78, no. 8, p. 1605–1618.

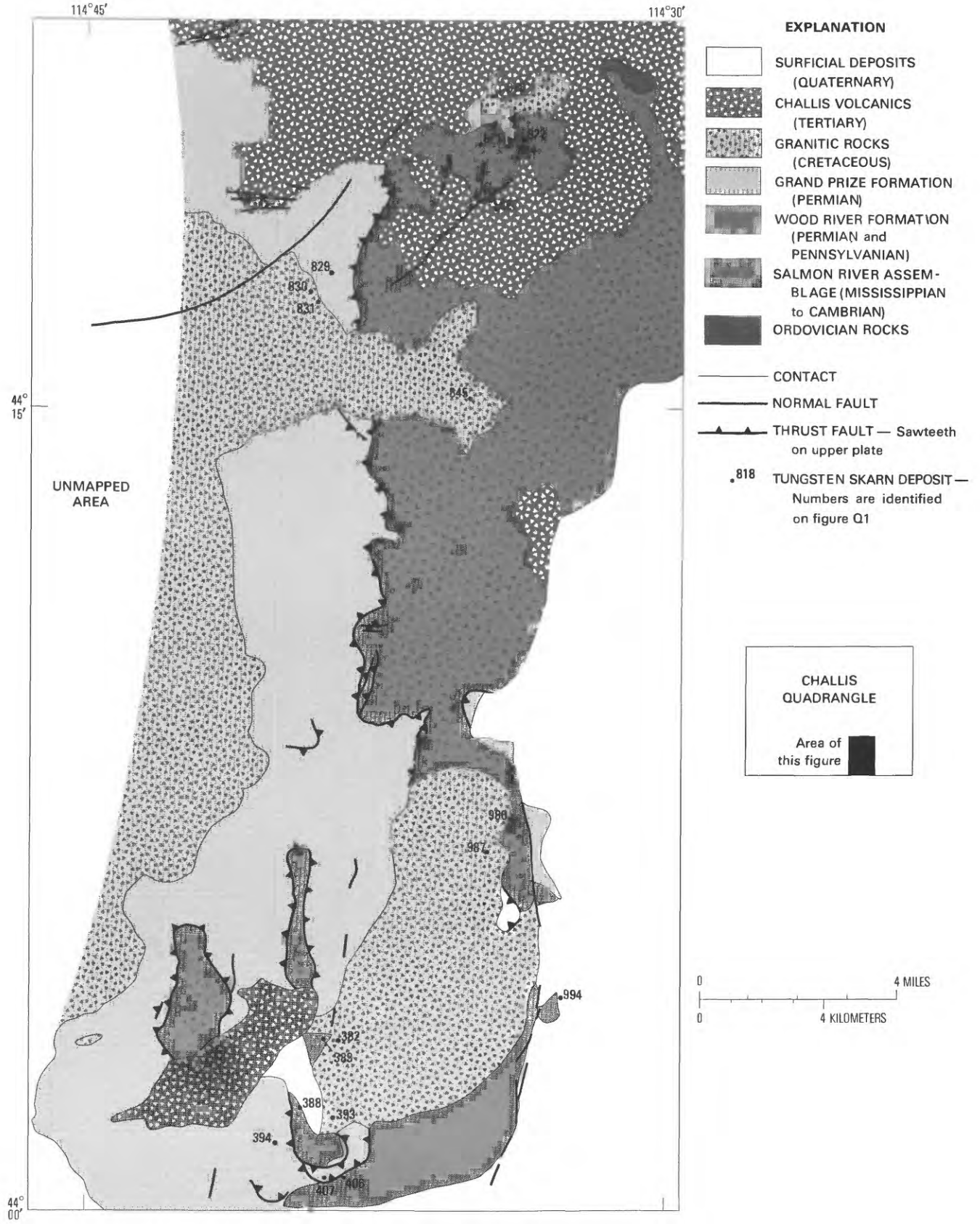

Figure Q6. Simplified geologic map showing the south-central cluster of tungsten skarn deposits east of Stanley, Idaho. Modified from Fisher and others (1983) and unpublished mapping of W. E. Hall and S. W. Hobbs (1983).

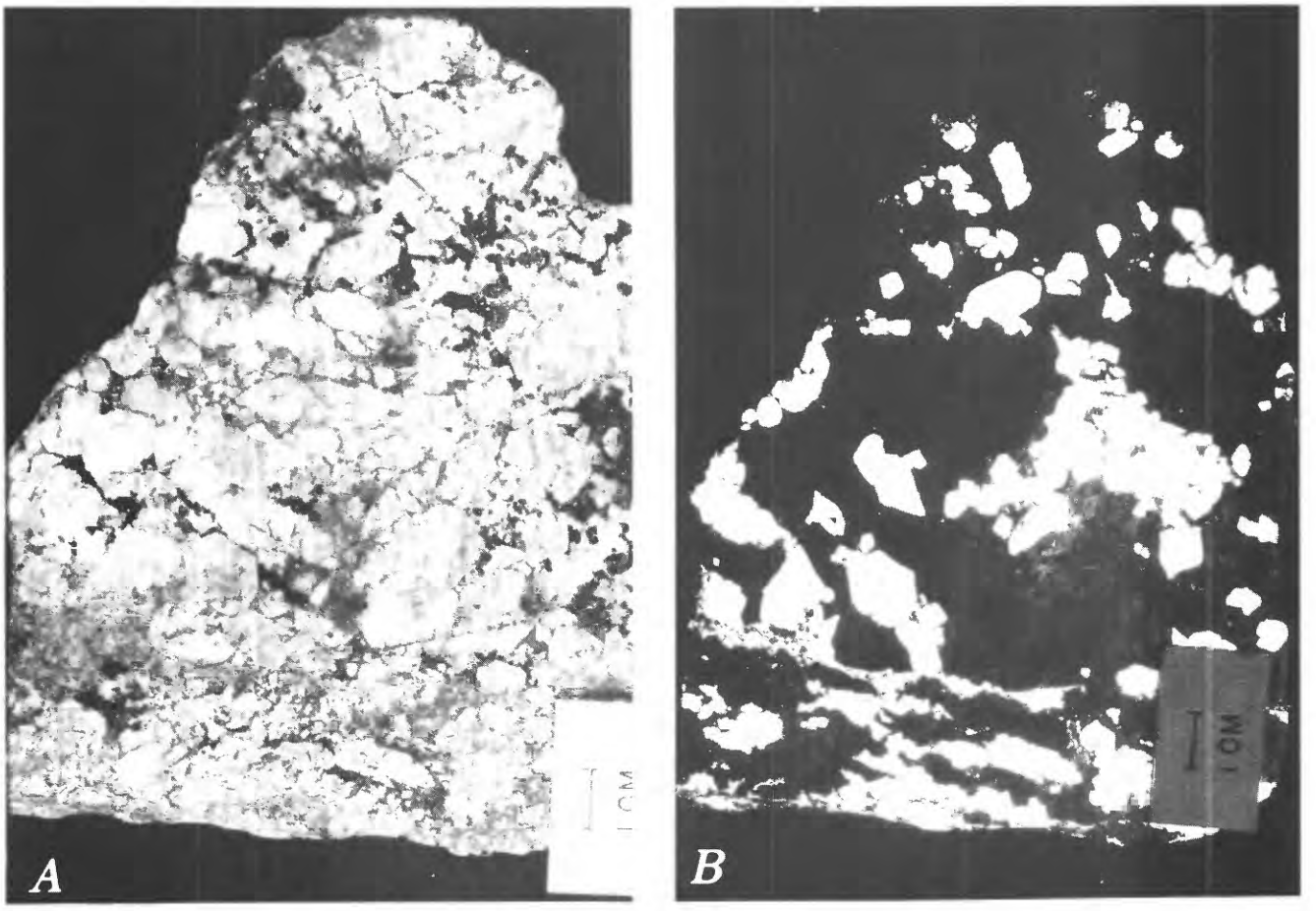

Figure Q7. Sample of ore from the Tungsten Jim mine, Challis quadrangle. *A*, in ordinary light. *B*, in ultraviolet light, showing fluorescing scheelite.

Leonard, B. F., 1983, The Golden Gate tungsten deposit and metal anomalies in nearby soils and plants, Yellow Pine district, Valley County, Idaho: U.S. Geological Survey Open-File Report 83–835, 26 p.

Mitchell, V. E., Strowd, W. B., Hustedde, G. S., and Bennett, E. H., 1981, Mines and prospects of the Challis quadrangle, Idaho: Idaho Bureau of Mines and Geology, Mines and Prospects Map Series, 47 p., 1 map, scale 1:250,000.

Petersen, M. A., 1984, Geology and mineralization at the Quartz Creek tungsten mine, Yellow Pine, Idaho: Kent, Ohio, Kent State University M.S. thesis, 80 p.

Symposium on the Geology and Mineral Deposits of the Challis 1°×2° Quadrangle, Idaho

Chapter R

Stratabound Cobalt-Copper Deposits in the Middle Proterozoic Yellowjacket Formation in and Near the Challis Quadrangle

By PETER J. MODRESKI

CONTENTS

FIGURES

TABLES

Abstract

Stratabound cobalt-copper-iron deposits occur within the Middle Proterozoic Yellowjacket Formation in the northeastern corner of the Challis 1°×2° quadrangle. These deposits form the southern end of the northwest-trending Idaho cobalt belt, which contains the currently inactive Blackbird mine, the major cobalt deposit in North America. The deposits in this belt consist of stratabound sulfide and arsenide minerals (pyrite, chalcopyrite, cobaltite, pyrrhotite, and arsenopyrite) in argillaceous quartzite. The ore minerals were recrystallized and remobilized to varying degrees during metamorphic and orogenic events that are inferred to have taken place mainly in Precambrian time. The metamorphic grade of the Yellowjacket Formation is lower greenschist facies within most of the Challis quadrangle but increases to the north and west. The metals appear to have been incorporated into the sediments syngenetically and represent a sea-floor exhalative, distal-volcanogenic process of mineralization. The source of the metals was probably related to the volumetrically minor basaltic volcanism in the basin.

The mineralized rock within the Challis quadrangle is along the North Fork of Iron Creek, where the Little No-Name mine explored strata containing chalcopyrite and cobaltiferous pyrite. Adjacent strata, which are high in magnetite and contain minor disseminated sulfide minerals, appear to have been deposited in a more oxidized environment, possibly farther from the source vents of the metal-bearing fluids. Veins and breccias of black fine-grained quartz-tourmaline rock occur sporadically throughout the district; they are not directly associated with ore in the Iron Creek area, although some occurrences near the Blackbird mine contain cobaltite. Specular hematite veins, which are essentially cobalt free, occur locally in the Yellowjacket Formation, Hoodoo Quartzite, and quartzite of the overlying Lemhi Group; they probably formed during metamorphism. The Twin Peaks mine, in the extreme northeastern corner of the Challis quadrangle, produced a small amount of lead and copper; the ore, with high silver values but essentially no cobalt, is apparently stratabound but concentrated mainly in shear zones. Its host rock may (questionably) be the Yellowjacket Formation.

Northwest of the Challis quadrangle, the cobalt belt includes the inactive Blackpine mine, the Blackbird mine and nearby prospects, several recently discovered cobalt occurrences within the Special Mining Management Zone-Clear Creek of the River of No Return Wilderness area, and the Salmon Canyon Copper Co. mine. Several stratabound copper deposits in the Salmon River Mountains and Lemhi Range west and south of Salmon may or may not be genetically related to the cobalt deposits. The gold and lead-zinc-silver deposits in the region, including the the Yellowjacket mining district, the Mackinaw district near Leesburg, and the Mineral Hill district near Shoup, probably originated through Tertiary igneous activity.

INTRODUCTION

This chapter describes the cobalt-copper deposits in metamorphosed sedimentary rocks of the Middle Proterozoic Yellowjacket Formation in the Salmon River Mountains in the northeastern part of the Challis quadrangle. The deposits are stratabound and appear to have formed during a syngenetic, volcanogenic-exhalative mineralizing event on the sea floor. They occur along a northwest-southeast trend, the so-called Idaho cobalt belt. Most of the cobalt belt and its principal deposit, the Blackbird mine, lie just north of the Challis quadrangle; for this reason, the scope of this chapter has been broadened to include the Precambrian rocks in parts of the adjoining Elk City, Dillon, and Dubois 1°×2° quadrangles. Field work by the author, principally in the Degan Mountain and Taylor Mountain 7½-minute quadrangles, was done in the summers of 1980–83; mines and mineral deposits in the adjacent areas were also examined during this time. E. B. Ekren also mapped parts of the Degan Mountain, Taylor Mountain, and adjacent quadrangles. In addition to field mapping, emission spectrographic analyses were obtained of mineralized and unmineralized rocks, and some samples were studied in thin section, polished section, with the electron microprobe, and with X-ray diffraction.

Acknowledgments.—I was fortunate to be able to draw on the extensive stratigraphic work done on the Yellowjacket Formation by D. A. Lopez. I thank G. A. Hahn and G. J. Hughes, Jr., of Noranda Exploration, Inc., for discussions about their detailed studies of the Blackbird deposit and adjacent areas, and for the opportunity to examine mining properties and rock samples. I also thank E. B. Ekren, K. V. Evans, S. W. Hobbs, B. F. Leonard, D. A. Lopez, Karen Lund, and E. T. Ruppel, all of the U.S. Geological Survey; Terry Webster and S. G. Peters, formerly of Noranda; and D. W. Peters of the U.S. Forest Service, for valuable discussions about the area and its geology. The collaboration with E. B. Ekren in mapping the Precambrian rocks within the Challis quadrangle is particularly appreciated. I thank R. A. Milne and E. F. Waterman for allowing access to their mining properties.

REGIONAL GEOLOGY

Precambrian rocks of Middle Proterozoic age occur mainly in the northern and northeastern part of the Challis quadrangle (fig. A2, chap. A, this volume; fig. R1). They include, from oldest to youngest, the Yellowjacket Formation, the Lemhi Group and the Swauger Formation (fig. R2). The Yellowjacket Formation consists principally of thin-bedded argillaceous quartzite; Shockey (1957) estimated its total thickness to be 10,000 m (meters). The top and base of the Yellowjacket Formation have nowhere been recognized in the field. The Hoodoo Quartzite of Ross (1934) is a clean medium-grained, feldspathic quartzite, which, according to recent mapping and interpretation by E. B. Ekren (written commun., 1984), forms a unit about 1,100 m thick within the upper part of the Yellowjacket Formation. The Hoodoo crops out in a broad area in and around Taylor Mountain and

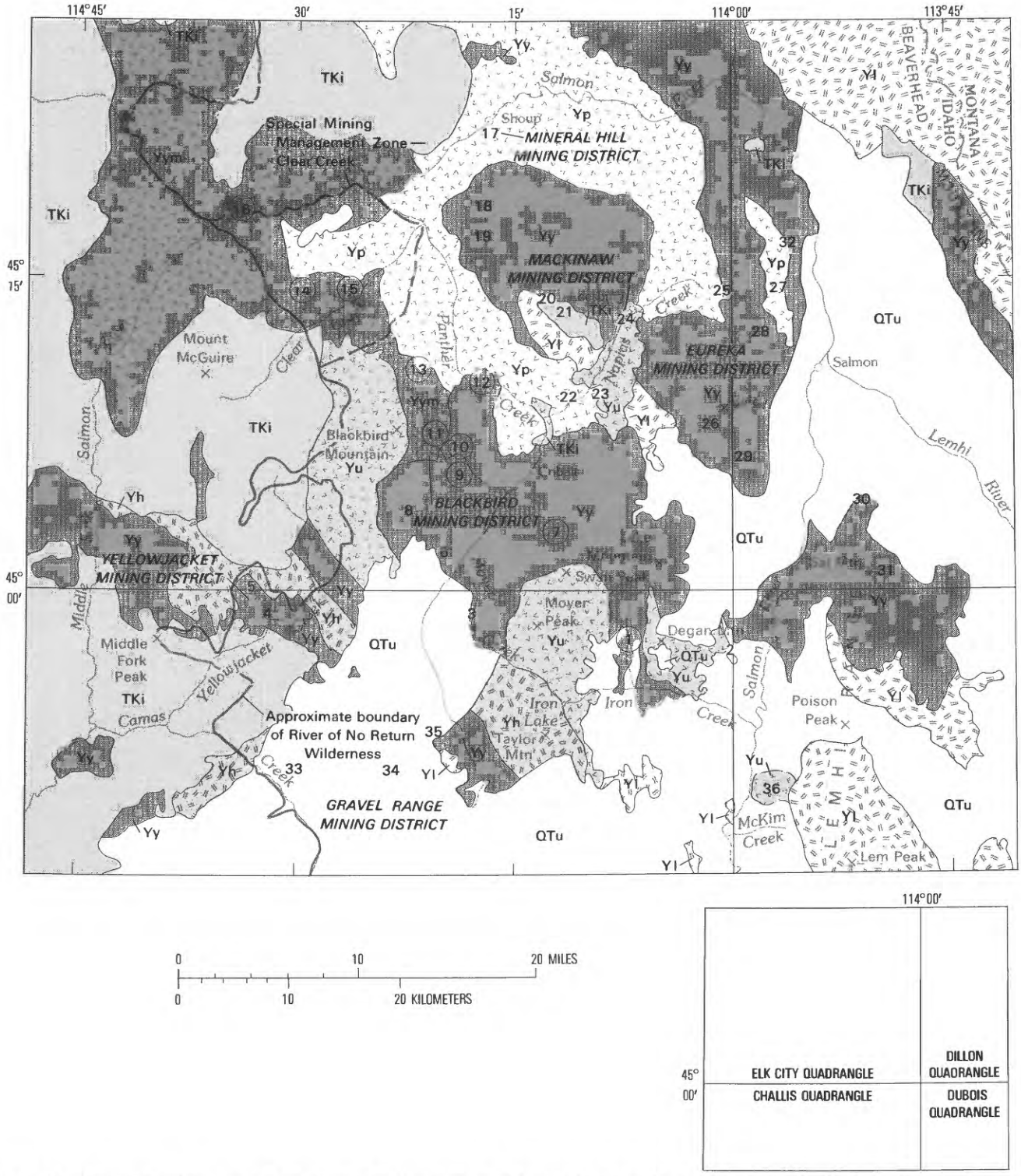

Figure R1. Generalized geologic map showing outcrop areas of Precambrian rocks and locations of selected mines and prospects in parts of the Challis, Elk City, Dillon, and Dubois quadrangles. Geology modified from Bennett (1977), Evans (1981), Fisher and others (1983), Lund and others (1983), Mitchell and Bennett (1979), Rember and Bennett (1979), Ruppel and others (1983), and unpublished mapping by E. B. Ekren and P. J. Modreski.

farther west in the Challis and Elk City quadrangles (fig. R1); it was earlier interpreted to overlie the Yellowjacket (Ross, 1934).

The Lemhi Group (Ruppel, 1975) consists of five formations. In ascending order, they are the Inyo Creek, West Fork, Big Creek, Apple Creek, and Gunsight Formations (fig. R2). Only the upper three have been recognized with certainty within the Challis quadrangle. The Lemhi Group lies in thrust contact on the Yellowjacket wherever it has been studied (Ruppel, 1975, 1978,

EXPLANATION

PHANEROZOIC

QTu — VOLCANIC AND SEDIMENTARY ROCKS — Includes small areas of Paleozoic sedimentary rocks

TKi — INTRUSIVE ROCKS, MAINLY EOCENE AND LATE CRETACEOUS

MIDDLE PROTEROZOIC

Yl — LEMHI GROUP — Includes Swauger Quartzite in Lemhi Range and Belt Supergroup in Beaverhead Mountains

Yu — METASEDIMENTARY ROCKS OF UNCERTAIN CORRELATION — Includes fine grained clastic rocks of Apple Creek or Yellowjacket Formations and quartzite of Big Creek, Hoodoo, or Yellowjacket Formations

Yp — PLUTONIC ROCKS — Includes granite, augen gneiss, and migmatite

Yh — HOODOO QUARTZITE

Yy — YELLOWJACKET FORMATION

Yym — YELLOWJACKET FORMATION — Metamorphosed to gneiss and schist

——— CONTACT — Dashed where approximately located

(16) 26 MINES AND PROSPECTS — Circled numbers show deposits that are part of the cobalt belt

1. Little No-Name mine (Cu, Co)
2. Twin Peaks mine (Cu, Pb)
3. Specular hematite prospect near Moyer Creek (Fe)
4. Yellowjacket mine, Yellowjacket mining district (Au, Ag, Cu, Pb)
5. Black Eagle mine, Yellowjacket mining district (Au)
6. Musgrove mine (Au)
7. Blackpine mine (Cu, Co)
8. Unnamed prospect at head of French Gulch (Cu, Co)
9. Patty B prospect, Blackbird mining district (Co)
10. Haynes-Stellite mine, Blackbird mining district (Co)
11. Blackbird mine, Blackbird mining district (Co, Cu)
12. Sweet Repose mine, Blackbird mining district (Co)
13. Tinker's Pride (Cu, Co) and Bonanza Copper (Cu) mines, Blackbird mining district
14. Cobalt occurrences near Garden Creek (Co)
15. Cobalt occurrences near Elkhorn Creek (Co)
16. Salmon Canyon Copper Co. mine (Cu, Co)
17. Clipper Bullion and other mines, Mineral Hill mining district (Au)
18. Copper King mine, Mackinaw mining district (Cu)
19. Mayflower mine, Mackinaw mining district (Cu, Au, Ag)
20. Haidee mine, Mackinaw mining district (Au)
21. Italian mine, Mackinaw mining district (Au)
22. Blue Jay mine, Mackinaw mining district (Pb, Ag)
23. Ringbone Cayuse mine, Makinaw mining district (Pb, Ag)
24. Gold placers near Leesburg, Mackinaw mining district (Au)
25. U.P. and Burlington mine, Eureka mining district (Au)
26. Bowman mine, Eureka mining district (Cu)
27. Queen of the Hills mine, Eureka mining district (Cu)
28. Silverton prospect, near Bob Moore Creek, Eureka mining district (Pb)
29. Tormey mine, Eureka mining district (Cu)
30. Pope-Shenon mine (Cu)
31. Harmony mine (Cu)
32. Thorium prospects near Diamond and Wallace Creeks (Th, U, rare earths)
33. Mines near Meyers Cove, Gravel Range mining district (Au, Pb, fluorite)
34. Singheiser mine, Gravel Range mining district (Au)
35. Rabbitfoot mine, Gravel Range mining district (Au, Cu)
36. Specular hematite prospects north of McKim Creek (Fe)

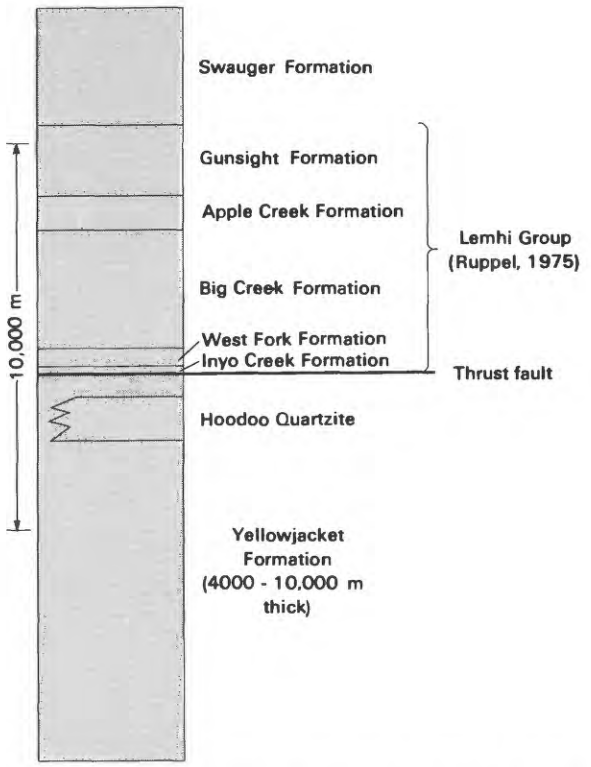

Figure R2. Stratigraphic column showing metasedimentary rock formations of Middle Proterozoic age in the Challis quadrangle and vicinity.

1980). The Apple Creek Formation resembles the Yellowjacket in many respects, and distinction of the two formations is difficult. Much of the upper part of the Yellowjacket(?) Formation north of Taylor Mountain and around Degan Mountain (fig. R1) may actually be the Apple Creek Formation and is shown as rock of questionable identity on figure R1. The Lemhi Group is overlain by reddish quartzite of the Swauger Formation (Ruppel, 1975; Hobbs, 1980). The Middle Proterozoic Lawson Creek Formation overlies the Swauger south of the area shown in figure R1 (Hobbs, 1980). The only Paleozoic rocks observed in the northeastern corner of the Challis quadrangle are in fault contact with the Yellowjacket(?) Formation in a very restricted area near Rattlesnake Creek and the Twin Peaks mine.

The Yellowjacket Formation is exposed for about 80 km (kilometers) northwestward from the Iron Creek drainage in the Challis quadrangle (fig. R1). Yellowjacket rocks also crop out to the east in the northern Lemhi Range and the Beaverhead Mountains. Cobalt occurrences, however, are restricted to a belt about 54 km long, extending northwestward from Iron Creek to the Salmon Canyon Copper Co. mine on the northern side of the Salmon River. Rocks within this cobalt belt strike generally northwest. They commonly dip to the northeast, but detailed mapping within the Challis quadrangle indicates that the Yellowjacket is extensively folded; in places it is isoclinally folded. The fold axes trend north-northwest. In areas of tight folding, axial-plane cleavage is prominently developed in the more argillaceous (phyllitic) beds of the Yellowjacket. Deformation is more intense in

the Elk City quadrangle to the north (Bennett, 1977; Evans, 1981; Maley, 1974). Because of the relative paucity of observable bedding-top criteria and the lack of distinctive, traceable beds, considerable repetition of strata through faulting or isoclinal folding is possible.

The absolute age of the Yellowjacket Formation is not well constrained. Evans (1981) dated one pluton that intrudes the Yellowjacket near the Salmon River at 1.37 b.y. (billion years), setting a lower limit on the age of the formation. Hughes (1983) reported a 1.7-b.y. potassium-argon age for rock interpreted to be mafic tuff within the Yellowjacket, but the limits of error on this age may be large (Karl Evans, oral commun., 1984). The possibility has long been considered (for example, Ruppel, 1975) that the Yellowjacket Formation correlates with the Prichard Formation of the Belt Supergroup, or at the very least that it represents a synchronous deposit in a similar environment in a separate depositional basin.

The metamorphic grade in the Precambrian rocks within the northeastern part of the Challis quadrangle is principally lower greenschist facies. The argillaceous quartzite and interbedded argillite commonly contain both green and brown biotite, sericite, and chlorite. Calc-silicate beds contain amphibole, scapolite, epidote, clinozoisite, and phlogopite. As mentioned earlier, metamorphic grade increases to the north and west, with amphibolite-grade rocks containing garnet, staurolite, and chloritoid occurring near the Blackbird mine, and sillimanite-grade rocks to the northwest, closer to the Precambrian augen gneiss plutons and migmatites along the Salmon River (Bennett, 1977; Evans, 1981). No detailed study of the metamorphic petrology of this region has ever been made. The regional metamorphism probably took place during the Precambrian (Tucker, 1975; Evans, 1981; Snee, 1983), with the possibility of thermal overprinting during Paleozoic, Cretaceous, and Eocene intrusive events.

Rocks of the region were thrust eastward during the Antler orogeny (mid-Paleozoic) and more particularly during the Sevier and Laramide orogenies (Cretaceous, and Late Cretaceous to early Tertiary) (Skipp and Hait, 1977; Ruppel, 1978, 1982). To the east in Idaho and adjacent Montana, Ruppel (1978) described as the "Medicine Lodge thrust system" the structure on which the Lemhi Group and younger rocks have been carried eastward over Yellowjacket and older basement rocks. The region was subsequently broken by predominantly north-south-trending, basin-and-range type normal faulting and (or) block uplift (Skipp and Hait, 1977; Ruppel, 1982), continuing today.

LITHOLOGY OF THE YELLOWJACKET FORMATION

The Yellowjacket Formation, which contains the ore deposits, consists of orthoquartzite (rare) to argillaceous quartzite, siltite, sandy or silty argillite, and argillite. The quartzites are mostly arkosic, containing both plagioclase and potassium feldspar, plus detrital tourmaline, zircon, garnet, sphene, and magnetite-hematite. Some of the quartzite is laminated and some is cross-laminated; alternating or interbedded quartzite and siltite-argillite are common. The grains making up the quartzite are typically poorly sorted. The most abundant sediment was probably very fine grained sand, but sediment sizes ranged from clay and silt through very fine to fine, medium, and some coarse sand. The original clay matrix has been recrystallized to sericite, biotite, chlorite, and iron oxide.

The Yellowjacket Formation was originally described by Ross (1934) from his type section along Yellowjacket Creek as consisting of 2,676 m of quartzite and argillaceous and calcareous quartzite. In the Leesburg and Blackbird Mountain 15-minute quadrangles (Shockey, 1957; Purdue, 1975; Bennett, 1977), the formation has classically been divided into a lower phyllite member and an upper quartzite member (fig. R3). Lopez (1981) divided the Yellowjacket into five members, generalized in figure R3, having an aggregate thickness of 7,100–8,100 m. Near the Blackbird mine, Hughes (1983) and Sobel (1981, 1982), distinguished three members totalling 6,000 m, coarsening upward from predominantly silty and sandy argillite (member A) to argillaceous quartzite and sandy argillite (member B) to quartzite (member C). The generalized maps of Hughes (1983) and Hahn and Hughes (1984) show most cobalt occurrences to be in or near their unit A, along what was inferred to be the axis of the depositional basin. Within the northeastern corner of the Challis quadrangle, the lithology varies upsection from argillaceous quartzite along Iron Creek, to more siltite and sandy argillite in the northern part of the Degan Mountain and Taylor Mountain 7½-minute quadrangles, to quartzite in the south-eastern part of the Leesburg 15-minute quadrangle. This sequence may represent as much as 7,000 m of section and probably corresponds to members B through E of Lopez (1981) and to members A through C of Hughes (1983).

Calcareous beds (now predominantly or entirely calc-silicate rocks) occur locally in the Yellowjacket section. Ross (1934) and Carter (1981) described calcareous beds or lenses near the base of the Yellowjacket section in the Yellowjacket Creek area. Leonard (1962) and Cater and others (1973) described calcareous beds in the Big Creek area further to the west. Calc-silicate and calcareous beds occur along Moyer Creek northwest of Taylor Mountain (fig. R1); some of these calcareous beds overlie the specular hematite deposit discussed in the section on "Specular Hematite Occurrences."

Rocks of igneous origin in the Yellowjacket Formation appear to be volumetrically more abundant north of the Challis quadrangle, where Hahn and Hughes (1984) mentioned finding tuffs and tuffaceous sediments, dikes, sills, and diatremes. The metamorphosed igneous rocks

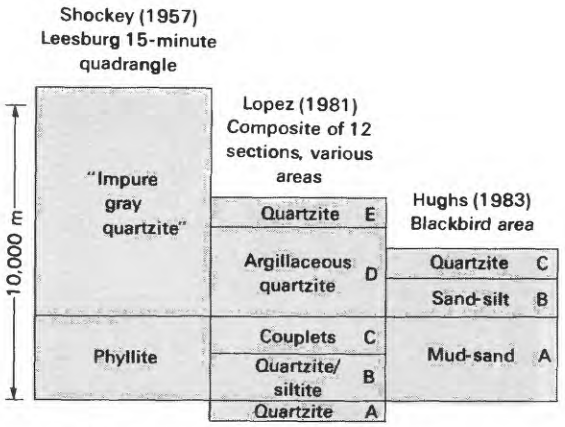

Figure R3. Comparison of informal stratigraphic units of the Yellowjacket Formation showing tentative correlation of rocks exposed in different areas near the northeastern corner of the Challis quadrangle.

Table R1. Contents of selected elements in the metavolcanic rocks of Yellowjacket Formation from the Challis quadrangle

[1, metamorphosed volcanic rock from the Yellowjacket Formation at about lat 44°56'46" N., long 114°06'07" W., about 1.8 km west-southwest of Degan Mountain. 2, metamorphosed volcanic rock (mafic tuff?) from the Yellowjacket Formation at about lat 44°56'47" N., long 114° 7'113" W., along North Fork of Iron Creek, about 3.2 km west-southwest of Degan Mountain (K. V. Evans, U.S. Geological Survey, unpub. data, 1984). 3, typical values for clastic sedimentary rocks of the Yellowjacket Formation, data from Lopez (1981) and this study. Values are in parts per million except where noted; >, greater than]

Element	1	2	3
		In percent	
Mg	3	5	0.3–1.0
Ca	1.5	7	.05–.7
Ti	.7	>1	.1–.5
Fe	5	15	.7–10
		In parts per million	
V	200	500	30–150
Cr	300	200	15–100
Mn	700	1,500	50–1,500
Co	50	70	5–15
Ni	150	150	5–30
Cu	2,000	70	5–50

can be distinguished by their high content of magnesium, titanium, vanadium, chromium, iron, nickel, and copper (table R1).

Depositional sedimentary structures are locally well preserved in the Yellowjacket Formation. Structures seen include parallel laminations and cross-laminations, oscillatory and current ripples, load casts, fluid-escape and sand-injection structures (fig. R4), soft-sediment slump folds, graded bedding, and others (Lopez, 1981).

Local bedding-plane polygonal structures that appear to be subaerial desiccation cracks in the Yellowjacket Formation (fig. R5) have been observed by the author at several locations north of Iron Creek in the Degan Mountain quadrangle, and by E. B. Ekren in three locations in and near the Yellowjacket mining district to the west (written commun., 1984). Ekren and I concur that these structures are distinct from the "pseudo-mudcracks" noted by Lopez (1981) as having been produced by the intersection of cleavage surfaces with deformed bedding surfaces in laminated rocks. If they are true subaerial desiccation cracks and not synaeresis (shrinkage) cracks formed underwater in buried sediments due to dewatering and changes in pore-fluid electrolyte balance, they indicate that at least locally and periodically the surface of deposition was emergent. This conclusion agrees with the interpretations of Ross (1934) and Carter (1981) that the Yellowjacket Formation was of shallow marine origin. Recently, however, Lopez (1981), Sobel (1981, 1982), and Hughes (1983) interpreted much of the Yellowjacket section to the north as consisting of distal, deep-water turbidites. This lithology may indicate a transition from the margin of the basin of deposition to the center.

MINERAL DEPOSITS

The most important ore deposits within the Precambrian rocks in the study area are the cobalt-copper deposits of the belt centered about the Blackbird mine. The southeastern end of this cobalt belt lies within the Challis quadrangle, in the Iron Creek area. The Twin Peaks lead-copper deposit, near the extreme northeastern corner of the Challis quadrangle, may be largely unrelated to the stratabound Blackbird-type deposits. Other small copper, gold, and base-metal deposits within the Precambrian rocks are likely to have been derived mainly as a result of post-Precambrian igneous activity.

Cobalt-Copper-Magnetite Deposits in the Iron Creek Area

Strata of the Yellowjacket Formation, mineralized with chalcopyrite and cobaltiferous pyrite, dip moderately (40–60°) to the northeast and strike northwest across the North Fork of Iron Creek (fig. R1) in the northeastern corner of the Challis quadrangle. This copper-cobalt deposit was discovered in 1967–68 during construction of a logging road up the creek. Several hundred feet of drifts and crosscuts, the Little No-Name mine, were driven into the hillsides from adits on both sides of the creek by Sachem Prospects Corp. in 1970–71 (Cohenour and others, 1973). Additional work by Sachem and succeeding companies included core drilling and induced polarization, resistivity, and ground magnetic geophysical surveys, soil and stream-sediment geochemical sampling, and additional drift construction (Cohenour and others, 1973; Peters, 1979). The patented claims along the North Fork of Iron Creek are currently (1985) held by Noranda Mining, Inc.

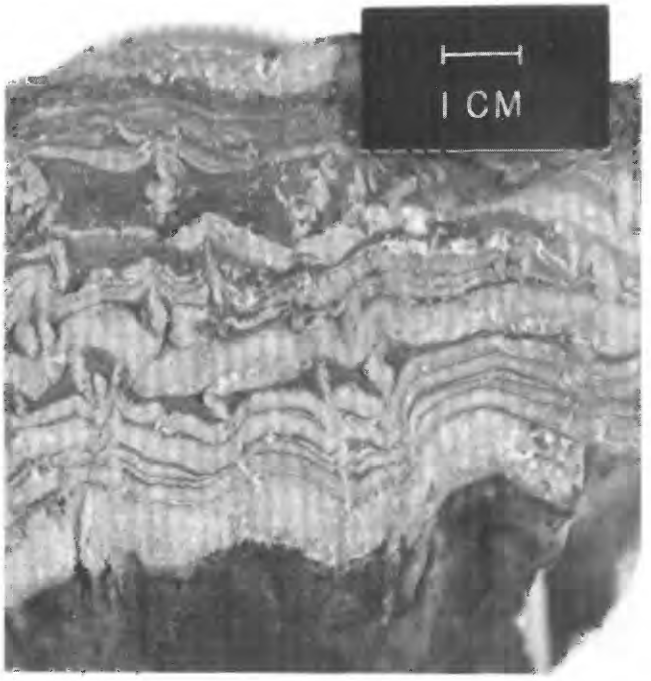

Figure R4. Laminated very fine grained argillaceous quartzite and silty argillite showing penecontemporaneous deformation and disruption of bedding by injection of sand during differential compaction and dewatering. Yellowjacket(?) Formation, Swan Peak, Leesburg 15-minute quadrangle.

Cohenour and others (1973) described the deposit as "fracture and cavity fillings as veins and veinlets and commonly as fine-grained disseminations," "concentrated in what appear[s] to be distinct lens-shaped bodies," and "associated with zones of brecciation and bedding plane fractures, possibly related to bedding plane faults." Roadcuts along the creek show that this mineralized zone is separated from a magnetite-rich zone about 500 m to the south and about 400 m stratigraphically lower by largely barren argillaceous quartzite and siltite. Microprobe analysis of pyrite in ore from the Little No-Name mine revealed as much as about 2–3 weight percent cobalt; no separate cobalt mineral phases have been recognized. Cohenour and others (1973) reported that systematic sampling from the adits and outcrops showed average metal contents of 0.76 percent copper, 0.19 percent cobalt (along 233 feet of the east adit); 0.87 percent copper, 0.30 percent cobalt (along a 124-foot drift off the east adit); 1.08 percent copper, 0.21 percent cobalt (120 feet along outcrops); and 0.16 percent copper and 0.08 percent cobalt (along 375 feet of the west adit). Samples analyzed by the U.S. Geological Survey (table R2, no. 8) showed as much as 2 percent copper and 0.3 percent cobalt.

Erdman and Modreski (1984) have described the utility of aquatic moss as a concentrator of and prospecting guide for cobalt and copper, based on a study done

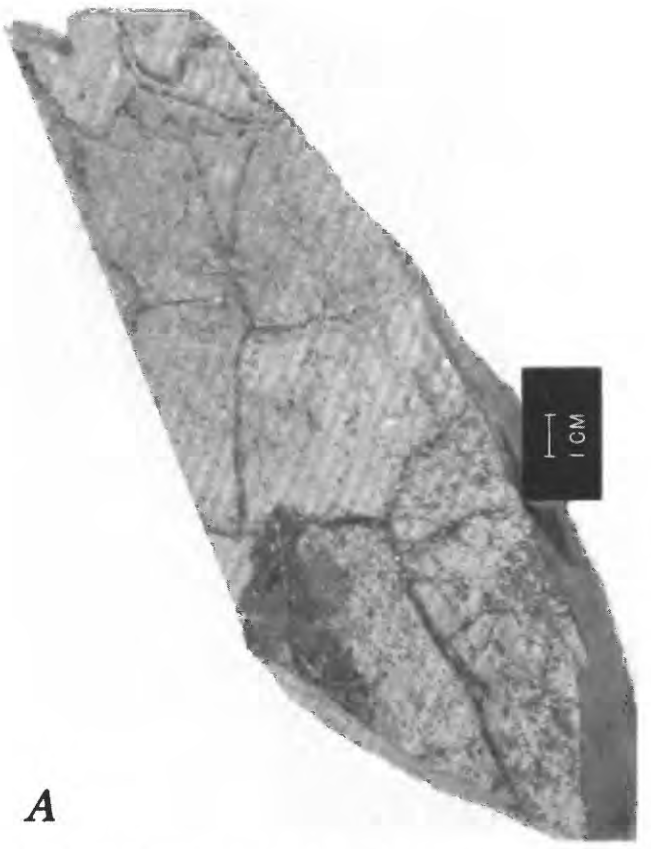

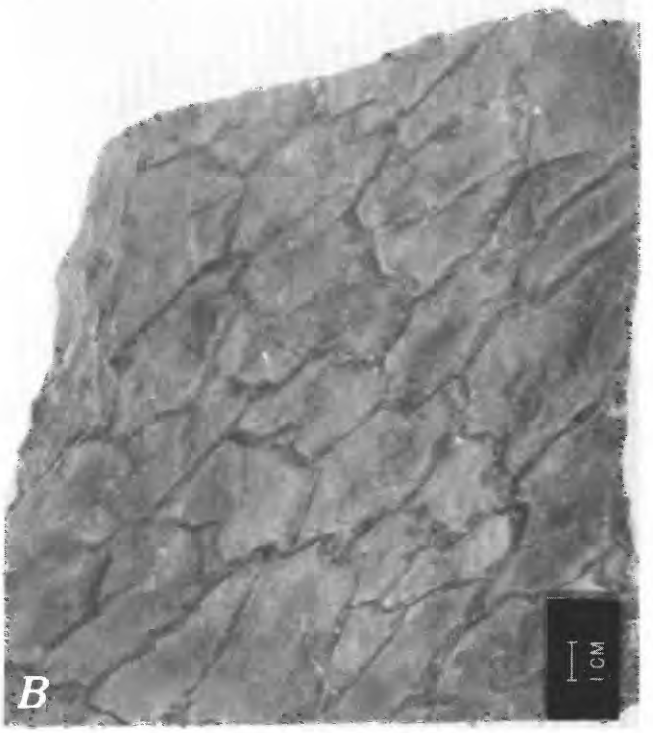

Figure R5. Bedding-plane polygonal structures inferred to be mudcracks of subaerial origin. *A*, undeformed polygons in argillaceous siltite from an outcrop about 1 km east of Yellowjacket Creek, within the Casto quadrangle, studied by Ross (1934). *B*, deformed polygons in argillaceous siltite of Yellowjacket(?) Formation north of Badger Creek in the Iron Creek area, Degan Mountain 7½-minute quadrangle.

in the North Fork Iron Creek drainage. They reported as much as 2,000 ppm cobalt and 35,000 ppm copper in dry-ash weight of aquatic mosses at and downstream from the deposits.

Cohenour and others (1973) distinguished four so-called "trends" or "zones" of mineralized rock across the North Fork of Iron Creek (see also Erdman and Modreski, 1984). From south to north these are a "magnetite-copper-cobalt trend;" a "copper-cobalt trend" that includes the Little No-Name mine; a "copper sulfate zone" named for copper sulfate bloom on surface exposures, said to overlie rock containing disseminated chalcopyrite; and an "arsenopyrite-gold zone" said to contain gold- and cobalt-bearing arsenopyrite veins that cut across bedding.

The strata rich in magnetite also locally contain some disseminated pyrite and chalcopyrite, and some tourmaline-quartz veins. Magnetite in these beds is in thin laminae along bedding planes, in irregular streaks and veinlets, and in layers composed entirely of massive magnetite. The magnetite is essentially pure Fe_3O_4 and is not particularly cobaltiferous; microprobe analysis showed 0–0.02 weight percent MgO, 0.13–0.18 percent Al_2O_3, 0.01 percent CaO, 0–0.02 percent TiO_2, 0–0.1 percent V_2O_3, 0–0.02 percent MnO, and 0–0.03 percent CoO. Emission spectrographic analysis of a fairly pure sample of magnetite showed only 30 ppm cobalt.

These magnetite-bearing strata are best exposed at three places along the road that follows the North Fork of Iron Creek and then circles eastward around the south side of Degan Mountain: (1) about 4.0 km north of the confluence of the North Fork of Iron Creek with Iron Creek; (2) about 3.4 km north-northeast of this confluence, on the north side of Jackass Creek; and (3) about 2.5 km northeast of this confluence, southeast of Jackass Creek. A prominent red gossan is near Jackass Creek, and the roadcuts on the northern side of the creek expose mineralized rocks that develop prominent efflorescences of blue chalcanthite (copper bloom) and pink to white and yellow efflorescences which have been taken to be erythrite (cobalt bloom), but which chemical analysis and X-ray diffraction studies actually show to be cobalt-bearing pickeringite (hydrous magnesium-iron aluminum sulfate containing about 0.5–1.0 weight percent CoO). At outcrops southeast of Jackass Creek and north of the road, black veinlets of fine-grained intergrown tourmaline and quartz cut the magnetite-bearing strata. Prominent tourmaline-quartz veins and breccias are also present closer to Iron Creek, and are discussed in the section below. This magnetite-rich horizon, and possibly additional strata containing minor amounts of magnetite more distant from the ore deposits, probably accounts for the strong, positive magnetic anomaly that trends northwest across this corner of the Challis quadrangle (Mabey and Webring, chap. E, this volume). Cohenour and others (1973) also suggested that sharp, local discontinuities in magnetic anomalies in this area may be due to a northwest-trending fault that offsets igneous rock at depth.

The "arsenopyrite-gold zone" of Cohenour and others (1973) is poorly exposed in bulldozer cuts on the hillside west of the North Fork of Iron Creek, about 2.0–2.2 km north of the Little No-Name mine. No specific cobalt minerals have been identified from there, but the arsenopyrite is cobalt bearing, and pale-pink cobalt bloom of cobaltoan pickeringite is on weathered samples. Cohenour and others (1973) reported that high-grade vein samples from the "arsenopyrite-gold zone" showed as much as 1 ounce of gold per ton, 0.4 percent cobalt, and 0.4 percent bismuth. Our analyses (table R2, no. 8) have shown as much as 0.3 percent cobalt, 0.15 percent bismuth, and 150 ppm nickel; we made no assays for gold.

Tourmaline-Quartz Veins and Breccias

Bodies and veins of black, fine-grained tourmaline in quartz occur in several places near the strata mineralized with cobalt and copper near Iron Creek, but not within the mineralized strata. They range from breccias composed of angular quartzite clasts in a fine-grained, flinty matrix of quartz-tourmaline (fig. R6), to spiderwebs of thin, black veinlets permeating the rock, to solid veins of fine-grained quartz and tourmaline as thick as 6 cm (centimeters). Prominent outcrops of breccia and veins occur just northeast of the confluence of Iron Creek and its North Fork, about 240–300 m (800–1,000 feet) above the creek level. Quartzite within and adjacent to the breccias is pale and bleached, and contains only sericite with no dark mica or chlorite. Similar quartz-tourmaline veins are present as outcrops and float in at least six other places in the Degan Mountain and Taylor Mountain quadrangles. A few exposures show thin veins containing quartz, tourmaline, and specular hematite. Tourmaline-quartz veins and breccias also occur near the Blackbird mine, particularly at the Patty B and Haynes-Stellite prospects, which contain fine-grained, silicified, tourmalinized breccia that also is mineralized with disseminated, fine-grained cobaltite. In the Iron Creek area, the tourmaline-quartz rock contains only near-background-level concentrations of cobalt and copper (table R2, no. 15).

Tourmaline, specifically magnesian tourmaline, has been noted as a prominent associate of massive sulfide deposits, notably at the Sullivan mine, British Columbia, and at several Appalachian sulfide deposits in volcanic terranes (Slack, 1982). The tourmaline at Iron Creek is intermediate in composition; preliminary microprobe analyses show atomic Mg:Mg+Fe to be about 0.35, and about 0.50 in coarser grained tourmaline in quartz near the Blackbird mine. At the Sullivan mine, extensive footwall tourmalinization is interpreted to represent boron metasomatism by fluids related to those that transported the metals to the deposit (Ethier and Campbell, 1977; Campbell and Ethier, 1983). In the Blackbird mine and Iron Creek areas, the boron-bearing fluids may have been laterally distant from those that carried the cobalt, copper, and iron, or they may have

Table R2. Contents of cobalt and other metals in mineralized

[Analyses by six-step semiquantitative emission spectrography, except zinc in 68 Yellowjacket Formation samples by atomic Conklin, M. Malcolm, U.S. Geological Survey. Value given as arithmetic mean and median (in parentheses) for each data in parts per million; iron in weight percent. Limits of detection are as indicated except zinc is 5 ppm for samples analyzed equal to; ≤, less than or equal to; ~, about]

Element Limit of detection	Co 5	B 20	V 7	Cr 1	Mn 1	Fe 0.001	Ni 5
1. Yellowjacket Formation (Lopez, 1981); 68 samples	9 (10)	70 (30)	82 (30)	52 (50)	370 (200)	4 (3)	21 (20)
2. Yellowjacket Formation, unmineralized; 12 samples	9 (8)	92 (30)	42 (30)	35 (25)	450 (250)	3 (2.5)	13 (10)
3. Lemhi Group; 3 samples	---	63 (70)	53 (30)	28 (20)	73 (100)	1 (1)	9 (7)
4. Blackbird mine (C. M. Tschanz, unpub. data, 1979); 10 samples	>6,000 (6,000)	<10	1 (<1)	5 (5)	490 (355)	>20	1,300 (1,200)
5. Blackbird mine; 4 samples	16,000 (18,000)	75 (<20)	10 (12)	7 (6)	150 (110)	>8	2,000 (425)
6. Blackpine mine; 3 samples	58 (20)	≤20 (≤20)	25 (30)	16 (15)	170 (150)	>7 (7)	77 (70)
7. Haynes Stellite mine and Patty B prospect; 3 samples	11,000 (1,000)	5,000 (7,000)	38 (30)	32 (30)	60 (70)	4 (3)	280 (100)
8. Iron Creek Area:							
Arsenopyrite zone; 5 samples	780 (150)	20 (<20)	88 (70)	18 (30)	750 (200)	6 (7)	64 (70)
Little No-Name mine; 3 samples	2,800 (2,000)	---	20 (15)	13 (10)	230 (300)	>10	150 (150)
Magnetite-rich rock; 5 samples	92 (30)	320 (200)	57 (70)	1 (1)	360 (110)	>10	15 (15)
Sulfide-bearing rock; 5 samples	690 (500)	650 (200)	22 (10)	7 (5)	220 (300)	6 (3)	21 (20)
9. Minor copper prospects and showings; 8 samples	46 (7)	20 (20)	42 (25)	28 (20)	390 (300)	2 (2)	17 (12)
10. Musgrove mine; 1 sample	10	---	20	15	70	5	20
11. Pope-Shenon mine; 3 samples	52 (70)	---	15 (15)	13 (7)	210 (300)	6 (7)	24 (15)
12. Salmon Canyon mine; 3 samples	2,700 (700)	100 (<20)	50 (30)	30 (30)	600 (500)	>9 (10)	420 (150)
13. Sweet Repose mine 2 samples	400	---	110	120	250	7	70
14. Specular hematite prospects:							
McKim Creek; 2 samples	5	---	30	4	83	>10	13
Moyer Creek; 2 samples	8	---	165	7	83	>10	10
15. Tourmaline-quartz veins and breccias; 8 samples	13 (5)	5,000 (2,000)	45 (40)	21 (18)	100 (100)	3 (3)	22 (15)
16. Twin Peaks mine; 5 samples	8 (7)	---	11 (10)	4 (2)	230 (300)	7 (7)	10 (7)

[1]Analysis by atomic absorption; limit of detection 5 ppm.

[2]Analysis by quantitative emission spectrography; limit of detection 10 ppm.

and unmineralized rocks, Challis quadrangle and vicinity

absorption (Lopez, 1981), and 10 Blackbird mine samples by quantitative emission spectrography. Analysts: L. Bradley, N. M. set. Only one value is given if data set was two samples or fewer, or if all values are below or above detection range. Values by atomic absorption (group 1). Leaders (---), value less than limit of detection; <, less than; >, more than; ⩾, more than or

Cu 1	Zn 300	As 1,000	Mo 3	Ag 0.5	Sn 10	Pb 10	Bi 10
17 (<5)	[1]48 (30)	---	1 (<5)	---	⩾2 (<10)	9 (5)	---
23 (8)	---	---	---	---	---	---	---
13 (5)	---	---	---	---	---	---	---
>17,000 (20,000)	[1]280 (285)	20,000 (15,000)	2 (<6)	9 (10)	10 (<10)	10 (9)	240 (190)
17,000 (18,000)	---	~50,000	---	4 (4)	---	---	920 (320)
28,000 (10,000)	>300 (<300)	---	---	23 (15)	10 (<10)	⩽10 (<10)	33 (30)
80 (70)	---	27,000 (7,000)	4 (5)	---	---	20 (30)	10 (10)
120 (150)	---	40,000 (<1,000)	---	1 (<0.5)	---	9 (<10)	330 (<10)
18,000 (20,000)	---	⩾500 (<1,000)	⩾3 (<3)	8 (10)	---	70 (30)	38 (50)
110 (110)	---	---	---	---	---	---	---
110 (70)	---	---	13 (10)	---	---	10 (10)	---
16,000 (4,000)	---	---	⩽3 (<3)	10 (2)	---	110 (30)	⩾14 (<10)
30	---	---	3	3	---	---	---
23,000 (20,000)	---	---	---	6 (7)	---	28 (15)	15 (15)
28,000 (30,000)	300 (300)	40,000 (15,000)	4 (5)	34 (50)	7 (10)	13 (10)	220 (150)
1,500	---	1,000	---	---	---	---	---
6	---	---	---	---	65	---	---
4	---	---	---	---	---	---	---
110 (22)	---	---	---	---	⩾6 (<10)	---	---
33,000 (3,000)	---	---	3 (<3)	63 (30)	---	5,000 (2,000)	---

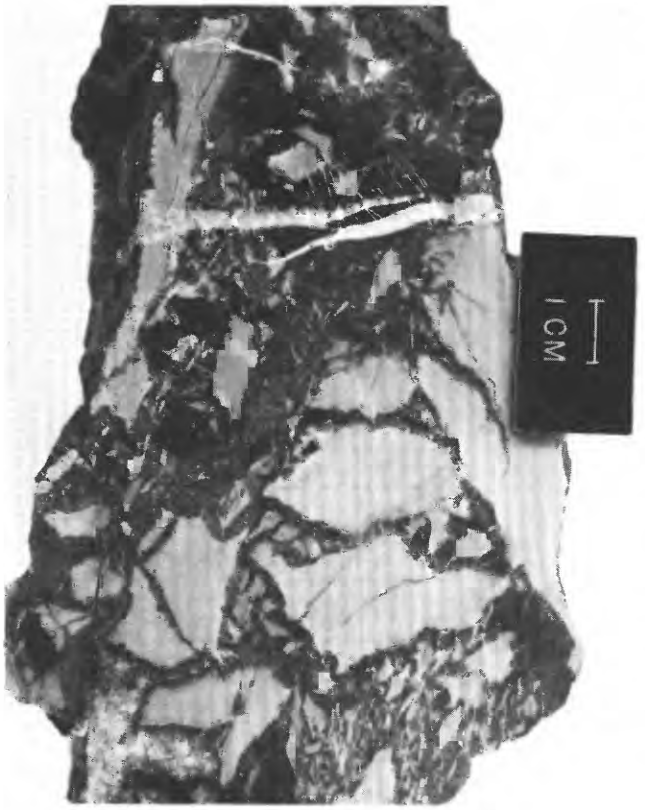

Figure R6. Breccia of sericite-quartzite with matrix of black, fine-grained tourmaline and quartz, cut by later veinlets of white quartz in tension cracks. Yellowjacket Formation, north of Iron Creek, Degan Mountain 7½-minute quadrangle.

been the same fluids at an earlier or later stage in their time-temperature-depth evolution. It is also possible that the fluids that formed these tourmalinites were exhaled from magma in unexposed Cretaceous or Eocene plutons (Purdue, 1975).

Lead and Copper Deposits at the Twin Peaks Mine

The inactive Twin Peaks mine, southwest of Rattlesnake Creek near the extreme northeastern corner of the Challis quadrangle (fig. R1), consists of four principal adits and drifts that were worked for lead and copper. The mine produced galena (with silver values) and copper (chalcopyrite-malachite-cuprite-pyrite), according to Starr (1955) and Peters (1979). Starr reported that the ore from the "lead adits" contained about 10 percent lead, 6 ounces of silver per ton, and 0.01–0.02 ounces of gold per ton, and ore from the "copper adit" contained about 10–12 percent copper and 9 ounces of silver per ton. Only a few hundred tons of ore were shipped. Starr's (1955) mine mapping showed that the minerals were mainly in shear zones that cut across bedding, with some disseminated minerals in the massive rock. The host rock is mainly gray or greenish-gray siltite and argillaceous quartzite. Although it is generally similar in appearance to the Yellowjacket sequence along the North Fork of Iron Creek, it is more argillaceous overall. The mine may actually be in strata of the Apple Creek Formation of the Lemhi Group. A possible indication that the rock is not Yellowjacket is the relative absence of cobalt and nickel from this deposit (table R2, no. 16).

Stratigraphic and Structural Framework of the Twin Peaks Mine Area

Just east of the mine, the Yellowjacket(?) beds terminate against a clean, massive, medium-grained, feldspar-free white quartzite. Much of the quartzite has a distinctly bimodal size distribution of quartz grains, resembling that described by McCandless (1982) in the Lower Ordovician Summerhouse Formation. The contact is not well exposed; some of the quartzite is fractured near the contact, but attitudes of the massive quartzite and the argillaceous quartzite and siltite beds are essentially conformable; both dip about 30–50° to the west. About 200 m of this massive quartzite is exposed in the steep canyon of Rattlesnake Creek, where a thin (50 m at most, generally much less) layer of gray, fine-grained dolomite lies atop the quartzite and appears to grade into the quartzite. The dolomite is poorly exposed for about 1 km north from Rattlesnake Creek. Landreth (1964) reported fossil corals in the dolomite and suggested that it and the underlying quartzite correlate with the Ordovician Kinnikinic Formation. A sample of the dolomite collected during the present study contained fragmentary brachiopods and conodonts, which indicate a probable Middle Ordovician age (J. T. Dutro, Jr., and John Repetski, U.S. Geological Survey, written commun., 1983, USGS sample no. 9666–CO). The dolomite and quartzite may be equivalent to the Middle Ordovician Ella Dolomite and the Lower Ordovician Summerhouse Formation (Hobbs and others, 1968; McCandless, 1982; Ruppel and others, 1975) or to the basal part of the Middle and Upper Ordovician Saturday Mountain Formation (Hobbs, chap. D, this volume) and an underlying quartzite such as the Kinnikinic.

These relations indicate that, despite a 30–50° dip to the west of both the dolomite-quartzite sequence and the adjacent argillaceous Yellowjacket(?), the two sequences are separated by a major fault. The trace of this fault contact indicates an average 60° dip to the west (Fisher and others, 1983). The dolomite-quartzite sequence appears to rest conformably on a thin- and thick-bedded sequence of green to red, feldspathic, sericitic quartzite and interbedded phyllite that most closely resembles quartzites of the Big Creek Formation of the Lemhi Group. These relations likewise suggest that, despite the apparent conformity of dip in the two sequences, the dolomite-quartzite sequence is separated from the underlying quartzite-phyllite sequence by a major fault. Both faults parallel the bedding, but the

direction of displacement is unknown. Landreth (1964) concluded that the fault above the dolomite-quartzite sequence was a high-angle reverse fault dipping about 60°. The fault may have been reactivated in early Tertiary time as a right-lateral strike-slip fault.

Minor Copper Occurrences

Several small showings of copper are present in the Yellowjacket Formation in the northeastern part of the Challis quadrangle. These showings are mostly malachite along bedding planes; a few include chalcopyrite associated with quartz pods. Prospect pits exposing minor amounts of malachite and chalcopyrite are in the Yellowjacket(?) Formation south of Rattlesnake Creek, west of the Twin Peaks mine. Several small pits and adits were dug into showings in Badger Basin, just north of Iron Creek and south of Degan Mountain (fig. R1). Other showings are along the North Fork of Iron Creek, along the east-facing cliffs about 2.8 and 3.8 km north-northeast of Iron Lake, and about 0.9 km east-southeast of Moyer Peak. Analyses (table R2, no. 9) show only minor amounts of cobalt in these occurrences, and no cobalt bloom was seen.

Specular Hematite Occurrences

Veins of specular hematite in rocks of the Yellowjacket Formation occur on the west side of Moyer Creek west-northwest of Moyer Peak (fig. R1). The hematite veins (fig. R7) are in a zone just beneath a series of calc-silicate beds; the quartzite containing the hematite is also somewhat calcareous. The zone is exposed by bulldozer cuts, known as the Iron King claims (Peters, 1979). Most of the hematite occurs as veins having various attitudes, but some layers in the calcareous quartzite appear to have been partly replaced by fine-grained flakes of hematite. The exposure is erosionally truncated and covered by Challis Volcanics.

A similar deposit occurs north of McKim Creek, just east of the Salmon River in the Lemhi Range (fig. R1, Dubois quadrangle). Here specular hematite veins were mined on a small scale from open cuts at the Black Angus deposits (Soregaroli, 1961). Some of the ore is said to have been sold around 1982 for use in heavy drilling mud (D. W. Peters, oral commun., 1983). The host rock of this iron deposit is a micaceous quartzite, commonly green (chloritic) near the deposit; it locally has a pinkish-white, bleached appearance near the veins. Its formational affinity is uncertain; Rember and Bennett (1979) have indicated that rocks near this area are part of the Lemhi Group. Anderson (1961) described additional hematite vein deposits (with minor associated magnetite and veins of white quartz) farther to the east in the Lemhi Range, in rocks he ascribed to his "Apple Creek Phyllite" and Swauger Quartzite.

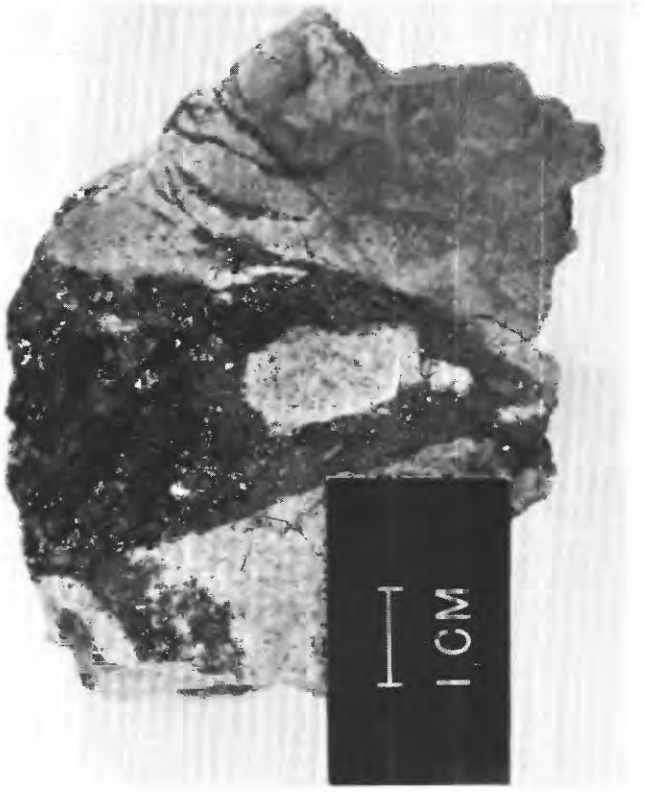

Figure R7. Specular hematite veins cutting calcareous (calc-silicate) quartzite. Yellowjacket Formation, west of Moyer Creek, Opal Lake 7½-minute quadrangle.

The specular hematite veins at both the above locations are essentially barren of cobalt and most other metals, although those at McKim Creek contain a notable amount of tin (table R2, no. 14). They show no unusual abundance of rare-earth elements; the presence of these elements would have suggested a relationship to the quartz-thorite-hematite-copper vein deposits of the Lemhi Pass thorium district of the Beaverhead Mountains (Staatz, 1979); those veins occur in rocks of the Yellowjacket Formation (and Lemhi? Group) but are probably related to Late Cretaceous-Tertiary plutons, according to Staatz. Bennett (1977) reported masses of hematite as float northwest of Leesburg along the projection of the Leesburg fault, and hematite is associated with some of the gold ores in the Mackinaw (Leesburg) district. Small veinlets of specular hematite or hematite and quartz are widely distributed throughout the Yellowjacket Formation and Hoodoo Quartzite in the Degan Mountain-Taylor Mountain-Opal Lake area. The hematite veins appear to be largely a product of metamorphism and intrusion of the Phanerozoic plutons.

Cobalt and Other Metals in the Blackbird District and Vicinity

The Blackbird mining district is about 30 km west of Salmon, in the Elk City 1°×2° quadrangle (Anderson,

1943b, 1947; Bennett, 1977; Umpleby, 1913; U.S. Bureau of Mines, 1943; Vhay, 1948). It comprised many nearby small mines and prospects, including the Belielle, Bohannon, Brown Bear, Bryan-Columbus, Chicago, Copper Queen, Dusty, Ella, Hawkeye, Haynes Stellite, High Five, Katherine, Ludwig, Patty B, St. Joe, Sunshine, Tom Jefferson, and Uncle Sam mines. Some of these were originally operated as separate mines but were later consolidated and connected through their underground workings as the Calera mine, and then as the Blackbird mine. Workings and ore horizons in the Blackbird mine (including the Idaho, Dandy, Chicago, and Brown Bear zones and the Blacktail open pit) strike N. 40° W. and dip 50–60° to the northeast (Bennett, 1977). The cobalt belt extends northwest and southeast from the Blackbird mine. To the northwest are additional cobalt occurrences recently found within the Special Mining Management Zone-Clear Creek of the River of No Return Wilderness, and one inactive mine containing copper and cobalt, the Salmon Canyon Copper Co. mine. To the southeast are a few small, inactive mines and prospects, including the Blackpine mine, and at the extreme southeastern end of the trend is the Iron Creek area previously discussed in this chapter. In addition to the deposits discussed in more detail below, the Tinker's Pride mine about 6 km north of the Blackbird mine was reported to contain minor cobalt (Bennett, 1977; Vhay, 1948), and an unnamed prospect at the head of French Gulch about 6 km south of the Blackbird mine was reported to have been worked for cobalt and copper (Bennett, 1977), although Vhay (1948) found no cobalt there.

Blackbird mine.—The inactive Blackbird mine is on the largest identified cobalt deposit in North America. The ore consists of cobaltite, chalcopyrite, pyrite, pyrrhotite, arsenopyrite, and minor amounts of other sulfides and arsenides, in biotite- to garnet-grade metamorphic rocks of the Yellowjacket Formation (Anderson, 1947; Roberts, 1953; Vhay, 1948; Purdue, 1975; Bennett, 1977; additional, unpublished, reports about the district are listed by Lund and others, 1983). The mine consisted of the Blacktail open pit and extensive underground workings. Preliminary work to reopen the underground mine, begun by Noranda Mining, Inc. in 1978, was suspended in 1982 due to a decline in the price of cobalt; reserves are said to be on the order of 4 million tons of ore containing 0.6 percent cobalt and 1.2 percent copper (Engineering and Mining Journal, 1980; table R2, nos. 4, 5). The mine produced about 14 million pounds of cobalt during the 1950's. The ore at the Blackbird mine is stratabound and appears to have been syngenetic (Lopez, 1981; Hahn and Hughes, 1984), but it has been extensively recrystallized and remobilized along shear zones and folds. Evident metamorphic changes include segregation of chalcopyrite into quartz pods at fold crests and the localization of the principal ore horizons along major zones of shearing or deformation (Purdue, 1975; Bennett, 1977). As was pointed out by Lund and others (1983), some of the gold and silver mineralization noted by Anderson (1947) may be a product of veins associated with Tertiary igneous activity rather than a part of the original Precambrian deposit.

The textural evidence for a syngenetic origin of the deposits is by no means as clearcut as it is in some of the world-famous volcanogenic massive-sulfide deposits, such as the Kuroko deposits of Japan. The actual preservation of syngenetic structures in the ore at the Blackbird mine has not been documented. Thin laminae of fine-grained cobaltite parallel to bedding may represent relict syngenetic layering. However, indirect evidence exists: some siliceous rocks in and near the ore zones may be exhalative cherts, silica that was vented into seawater by hot springs and subsequently precipitated (Hahn and Hughes, 1984). Black biotite-rich strata that occur close to ore horizons were interpreted as metamorphosed basaltic tuffs or sediments having an originally high tuffaceous component (Hahn and Hughes, 1984).

Hughes (1983) and Hahn and Hughes (1984) interpreted the basin into which the Yellowjacket sediments were deposited as a northwest-trending rift basin bordering the Archean craton to the east. They interpreted the Yellowjacket sediments to be a submarine fan complex that prograded into a deepwater basin, with the Blackbird and associated cobalt deposits lying near the axis of the basin.

Haynes Stellite mine.—This mine, about 2 km east-southeast of the main Blackbird mine (fig. R1), produced cobalt during 1917 to 1921 (Vhay, 1948). It was originally known as the Haynes Stellite mine and later as the Cobalt mine, and the adits are labeled "Cobalt Mine" on the current (1950) Blackbird Mountain 7½-minute topographic quadrangle. The rocks at this deposit (table R2, no. 7) include silicified and tourmalinized breccia containing disseminated cobaltite and mineralized biotitic strata that may represent former tuffaceous beds.

Patty B prospect.—This prospect, about 3.6 km southeast of the Blackbird mine (Vhay, 1948), includes a prominent outcrop of silicified, tourmalinized breccia containing disseminated cobaltite (table R2, no. 7).

Sweet Repose mine.—This privately held claim is on one of several small cobalt occurrences peripheral to the Blackbird deposit. It is about 6.5 km northeast of the Blackbird mine (fig. R1) (Anderson, 1943; Lopez, 1981). It contains fairly coarse grained cobaltite in biotite schist (two analyses are summarized in table R2, no. 13) that may represent mafic tuffaceous rock.

Blackpine mine.—This inactive deposit, about 14 km southeast of the Blackbird mine (fig. R1), contains pyrite-chalcopyrite-arsenopyrite ore similar to that of the Blackbird mine but lacks cobaltite (Shockey, 1957; Bennett, 1977). Ore samples collected on the dump had a low cobalt content (table R2, no. 6). Ore occurs as veinlets and stringers, grossly stratabound within chlorite-biotite-muscovite siltite-quartzite.

Salmon Canyon Copper Co. mine.—This deposit, in high-grade garnet-muscovite-biotite schist and gneiss, represents the farthest known extension of the cobalt belt to the northwest. It is at about 45°18′ N., 114°33′ W., on the north side of the Salmon River, 26 km northwest of the Blackbird mine (fig. R1). The minerals here include rather coarsely crystalline chalcopyrite, pyrite, arsenopyrite, and cobaltite, and are associated with quartz stringers and pods. Analyses of three ore samples are summarized in table R2, no. 12.

Cobalt occurrences in the Special Mining Management Zone—Clear Creek.—About 15–18 km northwest of the Blackbird mine, within the River of No Return Wilderness, geochemical cobalt anomalies were found in several drainages, principally along Garden Creek and Elkhorn Creek (Lund and others, 1983). This area is within the special mining management area designated by the U.S. Congress to permit continued development of cobalt resources. Outcrops containing cobaltite were found at one or more locations, near Elkhorn Creek.

Other Copper, Gold, and Base-Metal Deposits

The inactive Pope-Shenon copper mine is south of the town of Salmon, at the northern end of the Lemhi Range (fig. R1, Dillon quadrangle) (Anderson, 1943a). The ore was predominantly chalcopyrite, pyrite, and delafossite ($CuFeO_2$), with magnetite, hematite, actinolite, epidote, and quartz, and was said to occur mainly in east-trending shear zones within dark-green biotite-sericite-chlorite quartzite. Bodies of breccia, mineralized with pyrite and chalcopyrite, were probably associated with Tertiary dikes; the mine is near a Tertiary caldera mapped by Ruppel and others (1983). The ore contained mainly copper (2–15 percent) with only minor silver (0.1 ounce/ton or less) and a trace of gold (0.01 ounce/ton or less) (Anderson, 1943a). Our analyses showed minor cobalt (15–70 ppm, table R2, no. 11). The quartzitic host rock resembles Yellowjacket Formation, and a preliminary geologic map of the Dillon 1°×2° quadrangle (Ruppel and others, 1983) shows it as such. The possible relationship of this deposit to the cobalt belt is problematical; it may be solely a product of later events.

Similar copper deposits (the Harmony mine and others) occur elsewhere within the Lemhi Range (Anderson, 1943, 1956, 1961). Also, the Tormey, Bowman, Copper King, and Bonanza Copper mines are in the Salmon River Mountains west of Salmon (Umpleby, 1913; Vhay, 1948; Anderson, 1956; Shockey, 1957; Bennett, 1977; Peters, 1979).

The Musgrove mine, predominantly a gold deposit with quartz veins and limonitic breccia, is about 9.6 km south of the Blackbird mine (fig. R1; Umpleby, 1913). It is within rocks of the Yellowjacket Formation but is probably related to Tertiary intrusive activity. Analysis of one sample from the dump shows only a trace of cobalt (table R2, no. 10), though some prospects containing copper and cobalt occur elsewhere along Musgrove Creek (Vhay, 1948; Bennett, 1977).

The mines of the Yellowjacket district (fig. R1), about 21 km southwest of the Blackbird district, contain gold and some copper, lead, and silver. The deposits are in rocks of the Yellowjacket Formation but are probably related to the Crags and Casto Tertiary plutons (Anderson, 1953; Bennett, 1977; Carter, 1981; Peale, 1982). Likewise, lead-silver deposits (Ringbone Cayuse and Blue Jay mines) in the Mackinaw mining district near Leesburg, and gold deposits near Leesburg and in the Mineral Hill mining district near Shoup (all within the Elk City 1°×2° quadrangle, fig. R1), are all probably related to Tertiary (or possibly Precambrian) intrusions (Bennett, 1977; Shockey, 1957).

The gold, copper, and fluorite deposits of the Gravel Range mining district near Meyers Cove (Anderson, 1954; Ross, 1927; Umpleby, 1913) in the southwestern part of the area of figure R1 (nos. 33–35) are within the Challis Volcanics. The Eureka mining district, west of Salmon (fig. R1, nos. 26–29) includes gold and copper deposits, some near a Precambrian pluton and some lying within the Yellowjacket Formation (Peters, 1979; Shockey, 1957; Anderson, 1956, 1943a; Umpleby, 1913). Also within this mining district are some small wolframite-quartz veins reported west of Baldy Mountain (Peters, 1979; Shockey, 1957; near no. 26, fig. R1), and thorium-uranium-rare earth veins near Diamond and Wallace Creeks (Peters, 1979; Anderson, 1958; no. 32, fig. R1) that appear to represent the southwesternmost extension of the Lemhi Pass thorium-rare earth district (Staatz, 1979). Other gold-mining districts, not shown on figure R1, include the Carmen Creek mining district, north of Salmon (Anderson, 1956; Umpleby, 1913), and the Indian Creek mining district, east of Shoup (Umpleby, 1913).

GEOCHEMICAL COMPOSITION OF ROCKS

Lopez (1981) noted that the Yellowjacket Formation as a whole is characterized by anomalously high values of cobalt, copper, arsenic, antimony, bismuth, and strontium. Because of relatively high limits of detection, the analyses reported in this chapter (table R2) do not include useful new data for arsenic, antimony, and bismuth in unmineralized rocks. My very limited data set (table R3) suggests that the high strontium content of the Yellowjacket Formation (about 100–150 ppm (parts per million)) may be useful in distinguishing it from lithologically similar units of the Lemhi Group (15–50 ppm strontium). The high strontium content may reflect the more calcareous and feldspathic nature of the Yellowjacket Formation, because strontium geochemically replaces calcium in calcite and feldspar. However, mineralized

Table R3. Strontium content in mineralized and unmineralized rocks of the Yellowjacket Formation and Lemhi Group, Challis quadrangle and vicinity

[Analyses by semiquantitative emission spectroscopy. Values are in parts per million. Limit of detection 5 ppm, except 100 ppm for the 68 samples from the Yellowjacket Formation (Lopez, 1981). Although some ore minerals were present in the mineralized rocks, all the samples in this table were composed predominantly of clastic sedimentary or volcanic material. <, less than]

Source of sample	No. of analyses	Mean (median)	Range of data
Yellowjacket Formation			
Quartzite, siltite, and argillite	68	100 (100)	<100-300
Argillaceous quartzite and siltite	5	120 (150)	30-150
Calcareous rocks	2	420	150-170
Metavolcanic rocks	2	650	300-1000
Blackbird mine	3	22 (20)	15-30
Blackpine mine	3	20 (30)	<5-30
Iron Creek area mineralized rocks:			
Arsenopyrite zone	6	160 (60)	<5-700
North Fork of Iron Creek	4	40 (40)	30-50
North of Jackass Creek	5	5 (5)	<5-7
Southeast of Jackass Creek	4	88 (90)	20-150
Rocks with tourmaline quartz veins	3	80 (70)	70-100
Moyer Creek hematite prospect	2	135	70-200
Musgrove mine	1	15	15
Salmon Canyon Copper Co. mine	3	29 (30)	7-50
Sweet Repose mine	2	225	150-350
Lemhi Group			
Argillaceous quartzite	3	28 (20)	15-50
Uncertain affiliation, either Yellowjacket Formation or Lemhi Group			
Argillaceous quartzite and siltite	5	60 (70)	30-100
McKim Creek hematite prospect	2	42	15-70
Pope-Shenon mine	2	11	7-15
Twin Peaks mine	5	5 (<5)	<5-15

quartzite-argillite samples from the Blackbird mine and several others, firmly believed to belong to the Yellowjacket Formation, also show very low strontium contents (table R3), so more work needs to be done before this relationship can be verified. J. J. Connor (oral. commun., 1984) has begun a detailed survey of the chemical composition of the Yellowjacket Formation, with the goal of using statistically significant chemical parameters as a means of distinguishing the Yellowjacket from other formations and as indicators of the provenance of its sediments, as has been done for the St. Regis, Grinnell, and Spokane Formations of the Belt Supergroup (Connor, 1984).

GENESIS OF THE BLACKBIRD-TYPE DEPOSITS AND COMPARISON TO OTHER DISTRICTS

The Blackbird district deposits were originally interpreted to be hydrothermal, related to the Idaho batholith (Anderson, 1947; Roberts, 1953; Purdue, 1975). It now appears that the deposits represent original syngenetic, stratabound mineralization that has been modified by recrystallization, differentiation, and remobilization during regional metamorphism, and possibly by hydrothermal alteration or thermal metamorphism during subsequent intrusive events. Because of the present limited knowledge of the details of the process that formed Blackbird-type deposits, their formation can be modeled only in general terms. Metal-bearing fluids could have been derived either from cooling intrusions or from circulation set in motion by intrusive heat sources. Sulfide and arsenide minerals would have precipitated as the fluids cooled during venting on the sea floor. Silica in the fluids formed the exhalative chert, while quartz-tourmaline veins may have been forming at depth. The magnetite-rich deposits may have formed at a location laterally distant from the sulfides, in a more oxidized environment.

Compared to other deposits, the Blackbird-type cobalt-copper deposits appear to be partway between two extremes. One extreme (Franklin and others, 1981) is the volcanogenic, sea-floor massive sulfide deposits, such as the Kuroko, Besshi, and Cyprus-type base-metal and copper deposits, and the metal deposits presently forming at midocean spreading centers, all of which are in predominantly volcanic host rocks. The other extreme (Gustafson and Williams, 1981) is ore deposits within shallow-water clastic sedimentary rocks, such as the copper-silver deposits in Belt Supergroup rocks of Montana (Hayes, 1984), the copper and copper-cobalt deposits of Zambia and Zaire (Annels, 1974; Annels and others, 1983), and the deposits of the Kupferschiefer of eastern Europe. Many of these sedimentary deposits are thought to have formed during diagenesis of organic-rich, shallow-water sediments (Renfro, 1974; Brown, 1978), although the ultimate source of the metals may have been at least partly magmatic (Annels and others, 1983). Metamorphosed deposits that seem to have particular affinities to those of the Blackbird district include the cobalt-gold-copper deposit of the Standard mine, Quartzburg district, Oregon (Vhay, 1959), the copper-zinc-iron-cobalt deposit at Outokumpu, Finland (Koistinen, 1981), and several Appalachian sediment-hosted, stratabound massive sulfide copper-lead-zinc deposits such as those of Ore Knob, N.C.; Black Hawk, Maine; and Elizabeth, Vt. (Slack, 1982); Ducktown, Tenn. (LeHuray, 1984); and the Gossan lead district, Virginia (Gair and Slack, 1984). The Sullivan, B.C., lead-zinc deposit resembles the Idaho cobalt-copper deposits in several important ways: it is within a fine-grained sedimentary host rock (the Aldridge Formation, which is a possible though distant correlative of the Yellowjacket), it has indirect volcanic affinities, and it has tourmalinized footwall rocks (Hamilton, 1984; Hamilton and others, 1982). A unique and unmatched feature of the Blackbird district, however, is the high concentration of cobalt relative to other metals, particularly copper, nickel, and silver.

Better understanding of the genesis of the Idaho cobalt deposits may come from future mineral-chemistry

studies; trace-element geochemistry studies of the ore, chert, and sedimentary and igneous rocks; sulfur and oxygen isotopic measurements; fluid-inclusion studies; laboratory studies of the partitioning of cobalt, copper, and nickel between minerals and hydrothermal fluids; and continued detailed stratigraphic study and geologic mapping.

REFERENCES CITED

Anderson, A. L., 1943a, Copper mineralization near Salmon, Lemhi County, Idaho: Idaho Bureau of Mines and Geology Pamphlet 60, 15 p., 2 pl.

_____1943b, A preliminary report on the cobalt deposits in the Blackbird district, Lemhi County, Idaho: Idaho Bureau of Mines and Geology Pamphlet 61, 34 p.

_____1947, Cobalt mineralization in the Blackbird district, Lemhi County, Idaho: Economic Geology, v. 42, no. 1, p. 22–46.

_____1953, Gold-copper-lead deposits of the Yellowjacket district, Lemhi County, Idaho: Idaho Bureau of Mines and Geology Pamphlet 94, 41 p., 9 pl.

_____1954, Fluorspar deposits near Meyers Cove, Lemhi County, Idaho: Idaho Bureau of Mines and Geology Pamphlet 98, 34 p., 12 pl.

_____1956, Geology and mineral resources of the Salmon quadrangle, Lemhi County, Idaho: Idaho Bureau of Mines and Geology Pamphlet 106, 102 p., 3 pl.

_____1958, Uranium, thorium, columbium, and rare earth deposits in the Salmon region, Lemhi County, Idaho: Idaho Bureau of Mines and Geology Pamphlet 115, 81 p.

_____1961, Geology and mineral resources of the Lemhi quadrangle, Lemhi County, Idaho: Idaho Bureau of Mines and Geology Pamphlet 124, 111 p., 2 pl.

Annels, A. E., 1974, Some aspects of the stratiform ore deposits of the Zambian copperbelt and their genetic significance, *in* Bartholome, Paul, Gisments stratiformes et provinces cupriferes: Liege, Belgium, Societe Geologique de Belgique, p. 235–254.

Annels, A. E., Vaughan, D. J., and Craig, J. R., 1983, Conditions of ore mineral formation in certain Zambian copperbelt deposits with special reference to the role of cobalt: Mineralium Deposita, v. 18, p. 71–88.

Bennett, E. H., 1977, Reconnaissance geology and geochemistry of the Blackbird Mountain-Panther Creek region, Lemhi County, Idaho: Idaho Bureau of Mines and Geology Pamphlet 167, 108 p.

Brown, A. C., 1978, Stratiform copper deposits—evidence for their post-sedimentary origin: Minerals Science Engineering, v. 10, no. 3, p. 172–181.

Campbell, F. A., and Ethier, V. G., 1983, Environment of deposition of the Sullivan orebody: Mineralium Deposita, v. 18, p. 39–55.

Carter, C. H., 1981, Geology of part of the Yellowjacket mining district, Lemhi County, Idaho: Moscow, Idaho, University of Idaho M.S. thesis, 131 p.

Cater, F. W., and others, 1973, Mineral resources of the Idaho Primitive Area and vicinity, Idaho: U.S. Geological Survey Bulletin 1304, 431 p.

Cohenour, R. E., Fox, R. C., and Robison, W. D., 1973, Geology and geophysics of the Iron Creek copper-cobalt deposit, Lemhi County, Idaho: American Institute of Mining, Metallurgical, and Petroleum Engineers, 1973 Pacific Northwest Metals and Minerals Conference, Coeur d'Alene, Idaho 1973, 15 p.; available at U.S. Bureau of Mines, Western Field Operations Center, East 360 3rd Ave., Spokane WA, 99202.

Connor, J. J., 1984, Geochemistry of the Middle Proterozoic Spokane, Grinnell, and St. Regis Formations of the Belt Supergroup, *in* Hobbs, S. W., ed., The Belt: Montana Bureau of Mines and Geology Special Publication 90, p. 102–103.

Engineering and Mining Journal, 1980, Reopening of the Blackbird mine—a possible comeback for US cobalt: v. 181, no. 1, p. 29, 31.

Erdman, J. A., and Modreski, P. J., 1984, Copper and cobalt in aquatic mosses and stream sediments from the Idaho cobalt belt: Journal of Geochemical Exploration, v. 20, p. 75–84.

Ethier, V. G., and Campbell, F. A., 1977, Tourmaline concentrations in Proterozoic sediments of the southern Cordillera of Canada and their economic significance: Canadian Journal of Earth Science, v. 14, p. 2348–2363.

Evans, K. V., 1981, Geology and geochronology of the eastern Salmon River Mountains, Idaho, and implications for regional Precambrian tectonics: University Park, Pa., Pennsylvania State University Ph.D. thesis, 222 p.

Fisher, F. S., McIntyre, D. H., and Johnson, K. M., 1983, Geologic map of the Challis 1°×2° quadrangle, Idaho: U.S. Geological Survey Open-File Report 83–523, 41 p., 2 maps, scale 1:250,000.

Franklin, J. M., Lydon, J. W., and Sangster, D. F., 1981, Volcanic-associated massive sulfide deposits, *in* B. F. Skinner, ed., Economic Geology, 75th Anniversary Volume, 1905–1980: El Paso, Texas, Economic Geology Publishing Co., p. 485–627.

Gair, J. E., and Slack, J. F., 1984, Deformation, geochemistry, and origin of massive sulfide deposits, Gossan lead district, Virginia: Economic Geology, v. 79, no. 7, p. 1483–1520.

Gustafson, L. B., and Williams, Neil, 1981, Sediment-hosted stratiform deposits of copper, lead, and zinc, *in* B. F. Skinner, ed., Economic Geology, 75th Anniversary Volume, 1905–1980: El Paso, Texas, Economic Geology Publishing Co., p. 139–178.

Hahn, G. A., and Hughes, G. J., Jr., 1984, Sedimentation, tectonism, and associated magmatism of the Yellowjacket Formation in the Idaho Cobalt Belt, Lemhi County, Idaho, *in* Hobbs, S. W., ed., The Belt: Montana Bureau of Mines and Geology Special Publication 90, p. 65–67.

Hamilton, J. M., 1984, The Sullivan deposit, Kimberley, British Columbia—a magmatic component to genesis?, *in* Hobbs, S. W., ed., The Belt: Montana Bureau of Mines and Geology Special Publication 90, p. 58–60.

Hamilton, J. M., and others, 1982, Geology of the Sullivan orebody, Kimberley, B.C., Canada: Geological Association of Canada Special Paper 25, p. 597–665.

Hayes, T. S., 1984, The relation between stratabound copper-silver ore and Revett Formation sedimentary facies at Spar Lake, Montana, *in* Hobbs, S. W., ed., The Belt: Montana Bureau of Mines and Geology Special Publication 90, p. 63–64.

Hobbs, S. W., 1980, The Lawson Creek Formation of Middle Proterozoic age in east-central Idaho: U.S. Geological Survey Bulletin 1482-E, 12 p.

Hobbs, S. W., Hays, W. H., and Ross, R. J., Jr., 1968, The Kinnikinic Quartzite of central Idaho—redefinition and subdivision: U.S. Geological Survey Bulletin 1254-J, 22 p.

Hughes, G. J., Jr., 1983, Basinal setting of the Idaho cobalt belt, Blackbird mining district, Lemhi County, Idaho, *in* The genesis of Rocky Mountain ore deposits—changes with time and tectonics: Wheat Ridge, Colo., Denver Region Exploration Geologists Society, p. 21-27.

Koistinen, T. J., 1981, Structural evolution of an early Proterozoic stratabound Cu-Co-Zn deposit, Outokumpu, Finland: Royal Society of Edinburgh Transactions; Earth Sciences, v. 72, no. 2, p. 115-158.

Landreth, J. O., 1964, Geology of the Rattlesnake Creek area, Lemhi County, Idaho: Moscow, Idaho, University of Idaho M.S. thesis, 51 p.

LeHuray, A. P., 1984, Lead and sulfur isotopes and a model for the origin of the Ducktown deposit, Tennessee: Economic Geology, v. 79, no. 7, p. 1561-1573.

Leonard, B. F., 1962, Old metavolcanic rocks of the Big Creek area, in central Idaho, *in* Short papers in geology, hydrology, and topography: U.S. Geological Survey Professional Paper 450-B, p. B11-B15.

Lopez, David, 1981, Stratigraphy of the Yellowjacket Formation of east-central Idaho: U.S. Geological Survey Open-File Report 81-1088, 206 p.

Lund, Karen, Evans, K. V., and Esparza, L. E., 1983, Mineral resource potential map of the Special Mining Management Zone, Clear Creek, Lemhi County, Idaho: U.S. Geological Survey Miscellaneous Field Studies Map MF-1576-A, scale 1:50,000.

Maley, T. S., 1974, Structure and petrology of the lower Panther Creek area, Lemhi County, Idaho: Moscow, Idaho, University of Idaho Ph.D. thesis, 130 p.

McCandless, D. O., 1982, A reevaluation of Cambrian through Middle Ordovician stratigraphy of the southern Lemhi Range [Idaho]: University Park, Pa., Pennsylvania State University Ph.D. thesis, 157 p.

Mitchell, V. E., and Bennett, E. H., 1979, Geologic map of the Elk City quadrangle, Idaho: Idaho Bureau of Mines and Geology, scale 1:250,000.

Peale, R. N., 1982, Geology of the area southeast of Yellowjacket, Lemhi County, Idaho: Moscow, Idaho, University of Idaho M.S. thesis, 129 p.

Peters, D. W., 1979, Geology, mineral, and energy resources, *in* Source Document, Taylor Mountain Planning Unit, July 1979: unpublished report available at Forest Supervisor's Office, Salmon National Forest, Salmon, Idaho 83467.

Purdue, G. L., 1975, Geology and ore deposits of the Blackbird district, Lemhi County, Idaho: Albuquerque, University of New Mexico M.S. thesis, 49 p.

Rember, W. C., and Bennett, E. H., 1979, Geologic map of the Dubois quadrangle, Idaho: Idaho Bureau of Mines and Geology, scale 1:250,000.

Renfro, A. R., 1974, Genesis of evaporite-associated stratiform metalliferous deposits—a sabkha process: Economic Geology, v. 69, no. 1, p. 33-45.

Roberts, W. A., 1953, Metamorphic differentiates in the Blackbird mining district, Lemhi County, Idaho: Economic Geology, v. 48, p. 447-456.

Ross, C. P., 1927, Ore deposits in Tertiary lava in the Salmon River Mountains, Idaho: Idaho Bureau of Mines and Geology Pamphlet 25, 21 p.

_____1934, Geology and ore deposits of the Casto quadrangle, Idaho: U.S. Geological Survey Bulletin 854, 135 p.

Ruppel, E. T., 1975, Precambrian Y sedimentary rocks in east-central Idaho, Chap. A *in* Precambrian and Lower Ordovician rocks in east-central Idaho: U.S. Geological Survey Professional Paper 889, p. 1-23.

_____1978, Medicine Lodge thrust system, east-central Idaho and southwest Montana: U.S. Geological Survey Professional Paper 1031, 23 p.

_____1980, Geologic map of the Patterson quadrangle, Lemhi County, Idaho: U.S. Geological Survey Geologic Quadrangle Map GQ-1529, scale 1:62,500.

_____1982, Cenozoic block uplifts in east-central Idaho and southwest Montana: U.S. Geological Survey Professional Paper 1224, 24 p.

Ruppel, E. T., O'Neill, J. M., and Lopez, D. A., 1983, Preliminary geologic map of the Dillon 1°×2° quadrangle, Montana: U.S. Geological Survey Open-File Report 83-168, 1 map.

Ruppel, E. T., Ross, R. J., Jr., and Schleicher, David, 1975, Precambrian Z and Lower Ordovician rocks in east-central Idaho, chap. B *in* Precambrian and lower Ordovician rocks in east-central Idaho: U.S. Geological Survey Professional Paper 889, p. 25-34.

Shockey, P. N., 1957, Reconnaissance geology of the Leesburg quadrangle, Lemhi County, Idaho: Idaho Bureau of Mines and Geology Pamphlet 113, 42 p., 1 pl.

Skipp, Betty, and Hait, M. H., Jr., 1977, Allochthons along the northeast margin of the Snake River Plain, Idaho, *in* Heisey, E. L., and others, eds., Rocky Mountain thrust belt —geology and resources: Wyoming Geological Association, 29th Field Conference, Guidebook, no. 29, p. 499-515.

Slack, J. F., 1982, Tourmaline in Appalachian-Caledonian massive sulphide deposits and its exploration significance: Transactions of the Institution of Mining and Metallurgy, Section B, Applied Earth Science, v. 91, p. B81-B89.

Snee, L. W., 1983, Effects of thermal history on mineralization, *in* Lund, Karen, Evans, K. V., and Esparza, L. E., Mineral resource potential of the Special Mining Management Zone—Clear Creek, Lemhi County, Idaho: U.S. Geological Survey Miscellaneous Field Studies Map MF-1576-A, Pamphlet, p. 7.

Sobel, L. S., 1981, A stratigraphic model for Precambrian-Y turbidites of central Idaho [abs.]: Geological Society of America Abstracts with Programs, v. 13, no. 7, p. 557.

_____1982, Sedimentology of the Blackbird mining district, Lemhi County, Idaho: Cincinnati, Ohio, University of Cincinnati M.S. thesis, 235 p.

Soregaroli, A. E., 1961, Geology of the McKim Creek area, Lemhi County, Idaho: Moscow, Idaho, University of Idaho M.S. thesis, 53 p.

Staatz, M. H., 1979, Geology and mineral resources of the Lemhi Pass thorium district, Idaho and Montana: U.S. Geological Survey Professional Paper 1049-A, p. A1-A90.

Starr, R. B., 1955, Geology of the Twin Peaks mine, Lemhi County, Idaho: Ithaca, N.Y., Cornell University M.S. thesis, 38 p.

Tucker, D. R., 1975, Stratigraphy and structure of Precambrian Y (Belt?) metasedimentary and associated rocks, Goldstone Mountain quadrangle, Lemhi County, Idaho, and Beaverhead County, Montana: Oxford, Ohio, Miami University Ph.D. thesis, 221 p.

Umpleby, J. B., 1913, Geology and ore deposits of Lemhi County, Idaho: U.S. Geological Survey Bulletin 528, 182 p.

U.S. Bureau of Mines, 1943, Blackbird district, Lemhi County, Idaho—Supplement to War Minerals Report 78: War Minerals Report 131—Copper, Cobalt, 20 p.

Vhay, J. S., 1948, Cobalt-copper deposits of the Blackbird district, Lemhi County, Idaho: U.S. Geological Survey Strategic Mineral Investigations Preliminary Report 3-219, 26 p., 4 pls.

_____1959, Preliminary report on the copper-cobalt deposits of the Quartzburg district, Grant County, Oregon: U.S. Geological Survey Open-File Report, 20 p., 3 pls.

Symposium on the Geology and Mineral Deposits of the Challis 1°×2° Quadrangle, Idaho

Chapter S

Comments on the Development of Resource Assessment Models, Analogy, and Metaphor, and Their Use in Resource Evaluation, Challis Quadrangle

By FREDERICK S. FISHER

CONTENTS

Abstract

Modeling of ore deposits and other geological phenomena is a common practice, yet we seldom examine the underlying thought processes used in constructing and comparing models. Models are sets of information containing both facts and deductions that are based on our perceptions and on incomplete data. As abstractions, they are distorted from reality by deletion, inference, generalization, and the bias of our own experience. Knowledge of how models differ from reality is important in critically examining existing models and constructing new ones.

Analogy is a process by which we extend our ideas into new physical and conceptual territory, and may be classified as analogy by proportionality, by attribution, and by metaphor; all three types are commonly used in ore-deposit studies. Analogy by metaphor is particularly useful for introducing novel concepts, for working with uncertain products and processes, and for explaining ideas to nongeologists. Metaphor, by focusing attention on new combinations of facts and processes, helps to increase our understanding and perception. Increased understanding and perception reduces the bias of our own experiences and aids the thought process by consolidating information. Metaphor assists us in formulating ideas and extending those ideas into new areas. Metaphor is thus useful in creating new models and introducing them into the general body of geological knowledge.

Models of syngenetic stratabound vanadium-silver occurrences in the Paleozoic Salmon River assemblage and of mineralized high-level Eocene rhyolites in the Challis volcanic field illustrate the use of analogy and metaphor in their development as exploration and assessment guides.

INTRODUCTION

This chapter presents a summary of some of the conceptual processes underlying the study of ore deposits for the resource appraisal in the Challis 1°×2° quadrangle. Models of ore deposits are used for a variety of purposes in geology, including exploration guides, assessment methods, financial calculations, and program planning (Peters, 1978, p. 162, 360–362, 542–550). Much has been written about the types of data that should be included in ore-deposit and resource-appraisal models (Harris and Agterberg, 1981; Bailly, 1981; Singer and Mosier, 1981; Botbol and others, 1978; Wolf, 1976; and Cameron, 1975). The focus here is on what a model is, and how models are constructed and compared.

The use of models, analogies, and metaphors is inherent in the science of mineral-resource appraisal, but only models are commonly identified as such, and the thought processes involving analogies and metaphors are rarely if ever described. Models of ore-deposit types are created by selecting common factors from an assemblage of data on a number of ore deposits and occurrences, but those who create the models generally present the finished product and do not describe the process of selection and synthesis. The term "analogy" is sometimes used to describe the comparison of the model with data from a new area but again without explaining the type of comparison being made. The term "metaphor" is rarely seen in geologic literature, even though the use of metaphor in resource appraisal and elsewhere in geology is widespread. It is useful to examine some of the basic features of these concepts and how they are applied in geology.

MODELS

The models we construct are based on our perceptions and on incomplete data; as abstractions they differ and are distorted from reality. In general, our models can be thought of as differing from reality in three ways (Bandler and Grinder, 1975): through deletion, inference, and generalization. We delete because if we put all available facts into our models we are overwhelmed with detail, much of which would be valueless for the purposes of our model. We select the pertinent information by a process of deletion and simplification.

A second difference between models and reality is inference or distortion, which occurs when we shift from observed facts to inferred possibilities. For example, from a study of fluid inclusions, we determine the daughter products and measure filling and freezing temperatures, and then make inferences about the chemistry of the parent ore fluids; from stable-isotope measurements we postulate the sources of the metals in a given ore deposit. Our personal experience biases our thinking so that we select, delete, and evaluate data according to our own experience.

Ore-deposit models also differ from reality through generalization. Generalization is the process by which a model of a given ore-deposit type, based on a selected smaller group of deposits, comes to represent a much larger group of deposits. Generalization allows us to recognize deposits we have never seen before and to classify deposits into selected groups, facilitating the use and understanding of the model.

The most efficient model contains the least number of elements while still maintaining its usefulness. The effectiveness of exploration models is generally increased by focusing the model more toward genetic process than descriptive content. An accurate genetic model of ore deposition is a more powerful prospecting tool than a model based solely on empirical observations because it enables prediction of resource possibilities from less data and permits extension of knowledge into unexplored environments.

ANALOGY AND METAPHOR

We use a process of analogy to refine existing ore-deposit models, to extend them into new physical and

conceptual territory, and to develop new models. Hypotheses "are always suggested through analogy. * * * Analogic reasoning suggests that the desired explanation is similar in character to the known, and this suggestion constitutes the production of a hypothesis" (Gilbert, 1896).

Webster's Third New International Dictionary of the English Language Unabridged (1964) defined analogy as "a similarity of ratios or properties; inference that if two or more things agree with one another in one or more respects they will probably agree in other respects." The dictionary indicated that analogy may be divided into analogy by proportionality, by attribution, and by metaphor. Examples of the use of all three of these types in conjunction with ore-deposit modeling are not difficult to find. An example of analogy by proportionality is Lasky's cumulative tonnage-grade relationship (Lasky, 1950), whereby the tonnage of ore increases exponentially as the grade decreases arithmetically. Examples of analogy by attribution are widespread. In the simplest case we compare the attributes of an ore-deposit model with those of unexplored ground to assess its resource potential. Analogy by metaphor is fertile ground for developing and explaining new ideas. The use of metaphor is widespread in geology; examples include the description of intrusive bodies as "heat engines" driving hydrothermal convection cells, of certain kinds of faults as "trap-door" structures, and of veins as "plumbing systems," recognizing that the word "vein" itself in geologic usage started as a metaphor.

Metaphors introduce novel concepts by using familiar terms to make new ideas easier to understand. By focusing attention on new combinations of facts and processes, metaphor helps to increase our understanding, reduces the bias of our own experiences, and aids the thought process by consolidating information, making it easier to use and remember. Metaphor can be as simple as the substitution of a single word for another word in a given model. Most often, however, the use of metaphor is more general, involving numerous substitutions of fact and process and containing considerable unspecified implications (Black, 1962).

Commonly the most obvious implication or idea expressed is the underlying comparison of similar concepts in a metaphor. For example, in the phrases "trap-door fault" and "ladder vein," the similarity is the geometry of the structures; the shape of the ladder is compared to the vein and the trap door to the fault. In the phrase "heat engine," the comparison is thermodynamic; the production of heat by the engine is compared to that of the intrusive body. But all of these metaphors carry many more unspecified implications or implicit ideas; fluid movement, element dispersal, cooling rates, and convection cells are all associated with the heat-engine metaphor, and the trap-door-fault metaphor implies different structural styles associated with the hinge zone verses the sides of the trap door. These examples illustrate the power of metaphor to aid creative thought by leading our thinking into new areas and also illustrate the general idea of the importance of the unspecified implications or implicit information contained in a metaphor.

In short, metaphors depend very much on the user, each user possibly deriving a somewhat different array of ideas from the same metaphor. Metaphor is most effective when searching for new ideas and thinking broadly.

In the context of mineral exploration, models convey a sense of measurement, precision, scale, detail, boundaries, standards, and pattern. In contrast, when using metaphor, flexibility increases, precision decreases, unknowns are more common and acceptable, scale becomes less material, and details and boundaries are vague. Metaphor assists formulation of ideas and the extension of those ideas into new areas. Metaphor thus is useful for creating new models and for the introduction of those models into the general body of geological knowledge. The models themselves are required when evaluating and judging ideas and when focusing on practical application.

EXAMPLES OF MODELS

About 55 ore-deposit types requiring models for assessment and exploration have been identified in the Challis quadrangle. Two examples illustrating some applications of analogy and metaphor are a syngenetic stratabound vanadium-silver model for the Paleozoic Salmon River assemblage, and a high-level rhyolite model useful within the Challis volcanic field. High-level rhyolites are rhyolite intrusive bodies emplaced at or very near the Earth's surface; some may have breached the surface. In plan, shapes may be circular, linear, or very irregular.

Remobilized lead-silver deposits (Hall and others, 1975) and stratabound zinc deposits in rocks of the Devonian Milligen Formation (Hall, chap. J, this volume) are known south of the Challis quadrangle. The recognition of rocks in the Challis quadrangle that have gross similarities in lithology, color, structural setting, and possibly age to the Milligen (analogy by attributes) suggested a search for stratabound and remobilized deposits in all similar rocks in the Challis quadrangle, including the Paleozoic Salmon River assemblage. Geochemical data gathered from reconnaissance rock sampling to test this idea suggested vanadium and silver rather than lead and silver in the Salmon River assemblage. Thus a new assessment model (changed by substitution) was developed.

The deposits in the Salmon River assemblage are in a thick accumulation of dark-gray to black turbidites composed of argillite, siltstone, calcareous siltstone, quartzite, sandstone, and carbonate beds. These rocks are allochthonous, thrust eastward during the Sevier orogeny

(Armstrong, 1968), and are now exposed along the eastern side of the Idaho batholith (Fisher and others, 1983). Individual beds are generally 1–2 m thick but may be as thick as 10 m. Flute and groove casts, cross laminations, and graded bedding are common. The rocks have been highly deformed, and isoclinal folds are common. The exact thickness of the sequence is unknown but is estimated to be more than 2,000 m. Silver, barium, copper, molybdenum, vanadium, and zinc are all present in anomalous concentrations in these rocks (Fisher and May, 1983). Rock sampling in selected areas in the Salmon River assemblage indicated that stratabound concentrations of vanadium and silver are present and generally are associated with carbonaceous units (Fisher and May, 1983). Zinc and barite may also be present. Geologic mapping suggests that such units are relatively widespread. Details of the geological characteristics and settings of these and other deposits in upper Paleozoic rocks are discussed by Hall (chap. J, this volume). This assessment model indicates that much of the Salmon River assemblage may be favorable for syngenetic vanadium and silver resources.

Epithermal precious-metal deposits are associated with high-level Eocene rhyolites in the Challis volcanic field. A general model for mineral deposits associated with rhyolites (Berger, 1982; Silberman, 1982) was modified to fit data from three mineralized areas in the Challis quadrangle, the Sunbeam, Singheiser, and Parker Mountain gold-silver deposits (Fisher, chap. A, this volume). Many features are presently poorly defined in this model; the term "high-level" is useful because we do not know how close some of these intrusions came to the surface—some breached, others did not. Fracture patterns and directions of hydrothermal-fluid flow markedly control the zoning of ore deposits in these high-level intrusions (Peterson and others, 1977). The cooling history, hydrothermal-fluid flow, and mineralization of rhyolites that breached are probably different from those that did not breach. The rhyolite bodies are mostly domes and dikes that formed late in the volcano-tectonic sequence, probably less than 45 m.y. ago, but the exact time cannot be specified. Preliminary geochemical sampling suggests that silver, gold, arsenic, molybdenum, and zirconium are present in anomalous concentrations (Hardyman and Fisher, chap. N, this volume). These rhyolites are aphyric to porphyritic and are associated with the trans-Challis fault system (Kiilsgaard and Lewis, chap. B, this volume). Application of this exploration model to favorable areas identified by geological mapping by Hardyman (Fisher and others, 1983) has led to the discovery of new areas having high resource potential for gold, silver, and possibly molybdenum (Hardyman and Fisher, chap. N, this volume).

Awareness of the basic aspects of models, analogy, and metaphor focuses attention on some of the thought processes involved in the development of exploration and assessment models and in the search for new mineral resources. It helps avoid the mental traps of rigidly defined models that stifle the innovative thinking needed to see ore possibilities where some may see only barren rock.

REFERENCES CITED

Armstrong, R. L., 1968, Sevier orogenic belt in Nevada and Utah: Geological Society of America Bulletin, v. 79, no. 4, p. 429–458.

Bailly, P. A., 1981, Today's resource status—tomorrow's resource problems—The need for research on mineral deposits, *in* Mineral resources—Genetic understanding for practical applications: Washington, D.C., National Academy Press, p. 21–32.

Bandler, Richard, and Grinder, John, 1975, The structure of magic I: Palo Alto, Calif., Science and Behavior Books, Inc., 225 p.

Berger, B. R., 1982, The geological attributes of Au-Ag base-metal epithermal deposits, *in* Erickson, R. L., compiler, Characteristics of mineral-deposit occurrences: U.S. Geological Survey Open-File Report 82–795, p. 119–126.

Black, Max, 1962, Models and metaphors: New York, Cornell University Press, 267 p.

Botbol, J. M., Sinding-Larsen, R. S., McCammon, R. B., and Gott, G. B., 1978, A regionalized multivariate approach to target selection in geochemical exploration: Economic Geology, v. 73, no. 4, p. 534–546.

Cameron, E. M., ed., 1975, Conceptual models in exploration geochemistry, the Canadian cordillera and Canadian shield: Journal of Geochemical Exploration, v. 4, no. 1, 213 p.

Fisher, F. S., and May, G. D., 1983, Geochemical characteristics of the metalliferous Salmon River sequence, central Idaho: U.S. Geological Survey Open-File Report 83–670, 28 p.

Fisher, F. S., McIntyre, D. H., and Johnson, K. M., 1983, Geologic map of the Challis 1°×2° quadrangle, Idaho: U.S. Geological Survey Open-File Report 83–523, 39 p. and 2 oversize sheets, scale 1:250,000. Also available from Idaho Bureau of Mines and Geology, Moscow, Idaho 83843.

Gilbert, G. K., 1896, The origin of hypothesis, illustrated by the discussion of a topographic problem: Science, new series, v. 3, no. 53, p. 1–13.

Hall, W. E., Rye, R. O., and Doe, B. R., 1975, Wood River mining district, Idaho—Intrusion related lead-silver deposits derived from country rock source: U.S. Geological Survey Journal of Research, v. 6, no. 5, p. 579–592.

Harris, D. P., and Agterberg, F. P., 1981, The appraisal of mineral resources, *in* Skinner, B. J., ed., Economic Geology, 75th anniversary volume, 1905–1980: Economic Geology Publishing Co., p. 897–938.

Lasky, S. G., 1950, How tonnage and grade relations help predict ore reserves: Engineering and Mining Journal, v. 151, no. 4, p. 81–85.

Peters, W. C., 1978, Exploration and mining geology: New York, John Wiley and Sons, 696 p.

Peterson, Ulrich, Noble, D. C., Arenas, M. J., and Goodell, D. C., 1977, Geology of the Julcani mining district, Peru: Economic Geology, v. 72, p. 931–949.

Silberman, M. L., 1982, Hot-spring type, large tonnage, low-grade gold deposits, *in* Erickson, R. L., compiler, Characteristics of mineral-deposit occurrences: U.S. Geological Survey Open-File Report 82–795, p. 131–143.

Singer, D. A., and Mosier, D. L., 1981, A review of regional mineral resource assessment methods: Economic Geology, v. 76, no. 5, p. 1006–1015.

Wolf, K. H., 1976, Conceptual models in geology, *in* Wolf, K. H., ed., Handbook of strata-bound and stratiform ore deposits, v. 1, Principles and general studies: New York, Elsevier Scientific Publishing Co., p. 11–78.

*U.S. GOVERNMENT PRINTING OFFICE: 1986-676-047:26014